RADIO FREQUENCY INTERFERENCE FROM SMALL A.C. COMMUTATOR MOTORS

by

TIRLOCHAN SINGH BILKHU

A thesis submitted for the Degree of

DOCTOR OF PHILOSOPHY

THE UNIVERSITY OF ASTON IN BIRMINGHAM

October 1985

THE UNIVERSITY OF ASTON IN BIRMINGHAM

Radio Frequency Interference from small a.c. commutator motors

Submitted for the degree of Doctor of Philosophy.

By: Tirlochan Singh Bilkhu.

SUMMARY

Small a.c. commutator motors as used in domestic appliances inherently generate unacceptably high levels of Radio Frequency Interference (RFI) and thus require suppression. The factors affecting the generation of RFI in the motor design parameters and the influence of mechanical variations in the motor assembly have been studied by experimental means. The relative importance of various factors, in terms of the interference level which they generate is established by isolation of the individual RFI sources so far as is practicable. In addition a case-study of the manufacture of domestic appliance motors at Hoover plc (the industrial sponsors of this thesis) was carried out in order to identify the causes of motor to motor variability in RFI levels from mass produced motors.

It has been found that commutation even without the influence of the short circuited coil parameters generates high RFI levels. The additional influence of the short circuited coil parameters is to further increase RFI. It is shown that the construction of the armature and field can be engineered to reduce overall RFI levels from small motors.

The contact stability of the brushes has been isolated as a major factor in influencing RFI levels. The allowable mechanical tolerances in the motor construction to minimise brush vibration and thus reduce RFI have been determined and these are compared with those used in manufacture at Hoover plc. It has been found that motor to motor variability in RFI levels results from manufacturing tolerances achieved on the shop floor. Recommendations for the reduction of this variability are stated. It is concluded that improvement of brush stability by appropriate mechanical design improves commutation which in turn; reduces overall RFI levels, reduces suppression cost, minimuses motor to motor variations in RFI levels and reduces brush wear.

KEYWORDS commutator motors, RFI, radio frequency interference, case-study, commutation.

ACKNOWLEDGEMENTS

Acknowledgements are made to the origanisations which have collaborated with the IHD Scheme at Aston University to make this research possible, namely: Hoover plc, the Department of Electrical and Electronic Engineering and the Department of Production Engineering at Aston University, and the Science and Engineering Research Council.

Grateful acknowledgements are expressed to the project Supervisory Team for their invaluable contributions and enthusiastic support. Particular thanks to Mr. B. James for his encouragement and guidance throughout the research and in the preparation of this thesis, and to Mr. R. Binnie for his help and support within the Hoover plc organisation.

Finally sincere thanks to my family for their patience and understanding for which I shall be forever indebted.

T.S. Bilkhu

October, 1985

Supervisory Team

Mr.B.James (main supervisor), Dept. of Electrical and Electronic Eng.

Mr.D.S.Palmer (associate supervisor), Dept.of Electrical and Electronic Eng.

Mr. R. Binnie (industrial supervisor), Hoover plc.

Dr. R. Ethridge (associate supervisor),Dept.of Production Engineering

Mr. D. Hickson (tutor), IHD Schemes Office

Dr. D. Van Rest (tutor), IHD Schemes Office

CONTENTS

			Page No.
Summary			ii
Acknowledgements			iii
Contents			iv
List of Figures			viii
List of Tables			xxiii
List of Photographs			xxiv
Chapter 1		INTRODUCTION	1
	1.1	Problems caused by EMI	2
	1.2	The nature of electrical interference	4
	1.3	Interference generating mechanisms	6
	1.4	Interference from domestic appliances	9
	1.5	Development of RFI regulations	11
	1.6	Motor design and RFI	14
Chapter 2		THE PROJECT PROPOSAL - BACKGROUND AND OUTLINE	24
	2.1	Hoover plc	25
	2.2	Engineering at Hoover	26
	2.3	RFI work at Hoover	29
	2.4	RFI suppression components	32
	2.5	Economic considerations	35
	2.6	The project proposal	38
	2.7	Practical aspects of industry based research	40

Page No.

Chapter 3		SMALL A.C. COMMUTATOR MOTORS	48
	3.1	General construction	50
	3.2	Vector diagram	56
	3.3	The commutation process	59
	3.4	Brush EMFs	62
	3.5	Voltage equation of the short circuited coil	65
	3.6	Improvement of commutation	67
	3.7	The brush-commutator contact	68
	3.8	Effects of vibration on commutation	71
	3.9	Discussion on commutation	82
Chapter 4		RESEARCH LITERATURE REVIEW ON RFI	107
	4.1	Man-made RFI sources	109
	4.2	RFI from small commutator motors	115
	4.3	RFI detection methods	137
	4.4	RFI measuring techniques	144
	4.5	Discussion	148
Chapter 5		TEST EQUIPMENT AND EXPERIMENTAL PROCEDURE	176
	5.1	Motor test rig design	178
	5.2	Construction details	180
	5.3	Programme for experimental test woık	187
	5.4	Instrumentation and measurement	198

		Page No.
Chapter 6	TEST RESULTS AND DISCUSSION	232
6.1	RFI caused by the commutator switching action	233
6.2	RFI caused by the variation of the short circuited coil parameters	244
6.3	RFI due to the influence of the physical components of the armature and field	258
6.4	RFI due to the influence of mechanical variations in the motor assembly	286
Chapter 7	CASE STUDY TO DETERMINE THE SOURCES OF VARIABILITY IN RFI LEVELS FROM MASS PRODUCED MOTORS	408
7.1	Background to case study	409
7.2	Manufacturing tolerances	411
7.3	Factory structure	418
7.4	General quality monitoring	420
7.5	Objective manufacturing problems	421
7.6	Subjective manufacturing problems	445
7.7	Reduction of variability in RFI levels	450
Chapter 8	CONCLUSIONS AND RECOMMENDATIONS	467
8.1	Conclusions from experimental investigations	468
8.2	Conclusions from case-study	477
8.3	Recommendations for future work	479

Page No.

Appendix A1	TEST RIG DETAIL DRAWINGS	483
Appendix A2	TEST RESULTS	505
Appendix A3	PROPERTIES OF THE FOURIER TRANSFORM	588
Appendix A4	ESSON'S FORMULA	589
Appendix A5	THE USE OF THE MICROWAVES IN OBSERVING BRUSH MOVEMENT IN FRACTIONAL HORSEPOWER COMMUTATOR MOTORS	590
Appendix A6	PHOTOGRAPHS	603
References		611

LIST OF FIGURES

Page No.

Fig. 1.1	Spectral energy in the time and frequency domains	17
Fig. 1.2	Sources of electromagnetic interference	17
Fig. 1.3	Generation of RFI by the variation of circuit parameters	18
Fig. 1.4	Generation of RFI by the variation of stored energy by switching	18
Fig. 1.5	High frequency equivalent circuit of a series motor	19
Fig. 1.6	Symmetrical and asymmetrical components of interference currents	19
Fig. 1.7	Modes of RFI propogation	20
Fig. 1.8	Interference complaints received by the Post Office since 1949	21
Fig. 1.9	Limits on conducted RFI voltage (150kHz-30MHz) and radiated RFI power (30MHz-300MHz) applicable to household appliances	22
Fig. 1.10	International organisation for the control and abatement of RFI (from McLachlan et al [7])	23
Fig. 2.1	Equivalent circuit of a capacitor over a wide frequency range	43
Fig. 2.2	Effect of lead length on capacitor impedence	43
Fig. 2.3	Comparison of filtering performance of feed-through and lead-type capacitors	44
Fig. 2.4	Equivalent circuit of an inductor over a wide frequency range	45
Fig. 2.5	Frequency response of a T.V. choke inductor	45
Fig. 2.6	Maximum and minimum spread of RFI levels measured from production suction cleaners	46
Fig. 2.7	Comparison of prices of various 0.1μF suppression capacitors since 1973	47
Fig. 2.8	Percentage on-cost of fitting suppression on 'MC04' model motor	47
Fig. 3.1	Series motor connections	90

		Page No.
Fig. 3.2	Common stator configurations	90
Fig. 3.3	Range of stator variations found in small series motors	91
Fig. 3.4	Range of rotor variations found in small series motors	92
Fig. 3.5	Optimised shape of motor laminations	92
Fig. 3.6	Example of 12 slot rotor wound with 2 coil sides per slot	93
Fig. 3.7	Two typical commutator assemblies	93
Fig. 3.8	Common brush mounting arrangements used in small motors	94
Fig. 3.9	Vector diagram of series motor	95
Fig. 3.10	Comparison of speed-torque characteristics of a small motor on d.c. and 50Hz supply	95
Fig. 3.11	Characteristics of a 150W series motor	96
Fig. 3.12	Commutation of coils 1 and 4 as the rotor moves relative to the brushes	96
Fig. 3.13	Commutation in single phase machines	97
Fig. 3.14	Short-circuited winding element	97
Fig. 3.15	Resistance commutation and linear commutation	98
Fig. 3.16	Delayed commutation (a) and over-commutation (b)	98
Fig. 3.17	Flux circling the commutating coils	99
Fig. 3.18	Static and dynamic hysteresis loop of the laminations	99
Fig. 3.19	Distortion of the air gap flux by armature reaction	100
Fig. 3.20	Voltage and current components of the commutating coil	100
Fig. 3.21	Circuit diagram of the short-circuted coil	101
Fig. 3.22	Improvement of commutation by brush shift	101
Fig. 3.23	Variation of sparking intensity with increasing external vibration frequency	102
Fig. 3.24	Modes of vibration induced by static (A) and dynamic (B) unbalance	102

		Page No.
Fig. 3.25	Limiting curve for maximum eccentricity as a function of speed for small motors	103
Fig. 3.26	Simplified brush and eccentric commutator arrangement	103
Fig. 3.27	Optical arrangement to measure brush vibration	104
Fig. 3.28	Variation of current density at brush tip against time from the start of commutation	104
Fig. 3.29	Limiting curve for arcing voltage with increasing brush metallic content	105
Fig. 3.30	Variation of coil inductance with frequency	105
Fig. 3.31	Variation of the measured active inductance of the commutating coil with brush position	106
Fig. 4.1	Typical radiated noise spectra for r.f. stabalised arc welders	154
Fig. 4.2	Radiated noise spectra for a resistance welder at various distances from the source	155
Fig. 4.3	Radiated noise spectra of an electric discharge cutting machine	155
Fig. 4.4	Typical line orginated RFI	156
Fig. 4.5	Typical radiated RFI from automobile ignition systems	156
Fig. 4.6	Event sequence of the ignition system	157
Fig. 4.7	Typical RFI measured from fluorescent tubes	158
Fig. 4.8	RFI generated from mechanical switches	158
Fig. 4.9	Theoretical spectrum envelopes	159
Fig. 4.10	RFI from a commutator motor at 15000 r/min	160
Fig. 4.11	Comparison of RFI from (a) normal brush, (b) laminated brush on commutators and (c) normal brush on slip ring	160
Fig. 4.12	Comparison of standard and laminated brushes for various angles of brush shift	161
Fig. 4.13	Effect of slip ring material on sliding contact interference	161
Fig. 4.14	Effect of brush force on sliding contact interference	162

		Page No.
Fig. 4.15	Effect of speed variation on RFI from a commutator motor	162
Fig. 4.16	Comparison of RFI levels measured on the positive and negative conductors of a small motor on a.c. supply	163
Fig. 4.17	Comparison of RFI levels from a 24 and 12 bar commutators	163
Fig. 4.18	Comparison of RFI levels with increases in motor loading and armature unbalance	164
Fig. 4.19	High frequency equivalent circuit of a symmetrical series motor	164
Fig. 4.20	Measured variation of the asymmetrical internal impedance with frequency of two series motor appliances	165
Fig. 4.21	Examples of impedence measurements recorded from field and armature windings	165
Fig. 4.22	Equivalent circuit of a symmetrical series motor (above), showing measured stray capacitances and interference currents (below)	166
Fig. 4.23	High frequency equivalent circuit of a series motor postulated by Hall and Quelch	167
Fig. 4.24	Comparison of RFI levels from rectangular waves at various frequencies with those obtained from electrical machines	167
Fig. 4.25	Predicted RFI levels from repetitive trapezoidal, sinusoidal and triangular pulses	168
Fig. 4.26	Predicted RFI levels for a 28V step or pulses of various width and rise times	169
Fig. 4.27	Operating cycle of a simple switch	169
Fig. 4.28	Simplified h.f. equivalent circuit of an appliance connected to the mains supply via a V-network mains terminating impedence	170
Fig. 4.29	Block diagram of an RFI measuring receiver	170
Fig. 4.30	Quasi-Peak detector circuit	171
Fig. 4.31	Quasi-Peak pulse response curve	171
Fig. 4.32	Block diagram of instrumentation system for obtaining APD data of ignition noise	172
Fig. 4.33	Measured APD of ignition noise	172

		Page No.
Fig. 4.34	Block diagram of NAD counter	173
Fig. 4.35	Measured NAD due to vehicle traffic	173
Fig. 4.36	Measurement of radiated RFI by the "Swedish Method"	174
Fig. 4.37	Measurement of radiated RFI by the "Absorbing clamp method"	174
Fig. 4.38	Test arrangement used by Hall and Quelch to assess the influence of RFI of the commutator-brush contact	175
Fig. 5.1	Test rig framework	210
Fig. 5.2	Non-drive end plate assembly	211
Fig. 5.3	Test rig armature assembly	211
Fig. 5.4	Test rig base plate	212
Fig. 5.5	Brush box assembly	212
Fig. 5.6	Test rig field assemblies	213
Fig. 5.7	Location of field assembly in the test rig	214
Fig. 5.8	Test rig assembled with drive fan	215
Fig. 5.9	Fan-air drive arrangement	215
Fig. 5.10	Test- ig loading arrangement	216
Fig. 5.11	Rotor construction (a) and operation (b) for RFI tests described in section 5.3.1	216
Fig. 5.12	Test arrangement for measurement of RFI levels due to the commutator switching action	217
Fig. 5.13	Circuit diagram of the commutation model used in the RFI tests described in section 5.3.2	218
Fig. 5.14	Construction of rotor for use in the commutation model	218
Fig. 5.15	Special brush-box assembly	218
Fig. 5.16	Variable voltage source "e"	219
Fig. 5.17	Armature for static out-of-balance tests	219
Fig. 5.18	Armature for dynamic out-of-balance tests	219
Fig. 5.19	Brush holder movement to vary brush alignment on quadrature axis	220

		Page No.
Fig. 5.20	Variation of brush-brush box clearance a) tangential and b) axial to commutator rotation	220
Fig. 5.21	Brush overhang length	221
Fig. 5.22	Insertion of steel shims to produce vertical bearing misalignment	221
Fig. 5.23	Movement of non-drive end plate to produce horizontal bearing misalignment	222
Fig. 5.24	Insertion of steel shims to produce an asymmetric air gap in the direct axis	223
Fig. 5.25	Insertion of steel shims to produce an asymmetric air gap in the quadrature axis	223
Fig. 5.26	Asymmetric air gap (a) in the direct axis and (b) in the quadrature axis	224
Fig. 5.27	Test arrangement for measurement of conducted RFI	224
Fig. 5.28	RFI measurement test equipment	225
Fig. 5.29	Test arrangement for measurement of radiated RFI	226
Fig. 5.30	Simplified diagram of the r.f. bridge circuit	227
Fig. 5.31	Test arrangement for detection of interference currents	228
Fig. 5.32	Substitution of test rig for a signal generator to determine magnitude of interference currents	228
Fig. 5.33	Armature coils 1 and 7 undergoing commutation	229
Fig. 5.34	Test arrangement for measurement of active inductance	229
Fig. 5.35	Measurement of armature unbalance	230
Fig. 5.36	Measurement of spring force	230
Fig. 5.37	Measurement of commutator profile	231
Fig. 5.38	Block diagram of commutator roughness measuring equipment	231
Fig. 6.1	Construction of chart used for the graphical presentation of measured RFI data	304

Page No.

Fig. 6.2 Measured RFI levels from a 24 segment commutator at 1.5A supply current with varying shaft speed 305

Fig. 6.3 Measured RFI levels from a 24 segment commutator at 2.5A supply current with varying shaft speed 306

Fig. 6.4 Measured RFI levels from a 22 segment commutator at 1.5A supply current with varying shaft speed 307

Fig. 6.5 Measured RFI levels from a 21 segment commutator at 1.5A supply current with varying shaft speed 308

Fig. 6.6 Effect of speed variation on measured RFI levels from a 24 segment commutator at 1.5A supply current 309

Fig. 6.7 Effect of speed variation on measured RFI levels from a 22 segment commutator at 1.5A supply current 310

Fig. 6.8 Effect of speed variation on measured RFI levels from a 21 segment commutator at 1.5A supply current 311

Fig. 6.9 Comparison of measured RFI levels with the EEC limits from a 24 segment commutator (1.5A supply current) at (a) 16000 r/min and (b) 22000 r/min 312

Fig. 6.10 Measured brush movement with varying shaft speed using (a) 24, (b) 22 and (c) 21 segment commutator 313

Fig. 6.11 Effect of current variation on measured RFI levels from a 24 segment commutator at 14000 r/min 314

Fig. 6.12 Effect of current variation on measured RFI levels from a 22 segment commutator at 14000 r/min 315

Fig. 6.13 Effect of current variation on measured RFI levels from a 21 segment commutator at 14000 r/min 316

Fig. 6.14 Measured RFI levels from a 24 segment commutator at zero supply current with varying shaft speed 317

Fig. 6.15 Effect of speed variation on measured RFI levels from a 24 segment commutator at zero supply current 318

Page No.

Fig. 6.16	Measured RFI levels from a copper slip ring at 1.5A supply current with varying shaft speed	319
Fig. 6.17	Comparison of measured RFI levels from a copper slip ring and a 24 segment commutator rotating at 18000 r/min and 1.5A supply current	320
Fig. 6.18	Effect of speed variation on measured RFI levels from a copper slip ring at 1.5A supply current	321
Fig. 6.19	Effect of current variation on measured RFI levels from a copper slip ring at 18000 r/min	322
Fig. 6.20	Measured RFI levels with varying resistance, Rs, (Ls = 0, e = 0) at 5000 r/min and 1.5A supply current	323
Fig. 6.21	Measured RFI levels with varying resistance, Rs, (Ls = 0, e = 0) at 10000 r/min and 1.5A supply current	324
Fig. 6.22	Measured RFI levels with varying resistance, Rs, (Ls = 0, e = 0) at 15000 r/min and 1.5A supply current	325
Fig. 6.23	Measured RFI levels with varying resistance, Rs, (Ls = 0, e = 0) at 20000 r/min and 1.5A supply current	326
Fig. 6.24	Effect of varying resistance, Rs, on measured RFI levels at 5000 r/min	327
Fig. 6.25	Effect of varying resistance, Rs, on measured RFI levels at 10000 r/min	328
Fig. 6.26	Effect of varying resistance, Rs, on measured RFI levels at 15000 r/min	329
Fig. 6.27	Effect of varying resistance, Rs, on measured RFI levels at 20000 r/min	330
Fig. 6.28	Measured RFI levels with varying inductance, Ls, (Rs = 0.15 ohm, e = 0) at 5000 r/min and 1.5A supply current	331
Fig. 6.29	Measured RFI levels with varying inductance, Ls, at 10000 r/min and 1.5A supply current	332
Fig. 6.30	Measured RFI levels with varying inductance, Ls, at 15000 r/min and 1.5A supply current	333
Fig. 6.31	Measured RFI levels with varying inductance, Ls, at 20000 r/min and 1.5A supply current	334

		Page No.
Fig. 6.32	Measured RFI levels with varying inductance, Ls, on measured RFI levels at 5000 r/min	335
Fig. 6.33	Measured RFI levels with varying inductance, Ls, on measured RFI levels at 10000 r/min	336
Fig. 6.34	Measured RFI levels with varying inductance, Ls, on measured RFI levels at 15000 r/min	337
Fig. 6.34	Measured RFI levels with varying inductance, Ls, on measured RFI levels at 20000 r/min	338
Fig. 6.36	Measured RFI levels with varying supply current and Ls = 50μH at 15000 r/min	339
Fig. 6.37	Measured RFI levels with varying supply current and Ls = 100μH at 15000 r/min	340
Fig. 6.38	Measured RFI levels with varying supply current and Ls = 500μH at 20000 r/min	341
Fig. 6.39	Variation of un-commutated current at Tc with increasing armature current	342
Fig. 6.40	Measured RFI levels with varying circuit emf (e) at $\psi = 45^{o}$ with Ls = 230μH at 15000 r/min and 1.5A supply current	343
Fig. 6.41	Measured RFI levels with varying circuit emf (e) at $\psi = 45^{o}$ with Ls = 500μH at 15000 r/min and 1.5A supply current	344
Fig. 6.42	Measured RFI levels with varying circuit emf (e) at $\psi = 45^{o}$ with Ls = 1000μH at 15000 r/min and 1.5A supply current	345
Fig. 6.43	Influence of circulating current on commutation	346
Fig. 6.44	Measured RFI levels with varying phase angle, ψ , at e = 4V (Ls = 230μH) at 15000 r/min and 1.5A supply current	347
Fig. 6.45	Measured RFI levels with varying circuit emf (e) at $\psi = 45^{o}$ with Ls = 230μH at 15000 r/min and 0.5A supply current	348
Fig. 6.46	Measured RFI levels with varying circuit emf (e) at $\psi = 45^{o}$ with Ls = 230μH at 15000 r/min and 2.5A supply current	349
Fig. 6.47	Measured RFI levels from the U-type field system at 1, 1.5 and 2A	350

		Page No.
Fig. 6.48	Measured RFI levels from the U-type field system with loose fitting laminations at 0.5, 1, 1.5 and 2A	351
Fig. 6.49	Measured RFI levels from the U-type field with stationary unwound 12 slot armature at 0.5, 1, 1.5 and 2A	352
Fig. 6.50	Measured RFI levels from 12/24 armature (field system removed) at 1.5A supply current with varying speed	353
Fig. 6.51	Measured values of active inductance, L_{comm}, with varying brush position on 12/24 armature	354
Fig. 6.52	Test rig connections for single winding using (a) U-type field (b) O-type field	355
Fig. 6.53	Measured RFI levels with the field windings connected to the line side of the mains supply using a 12/24 armature and U-type field	356
Fig. 6.54	Measured RFI levels with the field windings connected to the neutral side of the mains supply using a 12/24 armature and U-type field	357
Fig. 6.55	Simple r.f. equivalent circuit of test rig with U-type field windings connected to the line side of the mains supply	358
Fig. 6.56	R.F. impedance of the U-type field	359
Fig. 6.57	Measured RFI levels with field windings connected to the line side of mains supply using a 12/24 armature and O-type field	360
Fig. 6.58	R.F. impedance of the O-type field	361
Fig. 6.59	Comparison of measured symmetric interference currents from the test rig fitted with (a) U-type field and (b) O-type field	362
Fig. 6.60	Comparison of measured asymmetric interference currents from the test rig fitted with (a U-type field and (b) O-type field	363
Fig. 6.61	Measured RFI levels with the field windings connected to the line side of the mains supply using a 12/24 armature and U-type field with the earth connection removed	364
Fig. 6.62	Measured asymmetric and symmetric interference currents from the test rig fitted with 12/24 armature and U-type field with the earth connection removed	365

Page No.

Fig. 6.63	Measured RFI levels with field windings connected to the line side of the mains supply using a 12/24 armature and U-type field with the earth connected to the field lamination stack	366
Fig. 6.64	Field connected as a split winding either side of the armature	367
Fig. 6.65	Comparison of measured RFI levels using the 12/24 armature and O-type field with the windings connected (a) to one side of the armature and (b) in the split winding configuration	368
Fig. 6.66	Comparison of measured RFI levels using the 12/24 armature and U-type field with the windings connected (a) to one side of the armature and (b) in the split winding configuration	369
Fig. 6.67	Comparison of measured summetric and asymmetric interface currents from the test rig fitted with (a) U-type field and (b) O-type field in the split winding configuration	370
Fig. 6.68	Comparison of measured asymmetric interference currents from the test rig fitted with (a) U-type field and (b) O-type field in the split winding configuration	371
Fig. 6.69	Measured R.F. impedance between split windings of (a) the O-type and (b) the U-type field	372
Fig. 6.70	Simple r.f. equivalent circuit of the test rig with O-type field windings balanced either side of the armature	373
Fig. 6.71	Comparison of measured RFI levels obtained using U-type field with different armature configurations	374
Fig. 6.72	Measured symmetric interference currents from the test rig with different armature configurations	375
Fig. 6.73	Measured asymmetric interference currents from the test rig with different armature configurations	376
Fig. 6.74	Measured R.F. impedance between armature windings and laminations using (a) 7/21 (b) 12/24 and (c) 11/22 armature	377
Fig. 6.75	Measured RFI levels with varying armature turns per coil using 12/24 armature and U-type field	378

		Page No.
Fig. 6.76	Measured RFI levels with varying armature turns per coil using 7/21 armature and U-type field	379
Fig. 6.77	Speed current characteristics of the test rig fitted with 12/24 armature and U-type field at 240V with varying motor load	380
Fig. 6.78	Measured RFI levels with varying motor load using 12/24 armature and U-type field	381
Fig. 6.79	Measured RFI levels with varying armature static out-of-balance at 18000 r/min	382
Fig. 6.80	Effect of varying static out-of-balance on measured RFI levels at 18000 r/min	383
Fig. 6.81	Measured RFI levels with varying armature dynamic out-of-balance at 18000 r/min	384
Fig. 6.82	Effect of varying armature dynamic out-of-balance on measured RFI levels at 18000 r/min	385
Fig. 6.83	Measured RFI levels with varying spring load at 18000 r/min	386
Fig. 6.84	Effect of varying spring load on measured RFI at 18000 r/min	387
Fig. 6.85	Measured RFI levels with varying brush alignment along the quadrature axis against the direction of rotation	388
Fig. 6.86	Effect of varying brush alignment along the quadrature axis against the direction of rotation on measured RFI levels	389
Fig. 6.87	Measured RFI levels with varying brush alignment along the quadrature axis with the direction of rotation	390
Fig. 6.88	Effect of varying brush alignment along the quadrature axis with the direction of rotation	391
Fig. 6.89	Measured RFI levels with varying heights of proud commutator segments at 18000 r/min	392
Fig. 6.90	Measured brush movement with varying height of proud commutator segments at 18000 r/min	393
Fig. 6.91	Measured RFI levels with varying commutator eccentricity at 18000 r/min	394

		Page No.
Fig. 6.92	Effect of varying commutator eccentricity on measured RFI levels at 18000 r/min	395
Fig. 6.93	Measured RFI levels with varying commutator surface finishes	396
Fig. 6.94	Effect of varying commutator surface finish on measured RFI levels	397
Fig. 6.95	Measured RFI levels with (a) under-cut commutator insulation and (b) flush commutator insulation	398
Fig. 6.96	Measured RFI levels with varying brush box and brush clearance in the direction tangential to commutator rotation	399
Fig. 6.97	Effect of varying brush box and brush clearance on measured RFI levels	400
Fig. 6.98	Measured RFI levels with varying brush overhang length at 18000 r/min	401
Fig. 6.99	Effect of varying brush overhang length on measured RFI levels	402
Fig. 6.100	Measured RFI levels with varying bearing misalignment at 18000 r/min	403
Fig. 6.101	Effect of varying angular brush shift on measured RFI levels at 13000 r/min	404
Fig. 6.102	Measured RFI levels with varying bearing journal diameter	405
Fig. 6.103	Movement of under-size armature bearing journal inside bearing inner race with rotation	406
Fig. 7.1	Maximum and minimum RFI levels recorded from a selection of production cleaners fitted with the MC14 motor	453
Fig. 7.2	Maximum and minimum RFI levels recorded from a selection of production cleaners fitted with the EURO motor	454
Fig. 7.3	Measured RFI levels from cleaner fitted with EURO motor a) with sticking brushes b) after correction	455
Fig. 7.4	Measured RFI levels from cleaner fitted with EURO motor a) with proud commutator b) after correction	456

Page No.

Fig. 7.5	Measured RFI levels from cleaner fitted with EURO motor a) with armature out-of-balance b) after correction	457
Fig. 7.6	Dirt fan assembly a) on MC14 armature shaft and b) on EURO armature shaft	458
Fig. 7.7	Lobed journal contours; a) theoretical three lobed journal of diameter "d" b) contour of armature bearing journal obtained from shop floor	459
Fig. 7.8	Examples of commutator profiles resulting from lobed bearing journals	460
Fig. 7.9	Brush box defects; a) distorted box cross-section, b) bowed constriction along box length, c) burr on front end of box	461
Fig. 7.10	Screw clamping of brush box to motor frame to reduce vibration	462
Fig. 7.11	Measured RFI levels from EURO motor constructed to specified tolerances a) without suppression, b) with parallel 0.1uF capacitor, c) with parallel 0.1uF capacitor and two in line 6uH inductors	463
Fig. 7.12	Maximum and minimum RFI levels recorded from cleaners fitted with EURO motors (suppressed) constructed to specified tolerances	464
Fig. 7.13	Maximum and minimum RFI levels recorded from clearners fitted with EURO motors constructed to specified tolerances and with brush boxes glued to motor frame	465
Fig. 7.14	Maximum and minimum RFI levels recorded from cleaners fitted with EURO motors constructed to specified tolerances and only 0.1uF parallel capacitor suppression	466
Fig. A1.1(a)	Test rig general layout 1 (Front elevation - section C/L)	484
Fig. A1.1(b)	Test rig general layout 2 (Plan view)	485
Fig. A1.2(a)	Test rig general layout 3 (Section A-A)	486
Fig. A1.2(b)	Test rig general layout 4 (Section B-B)	487

		Page No.
Fig. A1.3	Non-drive end plate	488
Fig. A1.4	Drive end plate	489
Fig. A1.5	Base plate	490
Fig. A1.6	Brush box assembly clamping ring	491
Fig. A1.7	Non-drive end plate detachable central disk	492
Fig. A1.8	Spacing posts	493
Fig. A1.9	Insulating back plate	494
Fig. A1.10	Insulating brush box holder block	495
Fig. A1.11	Insulating brush box holder block clamping nut	496
Fig. A1.12	Drive end plate bearing clamping disc	497
Fig. A1.13	Brush box clamping plate	498
Fig. A1.14	Non-drive end plate bearing cup finger clamp	499
Fig. A1.15	Test rig framework fixed stop	500
Fig. A1.16	Field assembly clamp	501
Fig. A1.17	Bottom half field assembly cradle (U-type field)	502
Fig. A1.18	Upper clamping half field assembly cradle	503
Fig. A1.19	Bottom half field assembly cradle (O-type field)	504

LIST OF TABLES

		Page No.
Table 3.1	Critical speeds of eccentric commutator for zero brush spring force	79
Table 3.2	Classification of the quality of commutation	83
Table 6.1	Measured values of active inductance L_{comm} for top and bottom armature coils	277
Table 6.2	Measured short-circuited coil transformer voltage on test armatures	279
Table 6.3	Measured short-circuited coil active inductance and transformer voltage on test armatures	283
Table 6.4	Summary of allowable mechanical tolerances on test rig assembly for minimum RFI	303
Table 7.1	Comparison of specified manufacturing tolerances on MC14 and EURO motor assemblies with test results	412
Table 7.2	Summary of maximum mechanical variations recorded from production motors	416

LIST OF PHOTOGRAPHS

		Page No.
Plate A6.1	Test rig assembly (with field removed)	604
Plate A6.2	Test rig (plan view)	604
Plate A6.3	U-type field assembly	605
Plate A6.4	Hoover MC14 motor	605
Plate A6.5	MC14 armature assembly	606
Plate A6.6	MC14 U-type field	606
Plate A6.7	MC14 brush assembly	607
Plate A6.8	MC14 dirt fan	607
Plate A6.9	Hoover EURO motor	608
Plate A6.10	EURO armature assembly	608
Plate A6.11	EURO O-type field	609
Plate A6.12	EURO brush assembly	609
Plate A6.13	EURO dirt fan	610

CHAPTER 1

INTRODUCTION

1.1 Problems caused by EMI

1.2 The nature of electrical interference

1.3 Interference generating mechanisms

1.4 Interference from domestic appliances

1.5 Development of RFI regulations

1.6 Motor design and RFI

CHAPTER 1

INTRODUCTION

Small a.c. commutator motors for domestic applicances have evolved over the years to a design which is considered suitable for the application, and also for mass manufacture at reasonable cost. These designs have been a compromise between performance, size and cost - but the motors inherently generate unacceptable levels of electromagnetic interference (EMI) and thus require suppression.

The study in this thesis concentrates on the radio frequency region of the electromagnetic spectrum, ranging from 150 kHz to 300 MHz. Interference in this region is commonly called radio frequency interference (RFI) or radio noise, in earlier works it has also been referred to as electrical noise and radio influence voltage (RIV).[1] This chapter serves as a general introduction to the problems caused by EMI, dsescribing the nature of electrical interference and the methods by which it is transmitted to the environment. The continuing changes in regulations concerning the control of EMI and the present limits applying to electric motors are considered and finally in section 1.6 the needs for RFI investigations in motor design are discussed.

1.1 Problems caused by EMI

Electromagnetic interference can impair the functioning of electrical equipment, White [2] describes EMI as a form of 'environmental pollution' capable of polluting the frequency spectrum from DC to about 40 GHz.

Most people are familiar with some common effects of EMI pollution; the ignition of an automobile idling outside the house can cause interference to a television picture by developing intermittent dash lines or bars, or even cause complete flipping (loss of synchronism) of the picture. A domestic appliance like an electric drill or a vacuum cleaner operating in the house (or a neighbours house) can result in buzzing or crackling noise on radio reception, causing distress to the listener. These situations can be of considerable nuisance, and thus EMI has a direct bearing on the enjoyment by millions of viewers and listeners to both radio and television broadcasting. The 'nuisance' of EMI cannot be taken too lightly, as is clear when we consider the result of EMI pollution in other areas, such as communications, defence and medical equipment.

Reduction of EMI is an important factor in the provision of intelligible telephonic communication and can be critical in connection with vital radio services such as those employed on ships and aircraft. For example, EMI can result in a jammed radio signal causing navigational errors in an aeroplane with catastrophic results.

EMI can result in the malfunctions of all types of electrical equipment affecting the lives of many people, e.g. burglar alarms and fire alarm systems also medical equipment such as heart pace-makers, dialysis machines, life support systems to name but a few. The corruption of signals to a radio scanner satellite tracking devices or digital systems such as computer equipment controlling the firing sequence of a nuclear war-head missile could affect the lives of many millions of people. It becomes apparent that EMI resulting in spectrum pollution is more than just an engineering problem, the abatement of interference has also major social and economic considerations.

1.2 The Nature of Electrical Interference

A single electrical pulse (transient) occuring in the time domain produces a continuous energy spectrum throughout a specific bandwidth in the frequency domain. The repetition of such a pulse in regular sequence produces phase cancellations in the time domain, which in turn gives rise to spectral lines occuring in the frequency domain. [5] In Figure 1.1, a geometrical interpretation of the planes of spectral energy appearing in the frequency and time domains is given. This illustrates the spectral planes produced by very narrow repetitive pulses.

When these discrete frequency components can be resolved within the bandwidth of the measuring equipment, then the effective energy distribution is defined as 'narrowband' noise (or 'coherent' noise). Conversley when these discrete frequency components cannot be resolved within the energy distribution it is defined as 'broadband' noise (also known as 'continuous' noise and 'non-coherent' noise). This latter class of impulsive interference is the type produced by commutator motors.

Any waveform can be described as a function of either the time domain or the frequency domain by using Fourier Transforms.[6] Equations defining the Fourier Transform and their associated properties are given in Appendix A3.

EMI is caused by both natural and man-made noise, some of the common sources are listed in Figure 1.2. Natural noise includes atmospheric noise and precipitation static as well as extra-terrestial emmissions originating from the sun. Man-made interference noise can be divided into four classes as listed below;[7]

(a) interference from other radio systems operating on the same frequency channel, (eliminiated by careful frequency assignment or time sharing between co-channel stations).

(b) interference caused by spurious out-of-hand radiation produced by both radio receivers and transmitters.

(c) interference caused by electrical equipment in which r.f. energy is deliberately generated for heating purposes.

(d) interference from electrical equipment of many different kinds in which r.f. energy is an unwanted by-product in the normal functioning of the apparatus.

RFI produced by small commutator motors in domestic appliances, which are the subject of this thesis, fall into this latter category of man-made noise.

Theoretically all systems of varying charges and currents radiates a certain ammount of energy.[8] In many cases in actual practice the radiation can be ignored, for example radiation from a 50 Hz power transmission line exists in theory, but the radiated power is so small that it can hardly be detected. In the case of high frequency transmissions e.g. from waveguides, the power is transmitted in the radiated wave but the currents in the walls of the waveguide are negligible. Interference covering the RFI spectrum band starts from only 150kHz where electrical power is transmitted by conduction, up to 300 MHz where much of the power exists in the radiated waves. Thus for the purposes of measurement the RFI spectrum is divided into a low frequency region from 150kHz to 30 MHz where conducted RFI is measured across a standard mains terminal impedance, and a high frequency region from 30 MHz to 300 MHz where radiated interference power is measured.[9]

Radio frequency interference is generated mainly where sharp or steep changes in currents or voltages occur i.e. when radio frequency harmonics are generated. The ammount of interference caused to a receiver is governed by the degree of coupling between the interference source and the receiver, the rate and amplitude of the current or voltage change, and also the bandwidth of the receiver.

1.3 Interference Generating Mechanisms

The basic interference generating mechanisms which produce EMI current components in electrical circuits have been summarized by Hall and Quelch [10] as follows;

(a) variation of circuit parameters

(b) variation of stored energy

(c) voltage transients

In addition to these there is also,

(d) electrical arcing. [11]

1.3.1 Variation of Circuit Parameters (Figure 1.3)

i) Resistance

Rapid variation of resistance can affect surges and dips in current which produces EMI current components. The brush to commutator contact in a motor is a typical example of this type of variation and even a simple switch can be considered as a variation of resistance i.e. from zero resistance when the switch is closed to infinite resistance when the switch is opened.

ii) Inductance

For an inductor (L) the induced e.m.f. 'e' is in part a function of the rate of change of Inductance.

$$e = - d(Li)/dt \qquad (1.1)$$

Thus a variation in Inductance, due to non-linearity of the magnetic circuit or varying air gap due to rotation of a slotted armature, gives rise to an induced e.m.f. which in turn can cause a current change leading to EMI.

iii) Capacitance

The generation of current 'i' in a capacitor (C) is in part a function of the rate of change of capacitance.

$$i = d(Cv)/dt \qquad (1.2)$$

Any variation of capacitance which can result from the movement of two conducting planes can generate EMI.

1.3.2 Variation of stored energy by switching

Electromagnetic energy can either be stored in an inductive or capacatative circuit, a transient change of energy due to switch operation causes interference currents to flow. These may be directly or inductively coupled to a nearby circuit or a receiver. Figure 1.4 which shows two circuits which are mutually coupled. Stored energy is suddenly released in circuit 'a' when the switch is closed. The electromagnetic field about 'a' changes correspondingly and sets the tuned circuit 'b' into oscillation. The degree of excitation depends on the degree of coupling between 'a' and 'b', as well as the rate and amplitude of the change in 'a' and the bandwidth of 'b'. An example of this type of interference is the sudden short-circuit applied to an armature coil at the start of commutation.

1.3.3 Voltage Transients

A rapid change of voltage applied to a circuit produces a corresponding change of current thus generating interference. The mechanism is the same as 1.3.2.

In a capacatative circuit the rate of change of voltage directly generates RFI currents as indicated by equation 1.2. In an inductive circuit the rate of change in current induces an e.m.f. which itself can cause a rapid change in current leading to RFI (see equation 1.1).

Voltage transients can occur in a periodic manner with electronic circuits or by a commutator.

1.3.4 Electrical Arcing

The formation and cessation of arcs can be considered as an impulsive type disturbance to a circuit and may cause considerable RFI. The arc itself radiates energy rich in harmonics, becoming another source of interference.

1.4 Interference from Domestic Appliances

A.C. Commutator Motors (also known as Universal Motors and A.C. Series Motors) are used extensively in small domestic appliances. In this thesis the term 'motor' will refer to this type of motor. Their applications include vacuum cleaners, food mixers, washing machines, sewing machines, law mowers, spin dryers, hair dryers, hand drills, carving knives and coffee grinders. These motors have ideal characteristics for these applications - a high starting torque, wide speed range and a good power to weight ratio, and it is unlikely that any other motor will replace the A.C. Commutator motor for many years to come.[12] The current world production of these motors is around 200 million per year (not including The Peoples Republic of China), of this about 70 million are made in the European Economic Community (EEC) and 10 million in the U.K.

The operation of these motors give rise to EMI as described in section 1.3. It is found that the interference is more pronounced at some frequencies than others. This is due in part to the intensity of certain harmonics in the frequency domain of the complex waveforms involved and also due to the attenuation of certain harmonics caused by the interaction of the complex inductance and capacitance components present in the motor.

Figure 1.5 shows the high frequency equivalent circuit of an A.C. commutator motor presented by Livshits [14] (the components of the circuits are more fully described in section 4.2.2). The stray capacitances of the windings have the effect of 'tuning' the interference at certain frequencies which gives the appliance an interference-frequency characteristic which is far from simple to interpret. In addition the overall extent of the frequency range of the interference is governed largely by these stray components.[15]

The mains lead connecting the appliance to the electrical supply may be regarded as a transmission line along which radio frequency currents are propogated with increasing attenuation depending on the physical constants of the conductors. The motor itself can be regarded as a radio frequency generator which produces r.f. voltages (a) between its terminals termed the 'symmetrical' component of interference and (b) between each terminal and its frame known as the 'asymmetrical' component. The symmetrical and asymmetrical component voltages produce currents in the conductors which circulate as shown in Figure 1.6. It can be seen that the symmetrical interference produces currents which at any instant are flowing outward in one conductor and returning via the other; the asymmetrical interference flows outwards through both conductors in parallel and returns by way of earth or through the capacitive coupling.

Stephens [15] suggested that the symmetrical interference currents do not produce a radiated field, but are propogated along the conductors, and being mainly responsible for the interference in the mains supply. The asymmetrical current path resembles that of an aerial and thus propogates 'Radiated Interference'. Radiation of this type can produce an interference at the receiver aerial. Radiated Interference can also induce interfering currents in other conductors, not necessarily connected to the electrical supply e.g. telephone wires, metal gas and water pipes, metal gutters or steel frames in buildings. These currents will produce further radiation fields which can affect a receiver. This last mode of propogation is referred to as 'Re-radiated Interference'. Figure 1.7 illustrates all three modes of interference propogation.

1.5 Development of RFI Regulations

The abatement of interference was on a purely voluntary basis in the United Kingdom until the passing of the Wireless Telegraphy Act 1949. [17] Regulations made under this Act prescribed requirements for limits of RFI from various electrical apparatus, but they applied chiefly to the users of such equipment. Committees set up by the Institution of Electrical Engineers (IEE) and the British

Standards Institution co-ordinated work carried out by broadcasting organisations and representatives of the electrical and radio industry in the study of RFI problems. The advice and guidance provided by this effort led to the production of relevant British Standards on the measurement of RFI (BS 727) [18] and limits of RFI (BS 800). [19]

The introduction of regulations encouraged manufacturers to use suppressor equipment for appliances during manufacture, the main attraction being able to advertise their products as 'complying to British Standards'. The effect of the regulations contributed to a fall in complaints to the Post Office of interference from a peak of 170,000 in 1955 to around 40,000 per year at present. [20] Figure 1.8 shows the rise and fall of interference complaints received by the Post Office since 1949.

Internationally, RFI regulations differed from country to country, and these differences represented a barrier to trade of electrical equipment. Thus the U.K. participated in the work of the International Special Committee on Radio Interference (C.I.S.P.R.) which operates under the aegis of the International Electrotechnical Commission (I.E.C.). The aims of C.I.S.P.R. are the establishment of internationally agreed methods of measurement and limits of RFI. It is interesting to note that in most cases U.K. regulations have been in line with the recommendations of C.I.S.P.R.

With the advent of the European Economic Community (EEC), all member nations were subject to EEC Directives to harmonize technical requirements concerning RFI. EEC Directive 76/889/EEC [22] relating to "electrical household appliances, portable tools and similar equipment" was agreed and adopted in November 1976. In August 1978, this Directive became enforceable by Law within the U.K.

The Directive sets out regulations stipulating the requirements on manufacturers (as well as others) to ensure that their equipment complies with RFI limits. The statutory requirement for domestic appliances is that equipment then shall be within the maxima of terminal voltage and interference power set out in BS 800: 1977 - since it is recognised that in volume production it is possible that a few appliances may fall outside the limits, and the Law allows statistical monitoring checks to be applied ensuring 80% of the production shall meet the limits with 80% confidence. [21]

Figure 1.9 shows the limits of conducted (curve 'a') and radiated (curve 'b') RFI from domestic appliances producing continuous interference in normal operation. Curve 'c' indicates the limits on conducted RFI using an alternative method of measurement as detailed in EEC Directive 82/499/EEC. [23] RFI measurement techniques and equipment are described in section 4.4. In this thesis the term "ClSPR/EEC limits" shall refer to the RFI limits relating to domestic appliances producing continuous interference in normal operation in EEC Directive 76/889/EEC and BS800: 1977.

The effect of the Law is such that if the Secretary of State is of the opinion that apparatus does not comply with the regulations then he may serve notice on any person or company who has manufactured, assembled or imported it in the course of business, prohibiting him from placing it in the U.K. market. Figure 1.10 shows the national and international organisation for the control and abatement of radio interference.

1.6 Motor Design and RFI

The level of radio frequency interference produced by a motor, determines how 'electromagnetically compatible' it is with the environment. The mechanisms by which RFI is generated and propagated by motors have been stated but very little additional literature on the subject is available. Thus the motor designer has no definite guide lines on how to achieve a compromise between the electromechanical performance and electromagnetic compatibility (EMC). The introduction of legislation to limit the levels of RFI from motors have made the solution of this problem a statutory requirement.

It has long since been known that the major source of interference is the commutation process. [71] Satisfactory improvement of commutation can be obtained in large motors with compoles and compensating windings but for small motors this is impracticable. The designer requires to know how changes in the commutation process will effect the level of RFI ultimately produced so that he may adjust the motor parameters to suit.

The design philosophy for commutator motors is well established and can be found in a number of standard text books. [24, 25, 26] The starting point generally used for the dimensioning of all commutator machines (including small commutator motors) is Esson's formula (see Appendix A4), but Schuisky [28] found this formula not directly applicable for small motors rated below 4kW. Investigations into the performance of small motors by Puchstein and Kimberley [27] led to practical design recommendations for of use by designers. These recommendations include acceptable values p.f., overall efficiency, specific magnetic and electric loading in air gap flux density and the armature.

Hoover plc, a major manufacturer of small commutator motors and domestic appliances, have adapted their design philosophy broadly around the recommendations of Puchstein and Kimberley. The motor design methods at Hoover plc, were studied to find out whether any special design procedures were adopted to minimise RFI but it was found that Hoover substantially used the standard design methods in common with other motor manufacturers.

The four stages of motor design are as follows:

(a) Description; describing performance of the machine as a function of the frequency, input voltage, motor speed and load.

(b) Detail design: choosing the main dimensions and the electrical winding and magnetic circuit design, this stage is influenced by progress in materials technology and the designers experience.

(c) Dimensioning; choosing the final values of parameters so that the design satisfies the performance specification.

(d) Test and Optimisation: Full prototype performance tests which may result in minor modification to design.

It was found that at Hoover the problem of RFI was considered only at the final stages of testing. At this point very little design modification would be possible to reduce RFI if it was found to be above the CISPR/EEC limits.

RFI suppression has thus been affected by fitting external r.f. filter networks to the mains terminals of the motor. This has for a long time proved to be satisfactory, since although RFI regulations did exist, motor manufacturers had no legal obligation to comply with them. The implementation of the EEC Directives and subsequent statutory regulations has led industry to re-appraise the design philosophy and costs with regard to RFI suppression. At Hoover plc it was found that in the case of some of their appliances the cost of suppression is a considerable proportion of the motor cost. Clearly a new and better solution to the problem has to be found.

Senior technical management at Hoover plc recognised that the answer to minimise RFI lay not in designing sophisticated and expensive r.f. filter circuits, but to design the motor itself so that it generates lower RFI. It was realised that the investigations could best be carried out as a university project. The University of Aston have been successfully operating an Interdisciplinary Higher Degrees Scheme for some years and this scheme caters for multidisciplinary industrial projects, the supervision being provided both by Industry and the urversity. Such projects are funded by Science and Engineering Research Council (SERC) and the decision was taken to carry out a detailed practical study of the effect of motor design parameters on the levels of RFI generation.

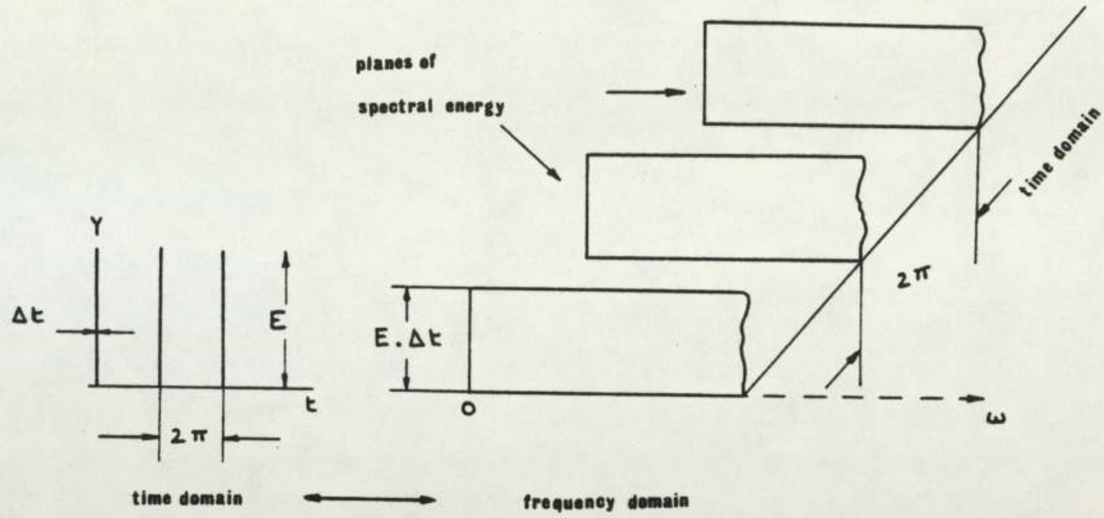

Spectral energy in the time and frequency domains
Fig. 1.1

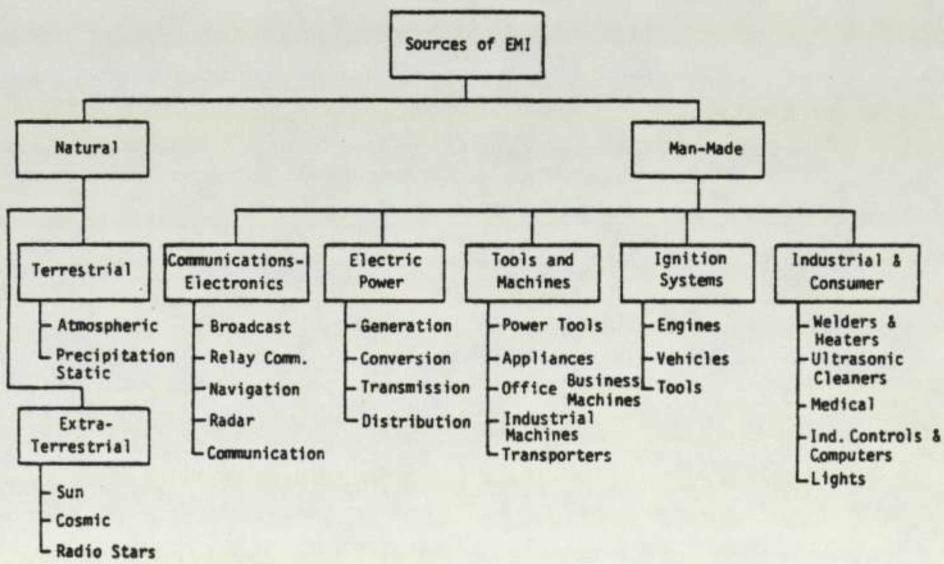

Sources of electromagnetic interference
Fig. 1.2

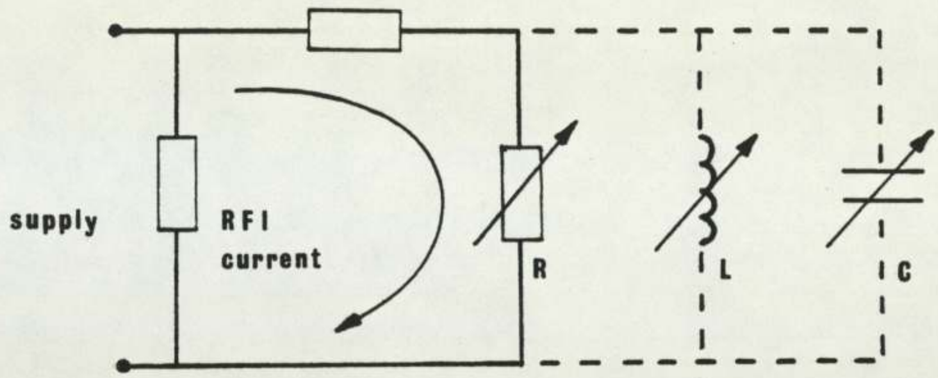

Generation of RFI by the variation of circuit parameters

Fig. 1.3

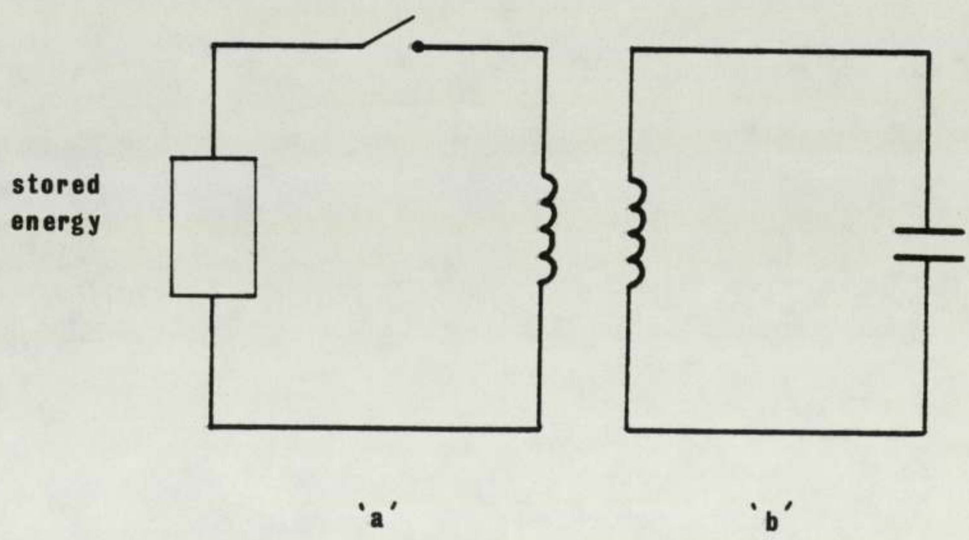

Generation of RFI by the variation of stored energy by switching

Fig. 1.4

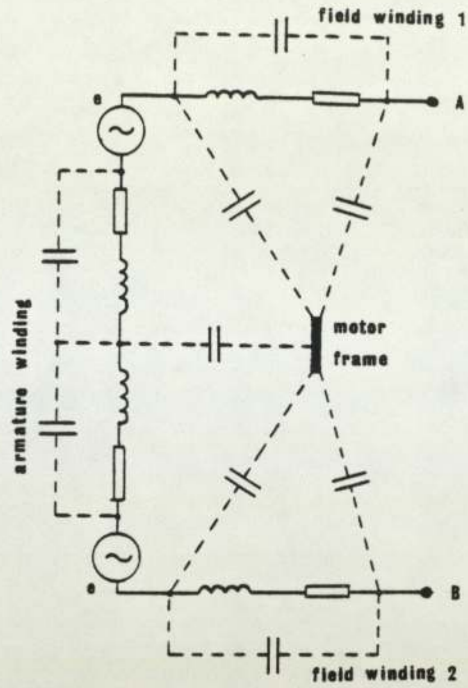

High frequency equivalent circuit of a series motor

Fig. 1.5

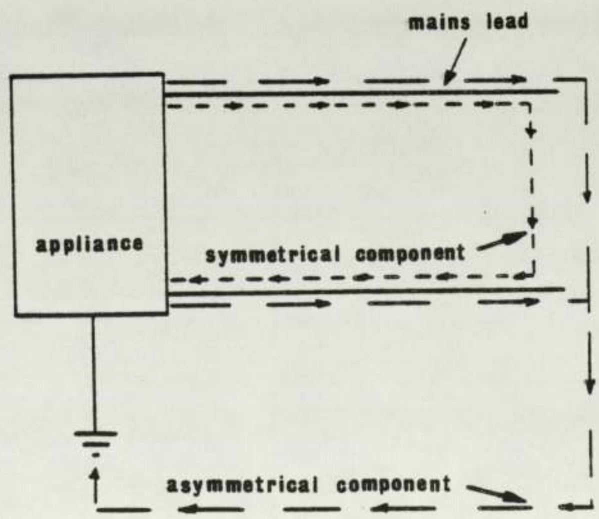

Symmetrical and asymmetrical components of interference currents

Fig. 1.6

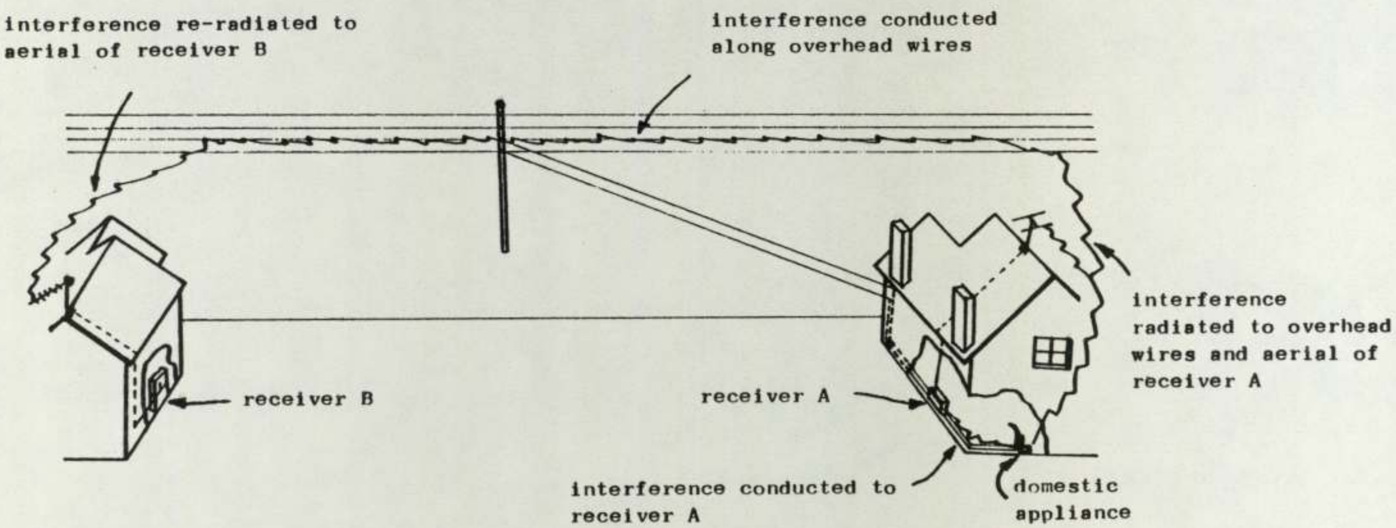

Modes of RFI propogation

Fig. 1.7

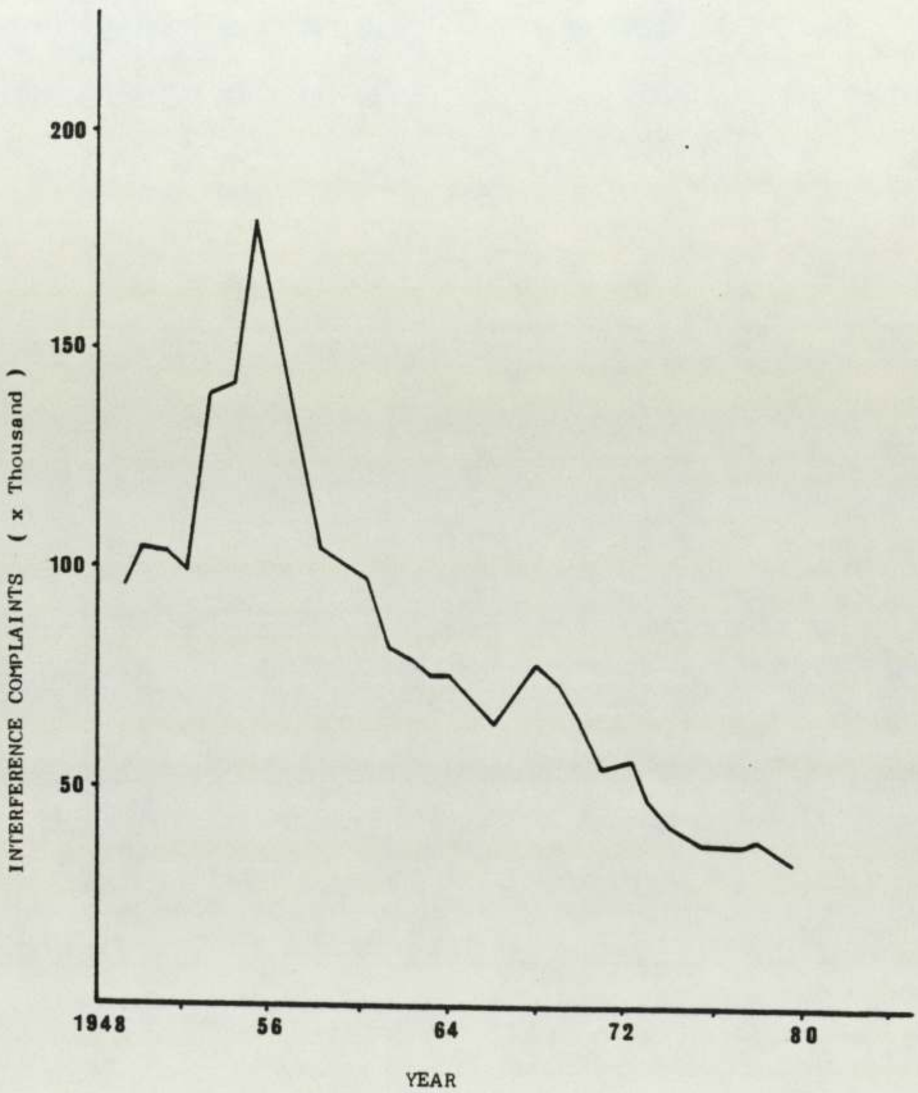

Interference complaints received by the Post Office since 1949

Fig. 1.8

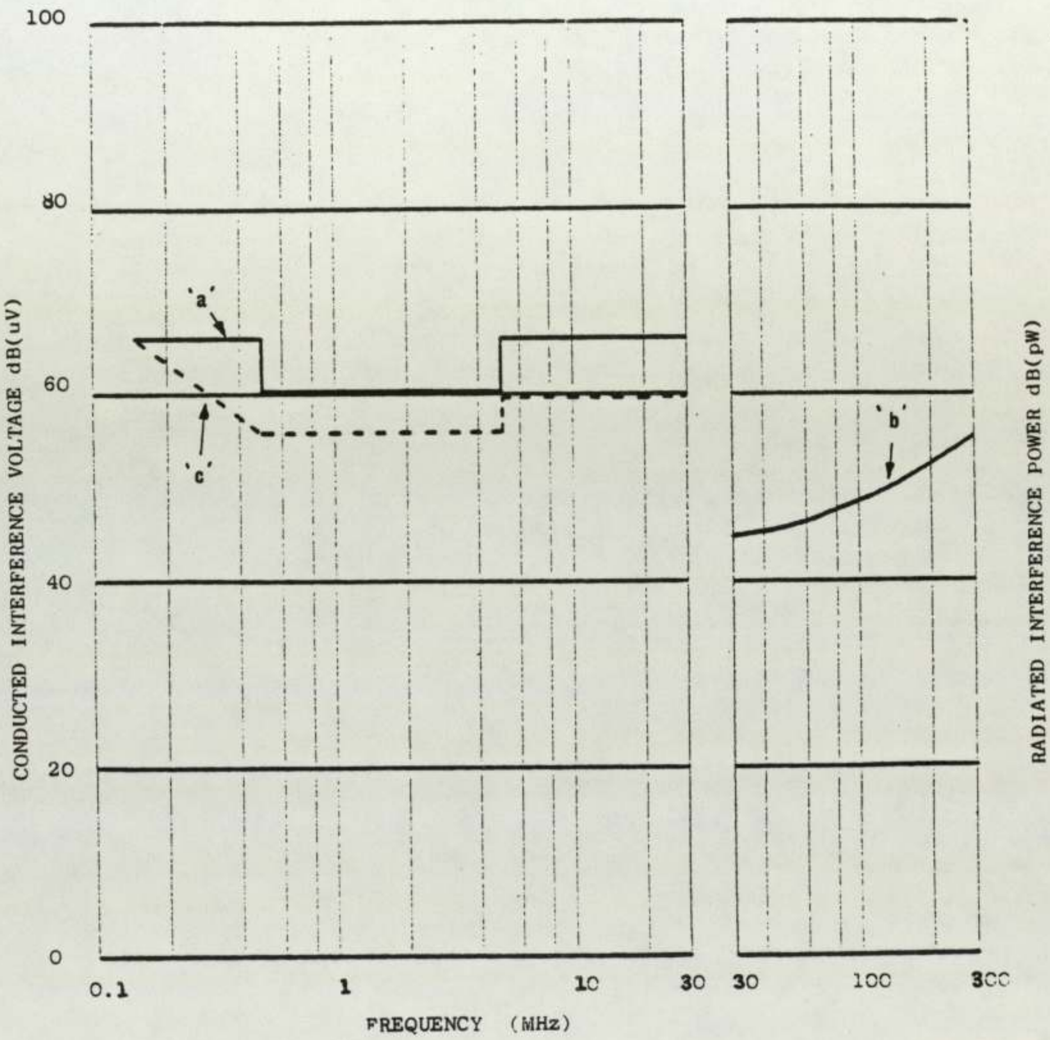

Limits on conducted RFI voltage (150 kHz - 30 MHz) and radiated RFI power (30 MHz - 300 MHz) applicable to household appliances

Fig. 1.9

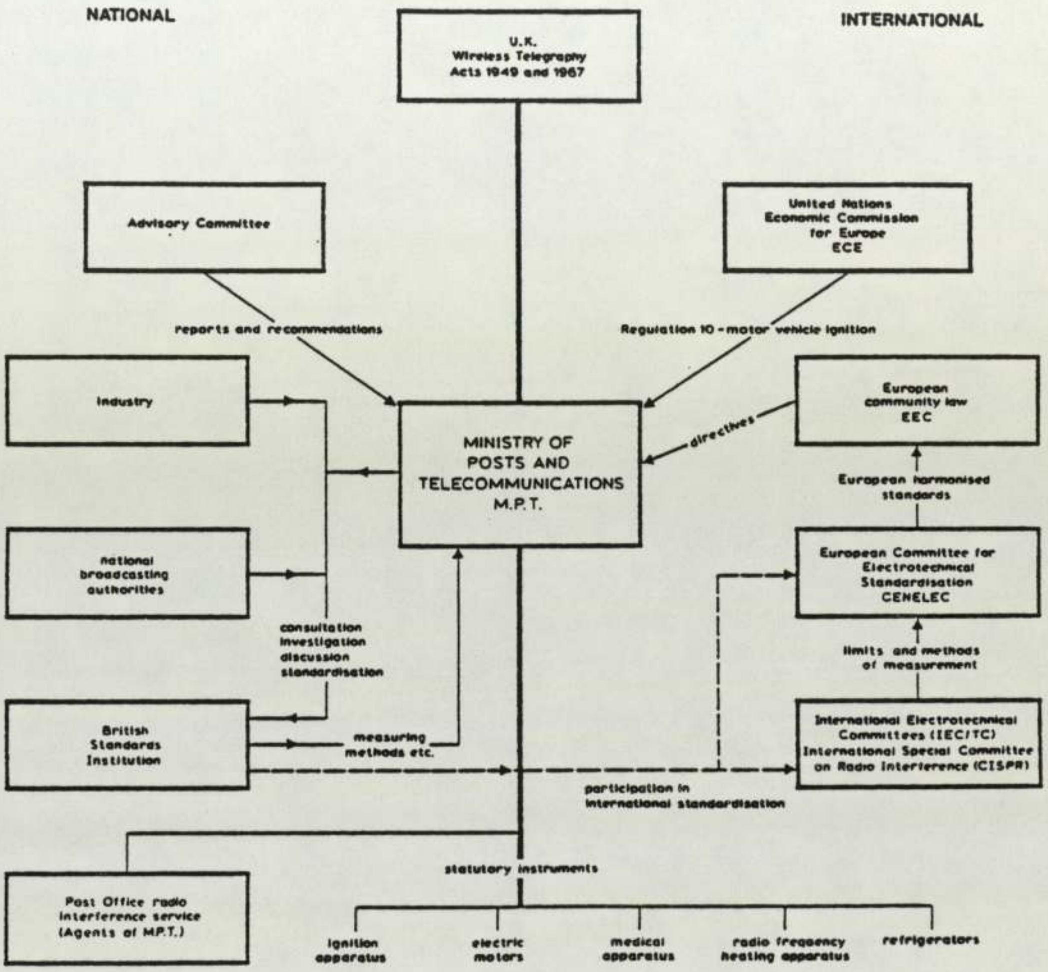

International organisation for the control and abatement of RFI (from McLachlan et al [7])

Fig. 1.10

CHAPTER 2

THE PROJECT PROPOSAL - BACKGROUND AND OUTLINE

2.1 Hoover plc

2.2 Engineering at Hoover

2.3 RFI work at Hoover

2.4 RFI suppression components

2.5 Economic considerations

2.6 The project proposal

2.7 Practical aspects of industry based research

CHAPTER 2

THE PROJECT PROPOSAL - BACKGROUND AND OUTLINE

This chapter presents an introduction to the Hoover company and its Engineering department at 'Headquarters' in Perivale, London. A study of Hoover's experience of RFI work, suppression methods and their costs are presented. In section 2.6 the original project proposal is presented and discusses the events which led to the revised work represented in this thesis.

2.1 Hoover plc

Hoover plc is the most widely known manufacturer of vacuum cleaners in the world and the worlds largest manufacturer concentrating solely on domestic appliances. The company began in 1908 in North Canton (then Berlin), Ohio, where the American Hoover Company was founded and the Hoover Worldwide Corporation is situated today.

The first British Hoover factory was built at Perivale, Middlesex in 1932; continuing demand for Hoover products in the U.K. and Europe, led the company to open new factories in Merthyr Tydfil, Mid-Glamorgan (1948), for the production of washing machines and Cambuslang, Lanarkshire (1946) to share the manufacture of small commutator motors and suction cleaners with the Perivale factory.

The product range sold in the U.K. includes vacuum cleaners, floor polishers, shampoo polishers, washing machines, tumble and spin dryers, refrigerators, freezers, electric irons and recently home security systems such as fire alarms and burglar alarms.

The total market of vacuum cleaners in the U.K. is presently around 2 million a year, of which Hoover holds nearly 50% of the upright cleaner market and 18% of the suction cleaner market. Similarly, in the total washing machine sales of approximately 1.5 million per year, Hoover holds over 25% of the market. Exports from the U.K. make up almost 30% of the output of the British factories, which comprises some 60% of Britains total export of vacuum cleaners.

During the course of this project, in October 1981, a decision to close the Perivale factory and transfer its work to the Cambuslang site was taken. (The effects of this move on the project are discussed in section 2.7). Perivale remains the Headquarters of the British Hoover organisation and the centre of Hoover engineering and design in the U.K.

Merthyr Tydfil is the production centre for Hoover washing machines, spin dryers and tumble dryers, with about 2,000 employees, it is the biggest factory of its kind in Britain.

Cambuslang, with some 1700 employees, is now the sole factory producing Hoover commutator motors and floor care products. Nearly 26 million Hoover vacuum cleaners have been made here since production started in 1946.

2.2 Engineering at Hoover

The manufacturing centres at Merthyr Tydfil and Cambuslang have their own Engineering departments and these are chiefly responsible for the smooth running of the respective factories supplying Engineering support for production. Engineering of new products their research and design is undertaken at Perivale, Engineering

Headquarters. This department has approximately 100 employees and is divided into six major sections as follows:

(a) Research and Development

(b) Industrial Design

(c) Motor and Controls laboratory

(d) Floor care laboratory

(e) Major appliance (white goods) laboratory

(f) Model shop

The Research and Development section is set up primarily to innovate new products and new product features. Once an idea is seen to have a marketable potential, it is passed on to the laboratories for further work. Industrial design employs designers and draughtsmen, producing designs for Hoover products, making them smart in appearance and easy to manufacture and assemble - incorporating new and eye-catching features that help sell the products in the market place.

The floor care and major appliance laboratories put new appliances through rigorous scientific tests to assess their performance and durability. Years of normal household use being compressed into days by non-stop operation. They test new materials and manufacturing methods for suitability. The motor and controls laboratory headed by Mr. R. Binnie (Industrial Supervisor to this project) carries out the design and test of motors and controls as used in Hoover appliances. The majority of test work presented in this thesis concentrated in this laboratory and is thus described in further details below (2.2.1).

Finally, the model shop serves all the other engineering sections, employing a number of highly skilled technicians to make prototype parts and models for use in the laboratories.

2.2.1 The Motor and Control Laboratory

The motor and controls laboratory is made up of the following sections:

(a) motors

(b) controls

(c) electronics

The motors section leader Mr. J. Harrington, is the Chief Motor designer at Hoover and has a staff of five engineers, involved in design and test of proto-type motor designs. Once the proto-type and pre-production motors have proved successful in laboratory conditions, the motors are fitted into appliances which undergo further tests both in the laboratory and in the field. When finally the motor goes into full production at Cambuslang, engineering responsibility is passed onto the resident engineering section at the production site - but the motor laboratory is still consulted on any design change or modifications.

The section leader of the controls and electronics section is Mr. N. Hamilton, these sections with approximately seven engineers are responsible for mechanical and electronic control systems as used in cleaners and washing machines made by Hoover. They design specifications for control devices manufactured by outside suppliers, then carry out their own performance tests in the laboratory. The electronics section, is also involved in the design or burglar and fire alarm systems.

RFI testing is technically under the control section, but for practical purposes, its work remains as an indepedent function in the motor and controls laboratory. There is one full time engineer responsible for RFI testing and design of suppression networks for all Hoover products. Personnel from the motor and controls laboratory are encouraged to join National and International Standard making Groups concerned with standards for the design and manufacture of electrical equipment and make the case for the particular requirement of the domestic appliance industry.

2.3 <u>RFI Work at Hoover</u>

The motor and controls laboratory at Engineering Headquarters, have carried out RFI test work since the mid 1940's, archived test records of RFI measurements date back to early 1947 - two years before the passing of the Wireless Telegraphy Act in 1949. This shows the concern and commitment of Hoover for the reduction of RFI, over the years. For many years they have funded independent RFI research carried out by the Electrical Research Association (ERA), this work has contributed chiefly in the area of RFI suppression network design, as well as work into the generation and propogation of RFI. But the results have had minimal effect on commutator motor design practice at Hoover. As mentioned earlier, it was the premise of this thesis, that technical management at Hoover decided to study reduction of RFI in motor design and manufacture itself.

Before the introduction of legislation on RFI limits in 1977, the function of RFI testing was mainly to specify suppression networks in new products at the pre-production stage of manufacture - this usually involved a great deal of trial and error to find optimum values of suppression components. Here the experience of the RFI engineer proved invaluable. However unsatisfactory this method may appear, it remains still the accepted practice throughout the industry.

RFI suppression has thus developed into more of an 'art' than a science. Once the new appliance went into full production, with no RFI test being carried out on the production floor, the motor section would carry out RFI checks as part of its normal reliability monitoring on one or two production samples per month. If these tests revealed that RFI levels exceeded the limits, the RFI engineer would be expected to carry out a thorough investigation of the offending appliance. Records show that in these cases the cause of high RFI levels was usually found to be due to a manufacturing fault in the motor. Among the faults recorded, are sticking brushes, loose brush boxes, high commutator bars, defective bearings and out of balance armatures. In the normal course of events, the fault would be reported back to the Quality Control staff on the shop floor. If no obvious fault could be found in the appliance and further tests on additional samples showed similar high results, the

RFI engineer would modify the suppression circuit. At this time there was virtually no feedback to the RFI engineer as to the quality of RFI performance of the appliance in service.

Legislation on interference, specifies that for series production line equipment, 80% of the production must meet the RFI limits with 80% confidence. This made it necessary for daily RFI tests to be carried out on the shop floor, thus the emergence of 'RFI test' sections in the Quality Control departments in the different factories.

Today, the function of RFI testing at Headquarters is primarily to specify suppression networks on proto-type, pre-production and first production samples of new products. Once in full production, there is very little feedback to the motor and control laboratory. Daily checking being carried out by the RFI testers in Quality Control. The only cases where the RFI engineer at Headquarters would be involved in production, would be RFI problems referred back by Quality Control, or if the motor section was reviewing an existing motor design for material or component changes.

Another aspect of RFI testing work, is to prepare data on appliance samples for 'Approvals tests'; when a product is launched in a new country, it is still necessary to satisfy the Approval Boards of that country that RFI limits are being met.

The direct responsibility for ensuring products conform to RFI regulations once the product is in full production is with Quality Control. A clause in the regulations requires that RFI test records must be made available on request, should any complaints of RFI from

Hoover appliances be required to be investigated. If Quality Control discover that appliances fall outside the limits, they would normally refer to the problem to the resident motor engineers - this is based on past experience of RFI testing at Headquarters, that the problem is more than likely a manufacturing fault. These Motor Engineers would investigate the problem and either deal with it themselves, but, if problems persist, Headquarters would be consulted.

2.4 RFI Suppression Components

There are two methods used extensively in the commutator motor industry to suppress RFI. One is to shunt the RFI away from the supply by means of a parallel capacitor, the other is to create a high impedance series path for the radio frequency currents using an inductor. Bond, [30] considers both these methods have their drawbacks; by providing a low impedance path with a shunt capacitor, high frequency currents are increased which could result in greater radiation. High frequency current in an inductor can give rise to magnetic fields and induce radio frequency voltages in nearby circuits. Thus, the use of these components can rarely eliminate RFI and careful design is necessary to ensure suppression performance across the RFI frequency band is achieved.

In any design, there may be a single component or a combination of components arranged in several circuit configurations to achieve the required level of suppression. A number of references [31, 32, 33] discuss the principles of filter design for RFI, but, coupled with this it is found that experience usually suggests the best form of suppression for a particular apparatus followed by empirical and heuristic methods for determining the optimum value of components.[7]

2.4.1 Capacitors

Figure 2.1 shows the equivalent circuit of a capacitor over a wide frequency range. It can be seen, that the inductance of the leads of a capacitor play a considerable part in determining the self resonant frequency of a capacitor and thus its overall performance. Below the resonant frequency the impedance of the capacitor gradually decreases with increase in frequency; above the resonant frequency, the capacitor behaves as an inductor and is therefore useless as a shunting component. Thus the requirement for capacitors used as RFI suppression components, is that the self inductance of the capacitor leads is as low as possible. Owing to the voltage ratings that are necessary on household appliance motors the capacitors tend to be bulky. Standard wound paper and foil type capacitors rely on dimensioning and terminal tab location for adequate control of self inductance. Figure 2.2 shows the typical effect of lead length upon capacitor impedance.

Ceramic capacitors, by virtue of their small dimensions have a much higher self resonant frequency hence good for suppression work, but, their performance deteriorates rapidly at high temperature and their use in RFI suppression is limited. Other types of capacitor designs which have evolved specifically for suppression of RFI in motors are; the 'feed through' or 'bushing' capacitor which reduce the self inductance by minimising lead effects and electrode inductance. Refinements in some types by inclusion of lossy ferrite materials, have been found to improve high frequency performance. Figure 2.3(a) shows the comparative effectiveness of a feed through capacitor with an ordinary stud-type. The 'delta' capacitor now a standard suppression component, is an arrangement of a shunt capacitor between live and neutral together with a capacitor from each line to ground. This incorporates the necessary elements for suppression by means of shunting, as well as saving material and space as indicated in Figure 2.3(b) and 2.3(c).

2.4.2 Inductors

Figure 2.4, shows the equivalent circuit of an inductor over a wide frequency band, the inductor exhibits inductance, resistance, capacitance between turns and capacitance between turns and ground. The distributed capacitance of an inductor acts as a lumped shunt capacitance, resulting in parallel resonance at high frequencies, beyond which an inductor can appear purely capacitative thus becoming totally unsuitable as a series component for the reduction of RFI currents. Figure 2.5 shows the typical frequency response of an inductor; it can be seen that its impedence peaks around the resonant frequency: thus the application of inductors in RFI work on commutator motors has developed for reduction of troublesome peaks of interference by selecting an inductor whose response will affect a reduction in that frequency region.

Inductors may be divided into two broad groups - single inductors and double inductors. An example of a single inductor is a 'T.V. choke', this type of inductor is used in domestic appliances to reduce interference in the television frequency bands. Double inductors are generally used for low frequency work, using a closed magnetic circuit to increase inductance. However, the core materials saturate at low flux densities - this is overcome by putting two windings on the same core, thus providing inductance in both live and neutral lines.

2.5 Economic Consideration

Suppression methods have changed little since the early days, relying heavily on the RFI engineers experience in dealing with similar appliances in the past, followed by trial and error of component values to select the optimum suppression circuit.

Suppressing a motor is not a difficult task, the 'art' of suppression however, lies in affecting 'economic suppression'. It is quite easy to over-suppress a motor - but the economics of motor production - as with all mass produced articles, is an extremely important factor in choosing the amount of suppression to be applied. The variability in the level of RFI generated from mass produced motors, as experienced at Hoover, further compounds the problem. The RFI engineer has to specify a single suppression network that ensures that all motor production achieves the specified RFI limits, allowing for the variability in RFI generated. Conflict arises in considering how much variability should be allowed for; Figure 2.6 shows the maximum and minimum RFI levels measured from samples of production suction cleaner fitted with suppression, it can be seen that the variability in RFI is such that at high frequencies the CISPR/EEC limits may be exceeded.

In the early 1960's, an increasing Hoover product range led to the manufacture of many different designs of small motors; each motor design is fitted with a suppression network considered suitable for that product. The first phase of a "cost saving" exercise in the early 70's led to the 'rationalisation' of suppression components. It was thought that one or two components should be specified to cover the whole range of small motors - thus simplifying RFI work and cutting the costs by reducing the range of components being purchased. The choice of the 'rationalised components' was one that would suppress the majority of motor designs to below the limits - any which fell outside the limits were either fitted with extra components or 'tolerated', since the RFI limits were not at this time enforcible by Law. This did not cause undue worry, since the number of complaints from Hoover appliances were rare.

The overall result of this approach was that many of the motor designs were over suppressed, although this did not concern the company too much at the time. Subsequent rising prices, increasing competition in the market place and the enforcement of RFI regulations, culminated in reviewing costs of RFI suppression once more. Now all the products had to conform to regulations, such that many of the motors had to have extra suppression components to cope with the variability of RFI generation in a particular model. Steadily the use of the rationalised components deteriorated and today all products are fitted with individually designed suppression circuits.

A study was made of costs of suppression from data dating back to 1974, made available by Hoover Costing and Purchasing Departments at Perivale. It was noted that before 1976 the majority of suppression components were bought from sources in Britain (Plessey) or West Germany (Funkton). The British components being in general slightly cheaper. From 1975 to 1977, prices of these components increased by almost 40% and this co-incided with the time when Hoover were already reviewing all costs and looking for alternative sources for suppression components. It was found that similar components from Eastern Europe and Scandinavia could be as much as 50% cheaper than in Britain or West Germany. Thus since 1976, to the present, the majority of capacitors and inductors have been bought from Yugoslavia (Iskra) and Sweden (Rifa). Figure 2.7 shows a comparison of prices of similar 0.1 μF capacitors as used on vacuum cleaner motors by Hoover.

The 'cost' of suppression as seen by Hoover is a combination of the actual price of the component, the price of any additional brackets or screws necessary to fix the components in place and two additional costs called 'fixed burden' and 'variable burden'. Fixed burden is a proportion of the fixed company overheads attributed to any manufacturing process. Variable burden relates to the time taken to complete the operation.

The result of this more frugal sourcing policy adopted by the Purchasing Department has not necessarily meant a reduction in costs of fitting suppression networks on motors. The studies show that the ratio of costs of fitting suppression to the total cost of motor manufacture have remained either fairly stable or show a slow increase over the past ten years. Figure 2.8 shows percentage cost of suppression to the cost of manufacture of the 'MC04' model motor as used in the Hoover Junior. Nine different motor designs were examined, the suppression costs ranged from the lowest at 6.3% of the overall cost to the highest at 22.3%, the overall average being 13%. In 1981 this represented a total of 2.7 million assorted suppression components at a cost of almost one million pounds.

Even after considerable savings by alternative sourcing of components the high 'on-cost' of suppression networks led Senior Technical Management at Engineering Headquarters to consider that suppression could only be effectively reduced if the motors could be designed to minimise RFI generation.

2.6 The Project Proposal

The previous sections of this chapter gave a background to the Hoover company, its experiences with RFI and the underlying causes which led to this project. As a summary it can be stated that small motors generate unacceptable level of RFI and to suppress this RFI to below the CISPR/EEC limits Hoover added external suppression circuits. The increasing relative costs of fitting suppression circuits to the overall costs of manufacturing motors, led the company to re-appraise its motor design philosophy. Their answer was to try to reduce the level of RFI inherently generated by the motor. Previous published work and past Hoover RFI records suggested that factors influencing the generation of RFI in motors fall into 3 categories.

(a) motor design features

(b) variations arising from the manufacturing process

(c) variations in the characteristics of the materials used.

The original proposals by Hoover, as discussed by the Supervisory Team on this project was to investigate the factors influencing RFI, the intent being to determine which are the most important factors contributing to RFI and thus evolve generalised recommendations that could be of use at the detail design stage of motor design. "It would be expected that the design improvements which lend to lesser generation of interference would bring (as a spin off) increased motor component life, it would reduce the variability between individual motors and would in turn reduce the variation in interference generated, and permit more economic designs for the suppression networks". [146] Additionally, it was also proposed to study the design of suppression circuits for specified performance for a minimum cost.

From the outset, Hoover made it clear that they were in search of 'practical knowledge' that could readily be acted upon and implemented in an industrial environment. This 'practical knowledge' thus emphasized the need for a practical approach to the project. The original project proposal embraced many areas of work which the Supervisory Team considered could not be adequately covered in a three year research programme. It was thus decided to omit the following;

a) Suppression network design and its optimisation

b) The influence on RFI due to variations in the characteristics of the materials used in motor manufacture.

The project was under regular review by the Supervisory Team and in many cases, the emphasis or direction of the work was changed in the light of events or results obtained. The final outline for work presented in this thesis can be summarised as follows:

(a) To study the factors affecting the generation and propogation of RFI in the motor design parameters.

(b) To study the influence on RFI levels due to mechanical variations arising from the manufacturing processes.

(c) To carry out a case study of the manufacture of a specific motor - to find the sources of variability in RFI levels from mass produced motors, to make appropriate recommendations such as reduce this variability and to see if a cost saving in suppression could be affected.

The scope of the work undertaken and the practical approach adopted is discussed more fully in Chapter 5. The construction and operation of small a.c. commutator motors is described in Chapter 3, with particular emphasis on commutation. The influence of mechanical variations on commutation is studied in Section 3.8. A literature review on the subject of RFI is presented in chapter 4; firstly with a brief introduction on general man-made noise sources, followed by a review of relevant work on RFI from small motors. The work presented in Chapters 3 and 4 provides a background for the studies undertaken and presented in the subsequent chapters.

2.7 Practical aspects of Industry based research

The IHD concept at Aston is to undertake industrial projects of an interdisciplinary nature suitable for research work with practical approach. [34, 35] The project, provides the collaborating organisation, the use of University facilities to research and solve problems in a manner which may not be otherwise possible. The project proposal by Hoover, fell broadly within this concept, its interdisciplinary nature combining motor design and RFI work in the Electrical department and manufacturing technology in the Production department.

Hoover offered research facilities in the form of test equipment and laboratory work space at its motor and controls laboratory in Engineering Headquarters. In the RFI test area, Hoover provided the necessary RFI measurement equipment and also a permanent RFI 'cage' to carry out RFI test work. The 'cage' is a specially constructed screened room of approximately 3 metres square, it had a filtered electrical supply such that no conducted interference from outside sources can corrupt test measurements. The walls of the 'cage' are made of steel mesh, this protects the room from any external radiated interference. The motor laboratory too, was well equipped with test apparatus.

The project having full support of the Engineering Director and with Mr. R. Binnie, Chief Engineer of motor and controls as 'industrial supervisor', was helped considerably in promoting the cause of the project within Hoover's organisation. So much so, that other departments in engineering and also production staff co-operated well with all aspects of the work. The model shop for example, was used extensively in the making of a test rig and for modification of motor parts to enable many design and manufacturing variations to be tested. At the beginning of the project the Perivale factory was in operation manufacturing motors and vacuum cleaners in the same building as the Engineering department - this proved to be of great value for learning production methods and observing practical problems in the manufacturing process. They also supplied motor parts for the test work. Without this supply, much of the work presented in this thesis would not have been possible - since the cost of manufacturing one-off parts in the model shop, was high. To make a special armature in the model shop, could cost almost £100, whereas by obtaining an armature from the production area and then modifying it to suit in the model shop, greatly reduced costs. It seemed natural at the early stages that the 'case-study' of the influence on RFI levels due to manufacturing variations proposed for the project, would be carried out in the Perivale factory. But the subsequent closure of the Perivale factory and transfer of its work and equipment to Cambuslang in 1981, followed by redundancies at Hoover Headquarters, led to a number of unforeseen problems.

Experimental work on the project, was disrupted for a short while due to lack of parts - but this was eventually offset by obtaining parts from Cambuslang once the transfer of production was completed. It became inevitable that any 'case study' of manufacturing variations would be undertaken at Cambuslang, but was delayed considerably; firstly because the Cambuslang factory itself was being re-organised and needed time to return to full production with the extra work from Perivale, secondly by industrial disputes. It was well into the final year of the project when conditions at Cambuslang allowed the case-study to commence.

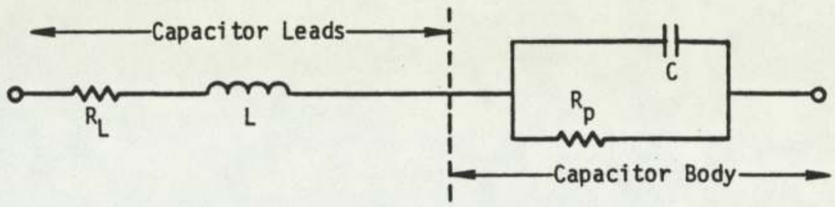

Where:
R_l = Series Resistance of leads and contacts
L = Inductance of Leads
R_p = Resistance Due to Dielectric Losses
C = Ideal Capacitance

Equivalent circuit of a capacitor over a wide frequency range

Fig. 2.1

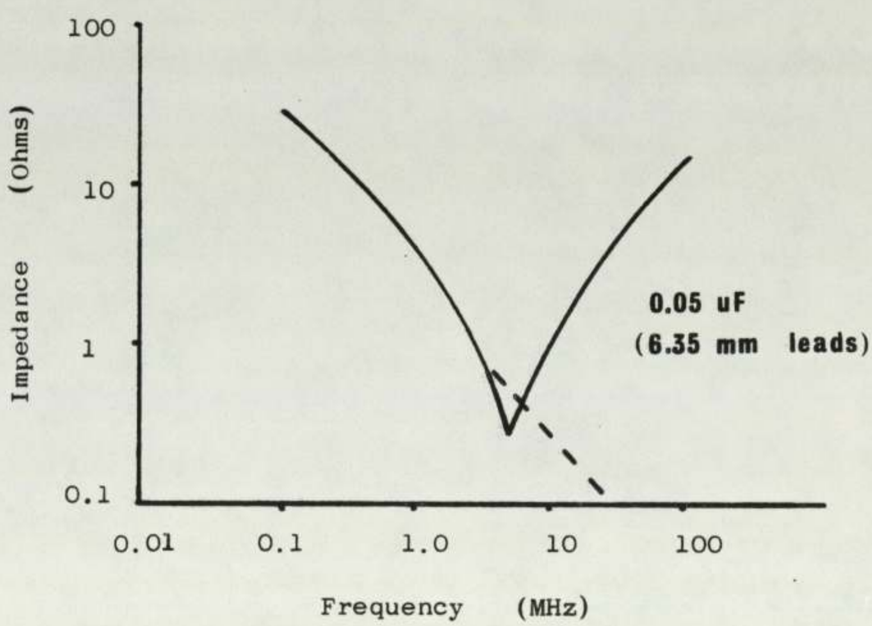

Effect of lead length on capacitor impedence

Fig. 2.2

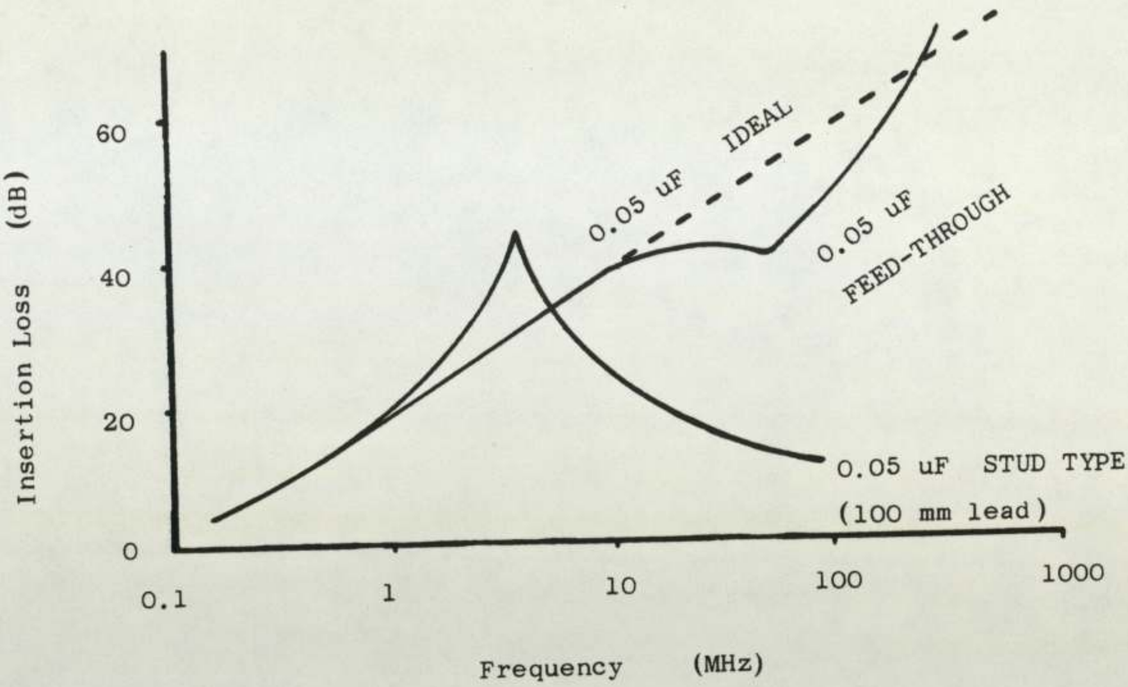

(a)

(b) shunt capacitor connections

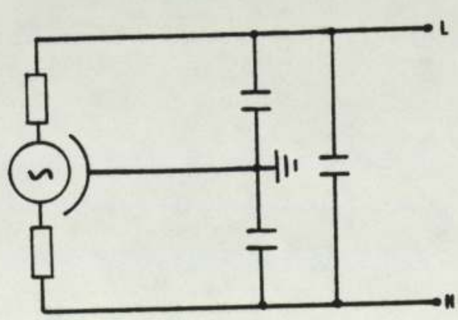

(c) delta capacitor connections

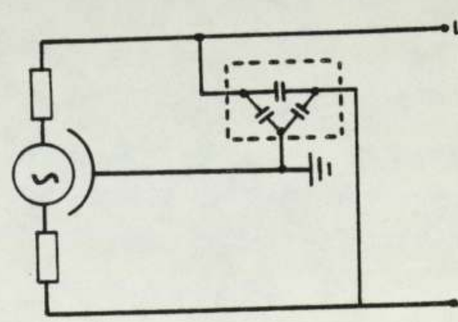

Comparison of filtering performance of feed-through and lead type capacitors

Fig. 2.3

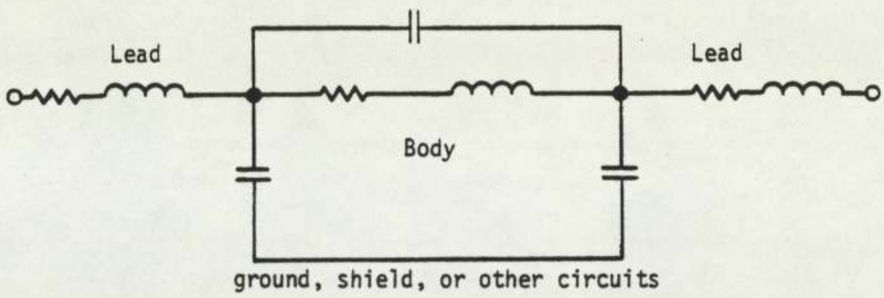

Equivalent circuit of an inductor over a wide frequency range

Fig. 2.4

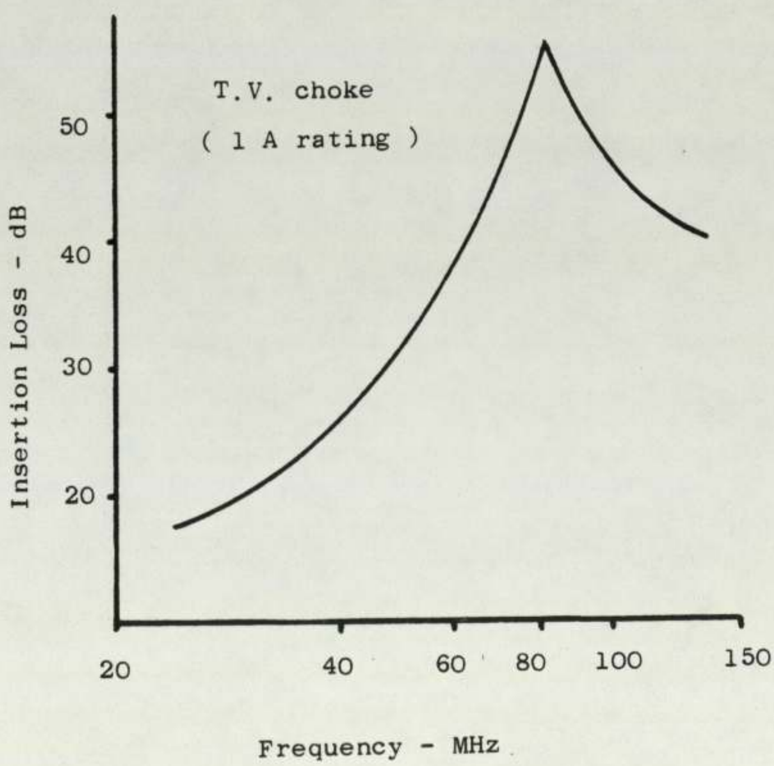

Frequency response of a T.V. choke inductor

Fig. 2.5

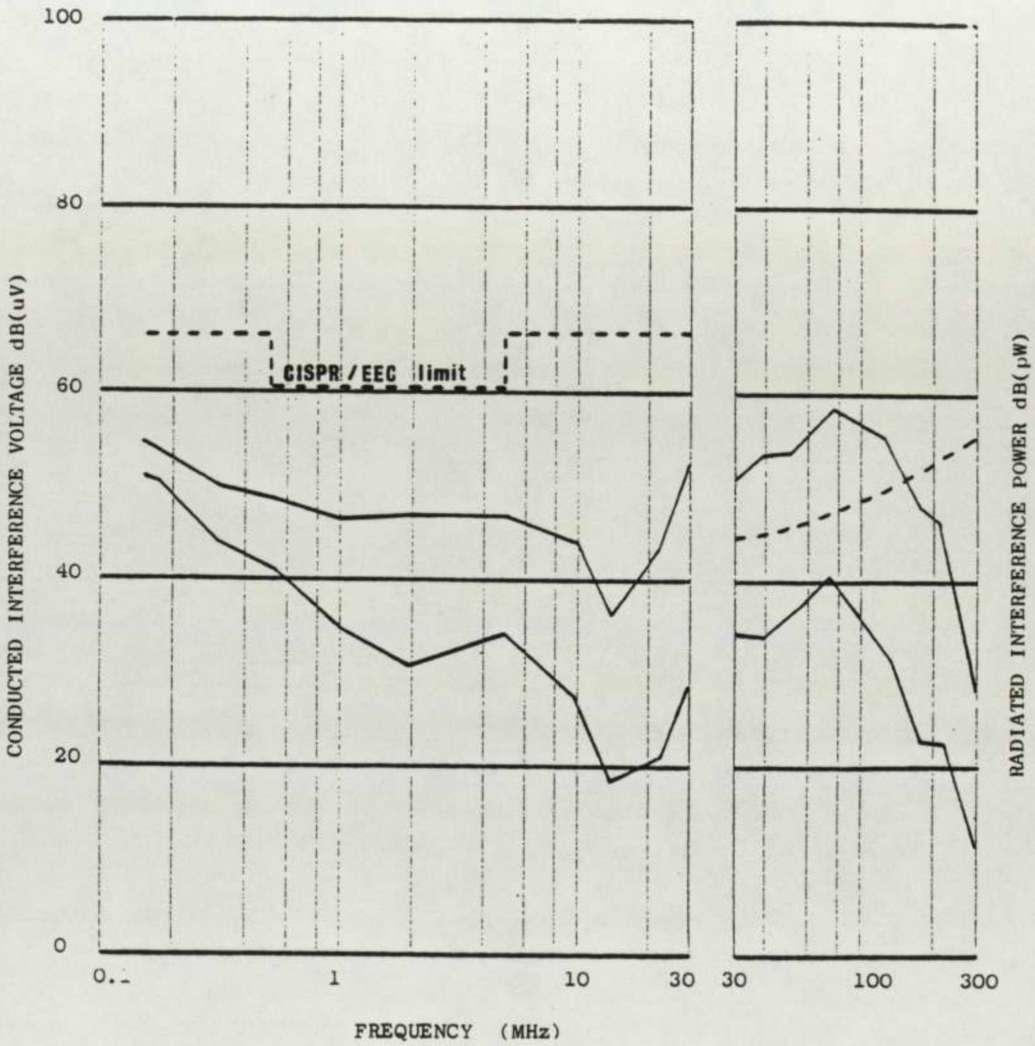

Maximum and minimum spread of RFI levels measured
from production suction cleaners

Fig. 2.6

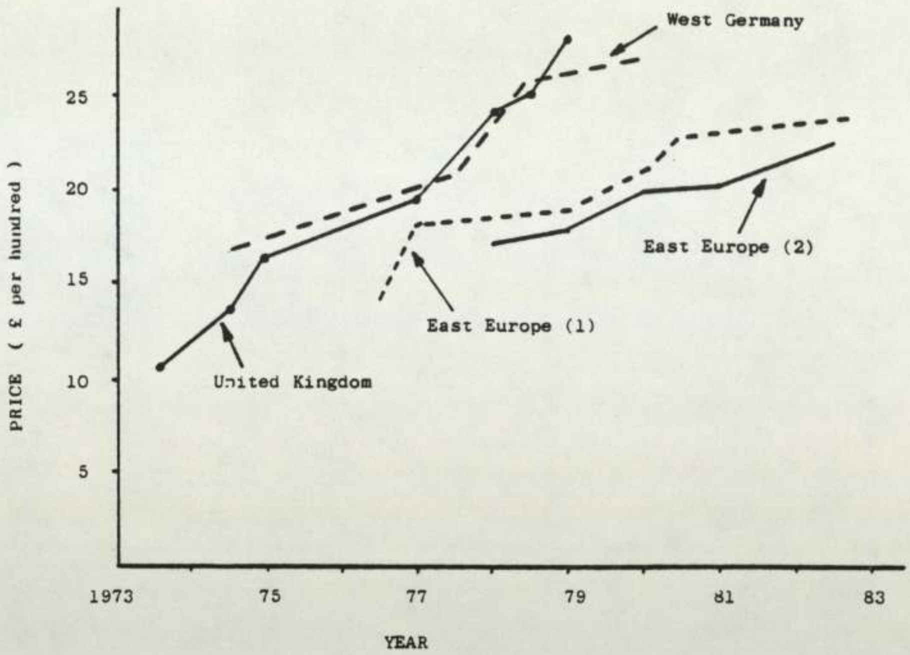

Comparison of prices of various 0.1 μF suppression capacitors since 1973

Fig. 2.7

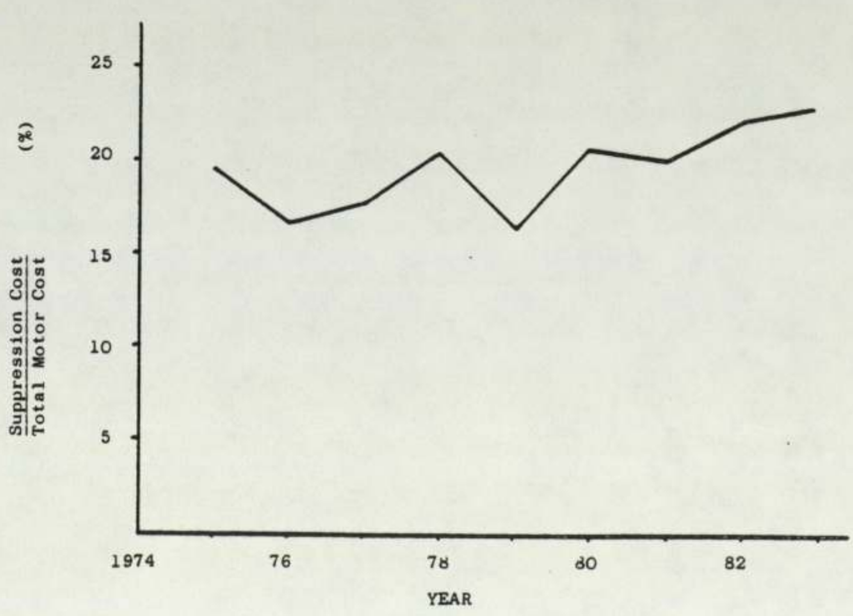

Percentage on-cost of fitting suppression on 'MC04' model motor

Fig. 2.8

CHAPTER 3

SMALL A.C. COMMUTATOR MOTORS

3.1 General construction

3.2 Vector diagram

3.3 The commutation process

3.4 Brush EMFs

3.5 Voltage equation of the short circuited coil

3.6 Improvement of commutation

3.7 The brush-commutator contact

3.8 Effects of vibration on commutation

3.9 Discussion on commutation

CHAPTER 3

SMALL A.C. COMMUTATOR MOTORS

This chapter presents a review of design and operational details of small a.c. commutator motors as used in domestic appliances. The main source of information for section 3.1 and 3.2, are Puchstien and Kimberley, [27] Garik and Whipple, [24] Say, [26] Taylor, [25] Knights [12] and Dijken. [28] Due to the lack of published material on these motors, work by Puchstein and Kimberley and Taylor is still the major source of reference of small a.c. motor design practice. Dijken considers the optimization of small motor design, he identified the critical design parameters to be (a) the effective rotor diameter (b) the relative stack length and (c) the ratio of the flux carrying width of the rotor teeth to the effective rotor diameter. A comparison of two motors one using the optimized method and the other conventional design practices showed that the cost of manufacturing the optimised motor was lower by nearly 8%. The inductance of the rotor coils was also reduced enabling improved commutation, less brush wear and longer motor life.

Section 3.3 to 3.6 discuss the theories of commutation in a.c. motors. Many of the ideas on commutation have evolved from work carried out on d.c. machines, but a number of references are identified which deal specifically with commutation in a.c. motors. Commutation is the reversal of current in a coil by means of a short-circuiting brush. In d.c. motors this reversal is opposed by an e.m.f., due to coil inductance resulting from its leakage flux.

In an a.c. motor commutation it is further complicated by other e.m.f.s. being induced in the short-circuited coil due to its rotation and also due to it being linked with the alternating components of the air-gap flux.

The brush-commutator contact and the factors that can affect it are studied in Section 3.7 and 3.8. Finally, in Section 3.9 a discussion on commutation is presented.

3.1 General Construction

Reversing the polarity of the supply on an ordinary d.c. series motor does not affect the direction of torque, thus such a motor can operate from an a.c. supply. However its operation at mains frequency would be unsatisfactory on account of high iron loss caused by the alternating flux in the solid poles and yoke. For motor outputs less than about 500 watts satisfactory operation can be obtained if the poles are laminated.

The earliest mention of the fact that a d.c. motor would, if its field system were laminated, operate on alternating current was made by Alexander Siemens in 1884 at a meeting of the Society of Telegraph Engineers. [25] A number of different types of single-phase motors were devised, but only a few have become commercially satisfactory. One of the most successful has been the small bi-polar a.c. series commutator motor, without compensation coils or commutating poles, has been in commercial use in domestic appliances since about 1905. [27] (These motors are still commonly referred to as 'fractional horse-power' commutator motors and 'universal' motors). Designs of series motors commonly used in domestic appliances can be generalised as having the following features: [28]

(a) Suitable for both a.c. and d.c. input voltage of about 100-240V.

(b) 7 - 16 rotor slots

(c) Output powers from 20 to 750W

(d) Speed range from 2000 to 20,000 r/min.

(e) Operating life not generally exceeding 1500 hours.

A market study, [12] showed that U.K. production of small commutator motors can be split into four power rating groups:

0 - 95W	-	electric shavers, sewing machines
95 - 190W	-	small vacuum cleaners, food mixers
190 - 750W	-	washing machines, power tools, vacuum cleaners, garden equipment

Motors of 190W to 750W, generally account for approximately 78% of the total production. The estimated world production of these motors for the 1980s is approximately 235 million units per year, of which almost 13 million are manufactured in the U.K.

Figure 3.1, shows the connections of a series motor, the field winding is connected in series with the armature by means of diametrically opposite brushes on a commutator. The field winding is in the direct axis which produces the excitation flux, Ød, the armature winding in the quadrature axis produces a quadrature flux, Øq.

The field system is of a salient pole type construction, this causes the space distribution of flux to deviate considerably from a sine wave. This has little effect on the motor behaviour since rotor torque and e.m.f. are dependent on the total flux and not on the distribution.

As mentioned earlier, the field stack is made up of laminations which may either be rivited or welded together. Figure 3.2, shows the two most common stator configurations. Figure 3.2(a), shows the U-type lamination profile, the windings are usually wound as a single coil on a bobbin or former, as indicated. The flux paths, through the air-gap at A are longer than those passing at B, so that the line C D is not a line of magnetic symmetry. The air-gap flux is concentrated at B and E, thus the neutral zone can vary considerably from the horizontal centre line. This profile is popular due to ease of winding, since the coils can be wound directly onto the stator due to the open end of the stack.

Figure 3.2(b), shows the O-type lamination profile, the flux paths here are symmetrical. The stator winding is split into two separate coils, and each mounted at the neck of the pole shoe as indicated. It can be made with pre-wound coils or coils may be directly wound on the stator, but generally requires specialised winding equipment to form the coil loops. The exact dimensions of the two profiles vary considerably in different motors. Figure 3.3, shows a range of stator variations that have been observed in small series motors.

The armature is composed of a solid steel shaft, rotor laminations, a commutator and windings. The rotor laminations and commutator are pressed directly onto the shaft, relying on the tightness of the fits to maintain their positions.

As with the stator laminations, the rotor slots too, vary considerably in slot profile. Figure 3.4, shows a selection of rotor profiles commonly used. Dijken's computer program optimized the shape of motor laminations for cost and performance. Figure 3.5, shows the result of his work, the stator uses an optimum amount of iron and copper (field windings) to produce the machine excitation. The rotor teeth and slot profile is optimized to reduce the inductance of the rotor coils and thus improve commutation (see section 3.3).

Armature windings are wound in a number of coils which are distributed around the armature in the rotor slots. The coils consist of many turns of thin insulated copper wire that can fill up almost any shape of rotor slot, (e.g. 20 - 40 turns in a 200W commutator motor). In each slot there can be either 2 or 3 coil sides, Figure 3.6, shows an example of a 12 slot rotor, indicating how slot 6 would be filled with two coil sides in position.

The coil ends are brought out and connected to a commutator segment, the commutator riser may either be slotted or hooked to enable easy fixing. Four different methods of connection have been used; soldering, brazing, arc welding and hot staking - this latter being the most common. The coils are connected such that they form a series closed loop around the commutator. Virtually, all small commutator motors use 'moulded' commutators. The commutator segments being moulded into an insulating resin are insulated from each other by the resin or intersegment mica wafers, this is normally undercut below the surface of the copper face. Naturally, the number of segments is equal to the number of coils on the armature and these have been found to range from 6 to 32 on small motors. Figure 3.7, shows two typical commutator arrangements.

The commutator surface is machined to give a smooth finish, enabling the brushes to make an intimate contact during operation. A few additional features common to the armature of small motors are;

(a) the practice to either tie down the windings to the shaft or varnish the windings to stop the centrifugal forces throwing them out of the slots.

(b) insulating paper inserts between the rotor laminations and the winding or epoxy coating of the rotor lamination in case the windings short circuit through the rotor.

The operating life of small motors varies from as little as 100 hours on coffee grinders, to about 1500 hours on vacuum cleaners. The operating life is determined by the brush life, which in turn, is a function of brush wear and the quality of commutation. New brush shapes, styles and grades of carbon are constantly being developed to meet modern application requirements and increasingly demanding specifications. Good brush design and selection of the appropriate brush grade are critical factors in machine design, in small motors they normally span either one or two segments on the commutator. The whole range of brush grades can be classified into the following groups. [13]

(a) Natural graphite grades; Have good lubrication properties. Used where high speeds are encountered or where silent running is important.

(b) Resin bonded grades; Based on natural graphite, but have a resin bond. This type of bond produces a high electrical resistance for good commutating ability. Current loading is limited.

(c) Hard carbon grades; Mechanically robust and long wearing, but limited to low and medium surface speeds and moderate current densities.

(d) Electrographite grades; Most widely used class of material. They have the characteristic high thermal and electrical conductivity of graphite and also are very resistant to burning. Capable of carrying heavy overloads and cause little commutator wear.

(e) Metal-impregnated graphite and metal graphite grades; High current densities and low contact voltage.

As mentioned above the brush must maintain an intimate electrical contact with the commutator surface, thus the design of the brush-holder and its spring assembly, require considerable attention. Figure 3.8, shows four of the most common methods of mounting brushes used in small motors. The springs used are of the helical compression type, these are relatively cheap to manufacture but spring pressure decreases as the brush wears and this can cause brush instability. Springs have been made of phosphor-bronze wire but these tend to fatigue at continuous operation of temperatures around 120°C. In some motors spring temperatures can exceed 150°C in normal operation. [36] At Hoover, tests on beryllium copper wire have shown considerable benefits as have copper clad steel wires. In large motors brush gear has been designed using constant force springs, [37] but their application in small motors has been minimal.

3.2 Vector Diagram (Figure 3.9)

The main current I, is the vector sum of the magnetizing current I_m and an iron loss component I_c, which leads the magnetizing current by 90°. The air-gap flux produced by Im thus lags the main current by the angle of hysteretic advance, γ and has two components, ϕ_d the exciting flux and ϕ_q the quadrature flux.

ϕ_d sets up an e.m.f. in the stator winding which lags the flux by 90° and is given by,

$$E_{tsd} = 2.\pi.f.Ts.\phi_d \qquad (3.1)$$

where Ts is equal to the number of turns of the field coil.

The stator current also sets up a leakage flux which gives rise to an e.m.f. which is conveniently treated as a leakage reactance drop of IX_1 leading the current by 90°.

ϕ_q sets up a transformer e.m.f. in the armature

$$E_{taq} = 2.\pi.f.\,(Ta/p).\,\phi_q \qquad (3.2)$$

Ta being the total turns on the armature and p the number of pole pairs. The rotation of the armature in the flux ϕ_d sets up a rotational e.m.f. between the brushes;

$$E_{raq} = 2.\pi\, f_r.(Ta/p).\,\phi_d \qquad (3.3)$$

where f_r is the rotation frequency. This e.m.f. has its peak value at the same moment as the peak value of ϕ_d but lags it by 180^o.

The applied voltage has to overcome all these e.m.f.'s and also the resistance Ir which is in phase with the main current.

The coils short-circuited by the brushes are linked with ϕ_d, and are rotating in ϕ_q, therefore, have e.m.f.'s induced in them, these are described later (section 3.4); these e.m.f.'s cause a circulating current I_b which lags by a considerable angle behind the fluxes as shown, thus a further component of main current, I_b' is necessary to neutralize the resulting m.m.f. (Figure 3.9, shows the vector diagram of the components described above with the air-gap flux as reference).

The power factor of the motor, $\cos\phi$, is inevitably less than unity, but the effect of the iron loss and brush circulating current, is to improve it slightly at the expense of efficiency.

3.2.1 Performance of Small a.c. Commutator Motors

The behaviour of the small a.c. commutator motor is similar to that of the series d.c. motor i.e.

(a) motor torque; $T \propto I\phi \propto I^2$

(b) motor output = Input - Copper losses - Iron losses - friction & windage

(c) motor speed; $n \propto 1/\phi$

The losses and inefficiency introduced by the alternating supply means performance on a.c. is inferior to that on d.c. supplies. Figure 3.10 shows the speed-torque curve of a small commutator motor on d.c. supply and a 50Hz main supply. The peak flux on a.c. is $\sqrt{2}$ x d.c. flux, the peak a.c. rotational e.m.f. E_{rad}, is $\sqrt{2}$ x d.c. rotational e.m.f. (i.e. $\sqrt{2} \times E_{dc}$). Since both e.m.f.'s are proportional to speed the relation between a.c. speed N_{ac} and d.c. speed N_{dc} can be written.

$$E_{rad}/E_{dc} = N_{a.c.}/N_{d.c.} \qquad (3.4)$$

On a d.c. motor $E_{dc} = V - Ir$, from the vector diagram of the a.c. motor (Figure 3.9)

$$E_{rad} \triangleq V \cos\phi - Ir \qquad (3.5)$$

so that,

$$N_{a.c.}/N_{d.c.} \simeq [\cos \phi - Ir/V]/[1 - Ir/V] \qquad (3.6)$$

The full load value of Ir/V is generally between 0.1 and 0.15 so that is this is neglected, the speed ratio becomes;

$$N_{a.c.}/N_{d.c.} \simeq \cos \phi \qquad (3.7)$$

Figure 3.11 shows a set of performance curves for a 150 W motor on a 250V, 50Hz a.c. supply, the shape of the curves can be assumed to be general for most motors of this type as used in domestic appliances.

3.3 The Commutation Process

Figure 3.12, shows three positions of the rotor of a commutator machine with 6 armature coils. Concentrating on coil 1; in Figure 3.12(a) this coil is in the right hand circuit, Figure 3.12(b) it is short circuited by the upper brush and 3.12(c) it is in the left hand circuit. The direction of current through the coil changes correspondingly as it moves in this way. Figure 3.13(a), shows an idealised view how the current in coil 1 changes as it moves round the armature if the supply current is constant. In single phase machines, the time of commutation being small compared to that of the cycle of the alternating current, there may be several current changes within one cycle (Figure 3.13(b)). It can be seen that the magnitude of the current change varies, depending on the moment in the cycle at which it occurs, from a value of twice the maximum current to zero.

The time of commutation is from the instant brush A just short circuits segments 1 and 2 to when brush A just leaves the surface of segment 1. If the peripheral speed of the commutator is V_c, the thickness of the brush t_b and the thickness of the insulation separation between the segment t_m, then the time of commutator T_c can be expressed as

$$T_c = (t_b - t_m)/Vc \tag{3.8}$$

In Figure 3.13, the change in current is shown as a linear function of time. Garik and Whipple [24] and others [41] showed that even if all e.m.f. effects in the short circuited coil are disregarded, linear commutation is impossible. Figure 3.14 represents the position of brush and commutator bars at a time t seconds after the short circuit begins, the following relations may be obtained;

$$i_1 = i_a - i \tag{3.9}$$

$$i_2 = i_a + i \tag{3.10}$$

$$A_1 = A_b \; t/T_c \tag{3.11}$$

$$A_2 = A_b \; (T_c - t)/T_c \tag{3.12}$$

where A_b - contact surface area of brush

A_1 - contact surface area of brush with commutator bar 1

A_2 - contact surface area of brush with commutator bar 2

If R_b is the contact resistance between brush and commutator then, R_b (A_b/A_1) is the contact resistance between brush and bar 1 and R_b (A_b/A_2) is the contact resistance between brush and bar 2.

In accordance with the assumption that no e.m.f.'s are present in the short circuit paths, applying Kirchhoffs law to the circuit gives;

$$i\, R_s + i_2 R_r + i_2 R_b \frac{Ab}{A_2} - i_1\, R_b \frac{Ab}{A_1} - i_1 R_r = 0, \tag{3.13}$$

letting $k = (R_s + 2R_r)/Rb$ therefore, the short circuit current i is a function of time t - given by;

$$i = \frac{i_a . T_c\ (T_c - 2t)}{T_c^2 + k.t\ (T_c - t)} \tag{3.14}$$

The general shape of the current change given by this result is sketched in Figure 3.15. As can be seen even in this simple case of resistance commutation, linear current change cannot be obtained. If the resistances R_s and R_r are assumed, to be zero, i.e. $k = 0$ then the current change is given by;

$$i = i_a \left(1 - \frac{2t}{T_c}\right) \tag{3.15}$$

this is the equation of a straight line between $+ i_a$ and $- i_a$, thus the required condition for linear commutation - but the assumptions are not valid for this to be true. In reality however, the short circuited coils is subjected to the influence of the following e.m.f.'s.

(a) Transformer e.m.f.; e_t, lagging the flux ϕ_d by 90^o.

(b) Rotational e.m.f.; e_{rot}, in phase with ϕ_q .

(c) Reactance e.m.f., e_r, in phase with the current.

They can either contribute to delay the current change (Figure 3.16a) or over commutate the current (Figure 3.16b), the result is that as the brush leaves segment 1 at the end of the time of commutation, commutation is incomplete. The additional current must change rapidly to i_a, the reactance voltage which is proportional to the rate of change of current increases to oppose the current change creating an arc from the trailing edge of the brush to the commutator segment. The arc completes the brush segment circuit allowing the current reversal in the coil to be completed.

3.4 Brush E.M.F.'s

As mentioned above the e.m.f. set up in the coils short-circuited by the brushes is made up of a reactance e.m.f., a rotational e.m.f. and a transformer e.m.f. This e.m.f. appears between the heel and toe of the brush as is discussed further below.

3.4.1 Reactance e.m.f.

Reactance voltage, e_r generated in the short-circuited coil, is a function of the total inductance of the coil and the rate of change of current in it i.e.

$$e_r = L\, di/dt \tag{3.16}$$

The total inductance is the sum of the inductance of the short circuited coil and the sum of the mutual inductance of the coil with other adjacent coils. Inductance is defined by the flux linkages i.e. the product of the flux and the number of turns linked with it. The definition of inductance is based on the concept of specific permeance which is the number of flux linkages per unit length of coil section consisting of one turn, through which a current of 1A is flowing.

The flux linked with the coil undergoing commutation is shown in Figure 3.17. It may generally be divided into three parts;

(a) the slot; consisting of flux lines, flowing across the slot from one side to the other, this flux section is distributed along the total active length of the coil section i.e. 21, having a slot permeance Λ_s.

(b) the tooth; consisting of flux lines closing between the heads of adjacent teeth, this part is also distributed along the length 21, having a tooth permeance of Λ_t.

(c) the end windings; consisting of flux lines closing around the coil end winding, portions along the length 21_{end} and has an endwinding permeance of Λ_{end}.

The total number of flux linkages of the coil section is;

$$2\,1\,\Lambda_s + 2\,1\,\Lambda_t + 2\,1\,\text{end}\,\Lambda\,\text{end} = 2\,1\,\Lambda' \qquad (3.17)$$

where Λ' is the equivalent specific permeance of the coil section. In the general case a coil consists W_c of turns, the flux linkages increase by W_c^2 therefore total inductance (L) is;

$$L = 2\, W_c^2\, l\, \Lambda' \tag{3.18}$$

The permeance Λ' is classically defined as function of the coil, slot and tooth dimensions, so it would appear that for any armature coil its inductance remains constant, and this result has been given in a number of text books. [42, 43] But this result fails to take into account the effect of eddy currents induced in the motor laminations. If a magnetic material is excited by an alternating current, eddy currents are induced in it, which affects the hysteresis loop of the material. The tendency of the induced currents is to prevent the flux from changing. Where the flux is increasing with time, the eddy currents tend to decrease the flux, and the flux decreases with time, the eddy currents tend to prevent this decrease. [44] Thus the hysteresis loop of the material is effectively increased as shown in Figure 3.18. The size of the dynamic loop is affected by the frequency of magnetization since the eddy currents are a function of frequency. The overall effects of a larger hysteresis loop is that the flux produced by an alternating current will be lower than that produced by a steady current of the same value - this in turn means that the flux linkages will be decreased, thus the coil inductance is also decreased. Dijken, showed the decrease in coil inductance with increasing supply frequency experimentally, and this is discussed further in section 3.9.

3.4.2 Rotational e.m.f.

The rotational e.m.f., e_{rot} generated in the short circuited coil attributed to the machine flux, is generated in the commutation zone, since the field free zone has zero width and does not coincide with the commutation zone because of the armature reaction m.m.f. The flux within this zone ϕ_c is alternating but stationary in space, the short circuited coil always occupies the same position relative to the flux, thus

$$e_{rot} = \pi . f_r . Tc. \phi_c . \sin(wt) \tag{3.19}$$

Armature reaction distorts the field flux in the air-gap as shown in Figure 3.19, the result is that the true magnetic neutral zone in the motor is at angle α away from the physical neutral position.

3.4.3 Transformer e.m.f.

The third of the e.m.f.'s that may be induced in the coils undergoing commutation is due to their being linked with an alternating flux by the relation;

$$e_t = T_c \, d\phi/dt \tag{3.20}$$

If the air-gap flux is assumed to be; $\phi = \phi_m \sin(wt)$ therefore;

$$e_t = T_c . w . \phi_m \cos(wt) \tag{3.21}$$

$$= 2\pi f . T_c \, \phi_m \cos(wt) \tag{3.22}$$

3.5 Voltage Equation of the Short-circuited coil

Figure 3.20, summarises the voltage and current components on the short circuited coil undergoing commutation. From above if the main current is;

$$i = I_{max} \sin(wt) \tag{3.23}$$

then the rotation e.m.f.;

$$e_{rot} = E_{rot} \sin(wt) \tag{3.24}$$

and the transformer e.m.f.;

$$e_t = E_T \cos(wt) \tag{3.25}$$

Mohr, [45] considered the influences of these two e.m.f.'s to be components of a single circuit e.m.f., e,

where; $$e = E_{max} \text{ Sin } (wt + \psi) \tag{3.26}$$

and, $$E_{max} = \sqrt{(E_{rot})^2 + (E_T)^2} \tag{3.27}$$

$$\psi = \tan^{-1} E_T/E_{rot} \tag{3.28}$$

This e.m.f. lags the main current by the angle ψ see Figure 3.20(b). Figure 3.21, shows the circuit diagram of the short circuited coil with all the circuit components represented as lumped parameters.

Applying Kirchhoffs law to this circuit gives;

$$i_1 (r_1(t) + R_v) - i_s R_s - L \frac{di}{dt} + e - i_n (R_v + r_n(t)) = 0 \tag{3.29}$$

In practive R_v is negligible and combining the two brush contact voltages drops to a single voltage, U_b the equation simplifies as shown below;

$$i_s R_s + L \frac{di}{dt} + e + U_b = 0 \tag{3.30}$$

3.6 Improvement of Commutation

The most widely used method of improving commutation in large machines is by the introduction of compoles or interpoles, first suggested by Metre in 1885. [43] These poles are arranged between the main poles to induce voltage opposing the reactance e.m.f. in the short-circuited coil. In small machines however this method is impractical due to both space and cost considerations.

In small motors a commutating field necessary to establish an e.m.f. to balance the reactance e.m.f. is created by means of shifting the brushes off the geometrical neutral axis. The true neutral axis in the motor is an angle α away from the geometrical neutral against the direction of rotation due to Armature reaction. To create a suitable e.m.f., the brushes must be shifted such that, the short circuited coils are under the influence of the main pole as shown in Figure 3.22. To satisfy this requirement it is necessary to shift the brushes further than the physical neutral by an additional angle of γ.

The main disadvantage of creating a commutating field in this manner, is that the angle of brush shift is dependent on the load current. Thus in small motors, the brushes are normally placed in some middle position corresponding to some average load.

3.7 The brush - commutator contact

The sliding brush-commutator contact creates a black film on the copper segments of the commutator. Davies, [46] describes the film as stratified with layers of graphite flakes overlaying one of cuperous oxide. Analysis shows that film is a complex mixture of water vapour, oxygen and numerous organic and inorganic compounds that permit sliding without excessive brush wear.

In the sliding contact at any instant only about 0.1% of the apparent brush area, actually makes up the electrical contact. Shobert [38] showed by experiment that there are only between five and twenty separate, simultaneously conducting areas for each brush within the mechanical contact surface. The spots are fine, highly conducting bridges formed by the process called 'fritting'. Two types of 'fritting' are defined.

(a) 'A' fritting; An avalanche breakdown of the surface film that occurs when the voltage gradient between the brush and commutator reaches approximately 10^8 V/m.

(b) 'B' fritting; Starts from an initially conducting spot which widens, thought to be due to electrostatic and electro-magnetic forces on the film.

Their number and cross-selectional area being dictated by an equilibrium between, on the one hand, the tendency of the brush and collector surfaces to oxidise and on the other for fritting to occur under the applied electric field and the cleaning action or abrasion of the brush against the commutator. In addition, there is a thin layer of moisture and oxide between the sliding surfaces through which current passes, by means of the tunnel effect, and which generally has ohmic resistance characteristics.

Brush polarity effects have been observed on slip rings. [39] Under the anode brush, the graphite film develops more uniformly; oxidation is inhibited by the direction of the current and fritting takes place at a lower temperature. Under the cathode brush, oxidation is enhanced, but less graphite is deposited and fritting must take place at a higher voltage, there is more disturbance of the conducting region thus increasing brush wear.

In a.c. commutator motors, the brush polarity is constantly changing. Watson [47] discussed that, conducting spots that occur at the anodic brush cease to conduct almost immediately the polarity is reversed, but remain as load bearing points. Thus, it is expected that brush wear would be increased due to increased fritting activity and the constant changing polarity.

3.7.1 Factors Affecting the brush-commutator contact

Reference 48, lists the following factors that can effect the brush-commutator contact;

(a) Temperature

(b) Brush pressure

(c) Speed

(d) Environment

(e) Mechanical factors

of these the latter, mechanical factors is the most significant and is discussed in detail in section 3.8.

Temperature rise can affect the contact resistance as well as the coefficient of friction of the sliding contact. The same is true of brush pressure. High commutator speeds reduce friction but can affect an increase in the contact voltage drop, the causes are thought to be;

(a) Aerodynamic - a boundary layer of air is formed between the brush and commutator.

(b) Mechanical - increasing the rate of production of wear particals effectively increasing the distance between the brush and commutator.

Shobert describes brush wear tests in different environments, the absence of water or oxygen suppresses oxidation and increasing brush wear. Active gases such as sulphur dioxide and chlorine causes the voltage drop to become unstable causing increased arcing. The most successful environments including the normal air/humidity were found to be organic vapours and inert gases like Nitrogen in the presence of water vapour.

3.8 Effect of Vibration on Commutation

Vibration affecting commutation in motors can result from

(a) Natural oscillation of the brush-commutator assembly.

(b) External vibration.

(c) Motor vibration.

(d) Commutator irregularities.

These are discussed below:

3.8.1 Natural Oscillation of brush commutator assembly

Every brush makes movements and oscillations relative to the brush holder, if the magnitude of this vibration is small it has practically no effect on the current transfer. However, excessive movements can lead to an adverse effect on the contact resistance of the sliding contact.

Grossman [49] considered that in the general case, the brush-commutator assembly represents a consecutive linkage of elastic components with coefficient of elasticity of K_1, K_2, K_3 and K_4 namely the spring, pressure bar, brush and contact layer respectively, such that the system coefficient of elasticity k is defined as;

$$\frac{1}{k} = \frac{1}{k_1} + \frac{1}{k_2} + \frac{1}{k_3} + \frac{1}{k_4} \tag{3.31}$$

The elasticity of the contact layer is described as a function of current density, rotational speed and the type of brush. Maslov [50] stated that the natural frequency of the spring-brush-contact layer oscillatory system is given by

$$W_{br} = \sqrt{(k_1 + k_4)/M_{br}} \tag{3.32}$$

(M_{br} = Mass of brush)

From theoretical and experimental studies, they presented the following conclusions:-

(a) When induced vibration frequencies approach the natural oscillation frequency of the brush, they increase brush displacement relative to the commutator and reduce the contact pressure. When the induced vibration frequencies coincide with the natural frequency of the brush a contact break is possible.

(b) The natural oscillation frequency of the brush is a function of the contact layer rigidity, as well as of the spring rigidity. However, in existing types of brush-gear the rigidity of the contact layer has a decisive effect on the natural frequency of the brush, and the rigidity of the springs can be discounted.

(c) Decreasing contact rigidity reduces the likelihood of a break in contact. However, the natural frequency of the brush, is reduced at the same time, which may cause the induced vibration frequency to coincide with the natural brush frequency, in which case a break in contact is possible even if contact rigidity is very low.

(d) When the brush is vibrating, the rigidity of the contact layer varies within a fixed range, the limits of which are not affected, either by the brush pressure or by a reduction in the brush contact area.

Vibration reduces the arc of brush contact and hence also reduces the commutating period. Ichnki [51] stated that the most influential factor in commutation is the contact stability of the brushes. Unstable brush contacts result in a stepped reversal of current that can cause severe arcing.

Friction of the sliding contact can induce brush vibration, the coefficient of friction is dependant on temperature and at high values has been observed to be responsible for brush chatter. This can be detected either by the brush emitting a whistling sound or by a glazed surface on the commutator. [37]

Volkman [52] concluded that there were basically three types of friction induced vibrations;

(a) Brush whistling or squealing which has a pure tone in the range of 2 to 5 kHz but this need not interrupt the electrical contact.

(b) Brush bounce or chatter from the impact force of the friction giving rise to considerable arcing. The vibration frequency generally in the order of 20 - 100 Hz.

(c) The vibration of the entire brush assembly, this occurs due to insufficient rigidity. Vibrations are again of the order of 100 Hz and have been observed to be responsible for severe arcing.

Other causes of brush assembly vibration have been attributed to excessive clearance between brush and holder, brush holder too far from the commutator or brushes too long and commutator irregularities (these are discussed in section 3.8.4).

3.8.2 External Vibration

Nellin [53] subjected several small motors to external vibrations at frequencies ranging from 50 to 1000 Hz, and observed their effect on commutation by measuring the degree of sparking produced. Test results (Figure 3.23) are presented for the following cases;

(a) the plane of vibration parallel to the brush axis.

(b) the plane of vibration perpendicular to the brush axis.

A sharp increase in sparking occurred at frequencies which coincided with the natural frequency of the armature (typically 100 - 400 Hz). As can be seen vibration parallel to the brush axis produced severe arcing near these frequencies and is attributed to relatively large changes in contact pressure.

3.8.3 Motor Vibrations

Hancock [54] describes motor vibrations being mainly due to

(a) the motor bearings

(b) rotor unbalance.

Bearings are considered to be the major cause of mechanical imperfection which distrubs the brush contact and degrades the quality of commutation. In ball and roller bearings the clearances between the balls or rollers and races can be large, any imperfection of these parts can excite motor vibrations. Dirty ball bearings have also been observed causing roughness in running producing increased sparking. Hancock stated that in machines with well fitted journal bearings these imperfections are generally smaller and the continuous film of lubricant provides better damping of disturbance.

The modes of rotor unbalance are defined as (a) static unbalance and (b) dynamic unbalance. [55]

Static unbalance is caused by the centre of gravity of the rotor not lying on the rotation axis. Centrifugal acceleration of this unbalance cause a nett radial force acting on the rotor, the magnitude of the force F is given by;

$$F = M.E.\omega^2 \qquad (3.33)$$

Where M is the mass of the rotor, ω its rotation speed and E the excentricity or radial distance from the centre of gravity from the axis of rotation. Figure 3.24(a), shows the mode of vibration caused by static unbalance forces.

Dynamic unbalance is created when the axis of rotation and the principle internal axis do not coincide, even if the rotor is statically balance, the distribution of the rotor mass may such that, vibration due to dynamic unbalance is affected as shown in Figure 3.24(b).

The causes of motor unbalance are;

- Dissymmetry
- Non homogenous material
- Shaft distortion at operating speeds
- Eccentricity
- Misaligned bearings
- Shifting of mass due to deformation at speed (e.g. winding lifting)
- Aerodynamic unbalance caused by turbulence

Figure 3.25, shows the limiting curve for maximum unbalance as a function of speed for small motors. [56] Under this curve the brush-commutator contact is stable whereas above the curve, the probability of contact separation and the resulting sparking is high. Weinart, [56] recommended that for mass produced armatures the maximum permissible value of rotor excentricity, should be 50% of that shown on the curve to allow for a known safety factor.

3.8.4 Commutator Irregularities

Commutators by the nature of their construction are a source of mechanical disturbance to the brush contact. The commutator segments separated by the intersegment insulation, incur regular impacts on the brush face as the commutator revolves. The rotational stresses enevitabily leads to variations in shape with increasing speed.

If a step is produced by an irreversible movement of a commutator segment, the brushes can ride completely clear of the surface after the step has passed until the brush spring moves the brush back into contact with the commutator. The magnitude of these effects are very small, in terms of machine dimensions, but, they may be sufficient to introduce a serious barrier to the transfer of current. [54]

Thermal forces too, can cause variation in commutator profile due to the different coefficient of expansion of the various materials used in its construction. The major commutator effects studied in the literature were as follows;

(a) commutator eccentricity

(b) surface finish

(c) variation in bar to bar heights.

Figure 3.26, shows a commutator of excentricity, $(R_2 - R_1)$, with a brush of mass M and spring force F. Shobert [39] used the following equation;

$$\text{speed, } n = \frac{30}{\pi} \sqrt{\frac{2F}{M(R_1 - R_2)}} \quad \text{r/min} \qquad (3.34)$$

to calculate the critical speed at which the effective force between the brush and commutator becomes zero. He stated that this expression should not be used as a direct measure of permitted eccentricities, since the condition for zero force should never be allowed and require a safety margin of about 5 to avoid uneven filming and commutator burning. At low speeds the brush is able to 'ride' the commutator eccentricity without affecting the contact too badly. Table 3.1, shows the values of n calculated for a small a.c. motor brush of mass 3.1g and spring force 200 g.

Knights [57] reported on results obtained on various small motors observing the commutator profile, brush life and quality of commutation. For eccentricities of 0.0051 mm the commutators showed no evidence of burning and brush life was normal, with higher eccentricities i.e. 0.025 mm and 0.051 mm, burning of the commutator was evident and brush life reduced by half. In some cases he reported that tests had to be stopped due to excessive brush burning.

Bates, [58] states that the initial finish of the commutator surface is known to have considerable effect on the performance of the brushes. Diamond tipped cutting tools although giving a good visual finish, leave mica insulation almost 0.005 mm proud on flush intersegmental insulation commutators. In this case it is reckoned that tungsten carbide tools give better results. Stability of the cutting tool is also essential, a vibrating tool can lead to 'flats' on the commutator surface, these give rise to destructive sparking and can also damage brush holders by vibration.

Variation in bar to bar heights is one of the most common mechanical causes of increased brush wear and increased sparking. Weinart [56]

Commutator Eccentricity $R_2 - R_1$	r/min for zero force
0.0025 mm	219,000
0.025 mm	69,600
0.25 mm	21,900

Critical speeds of eccentric commutator for zero brush spring force

Table 3.1

found that the maximum smooth repetitive impact was about 10 microns, the optimum value near 5 microns. Carson [60] carried out tests on small motors with bar to bar variations of less than 2.5×10^{-3}mm. The resulting erosions of the commutator segments was found to be due to excessive arcing, this erosion was found to shift around the commutator in the direction of rotation. The maximum allowable bar to bar height, such that the brush will follow the commutator profile by just touching each other is defined as, h, where;

$$h = Fg/2m(nC)^2 \tag{3.35}$$

where n speed in r/sec and C the number of commutator bars. Friction between brush and brush holder and the need for more than a momentary contact means that the maximum height will be less than that calculated by the expression.

3.8.5 Measurement of Brush Vibration

Brush vibration has been measured by means of small accelerometres or strain gauges inside or on the surface of a brush. [59] Clauss and Vogelsberg [60] used piezo-electric record player pickups attached to the brush, with the output from the crystal displayed on an oscilloscope. These methods although suitable for large machines where the mass of the brush is large relative to the transducer is unsatisfactory for small motors, where the brush weight is only of the order of a few grams. In this case, the brush behaviour can be significantly affected by the additional weight.

Ryan and Summers [61] described a method using microwaves and microwave components for observing irregularities on the commutator surface and state that this method can be used for measurement of brush vibration. But laboratory tests during the project, found that although this method could possibly be applied to measure brush vibration in large motors where the brush dimensions are of the order of the waveguide tube cross-section, for small brushes again this methods is unsuitable.

Knights [62] carried out brush vibration measurements on a washing machine motor by an optical method. The test-rig arrangement is shown in Figure 3.27. A hole drilled through the brush and brushbox is used as light-shutter sandwiched between rigidly mounted bulb (light source) and phototransistor. The vibrating brush causes variation of the light falling on the phototransistor which is detected on an oscilloscope. Laboratory tests again showed this method to be unsatisfactory, (a) because of the limited access to the brush and difficulty of installing the test arrangement with suitable rigidity and (b) since the RFI produced by the motor disturbed the vibration signal such that at high motor speeds, the required signal was totally obscured by the electrical noise.

The particular problems associated with observing brush movements in small motors can be summarised as follows;

(a) limited access to the brush

(b) high potentials on the brush during operation

(c) hostile local environment i.e. RFI, brush dust

(d) small size and weight of the brushes.

During the course of this project a new method of measuring brush vibration was developed and used in the test work, which satisfactorily overcomes the problems listed above. The design and principle of operation of this method is described in Appendix A5.

3.9 Discussion on Commutation

The theory of commutation gives little information as to the 'quality' of commutation. Quality is a measure of the level of sparking seen at the trailing edge of the brush during commutation. In practice quality is assessed by visual observation and classified as shown in Table 3.2.

Opinion as to which electromagnetic sources contribute most to sparking have changed over the years. [43] First it was thought that sparking was due to excessive current density under the brush, but tests proved that no arcing was visible even for current densities of 255 A/cm^2 per brush and up to 350 - 400 A/cm^2 under the trailing edge of the brush.

Another suggestion that failed critical examination, was that the existing switching voltage between the brush edge and commutator trailing bar was sufficient to create sparking. Today, it is widely accepted that sparking originates when the coil short circuited by the brush at the moment of interruption, stores sufficient amounts of electromagnetic energy $^1/_2 Li_s^2$ where i_s is the uncommutated current when the short circuit is opened. It is suggested that this energy should not exceed 50 W/cm length of brush.

Binder [63], showed that arcing occurs on a given brush if the product 'LIn' exceeds a limiting value, (where L is the leakage inductance, I the brush current and n the speed). This relation implies that the detaching contact can only withstand a voltage impulse of a limited intensity without drawing an arc.

Degree of sparking (class of commutation)	Degree of sparking	Condition of commutator and brushes
1	Absence of sparking (dark commutation)	No blackening of commutator or deposite on brushes
$1^1/_4$	Slight pin-point sparking under a small part of the brush	
$1^1/_2$	Slight sparking under major part of the brush	Black traces appear on commutator, easily removed by rubbing the commutator surface with petrol; deposits appear on brushes.
2	Sparking under entire edge of the brush Allowed only for short-time intermittent-duty loads and overloads.	Black traces which cannot be wiped off with petrol; deposits on brushes.
3	Heavy sparking under entire edge of the brush with large and flying sparks. Allowed only momentarily, with on-line starting or reversing, if the commutator and brushes afterwards are in condition allowing further operation.	Considerable blackening of commutator that cannot be wiped clean with petrol; burning and destruction of brushes.

Classification of the Quality of Commutation

Table 3.2

He discussed that the electrical breaking processes is determined by the brush contact resistance R_b, which depends on time, the leakage inductance, L, and the remaining circuit resistance r. If the contact resistance R_b is very rapidly taken up to infinity from its initial value, practically the whole flux $\phi = LI$ is applied as a voltage impulse across R_b. However, the circuit has an electric time constant $L/(R_b + r)$, if the breaking process is carried out slowly, the current will have decayed exponentially from its original value I before R_b takes large values and so no arc is drawn. He stated that somewhere between these extremes there is a limit at which 'just' no arc is set up any longer.

Dikin-Zanger [64] of the Hoover company in the early 1960's commented that the design of current reversal in small commutator machines is usually determined by considerations of brush life, since the brush life requirement is of the order of only a few hundred hours. Current reversal characteristics in such machines are pushed to the limit with the bulk of the reversal being completed by a trailing arc. He suggested that the arc is thus not an undesirable side effect. This attitude has however, changed and the reduction of arcing is a requirement in motor design.

A number of authors have made recommendations to improve commutation; Mohr, [65] presented graphical methods to calculate the sparking free load and speed limits of series motors, using their brush contact drop curve, parameters of the motor and working conditions. He stated that some of the assumptions made in classical commutator theory are quite impermisible for a.c. commutation. The use of the maximum rms values of voltage and current rather than the actual value of induced voltage and current which occurs when the trailing edge of the brush is stressed to its maximum. The point in the periodic current and voltage cycle in which commutation is most difficult, is not necessarily at the maximum current and voltage values, but at a point called the 'critical point' which coincides with the point at which the resultant circulating voltage 'e' is a maximum. He examined the conditions at the brush under the most unfavourable conditions and derived curves for spark-free commutation.

Weinart [56] examined the influence of the ratio of armature and field coils on commutation, by experimental studies he determined a factor X' expressed in terms of e_t the transformer voltage, e_F field voltage and C the number of commutator segments, i.e.

$$X' = e_t . C / e_F \tag{3.36}$$

and stated that for good commutation $X' \leqslant 1$.

Gray, [66] examined the brush current density for different ratios of the time of commutation Tc to electrical time constant of the short-circuited coil $L/R_b + r$; neglecting r (i.e. small compared to the resistance of the brush/commutator contact), curves were presented of the ratio $T_c/(L/R_b)$ against brush tip density/average brush density, see Figure 3.28.

He suggested for values of $Tc/(L/R_b)$ less than 1 the current density in the brush tip becomes infinite, and due to concentration of energy, sparking takes place, thus the criteria for commutation, is that $Tc/(L/R_b)$ is greater than 1.

In an a.c. motor the voltage generated in the short-circuited coil opposing the change in current, Vr, is a vectorial sum of all the voltages generated in the coil, i.e.

$$Vr = \sqrt{(e_r + e_{rot})^2 + e_t^2} \qquad (3.37)$$

Sources vary considerably on the limiting value of Vr between the trailing brush edge and the commutator segment that causes sparking. Values range from 2.5 volts, to 25 volts. [67] This variation is mainly due to the range of motors considered and the variety of brushes. For example, Binder [63] showed the variation of limit of Vr for grades of brush with different metallic content, (Figure 3.29). Dijken [29] and others [68] estimated that for small motors using electrographite brushes, the Vr limit is 12 volts. The Hoover design practice is to aim for an upper limit of Vr of approximately 10 volts. But designs where their calculated value of Vr is less than 10 volts, they still find sparking a problem. This leads to doubt about the calculated value of Vr; e_{rot} and e_t have been measured to show reasonable accuracy with design estimates, thus the value of e_r the reactance voltage is in doubt. The value of e_r commonly used in calculations to estimate V_r is the average reactance voltage (RV) as defined by Gray [66] i.e.

$$RV = L.2I/T_c \qquad (3.38)$$

But this value of reactance voltage is infact irrelevant since at no time during the commutator period, is this value applicable. It assumes a linear change of current from + I to - I in time Tc which has been shown above to be impossible. There follows a study of the parameters in this calculation.

(a) Effective Coil reactance (L)

The classical method for calculating the inductance of the rotor coils is given in section 3.4.1. The commutating coil is magnetically coupled with other rotor and stator coils and eddy current paths. Dijken [29] explains that the frequency influence on coil inductance shown in Figure 3.30, is due to these eddy currents. It is therefore, unclear as to what value of inductance should be taken into account during commutation. By experimental means Dijken obtained values for the active inductance which must be reckoned with at the end of commutation during sparking, 'L_{comm}'. (The method used to measure 'L_{comm}' is described in chapter 5).

Tests were carried out on small series motor rotor coils situated on the armature. His results showed that the actual 'L_{comm}' was dependent on the precise brush positions. Figure 4.31, shows the different positions selected and the values measured. It can be seen that the value of 'L_{comm}' varies between 312μH to 1920μH. In a motor, any jumping or movement of brushes would means that the 'L_{comm}' for any coil, can be different.

Comparing the measured and theoretical values of 'L_{comm}' for the 'normal' commutation condition as shown in Figure 3.31(f). The measured value of 'L_{comm}' is 336μH but the calculated value of inductance for the coil is 1750μH showing the wide discrepency that could occur in the calculation for

e_r using Grays formula.

(b) Change in Current

Grays formula used 2I as the change in current i.e. the full change from + I to - I. In practice, at the end of commutation, the current will have reduced from + I by the electric time constant of the coil i.e. $L/(R_b + r)$. But the contribution of 'e' the resultant of rotational and transformer voltages in the commutating coil which is out of phase with the main current by ψ can at some time be aiding the change in current and at others, oppose the change as indicated in Figure 6.43. Thus at any time, the final value of current in the coil that has to be commutated at the break of contact, is dependent on e.m.f. prevailing at that instant. Thus in estimating the reactance voltage it is reasonable to consider the 'worst case' of a current change of 2I.

(c) The Time of Commutation

Kostenko and Piotrovsky, [43] in a review of work on commutation, reported that Shefner had shown experimentally that the real time of commutation is much less than the calculated period Tc. A crude estimate of the time taken for commutation to complete after the contact break, is the duration of the arc itself.

The duration dependent on a number of factors i.e. the magnitude of the current, the speed of rotation and the electromagnetic energy to be dissipated. Dijken estimates the duration of an arc t_z of lenth 0.4 mm as seen in small series motors at 18000 r/min to be the order of 14 μsec. Whereas the value of Tc for this motor is 270μsec i.e. Tc is approximately equal to $20t_z$.

A comparison value of RV with the true reactance voltage e_r, which can be expressed as;

$$e_r = L_{comm} \times \frac{2I}{t_z} \qquad (3.39)$$

It appears that e_r is approximately four times greater than RV. Puchstein and Kimberley [27] appear to be aware of the limitation in using RV to estimate the true reactance voltage e_r and recommend that RV be multiplied by a 'weighting factor' of between 2.5 and 3.5, but they do not state any reason for this. From the discussion presented here, it appears that the higher weighting factor is more appropriate.

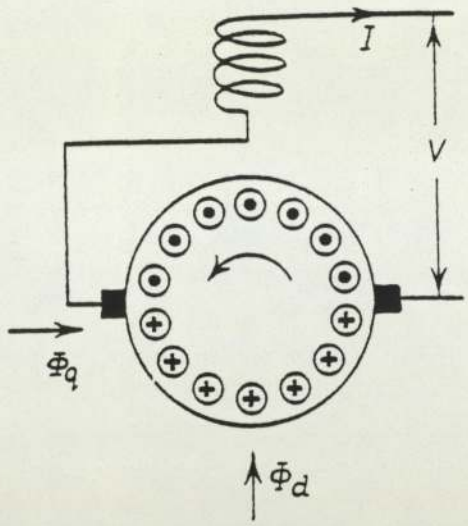

Series motor connections

Fig. 3.1

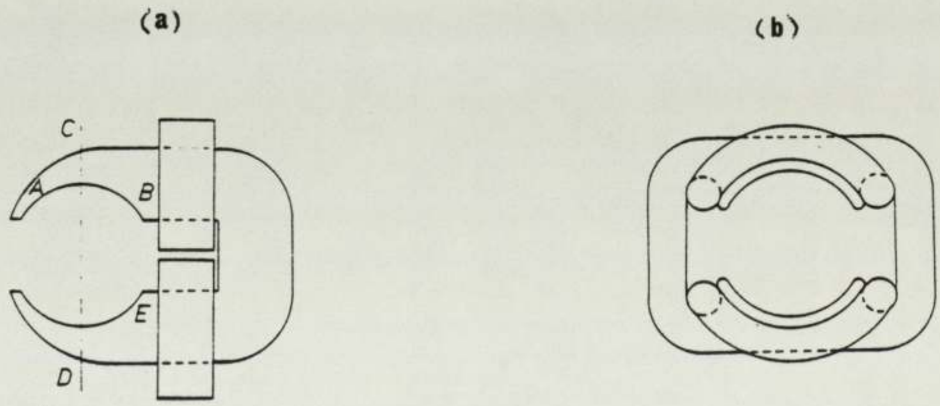

Common stator configurations

Fig. 3.2

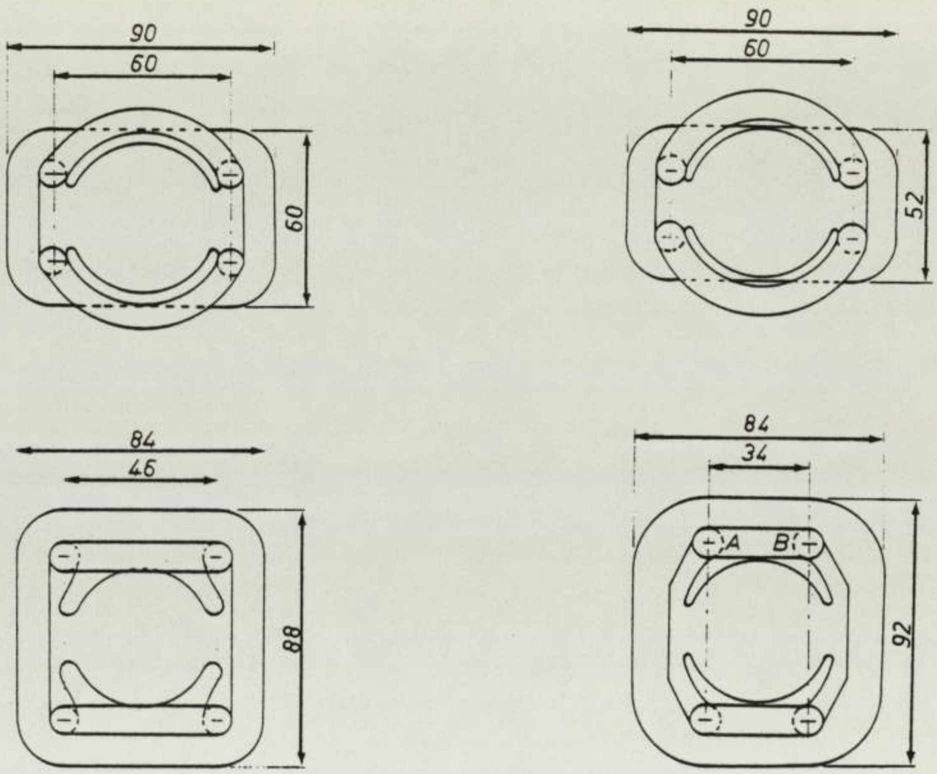

Range of stator variations found in small series motors

Fig. 3.3

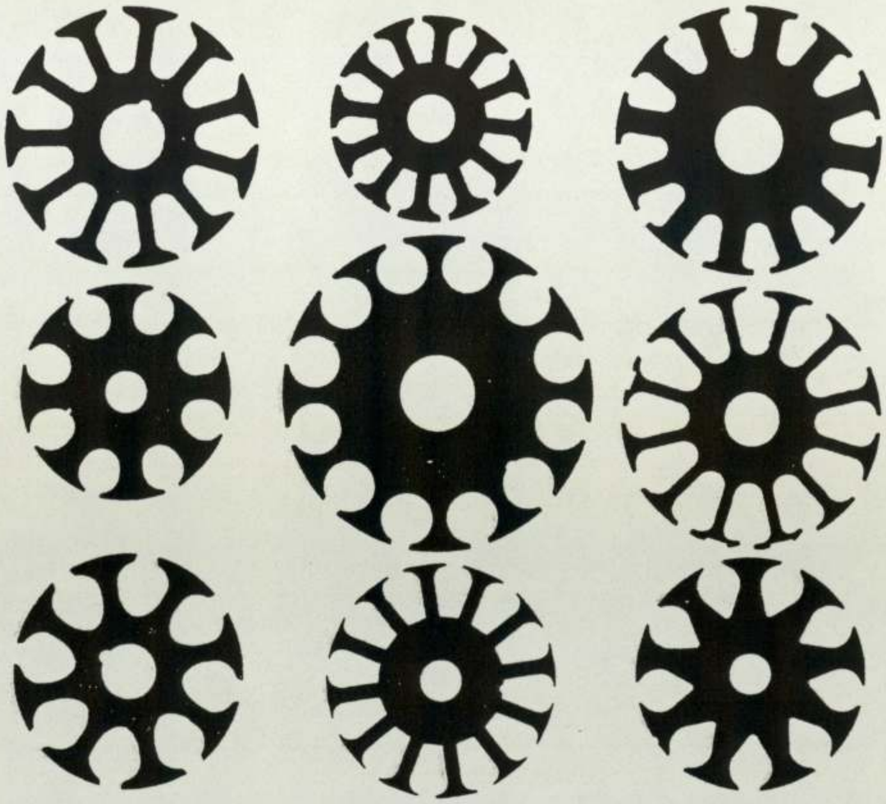

Range of rotor variations found in small series motors

Fig. 3.4

Optimised shape of motor laminations (from Dijken[28])

Fig. 3.5

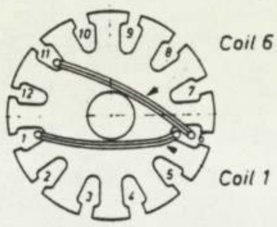

Example of 12 slot rotor wound with 2 coil sides per slot

Fig. 3.6

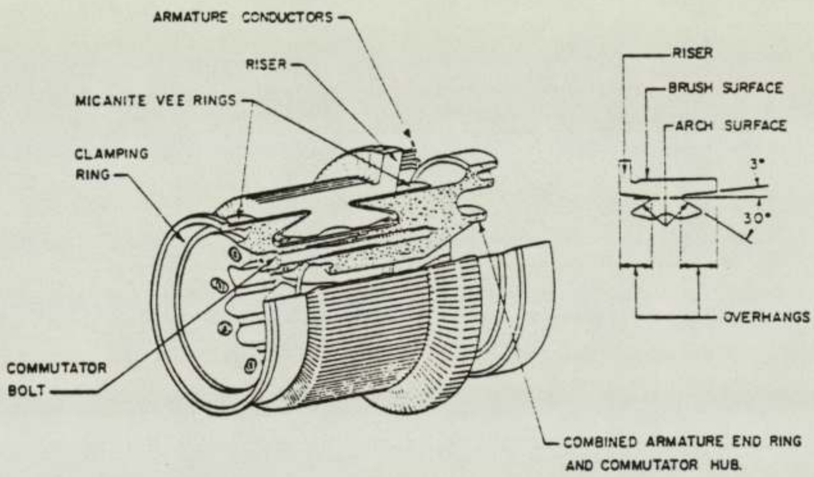

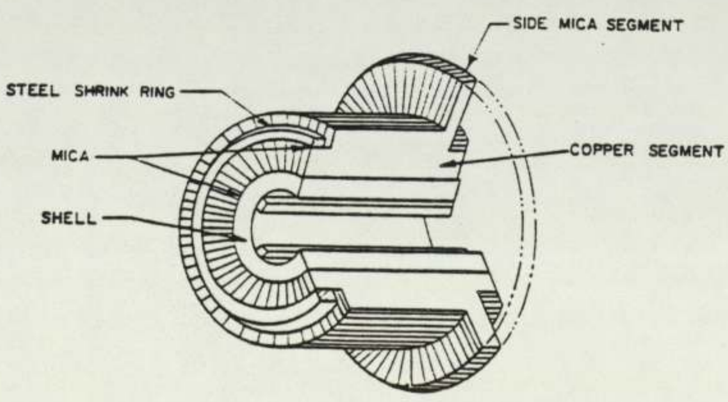

Two typical commutator assemblies

Fig. 3.7

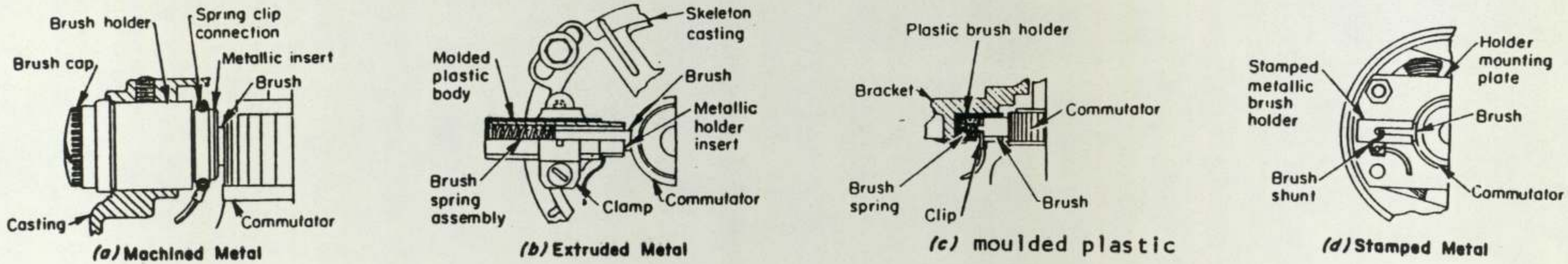

Common brush mounting arrangements used in small motors
(from Knights [12])

Fig. 3.8

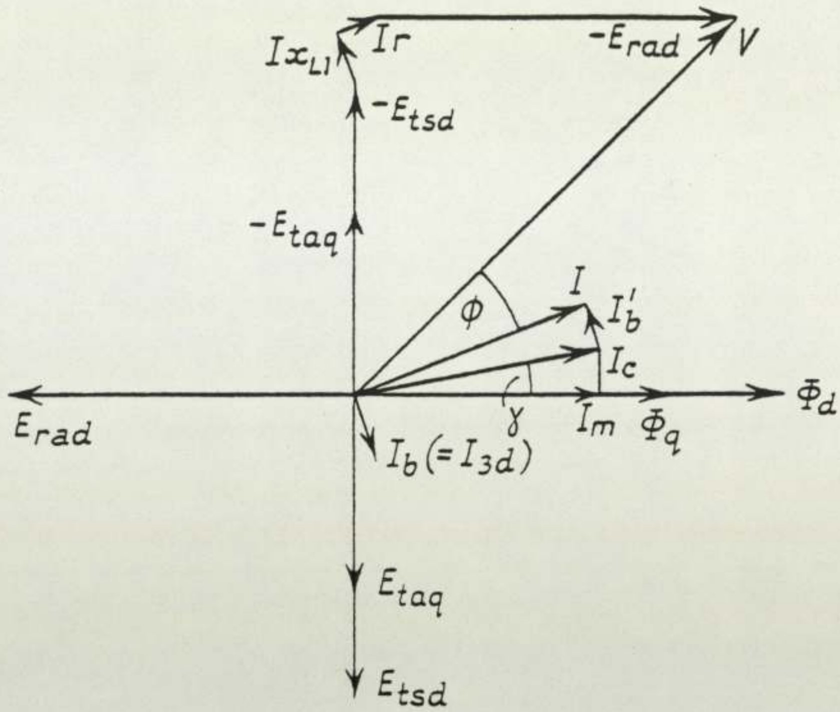

Vector diagram of series motor

Fig. 3.9

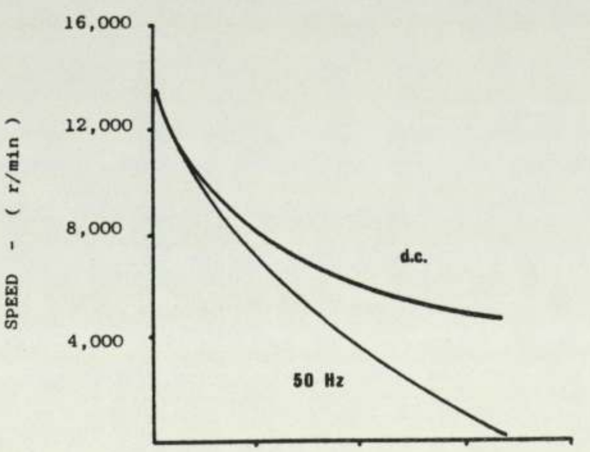

Comparison of speed-torque characteristics of a small motor on d.c. and 50 Hz supply

Fig. 3.10

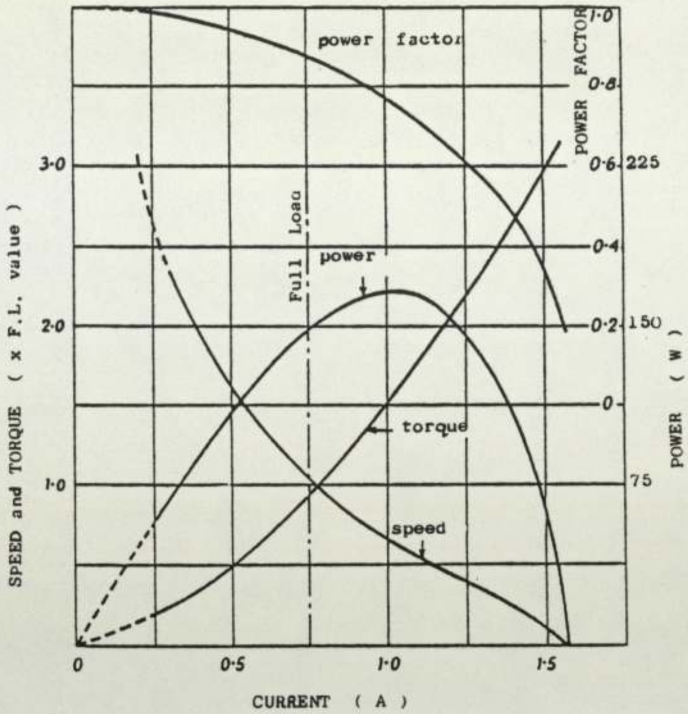

Characteristics of a 150 W series motor

Fig. 3.11

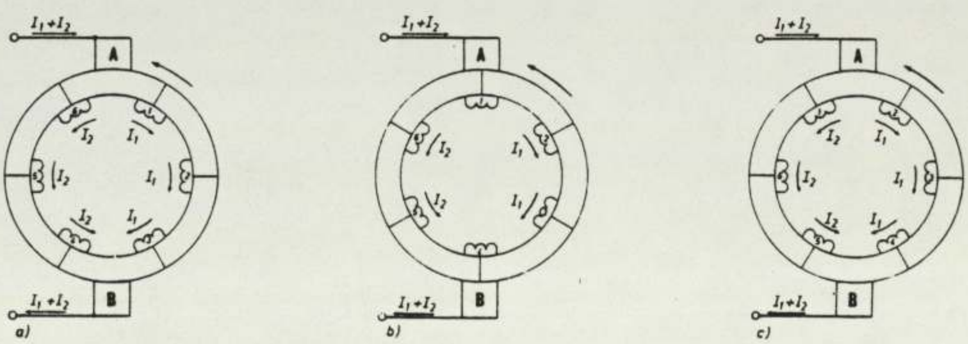

Commutation of coils 1 and 4 as the rotor moves relative to the brushes

Fig. 3.12

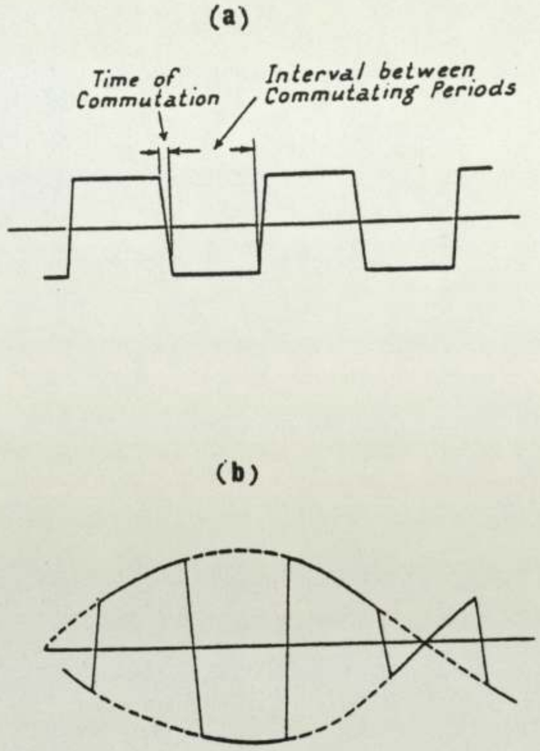

Commutation in single phase machines

Fig. 3.13

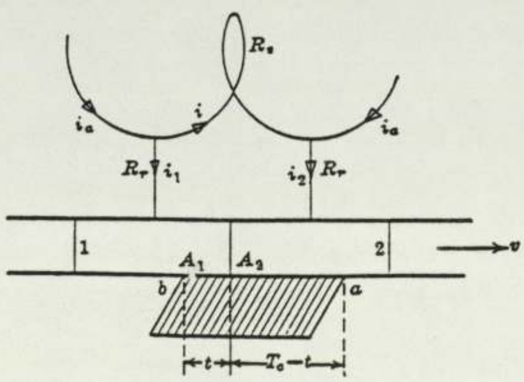

Short-circuited winding element

Fig. 3.14

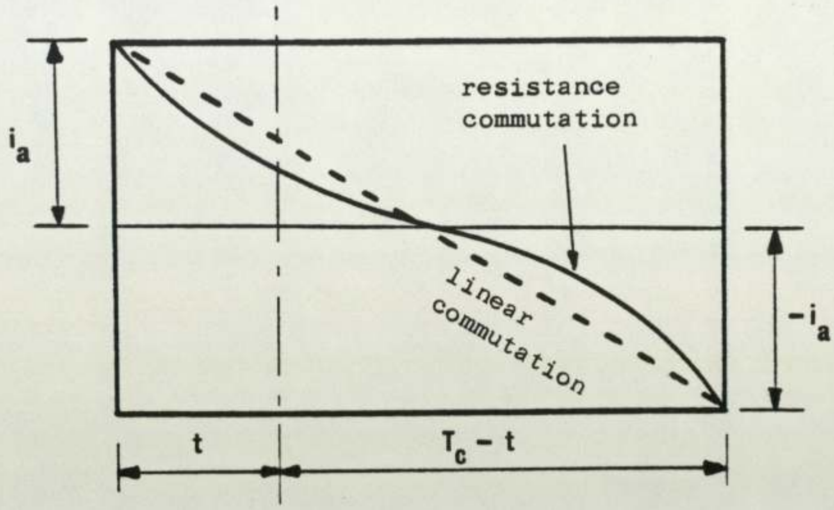

Resistance commutation and linear commutation

Fig. 3.15

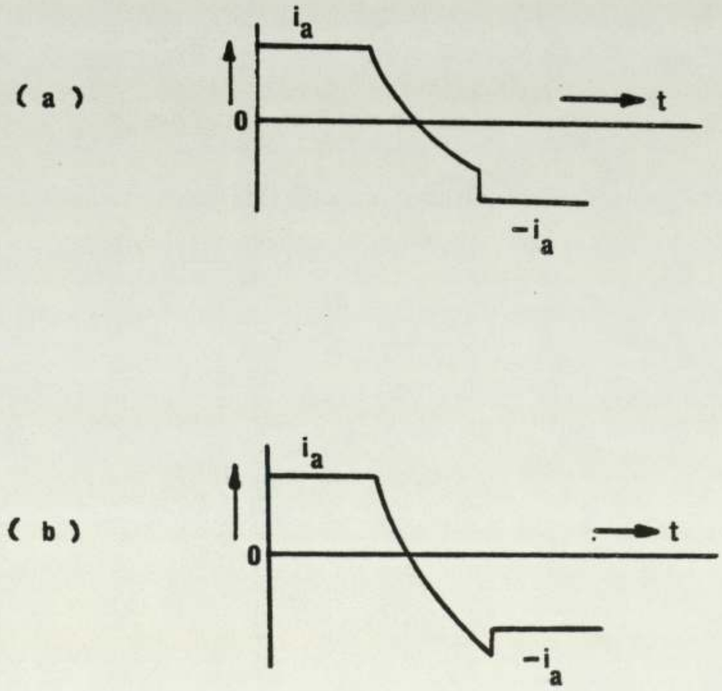

Delayed commutation (a) and Over-commutation (b)

Fig. 3.16

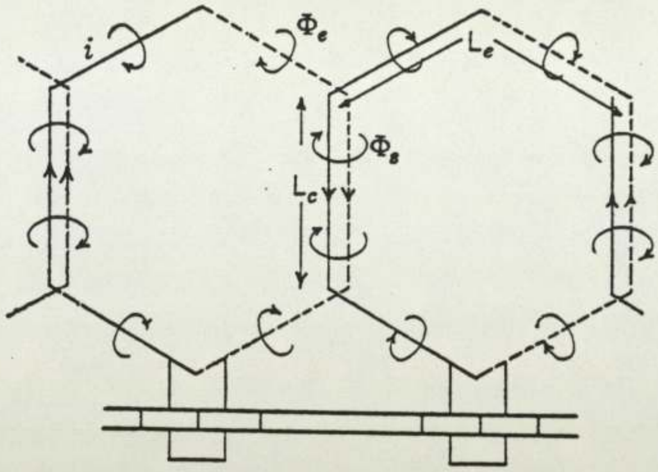

Flux circling the commutating coils

Fig. 3.17

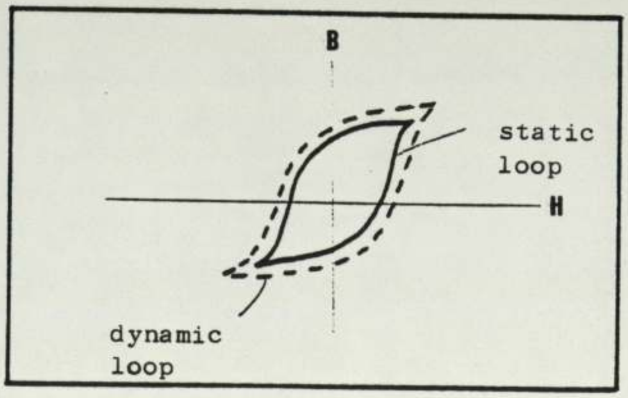

Static and dynamic hysteresis loops of the laminations

Fig. 3.18

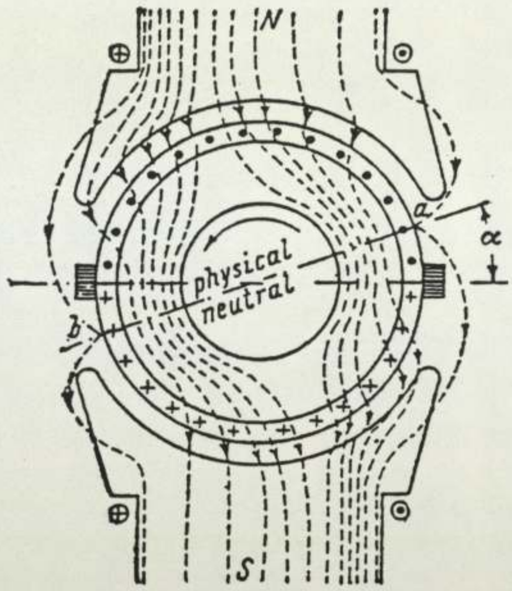

Distortion of the air gap flux by armature reaction

Fig. 3.19

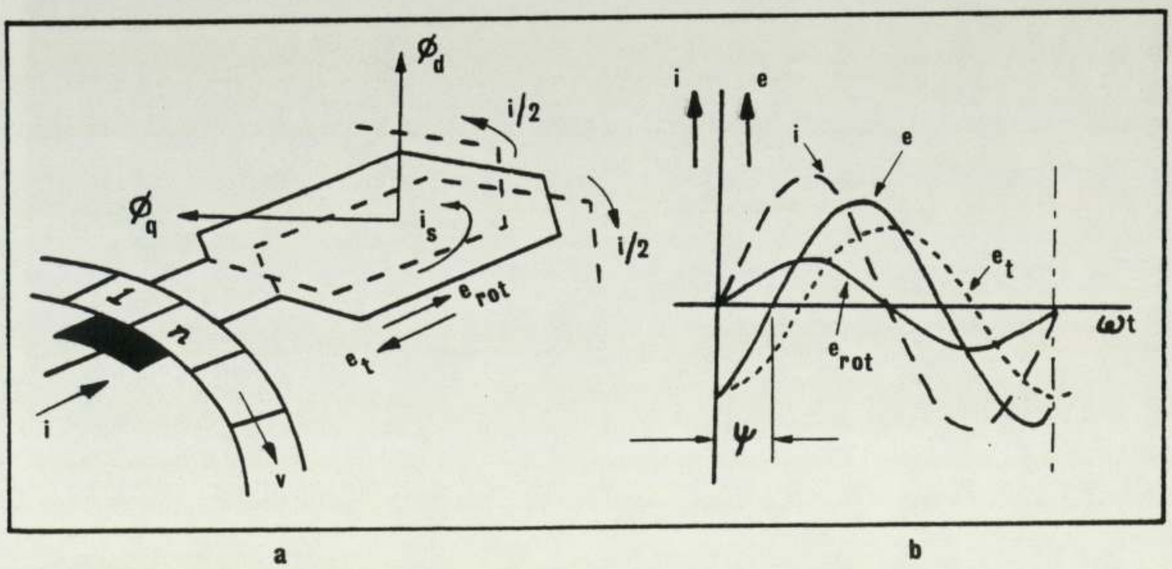

Voltage and current components of the commutating coil

Fig. 3.20

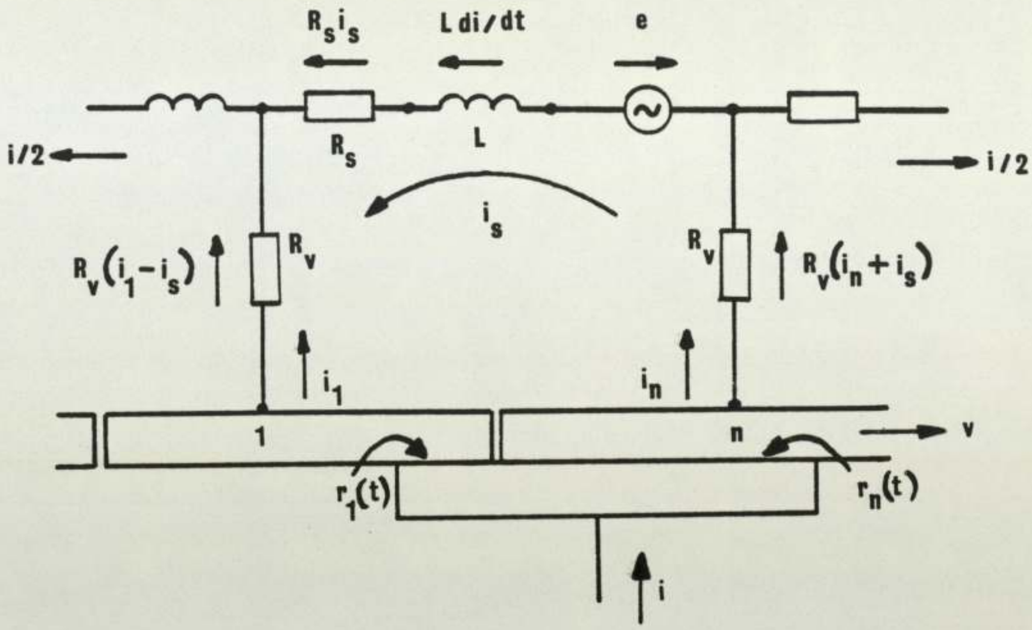

Circuit diagram of the short-circuited coil

Fig. 3.21

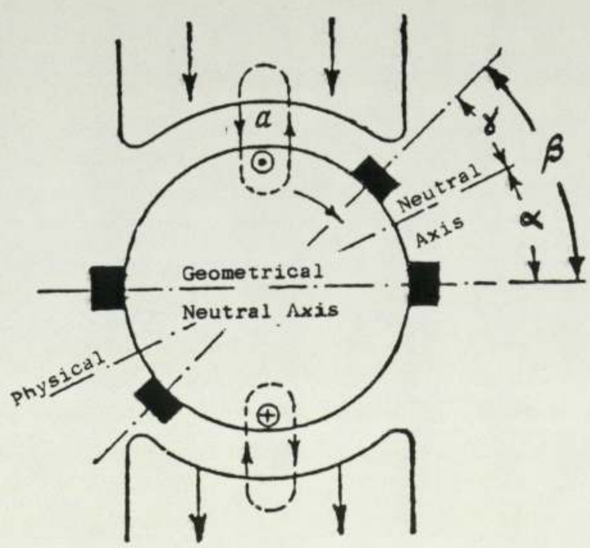

Improvement of commutation by brush shift

Fig. 3.22

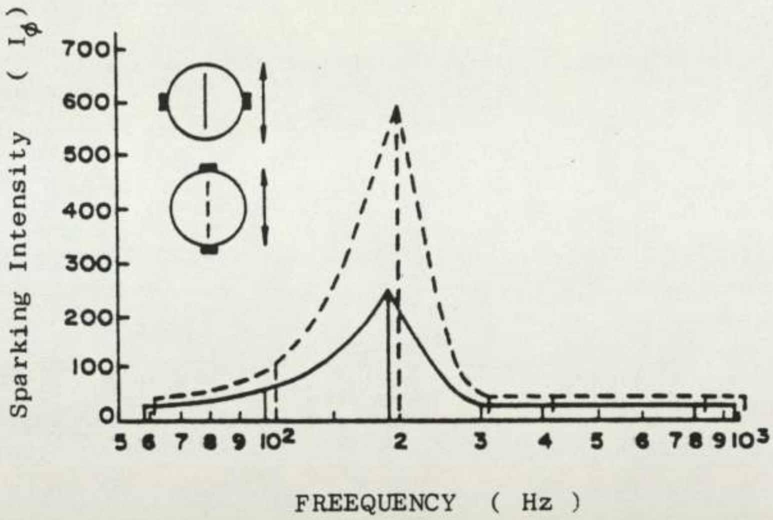

Variation of sparking intensity with increasing external vibration frequency (from Nellin [53])

Fig. 3.23

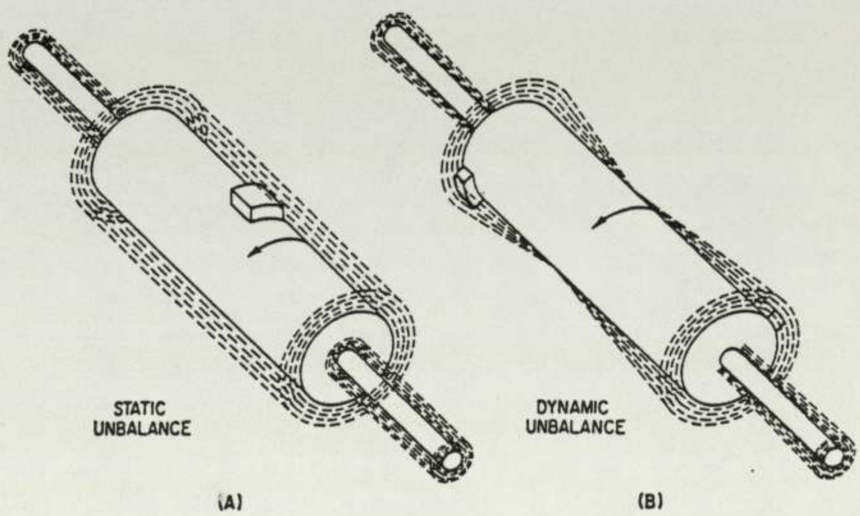

Modes of vibration induced by static (A) and dynamic (B) unbalance

Fig. 3.24

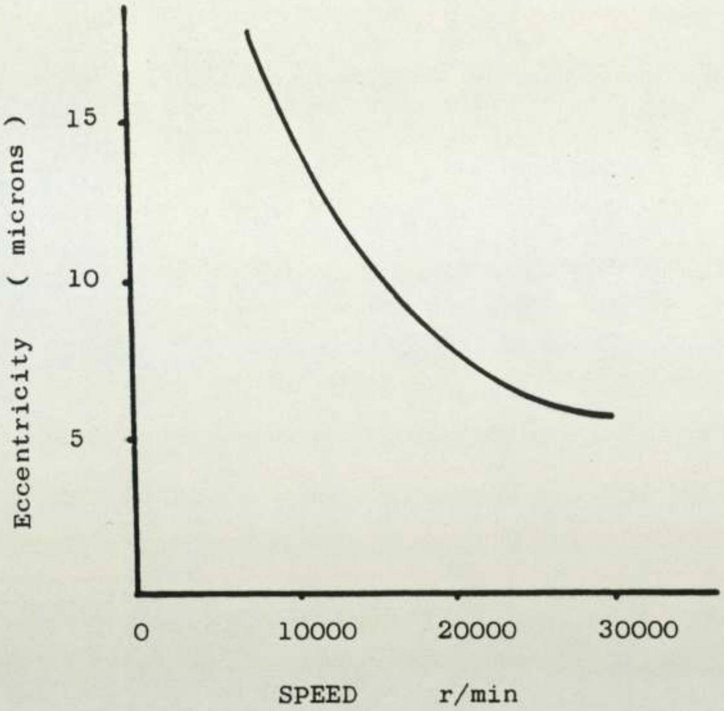

Limiting curve for maximum eccentricity as a function of speed for small motors (from Weinart[56])

Fig. 3.25

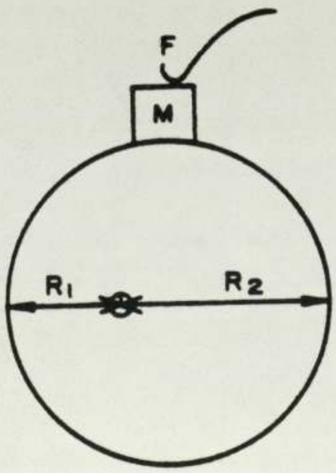

Simplified brush and eccentric commutator arrangements

Fig. 3.26

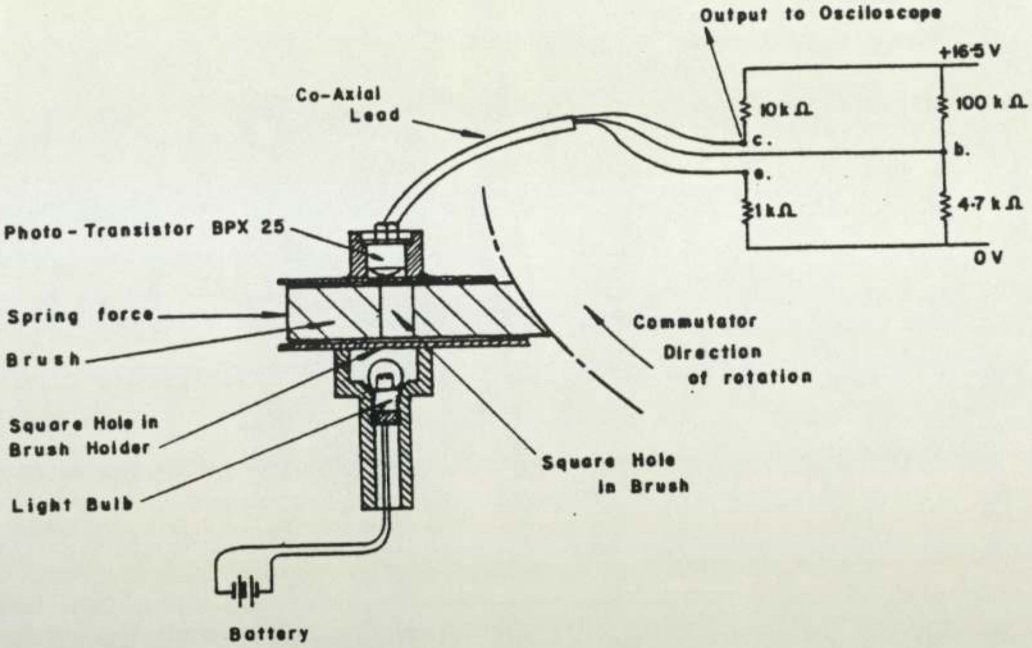

Optical arrangement to measure brush vibration (from Knights [62])

Fig. 3.27

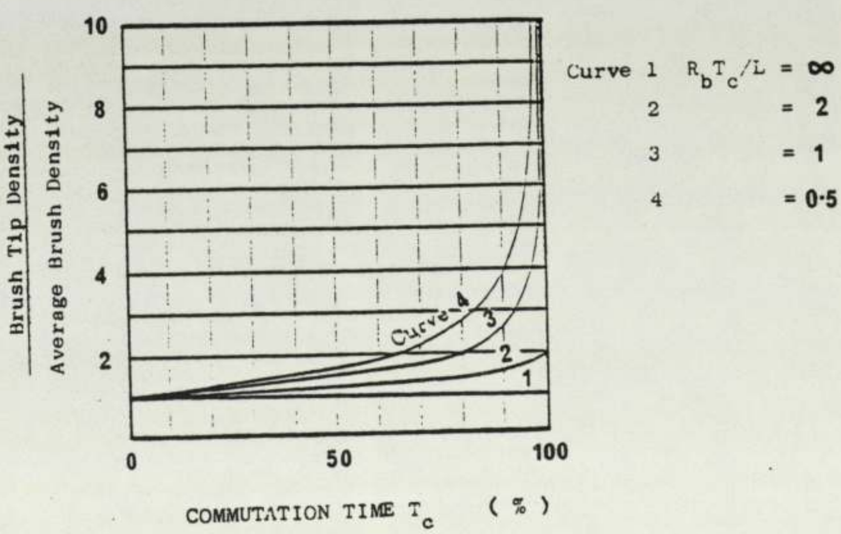

Variation of current density at brush tip against time from the start of commutation (from Gray [66])

Fig. 3.28

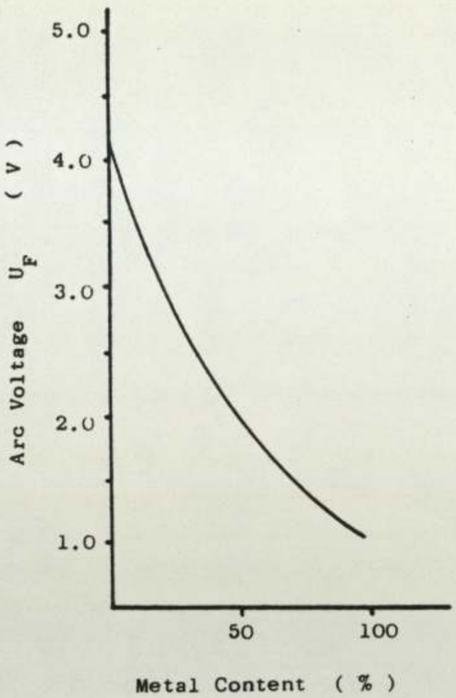

Limiting curve for arcing voltage with increasing brush metallic content (from Binder [63])

Fig. 3.29

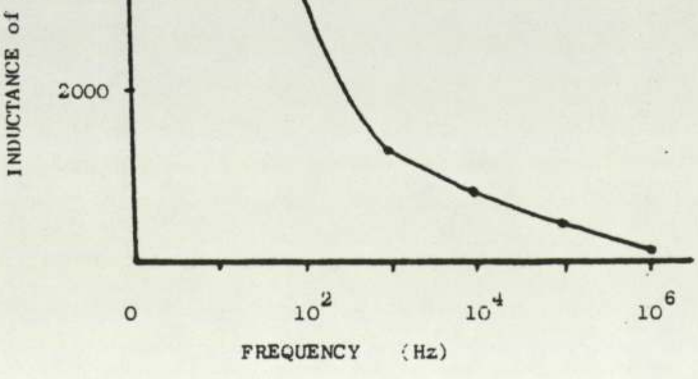

Variation of coil inductance with frequency (from Dijken [29])

Fig. 3.30

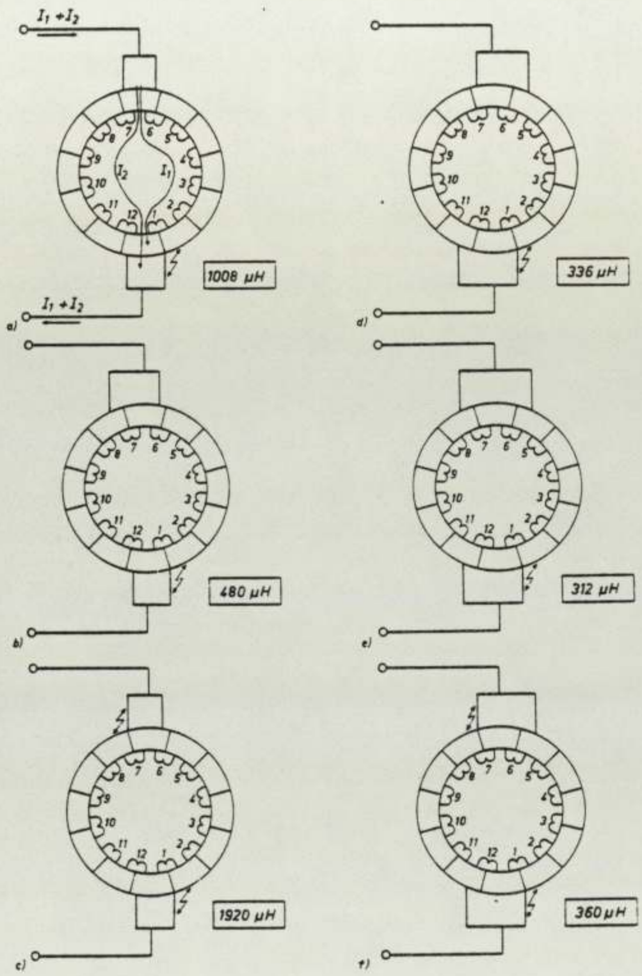

Variation of the measured active inductance of the commutating coil with brush position

Fig. 3.31

CHAPTER 4

RESEARCH LITERATURE REVIEW ON RFI

4.1 Man-made RFI sources

4.2 RFI from small commutator motors

4.3 RFI detection methods

4.4 RFI measuring techniques

4.5 Discussion

CHAPTER 4

RESEARCH LITERATURE REVIEW ON RFI

Much of the basic theory of electromagnetic radiation was worked out before 1900, and experiments had already demonstrated the validity of the work. The theory first appeared, in its fully developed form, in 1873 by Maxwell (1831-79) in his treatise of "Electricity and Magnetism". It was a corollary of Maxwell's theory that electromagnetic 'waves' should be generated by an electrical disturbance. [69] Hertz (1857-94) verified this prediction by experiment, demonstrated the existance of the radiation (1887) and determined many of its characteristics. [70]

The commutator switching action in d.c. machines was soon recognised as a source of electromagnetic radiation in the form of interference on telephone lines [71] and telegraph lines. [72] With the advent of broadcasting, the problem of radio frequency interference (RFI) from commutator motors became apparent. Early investigations were carried out by the General Post Office and in 1922, the Electrical Research Association (ERA) became actively interested in the study of interference. [73]

Most developed countries had a radio-telegraphy capability by the early 1930's. The main areas of work on RFI at this time, was the protection of sound broadcasting in the long and medium wavebands and methods of measurement of the complex and irregular waveforms being encountered. [74]

This chapter reviews literature on the subject of RFI; section 4.1

firstly examines some of the common sources of man-made noise other than motors. Section 4.2 reviews work on RFI from motors which form the background for the study presented in this thesis. RFI detection and measurement techniques are studied in Section 4.3 and 4.4. Finally, in section 4.5 a discussion on the approach to the study outlined in the project proposal (section 2.4) is presented.

4.1 Man-made RFI Sources

In section 1.2 it was stated that RFI can originate from both natural and man-made sources. This thesis is concerned with RFI from motors, which comes under the category of man-made noise emitted from apparatus as an unwanted by-product of their normal operation. This section examines a number of other electrical devices which also fall in this category and typical RFI levels are presented. The devices considered are;

a) Electrical Welding and cutting equipment

b) Electrical power lines

c) Ignition systems

d) Flourescent light

e) Switching devices

Thomas [75] considered that each of these devices had a distinct "spectrum signature". Spectrum signatures are defined as a summary and presentation of data showing all radio frequency energy radiations of electrical equipment. Meyers [76] and others [3, 77] compiled a number of spectrum signatures for a wide variety of apparatus from both previously published and unpublished material, many of the examples given below are taken from these references. The units of RFI measurement are dependent on the type of measurement equipment used. In interference reports, very often inadequate information regarding the units specified on graphical presentations is supplied, thus, making any meaningful comparision of RFI levels very difficult. Measurement techniques and equipment is presented in section 4.3 and 4.4.

4.1.1 Electric Welding and Cutting Equipment

Welding of metallic parts is commonly accomplished in industrial production by means of either r.f. stabilised arc welders, or, resistance welders. Each device generates intense heat in the work by the passage of large electric currents through the weld point. In an r.f. stabilised arc welder, the electrodes do not make physical contact with the work piece. A high frequency current signal is added to either a direct or mains frequency high power source of welding current which ionises a gaseous plasma between the electrodes and weld. The high electrical conductivity plasma provides a low impedence path for flow of the weld current. A spark-gap oscillator is used to produce the high frequency current component and the interference spectrum generated by the spark is superimposed upon the primary welding current. Fig.4.1, shows examples of a number of published r.f. stabilised arc welder radiated noise spectra. [78]

Electric resistance welders produce the necessary current density in the work piece by applying pressure to the electrodes that is sufficient to puncture the surface of the work piece, thereby admitting mains short circuit currents exceeding 10kA. Electrode diameter, pressure, current density are increased proportionally with the work metal thickness. Fig. 4.2, shows the radiated noise spectra for resistance welders at various distances from the source.[76, 78]

Metal cutting is performed by electrical discharge type apparatus. The work piece being electrically connected as an anode, and the cutting tool becomes the cathode, the two being separated by a narrow gap. High peak pulse discharge currents supplied to the anode, erode metal particles from the work-piece. Both the work-piece and the electrode are submerged in a circulating di-electric fluid which help sweep away the waste material. The average power rating of electric discharge cutting machine is 1-2 kW with pulse rates of approximately 3 kHz, the resulting noise spectra is shown in Fig. 4.3. [78]

4.1.2 Electrical Power Lines

Electrical power transmission lines have been found to produce electrical interference from mains frequencies up to the MHz frequency range. Fig. 4.4, shows the radiated typical noise spectrum from a transmission line. The RFI is attributed to a) Gap discharge radio noise and b) Line conductor corona discharge. [79] Gap discharge radio noise is produced by a rapid flow of electric current in the air-gap existing between two points of unequal potential occurring on electric power equipment. If the potential gradient is sufficiently great, in-elastic collisions occur between charge carriers and neutral molecules of the air-gap, resulting in the production of additional ions and electrons which separate into opposite charged clouds.

An excess of electrons creates an avalanche chain reaction in a current surge across the air-gap - radiation from this surge is observed as RFI and gas expansion produced by localized air heating produces an accompanying audible noise.

Corona discharge requires only a single charged object at sufficiently high potential, either positive or negative. As the potential increases, high mobility electrons in the vicinity are accelerated by the local electric field, which again by collisions with the air-gap molecules produce an excess of electrons. Onset of charge avalanching, coincides with corona-threshold attainment and initiation of both radio noise and visible spectrum emissions.

4.1.3 Ignition Systems

Many papers are available on the subject of automotive ignition noise, studies vary considerably on the method of RFI measurements. [82, 83, 84] Fig. 4.5 shows the typical RFI spectrums observed. The ignition system generates impulsive noise, the ignition circuit consists of a battery, induction coil, breaker points, by-pass capacitor, distributor and spark plugs.

Fig. 4.6, shows the event sequence (listed below) in the circuit producting RFI.

a) (Steady state) with the breaker points closed, no RFI produced.

b) Breaker-points open, the distributor gaps are excited by an inductive surge in induction coil and the spark plug gaps are ignited - RFI generated.

c) Breaker points again closing, the distributor and spark plug arcs are extinguished, the by-pass capacitor discharges through the breaker points - RFI generated.

The induction coil can produce voltage spikes exceeding 12 kV, creating current peaks of over 200 A. [80]

4.1.4 Flourescent Lights

Flourescent lights are typically designed with tungsten wire electrodes, separated by a length of a light glass column filled with a gas mixture containing argon or mercury. RFI emission is generated with the establishment of an alternating current electric discharge produced by pulses of high potential current from the electrodes. Pulsed current flow in the ionised gas column generates interference noise originating from the high current density region of the electrodes and which may be augmented in hot cathode tubes by random or impulsive emissions from material defects occurring on the electrode heaters. Fig. 4.7, shows a typical RFI spectrum measured from a domestic flourescent tube. [3]

4.1.5 Switching Devices

Switching of electrical current causes RFI, the switch may be either a simple key-switch or a solid state switching device, the level of interference is dependent on the magnitude and rate of current change as mentioned in section 1.2.

Howell, [85] presented a detailėd study of the mechanisms which generate noise in mechanical switches and Fig.4.8, shows the noise spectrum of these type of switches for different voltage and current supplies.

The Silicon Controlled Rectifier (SCR) and related bi-directional solid state switching devices, are widely used in power control. The noise sources in the semiconductor devices are well covered in the literature, [86] i.e. Johnson noise, shot noise and flicker noise. Hall and Palmer, [87] related these sources to SCR operation and stated that the noise produced is due to the following:

a) The generation and recombination of minority carriers in the device blocking state generating noise, owing to their passage across a reverse biased p-n junction. This carrier flow constitutes the leakage current.

b) The continuous generation and recombination of carriers during conduction and switch on.

c) The avalanche multiplication of carriers during the turn-on process.

d) The re-combination of carriers during turn-off.

e) Other causes about which little is known, which may be a function of the electrical operating conditions.

They observed noise generated by SCR control and summarized that the harmonics present in the waveform of the output voltage, are those as obtained by Fourier analysis of the waveform and constitutes a series of spectral lines of decreasing amplitude as the order of harmonic increases. Fig. 4.9, shows the theoretical spectrum of a number of voltage pulses of different shapes and repitition rates. In addition to these predicted spectral lines. Hall and Palmer noticed the existence of random signals between the harmonic lines at the higher frequencies resulting from the influence of cycle to cycle variation in a.c. supply voltage amplitude and period. They established that the most significant effect which produces noise is the random variation in the timing of the a.c. mains period (called time jitter).

Hall and Quelch [10] showed the increase in RFI from a hand-held drill motor, when fitted with SCR control as shown in Fig. 4.10. References 88, 89, 90, present numerous examples of RFI measurements with control devices switching current in both resistive and complex loads.

4.2 RFI from Small Commutator Motors

This section reviews the available literature on RFI from a.c. commutator motors, as very few published papers that deal directly with the subject were found, papers which deal with some aspects (i.e. d.c. machines) have been included. The work is presented as follows;

a) Factors affecting the generation of RFI

b) Factors affecting the propogation of RFI

c) Prediction of RFI

d) Suppression methods

4.2.1 Factors affecting the Generation of RFI

At the first conference on 'Radio Interference Reduction' held by the Armour Research Foundation (1954), Short [91] summarized the sources of noise to be found in commutator motors as the following;

a) <u>Noise due to commutation</u>: caused by the current switching action of the commutator is always present, and need not necessarily be accompanied by sparking. [15]

b) <u>Noise due to arcing at the end of Comutation</u>: The impluse type disturbance of the spark is rich in harmonics, the conducting leads act as a antenna causing radiation to occur over a wide frequency range. If the gap breaks down extremely rapidly, a frequency response up to the VHF band can be generated. [92] Additional frequencies known as the gyro and plasma frequencies are also generated. These do not represent RFI when considered alone, but German [11] suggested that it is possible when connected to an antenna system, the gyro and plasma 'generators' may radiate enough energy to become a source of RFI.

c) <u>Noise due to Arc conduction between commutator and brush</u>; current between the brush and commutator segments is carried by a group of parallel arcs that bridge a gaseous layer present between the brush and the bar. These arcs are continually forming and stopping, each time a new bar comes under the brush a new group of arcs must be established. This action results in an RFI noise source that is envelope modulated by the commutator frequency. Motter [1] called this, 'surface noise', and suggested that these transients are of a random nature, he showed that surface noise is present on slip ring motors as well as commutator motors, and produced curves showing the relative level of the two (Fig.4.11). Many factors affect the amplitude of the transients i.e. amplitude of current through brush face, brush material, brush pressure, commutator speed. Fig. 4.11, also shows that were attempts were made to improve commutation by means of laminated brushes, a lower level of RFI was generated.

d) <u>Armature Core and Shaft Noise</u>; Changes in current produced by commutation currents induce voltages in the shaft and armature core; these effects also transfer to the core through the high capacitance between the windings and the laminations. Short considered the entire machine structure as a cavity resonator, possibly becoming a very highly resonant circuit at certain frequencies. This noise would be of a narrow band nature and may be reduced by grounding the shaft.

Motter [93] observed that RFI generation could be reduced in d.c. motors by the improvement of commutation. This was affected by

a) The use of laminated brushes to aid the reversal of current and

b) by shifting the brushes with respect to the magnetic neutral.

The laminated brushes used on the test machine were made of four laminations of equal size but different resistivities the laminations were insulated from each other to reduce circulating current across the brush face. He concluded that for a given machine design, there is a finite laminated brush design to provide optimum performance by this method. Fig. 4.12, shows a comparison of test results with normal brush and with laminated brushes. By shifting the brushes from the magnetic netral he found that there is an optimum brush position where the RFI generated is a minimum, either side of which RFI is increased as commutation deteriorates.

Nelson and Diehl [94] further examined the brush operation with respect to RFI, their findings listed below state that brush polarity, brush-commutator contact, rotational speed and brush stability, have significant influence on RFI.

a) <u>Brush polarity</u>; tests on d.c. equipment showed that the interference level at the cathode brush is always higher than at the anode, this has been explained by the conduction characteristic of the copper oxide film on the commutator surface. Approximately ten times as much RFI generated at the cathode interface as at the anode. Experiments with chromium plated ring surfaces showed that the interferance of the cathode brush can be reduced, indicating that the influence of RFI at the brushes can be attributed partly to copper slip rings and commutation (See fig. 4.13).

b) <u>Variations of the sliding contact resistance</u>; RFI generally decreases with contact resistance and for a given type of brush composition the contact resistance generally decreases with the specific resistance of the material. Significantly lower brush resistance result in a corresponding reduction in brush temperature, which in turn decreases the level of RFI by retarding the rate of oxidation at the contact surface.

High brush current densities tend to hasten the formation of the oxide film on the sliding metal surface and coupled with the current switching was shows to increase RFI as shown. Random variations in contact resistance due to irregularities in the oxide film were found to give rise to increased RFI.

c) <u>Brush stability</u>; too low brush pressure results in high RFI from brush variation and chatter disturbing the electrical contact and is able to cause severe arcing. Too high pressures increase RFI levels because of rapid and non-uniform brush wear. Fig. 4.14, shown RFI measurements on slip ring contacts with varying brush pressure. Reference 95, reports similar findings on a.c. commutation and states that an optimum brush pressure can be selected form minimum radio interference. Nelson and Diehl stated that contact resistance variation resulting from brush bounce and chatter far over-shadow, the normal variations due to commutation surface film. Brush stability can also be increased with good brush holder design and they observed that in many cases the workmanship on brush holders is not nearly as good as that applied to other parts of the equipment.

d) <u>Rotational speed</u>; Noise levels increase as speed of rotation increases especially in commutator motors. This is thought to be due to increased current switching repetition rate. Hall and Quelch, [10] however, produced data (Fig.4.15) showing that RFI levels tend to level off beyond approximately 15,000 r/min, but the reason for this is not explained.

Schobert [40] reported work by Coquillette and others showing a series of tests on brush materials, ring materials and machines for which the conducted RFI spectra had been recorded, the main theme showing higher RFI at the cathode brush. Fig. 4.16 shows RFI levels on the 'Negative and Positive' conductor of universal motor on a.c. supply - but no explanation for the difference in RFI levels between the two is given.

Some additional sources of interference considered to be present in the brush - commutator circuit are listed below;

a) Interference from thermoelectric voltage generation increases with increased current density in the contact areas. As the current density is increased, more heat is generated in the contact resistance and the temperature of the brush surface and the commutator surface increases. This heat is generated in the small actual conducting surfaces which carry the current from the brush to the commutator, The magnitude of this interference is increased as the current density increases.

b) Thermal agitation is provided by current flow through a brush material and varies with brush temperature. Usually this effect is so small it is considered negligible.

c) Material transfer takes place when the arc, carrying current between the brush and the commutator, developes a temperature sufficient to melt microscopic metallic areas of the commutator. The metallic material may or may not be deposited on the brush face. The presence of this material, either on the face of the brush or in the space between the brush and the commutator, causes still greater irregularities in the contact areas and is conducive to an increase in interference. Loosened bits of brush material can also cause irregular contact areas.

In the early 1970's, ERA [96] attempted to correlate the r.f. voltages generated by a.c. commutator motors with their physical and dynamic properties. Information was collected on a number of motors, but results proved unsatisfactory for any relationships to be established. A steady reduction in r.f. voltage was however noticed during the continuous running of a motor, [97] but no correlation of RFI and motor parameters during continuous running emerged. It became evident that statistical investigations on RFI would not yield significant results.

A further study [98] into the properties of commutator motors was undertaken, the waveforms of interference voltage at the supply terminals were interpreted as consisting of three components:-

a) The voltage at the motor terminals due to the commutating current.

b) Emf's due to fluctuation in magnetic flux, caused by rotor slots passing the pole faces.

c) The voltage due to sparking at the brushes.

On testing motors generating excessive levels of RFI, examination of the machanical construction of the brush holders revealed that they were insecurely mounted in the main body of the motor, and the report concludes "All efforts to reduce sparking due to electrical effects would be wasted unless a stable mechanical design could be ensured".

Attempts were made to reduce RFI generated by fluctuations in magnetic flux caused by slotting of the armature by using "skewed" slots. [99] But comparisons made with normal slots showed no appreciable difference.

Comparison between 12 bar and 24 bar commutators [95] showed that the 24 bar produces a lower level of RFI see Fig. 4.17. This difference is attributed to the reduction of stored energy in the commutating coil that would occur for the higher number of commutator segments, where the inductance of the coil is thought to be less. No measurement of inductance was demonstrated, so this result is not considered to be conclusive. Significant increases in RFI levels were obtained with increase in motor loading and armature 'out of balance' tests as shown in Fig. 4.18. From these results it seems that an improvement in mechanical stability would reduce the inherent level of RFI.

Extensive studies have been taken by the ERA into the variation of RFI with different brush grades and brush lubrication. [100, 101, 102] Although improvements can be made with correct selection of brush grade and lubricant, the mechanical stability of the brush arrangement is still considered to be an over-riding factor.

Hall and Quelch [10] carried out a detailed study into the mechanisms affecting the generation of RFI in motors (listed in Section 1.3). They attempted to determine the importance of these mechanisms, in terms of the interference level which they generate and by isolating the individual RFI sources so far as is practicable, they established RFI levels by practical measurements. They concluded that the commutator brush contact variation and the commutation of the armature coils, are the main sources of RFI. Their work is discussed further in section 4.5.

4.2.2 Factors Affecting the Propogation of RFI

A commutator motor may be regarded as a radio frequency generator, which produces r.f. voltages between its terminals and also between each terminal and frame. The r.f.voltages between the terminals of the appliance is termed the symmetric mode of interference, the r.f. voltages between each terminal and frame are termed the asymmetric mode. These symmetrical and asymmetrical voltages produce r.f. currents in the supply wires. Most interference sources can be associated with both modes, and either mode may predominate in any particular frequency. This is in part, due to the nature of the generating voltages involved, but, chiefly as a result of inductance and stray capacitance present in the machine structure and supply wiring. These stray impedences have the effect of tuning the interference giving rise to resonant peaks and troughs of the interference spectrum.

Livshits, [14] formulated a high frequency equivalent circuit of a symmetrical series wound motor as shown in Fig.4.19. The commutating contacts between the brushes and commutator bars are considered as the interference generators. The circuit impedences are composed of:

a) the inductance (L_e) resistance (r_e) and self interturn capacitance (C_e) of the field windings.

b) The inductance (L_{ar}), resistance (r_{ar}) and self interturn capacitance (C_{ar}) of the armature.

c) the stray capacitance between the field winding and the motor frame C_e.

d) the stray capacitance between the armature winding and motor frame C_{ar}.

In Fig. 4.19(b), the field winding and armature winding impedences are combined into a common circuit with parameters L_i C_i and r_i. Livshits considered that the capacitance Ce may be neglected as it is fairly small. Thus the impedance between the external terminals of the motor A, B and the frame F is termed the asymmetrical internal impedance, Z_{ia} and that between terminal A and B is termed the symmetrical internal impedance, Z_{is}.

In order to assess the magnitude and nature of the internal impedences Livshits tested a number of domestic appliance motors. The measurements showed that the internal impedences of a commutator motor when it is on operation are very little different from their values in the absence of current, when not in operation. Fig. 4.20. shows the frequency dependence of Z_{ia} measured on two vacuum cleaner motors.

Conducted interference generated by an electrical device (i.e. in the low frequency range) is assessed by the interference voltage on the load (See section 4.4.1). Under practical conditions the high frequency load of the interference source is the supply circuit itself. The magnitude and nature of the high freuquency impedence of the supply circuit depends on factors such as the type of cable, the layout, its length, the number of branchings, the nature of the load and the presence of nearby conducting masses. It has been shown that over the frequency range, the supply circuit load can vary from a few ohms to the kilo-ohm ranges in a complex manner. References (92) and (103) show impedence measurements of field and armature windings for a number of appliances (Fig.4.21).

In 1972 a similar equivalent circuit was postulated by the ERA [92] as shown in Fig. 4.22(a). All the windings of the motor are shown to have interturn and interlayer capacitance and stray capacitance to the field laminations, which in turn has a stray capacitance to earth (or direct connection if the stack is earthed). It was concluded that the impedance measurements provide useful information on the r.f. performance of the motor and also provide an explanation for anomalous behaviour observed in the frequency spectrum.

Similar tests [104] were made on motors at frequencies above 10MHz. The symmetric impedences were found to consist of the self-capacitance and core loss of the armature and field windings, the asymmetric impedences consisted of the stray capacitance of field windings to earth.

A number of papers 105, 106, dealing with propogation from commutator motors were produced by the ERA in the mid 1970's. Investigations show that they stray capacitances present in small motors play a significant role in controlling the level of interference voltage measured at the mains terminals. The confining of interference currents to within the motor itself, is carried out to a certain extent already, and could possibly be improved much further by more thoughtful design. In general, stray capacitances in series with r.f. current paths should be minimized (thereby giving a high impedence to the r.f. current flow). Where the current can be diverted away from the mains terminal this capacitance should be maximized (thus giving a low impedence to the r.f. current flow). Extensive measurements of r.f. currents were made around the motor to find the flow paths. This resulted in a detailed equivalent circuit, showing actual stray capacitance values

(Fig. 4.22(b)).

Reference 107 proposes that suppresion measures are only effective if the filter components are installed to attenuate the dominant mode of r.f. current. Equally the impedance of the source is an important factor and can affect the performance of the suppressor. Measurement of the relative magnitudes of the two current modes provides valuable information and a comparison of both currents results in a more complete understanding of the overall situation.

Hall and Quelch [10] postulated an extremely detailed h.f. equivalent circuit of a commutator motor shown in Fig. 4.23. The circuit parameters are as follows;

a) Four components of the model that represent the metal parts (excluding windings), which with earth, are shown in heavy lines;

   (i) the rotor lamination stack

   (ii) the rotor shaft

   (iii) the gearbox

   (iv) the stator lamination stack

b) The fixed capacitances - with parallel resistors to allow for looseiness represent the capacitances of the insulation between the winding and metal parts, or between the metal parts themselves;

(v) Rotor winding to rotor lamination stack C_{rw-r} ;

(vi) Rotor winding to rotor shaft C_{rw-sp}

(viii) Stator winding to stator lamination stack, C_{sw-s} ;

(xi) Stator lamination stack to gearbox, C_{s-g}.

c) Other fixed capacitances, discrete components within the suppressor, or the mains isolating network and the artificial hand used for test purposes.

The variable capacitances are:

(x) Rotor lamination stack to stator with air dielectric, C_{s-r}, which varies periodically with rotation due to slotting;

(xi) Rotor shaft to gearbox with gearbox lubricant dielectric, C_{teeth}, which varies with rotor angle in a rather random way.

The randomly variable bearing resistance $R_{bearing}$ and brush contact resistances are shown.

d) Two stator windings are represented with transformer coupling to the rotor winding with further crossed-coil transformer coupling to allow for the rotationally induced e.m.f's. Each stator winding has an associated d.c. resistance R_{dc} and leakage inductance L_1 which are assumed constant. The magnetic properties of the iron path are accounted for by non-linear inductor L_1 in parallel with a non-linear resistor R_p. In parallel further is linear inductance L_a representing that due to the airgap. L_i and R_p vary throughout the operating cycle in a manner governed by the hysteresis loop.

e) The rotor winding of the test machine comprises 24 coils wound to form a closed loop, the rotor current flowing between the brushes in two parallel paths. Each brush shorts one or two rotor coils, depending on rotor angle. A pair of coils is shown 'shorted' by the contact resistance of each brush, each coil having an impedence Z_R. The remaining ten coils in each armature path have impedance 10 Z_R.

Measurements were made of the circuit parameters, but the complexity of the circuit made it difficult for any analytical assessment of the RFI mechanisms and accordingly they adopted an experimental approach to measure the relative importance of the interference sources and propogation modes.

4.2.3 Prediction of RFI

Motter [1] calculated the harmonic components of a rectangular wave using Fourier Analysis and compared them with those measured from RFI sources as shown in Fig. 4.24. He discussed that it is convenient to describe the nature of RFI in terms of this analogy and observed that increasing either the repetition rate or the voltage of the rectangular wave, increases the harmonic amplitude in direct proportion. This inferred that by knowing the amplitude and repetition rate of an interfering source, the RFI spectra of that source could be obtained by Fourier Analysis as in the case of the rectangular wave. It was recognised that in practical cases, the slower rise and fall time of the impulse noise would lead to lower harmonic amplitude than those predicted by this simple technique. Andone [108] presented a simple graphical technique to predict the levels of RFI for various pulse shapes. He utilized the properties of the Fourier transform to developed a piece-wise solution for the harmonic analysis of complex waveform shapes. Thus by solving the Fourier Integral for various frequency ranges is is possible to sketch its spectrum envelope across the frequency band, Fig. 4.25 shows a number of pulses and their associated RFI spectrum envelopes.

The use of this type of RFI prediction techniques is of limited use for predicting RFI from electric motors, even if the true pulse shapes could be estimated, the solutions obtained neglect the effects of the high frequency circuit parameters and their tuning effects across the frequency range. An attempt to allow for the attenuating effects of leads and source shielding was considered in a prediction technique proposed by Babcock and Sagasta. [109] They documented both conducted and radiated measured RFI levels for many voltage steps and pulses of varying rise times and different lead lengths. The final data presents a set of charts that can be used to calculate the level of RFI generated from a known pulse shape Fig. 4.26. Additional correction charts were included to allow for different configurations of lead wires.

Holownia [110] utilized state-space analysis techniques for the prediction of RFI from electrical networks. From the equivalent circuit of the noise source and with the generating sources represented by ideal electric switches the noise spectrum can be calculated. The network is characterised by the state of the switches at any instant. The state can be defined by means of a network state vector, considered in the n-dimentional space of network switches, where n is the number of switches in the network.

The full cycle of the switch operation is characterised by four states, (Fig. 4.27). The stationary states (where the switch is either open or closed) are denoted by C_s, such that:

$C_{S1} = C(x_1) = C(00)$, steady state switch open

$C_{S2} = C(x_3) = C(11)$, steady state switch closed

A change of switch state causes generation of transient pulses corresponding to a generation state C_g :

$C_{g1} = C(x_2) = C(01)$, switch closing

$C_{g2} = C(x_4) = C(10)$, switch opening.

In general, if the circuit contains n independent switches, then the total number of states of the network, C (x, y, z ...... n), to be taken into account in the analysis is:

$$C = 4^n \qquad (4.1)$$

with

$$C = C_s + C_g \qquad (4.2)$$

and

$$C_s = 2^n \qquad (4.3)$$

then $$C_g = 4^n - 2^n \tag{4.4}$$

with every different stationary state of the equivalent circuit there corresponds a different configuration of the network (i.e. different number of nodes and branches) and different values of node voltages and branch currents. Thus different generation states of the network are accompanied by the generation of different RFI spectra.

For the determination of the spectrum amplitude of impulses produced in the generation states, C_g, it is necessary firstly to carry out a 'steady-state' analysis. This is to determine the values of current flowing through closed switches and voltages across open switches for all stationary states C_s, of the circuit.

These values are easily calculated by application of normal circuit laws and circuit analysis techniques.

In the analysis of the generation of interference caused by a change in the networks stationary state C_{si} to the state C_{sk} as a result of the operation of the switches, all of the switches whose operation causes a change in network state are substituted by "spectral density sources" equivalent to the voltage or current step change invoked. Again by the application of normal circuit analysis techniques the resulting spectrum amplitude at any network node can be calculated.

Holownia showed that the spectrum amplitude obtained from the calculation could be converted to interference levels indicated by CISPR type Quasi-peak receivers. Ref. 111, ultilises the above method of analysis to predict the level of RFI produced from a greatly simplified equivalent circuit of an electric motor and its high frequency load (the supply circuit). It is stated that considerable progress in the solution of electromagnetic problems may be achieved by a more accurate identifiction of the equivalent circuit within the high frequency range. The calculated results obtained by applying the prediction technique, compared favourably with RFI levels obtained by measurement.

4.2.4 Suppression of RFI

The common RFI suppression components and suppression techniques have already been presented in section 2.4. In practice, suppression network synthesis utilises empirical and heuristic techniques to find the optimum circuit parameters. This section reviews some papers published on the subject of aiding the analysis and synthesis of suppression networks. Suppression networks are a form of low pass filters i.e. are able to pass the main supply current of 50 Hz but, impede the flow of RFI currents.

A number of text books consider practical filter network design methods. Reference (4, 112, 16) present RFI suppression circuit configurations for use on motors in various applications. Filter performance is assessed by the amount of RFI attenuation by the network. Attenuation, A, expressed in decibels (dB) is derived in the following manner;

$$A\ (\text{dB}) = 10 \log_{10} P_b/P_a \qquad (4.5)$$

Where P_b is the power delivered to the load before the insertion of the filter and, P_a the power delivered to the load after the insertion of the filter. Since the load impedence remains un-changed then;

$$A\ (dB) = 10 \log_{10} V_b/V_a \qquad (4.6)$$

V_b = voltage across the load before the insertion of the filter

and Va = voltage across the load after the insertion of the filter.

This is termed the 'insertion loss' of the filter. References 113, 114 examine a number of common suppression filter circuits to measure their insertion loss and thus the effectiveness of the suppression.

Ref. 115, summarised the information required for the optimisation of suppression components as follows;

a) Identification of the source; in a large system the specific source of noise may not be obvious and suppression at the source may be preferable to a filter at the mains input to the device.

b) Required attenuation: from a measurement of radio interference by the specified method the extent by which the interference exceeds the limit is determined and the required insertion loss, including factors allowing for production spreads, can be derived for all frequencies.

c) Mode of propogation: there are basically two modes of propogation, symmetric mode and asymmetric mode of which are of direct concern. Most interference sources can be attributed with both modes and either mode may predominate in particular frequency ranges. For many appliances, the symmetric mode tends to be dominant over the frequency range 150 kHz to 1 MHz. The importance of knowledge of the mode of propogation is that certain suppression components will only be effective for one mode and where limitations of suppression capacitance exist for example, more complex filters may be specified without the necessity for a prolonged series of tests.

d) Source impedance; A knowledge of source impedance is useful in that it allows calculations of insertion loss to be made, which provide prediction of the effectiveness of simple filters. It also determines the way in which complex LC filters should be installed and provides explanations for the interactions that sometimes occur between suppression components and the source usually due to series resonance.

Fig. 4.28, shows a simplified equivalent circuit of the motor and the mains supply. The motor is represented by e_1 and e_2 the interference voltage sources, Z'_1 and Z'_2 the symmetric impedance, Z_3 the assymmetric impedance. The mains circuit becomes the high frequency load of the RFI currents and is represented as a V-net-work of Z_n source impedance. From this simple diagram the symmetric (I_s) and asymmetric currents (I_a) can be estimated i.e.

$$I_s = \frac{e_1(1 + Z_2/2Z_3) + e_2(1 + Z_1/2Z_3)}{Z_1 Z_2/Z_3 + Z_1 + Z_2} \quad (4.7)$$

where $Z_1 = Z'_1 + Z_n$ and $Z_2 = Z'_2 + Z_n$

$$I_a = \frac{e_1 Z_1/Z_3 + e_2 Z_2/Z_3}{Z_1 Z_2/Z_3 + Z_1 + Z_2} \quad (4.8)$$

For high values of Z_3, the symmetric current reduces to $I_s = (e_1 + e_2)/(Z_1 + Z_2)$ which is the simple series current. The ratio of symmetric and asymmetric currents depends to a large extent on the ratio of impedence Z1/Z3 and Z2/Z3

Reference (115), uses this simple approach to calculate the response of different filter components for various combinations of interference source and impedences giving rise to the different modes of RFI current flow.

Shifman [33] presented a set of nomographs to obtain the insertion loss characteristics for any one, two or three element RFI filter configurations. He critisised the design equations for filters found in various textbooks since in practice the circuits synthesised from these equations rarely work satisfactorily. RFI filters are often subjected to current or voltage levels which make the element values determined by the handbook equations impractically large. For instance, the two element Butterworth filter with a cutoff frequency of 10 kHz calls for a capacitance of 0.45μF and an inductance of 1.13μH.

The design of such an inductor presents no problem if it is required to carry only 10 or 20 mA. However, if it must carry 20 amperes without saturating or overheating, it may become too bulky to be practical. It would be prefereable to use a different set of element values and still obtain the desired amount of insertion loss at frequencies above cutoff. Shifman states that this is possible; however, the equations which describe the insertion loss response of such modified or 'non-ideal' filters are not available in any readily usable form.

He developed a graphical method for the analysis and synthesis of RFI filters. By using standard charts and curves presented in the text the user is able to calculate suppression component values for a required degree of insertion loss. Cowdell [32] presented a graphical aid for the design of by-pass and feedthrough capacitor filters (the type commonly used on motors, see section 2.4). By studying the practical response of various designs of capacitors, he constructed a series of normalised performance charts and graphs. From the data the user is able to select the appropriate suppression capacitors.

4.3 RFI Detection Methods

The mechanism of RFI propogation is a complex mixture of conduction and radiation. In general, at the lower broadcast frequencies (i.e. 30 MHz) conduction is more important whereas at higher frequencies are conducted signals are substantially attenuated by supply wiring and radiation becomes more predominant. RFI measuring receivers have developed in a way bearing closely upon the method of propogation and the type of reception being protected, Fig. 4.29 shows the typical block diagram of a RFI measuring receiver. The broadband noise from commutator motors is a combination of impulse and random noise. [116] The approaches to measure broadband noise has led to the development of a number of different types of RFI receiver detector circuits i.e.

i) Quasi - Peak detection

ii) Peak detection

iii) R.M.S. detection

For the measurement of predominantly random noise sources, it has been necessary to develop statistical methods of evaluating the noise, i.e.

iv) Amplitude Probability Distribution (APD)

v) Noise Amplitude Distribution (NAD)

As mentioned earlier, most developed countries had a radio-telegraphy capability by the early 1930's, at this time it was only necessary to protect amplitude modulated sound broadcasting in the long and medium wavebands. The early interference measuring receivers used bandwidths of the order of 10 MHz, similar to the radio sets of the period. Subjective tests were made to determine the relation between the response of the measuring receivers and the 'annoyance' caused by different types of electrical interference. [117]

The Quasi-Peak receiver was found to give good agreement between measurement and subjective assessment of the effects of impulsive interference. Quasi-Peak pulse response is dependent on repetition frequency and the peak value of the input pulse. (See section 4.3.1).

RFI measuring equipment incorporating this type of detector are in use in most European countries, having been adopted by CISPR and British Standards Institution as the current measurement standard. Naturally, the RFI limits are specified, based in this type of measuring set. A number of papers 74, 118, 119, have been published correlating Quasi-Peak measurements with other types of detectors.

The peak detector (interference measuring equipment which responds only to the maximum amplitude of any complex waveform) is in use throughout the U.S.A. These receivers provide no additional information concerning the type of interference being measured and have not specified pulse response. Results of peak measurements are usually quoted in terms of unit bandwidth hence although it is not necessary to specify the bandwidth, the actual value must be known throughout the frequency range. Average detectors are often fitted to peak measuring sets as an addition facility to measure carrier wave or modulated signals.

In Sweden, the r.m.s. detector is perferred, this has a response proportional to the square root of the bandwidth and the square root of the pulse repetition frequency. It is considered to give a better correlation between subjective annoyance and response to interference from power lines and other interference of high pulse repetition frequency.

The statistical methods of noise evaluation (APD and NAD) have been used extensively in work on transmission lines [79] and ignition systems [83, 120], but as yet, these have not been applied to commutator motors.

4.3.1 Quasi-Peak Detection

The accepted definition of a Quasi-Peak measuring set, is one in which the detector indicates a fraction of the peak value and this fraction approaches unity as the pulse repetition frequency increases. [117] The response of any detection circuit is dependent on the receiver bandwidth and hence the bandwidth characteristics of the Quasi-Peak receiver are also specified. For measuring sets in the low frequency range from 0.15 - 30 MHz, the receiver bandwidth as specified by CISPR and BSI is 9 kHz and for the high frequency range from 30 - 1000 MHz the bandwidth used us 120 kHz.

Fig. 4.30, shows a simplified Quasi-Peak detector circuit. Rc is the circuit charging resistor giving a charging time constant Tc of $R_c C$ and R_D the capacitor discharge resistor giving a discharge time constant Td = $R_D C$. The choice of Tc and Td to give the best correlation between subjective annoyance and pulse response, has in the past, varied from country to country. The present EEC standards conform to values recommended by CISPR and BSI as follows;

a) In the frequency range 0.15 - 30 MHz

Tc = 1msec. Td = 160 msec.

b) In the frequency range 30 - 1000 MHz

Tc = 1 msec. Td = 550 msec

The response of the Quasi-Peak detector has been studied extensively both experimentally and theoretically 121, 122, 118. The general form of the pulse response curve is given in Fig. 4.31. Here the Quasi-Peak response Vqp is in terms of percentage of peak Vp i.e. P = 100 Vqp/Vp is plotted against factor α ,

where $$\alpha = \frac{\pi T_c B}{4 T_d N}$$

and N = pulse repetition frequency

B = receiver bandwidth

A theoretical derivation of this function is given by Haber. [118] Frick [123] calculated the response of a Quasi-Peak detector V_{qp}, to a train of rectangular pulses of amplitude A, duration d and period T where $d \ll T_c \ll T_d$ and $T \ll Td$ as;

$$V_{qp} = A/(1 + TR_c/dR_d) \qquad (4.9)$$

In this case, since the peak value $V_p = A$, therefore

$$P = 100. (1 + TR_c/dR_d) \qquad (4.10)$$

but this is only valid if a) the pulse repetition rate is constant and b) the pulse train is uniform in amplitude and waveform. Haber [118], considers the case for periodic pulses with random amplitudes for the case of broadband type noise.

Jackson [74] discussed that the response can be shown to be related to the subjective annoyance caused in sound and vision reception but may not be entirely adequate in relation to the error rate in digital transmission systems. Hsu [121] also critises the use of Quasi-Peak readings in relation to communication systems. As a summary, the output meter of a measuring set having a Quasi-Peak detector depends on;

a) the bandwidth of the receiver

b) the time constant of the detector

c) the repetition frequency of the pulses.

4.3.2 Peak Detection

Jackson [74] describes two forms of peak detection in common use;

a) the direct reading peak meter

b) the slide-back voltmeter

The direct reading peak meter is similar in design to the Quasi-Peak meter, except that the charge time constant is very much shorter typically Tc $\triangleq$ 10μsec., and the discharge time constant is much longer almost approaching 1 second. The pulse response may be evaluated by the same methods as the Quasi-Peak instrument and the values of time constant quoted yield a flat response over a wide range of pulse repetition frequencies.

The slide-back voltmeter functions by balancing the interference waveform against a known d.c. reference and is inherently capable of indicating the true peak of any waveform irrespective of pulse repetition frequency.

4.3.3 Statistical Methods of RFI Evaluation [81]

Random noise consists of frequency components which are random in amplitude and phase, the energy unlike broadband impulse noise, is not distributed in planes of spectral response, but, distributed randomly in the time and frequency spectrums. The nature of this type of noise has led to the development of statistical techniques in order to evaluate it.

The Amplitude Probability Distribution (APD) method, assumes that the radio noise signal X (t) observed at the output of a receiver-antenna circuit, tuned to a carrier frequency $\frac{\omega_0}{2\pi}$ has a temporal representation;

$$X(t) = V(t) \text{ Cos } (\omega_0 t + \emptyset(t)) \qquad (4.11)$$

Where both the voltage-envelope amplitude V(t) and the carrier phase, O(t) are time dependent variables. The cumulative probability that the instantaneous value of the envelope V(t) exceeds a specified value V during the measurement period T is designated the Amplitude Probability Distribution. The APD for the noise envelope voltage is written as an integral of the envelope density function, p(V);

$$\text{APD} = \int_{v(t)}^{\infty} p(V).dV \qquad (4.12)$$

Fig 4.32, shows the block diagram for an instrumentation system for obtaining pulse amplitude density data of ignition system noise. The measured noise is plotted in terms of the percentage measurements exceeding a specific noise level at preset frequency (see example Fig. 4.33) and this curve represents the APD of that noise source.

Hsu et al [120] compared ignition system APD with standard statistical distribution functions (i.e. log-normal distribution, Rayleigh distribution, Weibull distribution) to find which if any, represents the APD of the system tested, they concluded that the Weibull distribution provided the best fit.

Noise Amplitude Distribution (NAD) is an impulse counting technique and plots the measured interference at a preset frequency against the average number of noise pulses per second received. Fig. 4.34 shows an NAD counting arrangement presented by Oranc. [83] Fig.4.35 shows an example of measurements made using this technique of traffic noise.

4.4 RFI Measuring Techniques

RFI measuring techniques currently employed are as follows:

a) Measurement of conducted RFI in the low frequency range, 0.15 - 30 MHz

b) Measurement of radiated RFI in the high frequency range, 30 - 300 MHz

4.4.1 Measurement of Conducted RFI

In the frequency range 0.15 - 30 MHz radio frequency terminal voltage measurements are made across resistive impedences of 150 Ω connected in a V-network between live and earth and between neutral and earth. The technique is standard and is specified in B.S. 727 [18] and CISPR [124] documents.

The V-network is incorporated in an 'artificial mains network' (also called isolating unit, line impedence stabilising unit). The purpose of the artificial mains network is to enable r.f. voltage measurements to be made under controlled, repeatable conditions, providing sufficient isolation (from the mains) and to ensure that the impedence is unaffected by variations in mains impedence. Isolation is important to ensure that extraneous interference already present on the mains is adequately reduced in the measuring circuit to make errors negligible. [125]

The value of 150 ohms was selected as the mean value of a large number of measurements of impedences of domestic appliances. However recently is has been observed that the average mains impedance in the U.K. is better represented by a 25 μH inductance in parallel with a 50Ω resistance. Other countries show higher values, and as such a compromise of 50 μH in parallel with 50Ω has been accepted as an alternative artificial mains network based on world-wide measurements of mains impedence. [126] At present, the EEC and BSI allow the use of both this new artificial mains network and the standard 150Ω artificial mains network.

4.4.2 Measurement of Radiated RFI

In the frequency range above 30 MHz propogation of interference is a complex combination of conduction and radiation. For many years r.f. terminal voltage measurements were made in this range using a modified artificial mains network and supplemented where necessary by radiated field measurements. Terminal voltage measurements, however, did not give good correlation with the disturbances produced by an appliance under practical conditions, whereas measurements of radiated field strength do provide a good correlation but, require considerable laboratory space free from reflecting objects and free from extraneous interference. [127]

In the mid 1960's comparisons were made between various detection methods of measuring RFI in the VHF range, [128] the methods were;

a) Field strength measurements.

b) Field strength measurements by means of substitution.

c) Earth-current measurements by means of substitution.

d) Terminal voltage measurements.

An important step was taken when it was observed that the majority of interference produced by an appliance is radiated from the first few meters of the mains cable. [129] From this, Larrson of the Swedish Telecommunication Administration Laboratory, developed a method that could be used in an average sized laboratory subsequently called the 'Swedish Method' of measuring field strength. Coaxial Filters were slid over the mains cable to a position where a receiving dipole (placed several meters away from the source) detected a maximum field strength (Fig. 4.36). The interference capability of the source is defined in terms of the equivalent power which would have to be fed into a half wave dipole located in the same place in order to obtain the same reading.

Meyer 130, 131, replaced the co-axial filters with a ferrite tube, the major portion of the radiated interference is obsorbed by the ferrite material. Under these conditions, the input interference current is in direct proportion to the power obsorbed. This was developed by the Swiss Post Office and became known as the 'absorbing clamp' method. In 1967, CISPR adopted this method as a standard for VHF interference measurements.

With the 'absorbing clamp' method, the mains supply lead to an appliance , is loaded by a substantial amount of ferrite material, sufficient to provide a resistive termination to the interference in the frequency range. The interference is measured by a ferrite cored current transformer installed between the appliance and the load. The current transformer and ferrite load are constructed together in the form of a clamp or tube and the position on the mains lead is adjusted for maximum interference (generally obtained at or near quarter wave-length separation between clamp and appliance). (Fig. 4.37).

Fromy [132] proved mathematically that the maximum power that a given source can feed to a wire-type aerial can be expressed, as a first approximation by the same form equation as that giving the maximum power absorbed by the clamp.

Numerous comparative tests for the measurement of interference capability carried out in Switzerland, Sweden, U.K. and the Netherlands have shown good correlation between the results obtained with this method and field strength measurements. [133, 134,135, 136]

4.5 Discussion

Information on the subject of RFI from motors gathered in the Engineering Department at Hoover in the past had been of only limited practical use; infact, very little of it dealt with the kind of problems encountered by them in design and manufacture. Thus the first action taken on the project was to carry out a comprehesive literature review as presented in the earlier chapters and in particular section 4.2. This work provided a good background into the subject of RFI and and the present 'state of the art' as regards interference from small electric motors. From this study, possible avenues for research into the problems outlined by Hoover steadily emerged.

Broadly speaking the research for this project followed three distinct paths as the final project proposals described in section 2.6 i.e.

a) To study the factors affecting the generation and propogation of RFI in the motor design parameters

b) To study the influence on RFI levels due mechanical variations arising from the manufacturing processes.

c) A case-study to determine the sources of RFI variability from mass produced motors.

(The scope of the case-study (c) and the research methods adopted are detailed in Chapter 7).

In approaching the work for (a) it was initially thought that an analytical technique to predict the level of RFI from motors might be developed in order to calculate the interference due to different motor design parameters. Holownia [111] showed that his RFI prediction method from high frequency equivalant circuits could be applied to small motors and he presented results obtained from calculations which compared favourably with those measured in practice. He added, that better the conformity of the results could be obtained if a more representative equivalent circuit could be defined.

Hall and Quelch [10] postulated an equivalent circuit for a series motor incorporating the interference generating mechanism within the system. This they felt would only be representative up to a frequency of 1 MH_z; above this frequency the equivalent circuit would be greatly complicated by the fact that each parameter is "frequency dependent".

To apply Holownia's technique to this circuit, although not impossible, is extremely difficult and it was felt that the equivalent circuit would not reflect the subtle design changes and variations that required investigation. A further concern was that Holownia had used as his 'source' of interference, a simple on/off switch - this is too great a simplification of the commutation process which involves a complete reversal of current and is very difficult to model. As a result it was decided that although an analytical techniques had originally seemed possible, more detailed investigation showed that this was impractical. Accordingly, an experimental approach was decided on.

Hall and Quelch had presented a systematic test procedure for determining the different interference sources. The technique was to isolate the sources as far as possible and to measure the levels of RFI produced. To facilitate this, their test machine was specially mounted to give ready access for changing internal components. It was driven separately through a resilient rubber coupling by a similar drill motor. The physical isolation of the interference sources being affected by building up the machine in stages as follows:

i) The commutator brushes were removed and the two stator coils connected in series, thus eliminating the RFI generated by the rotor winding and commutator. This left only the interference mechanism incorporating the variation of the parameters of the field system, the stator stack to rotor stack capacitance and the gearbox to rotor shaft capacitance, together with their associated interference current paths.

ii) The additional influence of the commutator and brush contact resistance was assessed by using an unwound armature with opposite commutator segments shorted to provide a current path between the brushes. The effects of the e.m.f. induced in the armature coils by transformer action with the field coils and of coil commutation were therefore absent:

iii) The armature winding was included, connected to the commutator in the usual way;

iv) Thyristor control was introduced.

By this method they were able to assess the relative importance of the interference mechanism for a particular design of drill motor. It seemed reasonable therefore, to adapt Hall and Quelch's method and extend it to analyse the effect on RFI of a number of different possible design configurations as required in (a). The major problem with the test procedure was reported to be the non-repeatability of some of the test results. This was due to the fact that when the machine was taken apart and re-assembled it proved difficult to re-establish the same test conditions.

Close examination of Hall and Quelch's test method both in the laboratory during appraisal tests and from subsequent discussions revealed a number of faults in their procedure. Firstly, the use of the drive drill motor coupled to the test machine. It was found that the drive motor is capable of corrupting RFI measurements from the test machine, more so with increase in drive speed. Even with the use of extra filters and shielding techniques, the close proximity of the drive and the test machine rendered all attempts to be futile. Thus a number of the results and conclusions arrived at by Hall and Quelch are in doubt, this is further discussed in Chapter 6.

The second area of criticism is in their tests to assess the influence of the commutator-brush contact resistance. Figure 4.38 shows the arrangement described, it can be seen that as the commutator revolves and the trailing edge of the brush leaves a segment, contact through the short circuited path is instantly broken - in practice this is found to be accompanied by an arc. Thus any RFI measurements of this arrangement to assess the influence of the commutator - brush contact are clouded by the RFI generated from the arcing. Additionally, the arrangement is not valid since commutation is defined as reversal of current between the two adjacent commutator segments, not as in this case where the current is switched between opposite segments. Therefore it was decided to construct a multi-purpose test rig for the experimental work which effectively overcame the problems and faults identified above. The criteria applied to the design was as follows;

i) Rigidity of the motor test rig.

ii) Easy interchangability of the components.

iii) Easy accessability of the components.

iv) Easy measurement of critical dimensions.

v) To allow the simulation of manufacturing variations.

Adequate rigidity of the motor test rig was essential and this was obtained by using a strong aluminium frame.

The design was such that components could be readily changed with a minimum of dismantling of the framework. Easy measurement of critical dimensions was essential so that each component would be placed in exactly the required position. This would ensure the repeatability of the results.

In addition it was planned to use this rig to simulate mechanical variations resulting from the manufacturing process, thus implementing the experimental work for (b). This was achieved by designing the rig to allow the relative movement of parts of the motor. To overcome the problem of corruption of RFI measurements, due to an external motor drive source as observed in Hall and Quelch's arrangement, it was planned to rotate the rotor shaft by directing compressed air onto a fan fitted on the end of the shaft. Results obtained with this arrangement proved successful both in noise free drive and good speed control. The final motor test rig construction details and the programme of experimental tests to cover the planned area of study are described in Chapter 5.

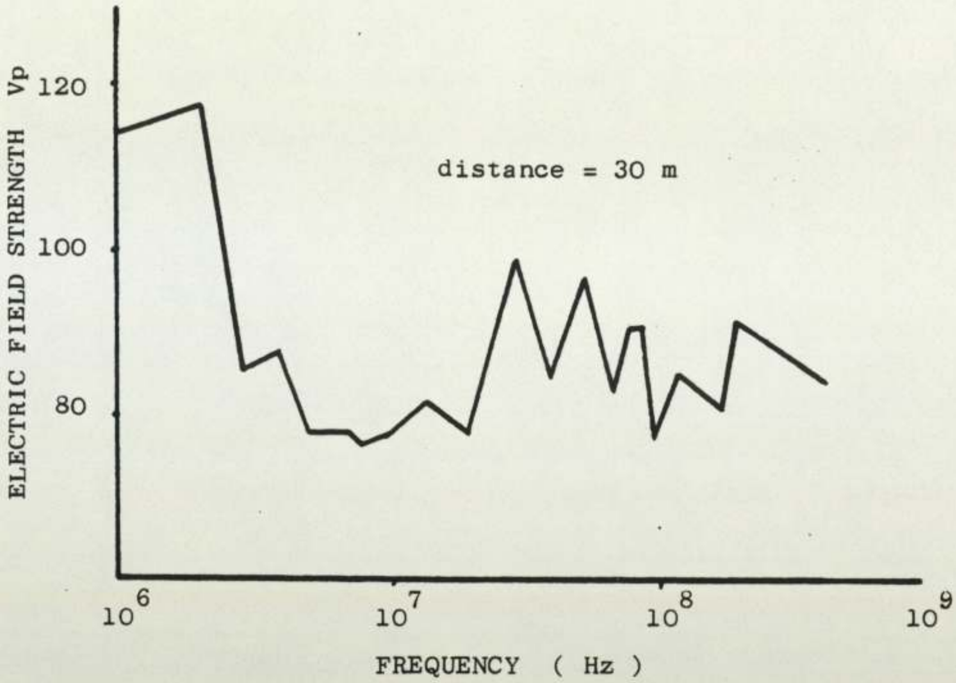

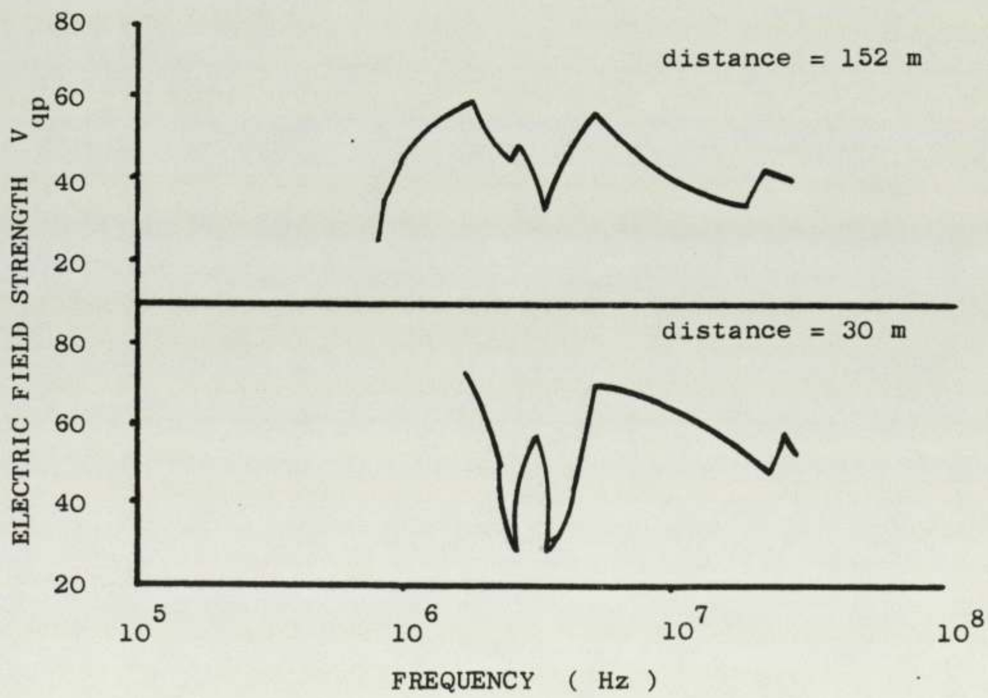

Typical radiated noise spectra for r.f. stabalised arc welders (from Skomal [78])

Fig. 4.1

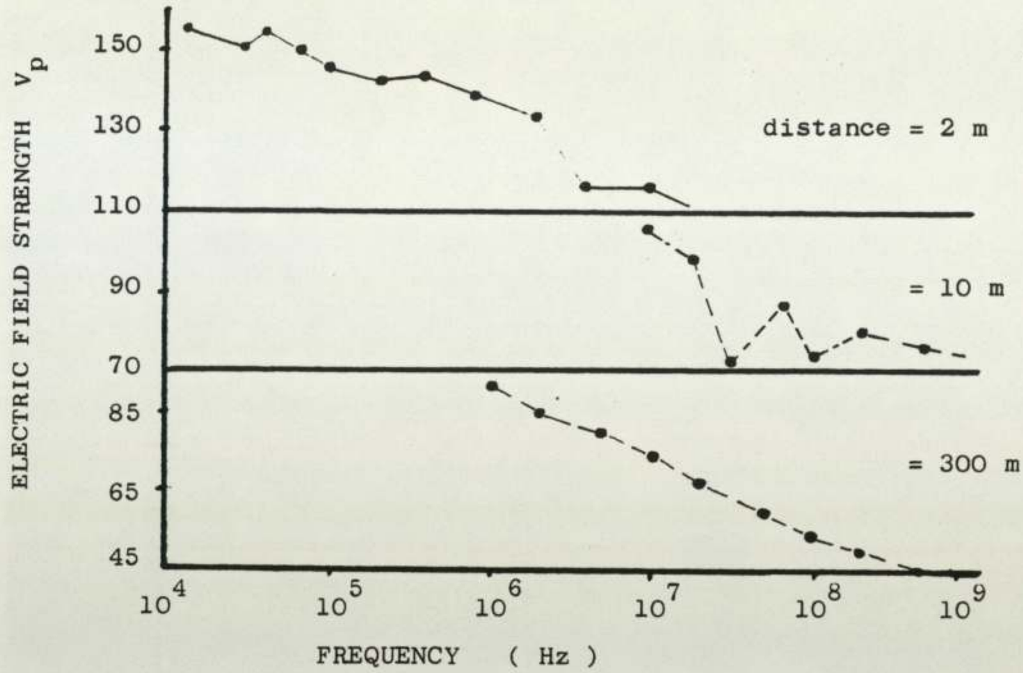

Radiated noise spectra for a resistance welder at various distances from the source (from Skomal [78])

Fig. 4.2

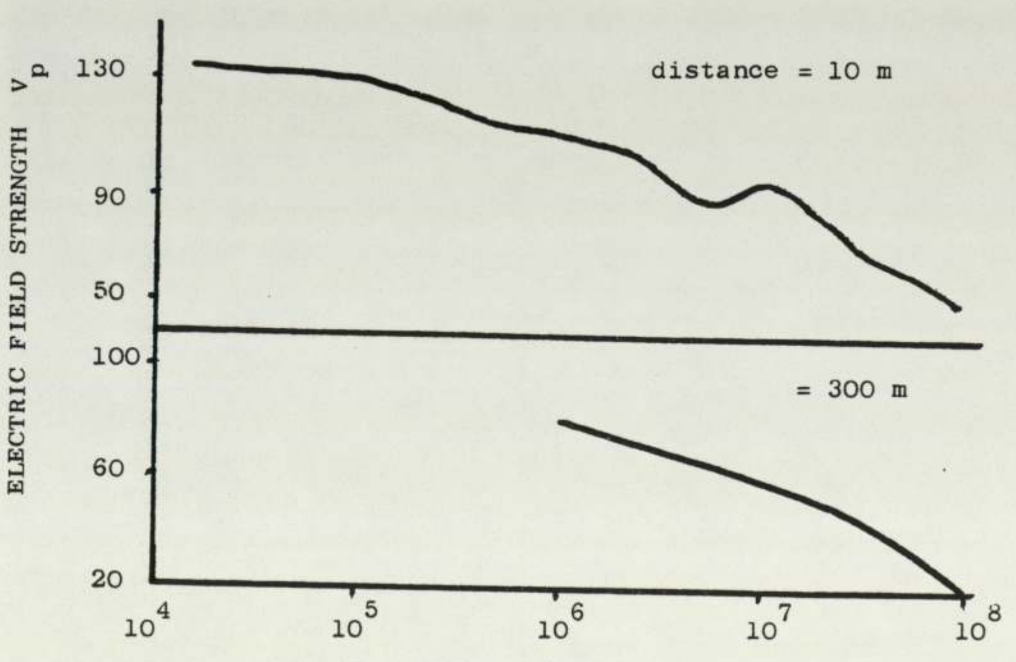

Radiated noise spectra of an electric discharge cutting machine (from Skomal [78])

Fig. 4.3

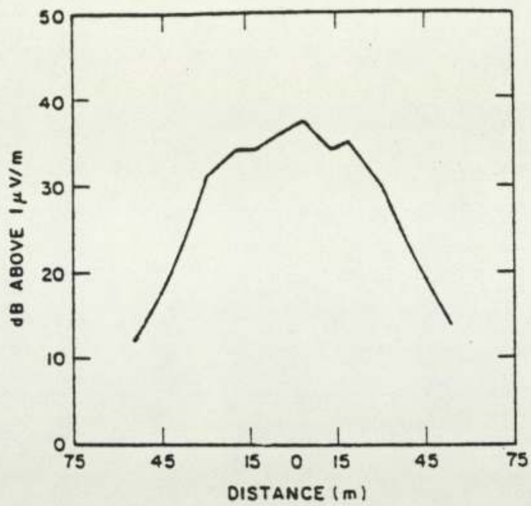

Typical line originated RFI (from Meyers[76])

Fig. 4.4

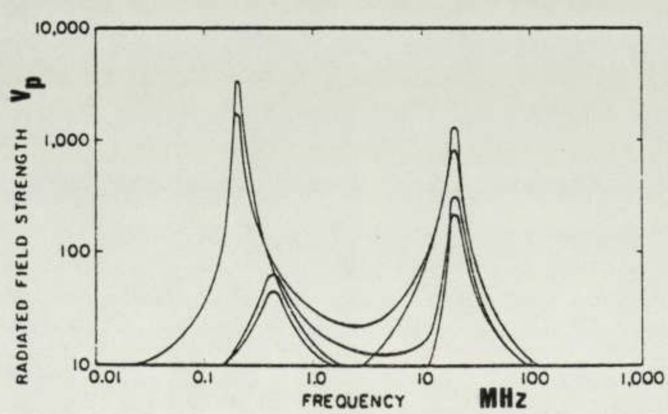

Typical radiated RFI from automobile ignition systems (from Meyers [76])

Fig. 4.5

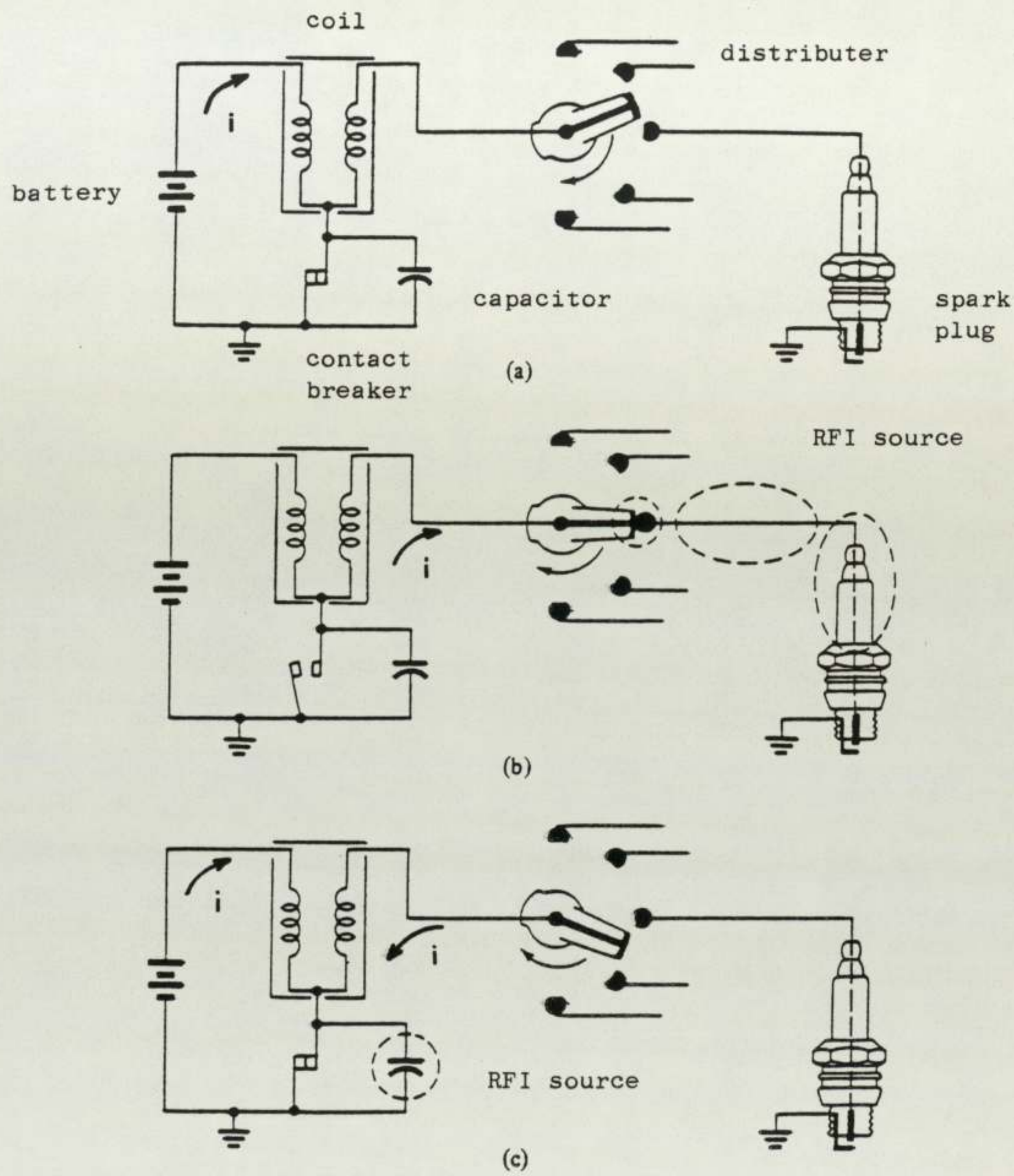

Event sequence of the ignition system

Fig. 4.6

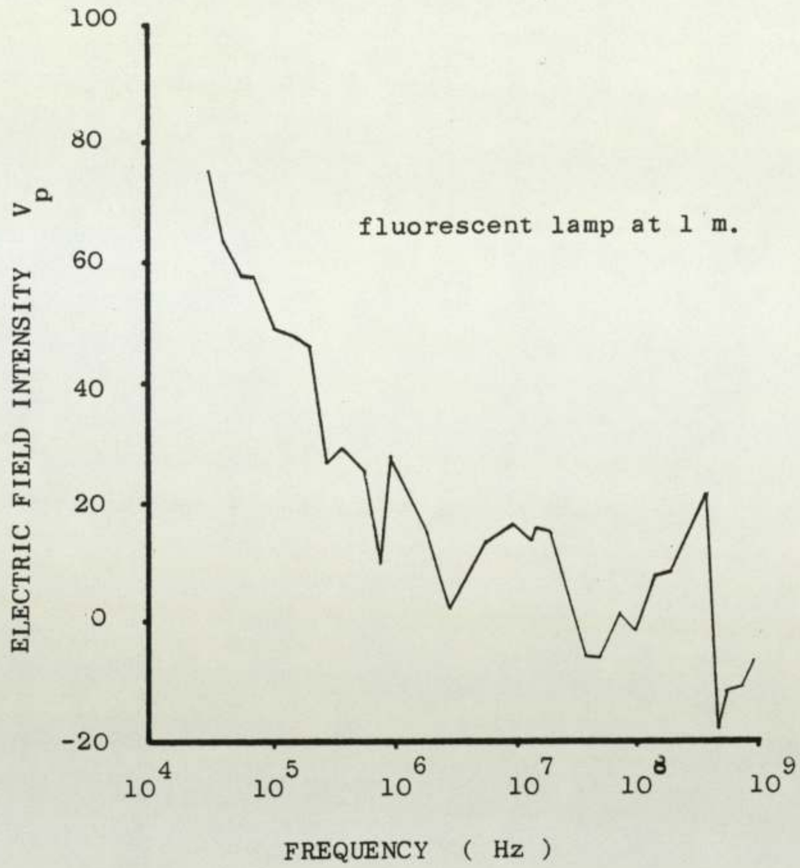

Typical RFI measured from flourescent tubes (from Skomal [77])

Fig. 4.7

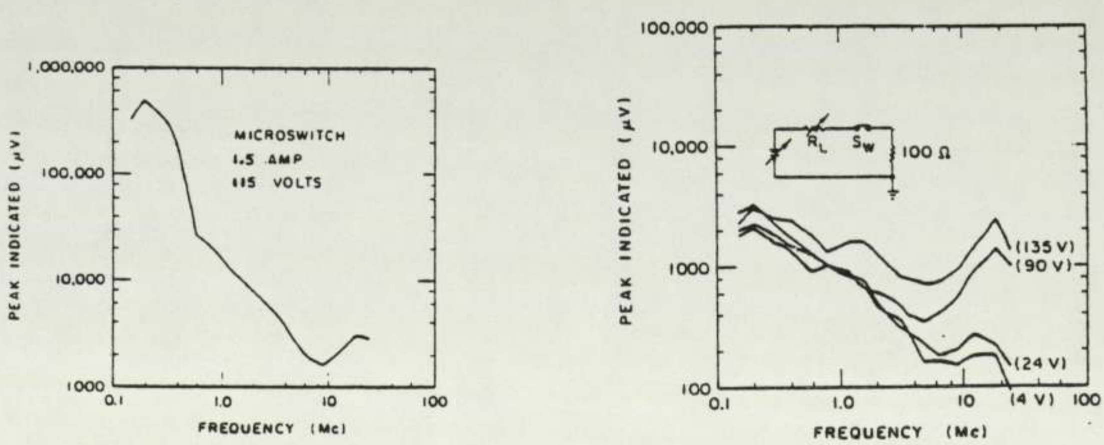

RFI generated from mechanical switches (from Meyers [76])

Fig. 4.8

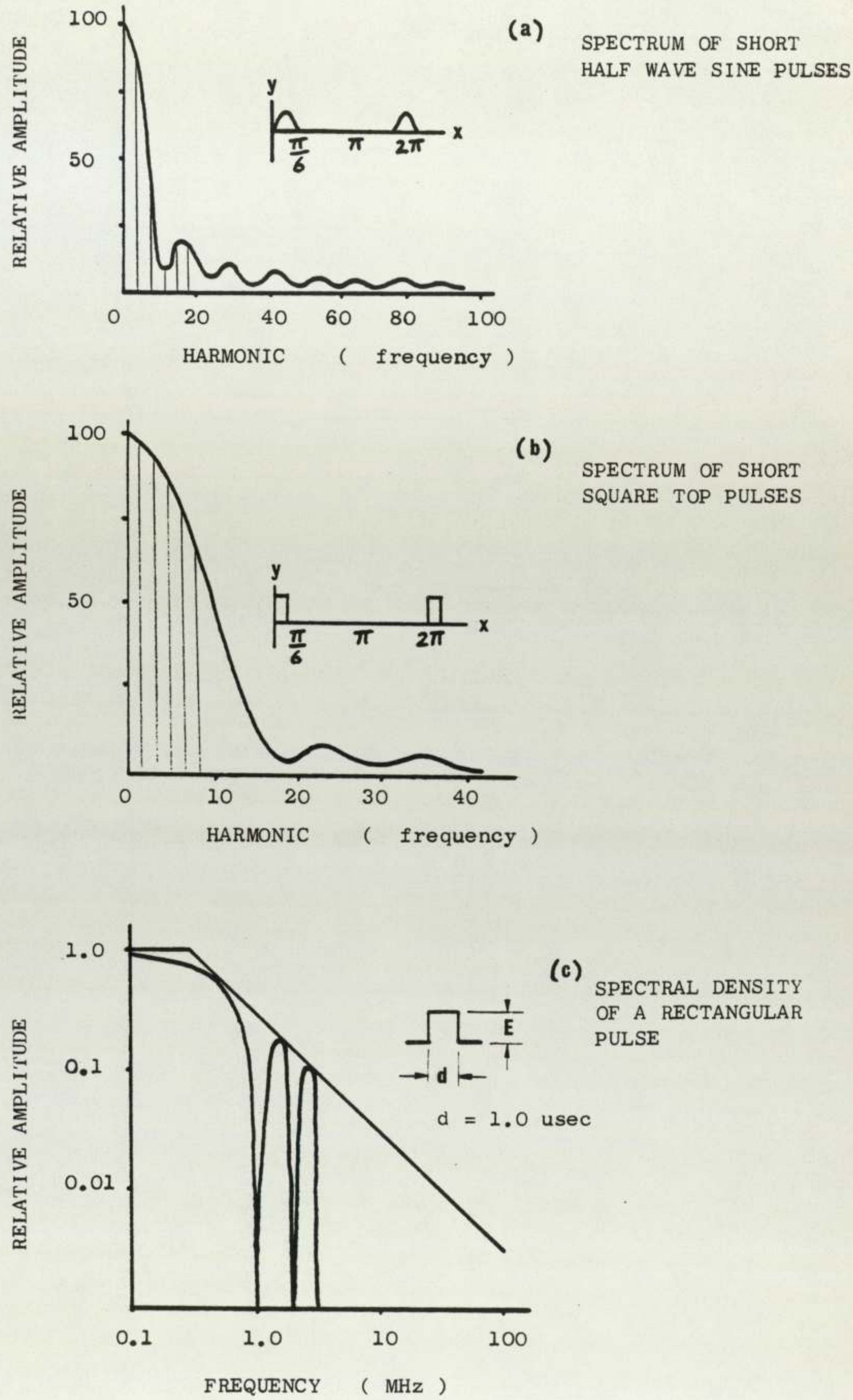

Theoretical spectrum evelopes

Fig. 4.9

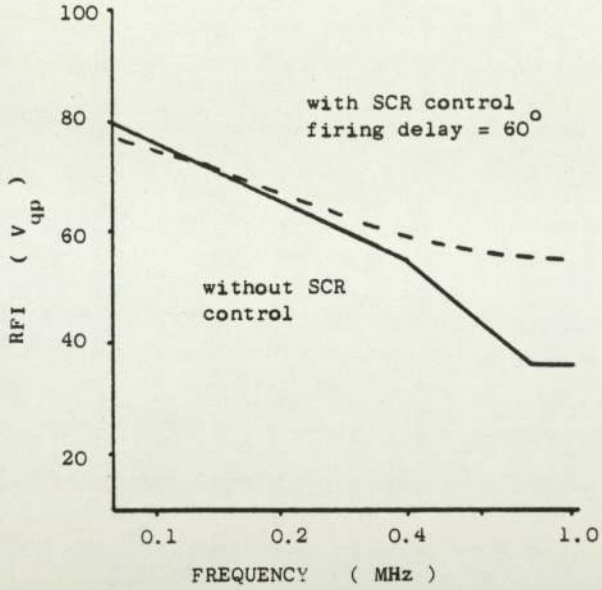

RFI from a commutator motor at 15000 r/min
(from Hall and Quelch [10])

Fig. 4.10

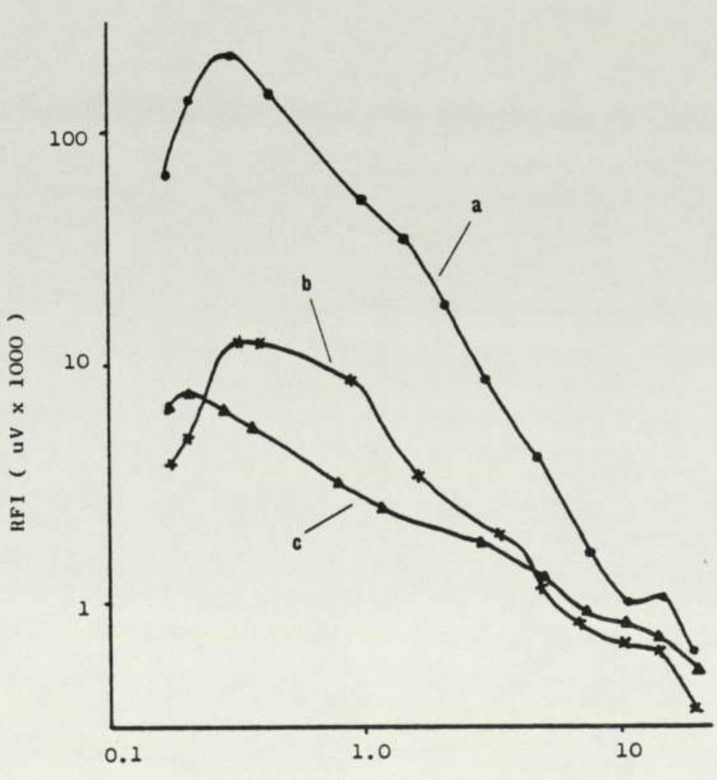

Comparison of RFI from (a) normal brush, (b) laminated brush on commutators (c) normal brush on slip ring (from Motter [1])

Fig. 4.11

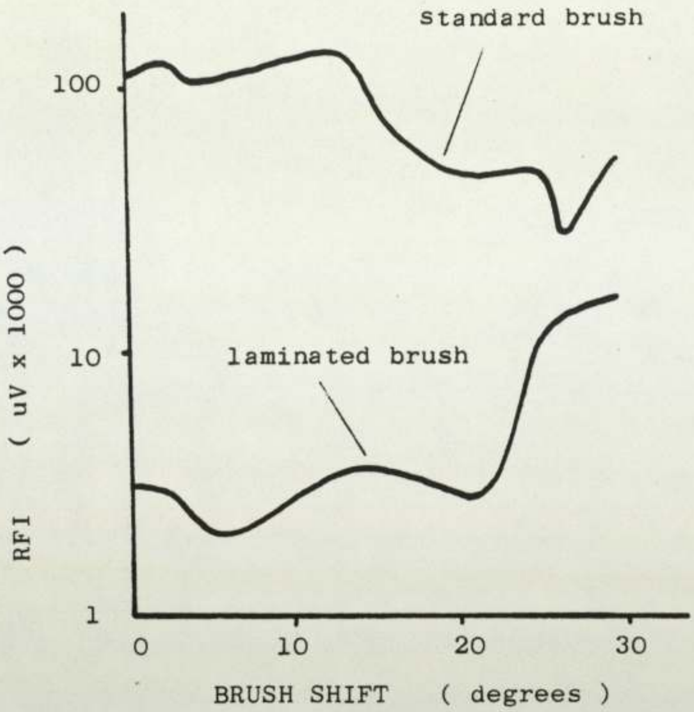

Comparison of standard and laminated brushes for various angles of brush shift (from Motter [93])

Fig. 4.12

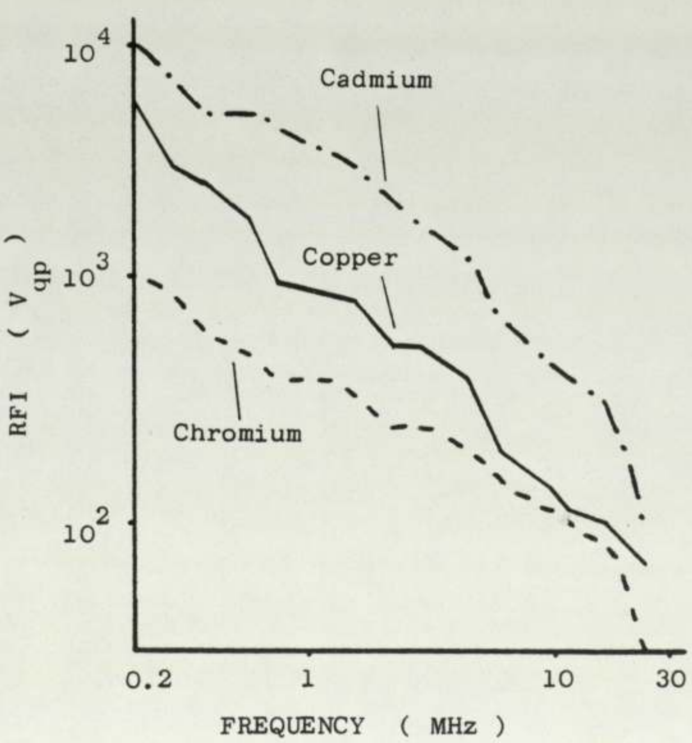

Effect of slip ring material on sliding contact interference (from Nelson and Diehl [94])

Fig. 4.13

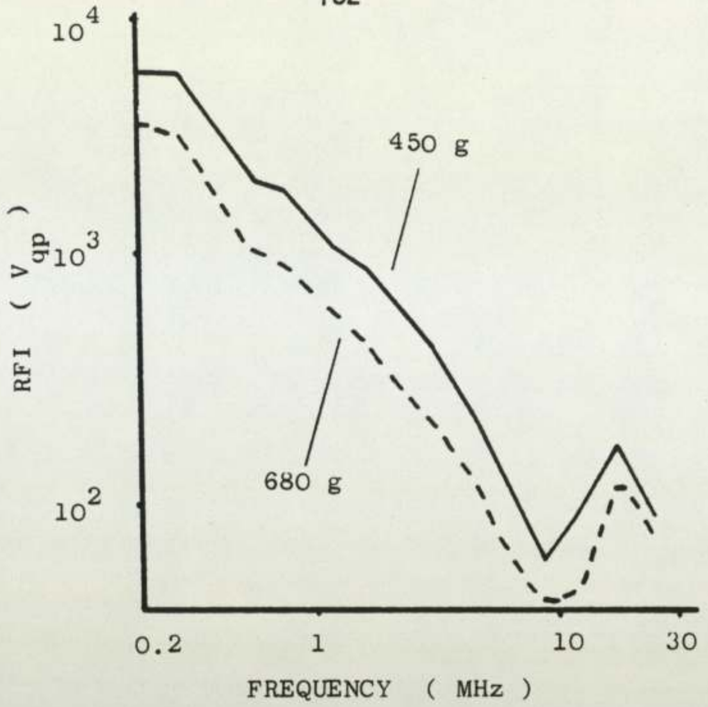

Effect of brush force on sliding contact interference (from Nelson and Diehl [94])

Fig. 4.14

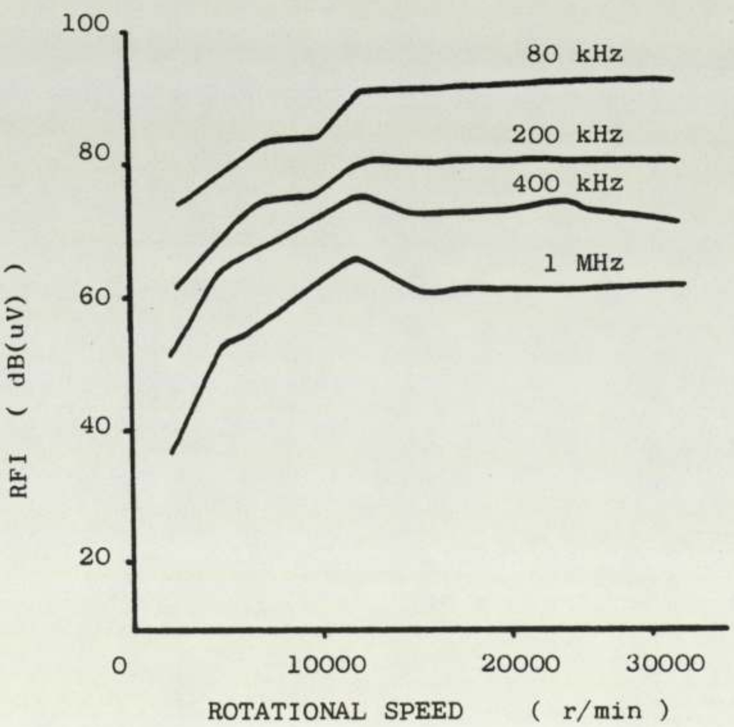

Effect of speed variation on RFI from a commutator motor (from Hall and Quelch [10])

Fig. 4.15

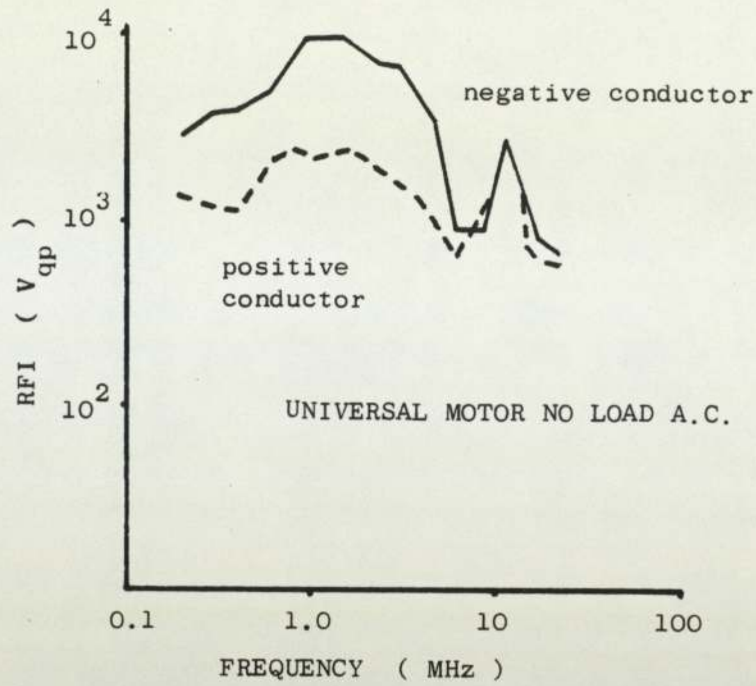

Comparison of RFI levels measured on the positive and negative conductors of a small motor on a.c. supply (from Schobert [40])

Fig. 4.16

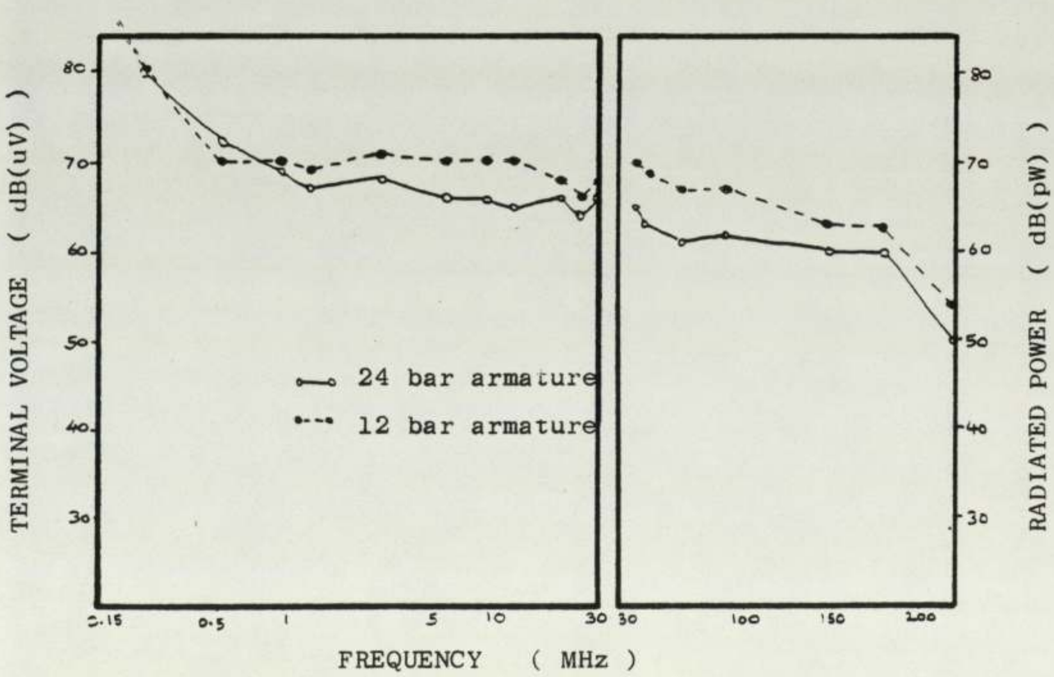

Comparison of RFI levels from a 24 and 12 bar commutators (from ERA [95])

Fig. 4.17

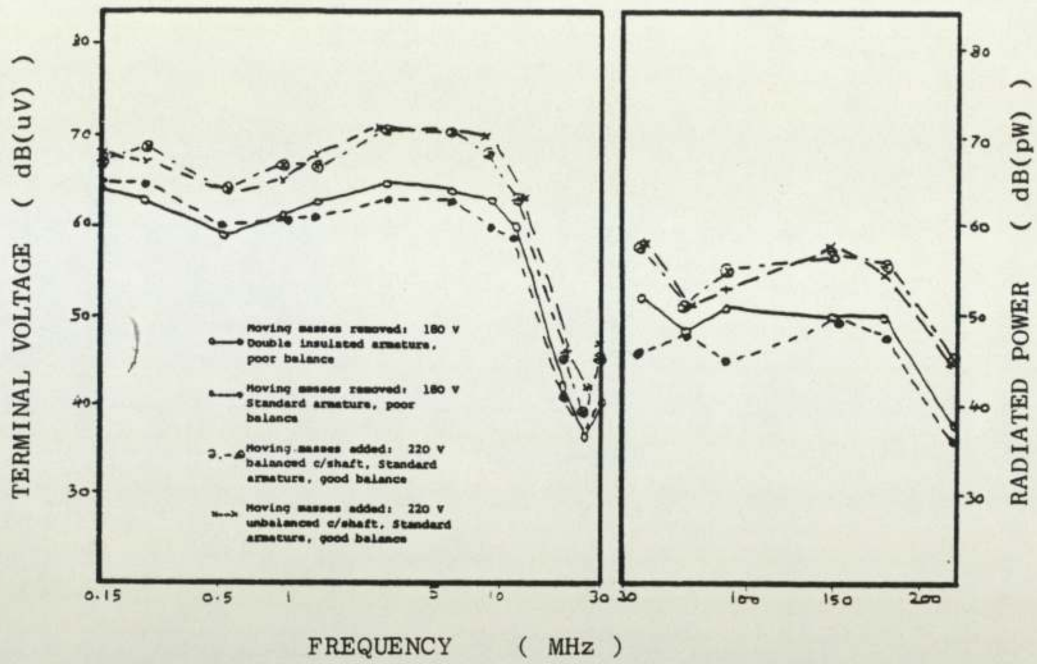

Comparison of RFI levels with increases in motor loading and armature unbalance (from ERA [95])

Fig 4.18

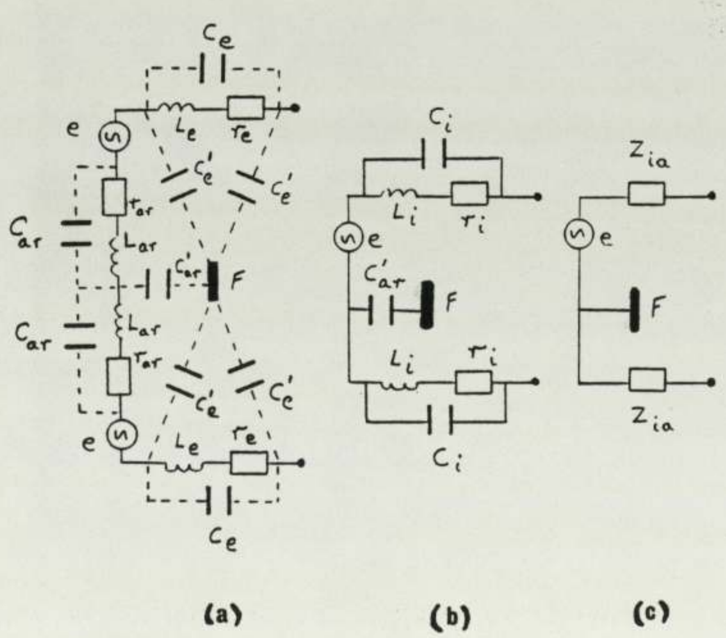

Equivalent high-frequency circuits of a symmetrical series motor as a source of radio interference.

(a) Complete.
(b) Converted.
(c) For radio frequency range.

High frequency equivalent circuit of a symmetrical series motor (from Livshits [14])

Fig. 4.19

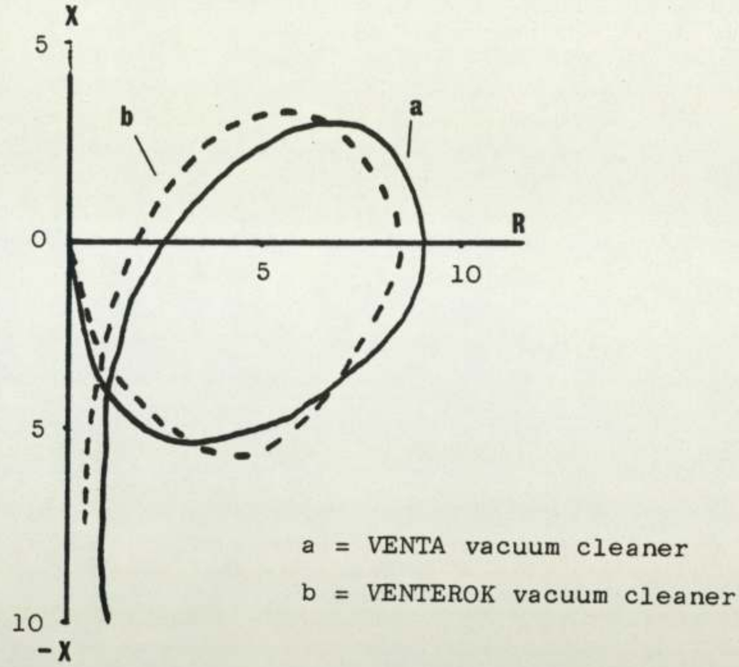

Measured variation of the asymmetrical internal impedance with frequency of two series motor appliances (from Livshits [14])

Fig. 4.20

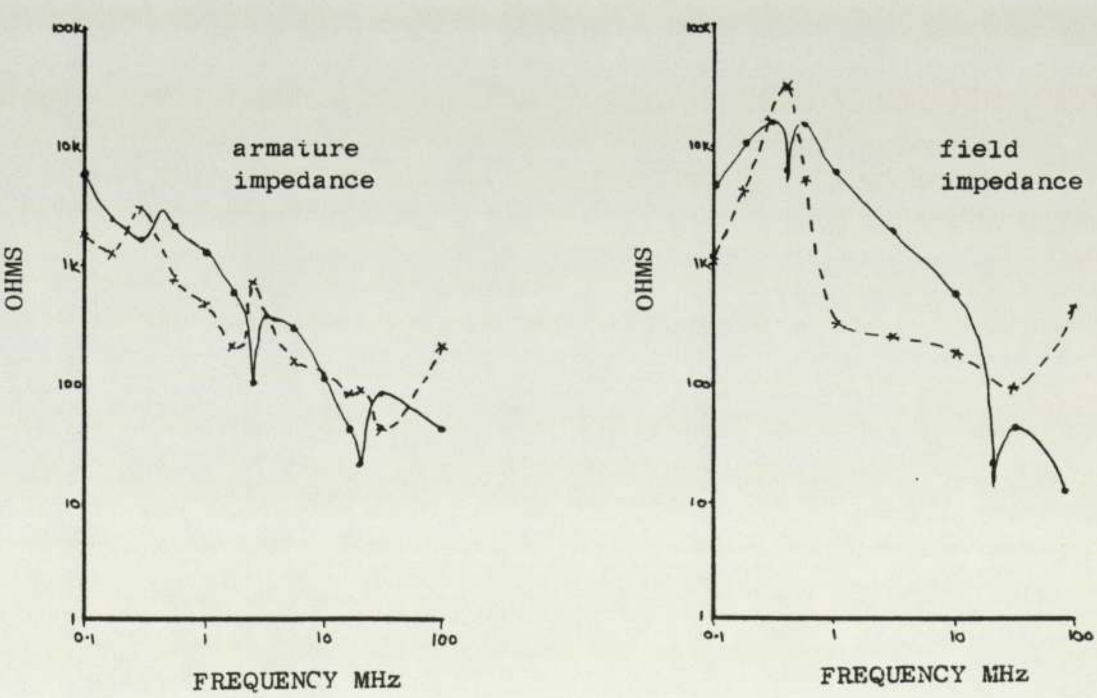

Examples of impedence measurements recorded from field and armature windings (from ERA [92])

Fig. 4.21

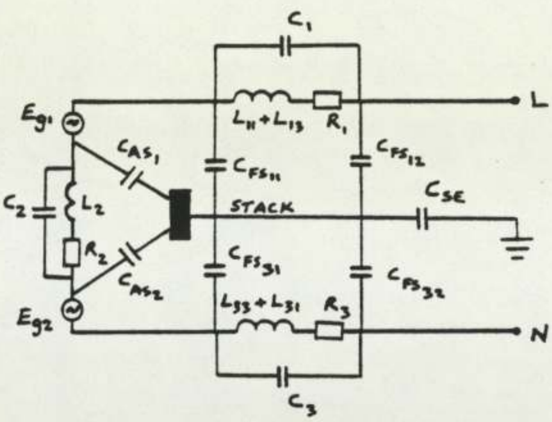

C_1, C_2, C_3 = self capacitance of windings
C_{AS} = self capacitance armature to stack
C_{FS} = self capacitance field winding to stack
C_{SE} = self capacitance stack to earth

Equivalent circuit of a symmetrical series motor (above), showing measured stray capacitances and interference currents (below) (from ERA [106])

Fig. 4.22

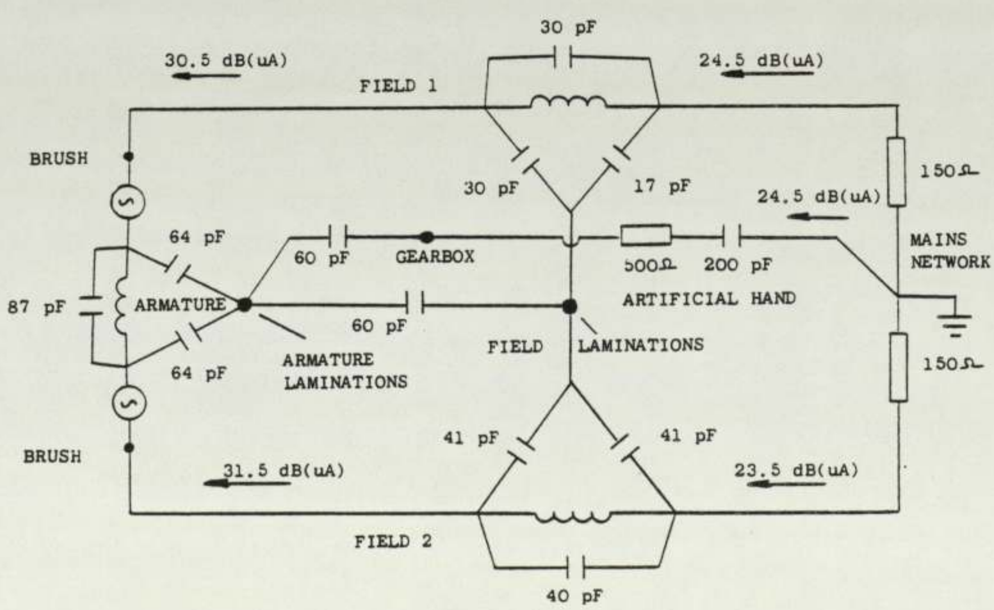

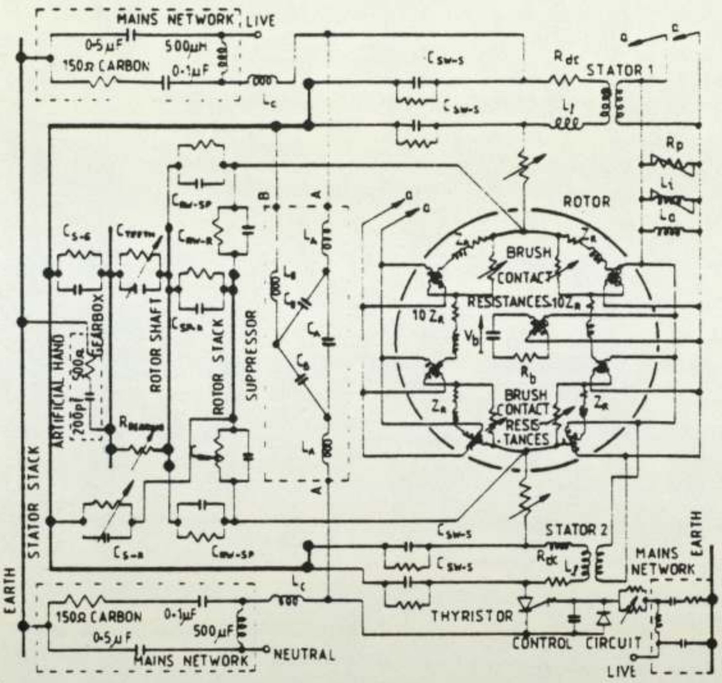

High frequency equivalent circuit of a series motor postulated by Hall and Quelch (from Hall and Quelch [10])

Fig. 4.23

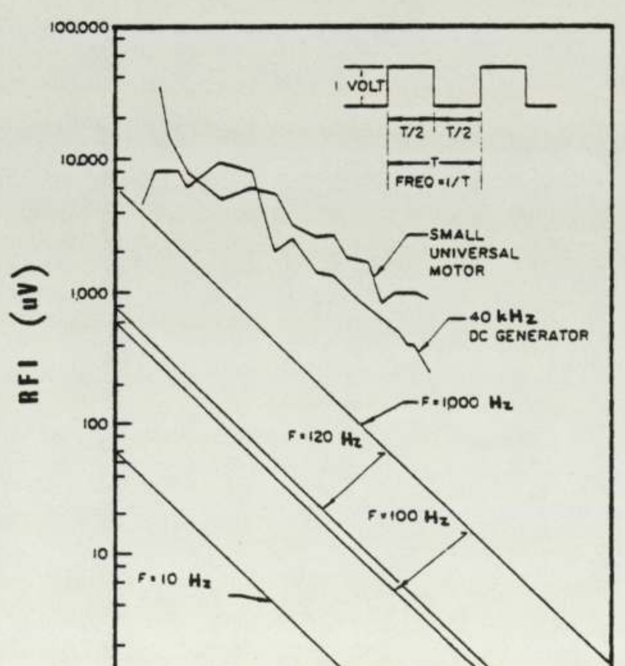

Comparison of RFI levels from rectangular waves at various frequencies with those obtained from electrical machines (from Motter [1])

Fig. 4.24

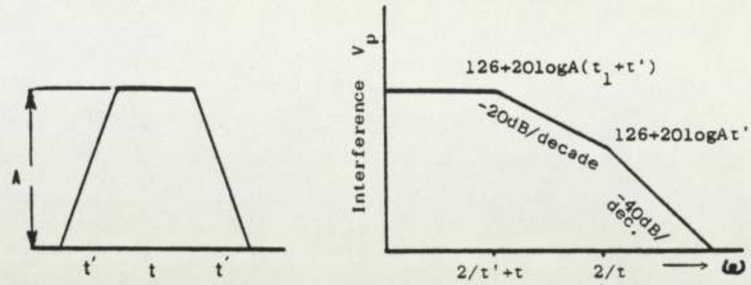

a) repetitive trapezoidal pulse with its interference spectrum envelope

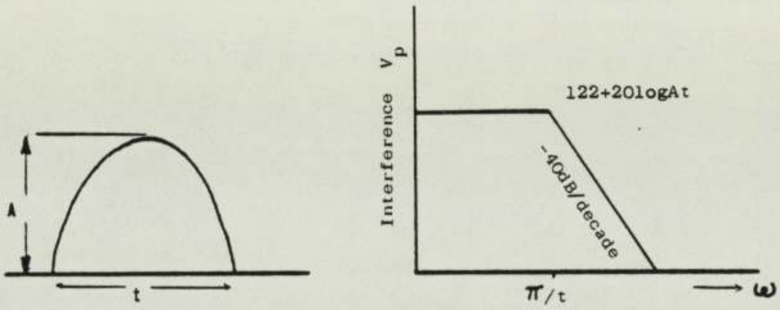

b) repetitive sinusoidal pulse with its interference spectrum envelope

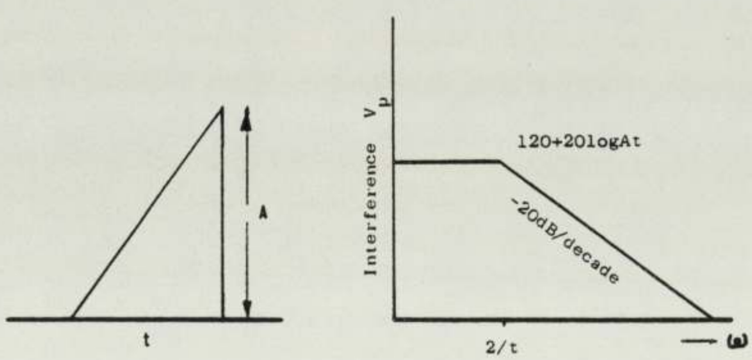

c) repetitive triangular pulse with its interference spectrum envelope

Predicted RFI levels from repetitive trapezoidal sinusoidal and triangular pulses (from Andone [108])

Fig. 4.25

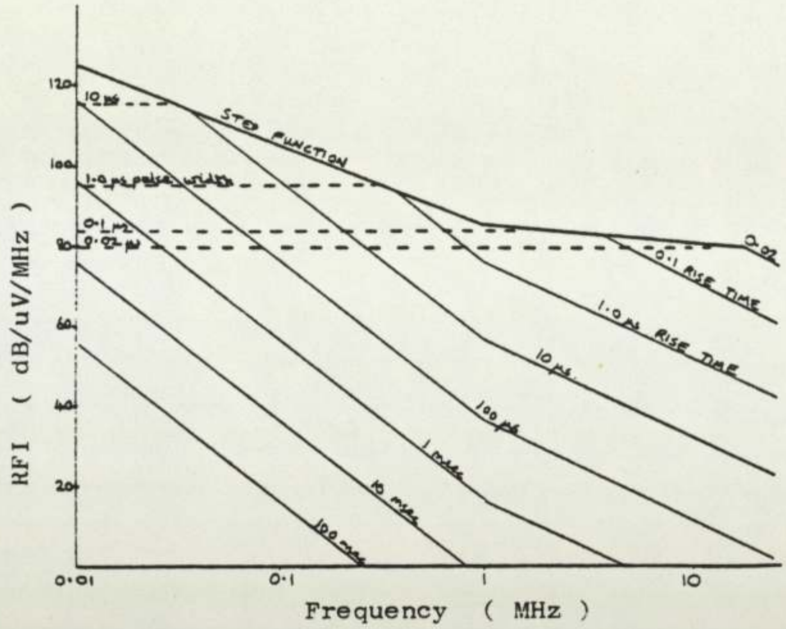

Predicted RFI levels for a 28v step or pulses of various width and rise times (from Babcock and Sagasta[109])

Fig. 4.26

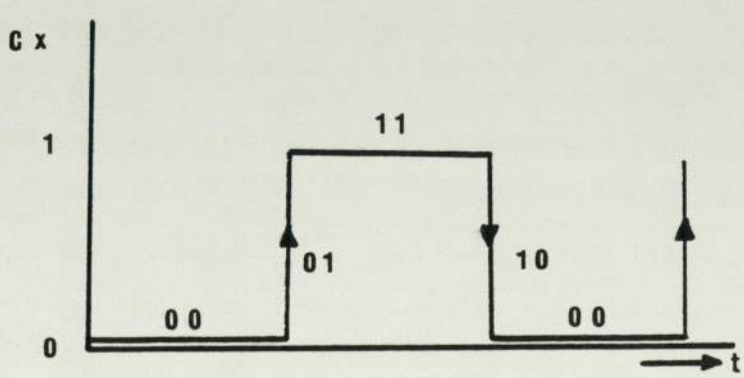

Operating cycle of a simple switch

Fig. 4.27

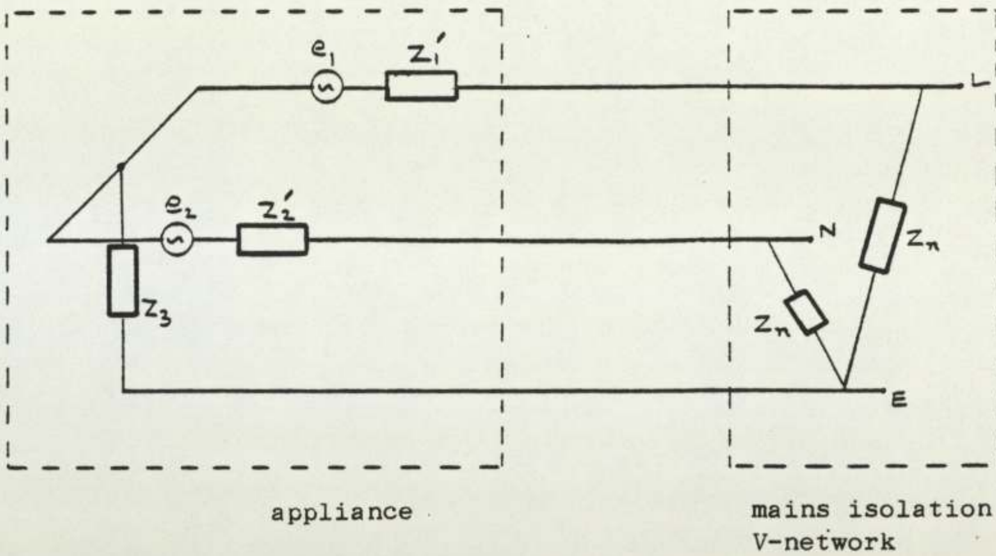

Simplified h.f. equivalent circuit of an appliance connected to the mains supply via a V-network mains terminating impedence

Fig. 4.28

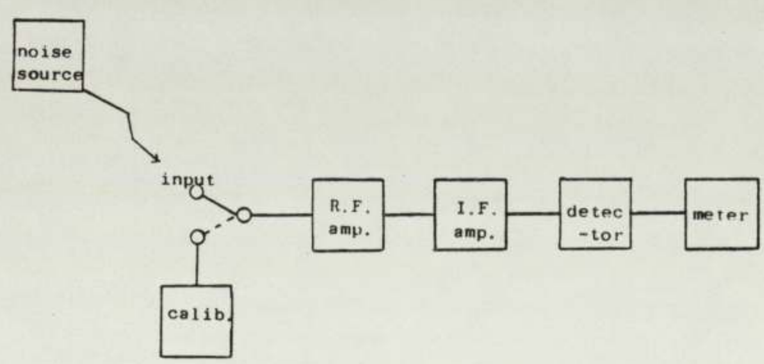

Block diagram of an RFI measuring receiver

Fig. 4.29

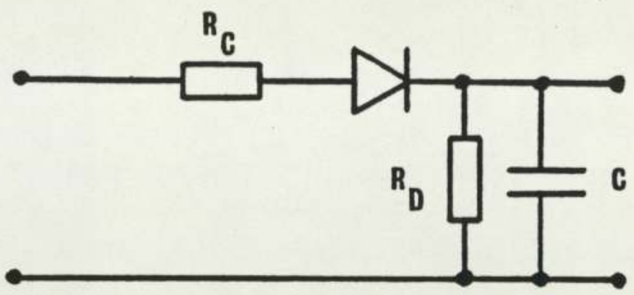

Quasi-Peak detector circuit

Fig. 4.30

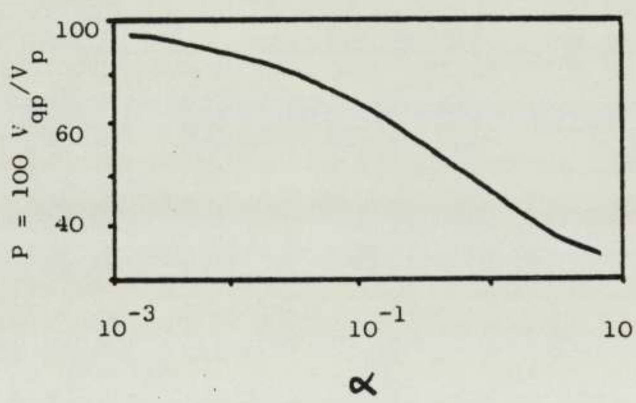

$\alpha = \pi T_C B_6 / 4 T_D N$

T_C , T_D = quasi-peak detector charge and discharge times respectively

B_6 = 6 dB bandwidth , N = pulse repitition frequency

Quasi-Peak pulse response curve

Fig. 4.31

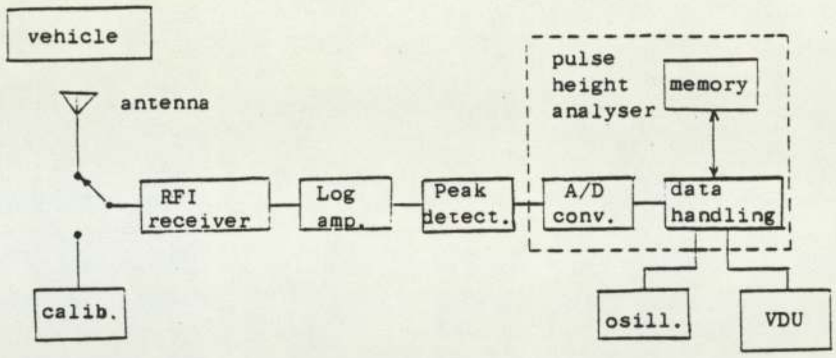

Block diagram of instrumentation system for obtaining APD data of ignition noise

Fig. 4.32

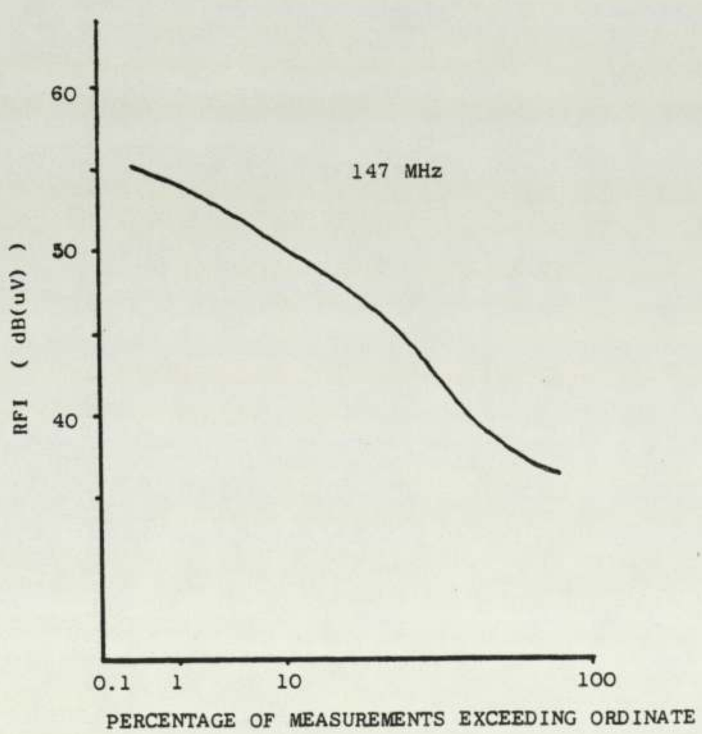

Measured APD of ignition noise
(from Skomal [81])

Fig. 4.33

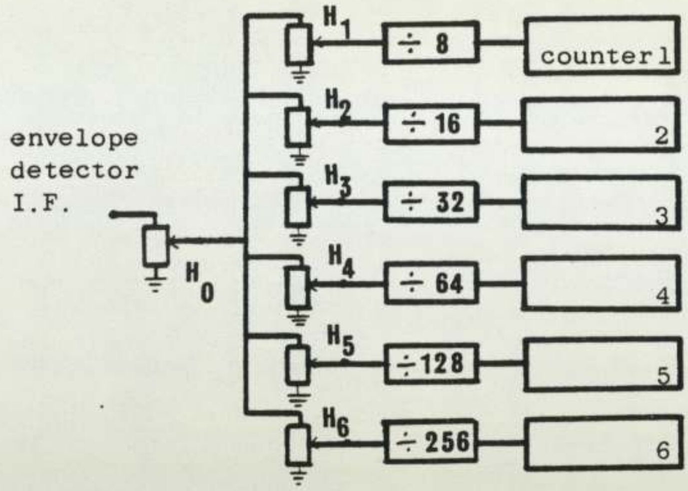

Block diagram of NAD counter

Fig. 4.34

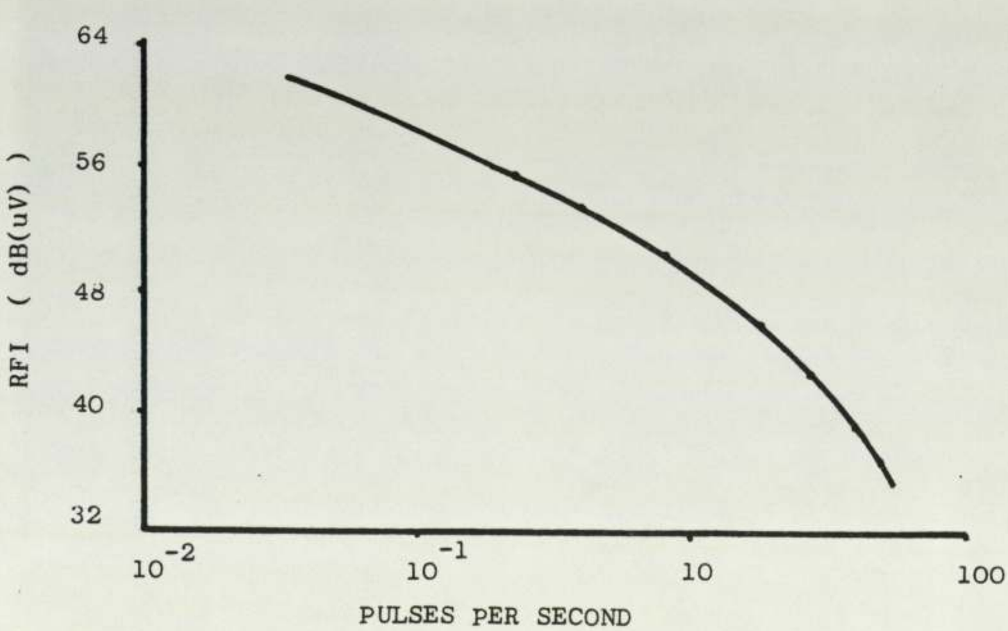

Measured NAD due to vehicle traffic (from Skomal [81])

Fig. 4.35

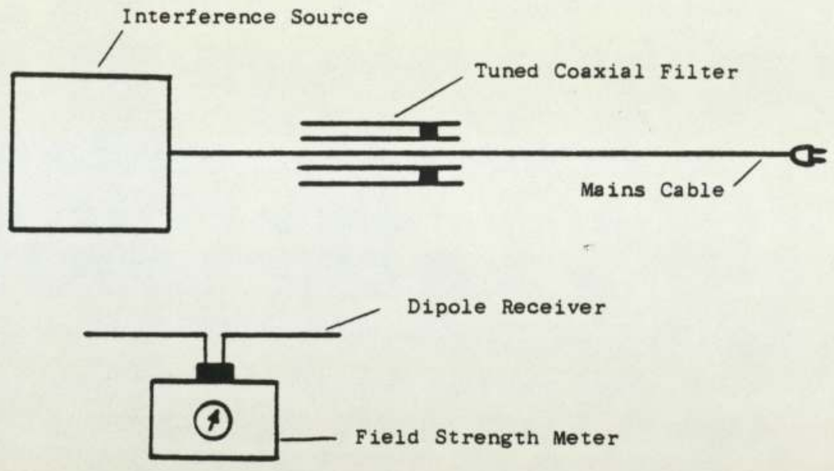

Measurement of radiated RFI by the "Swedish Method"

Fig. 4.36

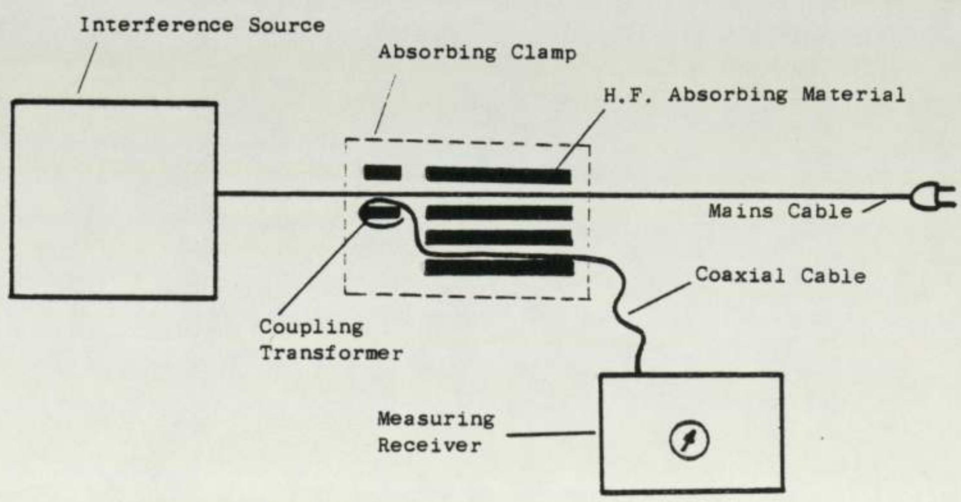

Measurement of radiated RFI by the "Absorbing clamp method"

Fig. 4.37

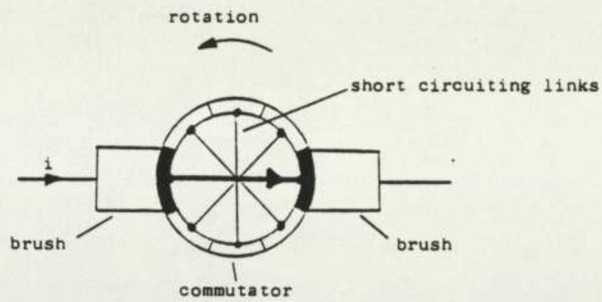

a

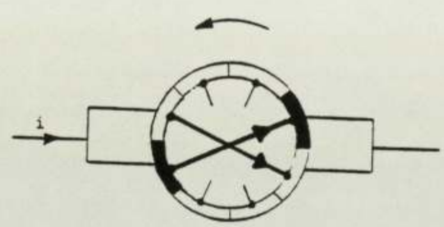

b

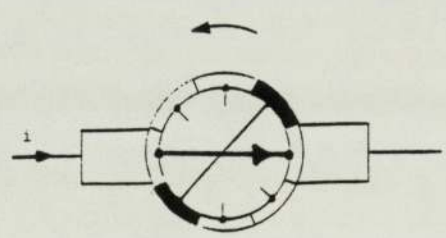

c

Test arrangement used by Hall and Quelch to assess the influence on RFI of the commutator-brush contact

Fig. 4.38

CHAPTER 5

TEST EQUIPMENT AND EXPERIMENTAL PROCEDURE

5.1 Motor test rig design

5.2 Construction details

5.3 Programme for experimental test work

5.4 Instrumentation and measurement

CHAPTER 5

TEST EQUIPMENT AND EXPERIMENTAL PROCEDURE

This chapter describes the test equipment and the experimental procedures adopted to investigate the electrical and mechanical factors contributing RFI in small motors. The majority of the experimental work was carried out at Hoover Engineering Department, in Perivale. To carry out the test work it was decided that a multi-purpose motor test rig should be constructed as discussed in section 4.5. A motor test rig was thus designed, the details of which are described in section 5.1 and 5.2. The programme for the test work is presented in section 5.3. In planning the programme, it became apparent that the work could be split into four main topics, i.e. to study the levels of RFI generated by:

i) the commutator switching action,

ii) the influence of the parameters of the short circuited coil undergoing commutation,

iii) the influence of the physical components of armature and field,

and iv) the influence of mechanical variations in the motor construction.

Topics (i), (ii) and (iii) form the basis of the investigation into the physical design of the motor. Topic (iv), covers the investigation into the influence on RFI levels due to mechanical variations arising from the manufacturing processes. It was planned to use these results to ascertain an acceptable limit for various construction tolerances, thus providing guide lines for the case-study to indentify the sources of high RFI levels in mass production. The case-study is presented in Chapter 7.

5.1 Motor test-rig design

Hoover made available a range of motor laminations to provide the basis for test-rig design, these were studied with a view to construct a rig that would offer the possibility of incorporating a number of design variations. As a result the test rig was based on a motor designed for use in the Hoover 'Junior' type vacuum cleaner (Model MC14). The motor being of a series field type construction, designed to run off a 240V, 50Hz mains supply with an output power of approximately 200W at 13000 r/min. A major consideration favouring this motor, included not only the design variation common to the standard model described below, but that this motor being in current production at the Perivale factory (subsequently moved to Cambuslang, Scotland) ensured an adequate supply of motor parts from the shop floor. This being especially important during the study of RFI generated due to the influence of mechanical variations, as these tests required a number of motor components from the factory (the details of which are described in section 5.4.4).

The standard MC14 design has a U-type field construction connected in series with an armature winding distributed in 12 rotor slots around a 24 segment commutator. The following armature design variations were available as direct replacement in the standard motor frame,

a) with armature windings distributed in 7 rotor slots around a 21 segment commutator.

b) with armature windings distributed in 11 rotor slots around a 22 segment commutator.

For simplicity, the armatures shall be referred to by their slot to commutator segment ratio i.e.

i) 12/24

ii) 7/21

iii) 11/22

The replacement armatures produced the same output performance as the standard 12/24 armature, the 7/21 having been used in an earlier design of the Hoover 'Junior'. The 11/22 armature was an early prototype armature construction that was never used in production, but a number of these armatures were constructed by the Model Shop at Perivale and made available for use on the test rig.

In addition to the standard U-type field construction, Hoover made available a prototype O-type stator lamination. This lamination had the same bore diameter as the standard U-type lamination, thus an O-type field system was constructed having the same stack length as the standard and fitted with field coils to give an equivalent motor performance when fitted in the test rig. The test rig was designed such that it could accommodate both these types of field configuration.

The criteria applied to the mechanical design of the test rig has been discussed in section 4.5. With these considerations detailed design drawings of the test rig components were produced and copies of these are presented in Appendix A1. The test rig components were made to high precision by technicians in the Model Shop and construction details of the test rig assembly are given below. (Photographs of the test rig assembly are presented in Appendix A6).

5.2 Construction Details

This section describes in the main components of the test rig as shown in the general layout diagram Fig. A1.1. Modifications to the test rig for the various experiments and the special features of its use are described in later sections. The components are as follows:-

a) test rig framework

b) brush box assembly

c) field assemblies

d) rotors

e) rotor drive arrangement

f) rig loading arrangement

5.2.1 Test rig framework

The test rig framework consists of two vertical end plates screwed in position onto a flat baseplate as indicated in Fig. 5.1. The components were machined from Aluminium stock material. To give the framework additional strength and ensure that the endplates remain equi-spaced, struts A and B were fitted between the inside faces of the vertical plates.

The end plates each house a motor bearing, the drive end bearing being a ball and race type with a sintered sleeve type bearing at the non-drive end. The distance between the plates corresponds to the position of the bearings on the rotor shaft when the armature is in position. To fit the armature without dismantling the main framework, the non-drive end bearing could be removed from the rear of the test rig by means of a detachable disc at the centre of the non-drive end plate as indicated in Fig. 5.2. The area of the disc was such that a fully wound armature could be 'threaded' into the test rig through the hole. The rotor shaft thus threads through the drive end bearing and is located in position on the bearing journal by means of a locating shoulder on the shaft, (see Fig. 5.3). The sintered sleeve bearing supports the weight of the armature and also aligns the rotor shaft in the test rig.

5.2.1.1 Baseplate, (Fig. A1.5)

The baseplate supports the vertical end plates as mentioned above. A recess cut parallel to the end plates as indicated in Fig. 5.4, is used to locate the field assembly described in Section 5.2.3. The depth of the recess ensures that the quadrature field axis coincides with the horizontal axis of the rotor stack. A fixed 'stop' (Fig. A1.15), positioned in the recess maintains the direct field axis coincident with the vertical rotor axis.

5.2.1.2 Drive end plate,(Fig. A1.4)

The drive end plate houses a ball and race bearing pressed into a hole on the inside face of the plate and secured by a clamping disc (Fig. A1.12). A circular recess concentric with the bearing locates the brush box assembly described in section 5.2.2.

5.2.1.3 Non-drive end plate, (Figs. A1.3 and A1.7)

The non-drive end plate as mentioned above has a detachable central disc which houses a sintered sleeve bearing. The sleeve bearing alignment is such that it lies directly opposite the ball and race bearing in the drive-end plate. The sintered sleeve is mounted in a bearing cup as used in the standard MC14 motor assembly.

The complete bearing assembly is fitted into a hole on the inside face of the detachable disc and secured in position in two 'finger' clamps (Fig. A1.14).

5.2.1.4 Spacing struts, (Fig. A1.8(a))

The spacing struts are used to ensure that the vertical end plates maintain a constant separation at all times and minimise plate flexture during motor operation.

5.2.2 Brush box assembly

The brush box assembly locates into a circular recess in the drive end plate and is held in place by a 'ring' clamp (Fig. A1.6) which screws onto the face of the plate, pressing the brush box assembly into the recess. The circular assembly profile allows the brush boxes to be rotated a full 360^{o} and clamps in at any desired angle. The assembly has the following components:

i) insulating back plate

ii) two insulating brush box holder blocks

iii) two brush box holders

5.2.2.1 Insulating back plate, (Fig. A1.9)

The insulating back plate is machined from a resin bonded fibre material. As mentioned above the back plate locates in a circular recess in the drive end plate. Two dove-tail grooves are cut across the back plate, these grooves are used to locate the brush box holder blocks directly opposite to each other, such that the brush boxes are located 180^{o} apart. The grooves allow the brush boxes to be moved above the below the quadrature axis without altering the angular position of the assembly. Once the desired brush box position is obtained it is secured by means of a screw from the rear of the back plate.

5.2.2.2 Insulating Brush box holder blocks, (Fig. A1.10)

These are machined from a resin bonded fibre material. The brush box holder blocks slide in the dove-tail groove of the insulating back plate and their primary function is to act as spacers from the back plate such that the brush boxes fitted in a groove on the surface of the block are able to position over the commutator surface.

5.2.2.3 Brush boxes, (Fig. 5.5)

The brush boxes are constructed from brass sheet to a design used in the standard MC14 motor. The basic design was reinforced by brazing the open edge of the brush box. The back of the box is open such that the brushes and brush retaining springs could be inserted with minimal dismantling of the rig. In order to secure the brush/spring assembly in the holder, a brass plate is secured into a flange at the back of the brush box as shown in Fig. 5.5 The brush box locates in a groove in the holder blocks described above and is fixed by means of a clamping plate (Fig. A1.13) screwed onto the holder block.

5.2.3 Field Assembly

There are two field systems common to the test rig; a U-type field lamination stack as used in the standard MC14 and an O-type field lamination stack especially constructed for use in the test rig. The O-type stack is equal in stack length and wound to give equal performance as the U-type field. Each field stack is clamped in an insulating cradle as shown in Fig. 5.6. The cradle ensured that the field iron is insulated from the rig framework and the bottom half of the cradle acts as a spacer of suitable height such that the horizontal axis of the field coincides with that of the armature stack. The field assembly is located in the framework by a recess in the baseplate and is secured in position by two clamps (Fig. A1.16) screwed into the baseplate pressing the cradle down as shown in Fig. 5.7.

5.2.3.1 U-type Field system, (Plate A6.6)

The U-type field stack is made up of laminations (Losil) which are rivitted together and the field coils wound on a plastic bobbin.

5.2.3.2 O-type Field System, (Plate A6.11)

The O-type field stack is made in the same fashion as the U-type stack, but with the laminations being welded together and the field coils wound in two equal halves at the neck of the pole shoes. A paper insert between the coils and the stack ensured suitable insulation.

5.2.3.3 U-type field assembly cradle

The U-type field assembly cradle is composed of a bottom half section Fig. A1.17, to support the field stack in position and locate it correctly in the test rig framework. The field stack is secured in position by means of an upper clamping half section Fig. A1.18(a), which is screwed into two vertical posts either side of the stack, as indicated in Fig. 5.6. The cradle sections are machined from resin bonded fibre, thus also insulating the field stack from the framework.

5.2.3.4 O-type Field assembly cradle

The O-type field assembly cradle is of similar design to that of the U-type field cradle (described above) being composed of a bottom half section Fig. A1.19, and upper clamping half section Fig.

A1.18(b).

5.2.4 The rotors

As mentioned earlier there are three armature designs common to the test rig i.e.

12/24

7/21

and 11/22 armatures

All the armatures being constructed on a standard rotor shaft as shown in Fig. 5.3. For the various experiments it was necessary to modify the basic armature such that isolation of the interference sources could be affected. Thus a number of special rotors were made and these are described in detail in the appropriate experiment description in section 5.3.

5.2.5 The rotor drive arrangement

For test conditions where it was necessary to drive the rotor shaft by external means a 'fan-air' drive arrangement was used.
A small metal fan was mounted on the drive-end of the rotor shaft and secured into position by means of a nut as shown in Fig. 5.8. The fan blades profile being such that the shaft is able to turn easily when the jet of compressed air is directed onto them.

Fig. 5.9, shows the drive arrangement. The nose of the air pipe is drawn to a narrow tip so that the compressed air could be directed precisely onto the fan blades. The volume of compressed air is controlled by a small tap at the end of the air-pipe. It must be noted that in order to obtain good speed control, it was necessary to ensure that the air-pipe was rigidly mounted being unaffected by external vibration.

Smooth speed control was obtained from approximately 500 r/min to 25,000 r/min, the high speed being limited only by the pressure of compressed air available from the air supply. At speeds below 500 r/min, bearing friction and the mass of the armature made smooth speed control difficult.

5.2.6 The rig loading arrangement

For the test conditions where the test rig is driven as an independent motor, the rotor shaft is loaded by means of a mechanical-brake arrangement as shown in Fig. 5.10. A small pulley-wheel is mounted onto the drive end of the shaft and secured by means of a nut as indicated. The brake was made by passing a leather strap under the wheel and connecting each end to a pair of spring balances mounted on an external frame. The brake was applied to the rotor shaft by tightening the wing-nuts A and B until the desired shaft speed was obtained.

5.3 Programme for Experimental Study

Electrical and Mechanical factors affecting the levels of interference in the motor were investigated by isolating them in the test rig as far as is practicable. In many cases this involved modifications to the rotor circuit or field components for which the test rig 'frame-work' served as the basic construction on which all the tests were performed. The experimental test programme was as follows:

5.3.1 RFI caused by the commutator switching action

To study the effects of current reversal during commutation without the additional effects of armature windings, a number of rotor shafts were prepared with only the commutators fitted in place (Fig. 5.11). The segments of the commutator were connected together with shorting links between the adjacent segments forming a closed ring as shown. The rotors were built into the test-rig framework with brushes fitted in place on the commutator surface in the normal manner. The test arrangement is shown in Fig. 5.12; current in the commutator links was limited by a pair of series resistors in the mains circuit, the total resistance of which was equal to the resistance of the field winding which these resistors replaced.

The fan-air drive arrangement described in section 5.2.5 was used to rotate the commutator at various speeds. In operation, current is conducted through the shorting links as shown in Fig. (5.11)(b) the commutator current switching action is the same as that in a normal motor. In this case it is possible to observe the levels of RFI generated without any additional affects of the emfs induced in armature circuit.

Commutators with 21, 22 and 24 segments were prepared for this test programme, in addition a rotor fitted with a copper slipring in place of the commutator was also tested. Measurements were made of conducted and radiated RFI and also of brush movement, the results of which are presented in section 6.1.

5.3.2 RFI caused by the variation of the short-circuited coil parameters

To study the effects of variations in the parameters of the coil undergoing commutation, i.e. coil resistance, inductance and induced voltage generated in the coil, it was necessary to have a means by which the effect of each parameter could be measured independently. This would be impossible with a normally wound armature, therefore, a "commutation model" was constructed. This model was first suggested by Konstannov [137] and subsequently used to study commutation by Mohr [45] and Binder [63]. Current direction is reversed by means of a commutator, through a circuit branch representing an armature coil. The branch is made up of the circuit elements of an ordinary coil and each element can be varied. Figure 5.13 shows a circuit diagram of the model.

The rotating part is composed of a 24 segment commutator and two slip rings fitted onto a standard rotor shaft as shown in Fig. 5.14. The segments of the commutator were collected into two groups (even and odd) and each group was connected to a slip ring. The shaft was assembled in the test rig framework and rotated using the fan-air drive arrangement described in section 5.2.5. A special brush box assembly (Fig. 5.15) had to be constructed to support brushes B and C to make contact with the slip rings, this assembly was clamped in the test rig framework in the baseplate recess cut for the field assembly.

The model of the armature circuit consists of a variable resistor, R_s, in series with a variable inductor, L_s, and a voltage source, e, variable in phase and magnitude, representing the induced transformer and rotational voltages generated in the short-circuited coil and connected across the slip rings, all in parallel with two resistances, R_a, representing the two halves of the armature winding. The series resistors, R_f, represents the resistance of the field coils.

The thickness of brush A making contact with the commutator was less than the width of one commutator segment. In the normal operation of the model, current is supplied to the system through brush A; when this brush contacts segment 1 only, current is fed to the circuit via brush B. As the commutator is rotated, segments 1 and 2 become shorted by brush A and the current in the branch representing the armature coil begins to commutate. With further rotation, commutation is completed as brush A leaves segment 1 on to segment 2 only, and current is fed to the circuit via brush C. In this manner current in the armature model is continually reversed in direction by the action of the commutator.

The test results showing the effect on conducted and radiated RFI due to the variation of the circuit parameters are given in section 6.2. The circuit components are described below.

5.3.2.1 Resistors R_s, R_a and R_f

The resistances used in the circuit were standard wirewound resistors. The resistance wire being wound on a fibreglass core and protected by a ceramic body. These resistors are small in size, approximately 5 cm in length yet capable of dissipating up to 11 watts. They were mounted between fixed terminal posts such that variation of resistance was achieved by replacing resistors rather than a potentiometer type arrangement. The ranges of values for the resistors were as follows

R_s; variable from 0.1 Ω to 20 Ω

R_a; variable from 1 Ω to 100 Ω

R_f; 25 Ω fixed

5.3.2.2 Inductance L_s

The inductance of armature coils used in small motors vary from a few μH to approximately 1mH. But since standard inductances (i.e. decade box type) in this range are only capable of conducting a few mA, it was necessary to construct suitable inductors for the circuit model. The core was made of a mild steel ring with an outside diameter of 8cm, a cross-sectional area of 1.5mm^2 and an air gap of 3mm. Two inductors were made in this way, one ring was wound with 100 turns of copper wire the other with only 10 turns. The coils were tapped at various points such that they could be connected in series, to give a variable inductance from 5μH to 1.3mH.

5.3.2.3 Variable voltage source 'e'

A voltage source, variable in magnitude and phase was obtained from a phase shifting transformer, the output of which was fed through a variac, as shown in Fig. 5.16. The inductance of the secondary of the variac was high (approxmately 10 mH), such that its inclusion in the circuit model would have adversely affected the performance of the model. Thus the voltage was fed to the circuit via a suitable transformer whose secondary coil had an inductance of only 230 μH and resistance 0.174 Ω. The output voltage was controlled from the variac and could be varied from zero to 8V max. By means of a control wheel on the phase-shifting transformer, the phase and the output voltage could be varied from zero to 2π.

5.3.3 RFI due to the influence of physical components of the armature and field

It was planned to build up the test rig introducing the different motor components in stages to measure their effect on RFI. In this way physical isolation of the interference sources could be affected, thus allowing an assessment of their relative importance in relation to the overall RFI levels from the complete test rig. The test programme was as follows:

a) Measurement of RFI levels from the field coils,

   i) without the field lamination stack
   ii) with the field lamination stack (complete field system)
   iii) complete field system with an unwound rotor in the air-gap.

b) Measurement of RFI levels across the motor brushes with,

   i) fully wound armature (field system removed)
   ii) fully wound armature and complete field system (complete motor) with different field profiles and winding configurations
   iii) complete motor with different armature profiles and

winding configurations

iv) complete motor with varying motor loads.

Measurements were taken of conducted and radiated RFI; assymetric and symmetric interference currents; armature and field impedences; active inductance 'L_{comm}'. The results of these tests are given in section 6.3.

5.3.4 RFI due to the influence of mechanical variations in the motor assembly.

To assess the effect on RFI due to mechanical variations in the motor assembly, the programme of tests described below were carried out. The test rig was built up as a complete motor using standard MC14 components, i.e. fitted with the standard U-type field assembly and using 12/24 type armatures. The motor was energised from a 240V supply via a standard 150 ohm artificial mains V-network and shaft load provided by the pulley type arrangement described in section 5.2.6.

5.3.4.1 Static armature out-of-balance

Static out-of-balance was introduced to a balanced 12/24 armature by adding weights to the rotor stack. Balancing putty was set onto the left and right hand planes of the rotor stack as shown in Fig. 5.17. In this manner, weights were added to increase static armature out-of-balance from zero to 3.0 gcm (30×10^{-6} kgm).

5.3.4.2 Dynamic armature out-of-balance

The preparation was similar to that described above, in this case, the putty weights were added such that the static out-of-balance remained zero, yet dynamic out-of-balance was steadily increased. This was done by setting the balancing putty to opposite points on the left and right hand planes of the rotor stack as shown in Fig. 5.18. In this manner, weights were added to increase dynamic out-of-balance from zero to 2.0 gcm (20×10^{-6} kgm).

5.3.4.3 Brush Pressure

The brush spring was of a simple helical compression type and the brush spring force was easily changed by varying the uncompressed length. In this manner the overall brush pressure onto the commutator surface was increased. Spring force was varied from 40g to 150g.

5.3.4.4 Brush alignment along quadrature axis

Alignment of the commutator and brush horizontal axis was altered by moving the insulating brush box holder blocks (section 5.2.2.2) along the dovetail groove in the insulating backplate (section 5.2.2.1) as shown in Fig. 5.19. Tests were carried out with increasing brush misalignment of up to 0.5 mm, firstly against and then in the same direction of commutator rotation.

5.3.4.5 Proud commutator segments

A number of finished armatures were selected at random from the shop floor. The commutator bar to bar heights of these armatures were measured from this it was possible to select armatures for tests with increasing bar to bar height variation in the range from zero to 12.5×10^{-3} mm.

5.3.4.6 Commutator eccentricity

The commutator surface was turned in a lathe such that the surface profile is concentric with the bearing journals. Thus to introduce commutator eccentricities, the commutators on a number of armatures selected at random from the shop floor, were machined in the tool room to have eccentricities in the range from zero to 80×10^{-3} mm. The armatures were then balanced to eliminate the influence of out of balance forces created by the eccentricity. These armatures were then fitted in the turn to the test rig and measurements of RFI were made.

5.3.4.7 Commutator surface finish

The commutator surface finish is controlled by the depth and speed of the finishing cut. Armatures from the shop floor were machined in the tool room to give different commutator surface finishes, the finishes range from 0.1×10^{-6}m Centre Line Average (CLA) to 5×10^{-6}m CLA. The armatures were fitted in turn into the test rig and measurements of RFI were made.

5.3.4.8 Commutator insulation depth

The 24 segment commutator being a 'bought in item', the slots were already cut to size, leaving little scope for variation. Thus the commutators on a number of 7/21 armatures were machined in the tool room to obtain a range of different insulation depths. The slot depth was increased from zero (i.e. flush insulation) to a depth of 2mm. The armatures were fitted in turn into the test rig and RFI measurements were made.

5.3.4.9 Brush box clearances

Clearance between the inside of the brush box and the brush is necessary to allow the brush to slide freely in the brush box. A number of brush boxes were made in the tool room to give an increasing clearance.

a) in the direction tangential to commutator rotation, (Fig. 5.20(a)).

and b) in the direction axial to commutator rotation, (Fig. 5.20(b)).

The clearances were increased up to 0.2 mm. Pairs of brush boxes with the same clearances were fitted in turn into the brush box holder assembly of the test-rig.

5.3.4.10 Brush overhang length, (Fig. 5.21)

The brush box could be slided towards and away from the commutator surface without affecting the brush box alignment by means of a slot in the brush box holder blocks. This movement allows the variations of the brush overhang length from the end of the brush box. Thus RFI measurements were made on the test rig for brush overhang lengths varying from 0.5mm to 3mm.

5.3.4.11 Bearing alignment

The test rig framework was constructed such that the bearings in the two end-plates were aligned both vertically and horizontally. Vertical misalignment was introduced by placing steel shims under the non-drive end plate as shown in Fig. 5.22. To facilitate horizontal misalignment, slots were cut in the framework baseplate such that the vertical plate could be shifted in position as shown in Fig. 5.23. In this manner bearing misalignments in the range zero to 0.2 mm were affected in both the directions indicated.

5.3.4.12 Air-gap

In the normal case the air-gap between the rotor and field stack is the same at both pole faces. The air-gap in the test rig was varied by adjusting the position of the field stack cradle relative to the armature. The air gap was varied in the direct axis by inserting steel shims under the field stack cradle as shown in Fig. 5.24. Variation of the air gap in the Quadrature axis was affected by inserting steel shims between the 'fixed stop' (fitted on the framework baseplate) and the field stack cradle as shown in Fig. 5.25. In this manner the air-gap was varied such that

a) the air-gap at the upper pole-face is increasing as the air-gap at the lower pole face decreases, Fig. 5.26(a).

and b) a non-uniform air-gap is present at both pole-faces,

Fig. 5.26(b).

5.3.4.13 Angular brush shift

The angle of brush shift was adjusted by rotating the brush box assembly relative to the armature in the test rig framework, as described in section 5.5.2. The neutral brush axis was found by applying a small alternating signal to the field coils and rotating the brush assembly until a maximum signal level was detected across the brushes by means of an oscilloscope. From this neutral position RFI results were taken as the brush axis was shifted against the direction of rotation.

5.3.4.14 Bearing Journal diameter

The bearing journals on a number of armatures obtained from the shop floor were precision ground in the tool room. The bearing journal diameters were decreased thus increasing the clearance between the bearing journal and bearing sleeve from an interference fit to a clearance of 0.016 mm. The armatures were fitted in turn into the test-rig and measurements of RFI were made on each.

5.4 Instrumentation and Measurements

This section details the instrumentation and measurement techniques employed to carry out the test programme outlined in the previous section.

5.4.1 RFI

Measurements of RFI levels were made using the standard equipment and techniques as described in BS 800 [19] and BS 727. [18] i.e.

a) Methods of Measurement of terminal voltages in the frequency range 0.15 - 30 MHz

and b) Methods of Measurement of interference power in the frequency range 30-300 MHz.

For these tests a mains supply lead of 10m was connected to the supply terminals of the test rig.

5.4.1.1 Measurement of terminal voltage, (Fig. 5.27)

The test rig is connected to a variable mains supply through a mains isolation network as shown. The isolation unit was a 'Schwarzbeck' standard artificial mains V-network of 150 Ω (model NNB M8 112). RFI measurements were made across the mains network as indicated using a 'Schwarzbeck' low frequency CISPR type Measuring Set (Model FSME 1515), this incorporated an r.f. receiver, Quasi-peak type detector circuit and an interference display meter. The two units are shown in Fig. 5.28. A selector switch on the isolation unit enabled RFI measurements to be made across Line and Earth or Neutral and Earth as required.

Tests were carried out in a screened room to eliminate external corruption of RFI measurements. The rig was placed on a wooden table satisfying the requirements of the British Standard. The mains lead was bundled and placed at a distance of at least 80 cm away from the measuring equipment. It was noticed that movement of the bundle could affect the results obtained, thus, during all testing it was ensured handling of the mains cable was kept to a minimum.

The receiver of the measuring set was tuned manually. Once the desired frequency was achieved, firstly it was necessry to calibrate the equipment, this being done by switching the set to 'Calibrate' mode and the calibration carried out automatically within the set. On completion of calibration the set is switched to 'Read' mode and the apparatus is ready to measure. With the test rig running, readings were taken by adjusting attenuators in the measuring set to give a null meter indication and the interference level being read from the attenuator scale in dB relative to 1μV. The procedure was repeated for each different frequency selected. The British Standard indicate the preferred frequencies that RFI readings should be taken i.e. 0.15, 0.16, 0.24, 0.55, 1.0, 1.4, 2.0, 3.5, 6, 10, 22 and 30 MHz. In addition, the frequency range is scanned to observe and record any peaks or troughs of RFI levels not evident from the preferred frequency readings.

5.4.1.2 Measurement of radiated power, (Fig. 5.29)

The test rig is connected to the mains supply through a variac, the connecting mains lead being stretched out in a straight line along a wooden bench as shown. A ferrite clamp (MDS20) is fitted around the mains lead, the clamp as mentioned in section 4.4.2 comprises of:

a) a number of ferrite rings surrounding the mains lead which serve both to absorb the power produced by the source and to isolate the source from the supply mains as far as high frequencies are concerned.

b) a h.f. coupling transformer whose output voltage is proportional to the h.f. current in the mains lead.

and c) a number of ferrite rings designed to prevent unwanted currents flowing in the surface of the co-axial cable connecting the transformer to the measuring receiver.

The ferrite rings of part (a) and (c) are split into half rings, each half being fitted into the jaws of the clamp. This enables the mains lead to be passed through the tunnel of rings without the plug having to be removed and re-fitted.

The measuring receiver used was a 'Schwarzbeck' high frequency CISPR type measuring set (Model VUME 1520 A). The set incorporates a high frequency receiver, Quasi-peak type detector circuit and interference display meter. The measurement techniques were as follows; the measuring receiver was tuned manually to the desired frequency and with the test rig in operation, the measuring set is firstly calibrated in a similar manner as described in Section 5.4.1.1. When calibration is complete the clamp is shifted along the cable until a maximum deflection is obtained on the display meter. Readings were taken with clamp left in position, by adjusting attenuators in the measuring set to give a null indication on the display meter. The interference level being read from the attenuator scale in dB relative to 1μV. The clamp is supplied with a calibration curve which has to be applied to the meter reading in dB (μV) in order to obtain the available power at the source expressed in dB relative to 1 pW.

The procedure is repeated for each different frequency selected. The British Standard indicates the preferred frequencies the RFI readings should be taken i.e. 30, 45, 65, 90, 150, 180, 220 and 300 MHz. Scanning of the frequency range for peaks and troughs of RFI levels is very difficult as the clamp position is frequency dependent, but where possible this was done.

5.4.2 R.F. impedance

The r.f. impedance measurements of various components of the test rig were made using a radio frequency admittance bridge (Wayne Kerr Model B801) in conjunction with a general purpose bridge source (Wayne Kerr Model SR 268). A simplified diagram of the bridge circuit is shown in Fig. 5.30, with the 'unknown' impedance connected across terminals A and B.

With the source set to the frequency of measurement required, the bridge is firstly balanced with the main controls set to zero and the test components not connected to the terminals. This reduces the effect of stray components in the test circuit to a minimum. With the test component connected, the bridge is then re-balanced using the main controls. Once the bridge is balanced the dials give a direct reading of the r.f. impedance in terms of the equivalent parallel components of conductance and capacitance. (Inductance readings being given in terms of equivalent negative capacitance). The procedure was repeated across the frequency band with sufficient readings taken such that an impedance curve could be drawn.

5.4.3 Interference currents

The Asymmetric and Symmetric interference currents conducted in the mains lead were evaluated from measurements made using probes fitted around the mains lead as shown in Fig. 5.31. This is a comparison method to observe interference currents, the details of which have been described in Reference 138. The test rig is connected to the variable mains supply through the standard mains 150Ω V network. The probe is a ferrite ring cored current transformer, the output of which is connected to a 'Schwarzbeck' low frequency CISPR type RFI measuring set (Model FSME 1515).

Probe A is shown connected such that the in-phase current i.e. twice the asymmetric current (2Ia) is measured, and probe B such that the current in one lead is reversed and the total current measured is twice the effective symmetric component (2Is). The interference level displayed on the measuring set is in dB relative to 1 μV. In order to evaluate the interference currents, the test rig was replaced by a h.f. signal generator and connected as shown in Fig. 5.32. With the signal generator tuned to the same frequency as the measuring receiver the output voltage, Vo, of the signal generator was increased until the interference level indicated by the measuring set corresponds to that measured from the test rig.

The interference current I can then be evaluated from;

$$2I = Vo/150 \qquad (5.1)$$

therefore the interference current in dB relative to 1μA can be expressed; I dB (μA) = Vo dB (μV) − 20 log 300 (5.2)

Interference current measurements were made in the screened room, with the test arrangement positioned as described in section 5.4.1.1. The measuring set was tuned and calibrated at the desired frequency, and with the rig running, the attenuators in the measuring set were adjusted to give a null meter indication. At this point, the mains supply was switched off and the test rig removed by disconnecting the mains lead connections at the rig, thus the mains lead and the probes are not disturbed in any way. As mentioned above, the rig was replaced by a h.f. signal generator which is tuned to the same frequency as that of the measuring receiver. The signal generator output voltage Vo was increased by a dial on the generator set (scaled in dB (μV)) until the reading on the measuring set again shows a null indication. At this point, Vo was recorded and subsequently converted to interference current in dB relative to 1μA. The procedure was repeated for a number of frequencies across the low frequency band for both asymmetric and symmetric current readings.

5.4.4 Active inductance

The active inductance 'L_{comm}' of an armature coil is defined as the value of inductance which must be reckoned with at the end of commutation during sparking. The method employed to measure L_{comm} described below was originally presented by Dijken [28] (See section 3.9).

The armature used for the measurement is indicated in Fig. 5.33. The armature coils 1 and 7 are shown commutating the main current from zero to I_1 and I_2 respectively.

In section 3.5 it was shown that the voltage equation of a coil undergoing commutation can be written:

$$i_s R_s + L di/dt + e + U_b = 0 \qquad (3.30)$$

L is defined as the active inductance of the coil L_{comm}, and if the supply current is constant and the rotor is kept stationery then 'e' can be eliminated. Further, if the brush is replaced by a soldered contact, U_b is effectively zero, thus the voltage equation simplifies to:

$$i_s R_s + L di/dt = 0 \qquad (5.3)$$

Considering coil 1, during sparking i_s varies from an initial value (assumed zero) to I, now i_s satisfies the equation:

$$i_s R_s + L di_s/dt - U_{spark} = 0 \qquad (5.4)$$

where U_{spark} is the voltage drop in the spark. Dijken estimated that U_{spark} is approximately 12 volts, if then the spark is simulated by a Zener diode of Zener voltage U_z and assuming $i_s R_s$ is negligible then:

$$L_{comm} . di_s/dt - U_z = 0 \qquad (5.5)$$

The time interval during which i_s increases from zero to I_1, is denoted by t_z, the spark decay time. Giving,

$$di_s/dt = I_1/t_z \qquad (5.6)$$

$$\text{therefore; } L_{comm} = U_z t_z / I_1 \qquad (5.7)$$

A schematic circuit for measurement of the active inductance is shown in Fig. 5.34. The coils 1-12 correspond to the rotor coils 1-12 in Fig. 5.33.

Commutation is simulated in coils 1 and 7, with the aid of transistors T_1, T_2, T_3 and T_4. Since the rotor is stationary the position of coil 7 remains the same, so it can be connected electrically below coil 12; this simplifies the switching of the four transistors. When T4 is conducting and T3 is cut off, coil 1 is short circuited. When T3 is conducting and T4 is cut off, I_1 passes through coil 1 and part of this current will temporarily pass through the zener diode. T_3 and T_4 are switched periodically, by means of a square wave voltage and U_z and i_z displayed on an oscilloscope. The time interval t_z is read off the time base of the oscilloscope trace. Similarly when transistor T_2 is conducting, T_1 is cut off, so I_2 passes through coil 7. The base of T_1 is connected to the base T_4 and the base of T_2 to that of T_3, such that simultaneous commutation of coils 1 and 7 could be simulated. Zener diodes of U_z = 12 volt were used and with the supply current adjusted by a potentiometer in the supply line, the active inductance thus being calculated from the expression above.

The various possible ways of short circuiting the rotor coil, depending on the position of the brushes as shown in Fig. 4.31 is simulated by connecting shorting links between the appropriate commutator segments where the brush is shown to be covering more than one segment. The method was adapted to measure the active inductance of the different armature designs used in the test programme.

5.4.5 Brush Vibration

The problems of measurement of brush movement in small commutator motors have been discussed in section 3.8.5. A number of the established techniques described were tried and rejected for various reasons and attempts were made to develop a suitable method to observe brush movement. The technique finally used turned out to be novel in concept involving the use of microwaves and waveguide components. The theory and operation of this new method of vibration measurement is described in Appendix A5.

5.4.6 Sparking at the trailing edge of the brushes

A visual assessment of the sparking at the trailing edge of each brush was made using an illustrated chart for reference. The quality of sparking was thus classified using Table 3.2.

5.4.7 Speed

The test rig rotor speed was measured with a photo-electric digital tachometer. The tachometer was mounuted so that its light beam was directed at the drive end shaft on which was fixed a strip of reflective tape. Each time the light beam was reflected to the tachometer, pulse was given. The digital display of the tachometer indicated shaft speed in r/min.

5.4.8 Armature Out-of-balance

Armature out-of-balance was measured using a Jackson and Bradwell Balancing Machine. The balancing machine consists of a spring suspended cradle for the armature, the armature being supported at the bearing journals in V-blocks. The armature is rotated by means of a pulley type drive, a light elastic pulley belt is passed over the rotor lamination stack and driven by a pulley wheel located under the cradle as shown in Fig. 5.35. As the armature is rotated, electro-mechanical sensors connected to the cradle detect vibrations caused by unbalances in the armature construction. The output of the sensors is indicated on an analog meter type display. The meter indication is calibrated to read armature unbalance in gcm and can be switched to read either dynamic out-of-balance on the left and right hand planes of the rotor lamination stack or give a simple indication of static out-of-balance.

5.4.9 Brush spring force

The brush spring force was measured using a push-on type spring balance calibrated to indicate spring weight in grams. The spring balance piston was pressed directly onto the brush thus retaining the spring at the back of the brush box, enabling the spring balance to measure the reaction force of the brush spring arrangement in situ as shown in Fig. 5.36.

5.4.10 Commutator profile

Commutator bar to bar heights and overall eccentricity measurements were made using a precision dial gauge arrangement as shown in

Fig. 5.37. The armature was rotated slowly by hand and commutator profile measurements were taken from the dial gauge meter indication.

5.4.11 Commutator surface finish

Commutator surface finish was measured using a Taylor-Hobson 'Surtonic' roughness measuring system. Fig. 5.38, shows a block schematic diagram of the measuring equipment. The drive unit traverses the pick-up and stylus along the commutator segment surface. The stylus moves vertically as it rides over the surface irregularities and in the pick-up this movement is converted to a corresponding electrical signal. The signal is filtered and amplified before being displayed as a rectified-meter indication. The roughness reading is given as a centre line average, (CLA), height of the roughness irregularities. The CLA measurement is defined as the average value of the departure, both up and down, from its centre line, throughout the sampling length.

5.4.12 Test Rig Dimensions

All test-rig dimensions were measured using standard tool room metrology equipment, i.e. height gauges, depth gauges, slip gauges, micrometers, etc. Using this equipment, brush alignment; bearing alignment; angular brush shift; brush box clearance; brush overhang and bearing journals were adjusted and measured to an accuracy greater than 2.5×10^{-4} mm.

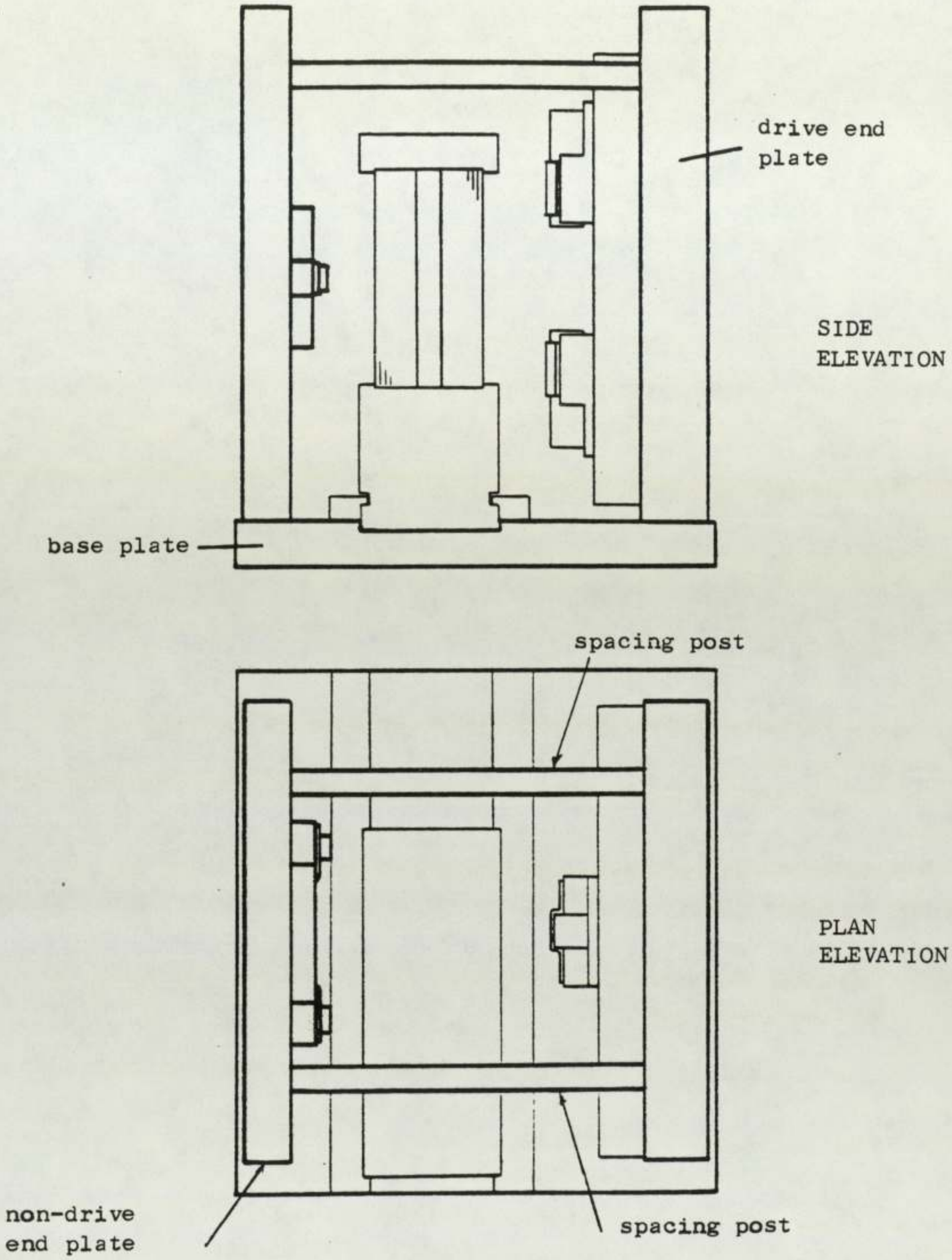

Test rig framework

Fig. 5.1

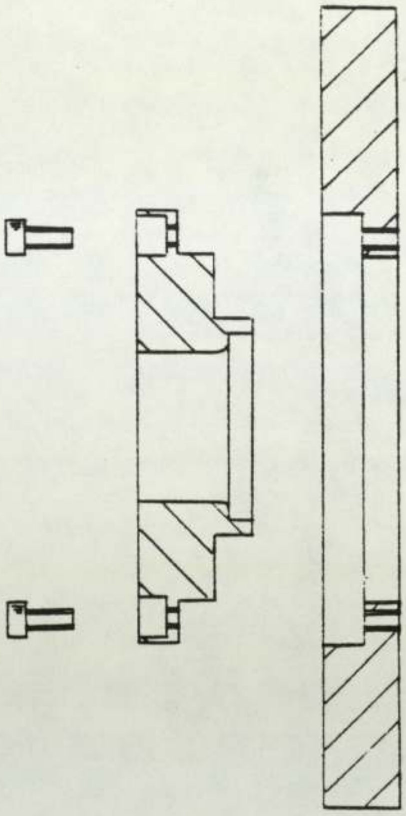

Non-drive end plate assembly

Fig. 5.2

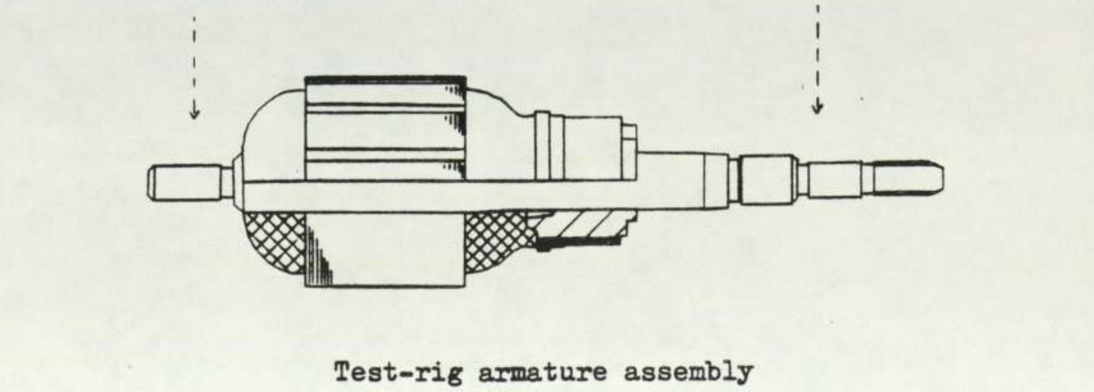

Test-rig armature assembly

Fig. 5.3

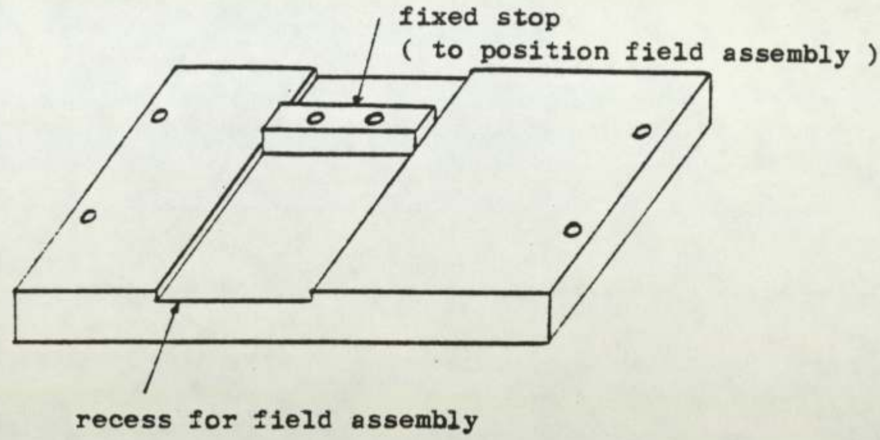

Test-rig base plate

Fig. 5.4

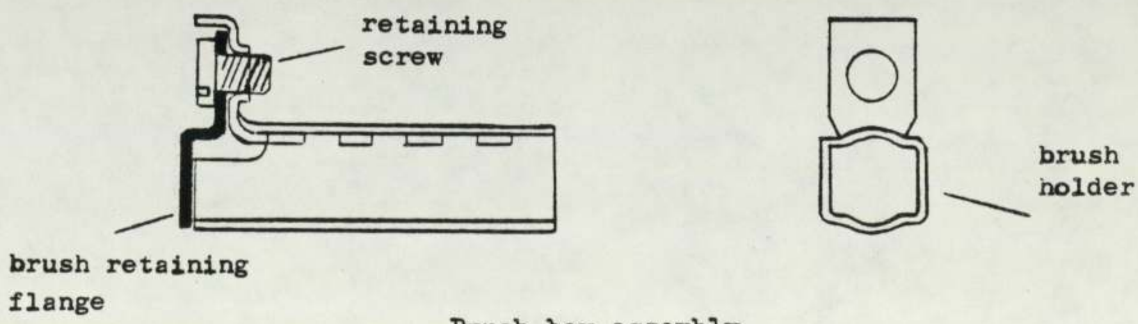

Brush box assembly

Fig. 5.5

(a) U-type field assembly

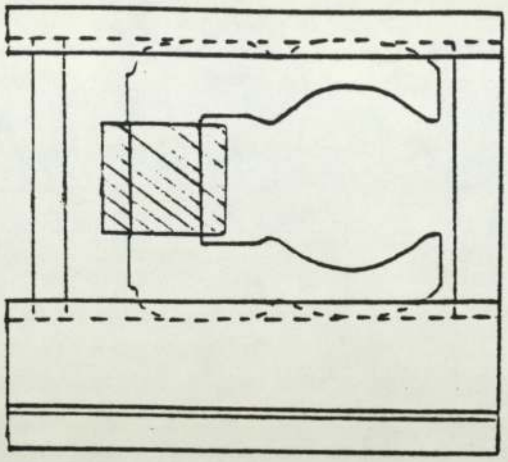

Test-rig field assemblies
Fig. 5.6

(b) O-type field assembly

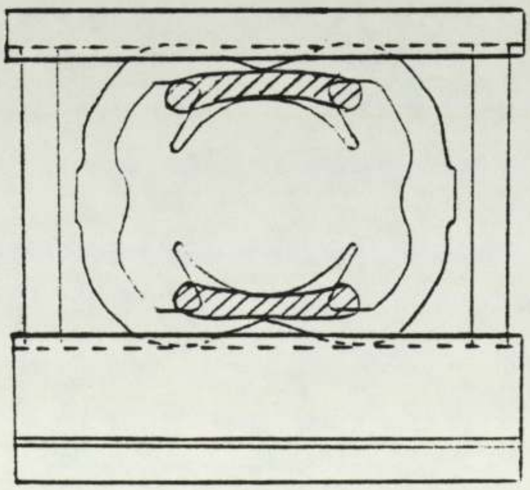

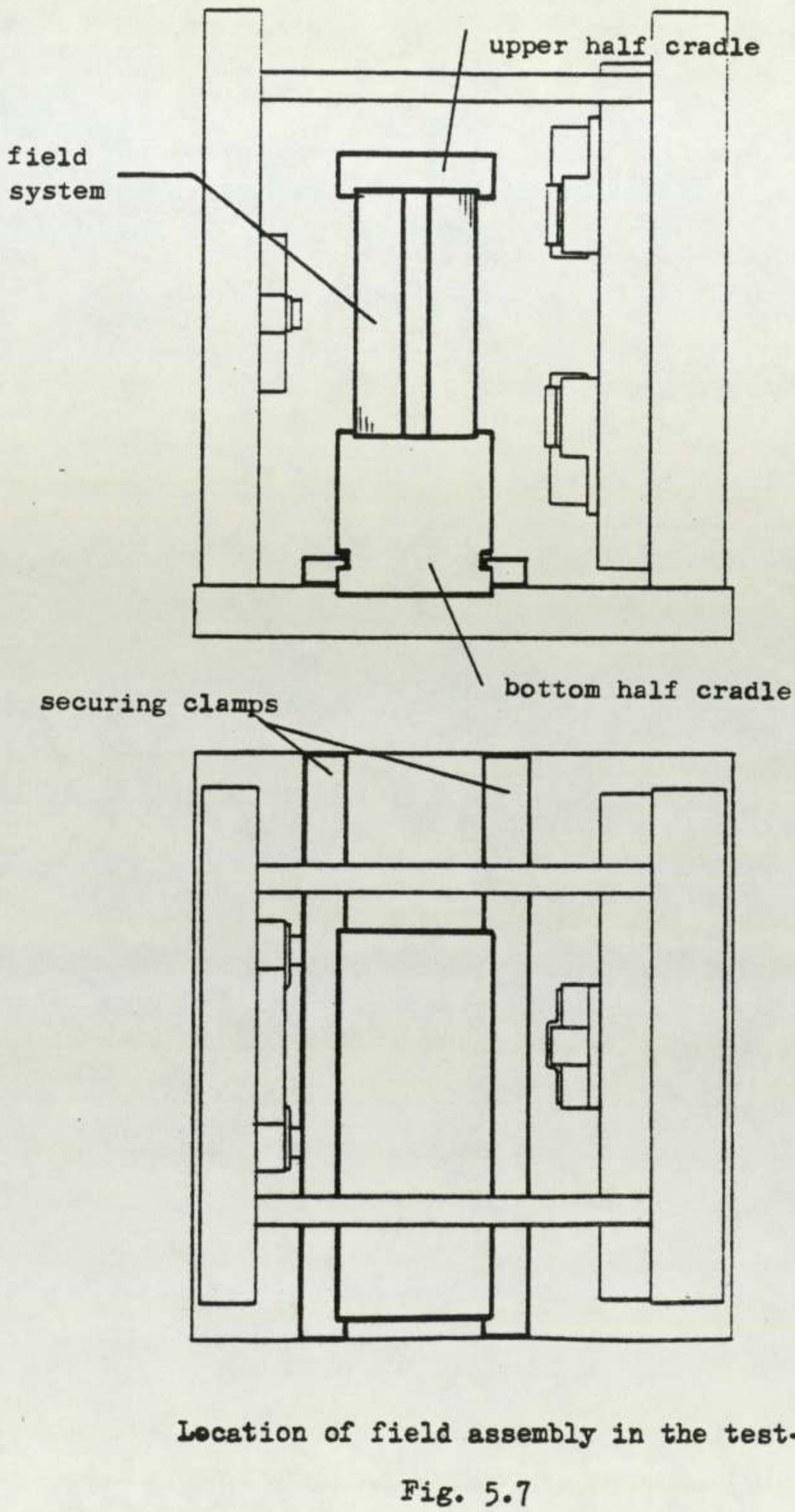

Location of field assembly in the test-rig

Fig. 5.7

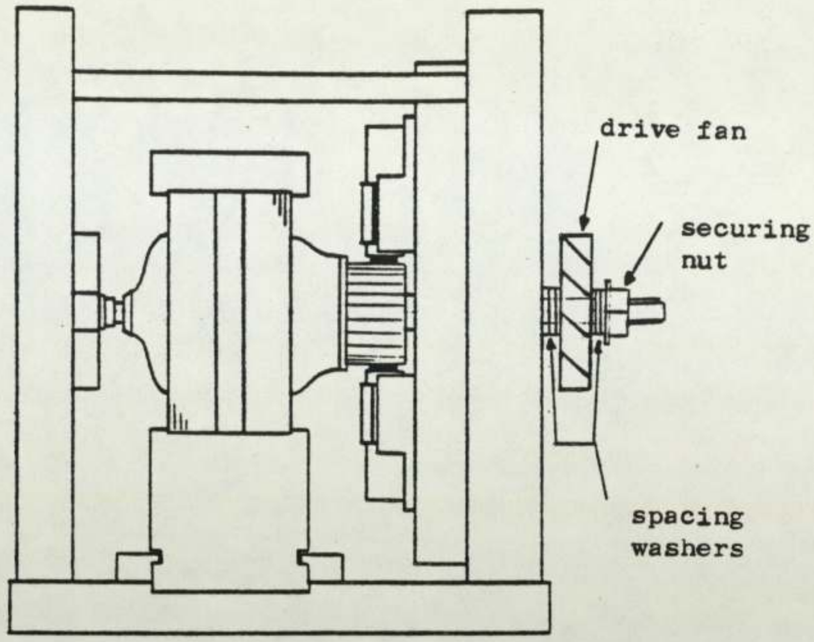

Test-rig assembled with drive fan

Fig. 5.8

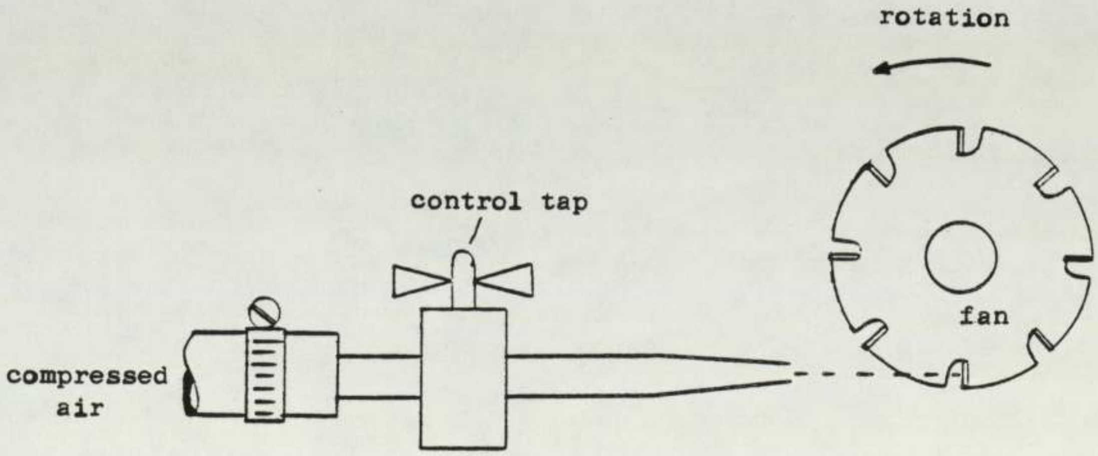

Fan-air drive arrangement

Fig. 5.9

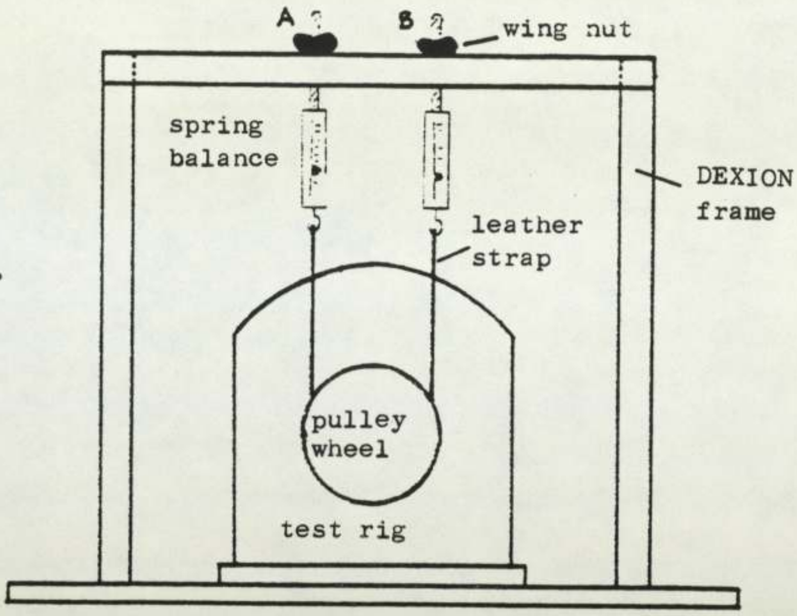

Test-rig loading arrangement

Fig. 5.10

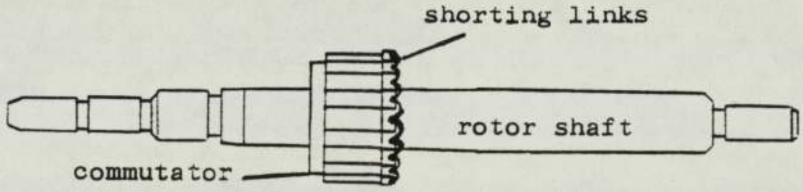

(a)

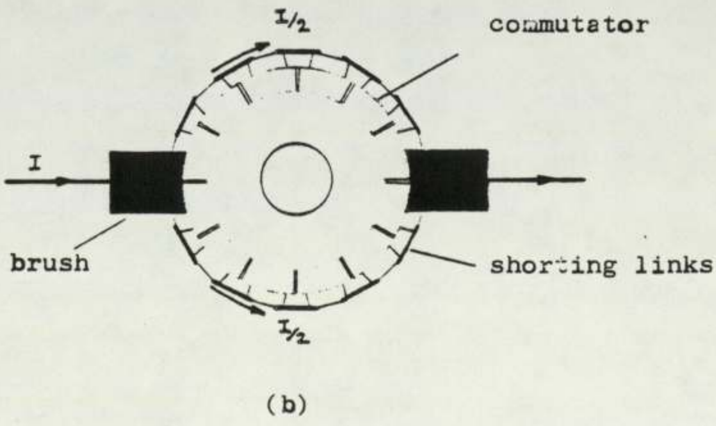

(b)

Rotor construction (a) and operation (b) for RFI tests described in section 5.3.1

Fig. 5.11

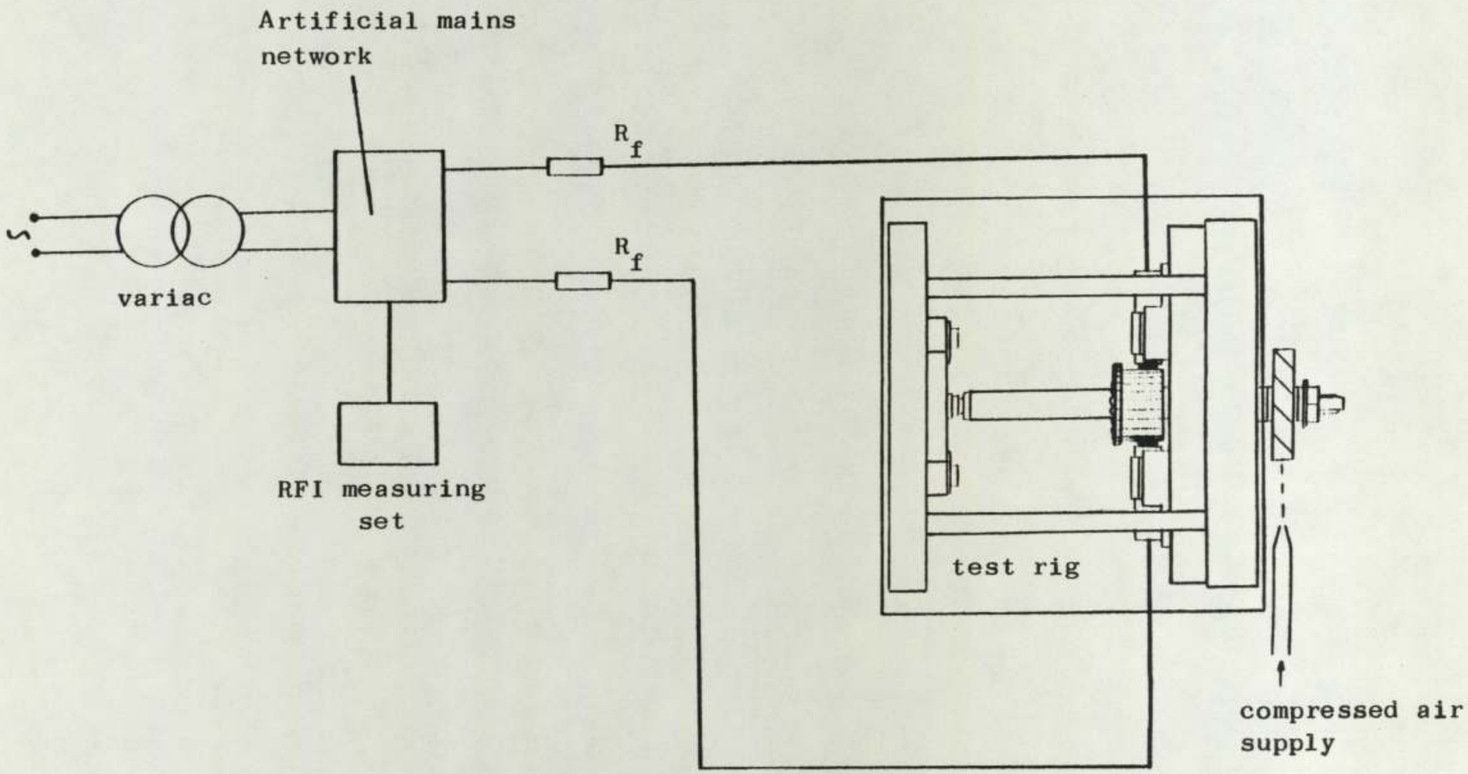

Test arrangement for measurement of RFI levels due to the commutator switching action

Fig. 5.12

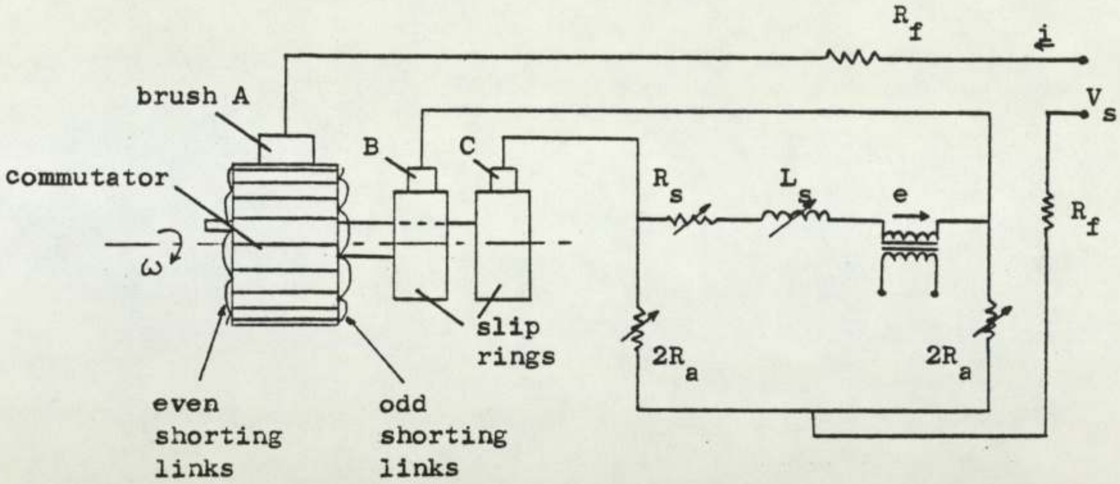

Circuit diagram of the commutation model used in the RFI tests described in section 5.3.2

Fig. 5.13

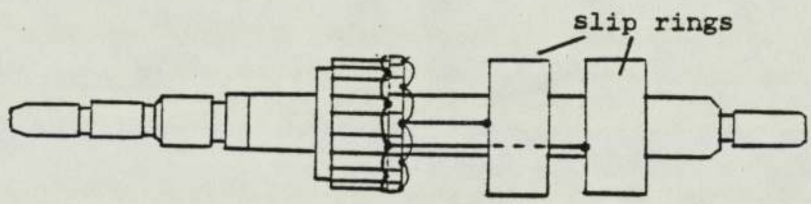

Construction of rotor for use in the commutation model

Fig. 5.14

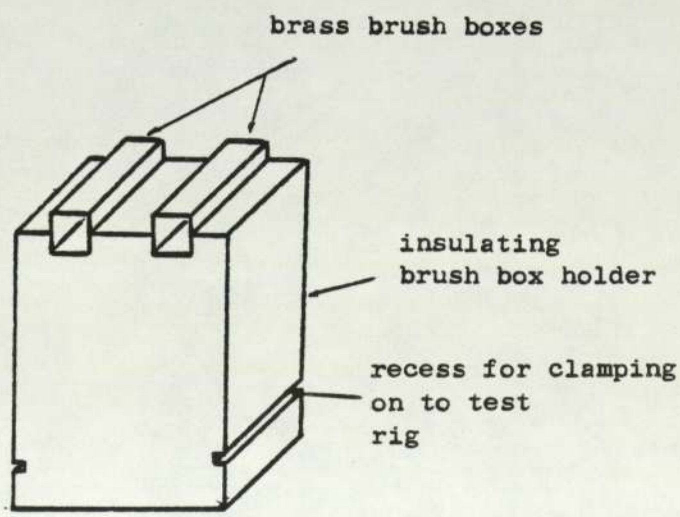

Special brush-box assembly

Fig. 5.15

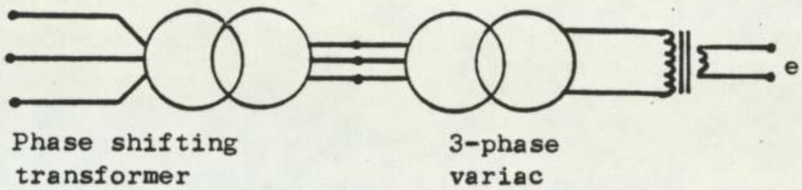

Variable voltage source

Fig. 5.16

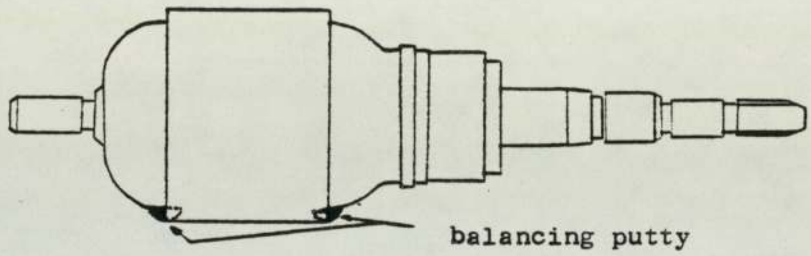

Armature for static out-of-balance tests

Fig. 5.17

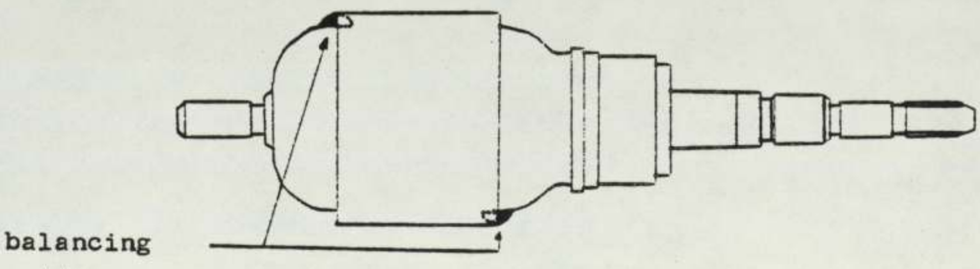

Armature for dynamic out-of-balance

Fig. 5.18

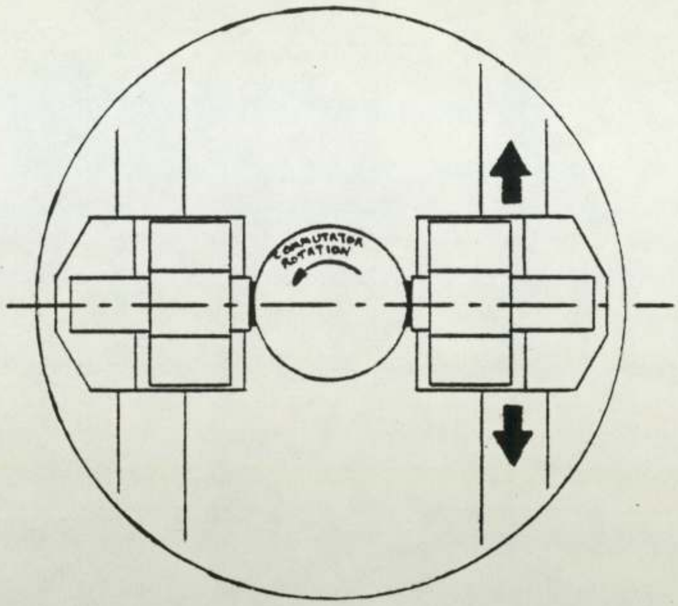

Brush holder movement to vary brush misalignment on quadrature axis

Fig. 5.19

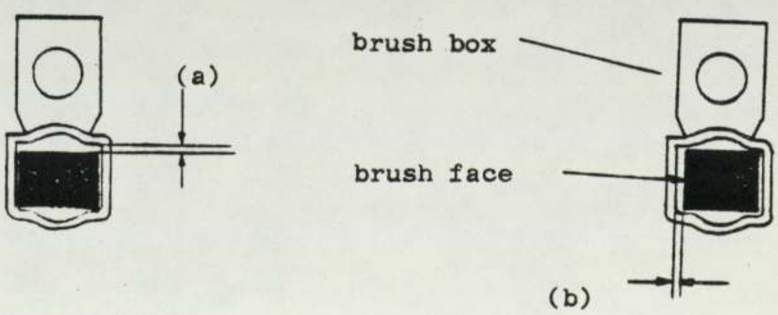

Variation of brush-box clearance (a) tangential and (b) axial to commutator rotation

Fig. 5.20

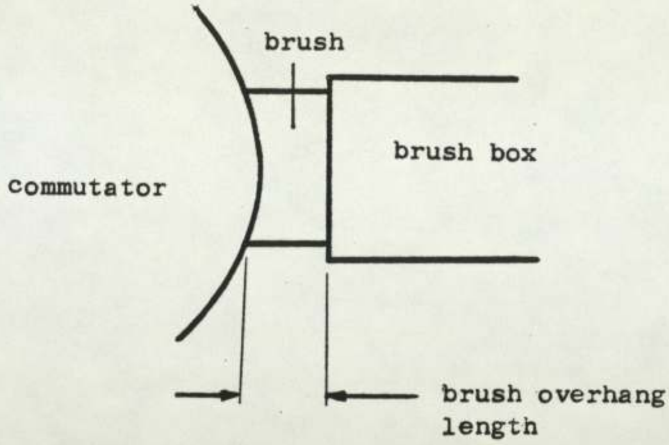

Brush overhang length

Fig. 5.21

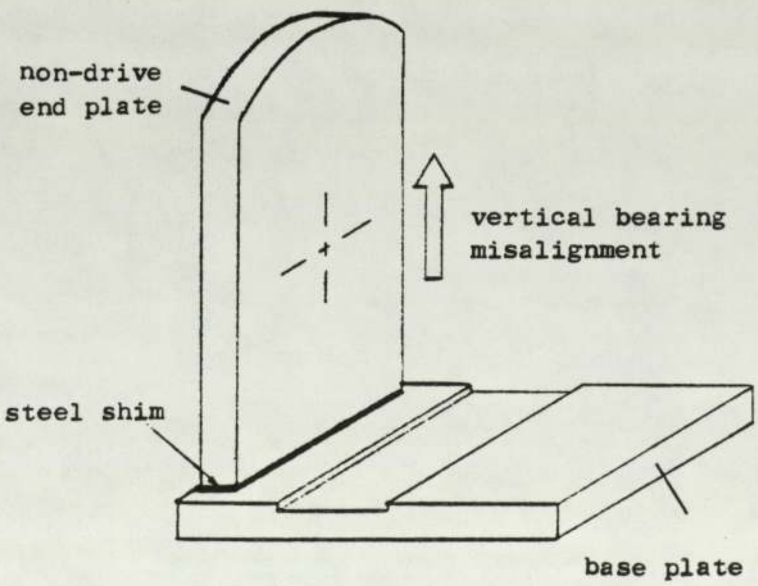

Insertion of steel shims to produce vertical bearing misalignment

Fig. 5.22

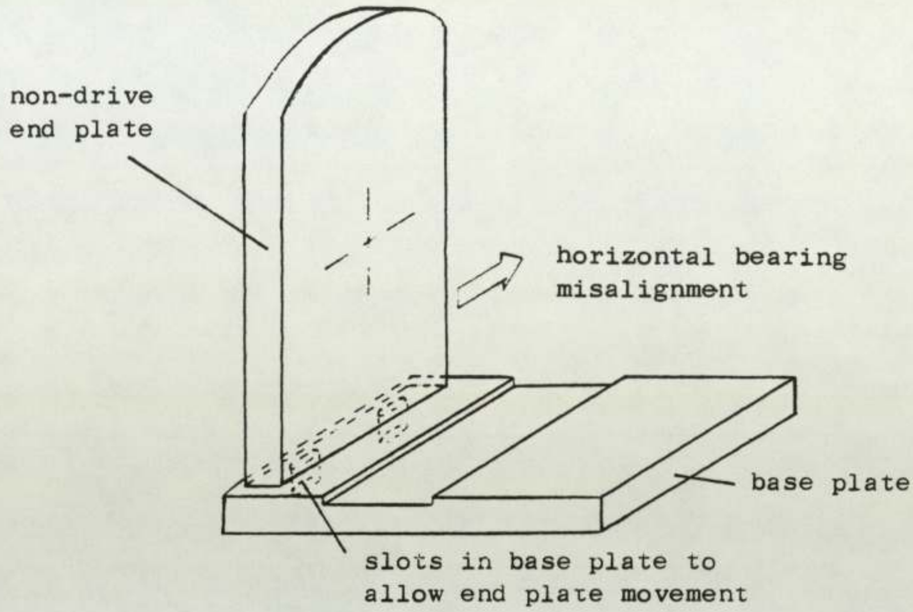

Movement of non-drive end plate to produce
horizontal bearing misalignment

Fig. 5.23

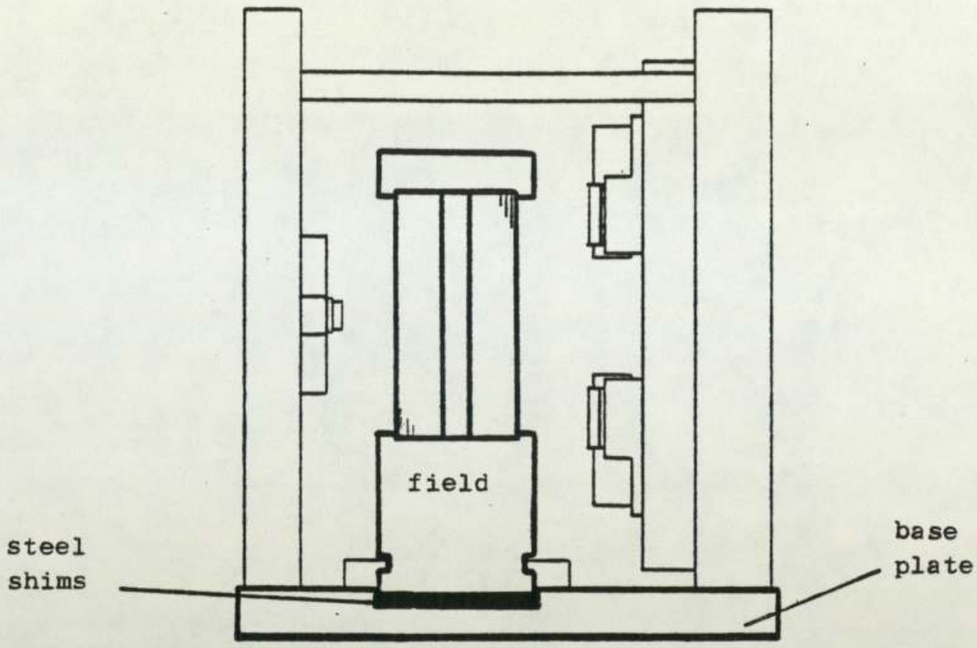

Insertion of steel shims to produce an asymmetric air gap in the direct axis

Fig. 5.24

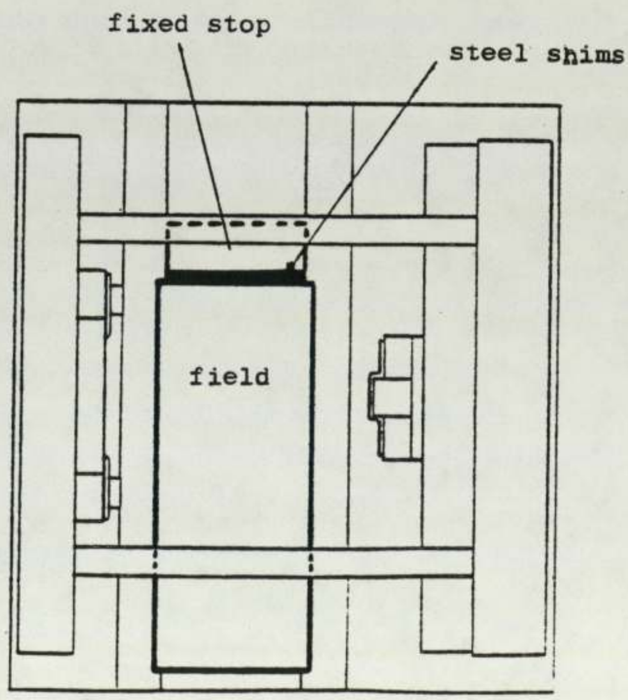

Insertion of steel shims to produce an asymmetric air gap in the quadrature axis

Fig. 5.25

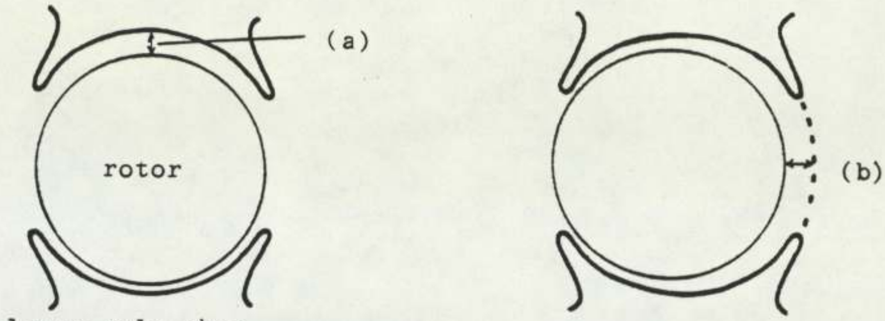

Asymmetric air gap (a) in the direct axis and (b) in the quadrature axis

Fig. 5.26

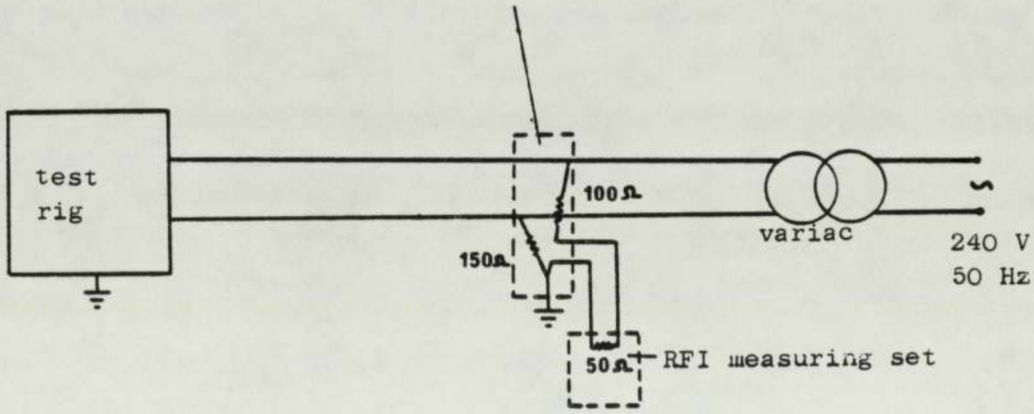

Test arrangement for measurement of conducted RFI

Fig. 5.27

INTERFERENCE (RFI/EMI) MEASURING RECEIVER, CISPR

FSME
1515

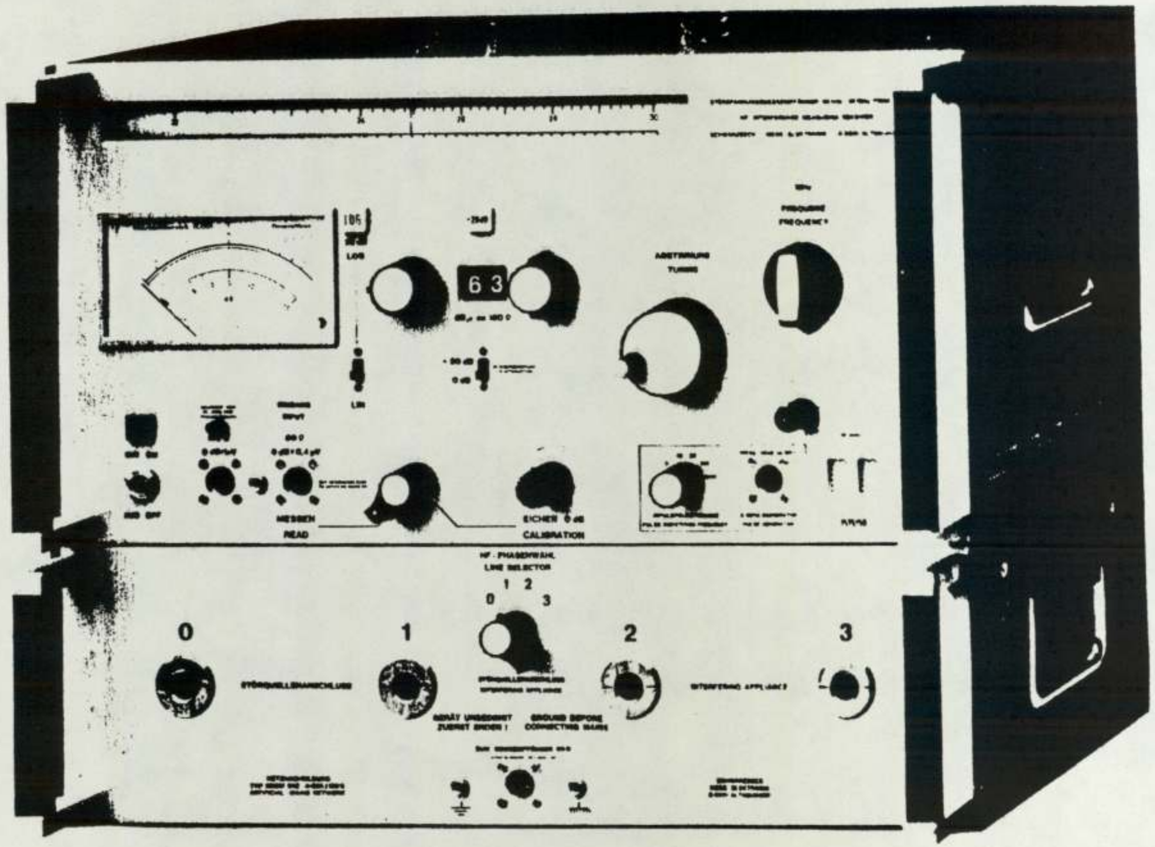

NNBM
8112

STANDARD ARTIFICIAL MAINS NETWORK

RFI measurement test equipment

Fig. 5.28

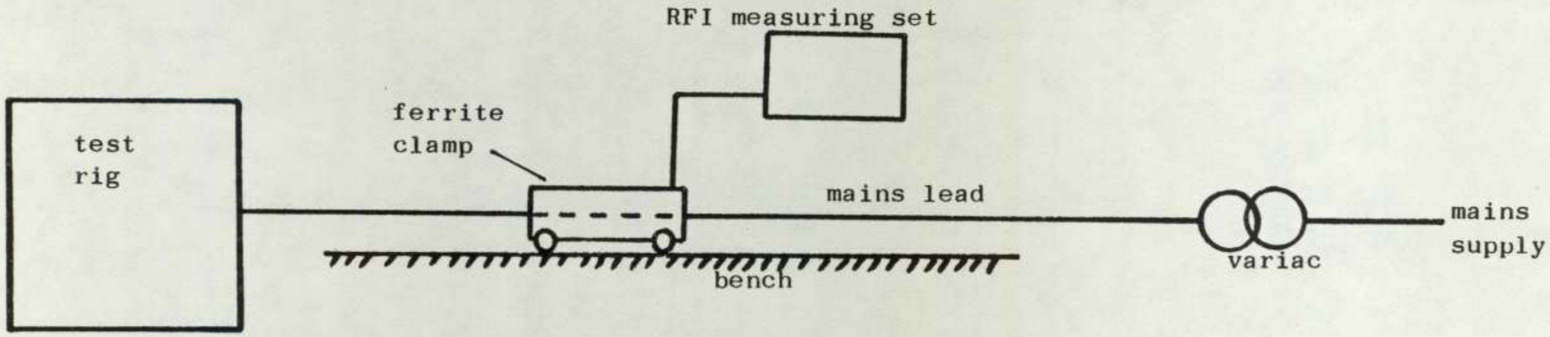

Test **arrangement** for measurement of radiated RFI

Fig. 5.29

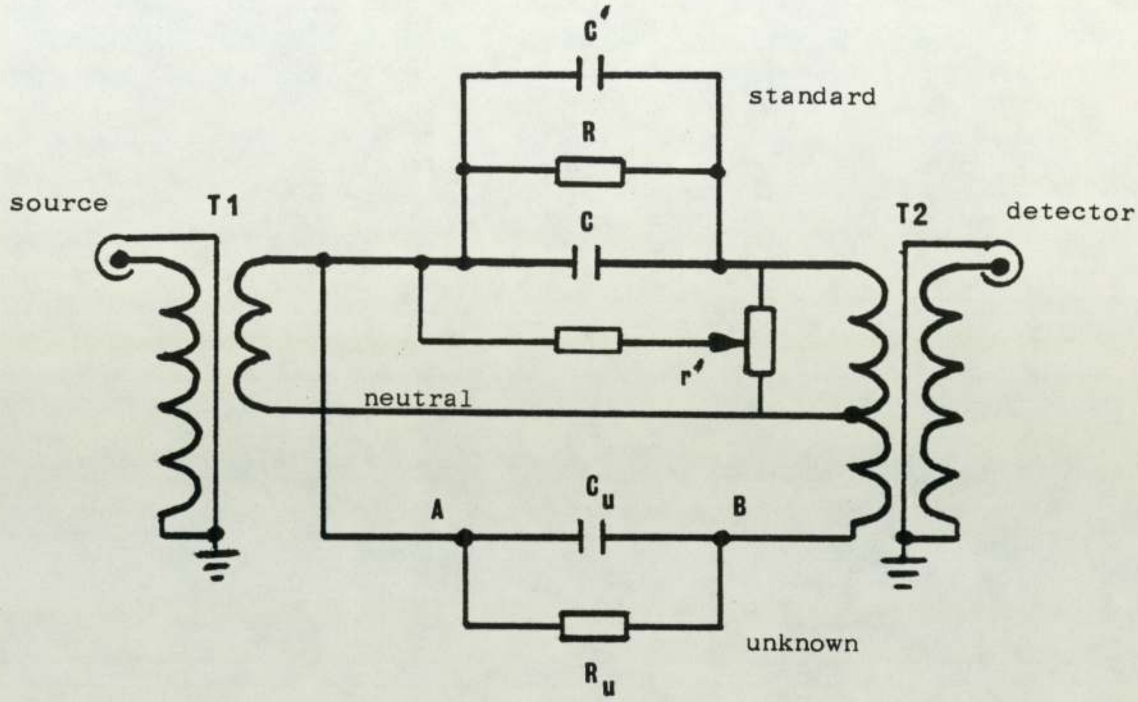

Simplified diagram of the r.f. bridge circuit

Fig. 5.30

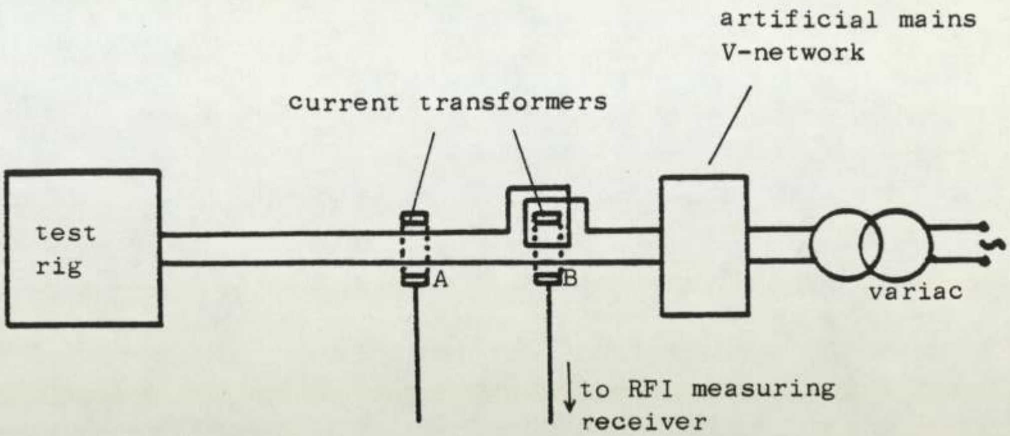

Test arrangement for detection of interference currents

Fig. 5.31

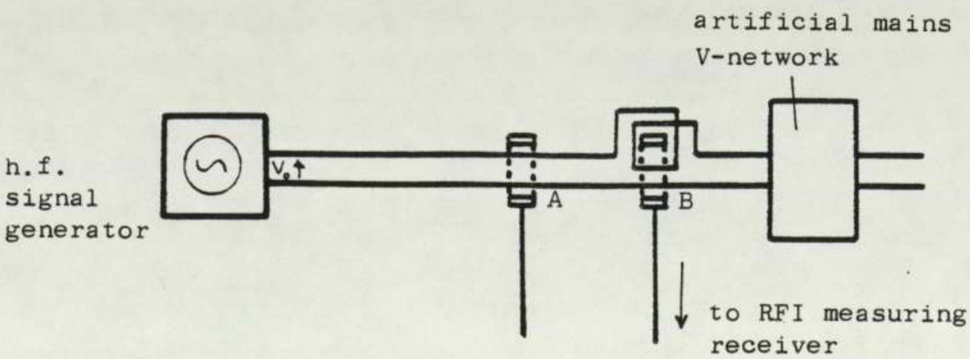

Substitution of test rig for a signal generator to
determine magnitude of interference currents

Fig. 5.32

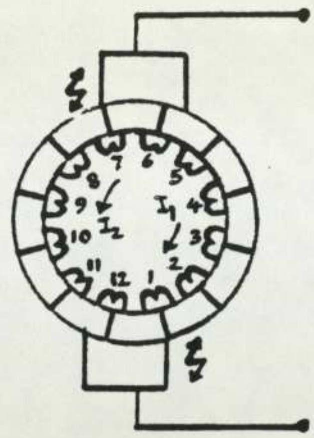

Armature coils 1 and 7 undergoing commutation

Fig. 5.33

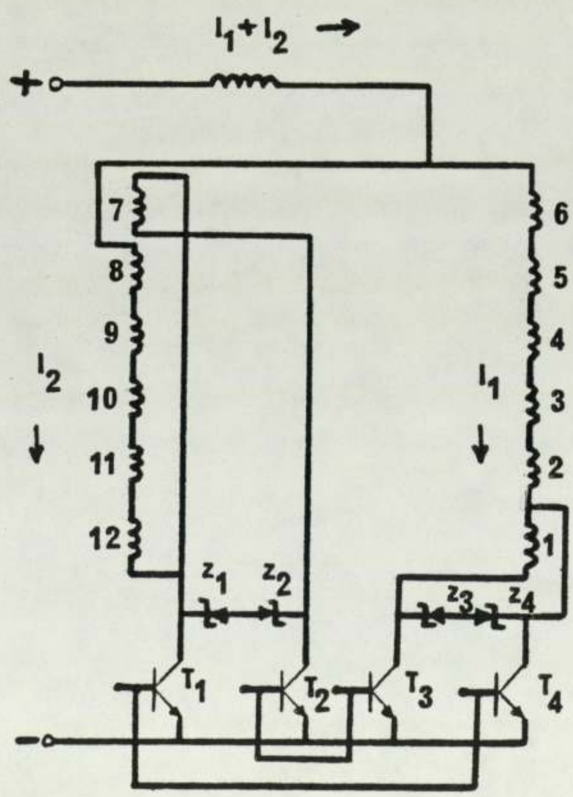

Test arrangement for measurement of active inductance (from Dijken [28])

Fig. 5.34

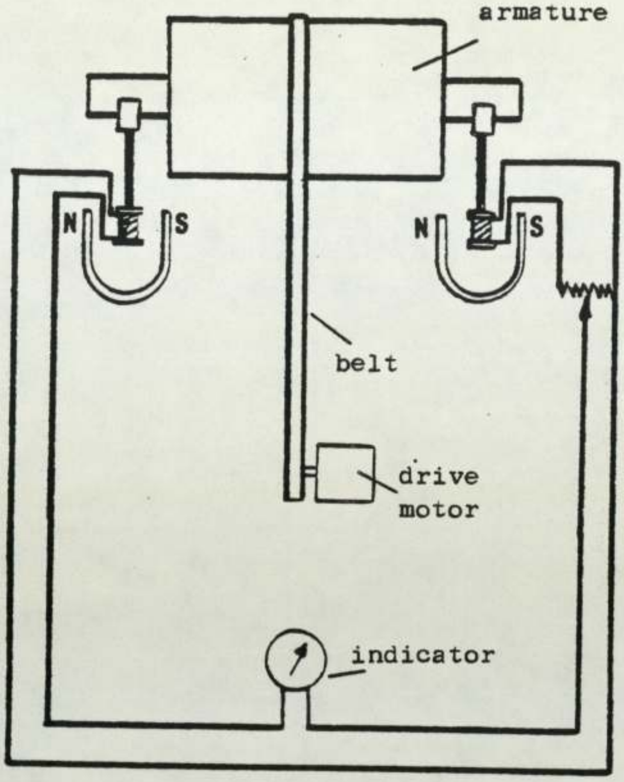

Measurement of armature unbalance

Fig. 5.35

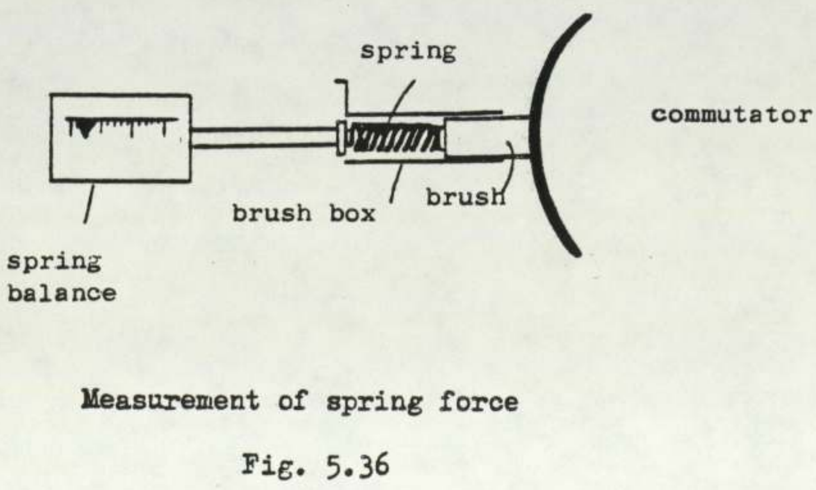

Measurement of spring force

Fig. 5.36

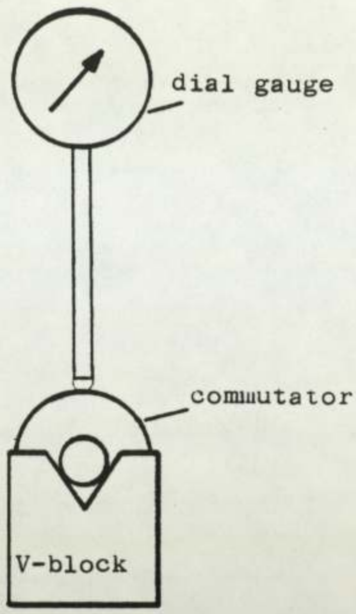

Measurement of commutator profile

Fig. 5.37

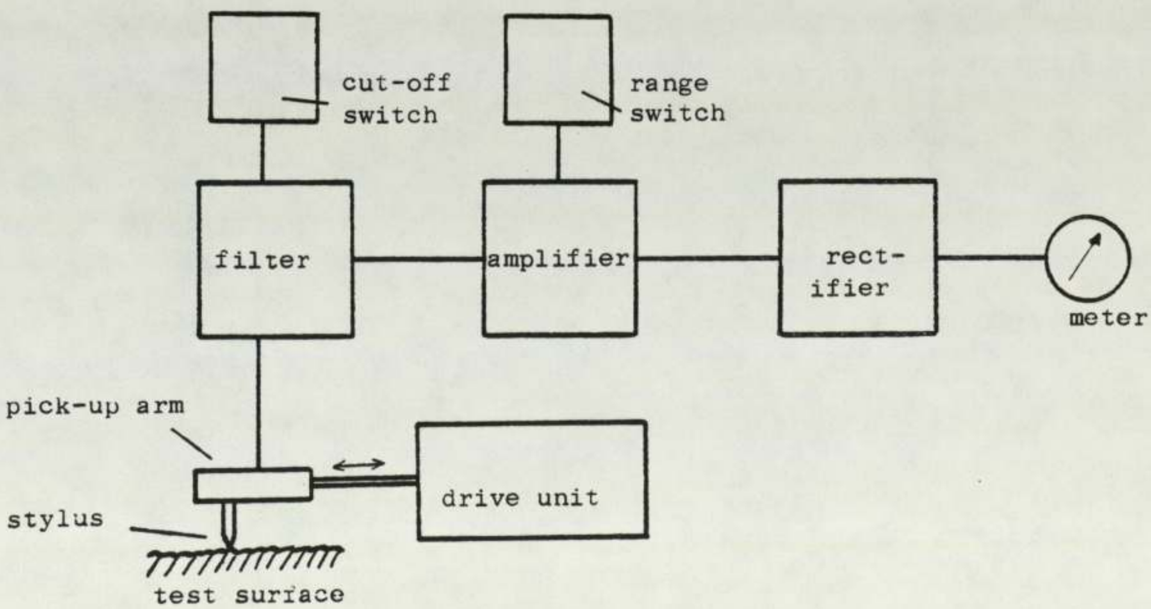

Block diagram of commutator roughness measuring equipment

Fig. 5.38

CHAPTER 6

TEST RESULTS AND DISCUSSION

6.1 RFI caused by the commutator switching action

6.2 RFI caused by the variation of the short circuited coil parameters

6.3 RFI due to the influence of the physical components of the armature and field

6.4 RFI due to the influence of mechanical variations in the motor assembly

CHAPTER 6

TEST RESULTS AND DISCUSSION

This chapter presents the results of the experimental study detailed in the previous chapter and the various points emerging from the results are discussed. The general test conditions were those as outlined in the 'Programme for Experimental Study', section 5.3, and measurements were made using the instrumentation and techniques described in section 5.4. The results of the measurements are tabulated in Appendix A2, for clarity data in this chapter is presented in graphical form. The graphs are constructed by firstly, plotting the actual test measurement points and then connecting the points by a series of straight lines, this is to represent the continuous nature of the interference spectrum across the frequency band. The frequency band of interest extends from 150 kHz to 300 MHz, for measurement purposes the band is divided into a) the low frequency region from 150 kHz to 30 MHz where the conducted RFI is measured in dB relative to 1 μV, and b) the high frequency region from 30 MHz to 300 MHz, where the radiated RFI is measured in dB relative to 1 pW. Thus in actual fact, the complete frequency band has to be represented by two graphs - one for each region. Again for clarity it proved more convenient to draw the two graphs adjacent to each other as shown in Figure 6.1.

The test results are detailed in the subsequent sections.

6.1 RFI caused by the Commutator Switching Action

It was intended to observe the levels of RFI generated by commutation without the influence of the e.m.f.'s generated in the armature coils. The test arrangement employed to do this is described in section 5.3.1. With the commutator rotated using the fan-air drive, RFI levels generated from the test rig were recorded at various speeds and brush current densities.

Tables A2.1 to A2.12 present the results obtained for increasing speed at 0.25, 1, 1.5, 2, 2.5 and 3 amps, using the 24 segment commutator. Similar measurements were made using the 22 and 21 segment commutators and these results are presented in Tables A2.13 to A2.24 and Tables A2.25 to A2.36 respectively.

Figs. 6.2 and 6.3, show sketches of the interference spectrums obtained at various speeds using the 24 segment commutator at 1.5A and 2.5A respectively. It can be seen that although the overall level of the RFI measured varies, the shape of the interference spectrum remains fairly consistent; the conducted RFI falls steadily by approximately 30 - 50 dB from 150 kHz to a minimum between 1 and 2 MHz, beyond which the RFI increases slightly with occasional peaks of interference up to 30 MHz.

The radiated RFI falls steadily by approximately 10 - 15 dB from 30 MHz to 300 MHz, showing only small variations of interference in the h.f. hand. The shape of the interference spectrum is governed predominantly by the stray capacitances and inductances in the test set-up. As discussed in section 1.4, these have the effect of 'tuning' the interference giving rise to the peaks and troughs of interference throughout the frequency band. The shape of the interference spectrum from the 24 segment commutator shown in Fig. 6.2 was also found to be common to the 22 and 21 segment commutators as indicated in Fig.6.4 and Fig.6.5, thus can be considered as the 'characteristics' shape of the test set-up.

The factors affecting the generation of RFI at the commutator was summarised by Short [91] as;

(a) Noise due to current switching

(b) Noise due to arcing at the end of commutation

(c) Noise due to arc conduction between the sliding copper and carbon contact, 'surface noise'.

(a) and (b) are inherent in commutation, but Motter [1], showed that surface noise (c) was also present on slip rings, where commutation is absent. Thus, in order to assess the influence of surface noise in relation to the RFI generated by the switching action of the commutator in the test set-up; RFI measurements were made using a rotating slip ring brush contact in the test-rig. The test results are presented in Table A2.37 to A2.40.

The main features of the test results are discussed below.

6.1.1 Speed Influence

Fig. 6.6, shows the influence of increasing speed on RFI levels generated using the 24 segment commutator at 1.5A. There is a sharp rise in interference from standstill to approximately 5000 - 6000 r/min, at this point the rise in interference levels off rapidly, such that beyond approximately 8000 r/min the levels of RFI remain fairly constant. At 20,000 r/min the levels of RFI can again be seen to rise rapidly, during testing, it was observed that this rise was accompanied by severe arcing at the brush contact. With further increase in speed the arcing worsened to produce ringfire. It was apparent that this latter increase in RFI was due to noise generated by arcing resulting from the instability of the commutator/brush contact at high speeds. The noise due to arcing overshadows the noise due to current commutation, which appears to have levelled off at around 8000 r/min.

Tests carried out on the 22 and 21 segment commutators showed no stability problems and as can be seen in Fig.6.7 and Fig.6.8 showing the speed influence on RFI for the 22 and 21 commutators respectively; there is no sudden increase in RFI at high speeds as observed in Fig.6.6. Figs.6.7 and 6.8 are similar in shape, there is an initial rapid rise in RFI from standstill to around 8000 r/min, at which point the rise in RFI levels off such that beyond approximately 10,000 r/min the RFI remains fairly constant.

Disregarding the effect of contact instability in Fig.6.6 at present, it can be seen that the speed influence on RFI levels for the three commutators show a similar trend, the only difference being the initial rate of rise of RFI from standstill. The shape of these curves can be explained by examining the response of the RFI measuring set Fig. 4.31 shows the pulse response curve of the Quasi-peak, measuring receiver, for pulse repitition frequencies (PRF's) greater that approximately 5kHz the pulse response curve is almost flat, such that the output of the Quasi-peak detector becomes relatively independent of the PRF.

It would be expected that the levelling off of RFI at around 5000 - 6000 r/min on the 24 segment commutator as shown in Fig.6.6, would correspond to a PRF around this frequency. The simple calculation shown below shows that this is in fact true;

Impulsive noise is generated as current is switched by the rotating commutator, for each revolution of the 24 segment commutator, there are 24 switchings at each brush, thus a total of 48 RFI pulses per revolution.

Therefore at 6000 r/min

$$PRF = (6000/60) \times 48 \text{ kHz}$$

$$= 4.8 \text{ kHz}$$

Similar calculations for the 22 and 21 segment commutator show that the levelling off of RFI in Figs.6.7 and 6.8, also correspond to PRF's of this order.

The shaft speed of motors used in household appliances varies from between 10,000 to 20,000 r/min, it can be seen from these results that, due to the pulse response characteristic of the RFI measuring set, RFI levels due to the commutating current in this speed range remain relatively independent of speed.

In Fig.6.9, the CISPR/EEC limits to RFI levels from motors is superimposed onto the interference spectrum of the 24 segment commutator at 16,000 r/min (curve (a)). It can be seen that even without the influence of armature coils the commutating current generates high levels of RFI. At low frequencies (below 500 kHz) the RFI levels fall outside the statutory limits. The excessive arcing due to brush instability at high speeds on the 24 segment commutator generates additional RFI which exceeds the limits over much of the frequency band (curve (b)). Thus it can be seen that the commutator action itself is capable of generating unacceptable levels of RFI. The commutator is an inherent feature of this type of motor and thus high levels of RFI can be expected from its operation. By adequate mechanical design however the additional RFI due to arcing caused by brush instability can be prevented.

In the design of the test rig, attention was given to the possibility of brush instability and thus the brush box assembly was mounted rigidly to overcome these problems. It can be assumed therefore, that the brush instability observed using the 24 segment commutator resulted from irregularities of the commutator (this is supported by the fact that no instability problems were observed on using the 22 and 21 segment commutators at high speeds). Tests were carried out to measure the brush movement on the three commutators and the results are presented in Fig.6.10. Curves (b) and (c) of the 22 and 21 segment commutator respectively, show the maximum brush movement increased from approximately 0.025 mm to 0.075 mm across the speed range without causing any contact problems. Curve (a) of the maximum brush movement of the 24 segment commutator shows that in the region where heavy sparking was observed, the brush movement increases rapidly to around 0.15 mm.

As described in section 4.2.1, the normal conduction between the commutator and brush is by a series of conducting arcs at the brush surface. When the contact separation is increased many of the conducting arcs are broken such that conduction is maintained only by one or two arcs. With greater separation as in the case of the excessive brush movements on the 24 segment commutator, the arcs are drawn until the electric field intensity is reduced sufficiently for the arcs to break momentarily thus breaking the actual commutator-brush contact resulting in the high levels of RFI observed in Fig.6.2. Further tests on the variation of RFI due to commutator irregularities, are presented in section 6.4.

6.1.2 Influence of current

The brushes used were capable of conducting currents up to approximately 2.5A, but tests were carried out increasing the current from 0.25A up to 4A to observe the effects on RFI at the high current densities as well as in the normal operating region of between 1 and 2A. Fig.6.11, shows the influence of increasing brush current on RFI levels generated using the 24 segment commutator at 14,000 r/min.

The RFI levels remain nominally constant across the frequency range, varying only by approximately 2dB from 0.25A up to 2.5A. At higher currents there is a significant rise in RFI, during testing this increase was noted to have been accompanied by arcing and occasional streamers at the brushes. It was evident that the excessive heat generated at the brushes at the higher currents caused contact bursting, resulting in arcing at the face of the brushes. The streamers were particles of white hot brush material thrown out from under the brushes by the rotation of the commutator. These effects cause excessive brushwear and irregular contact areas, which along with the noise generated by the arcing, is condusive to an increase in the levels of RFI observed in Fig.6.11 [94].

The main feature of interest in Fig.6.11, is in the normal brush operating region below 2A, the RFI levels are unaffected by changes in the brush current. The results indicate that the magnitude of current switched at the commutator does not influence the levels of RFI produced. Similar results were obtained on the 22 and 21 segment commutators as shown in Fig.6.12 and 6.13, respectively. Quelch and Hall [10], concluded from their tests that it is the variation of brush contact resistance during commutation that is of importance, and it appears that it is this variation rather than the magnitude of the switching current which leads to high levels of RFI at the commutator. It is true that contact resistance is dependent on the brush current, but the test results show that this variation seems to have little affect on the ultimate levels of RFI obtained.

RFI levels were observed as the brush current was reduced from 0.25A, it was found that the RFI levels remain fairly constant at the high levels shown in Fig. 6.11, falling rapidly only when the current is reduced to a few mA. An interesting observation made was that even when no current was supplied to the test rig, rotation of the commutator caused low levels of RFI to be generated. No report of this phenomena has been found in the literature, it is of interest since it shows that the brush-commutator arrangement is in fact itself a generator of RFI - albeit very small.

Measurements were made of this interference for increasing commutator speeds and the results are presented in Tables A2.41 to A2.46.

Fig.6.14, shows the interference spectrum generated by rotation of 24 segment commutator with zero current at various speeds. It can be seen that the RFI is rapidly attenuated in the low frequency band below 1MHz. At around 150kHz though, the RFI levels are significant, the RFI levels increase with speed, rising to over 25 dB at 22,000 r/min. Fig.6.15, shows the influence of speed on the RFI levels at various frequencies, the main observation is that the increase in RFI is almost linear with speed above 2000 r/min, such that with further increases in speed above 22,000 r/min, it would be expected that the levels of RFI in the low frequency region would become even higher.

A number of possible explanations as to the source thus this RFI are listed below, but it was decided that since the levels of RFI generated were low, no further detailed study to verify the explanations were carried out. The work is thus suggested as an area requiring further study in chapter 8.

The RFI could be generated by:-

(a) static electricity produced by 'contact charging' [139].

(b) thermelectric p.d. generated by friction at the sliding contact [94].

(c) The copper-moisture - air carbon contact resulting in the conditions required to produce a crude metal-air battery.[140]

Note: These are tenous hypothesis for an unexpected observation and require further detailed study for verification or otherwise of the source.

6.1.3 Surface Noise

As mentioned earlier part of the noise generated at the commutator is a result of normal arc conduction noise. This noise is equally present on slip ring contacts as on the commutator; thus tests were carried out on the test-rig using a slip ring in place of the commutator to observe, the amount of interference contributed by surface noise to the overall levels of RFI measured from the commutator.

Fig. 6.16 shows, the interference spectrums obtained using the slip ring with increasing speed at 1.5A. It can be seen that the RFI produced by surface noise is much less than that obtained on the commutator as seen in Fig. 6.2. Fig. 6.17, show the RFI spectrums for the slip ring and 24 segment commutator at 18000 r/min, it can be seen that surface noise is as much as 30 dB below the commutator RFI across the frequency band. Motter [1] considered that the factors affecting the amplitude of surface noise transients included, the brush material, brush pressure, rotation speed and brush current. The influence of slip ring speed is shown in Fig. 6.18, it can be seen that the RFI levels rise steadily as the rotation speed is increased. At the slip ring-brush contact there is a continuous formation and cessation of the conducting arcs during rotation, with increasing speed the rate at which this happens is also increased thus resulting in higher levels of RFI.

Fig. 6.19, shows the influence of brush current on surface noise, the RFI levels can be seen to increase with higher brush current, it is likely that the higher currents produce a greater number of conducting arcs which generate larger current disturbances during the process of arc formation and cessation again resulting in higher levels of RFI.

6.1.4 Summary of test results

(a) Commutation even without the influence of the short circuited coil parameters and the presence of the armature and field components can generate RFI levels which exceed the CISPR/EEC limits in the low frequency region.

(b) Surface noise generated between the rotating copper commutator and carbon brush face contributes as much as 20-30 dB RFI in the low frequency region to the overall RFI measured from commutation.

(c) At commutation pulse repitition frequencies of greater than around 5kHz the measured RFI levels remain relatively constant. Thus for small motors normally operating at speeds greater than 10000 r/min the measured RFI levels are independent of the number of commutator segments.

(d) Variation of brush current densities in the normal operating region of small motors has no observable influence on measured RFI levels from the commutator. However, at high current densities RFI levels are increased due to excessive heat generated at the brush face causing contact bursting and arcing resulting in increased brush wear and damage to the commutator surface.

(e) Low levels of RFI are generated from the rotating brush-commutator contact even when there is no external current source connected. These RFI components increase with speed but are attenuated above around 1 MHz.

6.2 RFI Caused by the Variation of the Short-circuited coil Parameters

In section 6.1, the RFI generated by the commutator switching action was observed, in this section the additional influence on RFI levels due to the parameters of the short circuited coil are examined. The test arrangement employed to observe this influence is described in section 5.3.2. Current in a circuit branch BC, representing the armature coil, is commutated by means of a commutator and slip rings arrangement as shown in Figure 5.13. The short-circuited coil parameters include:

a) coil resistance, (Rs)

b) coil inductance, (Ls)

and c) a circuit e.m.f. composed of the transformer e.m.f. and rotational e.m.f. generated in the coil during the time of commutation, (e).

With the commutator rotated using the fan-air drive, these parameters were introduced to branch BC in turn and varied to observe their influence on RFI. Measurements of RFI were taken at 5000, 10,000, 15,000 and 20,000 r/min for brush current of 0.5, 1.5 and 2.5A respectively. Details of the test condition and the results obtained are presented in the sections below. In section 6.1 it was found that RFI levels from the commutator without the influence of the armature coil parameters in this current range and at speeds above 10,000 r/min remain relatively constant. Thus any significant changes in RFI levels observed during the variation of branch BC could be related to the appropriate parameters under test.

The surface noise generated at the slip ring pair, is small in comparison with the noise generated at the commutator as shown in section 6.1.3, thus their effects can be neglected in tests presented in this section.

6.2.1 Resistance Commutation

The inductance elements of the circuit branch BC, were removed leaving only a resistive commutation circuit. The resistance was increased in stages from zero to 20Ω, RFI measurements were recorded and the results are presented in Tables A2.47 to A2.70. Figs. 6.20 to 6.23 show the interference spectrums obtained for increasing resistance at 5000, 10000, 15000 and 20000 r/min using 1.5A brush current.

It is evident from the sprectra obtained that RFI levels rise with increasing resistance. At the low speed (Fig. 6.20), below 5Ω where sparking at the brushes was minimal, it can be seen that the increases in RFI levels are greatest in the low frequency region at 150 MHz but the levels reduce steadily as the frequency is increased, such that above 3.5MHz, there is a variation of less than

2 dB in overall RFI levels extending into the h.f. region to 300 MHz. Further increases in resistance were accompanied by an increase in sparking at the brushes, this contributed to an increase in RFI particularly at frequencies above 1 MHz, with the greatest rises appearing around 10 MHz, but in the h.f. region the RFI levels continue to rise, becoming very erratic and difficult to measure. Fig. 6.24, shows the manner in which RFI increases at various frequencies across the r.f. band with increasing resistance at 5000 r/min. RFI rises steadily with small increases in resistance but levels off at around 6Ω. In the h.f. region at 90 and 300 MHz, there is a negligible change in RFI levels at these low resistance values and appear only to rise with the onset of sparking at the higher resistance. Similar observations can be made from the interference spectra obtained at the higher speeds; the influence of resistance variation is to increase RFI levels in the low frequency region - but the increases are attenuated as the frequency increases above around 3.5 MHz. With the onset of heavy sparking at the brushes at the higher resistance values, there is a further increase in RFI levels, but this increase appears to be most affected in the r.f. band above 1 MHz extending through to the h.f. power measurement region from 30 to 300 MHz. The manner in which RFI levels increase at various frequencies due to the influence of resistance commutation at the higher speeds is shown in Fig. 6.25 to 6.27.

The effect of variation of brush current showed an increase in overall RFI levels by approximately 6 dB from 0.5A to 2.5A, at the lower speed, although at the higher speeds this increase was greatly reduced to within 2 dB.

The influence of varying resistance on RFI levels can be explained in terms of the noise generated due to current reversal during commutation and also the noise generated by the sparking at the brushes as commutation is completed. The theory of resistance commutation was described in Section 3.3, it was discussed that linear current reversal can only be obtained if the resistance of the short circuited coil is zero. As resistance is increased the reversal of current is distorted as shown in Fig. 3.15. The rate of current reversal is a maximum at the beginning and end of commutation. Increasing the resistance leads to condition where the current is switched in two abrupt steps at the beginning and end of commutation.

Andone and others [108, 76] show that the more abrupt the changes in current, the greater the components of RFI generated. Their results also predict that the RFI components are greatest in the low frequency region and become attenuated at the higher frequencies. These features were observed in the interference spectra obtained from the test measurements described above; the increasing resistance causing an increasing distortion in current reversal which in turn increases the levels of RFI measured.

It becomes apparent that the increases in RFI levels observed in the h.f. region as the resistance values were increased above 6Ω, cannot be explained from Andone's results - but the observations made during testing, infer that these latter increases were due to noise generated in the sparking - which itself is caused by the abrupt changes in current.

In practice, armature coil resistance in small motors is less than

0.5Ω , thus it can be seen from the results, increases in RFI levels due to armature resistance in the normal operating region are only of the order of 2-3 dB in the low frequency region below 3.5 MHz. The case for resistance commutation is purely hypothetical, since coil inductance will always be present, test results presented in the following sections study the case for delayed commutation.

6.2.2 The Influence of Coil Inductance

Tests were carried out to observe the influence on RFI levels due to inductance in the commutating branch BC. Firstly, with the fixed resistor removed, inductance was introduced by connecting variable inductors in the circuit. Design details of the inductors are given in section 5.3.2.2. The resistance of the inductance coils was measured to be less than 0.15Ω, with all the coils in circuit. RFI measurements were recorded as the branch inductance was increased up to 1.3 mH, the results are presented in Tables A2.71 to A2.88. The tests were subsequently repeated with the addition of small fixed resistances in series with the inductor. Table A2.89 to A2.100, show the results obtained using fixed series resistances of 0.25 and 0.5Ω. The values of resistance were limited to these values since these were considered to be the typical order of magnitude expected for armature coils in the motors. Figs. 6.28 to 6.31, show sketches of the interference spectrums obtained using a brush current of 1.5A at 5000, 10,000, 15,000 and 20,000 r/min respectively. At 5000 r/min, (Fig. 6.28) it can be seen that even for inductance of only a few μH, the RFI levels increase significantly. At 25 μH, the greatest increase in RFI levels is below 10 MHz, increasing by approximately 10 dB at 1.4 MHz.

Above 10 MHz, in the high frequency region the increases in RFI levels are small. Intermittent pin-point sparking was evident at the trailing edge of the commutating brush. Increasing the inductance to around 500 µH, caused further increases in RFI levels but the shape of the interference spectrum, remains consistent. The degree of sparking also worsened with heavy sparking across the full width of brushes. For higher values of inductance the RFI levels remained fairly constant below around 6 MHz, but above this frequency the RFI levels continued to increase, becoming very erractic. At 10,000 r/min, (Fig. 6.29), again at low values of inductance the greatest increase in RFI levels was in the region below 10 MHz and this trend continued up to around 250 µH. At the higher inductances, the RFI levels continue to increase above around 6 MHz, whereas at the low frequencies, this rise is greatly reduced. At higher speeds it was observed that increases in RFI levels occur at inductances of only 10 µH, and rise further as the sparking worsens considerably with inductance. The greatest increase in RFI occur in the h.f. region where the RFI measurements became more difficult to measure due to the erratic nature of the readings obtained.

The influence of armature coil inductance is to delay the commutating current such that at the end of the time of commutation, current reversal is incomplete. The uncommutated current must fall rapidly to zero, but the change of current is opposed by a reactance voltage (i.e. Ldi/dt). if the reactance voltage is great enough ($\simeq$ 12V Ref: Dijken [28]), an arc is drawn between the leading commutator segment and the trailing edge of the brush as the current declines. In section 6.2.1, it was discussed that rapid changes in current, such as those experienced at the end of commutation, generate RFI components and have been referred to as the "noise of commutation". These RFI components are greatest in the low frequency region, decreasing steadily at higher frequencies. Thus the increases in RFI levels in the low frequency range observed in the test results is due to the increasing "noise of commutation", resulting from the influence of inductance on the commutating current. The effect of the sparking is to cause further RFI components referred to as the "noise of arcing". It is apparent from the test results that the RFI components of this latter noise are dominant in the high frequency region above around 6 MHz. The range of inductance used in these tests are typical of the values measured on small motors. It is clear that armature coil inductance causes significant increases in the RFI levels generated at the commutator, the following sections discuss the various influences observed.

6.2.2.1 Influence of speed

Fig. 6.32, shows the manner in which RFI levels increase at various frequencies as the inductance is increased at 5000 r/min. As observed from the interference spectrums above, at 0.15 MHz and 1 MHz RFI levels rise rapidly initially but become steady at around 500 μH. At the high frequencies, the RFI levels continue to rise although the rate of rise is reduced. Figs. 6.33, 6.34 and 6.35, show similar curves at 10,000, 15,000 and 20,000 r/min. It is evident that the initial rate of rise of interference increases with speed. Thus at high speed small values of inductance in the commutating circuit can cause significant increases in RFI.

In section 6.1.1, it was found that without the influence of armature coil parameters, RFI generated at the commutator remains fairly constant at high speeds. Thus the speed influence observed from the test results, can be attributed to the inductance of the commutating circuit and its effect on the commutating current. The rate of current decay during commutation is predominantly governed by the ratio (L/R_b). During commutation, the current falls exponentially at this decay rate until the time of commutation elapses. The reversal of the remaining uncommutated current I_c, causes the increases in the levels of RFI indicated in Figs. 6.28 to 6.31. The time of commutation is inversely proportional to the rotational speed of the commutator; thus as the speed increases the time of commutation T_c is reduced. This decrease in T_c, means that at the end of commutation, the amount of uncommutated current, Ic, increases. The increase of Ic at higher speeds explains the speed influence on the RFI levels evident from the test results. The higher the value of Ic, the more abrupt the final change in current at the end of commutation, as discussed above this causes an increase in RFI components due to the "noise of commutation". If the reversal of Ic results in sparking this further increases RFI due to the "noise of arcing".

6.2.2.2 Influence of current

Figs. 6.36, 6.37 and 6.38, show the interference spectrums obtained at 15000 r/min, for increasing brush currents at 50 μH, 100 μH and 500 μH respectively. At low inductance RFI levels remain relatively unaffected by increases in brush current, but at 100 μH, it can be seen that RFI increases in the frequency region above 6 MHz at the higher brush currents. It was observed that the degree of sparking is also worsened at the high brush currents. Similar results were observed at 500 μH where again the RFI levels above around 6 MHz are increased at the higher brush currents.

The current influence on RFI levels can again be explained by the commutating current; Fig. 6.39 shows the commutation of currents Ia_1 and Ia_2, where Ia_2 is greater than Ia_1. The rate of decay $e^{-(R_b/L)t}$, is the same, thus at time T_c the currents have fallen to Ic_1 and Ic_2 respectively. Although the ratio of Ia_1/Ic_1 and Ia_2/Ic_2 are the same. It can be seen that Ic_2, is obviously greater than Ic_1. It is thus apparent that increase in brush current results in an increase in the amount of uncommutated current at the end of the time of commutation. As described in section 6.2.2.1, the high uncommutated current results in increased brush sparking and also higher RFI levels. Nelson and Deihl [94] commented that as brush current density is raised, more heat is generated at the brush-copper contact, this hastens the formation of the oxide film on the commutator which can alter the brush contact resistance. The variation of brush contact resistance can affect the "surface noise" generated at the commutator and also the current decay time constant (L/R_b) which in turn directly affects the "noise of commutation".

6.2.2.3 Influence of series coil resistance

The results presented in Tables A2.89 and A2.100, show that there is minimimal influence on RFI levels due to the addition of small resistors in series with the variable inductors in branch BC. The series resistance Rs has negligible effect on the decay time constant and hence negligible effect on commutation and RFI.

6.2.3 RFI Caused by the Influence of Transformer e.m.f.'s and Rotational e.m.f.'s generated in the commutating coil

In Section 4.4, it was discussed that during commutation, the short circuited coil is subjected to influence of a transformer e.m.f., e_t and a rotational e.m.f., e_{rot}, generated within it. These e.m.f.'s can be considered to be components of a single 'circuit' e.m.f., e, where;

$$e = E_{max} \sin (wt + \psi) \tag{3.26}$$

$$E_{max} = \sqrt{(E_{rot}^2 + E_t^2)} \tag{3.27}$$

and $$\psi = \tan^{-1} E_t/E_{rot} \tag{3.28}$$

The circuit e.m.f. is alternating at the main current frequency, but lagging behind it by an angle ψ. Depending on the magnitude of the two e.m.f.s, e_t and e_{rot}, ψ, can lag from 0^o to 90^o, behind the main current.

Tests were carried out to observe the influence of the combined circuit e.m.f. on RFI levels due to commutation. A voltage variable in magnitude and phase, was injected into the commutating branch BC by means of a transformer arrangement described in section 5.3.2.3. Firstly, with the series elements in branch BC removed, such that the branch impedance comprised only of the inductance and resistance of the transformer coil, (these were 230 μH and 0.13Ω respectively). Measurements of RFI were recorded at 15,000 r/min using brush current of 1.5A for increasing circuit e.m.f.'s up to 8V (peak).

The results obtained are presented in Tables A2.101 to A2.103, for phase shifts (ψ) of 0^o, 45^o and 90^o, respectively. The tests were subsequently repeated after adding the variable inductors in the commutating branch and adjusting them to give total inductances of 500 μH and 1 mH. The results obtained are presented in Tables A2.104 to A2.109.

Figs. 6.40, 6.41 and 6.42, show sketches of the interference spectrum obtained with the different inductances at $\psi = 45^o$. At 230 μH, (Fig. 6.40) circuit e.m.f.s. of less than approximately 4V have minimal affect on the RFI levels measured. Further increase in voltage tend to increase the RFI levels across the frequency band and as the voltage exceeds 6V, the RFI levels rise significantly in the high frequency region. This latter increase in RFI was observed to be accompanied by severe arcing at the brushes. Similar results were obtained at the higher inductances as indicated in Figs. 6.41 and 6.42.

Figure 6.43, indicates the influence of the combined transformer and rotational e.m.f.s. on the reversing current, which is continually changing as the commutator rotates. At any instant if the circuit e.m.f. is opposing the direction of commutation, then the reversing current is delayed, as it is with the reactance e.m.f., thus as the end of the time of commutation the reversal of the uncommutated current contributes to increases in the levels of RFI. If the circuit e.m.f. is such, that it is in the same direction as the reversing current, then commutation can actually be improved as the current generated by the circuit e.m.f. assists the reversal of current. This case would obviously contribute to 'reduce' RFI. If, however, in this latter case the circuit e.m.f. is too large, the reversing current is over-commutated such that at the end of the time of commutation, the reversal of the over-commutated current can again cause increases in RFI levels.

It is apparent from the test results that there is a minimum 'threshold voltage', at which commutation is not adversely affected by the circuit e.m.f. and the RFI levels remain unaffected. Above this threshold voltage (round 4V), commutation is worsened, resulting in increased sparking and higher levels of RFI. At the onset of arcing at the brushes, the additional "noise of arcing" generated causes further RFI increases in the the h.f. region. The influence of variations in phase shift ψ and the magnitude of brush current are discussed below.

6.2.3.1 Phase Shift (ψ) Influence

With increasing phase shift the peaks of the circuit e.m.f. coincide with the zero crossing of the main current, as shown in Fig. 6.43 this has an adverse effect on commutation in this region. Fig. 6.44 shows the interference spectrums obtained using a branch inductance of 230 μH, with an injected circuit e.m.f. of 4V at 0^{o}, 45^{o} and 90^{o}. It can be seen from the curves that RFI levels increase with phase shift as expected. At $\psi = 90^{o}$, it was observed that sparking at the brushes was also worsened, becoming heavier. This is also evident from the RFI spectra showing the greatest increases in RFI levels in the h.f. region.

In small motors the phase shift results from the transformer e.m.f. component of the circuit e.m.f; this lags the main current and the rotational e.m.f. by 90^{o}. It is evident from the results that the transformer e.m.f. must be minimised to reduce increases in RFI levels and brush sparking.

6.2.3.2 Current Influence

RFI measurements were recorded at brush currents of 0.5A and 2.5A as the circuit e.m.f. was increased with the phase shift set at $\Psi = 45^{\circ}$, using a branch inductance of 230 μH. The results obtained are presented in Tables A2.109 to A2.111. Figs. 6.45 and 6.46 show sketches of the interference spectrums obtained. At 0.5A (Fig. 6.45), it can be seen that RFI levels begin to show an increase as the circuit e.m.f. is increased to only 2V, (in the test results shown earlier in Fig. 6.40, where a brush current of 1.5A was used, RFI levels remained relatively unaffected until the circuit e.m.f. was increased to 4V). At the higher brush current of 2.5A (Fig. 6.46), RFI levels are similar to those obtained at 1.5A, until the circuit e.m.f. is increased to around 6V where it can be seen there is a greater increase in RFI levels in the h.f. region.

It is clear from Fig. 6.43, that if the circulating current produced by the circuit e.m.f. is larger than the commutating current, the reversal of current can be so adversely affected that commutation can only be completed by severe sparking at the brushes - it is essential therefore, to minimise the magnitude of the circuit e.m.f.

Puchstien & Kimberley [27] summarised the findings of other authors as to the permissible levels of transformer voltages in the short circuited coil to give an acceptable quality of commutation in various motors and generators. The values range from 2V to 6.9V depending on the size of motor tested. From the results it appears that for small motors there is a threshold voltage of around 4V below which the circuit e.m.f. has minimal effect.

6.2.4 Summary of test results

(a) Distortion of current by resistance commutation increases overall RFI levels, however the values of coil resistance normally measured on small motors (less than 1 ohm) would only cause increases of the order of 2-3 dB in the low frequency region.

(b) The influence of reactance voltage (Ldi/dt) generated by the commutating current in the presence of coil inductance is to increase RFI as follows:

i) the reactance voltage delays the commutating current such that there is an abrupt change in current at the end of commutation. This distortion of the commutating current leads to increased RFI components in the low frequency region, attenuating as the frequency is increased.

ii) arcing at the end of commutation as the stored inductive energy ($1/2\ Li^2$) is dissipated generates further RFI components and these have been found to predominate in the region above 10 MHz extending across the high frequency region.

The magnitude of reactance voltage is dependent both on rotational speed and the magnitude of the switching current, thus an increase in either parameter further increases the overall RFI levels.

(c) The influence of the circulating current generated by the transformer and rotational voltages generated in the commutating coil is to periodically overcommutate and undercommutate the switching current. As above the resulting distortion of current and arcing generate RFI components which increase the overall RFI levels.

6.3 RFI due to the influence of the physical components of the armature and field

Commutation and the influence of the parameters of the short circuited coil have been isolated and the measurements of RFI obtained have been detailed in the previous sections. This section presents the results of RFI measurements associated with the armature and field components of small motors. Section 5.3.3 details the tests carried out to determine the levels of RFI generated by the various motor components.

The technique used was to build the test rig up in stages, measuring RFI levels at the addition of each component, such that the influence of that component on the overall RFI levels could be assessed. Measurements were recorded for the following test arrangements:-

a) Field windings only (section 6.3.1)

b) Field winding and field lamination stack (section 6.3.2)

c) Complete field system and unwound armature in the field air gap (section 6.3.3)

d) Fully wound armature with field system removed (section 6.3.4)

e) Complete motor; fully wound armature and complete field system (section 6.3.5)

For arrangements (c) and (d) it was necessary to rotate the armature externally by means of the fan-air drive described in section 5.2.5. The various components made available by Hoover plc for these tests include:

i) a single coil U-type field system

ii) a twin coil O-type field system

iii) 12/24 armature (i.e. armature windings distributed in 12 slots around a 24 segment commutator).

iv) 7/21 armature

v) 11/22 armature

Test conditions and the components used are detailed with the results in the sub-sections below.

6.3.1 Field Windings only

The standard Hoover U-type field windings consist of a plastic bobbin wound with 670 turns of 0.4 mm gauge copper wire. These windings were excited at various currents via the artificial mains network as indicated in Fig. 5.27. No detectable levels of RFI were observed either by conducted interference or radiated power measurements.

6.3.2 Field Windings and Field lamination stack

Tables A2.112 to A2.114, show the RFI levels obtained from the U-type and O-type field arrangements at excitation currents of 0.5, 1, 1.5 and 2A. Fig. 6.47, shows sketches of the interference spectrums obtained from the U-type field. At 0.5A the levels of RFI observed were negligible, but as the current was increased then it can be seen that the measured RFI at 0.15 MHz increases to a maximum of approximately 6dB at 2A. The RFI is rapidly attenuated at higher frequencies such that beyond around 0.25 MHz the levels cannot be detected. In the previous section, it was found that exciting field windings alone does not produce RFI, thus it is clear that the interference is caused by the magnetisation of the field laminations. When a steel sheet is magnetised an elongation takes place in the direction of magnetisation called 'magnetostriction'. [141] Excitation of an alternating magnetomotive force caused by elongations to be translated into periodic vibrations usually recognised as an audible 'hum' from the field stack.

Magnetostriction causes the field to appear as a periodically varying load to the mains supply generating the low frequency RFI components as observed above in the test results. It was considered that if the field vibration was increased, the RFI levels would also increase, this was confirmed by exciting a field with 'loose' fitting laminations, the measured results are sketched in Fig. 6.48. It can be seen that higher RFI levels are obtained as expected and it was also noted that the audible noise from the field was also increased.

6.3.3 RFI caused by the influence of rotor slots

The U-type field arrangements was mounted in position in the test rig and unwound armature rotors with 7, 11 and 12 slots were then assembled in the air gap in turn. Measurements of RFI were recorded across the field windings at increasing excitation currents with:-

(a) the rotors at standstill

(b) the rotors rotated (using the fan-air drive arrangement).

The test measurements are presented in Tables A2.115 to A2.124, the main features of the results are discussed below.

6.3.3.1 Rotor at standstill

The introduction of the rotors to the air gap caused a noticeable increase in audible magnetostriction noise from the test rig.

Observation of the measured RFI levels showed an increase of over three times the levels detected on the field alone. Fig. 6.49, shows a sketch of the interference spectrums obtained using the 12 slot rotor. It was noticed that the RFI measured with the rotor tooth under the centre of the pole was approximately 5dB higher than those measured with the slot under the centre of the pole. Wainart, [56] showed that the magnetic flux increases by approximately 15% with the tooth under the centre of the pole, causing a greater amplitude of magnetrostriction of the rotor laminations and thus a higher level of generated RFI. With loose fitting armature laminations again the magnetrostriction noise was found to increase further causing RFI levels to rise by as much as 20 - 25dB at the lower frequencies. In all cases, however, the levels are attenuated to zero at frequencies of above approx. 0.5 MHz. Measurements on the 7 and 11 slot rotors showed similar results although no influence of the slot number was evident.

6.3.3.2 Rotor at speed

Measurements of RFI levels were recorded with the rotors at 5000, 10000 and 20000 r/min and the field windings excited at 1.5A; the results are presented in Tables A2.122 to A2.124. It can be seen from the results that there is no detectable speed influence on the measurements. Rotating the unwound armatures by means of the fan-air drive caused the RFI levels to settle approximately mid-way between the maximum and minimum values observed at the two extreme stationary rotor positions discussed above. At the higher speed it was noted that the RFI even shows a slight decrease across the frequency range. The observations are in direct contradiction to the results presented by Quelch and Hall [10] for similar tests carried out on their test rig arrangement.

Although no information was given as to the number of slots on their rotor arrangement, their results show an increase with speed of up to 60 dB at 40,000 r/min with hardly any attenuation with frequency up to 1MHz, which led them to postulate that the interference was due to the mechanism of periodically varying capacitance between the metal parts of the machine caused by slot rotation. All three rotors tested above do not support the conclusions of Hall and Quelch with no significant difference in the RFI measured for each slot configuration.

It is felt that Hall and Quelch's conclusions result from the fact that they used a commutator motor to drive their test rig and the interference transmitted by this motor far out weighed the RFI generated within the test rig. The increase in RFI with speed, is probably the result of increased arcing at the brushes of the drive machine.

6.3.4 Wound armature with the field removed.

A 12/24 wound armature was fitted into the test rig with the field system removed. The windings were energised from the supply via brushes fitted in the normal position and the shaft rotated by means of fan-air drive. RFI measurements were recorded from the test rig at speeds of 5000, 10000, 13000 and 20000 r/min at 1.5A, the results are presented in Table A2.125.

Shaft rotation causes commutation of the main current in the armature windings, thus RFI is generated both due to the switching current and the resulting sparking at the trailing edges of the brushes. The quality of commutation is determined by the active inductance of the short circuited armature windings. The influence of transformer and rotational voltages in the commutating coil are absent since these are a function of the air gap flux, which has been eliminated by the removal of the field. Fig. 6.50, shows a sketch of the interference spectrums obtained. It can be seen that the shape of the spectrums is similar to those obtained from the commutation studies described in section 5.2.

The overall levels of RFI are as much as 30dB greater then the statutory CISPR/EEC limits at the higher speeds confirming earlier results that commutation is the major source of RFI in small motors. The speed and current influence of inductance commutation has been discussed in the earlier sections, the main point of interest observed during testing was that the RFI detector indication was very erratic, making precise measurements of RFI levels difficult. This type of erratic indication had been observed in the high frequency region in earlier tests where heavy sparking or arcing were particularly dominant. But in these tests, the erratic indication extended into the low frequency region even at 0.15 MHz, where the levels were varying by up to 5dB. In the earlier commutation studies, the parameters of the short circuited coil had been simulated by fixed circuit parameters. It was considered that the erratic variation of RFI levels could be associated with the variation parameters of the commutating coils by rotation. Dijken [28] showed that the active inductance, L_{comm} of the coils undergoing commutation was dependant on the precise brush contact at any instant, as this would affect the magnetic coupling of the armature coils. Armature rotation causes the brush contact to continually change thus the active inductance that the switching current must overcome at the end of commutation is also a variable. Measurements of L_{comm} were taken at various brush positions on the 12/24 armature as indicated in Fig. 6.51, it can be seen that the value of L_{comm} ranges between 124 μH and 379 μH.

From the RFI measurements presented in section 6.2.2 it can be seen that a variation of active inductance of this order can cause the RFI levels to change by approximately 10 - 15dB across the frequency spectrum. Thus the erratic RFI indication from the commutating armature is explained - the variation of active inductance of the commutating coils with rotation causes the generated RFI to deviate between the maximum and minimum levels determined by the maximum and minimum value of active inductance. The variation in RFI levels indicated by the Quasi-peak type detector are lower than the variation estimated from the interference spectrums shown in Fig. 6.31 since the detector output is a function not only of the amplitude of interference, but also its shape and repitition rate as described in section 4.3.1.

Further RFI tests to assess the influence of different armature designs is presented in section 6.3.5.3.

6.3.5 Fully wound armature and field systems (complete motor).

Test work described in this section was carried out in order to examine the levels of RFI produced due to different armature and field configurations. By connecting the armature and field windings in series via the brushes the test rig was driven as an independent motor, with motor load applied using the pony-brake arrangement described in section 5.2.6. As mentioned earlier, the test rig was designed to accommodate a U-type or O-type field stack and the choice of three different armature designs (i.e. 7/21, 11/22 and 12/24). The designs of these components was such that any combination of field and armature would give almost identical motor performance. The influence of the different components on the levels of RFI produced, was assessed from tests using the following test rig configurations:-

i) the field connected as a single lumped winding in series with a 12/24 armature.

ii) the field connected as a split winding connected in series either side of a 12/24 armature.

iii) configuration (i) with the 7/21 and 11/22 armatures.

The test rig was energised from a 240V, supply via a standard 150 Ω artificial mains terminating impedance. Motor load was adjusted to give a rated speed of 13000 r/min.

With this armature and field arrangement, all the interference generating sources isolated in the previous tests each make their contribution to the total RFI produced by the motor. The ultimate level of RFI detected by the measuring apparatus is subject to considerable modification as a result of the effects of stray capacitances and inductances which are present in the motor structure. These parameters may either attenuate interference currents by presenting a high impedance to their flow, or cause high peaks of interference where the interaction of capacitance and inductance gives rise to resonance conditions. The RFI measurements from the tests are presented in the subsequent sections. To explain the results it became necessary to make further measurements of various motor r.f. impedances and the asymmetric and symmetric RFI currents.

RFI current paths within the motor can only be effectively shown using a representative r.f. equivalent circuit of the motor and its associated wiring. Thus the use of simple r.f. models of the test rig arrangements have been made in order to discuss the essential features of the results obtained.

6.3.5.1 Field connected as a single lumped winding.

In this case, the field windings were lumped onto one side of the armature as indicated in Fig. 6.52(a). This is the normal connection arrangement for the U-type field system, but may equally well be used on the O-type field - connecting the two coil halves in series as shown in Fig. 6.52(b). RFI measurements were recorded using both field arrangements with:-

(a) the field windings connected to the line side of the mains supply (test rig frame connected to earth).

(b) the field windings connected to the neutral side of the mains supply (test rig frame connected to earth).

(c) repeat (a) with the earth connection removed.

(d) repeat (a) with the earth connected to the field laminations.

The results are presented in Tables A2.126 to A2.135. Fig. 6.53 shows a sketch of the interference spectrums obtained across line and earth (L-E) and across neutral and earth (N-E) using the U-type field system in arrangement (a). It can be seen that in the low frequency region, that the overall RFI levels are higher across N-E, but this level is still approximately 5 - 10dB lower in the low frequency region and almost 20 dB lower in the high frequency region than that measured on the 12/24 armature with the field removed in section 5.3.4 as indicated in Fig. 6.50. Thus the influence of the field is to reduce the measured RFI levels from the test rig, this reduction is primarily due to the field windings impeding the flow of interference currents generated at the motor brushes and is discussed further below. Another factor in reducing RFI levels with this arrangement, is the position of the brushes relative to the main flux; the armatures had been wound on conventional winding machines in the Hoover factory, the windings were displaced such that a brush shift of approximately 25^{o} is introduced when the brush axis is coincident with the quadrature axis. The brush shift improves commutation and its influence of RFI levels is examined later in section 6.4.13.

As mentioned above, with the field connected to the line side of the mains supply, the conducted interference measured across L-E is approximately 10 dB lower than that measured across N-E. Changing the field connections to the neutral side of the mains supply (arrangement (b)), also results in changing of the two RFI levels. In this case, the conducted interference measured across N-E is approximately 10dB lower than that measured across L-E (see Fig. 6.54). The shape of the interference spectrum in both cases is unchanged and the radiated interference spectrum remains unaffected by any change in field connections. These results can be explained with reference to the simplified r.f. equivalent circuit of arrangement (a) shown in Fig. 6.55. Neglecting the impedance of the mains cable, the only impedance to the flow of interference currents along the neutral lead is the r.f. armature impedance and the 150 Ω

terminal mains impedance, whereas the impedance to the interference currents along the line connection includes the r.f. impedance of the field windings. Fig. 6.56(a) shows the measured r.f. impedance across the U-type field windings. Below 1MHz the impedance varies between 10 and 20kΩ, at the higher frequencies the field windings appeared as a 60 pF capacitance as the impedance decreases steadily with frequency. This impedance has been attributed to the reactance of the interturn and interlayer self capacitance of the windings. It is clear that the r.f. impedance of the field is large in comparison with the 150Ω of the terminating mains network and is thus responsible for the difference in RFI levels measured at the line and neutral.

A further reduction in the RFI measured on the side at which the field is connected is caused by the diversion of the interference currents from the mains lead by the stray capacitance of the windings to the field lamination stack. Fig. 6.56(b) shows the measured r.f. impedance between the windings of the U-type field and the field lamination stack, it can be seen that although this impedance is higher than that of the windings, it is of comparable magnitude and thus offers an alternative path for the interference currents to flow. Fig. 6.57, shows the measured levels of RFI using the 0-type field there is a difference of around 5 - 10dB between the conducted interference levels across L-E and N-E, but it was noted that the levels of RFI at both sides was lower than that seen in Fig. 6.54. Thus it was expected that the two half coils connected in series on the 0-type field would exhibit a higher r.f. impedance than that observed from the single U-type field winding. This was confirmed by measurement as indicated in Fig. 6.58. Reference (103) states that mutual coupling between coils via the laminations is negligible, hence it was considered that the higher impedance results from the physical separation of the two coils causing a reduction in the total self capacitance of the windings. If we consider C to be the self capacitance of the single U-type field winding and C' to be the self capacitance of each of the half coils on the O-type field. It is obvious that C' is less than C because each half coils has less interturn and interlayer self capacitance. Connection of the two half coils in series results in the total self capacitance of the windings to be halved i.e. C'/2.

The lower self capacitance and hence higher series r.f. impedance of the field windings is desirable for the suppression of RFI. As shown above, in the case of the twin coil O-type field, there is a reduction in self capacitance by virtue of the series connection of the two half coils. Single (U-type field) winding self capacitance may be reduced by sectionalising the coils, thus reducing both their inherent interturn and interlayer self capacitance.

Measurements were further made of the asymmetric and symmetric interference current components for the two field systems, the results are shown in Figs. 6.59 and 6.60. The symmetric interference (Fig. 6.59) from the series twin coils is lower than that measured from the single coil, but the asymmetric components (Fig. 6.60) remains unaffected by the different fields. Thus it is likely that the reduction in RFI levels seen in Fig. 6.57 using the O-type field arrangement is due to a reduction in symmetric interference currents due to an increase in the field impedance discussed above. The lack of change in the asymmetric current suggests that most of this current flows via the neutral to earth (being unaffected by the change in field which is connected to the line side of the mains supply).

With arrangement (c), RFI measurements were repeated with the earth connection removed from the motor frame, thus removing the electrical connection allowing the asymmetric interference current to flow. Fig. 6.61, shows the measured RFI levels from the U-type field with this arrangement. It can be seen that the RFI levels at the line and neutral are the same and in fact 2-3dB lower than measured on the line in arrangement (a). Measurements of the asymmetric and symmetric currents for this case are shown in Fig. 6.62. The symmetric interference current is at the same level as detected in arrangement (a), but the asymmetric interference current is reduced as expected by the removal of the earth connection. The asymmetric interference is not totally eliminated since at radio frequencies, these currents are able to flow via the stray capacitance between the motor frame and field laminations to earth, although the very high impedance ensures that they are minimal. It also becomes apparent that the difference in RFI observed across L-E and N-E in the earlier tests was due to the asymmetric current component, the reduction of which causes the RFI at the two lines to be the same.

Finally, RFI measurements were taken with the test-rig connected as in arrangement (d) with the earth lead connected to the field laminations. Fig. 6.63, shows the interference spectrum obtained, the RFI levels as expected increase due to the low impedance path provided for the asymmetric currents to flow via the field lamination stack. But it is interesting to note that these RFI levels are lower than those obtained with the earth connected to the test rig frame, indicating that the majority of asymmetric currents flow via the armature laminations thus it is important to ensure there exists a high impedance between the armature windings and the armature laminations. The influence of this impedance is discussed in detail in section 6.3.5.3.

6.3.5.2 Field connected as a split winding either side of the armature

Fig. 6.64, shows a sketch of the field and armature connections, this is the normal configuration for the O-type field system. A special U-type field stack was wound with two coil halves such that it too could be connected in the split winding configuration for comparative tests. RFI measurements were recorded using both field arrangements both with and without the earth connection to the test rig frame, the results are presented in Tables A2.136 and A2.137.

Fig. 6.65, shows a sketch of the interference spectrum obtained using the O-type field system. The conducted interference at the line and neutral were virtually identical and the removal of the earth connection too, had negligible effect on the measured RFI levels. The main feature of these test results, is that with the split winding arrangement, overall RFI levels from the test rig are attenuated over much of frequency range to well below the CISPR/EEC limits. Fig. 6.65 shows a comparison with RFI levels obtained using the lumped winding configuration described in the previous section. It can be seen that the split winding reduces RFI levels by as much as 20dB in the low frequency region. At 0.15 MHz the interference is high, almost at the same level as that with the lumped winding; but as the frequency increases there is a rapid fall in interference by approximately 20dB up to 1 MHz. The downward trend continues at the higher frequencies but the fall in RFI is greatly reduced. A number of small peaks and troughs of interference can be seen at the higher frequencies, suggesting resonances of the stray capacitances and inductances within the test rig but even these do not cause the RFI level to exceed the CISPR/EEC limits. A similar large reduction in RFI was obtained using the special split winding wound on the U-type field stack as shown in Fig. 6.66. In this case, there is a much more rapid fall in interference in the frequency region below 1 MHz, but at the higher frequencies, the resonance peaks of interference are much more pronounced causing very little further reduction in RFI up to 30 MHz. In the high frequency region, there is very little reduction in RFI from that obtained using the lumped winding and the levels fall outside the CISPR/EEC limit up to around 100 MHz.

Figs. 6.67 and 6.68, show the measured levels of asymmetric and symmetric interference currents for both field arrangements. In both cases it can be seen that the asymmetric interference (Fig. 6.68) is very low, thus the balanced winding configuration causes the interference currents returning to earth to be minimised. This result also accounts for a negligible change in RFI observed with the removal of the earth connection. The symmetric interference currents (Fig. 6.67) are also much lower than those obtained on the lumped winding, it is this reduction which explains the lower levels of RFI obtained with the split balanced winding. Since the armature and motor supply have remained unchanged, it can be assumed that the amount of interference generated at the brushes is unchanged. Thus, the reduction in the symmetrical currents can only have been brought about by the winding configuration causing a short circuiting of the interference from the mains terminals. Measurements were made of the r.f. impedance between the two coils of both the field arrangements the results are shown in Fig. 6.69 a & b. In Fig. 6.69 (a) it can be seen that there is a large stray capacitance between the coils of the O-type field of the order approximately 800 pF. At radio frequencies this stray capacitance acts as a low impedances path to the symmetric interference currents - effectively removing this interference from the mains cable and thus reducing the overall measured levels of RFI. Fig. 6.70, shows a sketch of the r.f. equivalent circuit of the split winding arrangement indicating how the RFI generated in the motor is contained by the stray capacitance between the balanced windings. The r.f. impedance measured across the split coils wound on the U-type field stack is much higher than that on the twin coil field and also appears to increase at higher frequencies (see Fig. 6.69 (b)) thus accounting for the lack of RFI reduction obtained at the higher frequencies with this field stack. From these results it appears that the physical separation of the split coils on the O-type field contribute to reduce RFI levels by having a higher parallel stray capacitance whose value appears to be relatively constant over the radio frequency range.

6.3.5.3 The influence of Armature variations

It was intended to examine the levels of RFI obtained from the three different armature designs (i.e. 7/21, 11/22 and 12/24) in order to assess the influence of their design configurations. The test rig was fitted with the U-type field and measurements of RFI were recorded using each armature in turn; the results obtained are presented in Table A2.138. Fig. 6.71, shows the interference spectrums obtained from the three armatures. Below 0.5 MHz the RFI levels are very similar (within 1-2 dB) but at the higher frequencies the armatures each exhibit different spectrum levels. The interference from the 11/22 armature exhibited the highest overall RFI levels; falling by only 10dB up to around 10 MHz, but then decreasing by a further 15 dB up to 30 MHz. The RFI levels are again higher than the other armatures in the h.f. region but attenuate rapidly above 65 MHz. The interference from the 12/24 armature is approximately 5-6 dB lower than the 11/22 armature in the region between 1 MHz and 10MHz, but at higher frequencies up to 30 MHz the difference decreases to only approximately 3-4 dB and the shape of the interference spectrum becomes almost identical. In the h.f. region, resonance peaks and troughs cause the RFI levels to deviate by over 10 dB from the 11/22 spectrum and beyond 150 MHz the RFI attenuates rapidly to very low values of only 22 dB at 300 MHz. Finally, the 7/21 armature, in this case, the measured interference levels were slightly higher than the 12/24 at frequencies below 1 MHz, but at higher frequencies in the conducted interference region the RFI levels falls to lower than those exhibited by either of the other armatures. The interference falls steadily by approximately 25 dB up to 30 MHz being over 10 dB lower than the 11/22 armature between 2 MHz and 10 MHz. In the h.f. region up to 200 MHz, again the interference from the 7/21 armature is lower than the other armatures and the levels lie below the CISPR/EEC limits throughout the h.f. region. Above 200 MHz the interference from the 12/24 armature attenuates much more rapidly than the 7/21 armature. To determine the factors contributing to the differences in RFI levels of the three armatures it was decided to examine the various differences in their design and construction:-

(a) The number of commutator segments.

The interference spectrums do not show any trend of depending on the number of commutator segments. In section 6.1.1 it was found that at speeds greater than around 10000 r/min the commutation pulse repitition frequency (p.r.f.) from 21, 22 and 24 segment commutators has no significant effect on measured RFI levels.

(b) The number of rotor slots.

Again the test results do not show any trend of depending on the number of rotor slots. In section 6.3.3.2, it was found that the variation of rotor slotting had no detectable influence on measured RFI levels.

(c) Active inductance of the short circuit coils L_{comm}.

The active inductance of the armature coils can vary significantly depending on the precise brush contact at the point of commutation. Dijken [28] showed that there was also a considerable difference in active inductance between the armature coils wound at the bottom of the rotor slot and those at the top. Table 6.1, shows the maximum and minmimum values of L_{comm} recorded on each armature for coils wound at the bottom and top of the rotor slot.

The 11/22 and 12/24 armatures have two coil sides per slot whereas the 7/21 has three coil sides per slot. From the measurements of L_{comm} for each armature it is apparent that there is only a 10 - 15% difference between the top and bottom coils of the 11/22 and 12/24 armatures. But the coils in the 7/21 armature show a much wider variation; the top coils have values of inductance lower than both the other

Armature	Max. L_{comm} (μH)	Min. L_{comm} (μH)
12/24 Top Coil	330	112
12/24 Bottom Coil	379	124
11/22 Top Coil	396	115
11/22 Bottom Coil	460	127
7/21 Top Coil	324	76
7/21 Bottom Coil	470	130

Measured values of active inductance L_{comm} for top and bottom armature coils

Table 6.1

armatures, conversely the bottom coil has values of inductance far higher than the other armatures. Dijken, states that this variation in inductance explains why in small motors the commutator segments of the coils which are wound first often look worse than those wound last.

The wide variation in the values of L_{comm} obtained, makes it difficult to relate these values to the levels of RFI obtained. Suffice to say from the test results presented in section 6.2.2, that it is essential that coil inductance be kept to a minimum to reduce RFI.

It is likely that the differences in the interference spectrum is due in part to the different active inductances of the three armatures. This is not considered as the only factor contributing to the differences - increasing inductance of the short circuited coil was found to increase the measured RFI levels, but in most cases the overall shape of the interference spectrums remains unchanged. In Fig. 6.71, it can be seen that as well as the RFI levels being different for each armature, so also is the shape of overall interference spectrums - and this cannot be explained by increasing active inductance alone.

(d) <u>Transformer voltage generated in the short circuited coil.</u>

The transformer voltage generated in the short circuited coil undergoing commutation was measured on each armature, the results are presented in Table 6.2. Although the values can be seen to be much higher than those recommended in section

Armature	Transformer Voltage
11/24	9.24 V
11/22	10.47 V
7/21	9.88 V

Measured short-circuited coil transformer voltage on test armatures

Table 6.2

6.2.3 there is no trend emergency relating to the interference spectrums.

(e) Symmetric interference currents.

Fig. 6.72, shows the measured levels of symmetric interference currents generated from the test rig with the different armatures; again there is no significant difference in the levels to explain the differences in the measured RFI levels.

(f) Asymmetric interference currents.

Fig. 6.73, shows the measured levels of asymmetric interference currents generated from the test rig with the different armatures. The variation of these currents follow closely with the variation in RFI levels in the conducted interference region. Thus it becomes apparent that the major factor resulting in the differences in the three interference spectrums is the r.f. impedance of the armature windings to the armature laminations - since it is this impedance which contributes to a variation in the asymmetric impedance of the test rig. These impedances were ultimately measured and the results obtained from the three armatures are presented in Fig. 6.74. The impedances appear as stray capacitances between the windings and the rotor lamination stack. On the 11/22 armature the stray capacitance is of the order of 200 pF which at high frequencies results in a low impedance path for the asymmetric currents to flow. On examination it was found that the 11/22 armature coils had been wound directly on to the armature laminations, the only insulation being provided by the laquer insulation on the copper windings. The 12/24 and 7/21 armatures exhibit stray capacitances of approximately 150 pF and 95 pF respectively. The 7/21 armature was constructed with a cardboard slot insulation between the windings and laminations, it appears that this has a major influence on the reduction of the armature stray capacitance thus effectively causing a high asymmetric impedance reducing the RFI levels below those measured from the other two armatures. The 12/24 armature was coated with plastic epoxy insulation, this too is effective, but from the results obtained, it can be seen not to be as effective as the cardboard insulation.

6.3.5.3.1 Influence of armature turns per coil

During the development stage of motor design it is often necessary to change the number of armature turns per coil in order to obtain a specific motor performance. It was decided to observe how RFI levels would be affected by small changes in the armature windings. To this end, a number of 12/24 and 7/21 armatures were constructed with different turns per coil (T/C). The standard 12/24 armature had 40 T/C and armatures with 36 T/C and 34 T/C were constructed. Similarly the standard 7/21 armature had 39 T/C and armatures with 41 T/C and 43 T/C were constructed.

The armatures were fitted in turn into the test rig and with the pulley load adjusted to give a motor speed of 13000 r/min, measurements of RFI levels were recorded. The results obtained are presented in Tables A2.139 to A2.140.

Figures 6.75 and 6.76, show the interference spectrums obtained for the different armatures. It can be seen that there is a general trend for the RFI levels to increase with the larger number of armature turns. No detailed comparison of the tests is possible since by changing the armature turns, the motor performance is also altered. The main factors affected by changing the number of turns per coil i.e. coil inductance and transformer voltage, have both been shown in earlier tests to influence the RFI levels obtained. Transformer voltage is proportional to the number of turns per coil and the coil inductance is proportional to the square of the number of turns per coil - thus both factors are increased with increase in turns per coil leading to the higher RFI indicated in the test results.

Table 6.3, show the maximum and minimum values of L_{comm} and the transformer voltages measured from each armature.

6.3.5.4 Influence of varying motor load

RFI levels generated by commutation have been found to increase both with speed and supply current. The effect of varying motor load on the speed-current characteristics of the test rig are shown in Fig. 6.77. Increasing motor load gives rise to increasing supply current but decreases the motor speed. The influence of varying motor load on RFI levels is difficult to predict, since although the increasing current would tend to increase RFI - the decreasing speed would tend to reduce RFI. Measurements of RFI levels were thus recorded with the motor load adjusted to give speeds of 10000, 13000, 16000 and 20000 r/min. The results are presented in Tables A2.141. Fig. 6.78, shows a sketch of the interference spectrums obtained at the

Armature	Turns/coil	Max. L_{comm}	Min. L_{comm}	Transformer Voltage
12/24	40	379 μH	124 μH	9.24 V
12/24	36	309	103	9.07 V
12/24	34	277	91	8.50 V
7/21	43	568	159	10.71 V
7/21	41	517	145	10.27 V
7/21	39	470	130	9.88 V

Measured short-circuited coil active inductance and transformer voltage on test armatures

Table 6.3

different speeds. At 10000 r/min and 13000 r/min the RFI levels were unaffected, at 16000 r/min there is a 2-3 dB increase in h.f. region and in the conducted interference region above 10 MHz. Finally, at 20000 r/min the overall RFI levels increases by a further 1 or 2 dB across the frequency spectrum. It was noted that at the higher speeds the degree of sparking at the brushes worsened and it is likely it was this increase which produced the higher levels of RFI. Thus from these results it appears that varying motor load on small motors does not significantly effect RFI levels. The overall effect of the increasing current but reducing speed is to maintain the measured RFI levels relatively constant.

6.3.6 Summary of test results

(a) Magneto-striction of the armature and field laminations causes low levels of RFI to be generated.

(b) RFI levels measured with the rotor tooth at the centre of the pole face are approximately 5 dB higher than those with the rotor slot in the same position.

(c) There is no observable influence of slot number or slot rotation on measured RFI levels.

(d) Field windings aid the suppression of RFI generated at the brushes by presenting a high impedance path to the flow of interference currents and thus reduce the overall RFI levels measured from the motor. The h.f. impedance of the windings can be increased by sectionalising the windings in order to reduce the inter-layer capacitance.

(e) Stray capacitance between the field windings and the field laminations provide a path for the interference currents to be diverted away from the motor terminals and thus reduces measured RFI levels.

(f) A symmetrical split field winding configuration impedes the flow of both the asymmetrical and symmetrical interference currents such that, RFI levels above around 1 MHz are suppressed to below the CISPR/EEC limits without the aid of external suppression components.

(g) The single coil field arrangement although reducing the symmetric interference currents only has minimal effect on asymmetric currents.

(h) Asymmetrical interference currents flow via the stray capacitance between the armature windings and the armature laminations.

(i) The earth connection to the motor frame provides a low impedance path to the flow of asymmetric interference currents.

(j) Variation of motor load has negligible effect on measured RFI levels due to the speed-current characteristic of small motors.

6.4 RFI Due to the Influence of Mechanical Variations in the Motor Assembly

Commutation has been shown to be a major factor in the generation of RFI from small motors. In chapter 3, it was discussed that the quality of commutation can be affected both by electrical and mechanical factors in the motor construction. Electrical influences on commutation and the resultant levels of RFI generated have been studied in Section 6.2 and 6.3. The tests presented in this section investigate the influence of mechanical variations on RFI levels. In the main mechanical variations in the motor assembly directly affect the quality of commutation. The purpose of these tests, was two-fold; firstly to observe the influence of various mechanical variations and determine the limits on these variations such that RFI is not significantly affected, secondly, to compare the limits observed with the mechanical tolerances being allowed in the manufacture of a specific motor - this latter work is presented as part of a case-study in Chapter 7. Test conditions and the mechanical variations introduced to the test rig, are detailed in section 5.3.4, the results obtained from these tests and details of the points emerging are discussed in the subsections below.

The experiments required that RFI measurements be recorded from a number of specially prepared armatures. The armatures were fitted in turn into the test rig, the design which allowed the armature to be replaced by simply unscrewing a detachable central disc in the non-drive end-plate as described in Section 5.2.1.3. In this way, the different armatures could be introduced with negligible disturbance to the test set-up. This was essential to ensure repeatability of the test measurements and also in making valid comparisons between RFI levels from different armatures. In each case, the rig was fitted with a new set of brushes and adequate brush bedding time was allowed before measurements were recorded. In some cases, the mechanical variation introduced impaired the quality of commutation so much as to make it impractical for the motor to be run for long periods without severe burning or arcing at the brushes - in these cases, the supply voltage was reduced to achieve a condition where the armature could rotate reasonably satisfactorily to allow some sort of brush bedding to develop.

6.4.1 Static Armature out-of-balance

Tables A2.142 to A2.145, show the influence of increasing static armature out-of-balance on the measured RFI levels at 13000 and 18000 r/min. Fig. 6.79, shows a sketch of some of the interference spectrums observed at 18000 r/min, it can be seen that the overall RFI levels increase as the out-of-balance is increased. In section 3.8, it was discussed that out-of-balance causes vibrations of the armature which affects brush stability. Brush instability impairs the quality of commutation leading to increased sparking and arcing at the brushes, this has been shown to increase RFI levels between 1 MHz and 30 MHz in the conducted interference region and also cause increases throughout the radiated interference h.f. region. The test results reflect the worsening brush sparking as the out-of-balance is increased, Fig. 6.80 shows a graph of the manner in which the interference levels, are influenced by the unbalance at various frequencies in the r.f. spectrum. It can be seen that for out-of-balance of less than 0.4 gcm there is negligible change in RFI levels, but with further increases in out-of-balance the RFI levels began to increase significantly at the higher frequencies.

It was also noted that brush sparking worsened considerably at out-of-balances above 1.5 gcm increasing from a few intermittent sparks at around 0.4 gcm to heavy continuous sparking at values greater than 1.5 gcm. At the slower speed, RFI levels are unaffected for out-of-balances up to around 0.6 gcm but at the higher speed they increase with brush sparking as the out-of-balance is increased. The out-of-balance centrifugal forces, are proportional to the square of the rotational speed of the armature thus explaining the speed influence observed on the measured RFI levels.

In determining a limit for the allowable static armature out-of-balance, from the results it appears that values up to around 0.5 gcm at 18000 r/min would be permissible. This would ensure that both sparking and RFI levels are kept to a minimum. Out-of-balance is also undesirable due to its long-term affects on the motor. The continual armature vibration can damage the motor bearings leading to further vibrations and even complete failure of the motor.

6.4.2 Dynamic Armature out-of-balance

As with static out-of-balance, dynamic out-of-balance also causes vibration of the armature shaft, the mode of vibration is shown in Fig. 3.24 (b). Measurements of the RFI levels were recorded with increasing dynamic out-of-balances at 13000 and 18000 r/min, the results are presented in Tables A2.146 to A2.149. Fig. 6.81, shows a sketch of some of the interference spectrums observed at 18000 r/min. As in the previous case, RFI levels increase as the out-of-balance is increased and is accompanied by worsening sparking at the brushes. It can be seen that a dynamic out-of-balance of only 0.3 gcm can cause RFI levels in the h.f. region to increase, (whereas static unbalance of this value had no observable affect). Fig. 6.82, shows a graph of the manner which the RFI levels vary with dynamic armature out-of-balance. Again the speed influence is evident with RFI levels unaffected until dynamic out-of-balance is increased to above 0.4 gcm at 13000 r/min. From these results it is clear that dynamic out-of-balance is much more harmful to motor operation than the effects of static out-of-balance and should be limited to around 0.3 gcm.

6.4.3 Brush Pressure

Measurements of RFI levels were recorded with varying brush pressure the results are presented in Tables A2.150 and A2.151. Fig. 6.83, shows a sketch of the interference spectrums it can be seen that the highest RFI levels were measured at the lower spring load. The pressure exerted by this low spring load was clearly insufficient to damp out brush vibrations and chatter caused by the commutator rotation. The high levels of RFI were accompanied by severe arcing at the brushes which on later examination, showed evidence of burning at the trailing edge. The resulting commutator surface film was also very poor appearing highly glazed in parts and in other areas showing signs of exposed bare copper. At the trailing edge of the segments, there were heavy deposits of carbon and a number of segments showed signs of wear due to heavy arcing and burning. Both the increased arcing and the irregular brush commutator contact caused by vibration and brush wear are condusive to the increased RFI levels observed. Measurements of maximum brush movement at 40 g spring load revealed brush movements in excess of 0.3 mm, brush-commutator separations of this order leads to a complete contact break thus it is likely that much of the arcing at the brushes is due to transient spikes of the mains supply caused by the contact break.

As the spring load was increased, the arcing ceased and the overall RFI levels reduced to a minimum at spring loads of between 90 g and 110 g. At these loads, there was a general improvement in the quality of commutation (only intermittent light sparking) and also in the appearance of the resulting commutator film. Maximum brush movements of only 0.05mm, were detected. Further increases in spring load up to 150 g again caused an increase in the RFI levels as indicated in Fig. 6.83. The sparking at the brushes became heavy and continuous and the commutator film dull and powdery. Excessive brush pressure is known to increase the rate of brush wear. As the brush material wears away, there is an increase in the rate of formation and cessation of contact arcs at the face of the brush causing an increase in RFI levels. The increased pressure also generates friction excited vibration at the brush commutator interface which again impairs the quality of commutation and hence a factor in causing the increasing RFI levels. Measurement of the maximum brush movement at 150 g, spring load, confirmed this showing that the brush movement had increased to almost 0.15mm. Fig. 6.84, shows a graph of the manner in which RFI levels vary with increasing spring load at various frequencies, from these results, the upper and lower limits on spring load for minimum RFI can be determined to be 110 g and 90 g respectively. A source of concern in specifying limits on spring loads, is that coil type springs as used in small motors are found to 'age' relatively quickly. Work carried out by Kitter [142] showed that phosphor bronze springs lose as much as 54% of their spring load during running. It can be seen from the results above, that low spring loads can cause motor failures. Beryillium copper springs, showed a loss in spring loads of 39% whereas copper coated steel spring, faired the best showing a fall of only around 25%. Spring load also decreases with brush wear as the spring gradually decompresses. In large machines, constant force spring arrangements are common place, but they are not generally used in small motors.

6.4.4 Brush Alignment along the Quadrature Axis

The brushes were misaligned vertically above and below the quadrature axis as indicated in Fig. 5.19. Above the quadrature axis, the brush movement was against the direction of rotation and conversley below the quadrature axis the brush movement was with the direction of rotation. The results of the RFI measurements recorded are presented in Tables A2.152 and A2.153. Fig 6.85, shows a sketch of the interference spectrums obtained as the brush was misaligned against the direction of rotation. For brush movements of up to around 0.125mm, there was no detectable influence on the RFI levels. Examining the brush face, showed that the brushes were able to re-align themselves in the brush box to keep an intimate contact with the commutator surface. Further movements against rotation led to a deterioration of brush sparking and thus affecting an increase in the overall RFI levels. The brush face was found to have only bedded in an area less than the width of one commutator segment. This would not only affect brush stability, but in section 6.3.4, it was shown that if the brush spans less than one commutator segment the active inductance L_{comm} of the short circuited coil can increase by a factor of four or five thus increasing the measured levels of RFI. The manner in which the RFI levels increase is shown in Fig. 6.86.

Fig. 6.87, shows sketches of the interference spectrums obtained as the brushes were moved in the same direction of rotation. It is evident from the spectrums that RFI is much more adversely affected by this movement. For brush movements of up to around 0.075mm, the RFI levels were unaffected and thus it appears that the brush was able to re-align itself in the brush box as before. With further brush movement the regular commutator impacts on the trailing edge of the brush cause it to bounce and chatter resulting in severe brush arcing. The RFI levels increase because of this and it was noticed that the RFI detector readings became erratic and difficult to measure especially in the h.f. region. For brush movements greater than 0.375mm brush bedding was almost impossible due to the excessive brush chatter even at slow motor speeds. Examination of the brushes showed signs of burning and chipping due to the repetitive commutator impacts at the trailing edge. Fig. 6.88, shows the manner in which the RFI levels increase as the brush is misaligned in the direction of rotation at various frequencies. From the results presented, it is evident that the tolerance on brush alignment should not exceed 0.125mm against and 0.075mm in the same direction of shaft rotation.

6.4.5 Proud Commutator Segments

Table A2.154 and A2.155 show the results of RFI measurements recorded on a number of armatures with different heights of proud commutator segments at 13000 and 18000 r/min. Fig. 6.89 shows a sketch of the interference spectrums obtained at 18000 r/min. Proud segments of up to 3.75×10^{-3}mm produced RFI levels within 1 or 2dB across the r.f. spectrum. But at 5×10^{-3}mm the RFI levels rise by almost 10 dB above 10 MHz. It was noted that brush sparking had deteriorated considerably. Examination of the commutator showed that the proud commutator segment had heavy black deposits on the surface. Tests on further armatures with higher proud segments up to 12.5×10^{-3}mm led to much higher levels of RFI being generated by flash over and ring fire at the brushes. The proud segments showed signs of erosion and melting at the trailing edge. Further tests at high speed were abandoned due to the danger of damaging the test rig.

Tests carried out at 13000 r/min showed that proud segment of less than 7.5×10^{-3}mm, could be tolerated without significantly affecting the RFI levels, but as at the higher speed, armatures with proud segments greater than 15.0×10^{-3}mm, caused severe arcing and ring fire that RFI levels increased by over 15-20 dB in the h.f. region; becoming difficult to measure because of their erratic nature. Measurements were also made of brush movement for each of the armatures tested; Fig. 6.90, shows a graph of the maximum brush movement with increasing height of proud commutator segment. Where the proud segments is less than 3.75×10^{-3}mm the maximum brush movement is around 0.05mm, but the higher proud segments cause the maximum brush movement to increase to 0.4mm, it is likely that the impact of the proud segment causes the brush to be knocked away from the commutator causing a contact break resulting in the heavy arcing and high RFI levels observed. Proud commutator segments is one of the most common causes of increased brush wear and increased sparking, the maximum allowable difference between adjacent segments is such that the brush can follow the commutator profile without breaking electrical contact with the segments.

In chapter 3, an approximate expression to calculate the maximum allowable difference between two adjacent segments was stated as;

$$h = Fg / 2m (nC)^2 \qquad (3.35)$$

Inserting the approximate values from the test rig, gives the theoretical value of h to be approximately 2.5×10^{-3}mm; the test results reveal however, that values up to around 3.75×10^{-3}mm could be tolerated on the test rig without significantly influencing RFI levels.

6.4.6 Commutator Eccentricity

Tables A2.156 and A2.157, show the influence of increasing commutator eccentricity on the measured RFI levels at 13000 and 18000 r/min. Fig. 6.91, shows a sketch of some of the interference spectrums obtained at 18000 r/min. At this speed commutator eccentricities of up to 0.02mm had negligible affect on the RFI levels observed. It appears that the brushes are able to ride the commutator profile without any adverse effects on commutation. With further increases, in the eccentricity, the brush sparking worsened causing the RFI levels to increase. Examination of the brushes at 0.05mm eccentricity showed signs of increased wear and burning at the trailing edge. The commutator surface appeared uneven, showing patches of dark powdery film on the high eccentric side and almost bare copper on the other. Fig. 6.92, shows a graph of the variation of RFI levels with increasing commutator eccentricities at 18000 r/min. At the slower speed, eccentricities of up to 0.05mm had little effect on RFI; thus the speed influence on the effects of commutator eccentricity as predicted by Shobert (see section 3.8.4) is evident.

Knights [57] reported that the accuracy of commutator contour profile had considerable influence on brush life and final commutator conditions. Brush life tests on small motors had indicated that commutators should be finished to a tolerance not exceeding 0.0127mm maximum eccentricity. It can be seen that this value is almost half the value suggested by the RFI tests above. The discrepancy is explained by the fact that the armatures prepared for the RFI tests had been individually balanced to eliminate the effect of out-of-balance forces created by the commutator eccentricity and thus, a limit of approximately 0.02mm is not excessive.

6.4.7 Commutator Surface Finish

Surface finish is controlled by the depth and speed of the finishing cut as the commutator is machined down to size. Surfaces of less than 0.4×10^{-6}m CLA appear as a 'wet' mirror finish, the normal bright copper finish is obtained from around 0.5×10^{-6}m CLA to 1.5×10^{-6}m CLA. Surfaces greater than 2×10^{-6}m CLA appear grooved and have burrs at the edge of the copper segments. RFI measurements were recorded on armatures with different surface finishes and the results are presented in Table A2.158.

There was no discernable difference in RFI levels for surface finishes below 1×10^{-6}m CLA but it was noted that brush bedding on the 'wet' mirror finishes, took much longer to establish. It is likely that the slightly abrasive finishes above 0.4×10^{-6}m CLA actually aid brush bedding. The final commutator film for these armatures appeared smooth and even around the surface, brush sparking was also light and intermittent. Fig. 6.93, shows a sketch of the interference spectrums obtained from armatures with surface finishes above 1.5×10^{-6}m CLA. It can be seen that the RFI levels increase as the commutator surface is made more abrasive. The increased contact friction, can lead to brush vibrations as discussed in section 3.8. It was noted that brush sparking also became successively heavier and the commutator film became less even. The trailing edge of the commutator segments appeared blackened whereas the remaining surface only exhibited light patches of blackening. For finishes above 2×10^{-6}m CLA, the brush surface became heavily scored and also showed signs of burning at its trailing edge, resulting from arcing. The arcing is likely to be due to the chipping and melting of burrs on the commutator segments which not only led to increased levels of RFI, but also caused severe damage to the brushes. At these rough finishes, a commutator film cannot be formed since the 'screw thread' type action of the surface causes all the deposited brush material to be forced away from under the brush by rotation. Fig. 6.94 shows the manner in which the varying commutator surface finishes cause RFI levels to increase at various frequencies. From the RFI results, it appears that the upper limit on commutator surface finish, is around 1×10^{-6}m CLA and due to the brush bedding difficulties encountered with the 'wet' mirror surface finishes, it is recommended that a lower limit of 0.5×10^{-6}m CLA be also applicable.

6.4.8 Commutator Insulation Depth

A number of 7/21 armatures were tested with increasing depths of under-cut commutator insulation, but no influence on the measured RFI levels was detected. There was however, an increase in RFI levels of between 5-10 dB from an armature with the insulation machined flush with the commutator segments. The test results are presented in Table A2.159 and the interference spectrums obtained are shown in Fig. 6.95. Brush wear is greatly increased by flush insulation; with continuous running the commutator segments wear faster than the insulation, thus it stands proud preventing an intimate brush-commutator contact. This leads to more rapid brush wear and increased arcing as brush stability is impaired. Bates [58] suggests that diamond tipped cutting tools of the type used for commutator finishing, although giving excellent visual finish to the segments leave flush intersegment insulation almost 5×10^{-3}mm proud on small motors. From the test results, it is clear that under-cut insulation is desirable for the reduction of RFI, however, the depth of undercut appears insignificant.

6.4.9 Brush Box Clearances

Tables A2.160 and A2.161, show the influence on RFI levels of varying brush box clearances in the direction tangential to commutator rotation as indicated in Fig. 5.2.2(a). Fig. 6.96, shows a sketch of the interference spectrums obtained at clearances of 0.01mm, 0.1mm and 0.2mm. At the very narrow clearances of 0.01mm and 0.02mm high RFI levels were recorded across the r.f. spectrum resulting from heavy arcing at the brushes. The cause of this was found to be that the brushes were 'sticking' in the holders, possibly due to loose brush material fouling their movement. As the clearance was increased, to between 0.05mm and 0.1mm, the RFI levels reduced to a minimum level as the quality of commutation was improved. Further increases in clearance cause the RFI levels to increase as indicated by the interference spectrum in Fig. 6.96.

Measurements of brush movement showed that the increased brush box clearance leads to a decrease in brush stability with maximum brush movements increasing from 0.06mm at 0.05mm clearance to almost 0.25mm at 0.2mm clearance. Fig. 6.97, shows the manner in which RFI levels increase with variation of brush box clearance in the direction tangential to rotation. Tests carried out with varying brush box clearances in the direction axial to commutator rotation as indicated in Fig. 5.2.2(b), showed no influence of the measured RFI levels for clearances up to 0.2mm. Although as above, very narrow clearances (less than 0.02mm) again caused sticking of the brushes and thus higher RFI levels were observed. Clearance between brush and brush box is necessary to allow the brush to slide freely in order to follow the exact commutator profile as it rotates. From the results above, it can be seen that too small a clearance can cause the brush to 'stick' and momentarily break contact with the commutator causing arcing. Clearances of the order of 0.05mm to 0.1mm, as well as allowing the brush free movement also restrain its mechanical vibrations to a satisfactory level thus keeping RFI to a minimum.

6.4.10 Brush Overhang Length

The influence of increasing brush overhang length on measured RFI levels is presented in Table A2.162. Fig. 6.98, shows a sketch of some of the interference spectrums observed at 18000 r/min. There is no significant influence on RFI levels for brush overhang lengths of up to 1mm. Further increases in overhang cause the RFI levels to increase as the stability of the brush contact becomes impaired.

The brush box is unable to restrain brush vibrations caused by the regular impacts of the rotating commutator segments. The high tangential forces imparted to the brush face, can also twist the brush in such a manner as to inhibit the radial sliding motion necessary for the brush to follow the commutator profile. Tests were abandoned with the brush overhang lengths of 4mm where during the period allowed for brush bedding it was found that one of the brushes was broken by the excessive vibrations. The effect of varying brush overhang length on measured RFI levels at various frequencies is shown in Fig. 6.99. It appears from the results, that satisfactory RFI levels can be maintained with the brush overhang length limited to 1mm. Observations at Hoover in the past, have shown that too a short brush overhang length can also be a cause of motor failure. Heat generated at the trailing edge of the brush by the excessive sparking, has been known to melt the lip of the brush boxes resulting ultimately in motor failure. Although this fault has actually been compounded by other motor problems giving rise to the excessive arcing in the first place, it is felt that a minimum brush overhang length of 0.5mm would be appropriate.

6.4.11 Bearing Alignment

Tables A2.163 and A2.164 shows the influence of vertical (direct axis) and horizontal (quadrature axis) bearing misalignment on measured RFI levels at 18000 r/min. In both cases, it was found that there was no significant influence on RFI levels for bearing misalignments up to around 0.125mm. Further misalignments however, caused the twisting of the end bearings such that armature shaft could not rotate freely. Running the motor at vertical misalignments of 0.2mm caused increased arcing at the brushes and the measured RFI levels obtained can be seen from the sketches of the interference spectrum in Fig. 6.100. Tests on horizontal misalignment at 0.2mm caused the drive-end bearing to fail during testing and thus further tests on bearing misalignment were abandoned. The maximum permissible bearing misalignment is dependant both on the compliance of the end bearings and the distance between their centres; thus it is obvious that the tolerable limits for misalignment of approximately 0.125mm observed from the RFI test results would only be applicable to motors of similar design and dimensions.

6.4.12 Air-gap

In large machines asymmetric variation of the air-gap is known to cause vibrations due to the unbalanced magnetic pull experienced on the armature. It had been thought that similar forces in small motors may affect commutation and thus have an influence on the measured RFI levels but, asymmetric variation of the air gap both in the direct and quadrature axis had no detectable influence on the measured levels of RFI both at 13000 and 18000 r/min.

6.4.13 Angular Brush Shift

With brushes adjusted to the magnetic neutral axis, the influence of angular brush shift against the direction of rotation was examined. Tables A2.165 and A2.167, shows the measured levels of RFI for increasing brush shift at 13000 r/min. The results show a steady reduction in overall RFI levels as the brush shift is increased up to minimum at around 20^{o}. With further brush shifts the RFI levels begin to increase once more. The manner in which the RFI levels vary with brush shift can be clearly seen in Fig. 6.101. In section 3.6, the use of angular brush shift to improve commutation was discussed. From the results above it can be seen that the steady improvement in the quality of commutation with brush shift, causes a reduction in RFI of as much as 10 - 15 dB from the neutral axis. As the brush shift becomes excessive, and commutation is again impaired and the RFI levels again tend to increase. The use of RFI levels to determine the correct brush shift was first suggested by Motter [93]. From Fig. 6.101, it can be seen that limits on the position for minimum brush shifts are only of the order of around 2 degrees.

6.4.14 Bearing Journal Diameter

The nominal drive-end bearing journal diameter for an interference fit in the bearing race was 8.987mm. A number of armatures were machined with successively smaller bearing journal diameters to determine the influence of increasing bearing journal clearance on RFI levels - the measurements recorded from the different armatures are presented in Table A2.168. Fig. 6.102, shows a sketch of some of the interference spectrums obtained. It can be seen that for bearing clearances up to 0.008mm, the RFI levels are unaffected, but at higher clearances the RFI levels are increased. For clearances in excess of 0.014mm, it was noted that the audible shaft noise was increased and brush sparking became worsened with intermittent arcing also evident. The under-size bearing journals cause vibration of the armature due to movement of the centre of rotation as indicated in Fig. 6.103. As seen in earlier tests, armature vibrations impair the quality of commutation which results in the higher levels of RFI observed.

Motor life tests carried out by Radia [143] show that armature vibrations caused by under-size bearing journals, invariably lead to motor failure within 100 hours of continuous running. Subsequent examination of the bearing journal and the bearing race showed evidence of fretting at both surfaces caused by movement of the journal within the race during rotation. Further tests were recorded for increasing bearing journal clearances at the non-drive end and again it was observed that RFI levels are increased for clearances in excess of 0.008mm.

6.4.15 Summary of test results

Mechanical variations in the motor assembly can impair brush stability such that the quality of commutation is deterred. As a result of poor commutation RFI levels from the motor are increased. Brush stability is influenced by the following mechanical factors in the motor assembly;

i) armature out-of-balance
ii) commutator profile
iii) commutator surface finish
iv) brush box construction
v) brush box alignment
vi) bearing alignment
vii) spring pressure
viii) bearing journal - race clearance

The maximum allowable tolerances of the mechanical variations introduced to the test rig in order to minimise increases in RFI levels are summarized in Table 6.4.

Mechanical Variation	Allowable tolerance (from test work)
Static armature out-of-balance	0.5 gcm
Dynamic armature out-of-balance	0.3 gcm
Spring Load	110g, 90g (min)
Brush misalignment(with rotation)	0.125 mm
Brush misalignment(against rotation)	0.075 mm
Proud commutator segment	3.75×10^{-3}mm
Commutator eccentricity	0.02 mm
Commutator surface finish	1.0×10^{-6} m CLA, 0.5×10^{-6} m (min)
Brush box clearance	0.1 mm, 0.02 mm (min)
Brush overhang length	0.5 mm to 1.0 mm
Bearing misalignment	0.125 mm
Angular brush shift (from nominal)	2^{o}
Bearing journal (diameter)	0.008 mm

Summary of allowable mechanical tolerances on test rig assembly for minimum RFI

Table 6.4

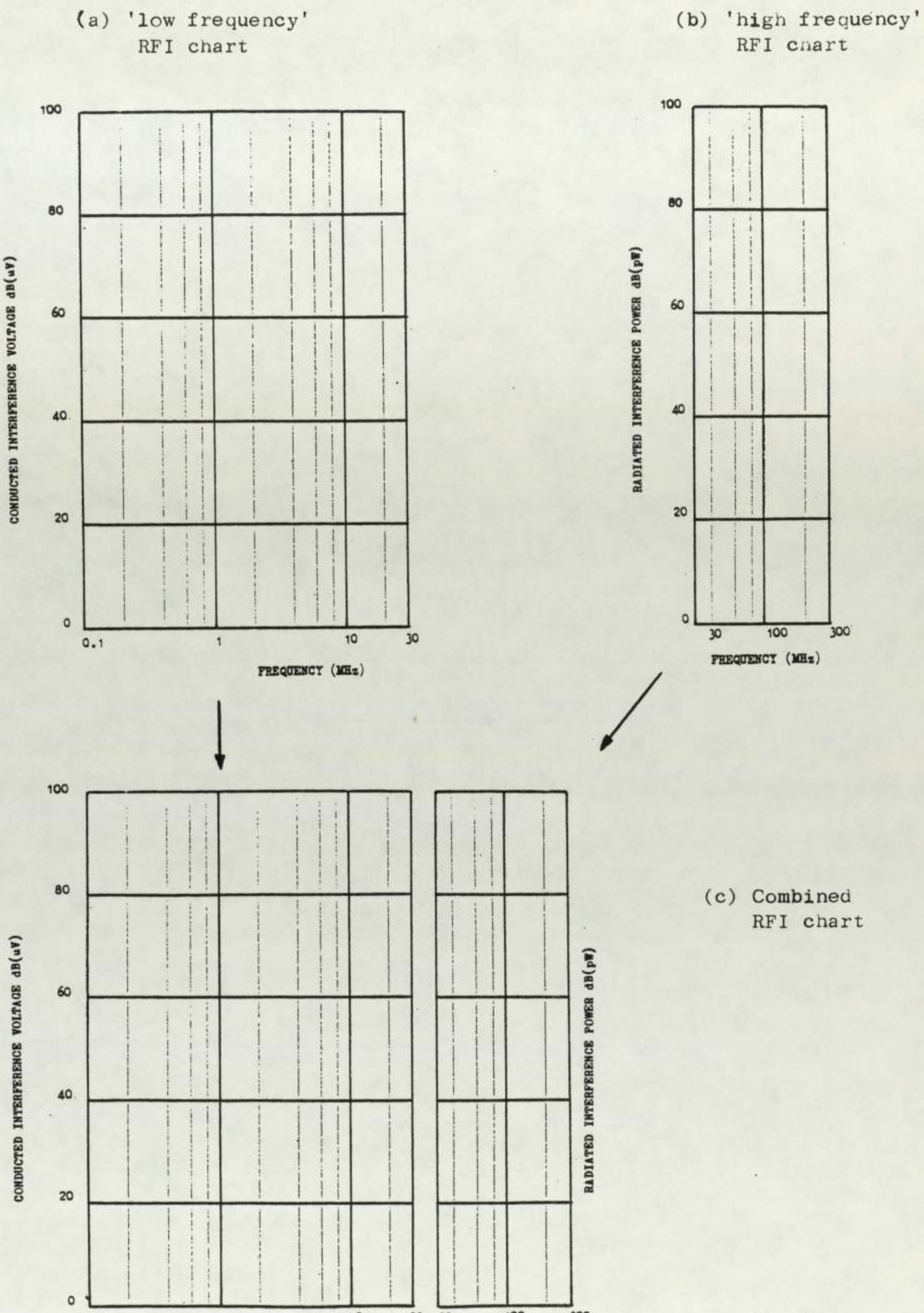

Construction of chart used for the graphical presentation of measured RFI data

Fig. 6.1

RFI caused by the commutator switching action:
Measured RFI levels from a 24 segment commutator at 1.5A supply current with varying shaft speed.

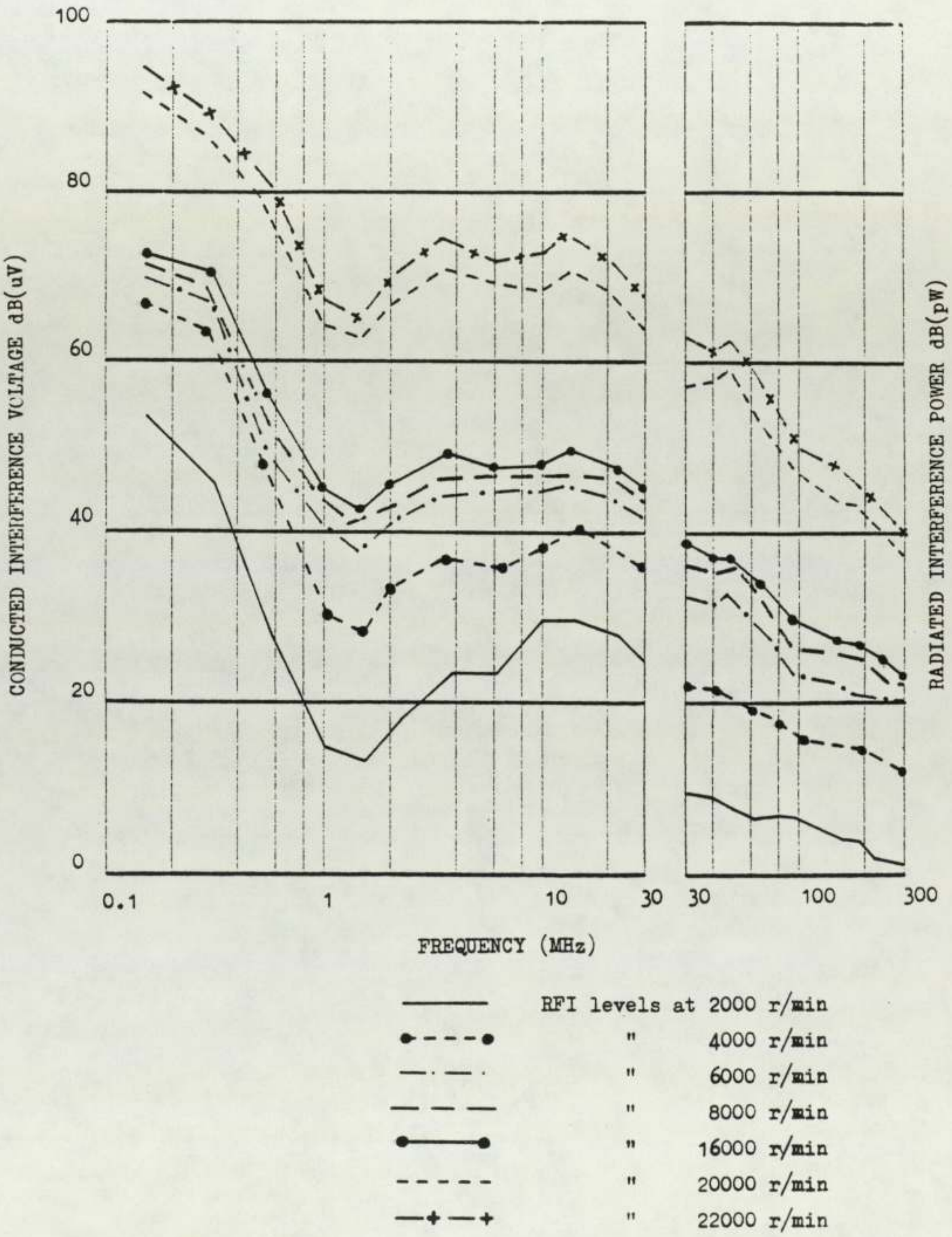

Fig. 6.2

RFI caused by the commutator switching action:
Measured RFI levels from a 24 segment commutator
at 2.5A supply current with varying shaft speed.

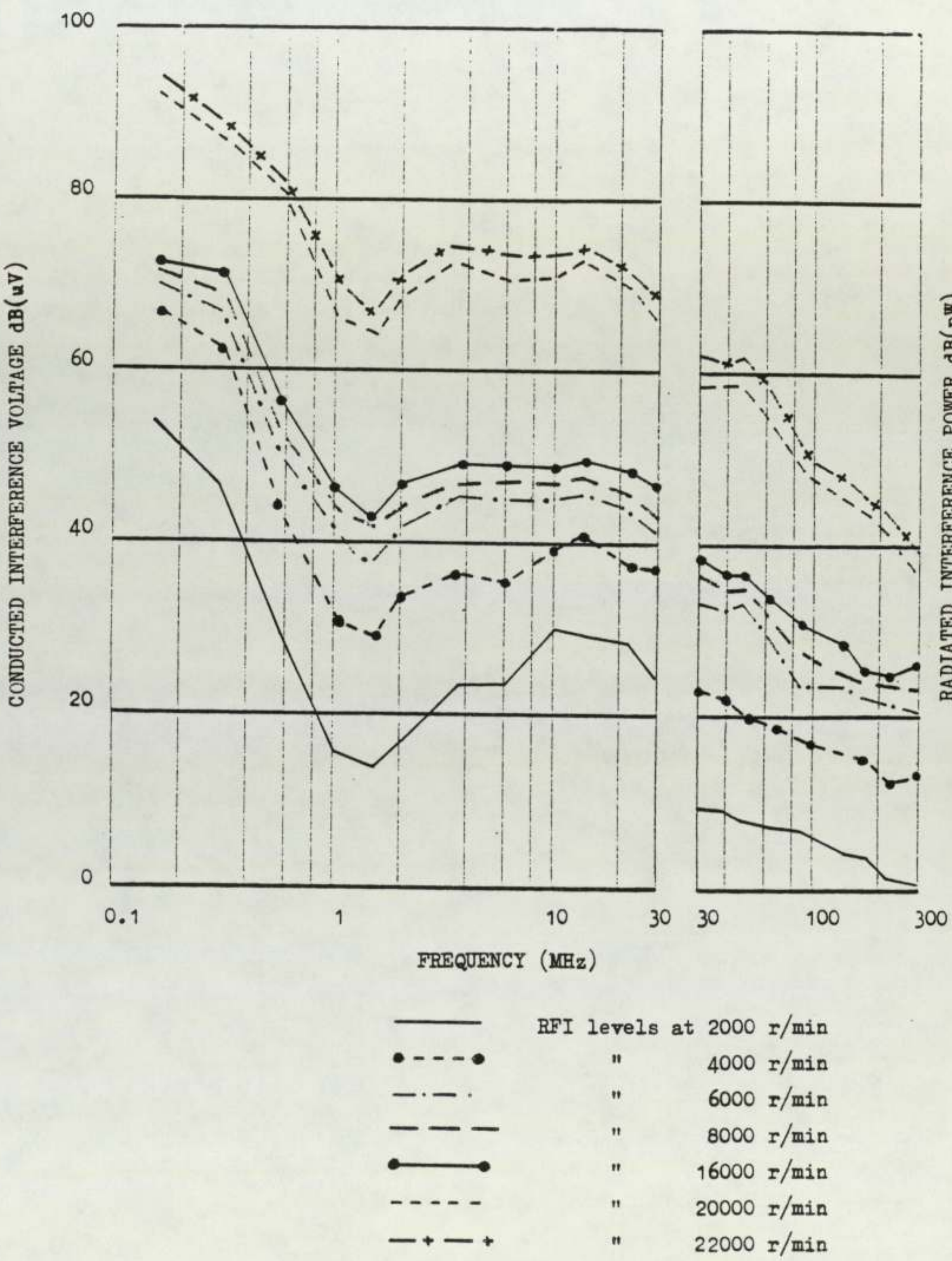

Fig. 6.3

RFI caused by the commutator switching action:
Measured RFI levels from a 22 segment commutator
at 1.5A supply current with varying shaft speed.

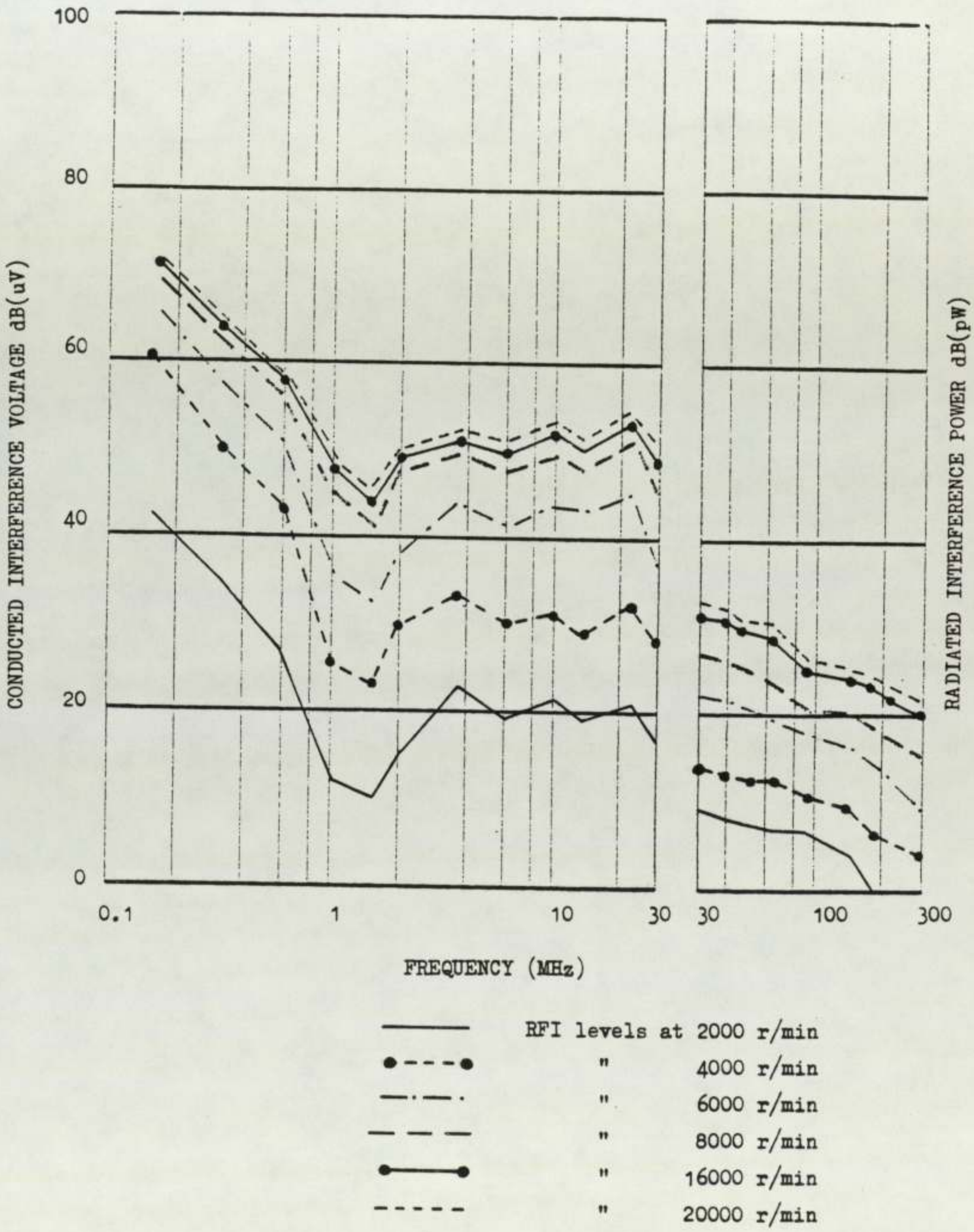

Fig. 6.4

RFI caused by the commutator switching action:
Measured RFI levels from a 21 segment commutator at 1.5A supply current with varying shaft speed.

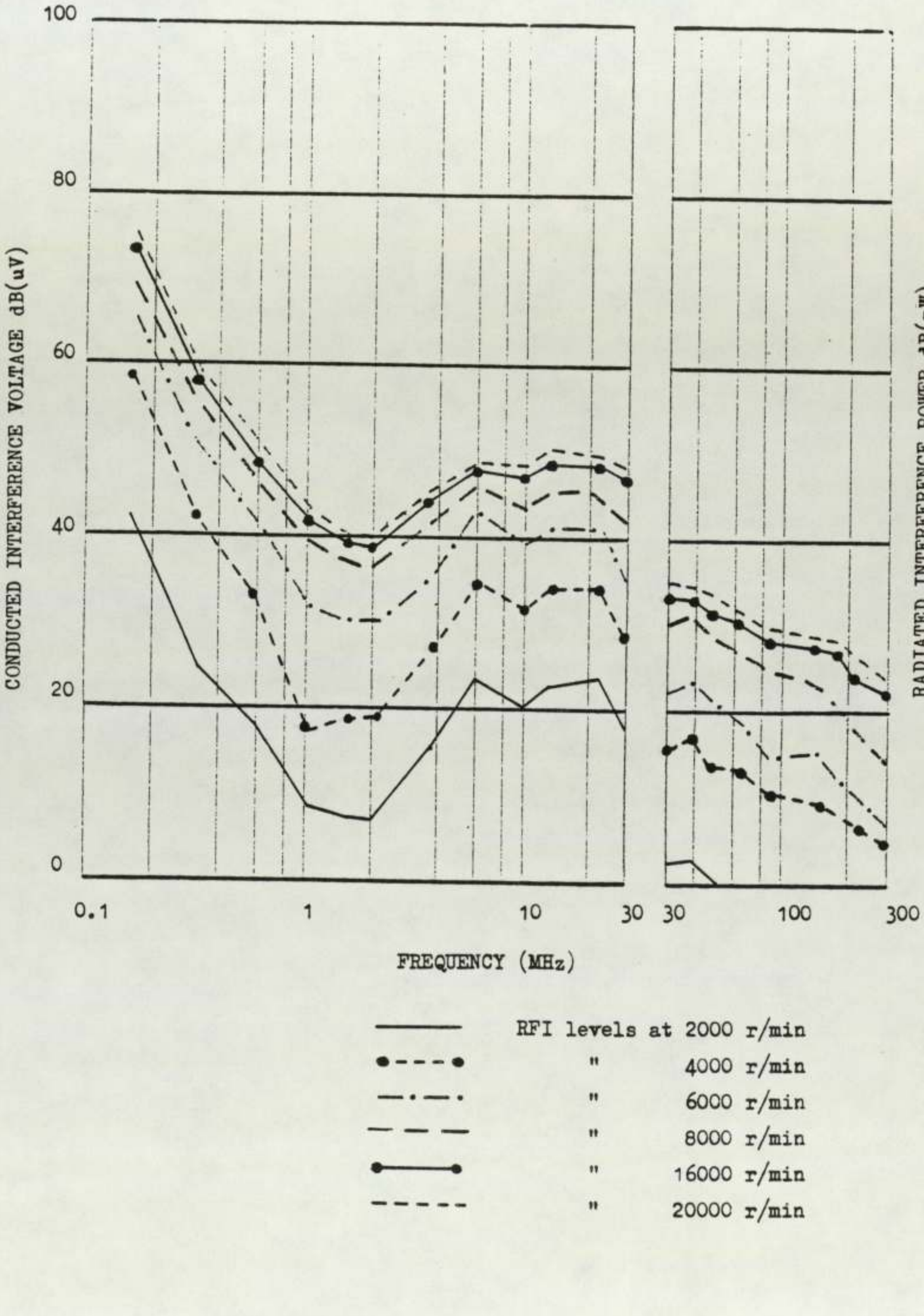

Fig. 6.5

Effect of speed variation on measured RFI levels
from a 24 segment commutator at 1.5A supply current.

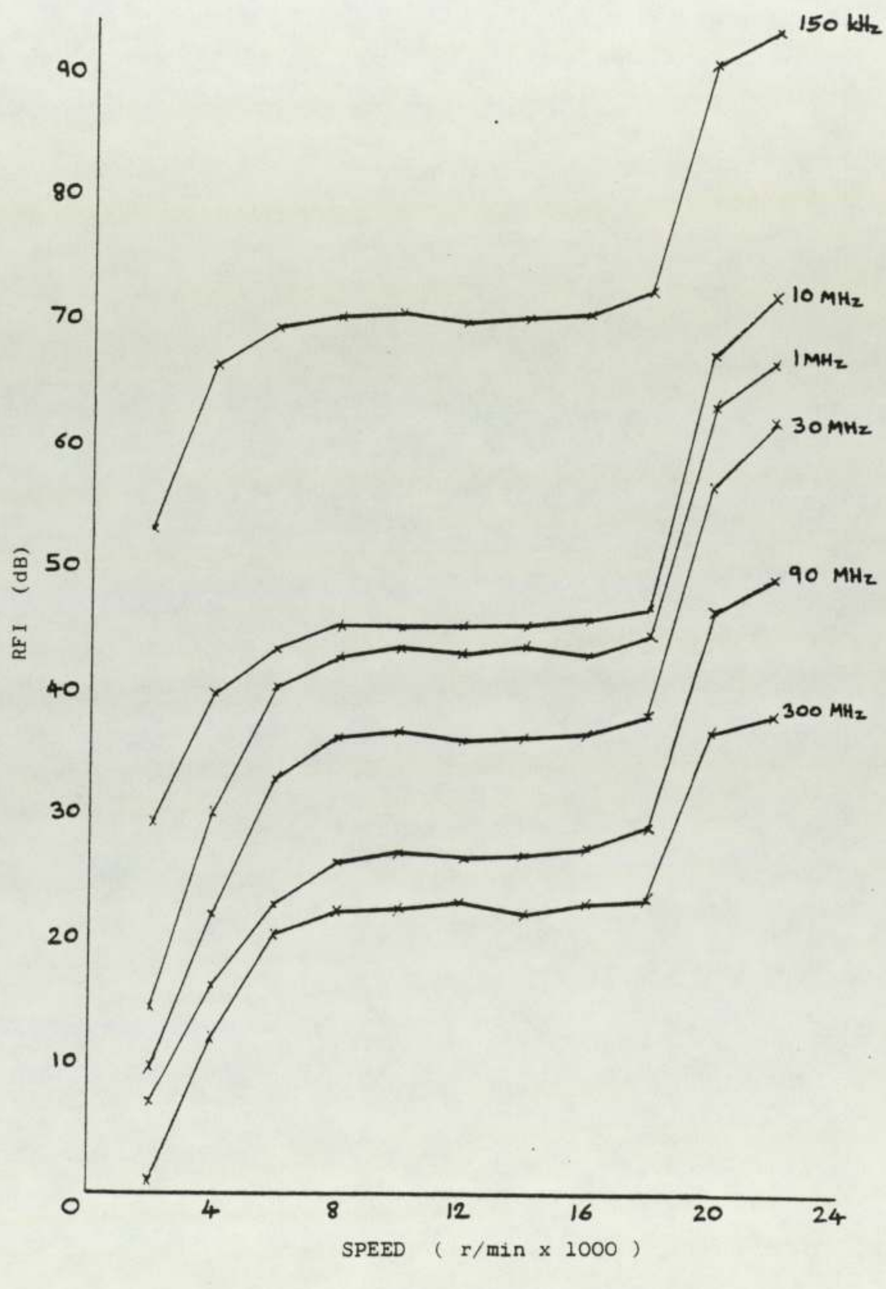

Fig. 6.6

Effect of speed variation on measured RFI levels
from a 22 segment commutator at 1.5A supply current.

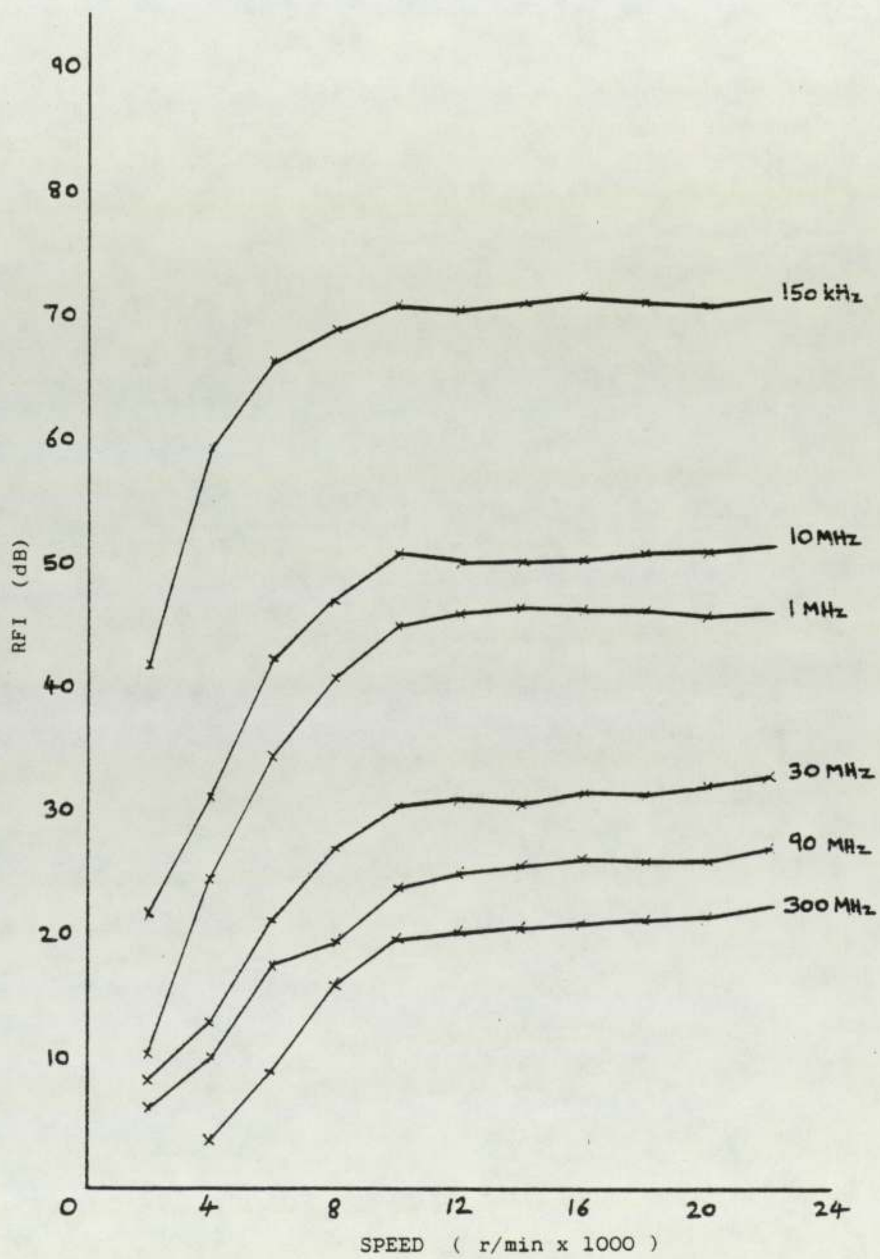

Fig. 6.7

Effect of speed variation on measured RFI levels
from a 21 segment commutator at 1.5A supply current.

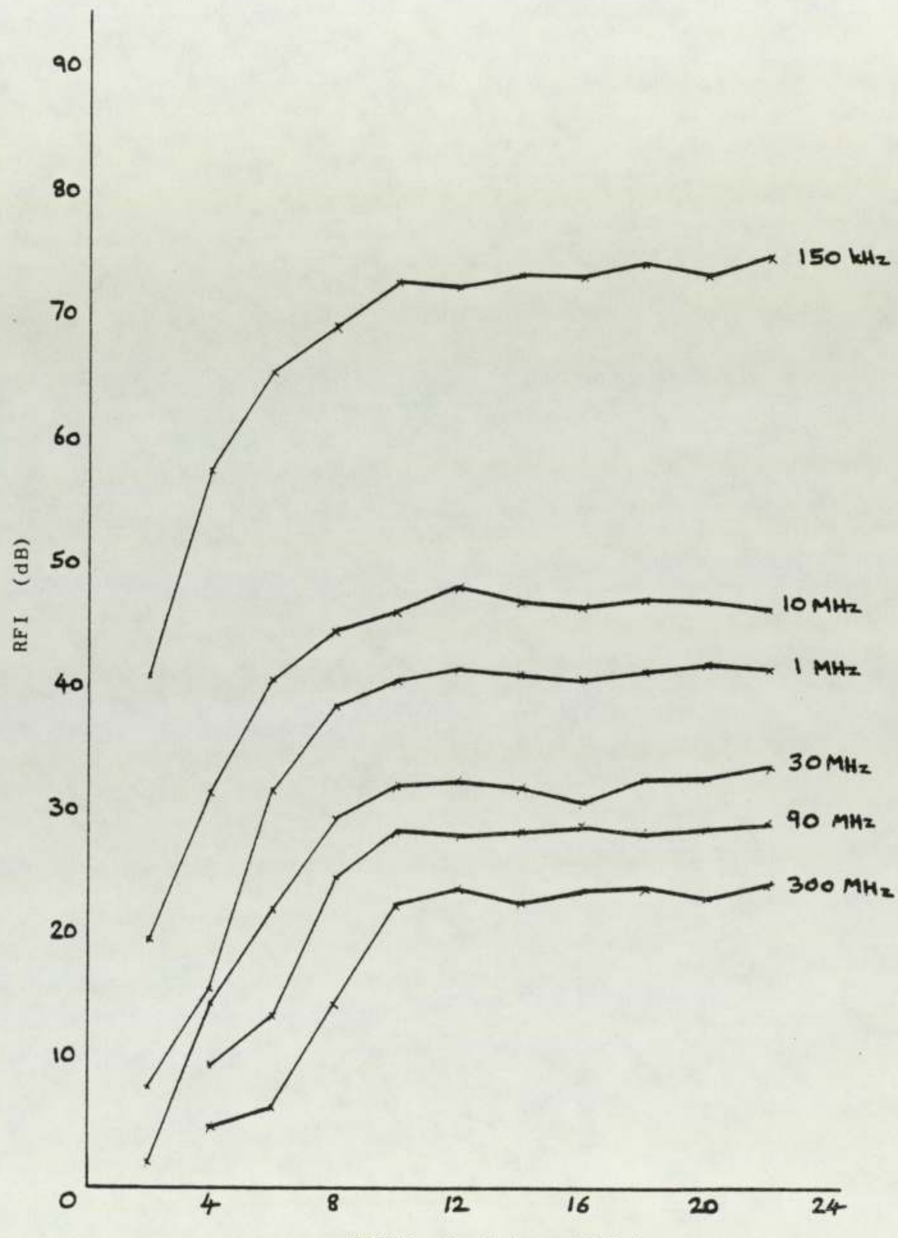

Fig. 6.8

Comparison of measured RFI levels with the EEC limits from a 24 segment commutator (1.5A supply current) at (a) 16000 r/min and (b) 22000 r/min.

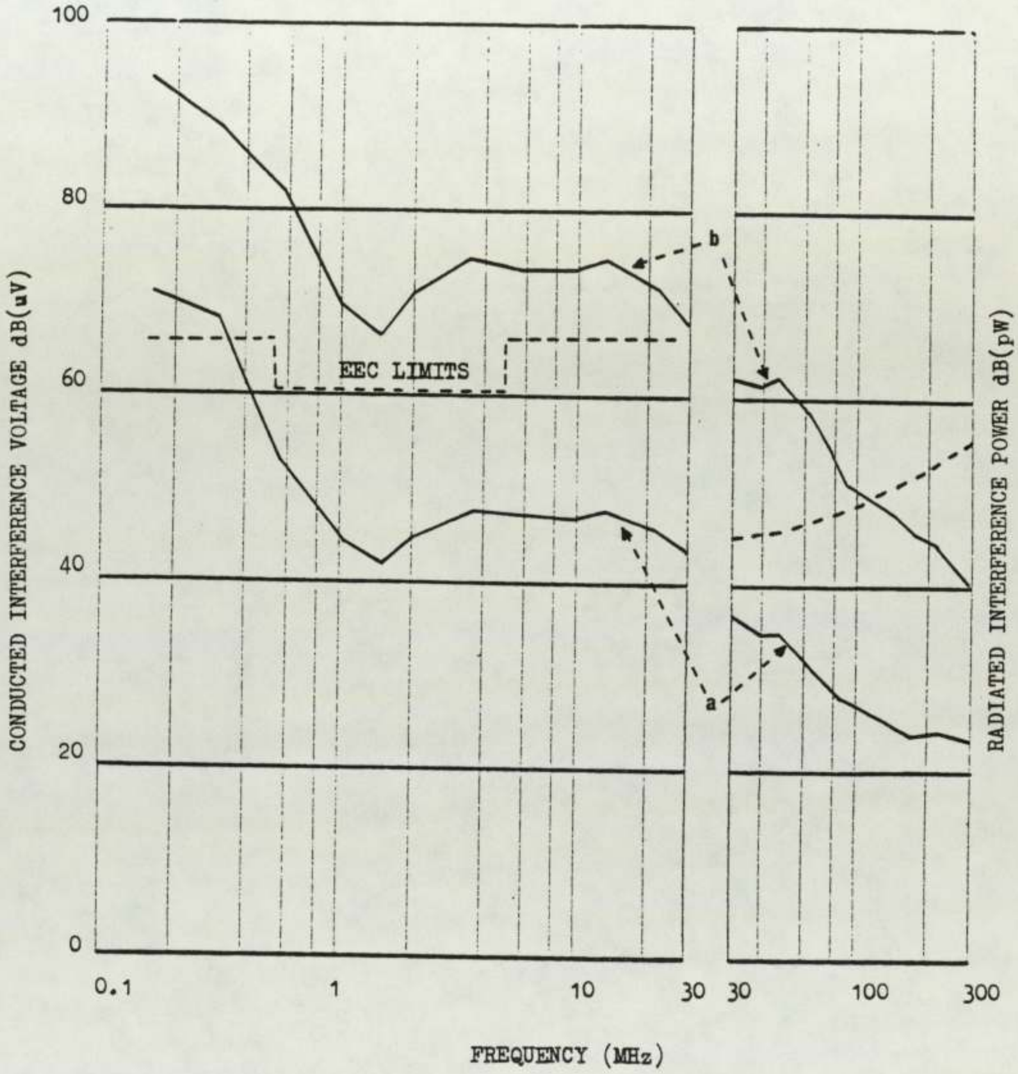

Fig. 6.9

Measured brush movement with varying shaft speed using
(a) 24 segment commutator,
(b) 22 segment commutator,
and (c) 21 segment commutator.

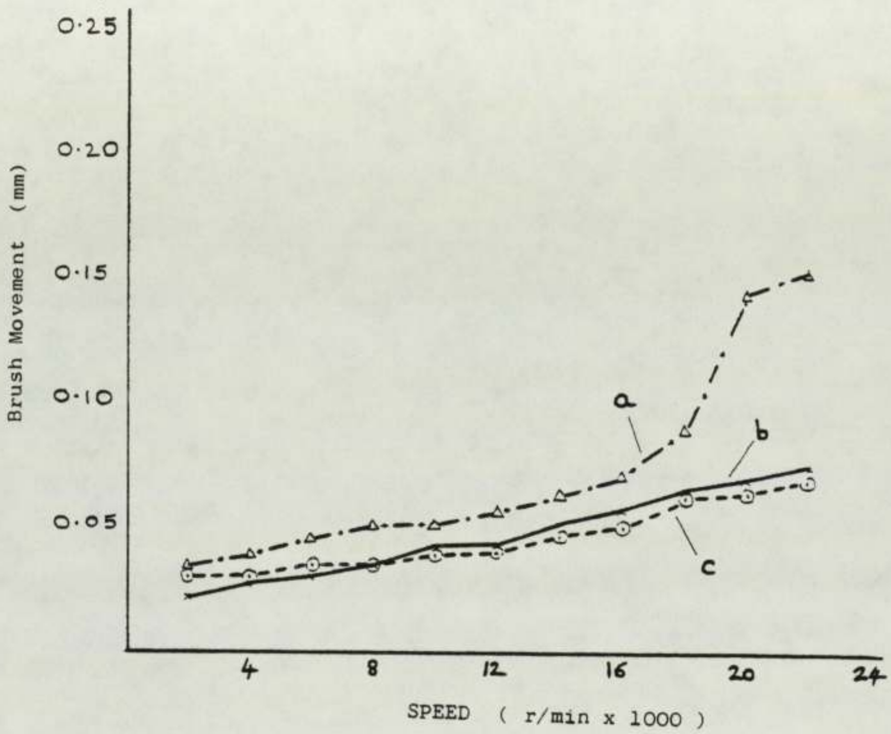

Fig. 6.10

Effect of current variation on measured RFI levels
from a 24 segment commutator at 14000 r/min.

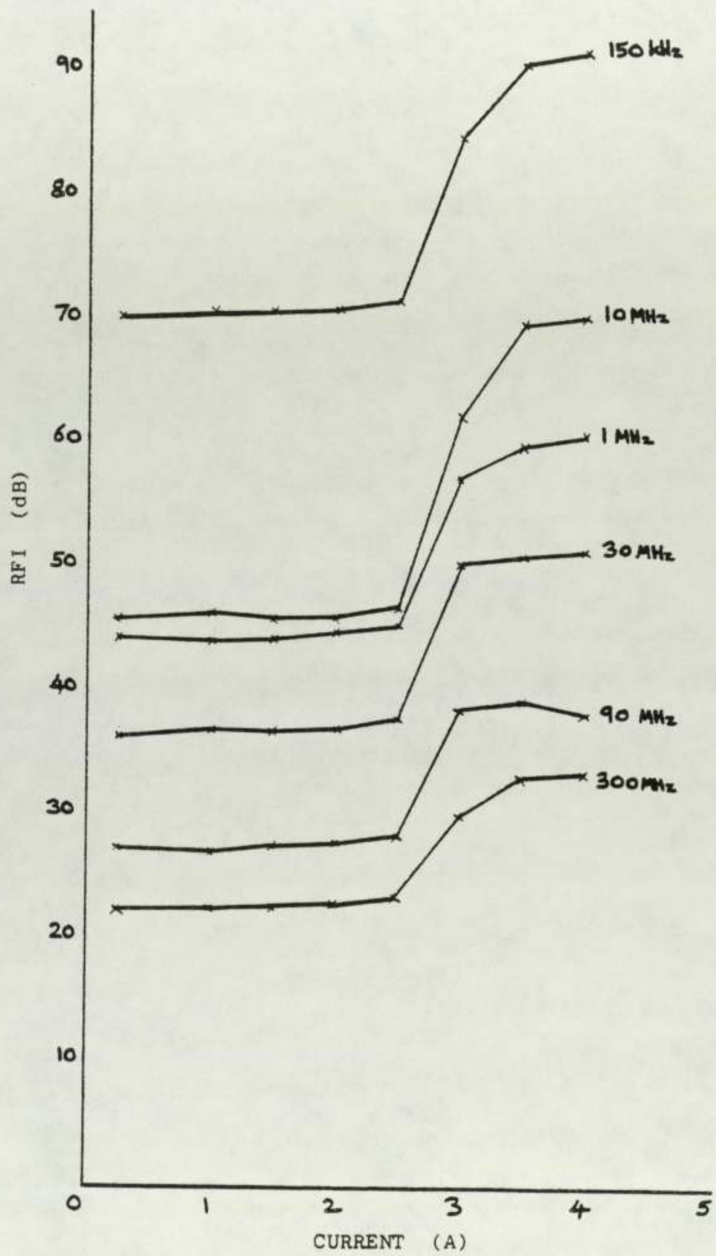

Fig. 6.11

Effect of current variation on measured RFI levels
from a 22 segment commutator at 14000 r/min.

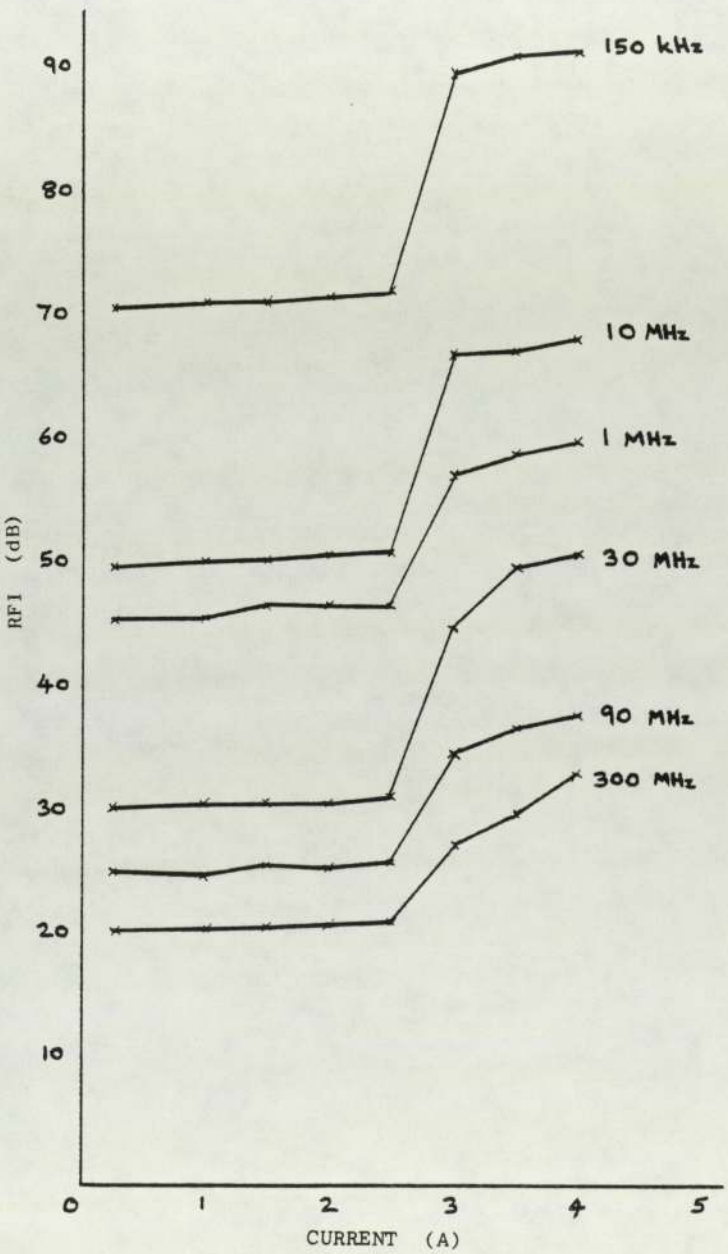

Fig. 6.12

Effect of current variation on measured RFI levels
from a 21 segment commutator at 14000 r/min.

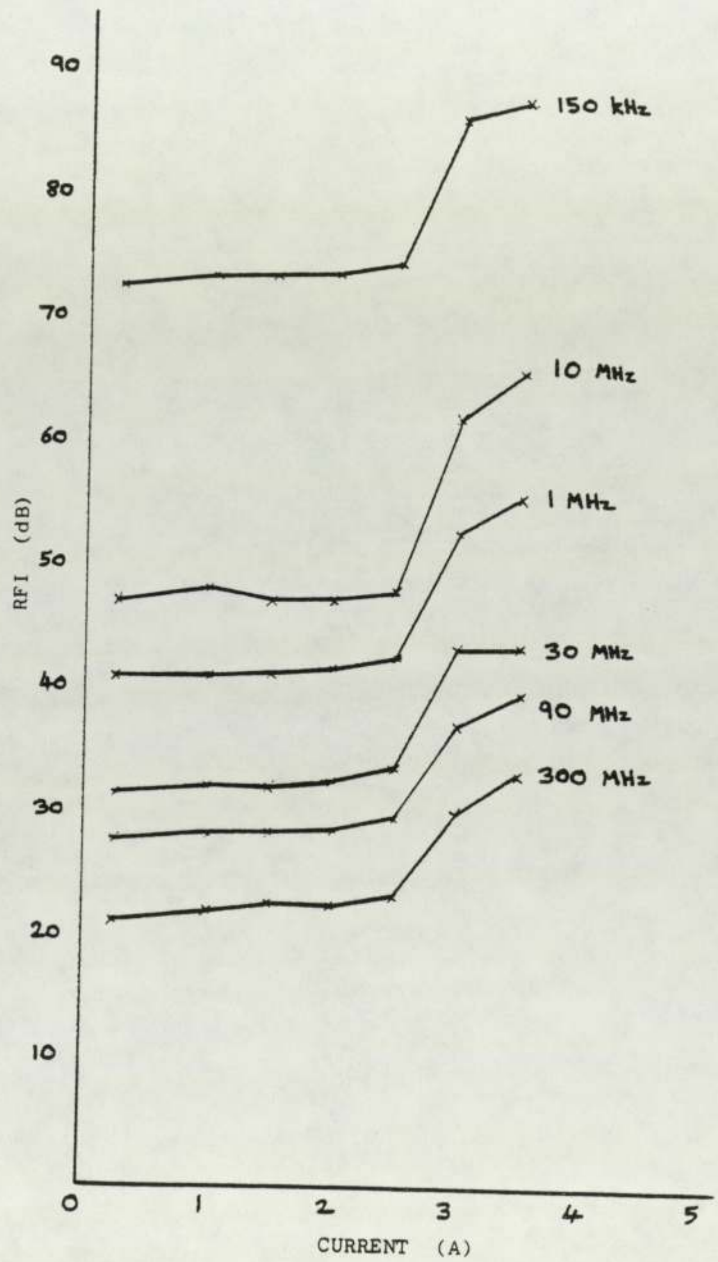

Fig. 6.13

RFI caused by the commutator switching action:
Measured RFI levels from a 24 segment commutator
at zero supply current with varying shaft speed.

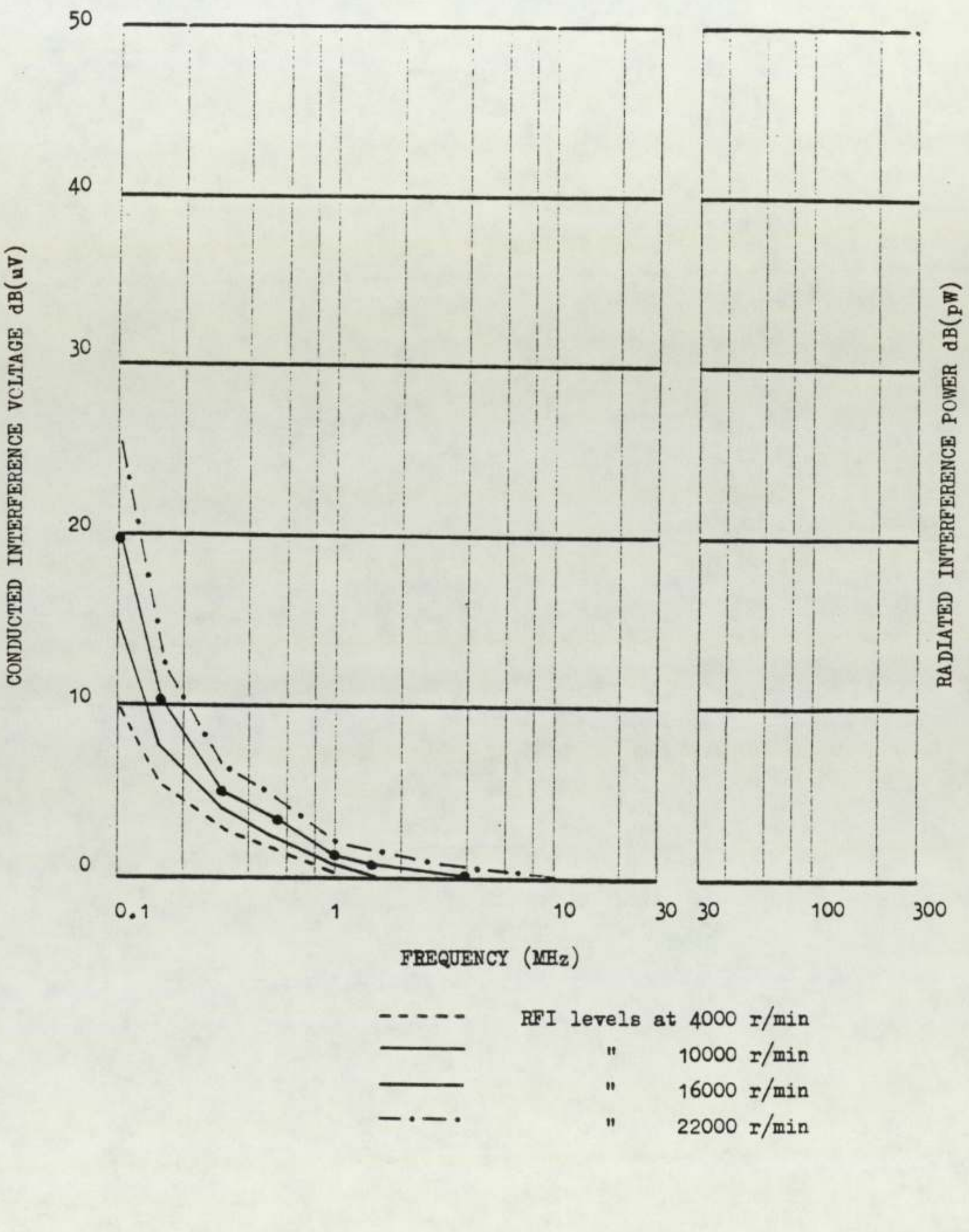

Fig. 6.14

Effect of speed variation on measured RFI levels
from a 24 segment commutator at zero supply current.

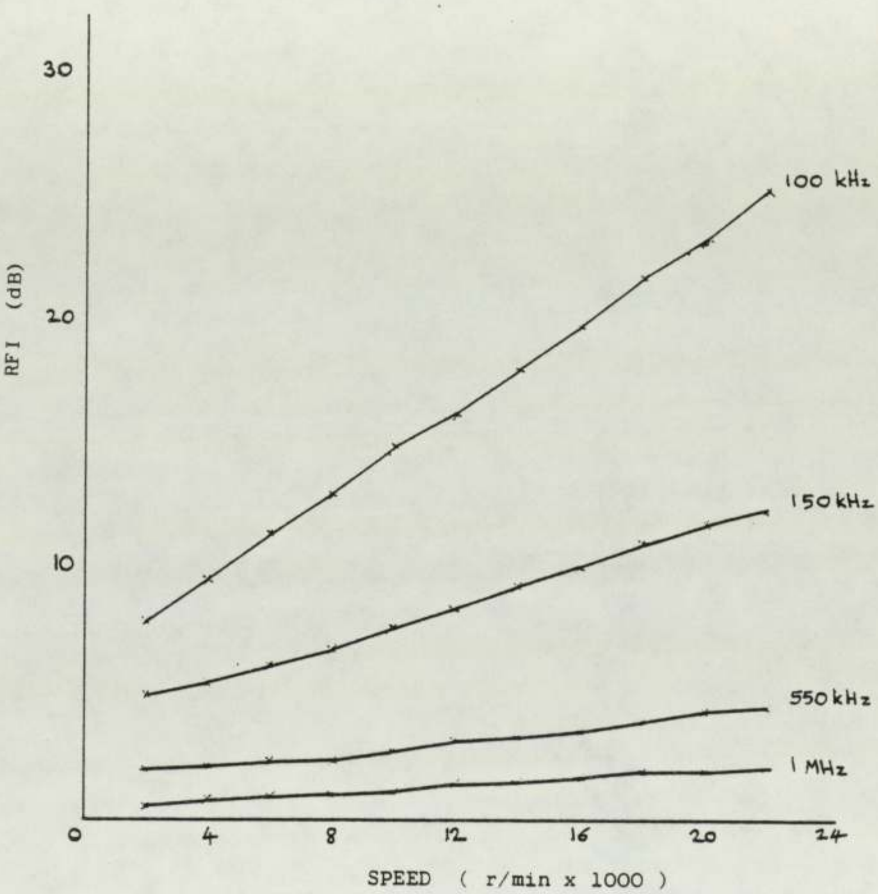

Fig. 6.15

Measured RFI levels from a copper slip ring at
1.5A supply current with varying shaft speed.

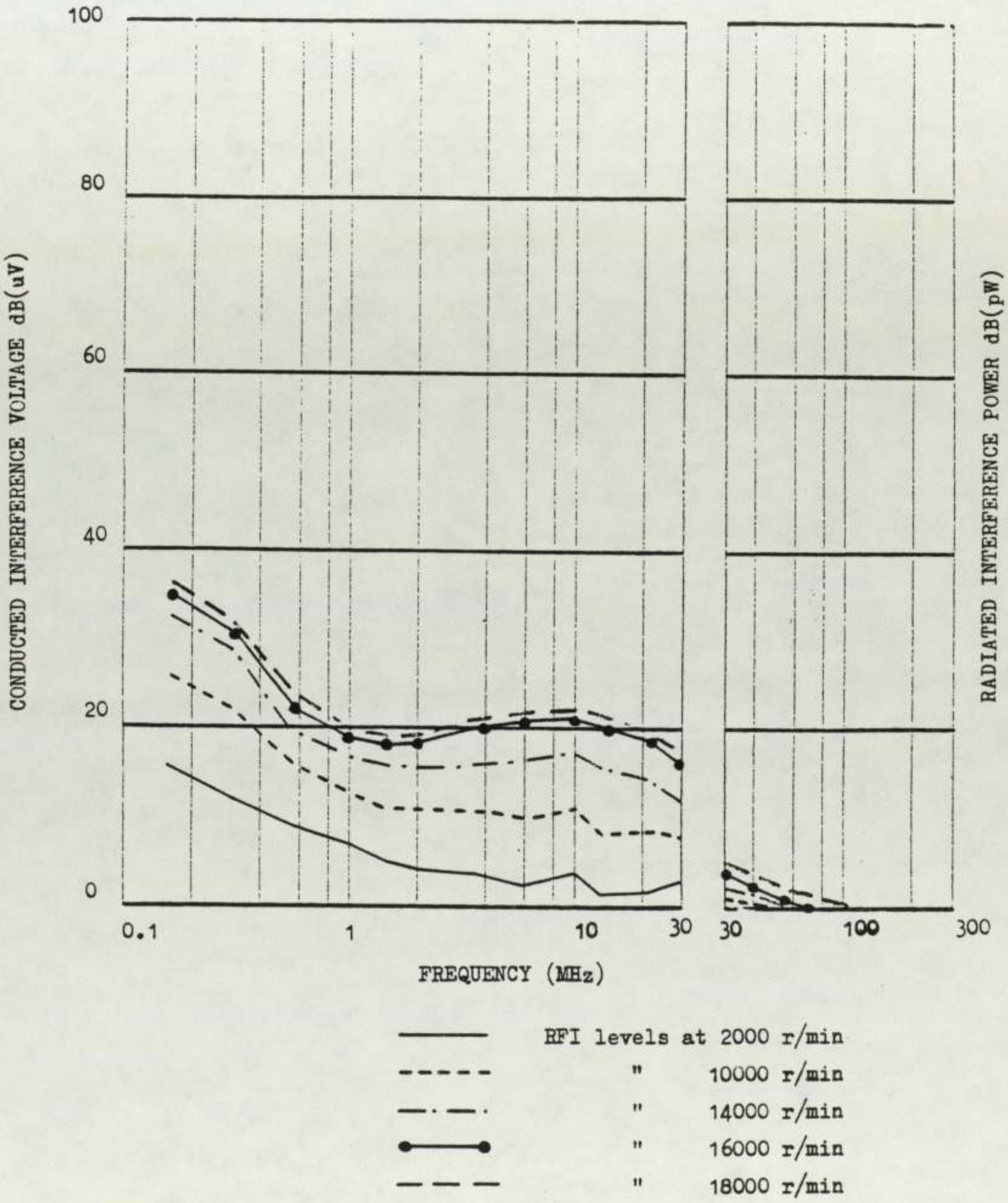

Fig. 6.16

Comparison of measured RFI levels from a copper slip ring and a 24 segment commutator rotating at 18000 r/min and 1.5A supply current.

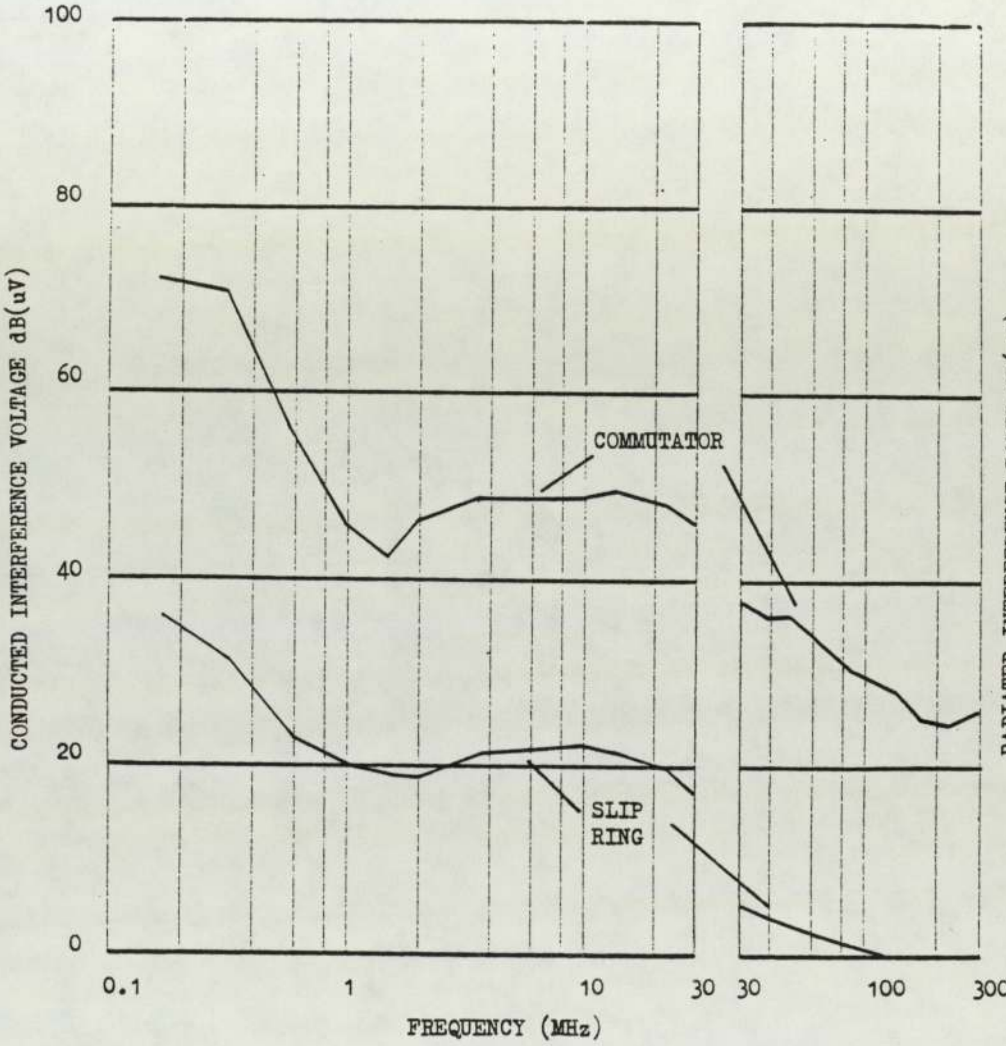

Fig. 6.17

Effect of speed variation on measured RFI levels
from a copper slip ring at 1.5A supply current

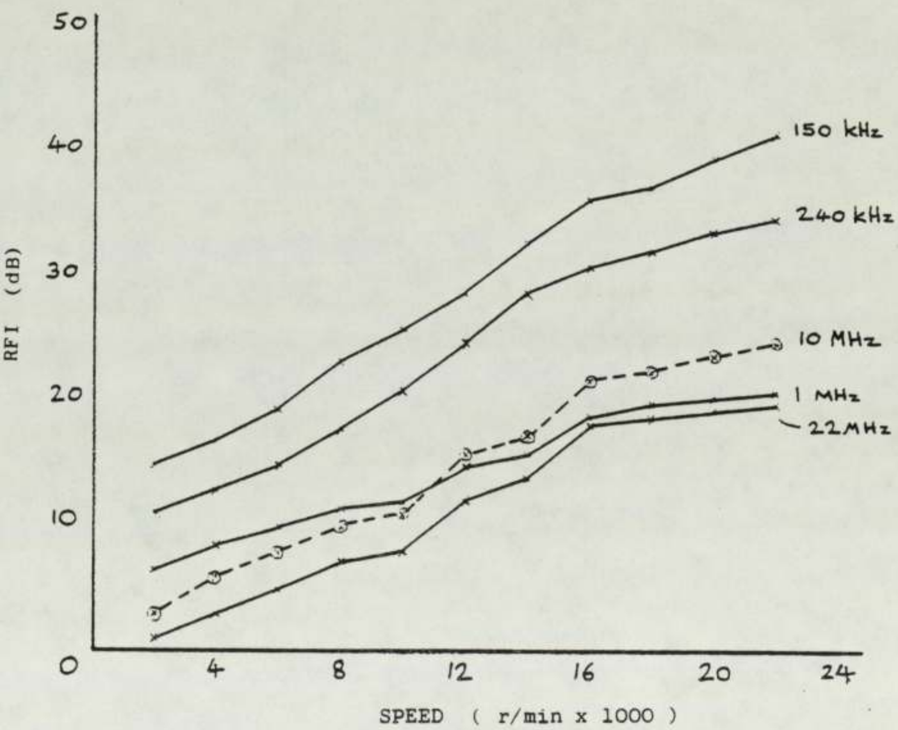

Fig. 6.18

Effect of current variation on measured RFI levels from a copper slip ring at 18000 r/min.

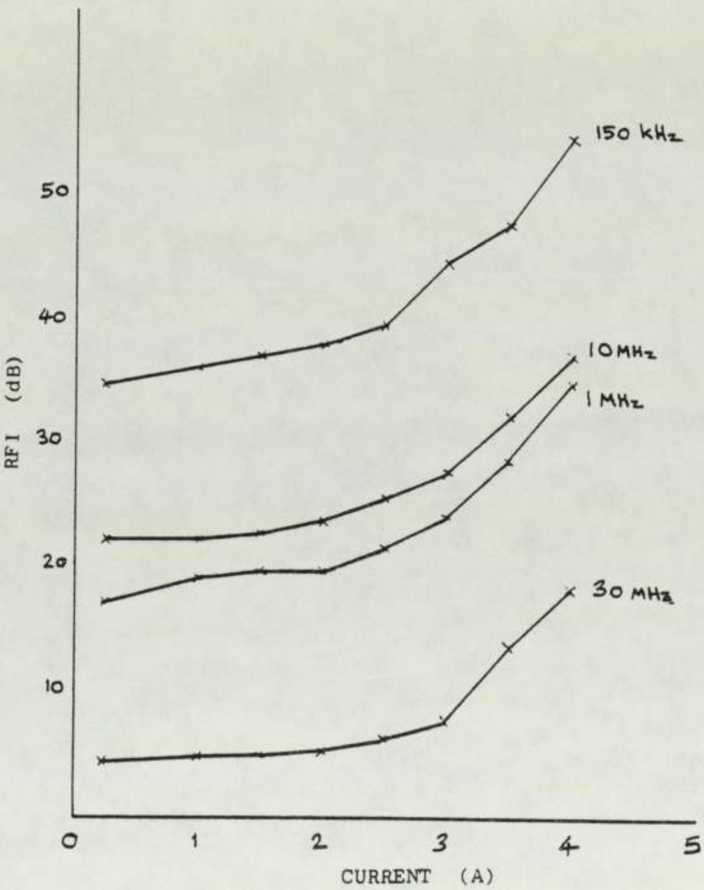

Fig. 6.19

RFI caused by the variation of the short circuited coil Parameters:
Measured RFI levels with varying resistance, R_s, (L_s = 0, e = 0) at 5000 r/min and 1.5 A supply current.

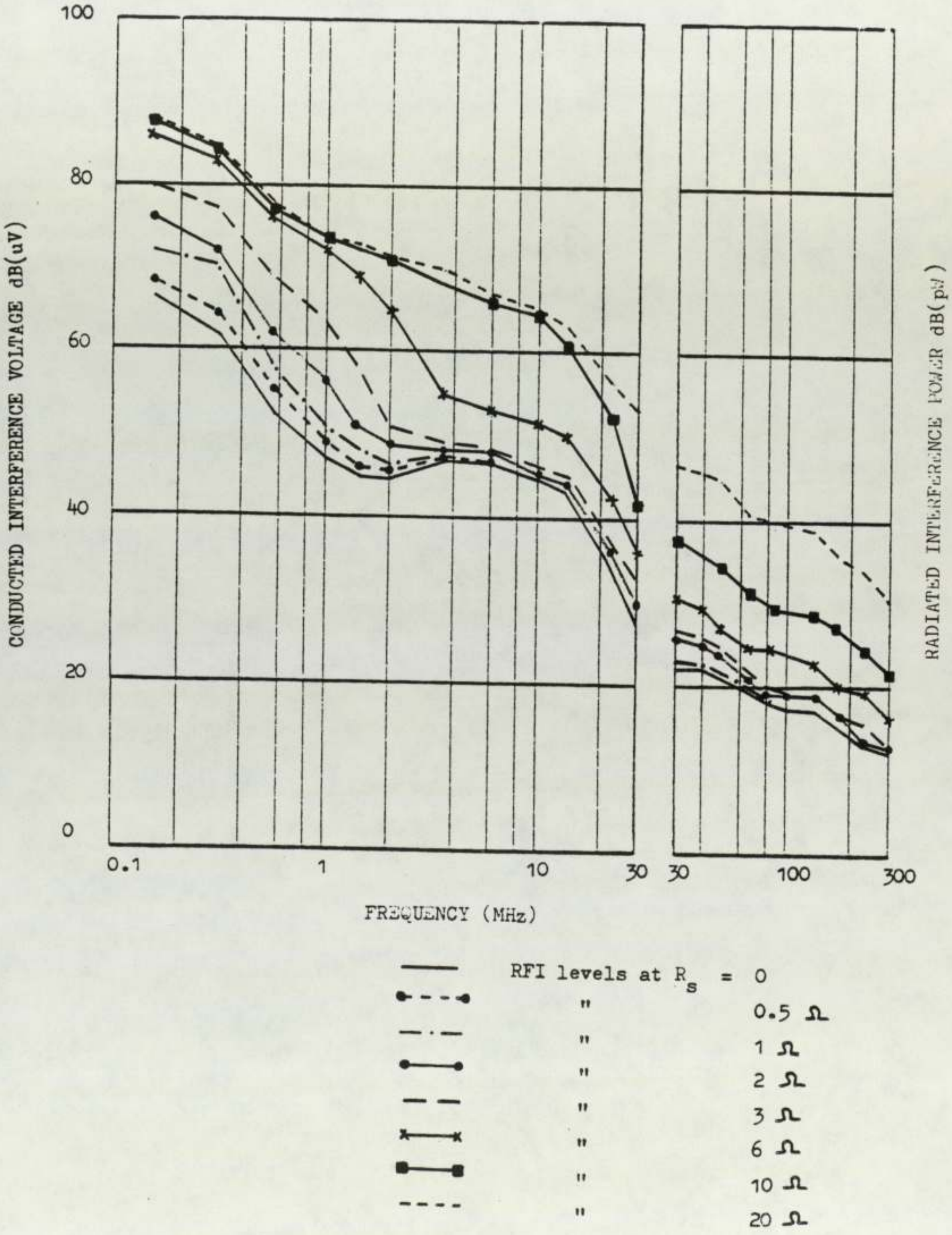

Fig. 6.20

RFI caused by the variation of the short circuited coil parameters:
Measure RFI levels with varying resistance, R_s, (L_s = 0, e = 0) at 10000 r/min and 1.5 A supply current.

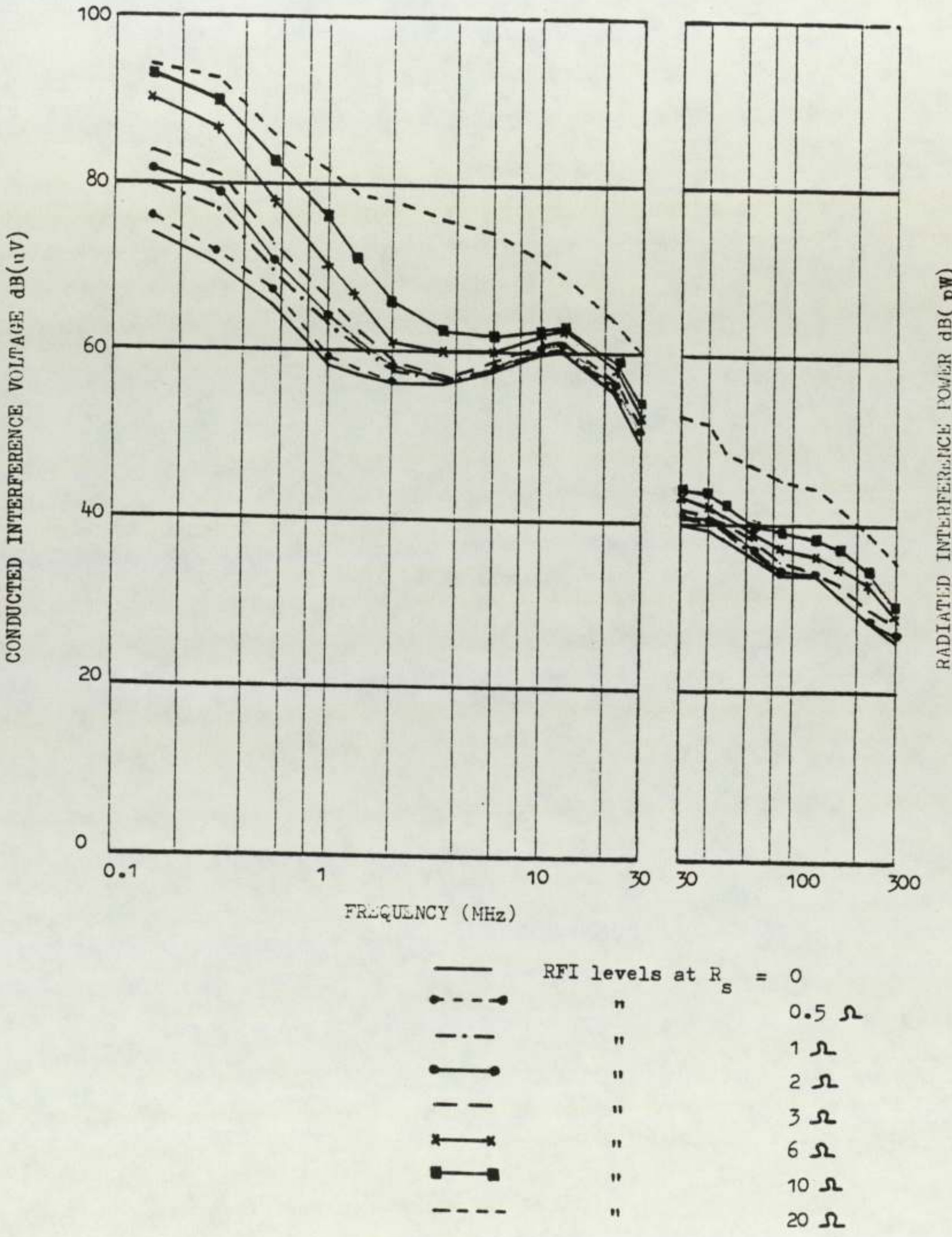

Fig. 6.21

RFI caused by the variation of the short circuited coil parameters:

Measured RFI levels varying resistance, R_s, (L_s = 0, e = 0) at 15000 r/min and 1.5 A supply current.

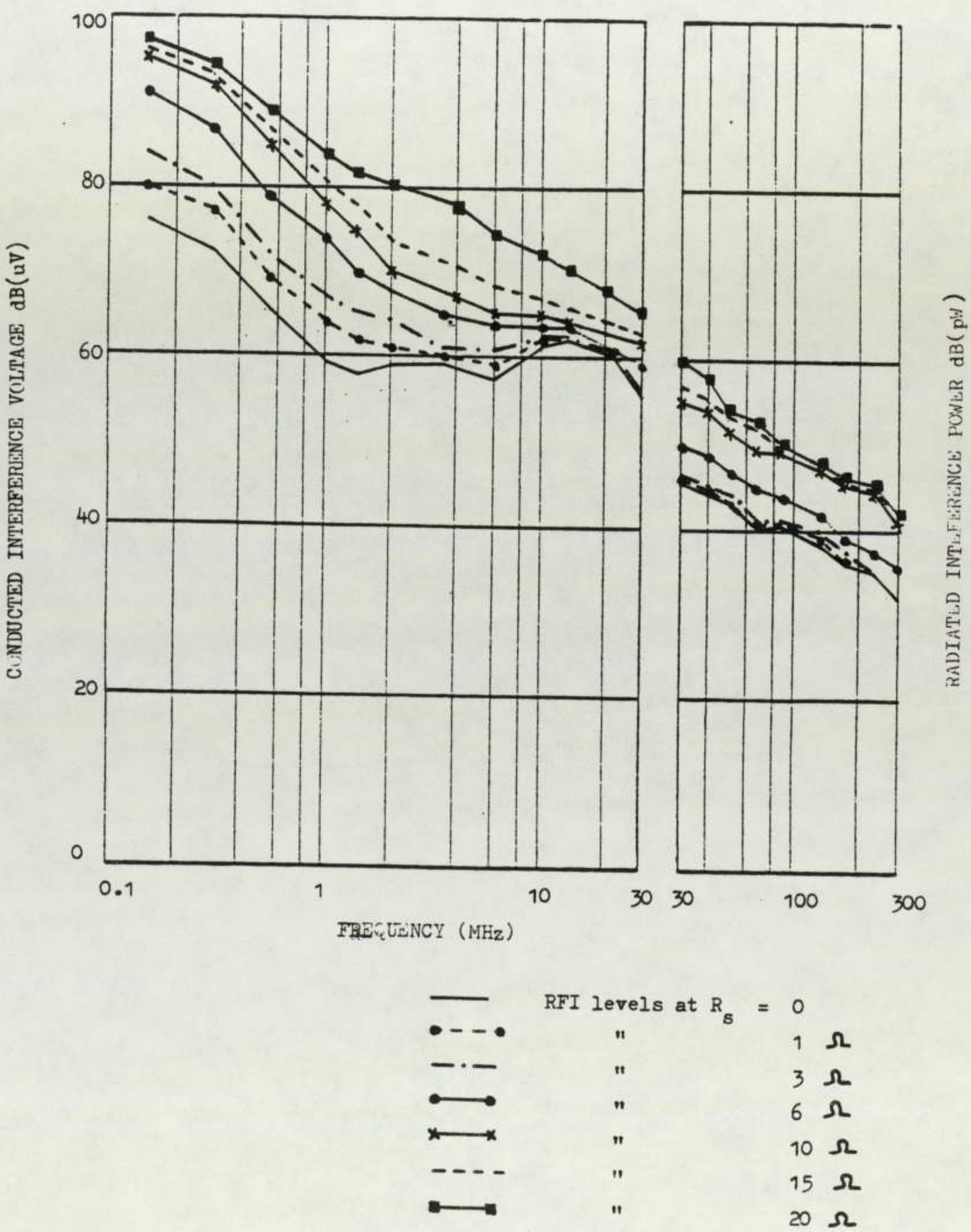

Fig. 6.22

RFI caused by the variation of the short circuited coil parameters;

Measured RFI levels with varying resistance, R_s, (L_s = 0, e = 0) at 20000 r/min and 1.5 A supply current.

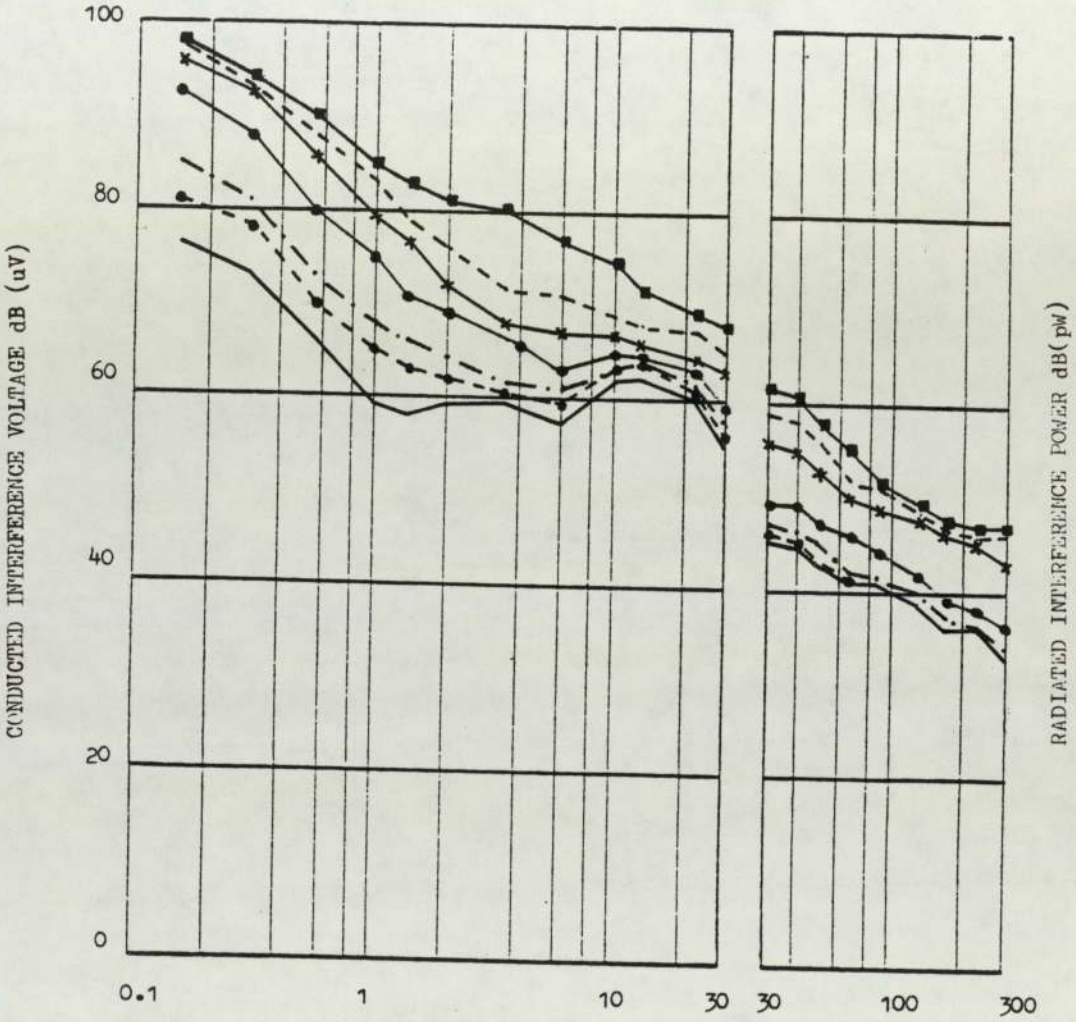

———	RFI levels at R_s =	0
•- - -•	"	1 Ω
—·—	"	3 Ω
•——•	"	6 Ω
×——×	"	10 Ω
- - - -	"	15 Ω
■——■	"	20 Ω

Fig. 6.23

Effect of varying resistance, R_s, on measured RFI levels at 5000 r/min.

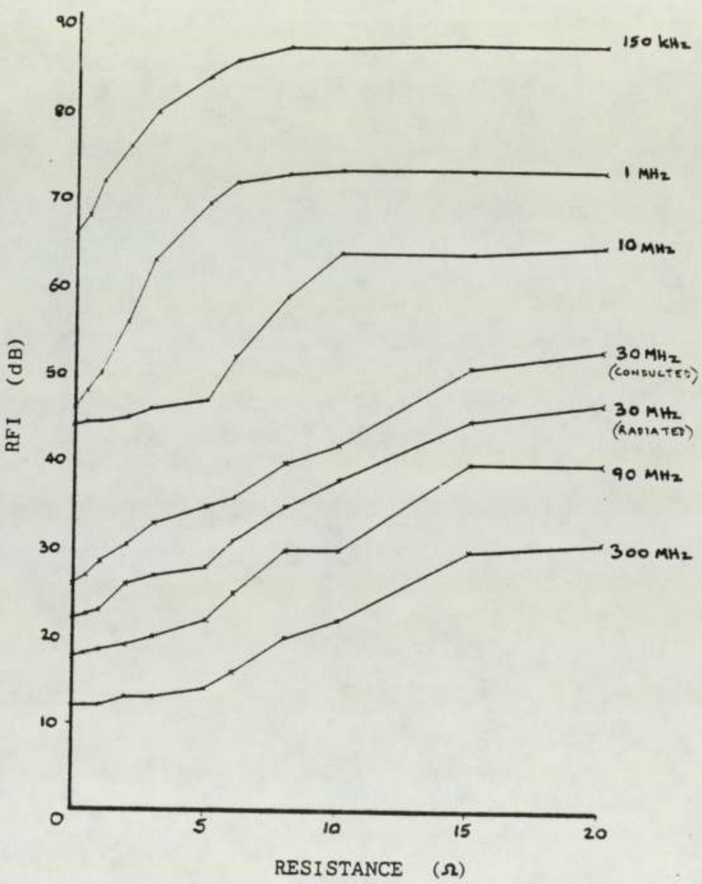

Fig. 6.24

Effect of varying resistance, R_s, on measured RFI levels at 10000 r/min.

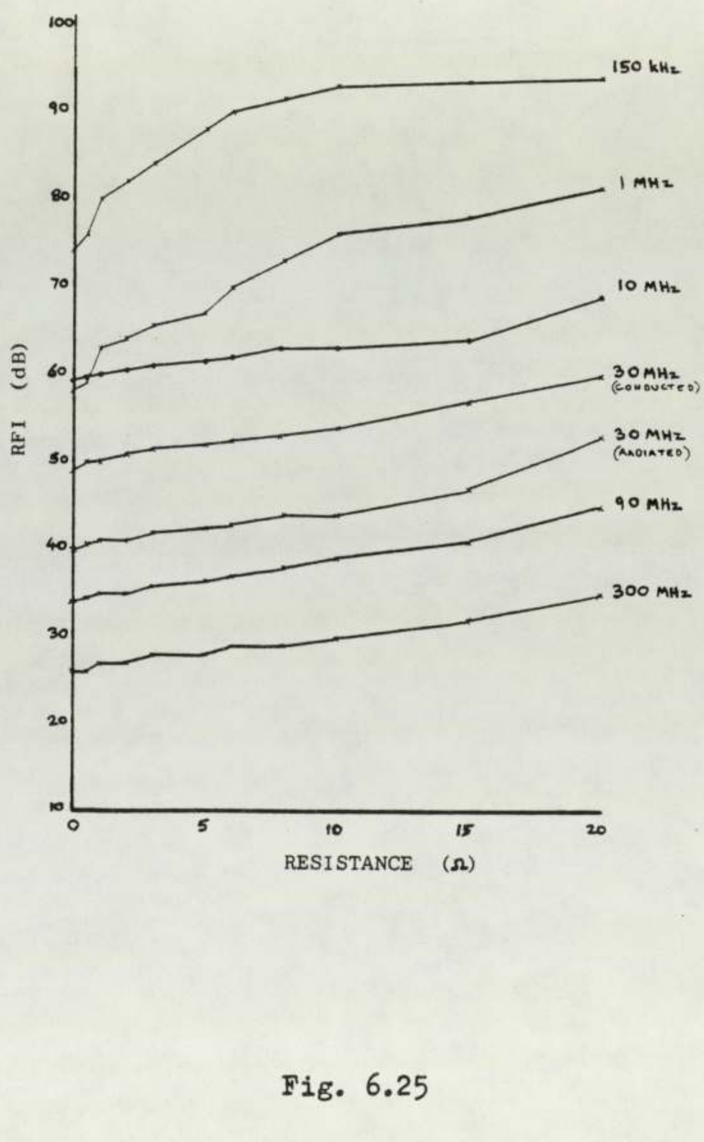

Fig. 6.25

Effect of varying resistance, R_s, on measured RFI levels at 15000 r/min.

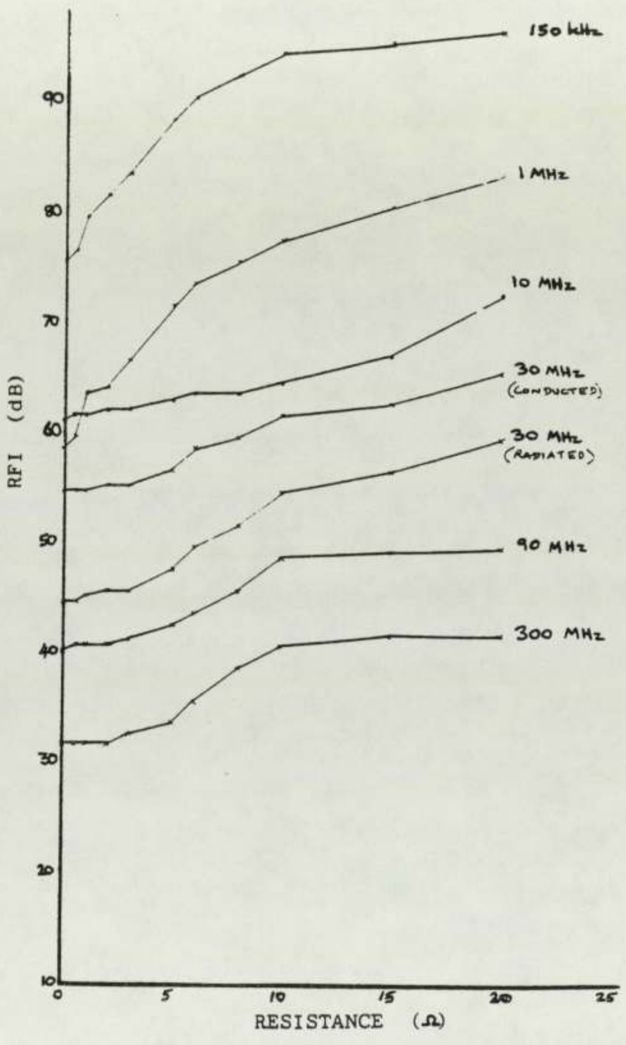

Fig. 6.26

Effect of varying resistance, R_s, on measured RFI levels at 2000 r/min.

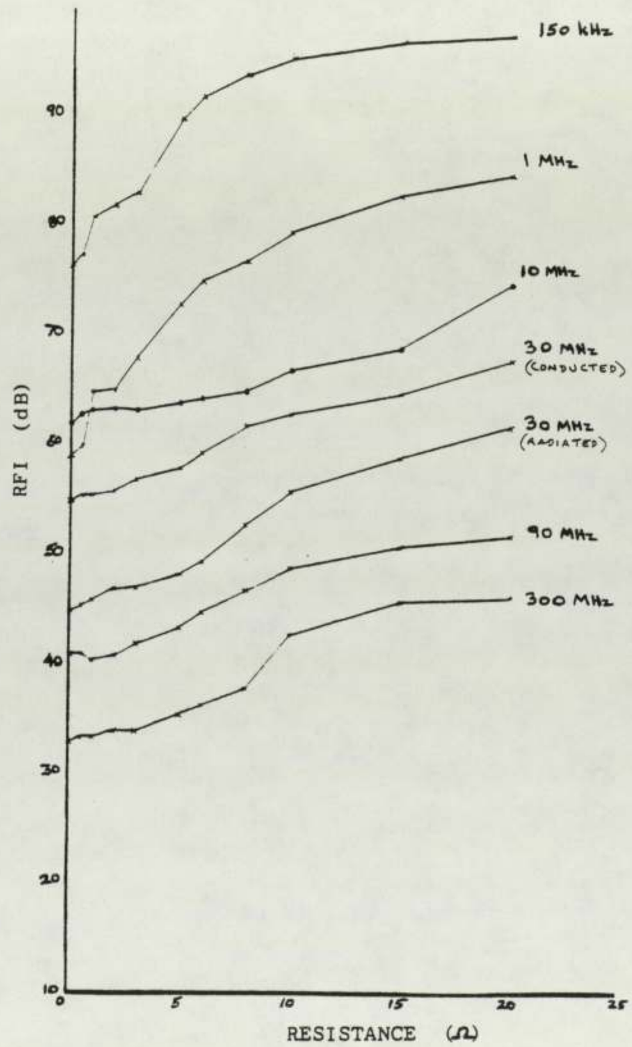

Fig. 6.27

RFI caused by the variation of the short circuited coil parameters:

Measured RFI levels with varying inductance L_s, ($R_s = 0.15\Omega$, $e = 0$) at 5000 r/min and 1.5 A cupply current.

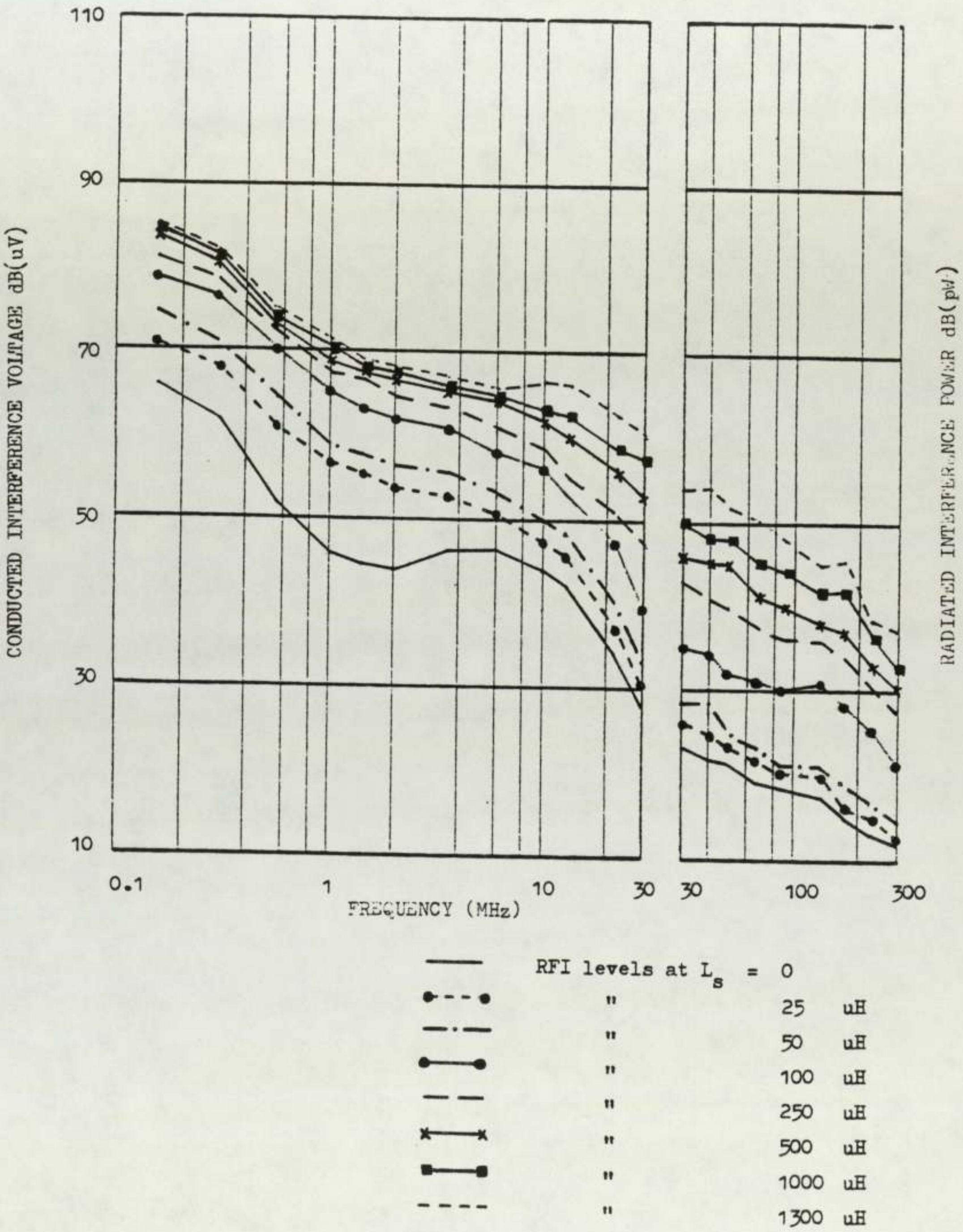

Fig. 6.28

RFI caused by the variation of the short circuited coil parameters:
Measured RFI levels with varying inductance, L_s, ($R_s = 0.15\Omega$, $e = 0$) at 10000 r/min and 1.5 A supply current.

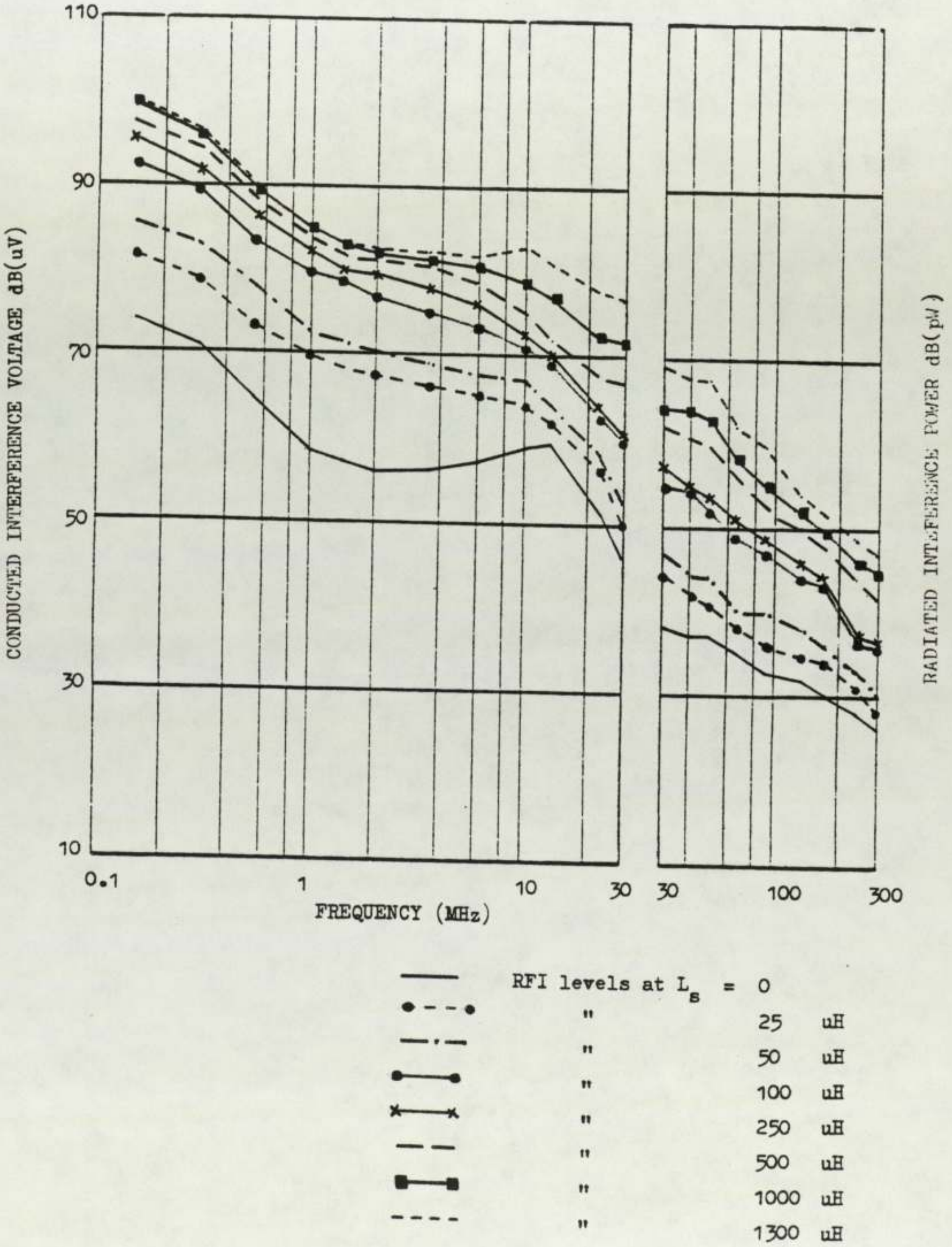

Fig. 6.29

RFI caused by the variation of the short circuited coil parameters:

Measured RFI levels with varying inductance, L_s, (R_s = 0.15 Ω e = 0) at 15000 r/min and 1.5 A supply current.

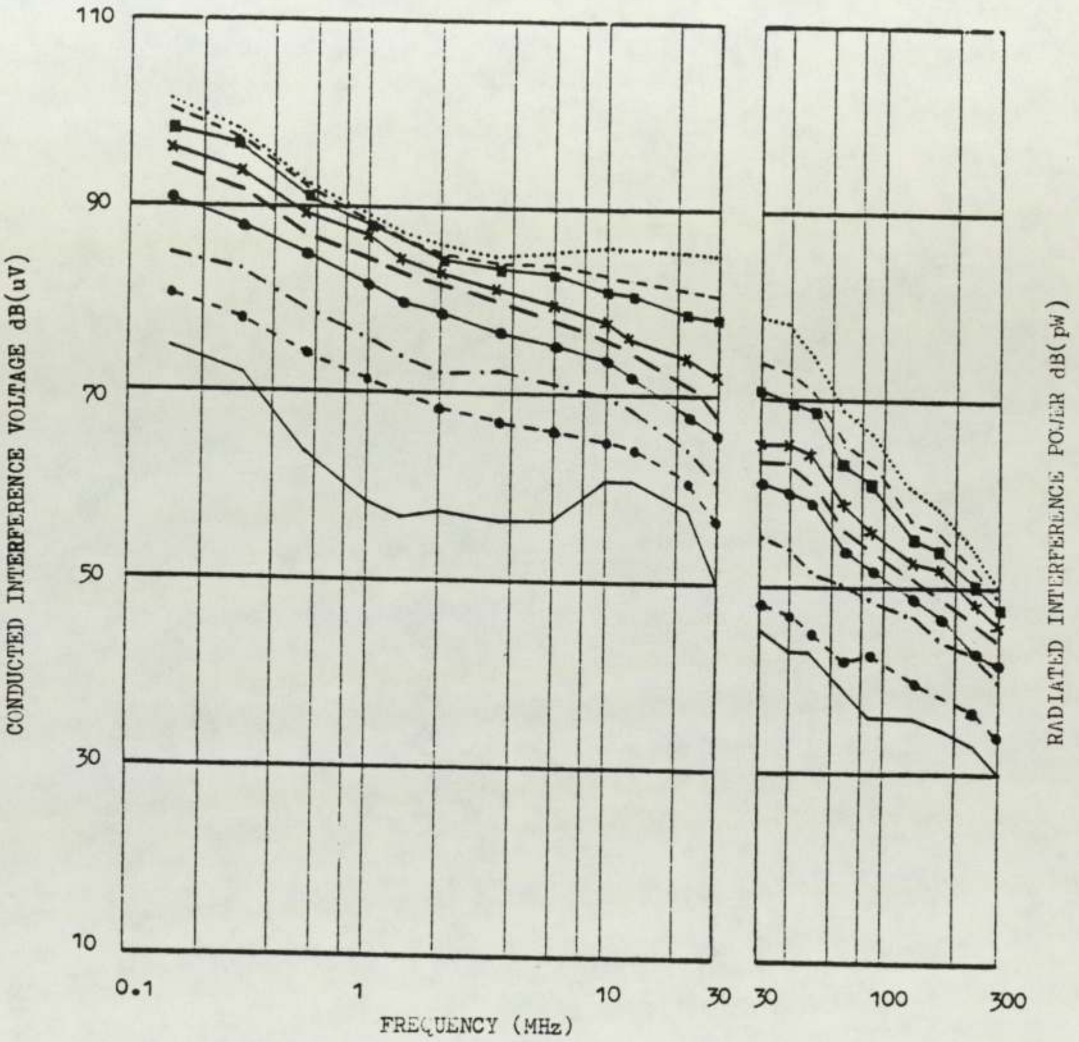

——	RFI levels at L_s =	0	
•- - -•	"	10	uH
—·—	"	25	uH
•——•	"	50	uH
— —	"	100	uH
×——×	"	250	uH
■——■	"	500	uH
- - - -	"	1000	uH
········	"	1300	uH

Fig. 6.30

RFI caused by the variation of the short circuited coil parameters:

Measured RFI levels with varying inductance, L_s, (R_s = 0.15 Ω, e = 0) at 20000 r/min and 1.5 A supply current.

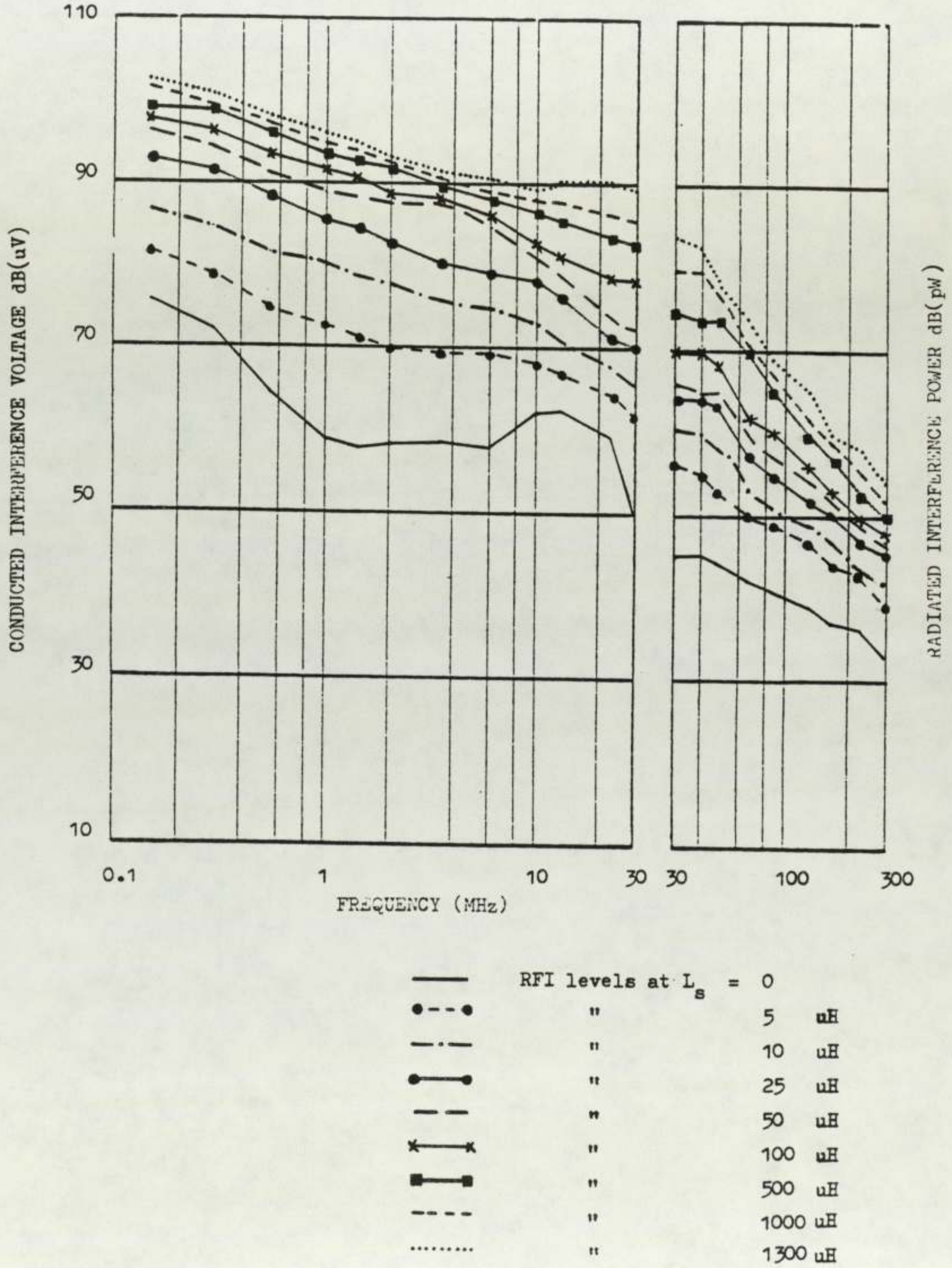

Fig. 6.31

Effect of varying inductance, L_s, on measured RFI levels at 5000 r/min.

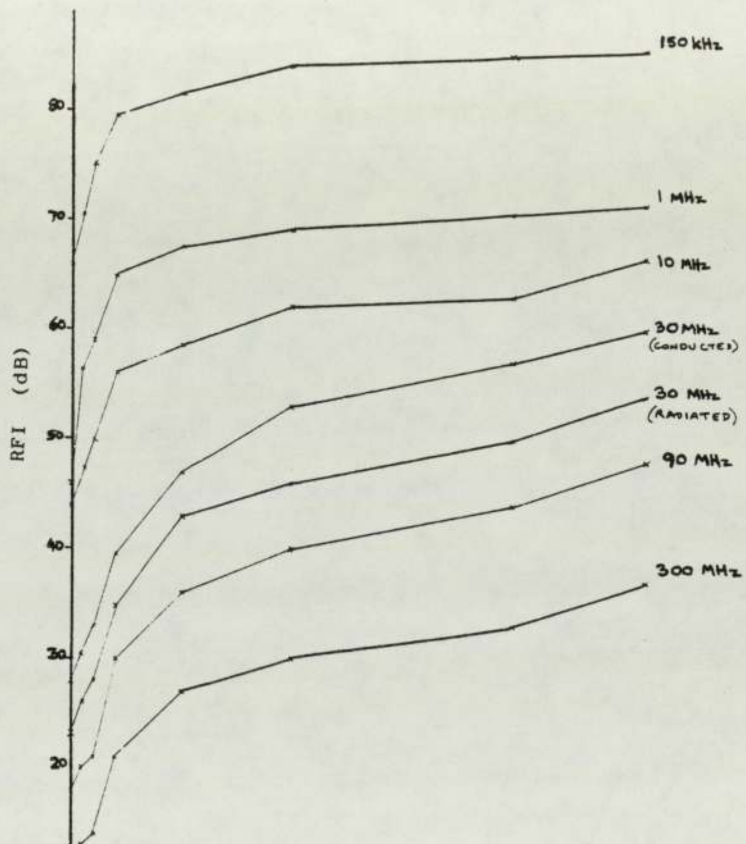

Fig. 6.32

Effect of varying inductance, L_s, on measured RFI levels at 10000 r/min.

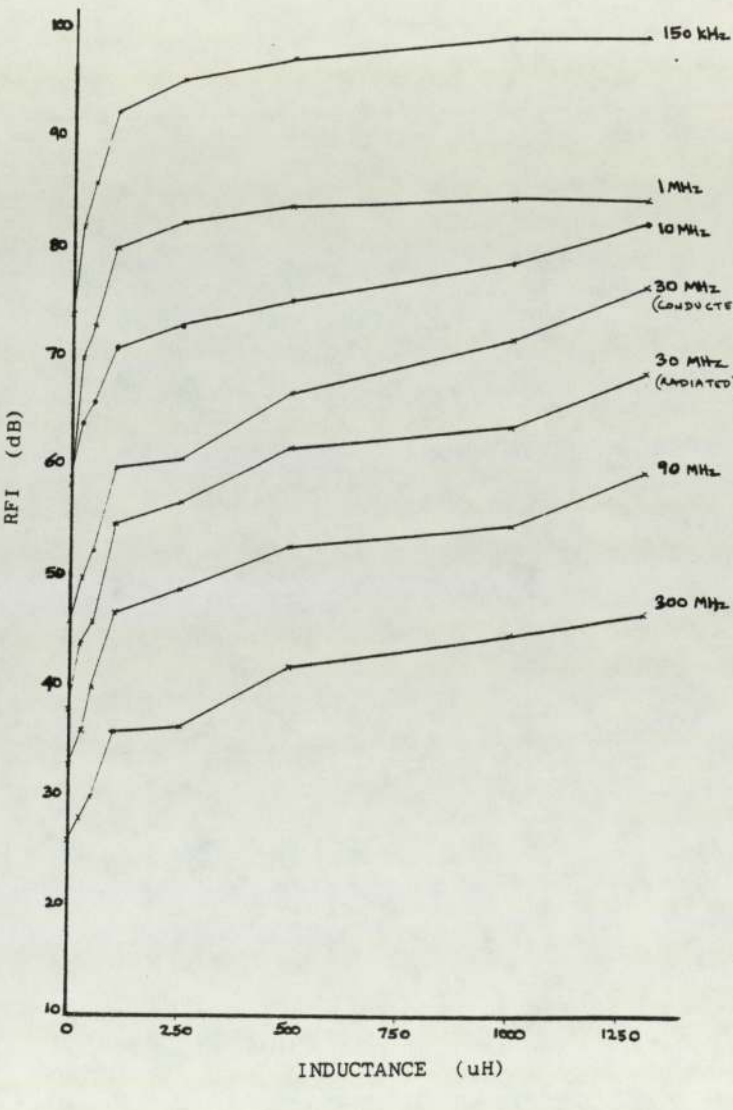

Fig. 6.33

Effect of varying inductance, L_s, on measured RFI levels at 15000 r/min.

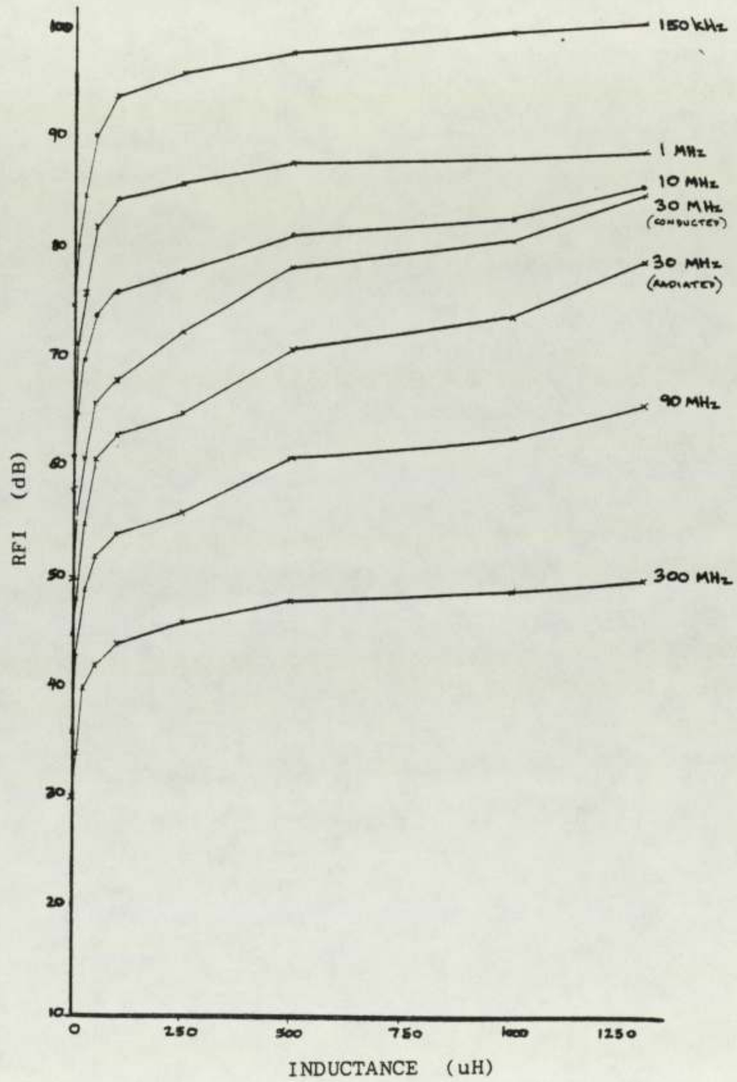

Fig. 6.34

Effect of varying inductance, L_s, on measured RFI levels at 20000 r/min.

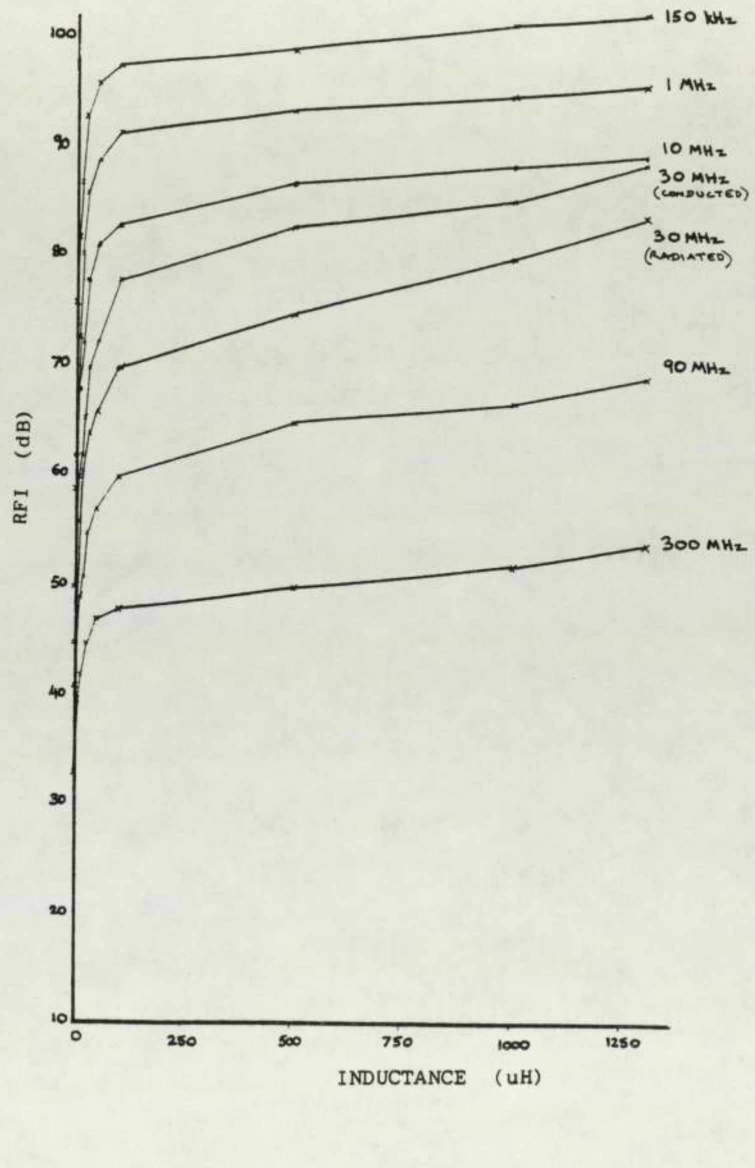

Fig. 6.35

RFI caused by the variation of the short circuited coil parameters:

Measured RFI levels with varying supply current and L_s = 50 μH (R_s = 0.15 Ω , e = 0) at 15000 r/min.

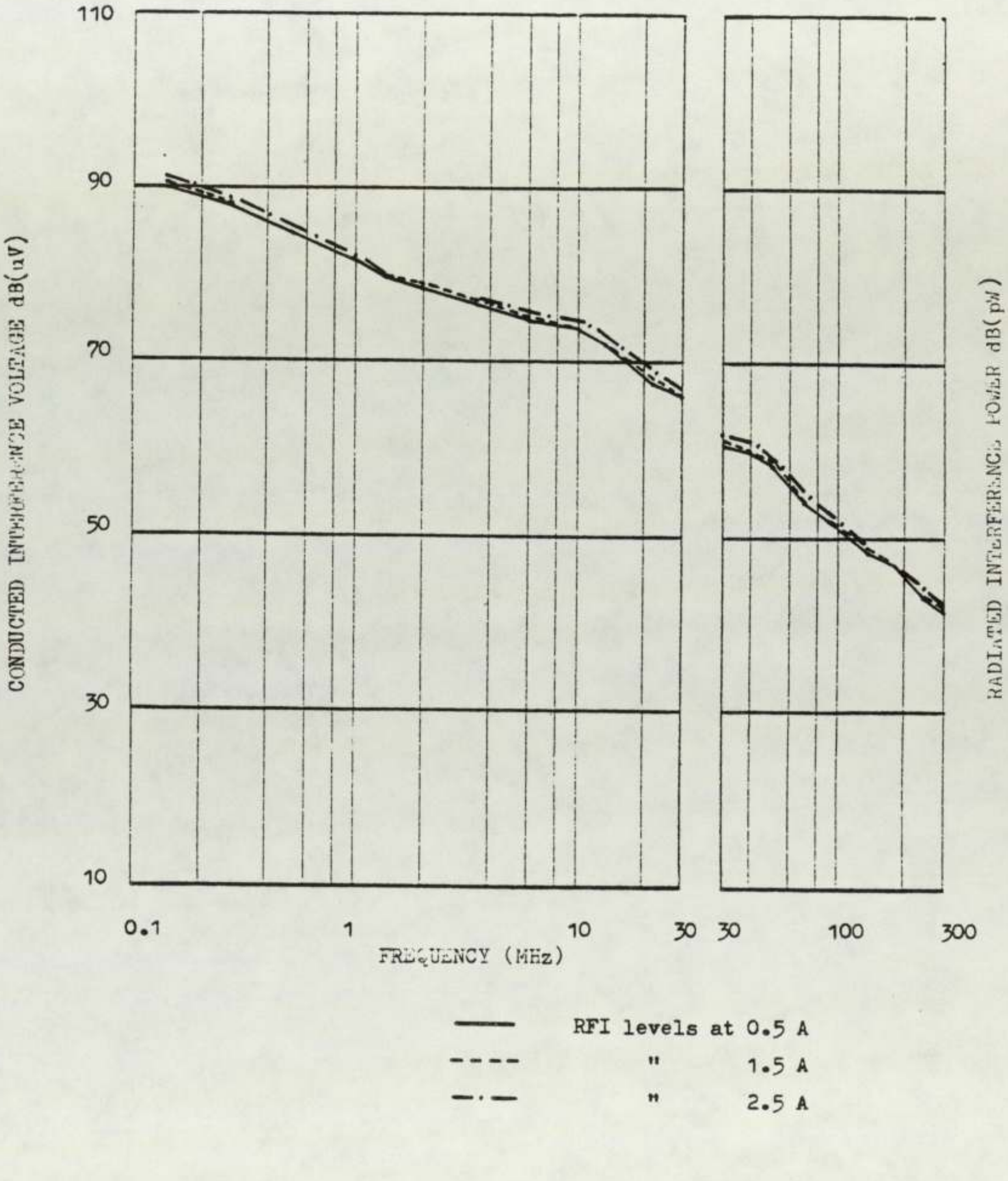

Fig. 6.36

RFI caused by the variation of the short circuited coil parameters:

Measured RFI levels with varying supply current and L_s = 100 μH (R_s = 0.15Ω, e = 0) at 15000 r/min.

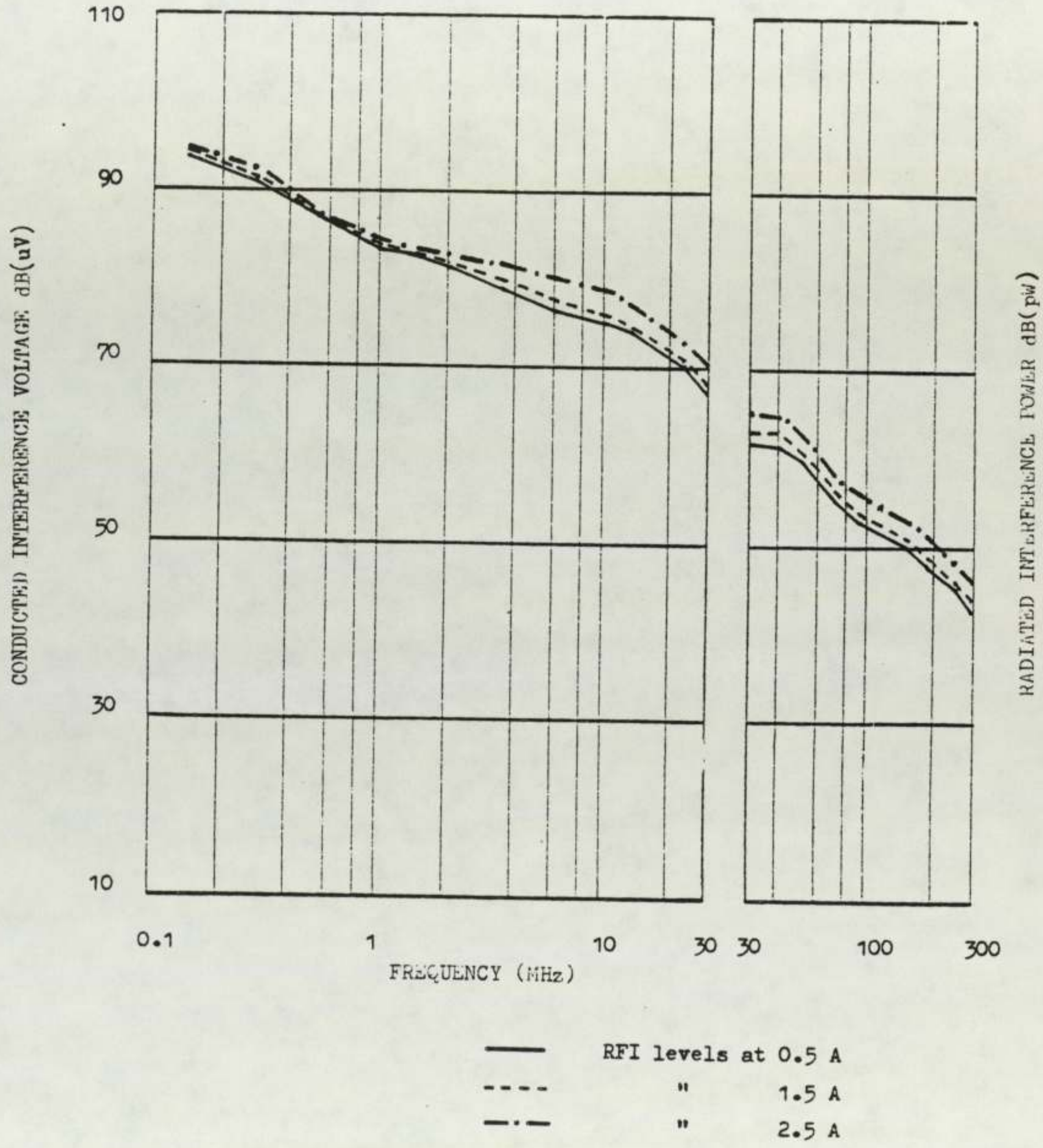

Fig. 6.37

RFI caused by the variation of the short circuited coil parameters:

Measured RFI levels with varying supply current and L_s = 500 μH (R_s = 0.15Ω, e = 0) at 20000 r/min.

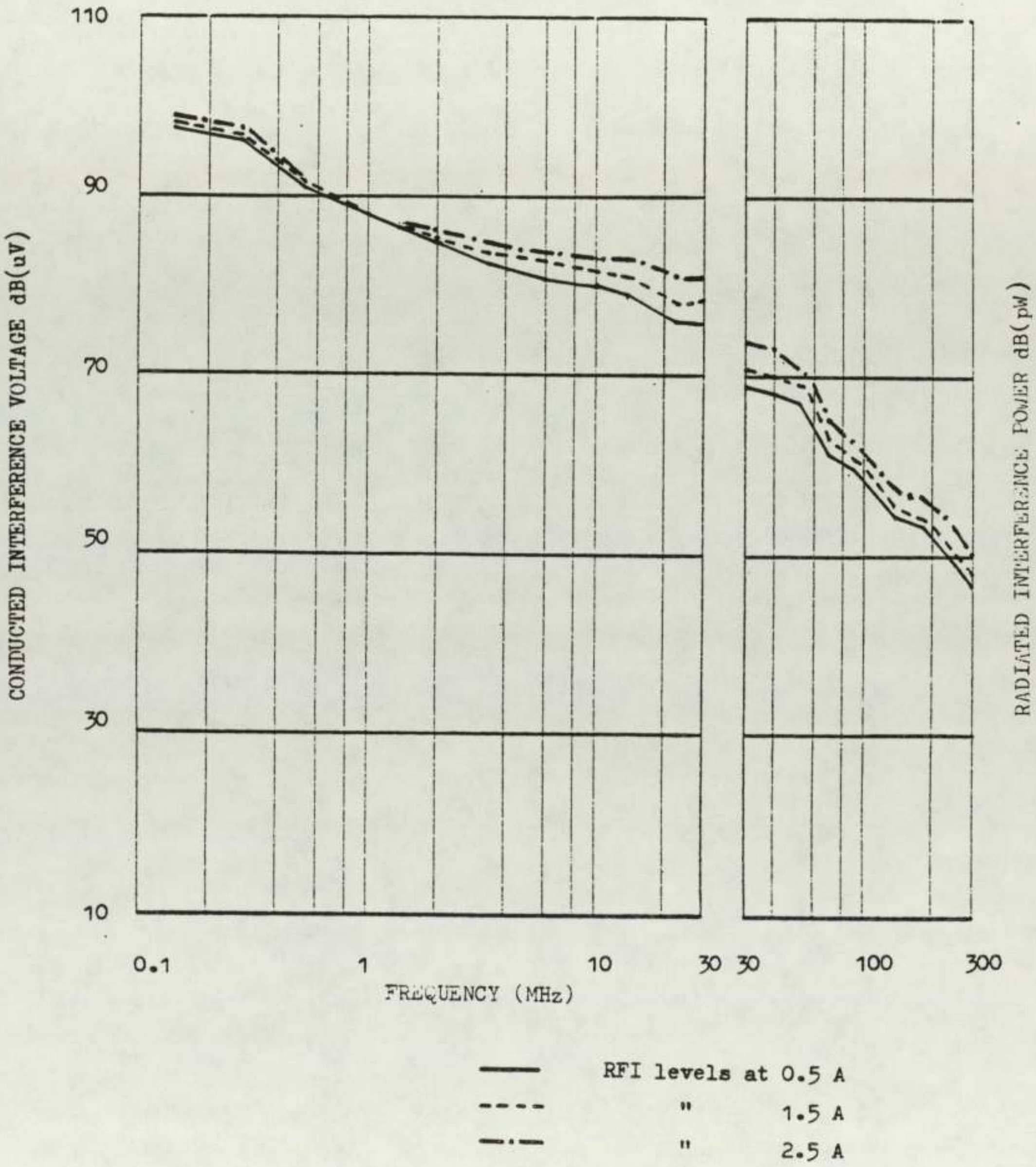

Fig. 6.38

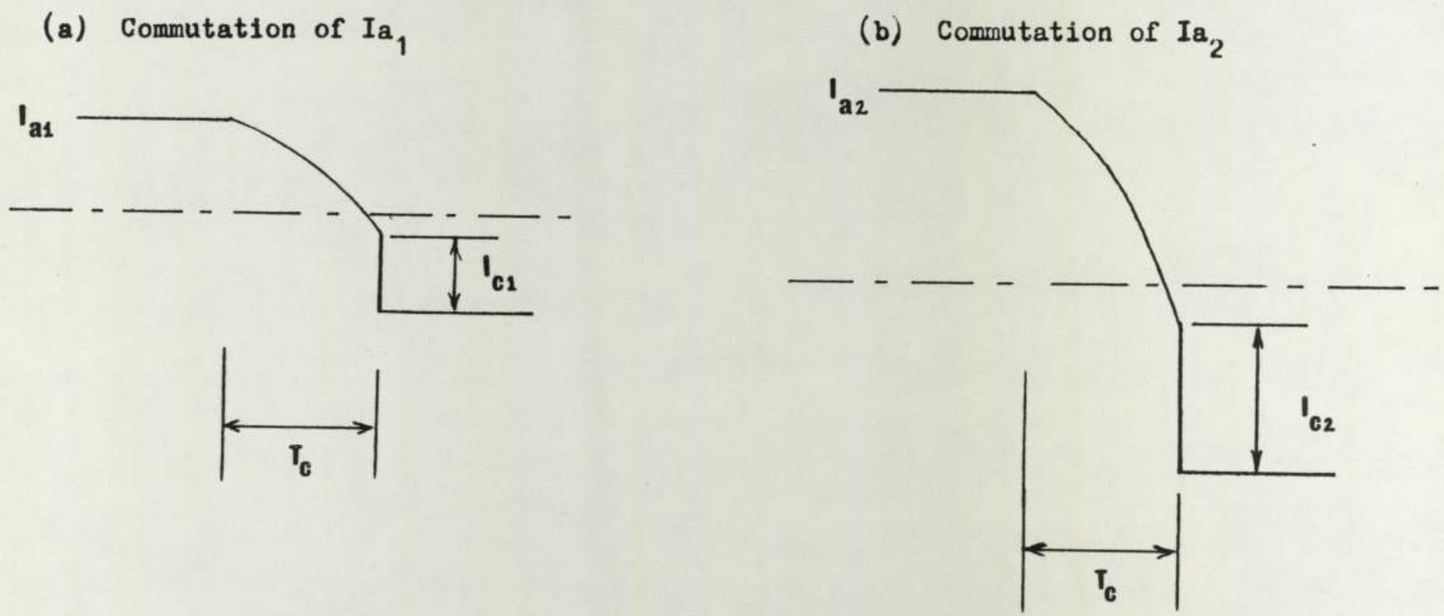

Variation of un-commutated current at Tc with increasing armature current

Fig. 6.39

RFI caused by the variation of the short circuited coil parameters:

Measured RFI levels with varying circuit e.m.f., (e), at $\Psi = 45^{\circ}$ with $L_s = 230\mu H$, $R_s = 0.174\,\Omega$ at 15000 r/min and 1.5 A supply current.

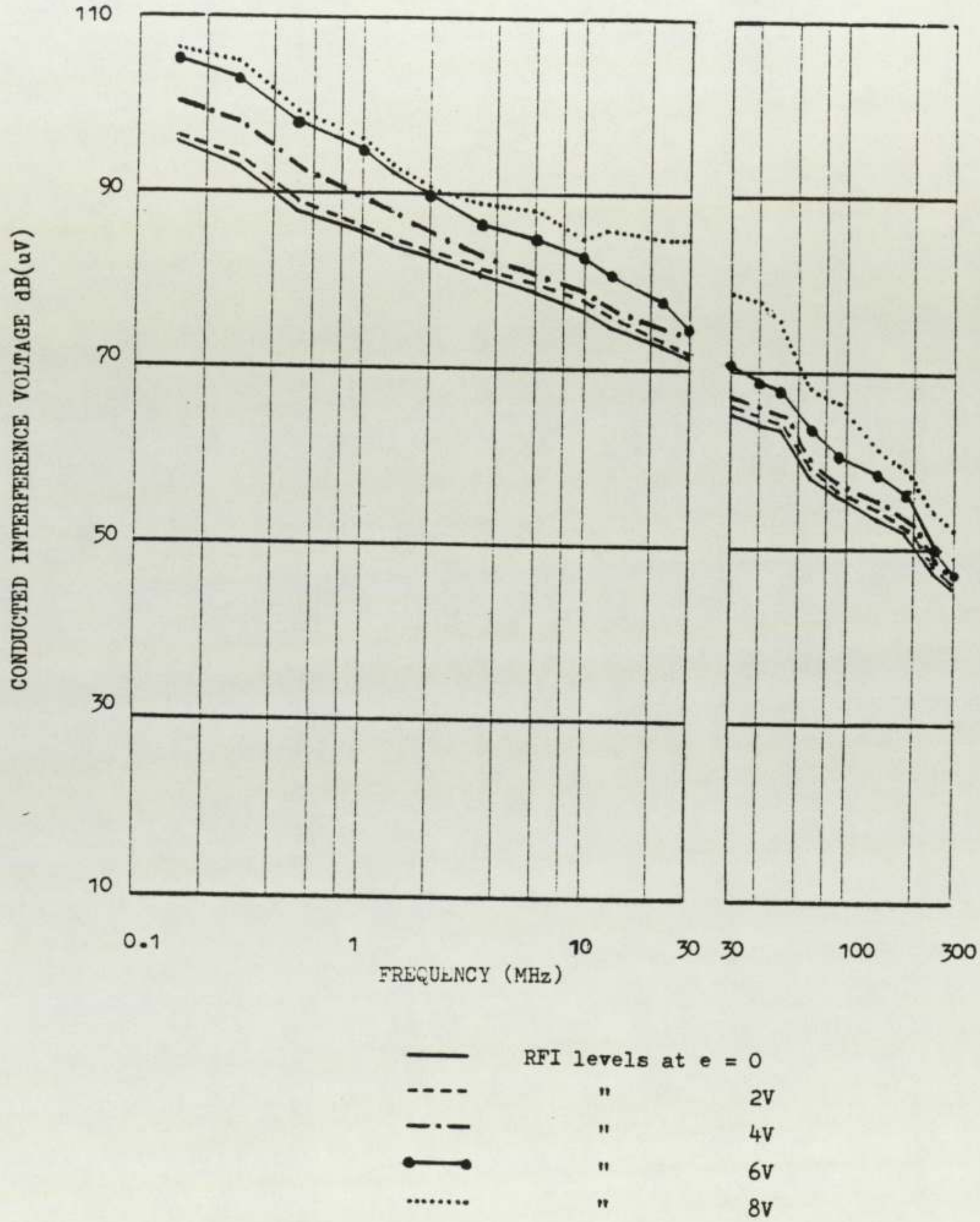

Fig. 6.40

RFI caused by the variation of the short circuited coil parameters:

Measured RFI levels with varying circuit e.m.f., (e) at $\psi = 45$ with $L_s = 500\mu H$, $R_s = 0.32\,\Omega$ at 15000 r/min and 1.5 A supply current.

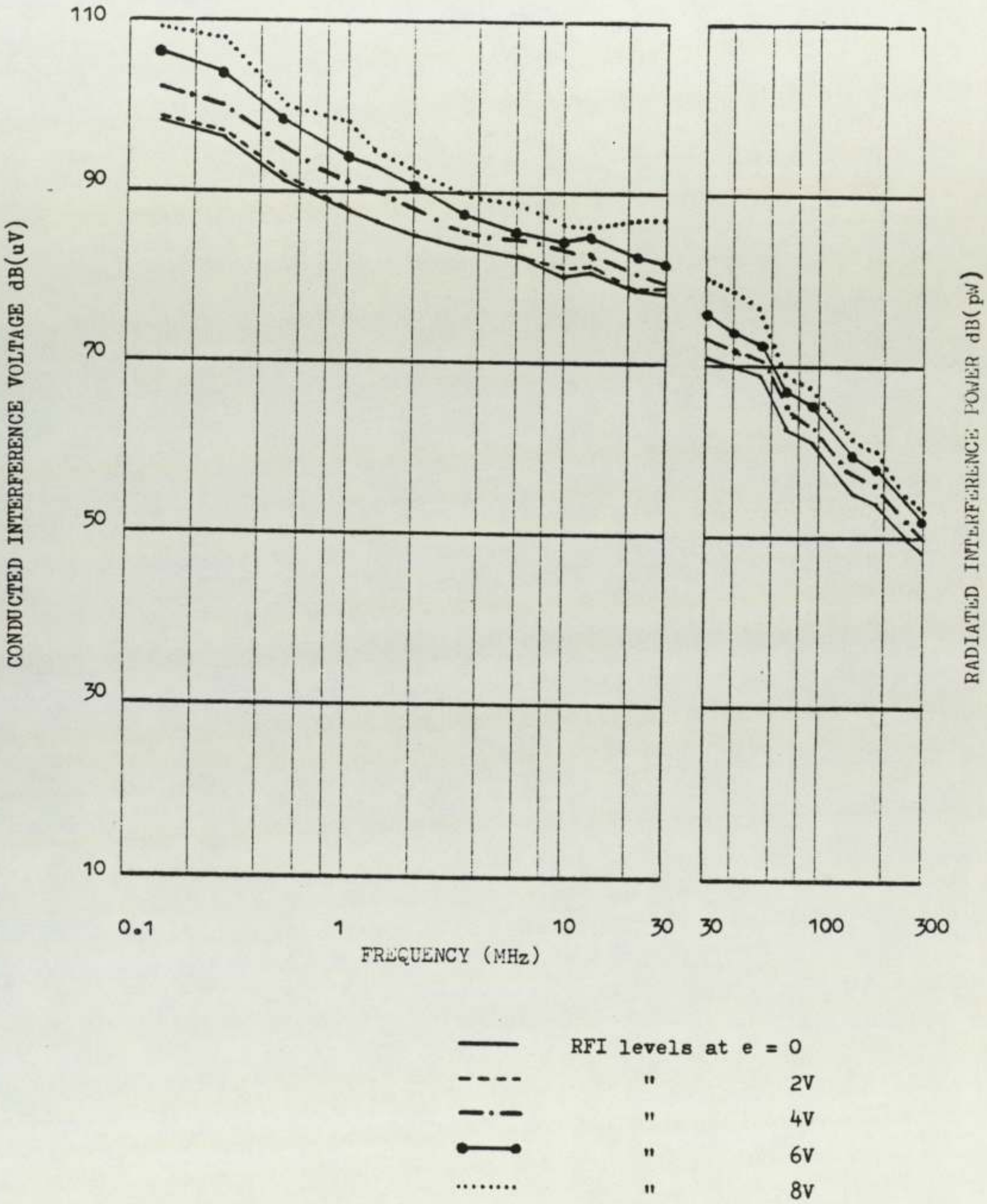

Fig. 6.41

RFI caused by the variation of the short circuited coil parameters:

Measured RFI levels with varying circuit e.m.f., (e), at $\psi = 45^{\circ}$ with $L_s = 1000 \mu H$, $R_s = 0.32 \Omega$ at 15000 r/min at 1.5 A supply current.

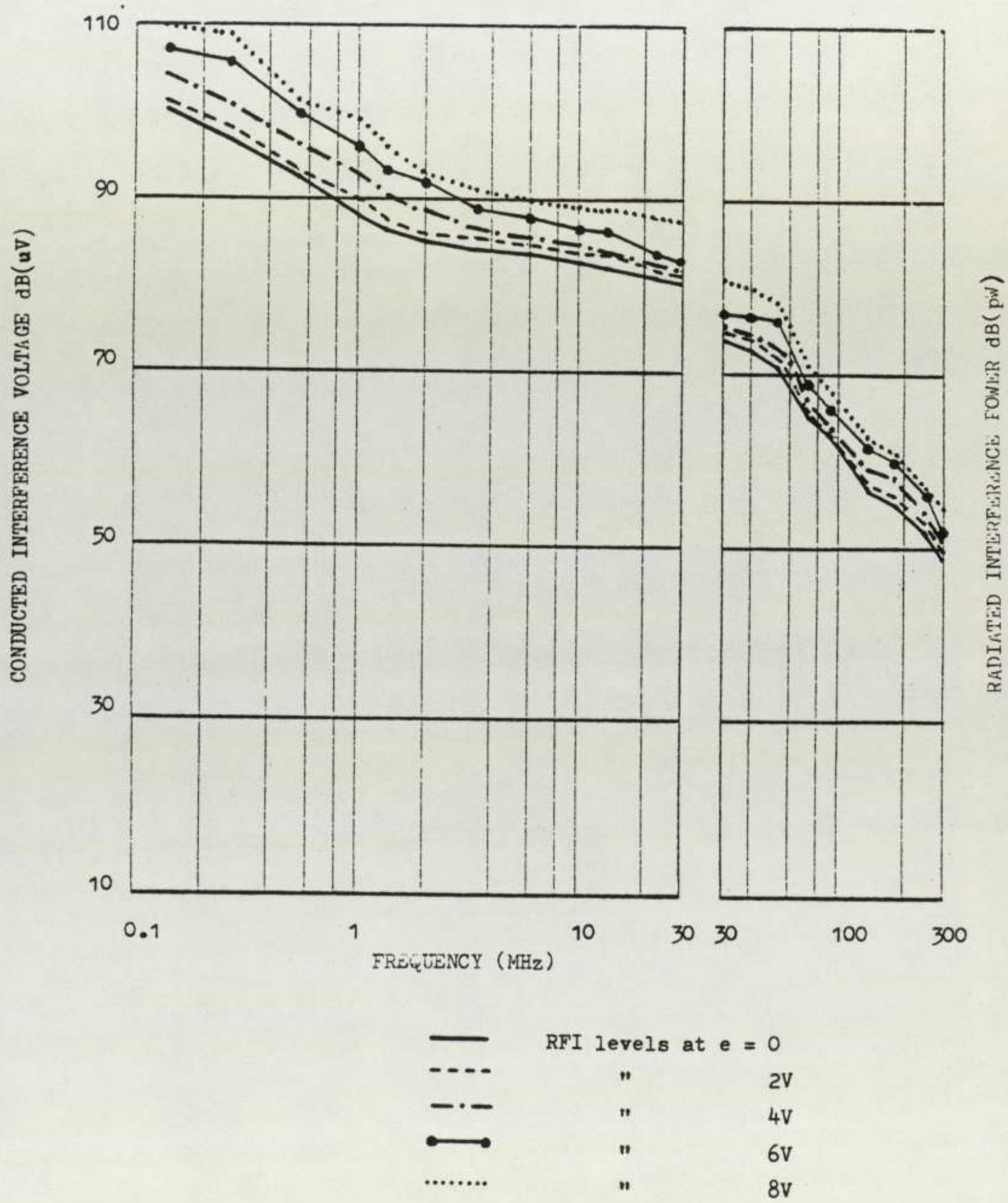

Fig. 6.42

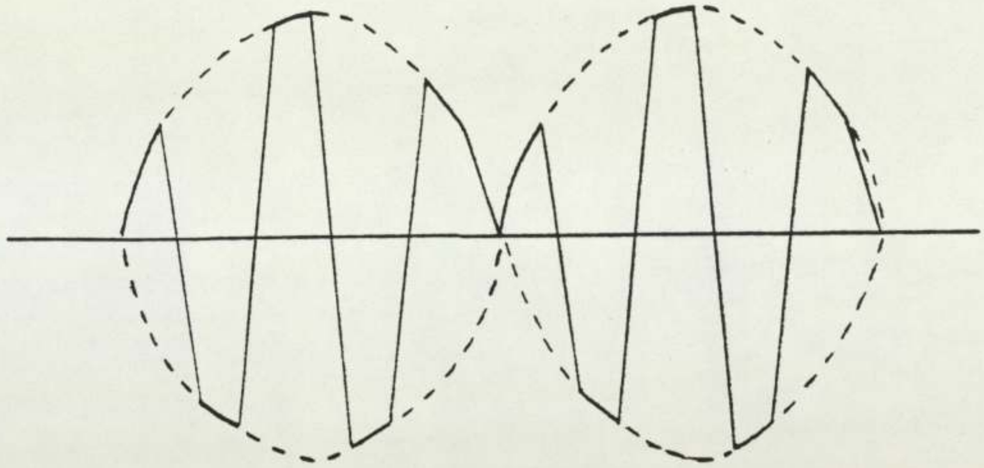

(a) Simplified sketch of commutating current

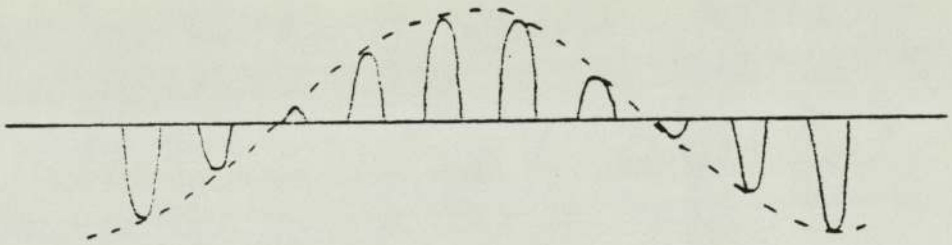

(b) Circulating current component at 90° lag with main current

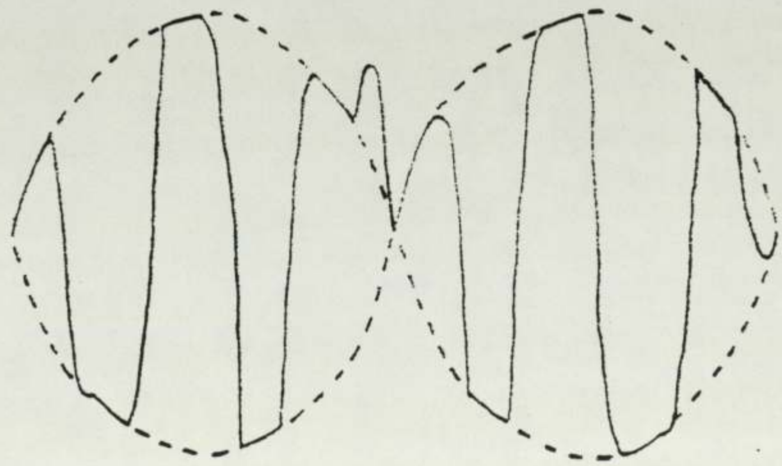

(c) Resultant commutating current; (a) (b)

Influence of circulating current on commutation

Fig. 6.43

RFI caused by the variation of the short circuited coil parameters:

Measured RFI levels with varying phase angle, ψ, at e = 4V with L_s = 230μH, R_s = 0.174 Ω at 15000 r/min and 1.5 A supply current.

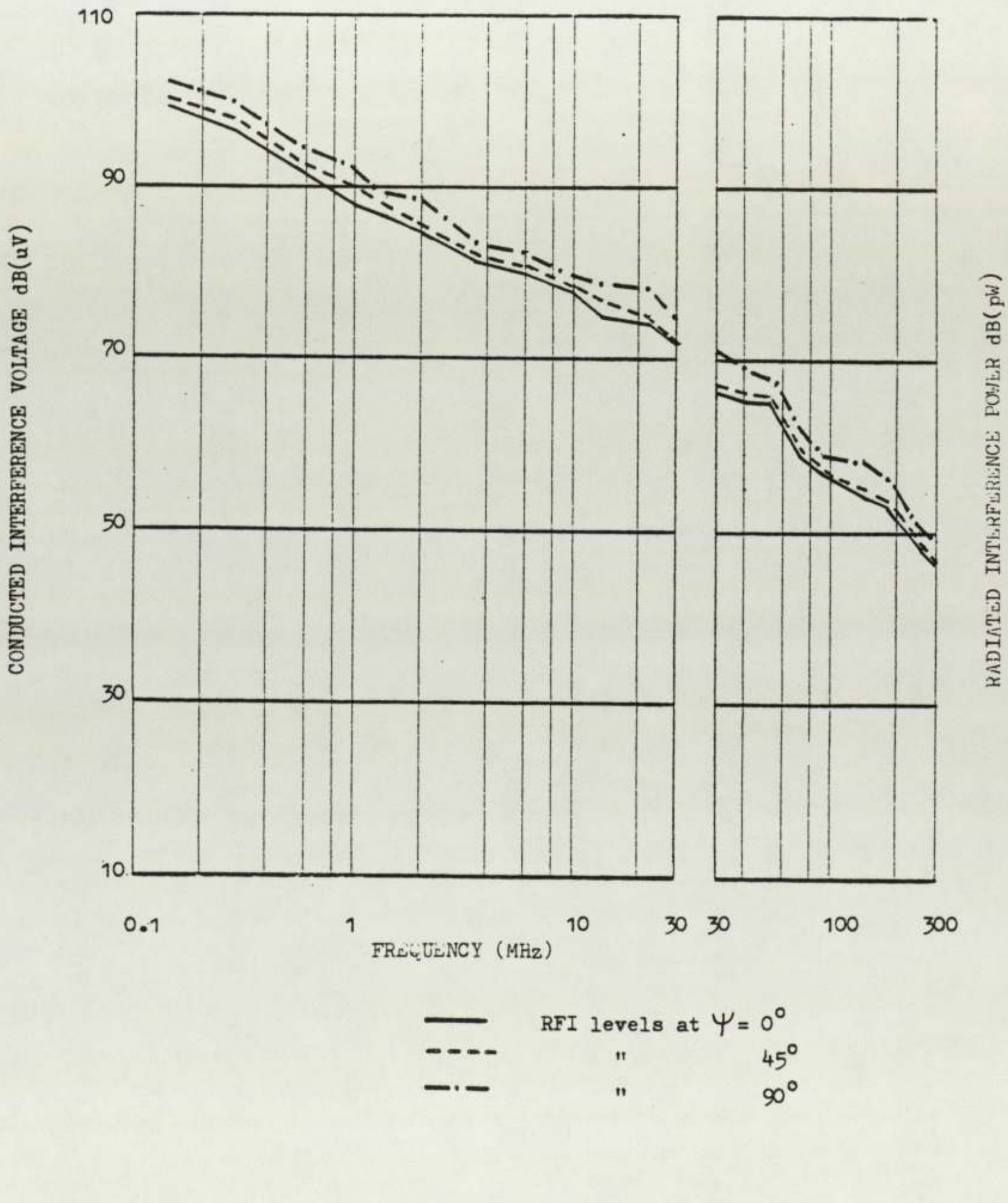

Fig. 6.44

RFI caused by the variation of the short circuited coil parameters:

Measured RFI levels with varying circuit e.m.f., (e) at $\psi = 45^{\circ}$, with $L_s = 230 \mu H$, $R_s = 0.174\,\Omega$ at 15000 r/min and 0.5 A supply current.

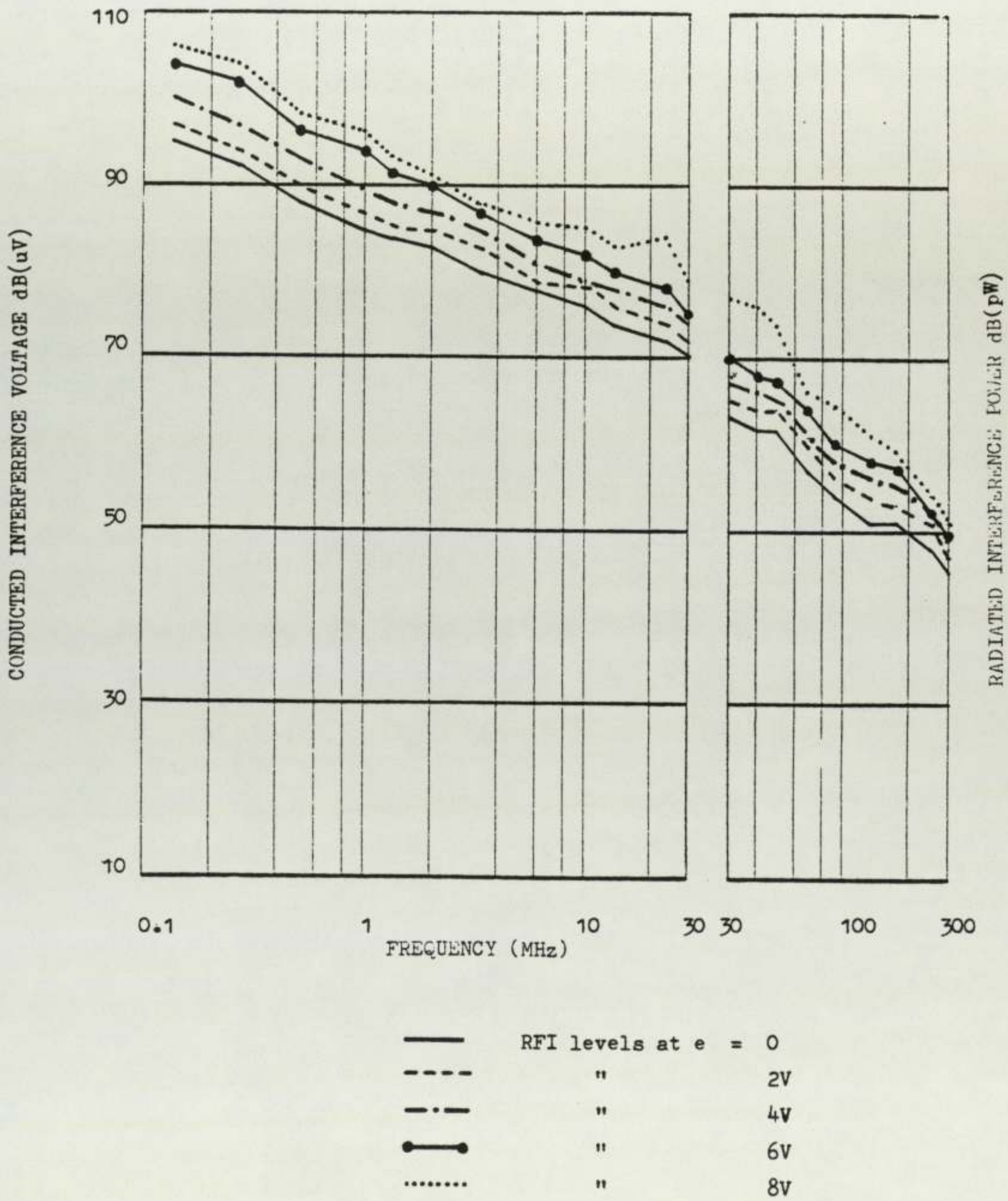

Fig. 6.45

RFI caused by the variation of the short circuited coil parameters:

Measured RFI levels with varying circuit e.m.f., (e) at $\psi = 45^{\circ}$, with $L_s = 230\mu H$, $R_s = 0.174\,\Omega$ at 15000 r/min and 2.5 A supply current.

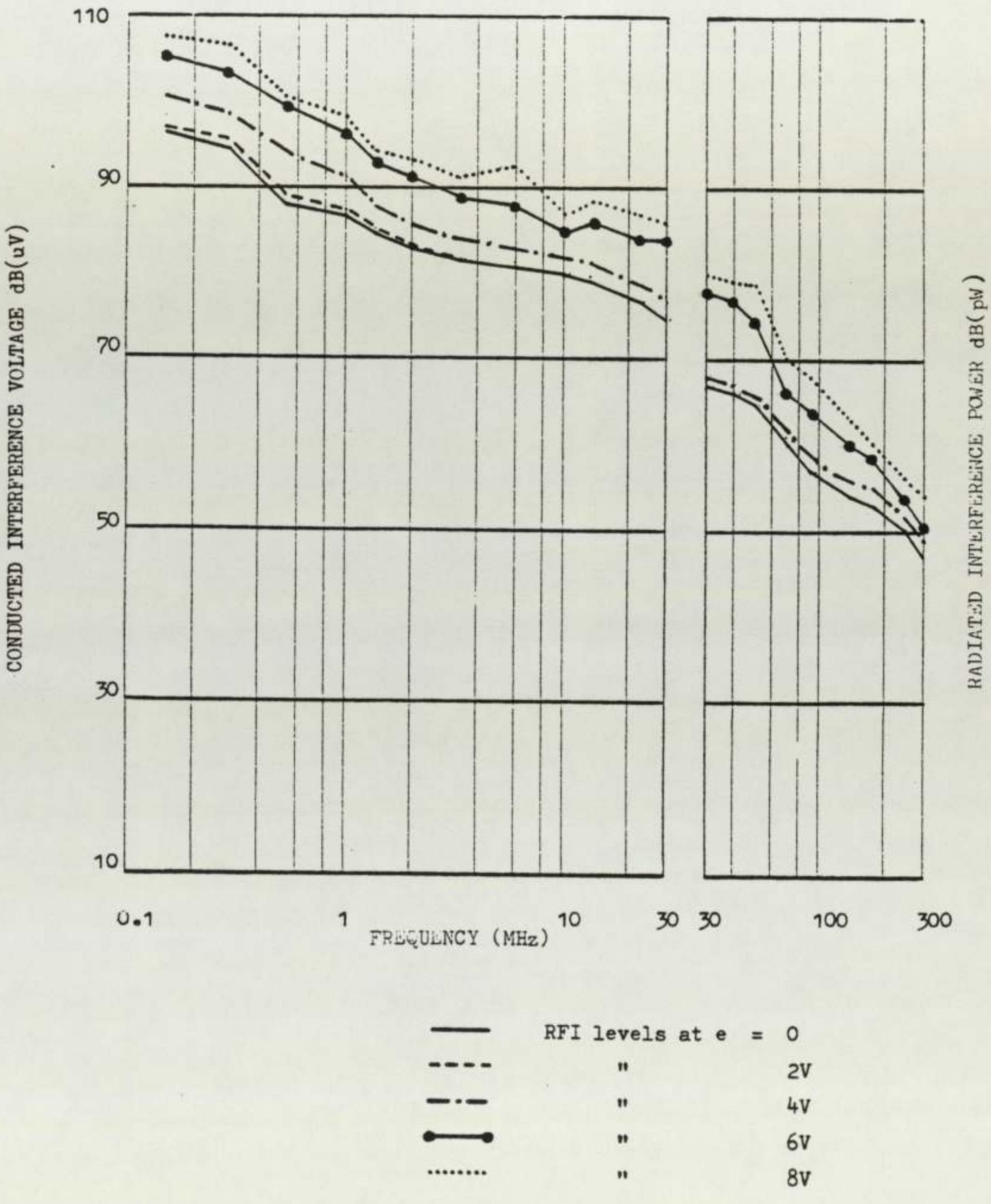

Fig. 6.46

RFI due to the influence of the physical components of the armature and field:
Measured RFI levels from the U-type field system at 1, 1.5 and 3 Amps.

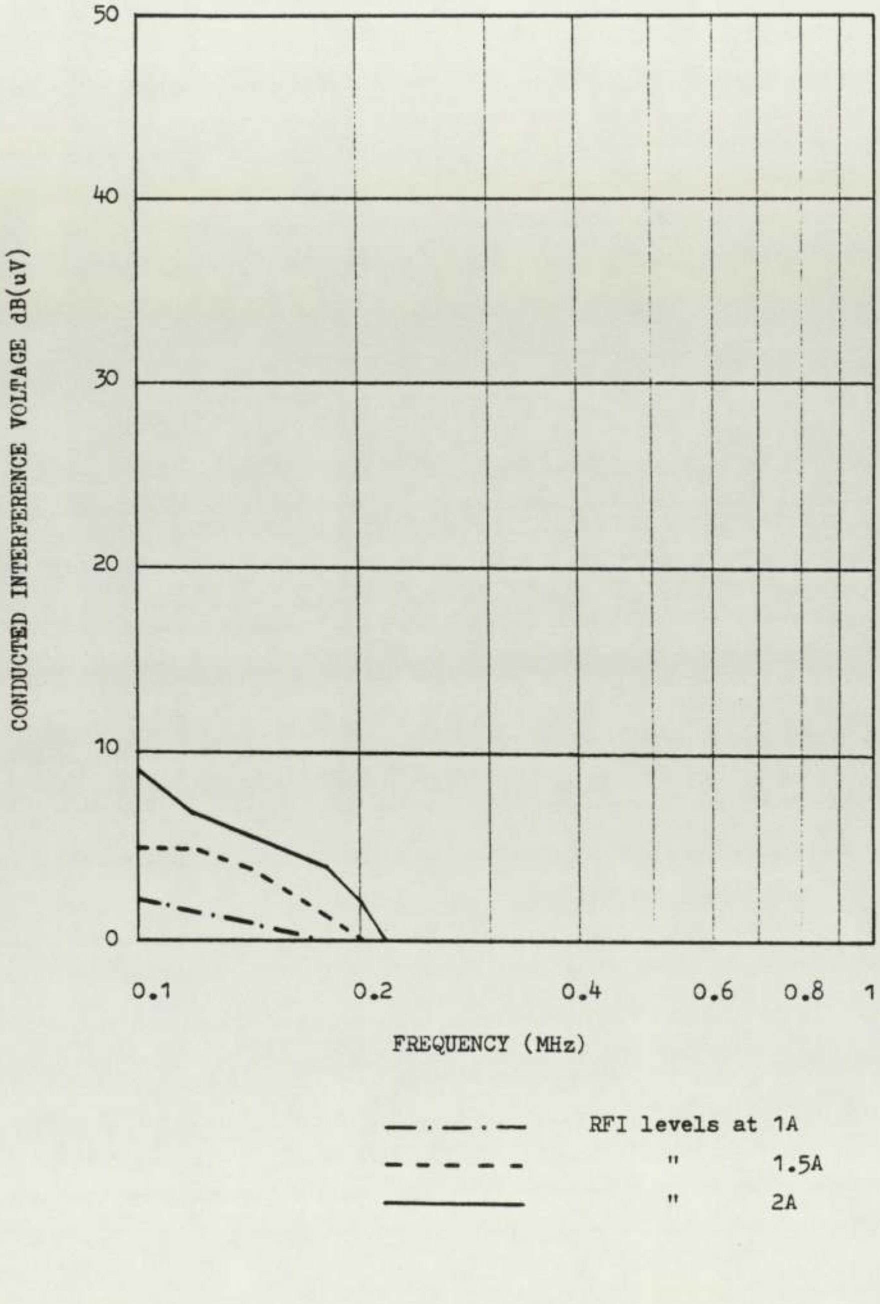

Fig. 6.47

RFI due to the influence of the physical components of the armature and field:
Measured RFI levels from the U-type field system with 'loose' fitting laminations at 0.5, 1, 1.5 and 2A.

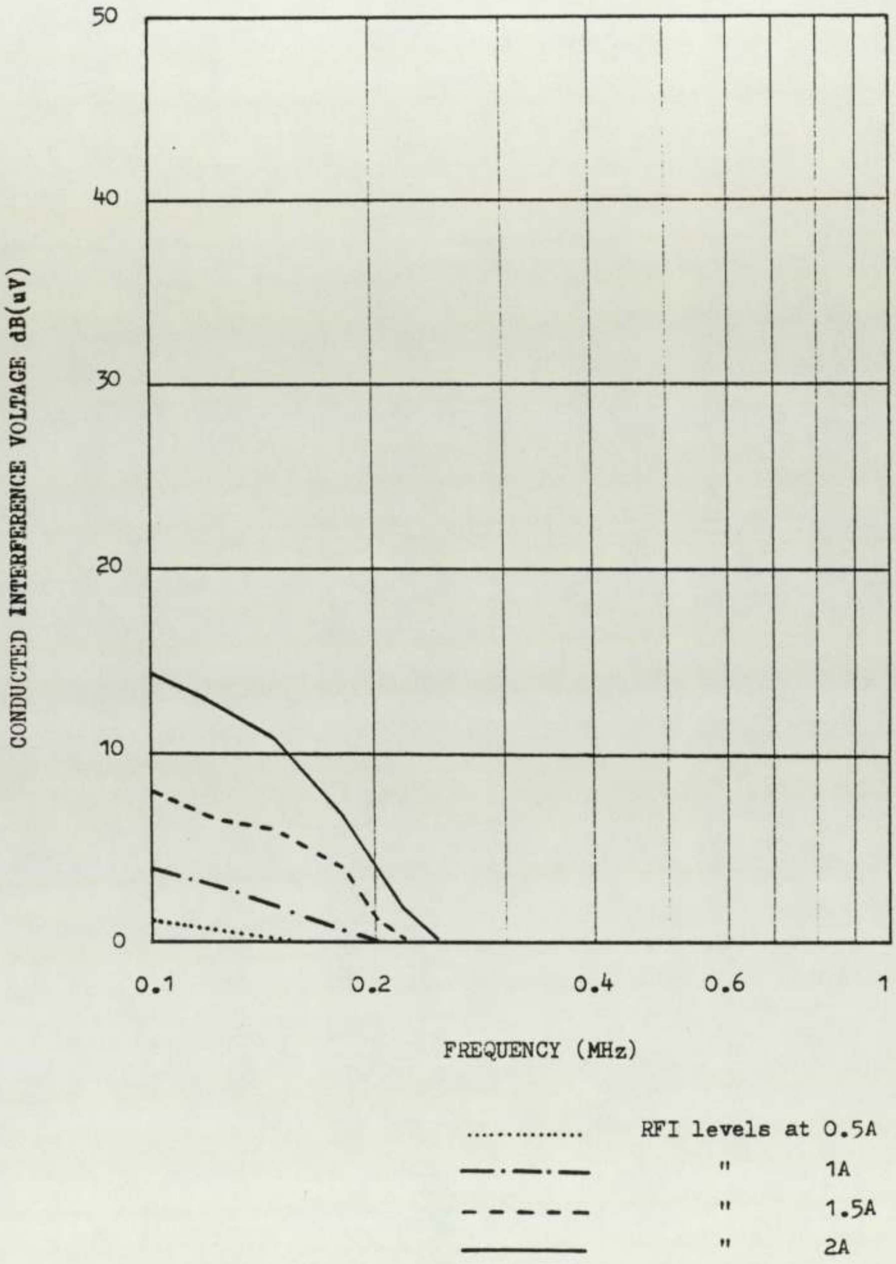

Fig. 6.48

RFI due to the influence of the physical components of the armature and field:
Measured RFI levels from the U-type field with stationary unwound 12 slot armature at 0.5, 1, 1.5 and 2A.

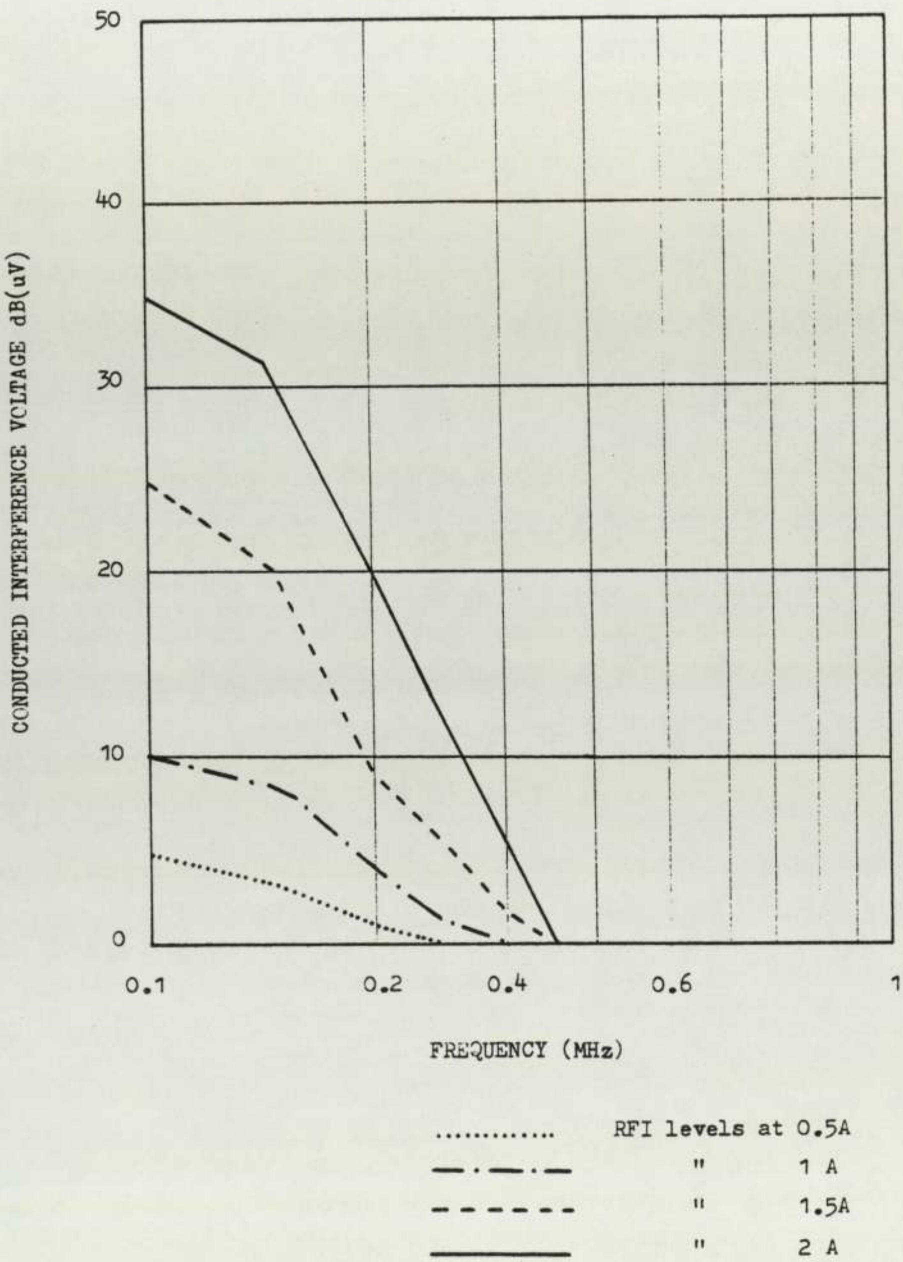

Fig. 6.49

RFI due to the influence of the physical components of the armature and field:
Measured RFI levels from 12/24 armature (field system removed) at 1.5A supply current with varying speed.

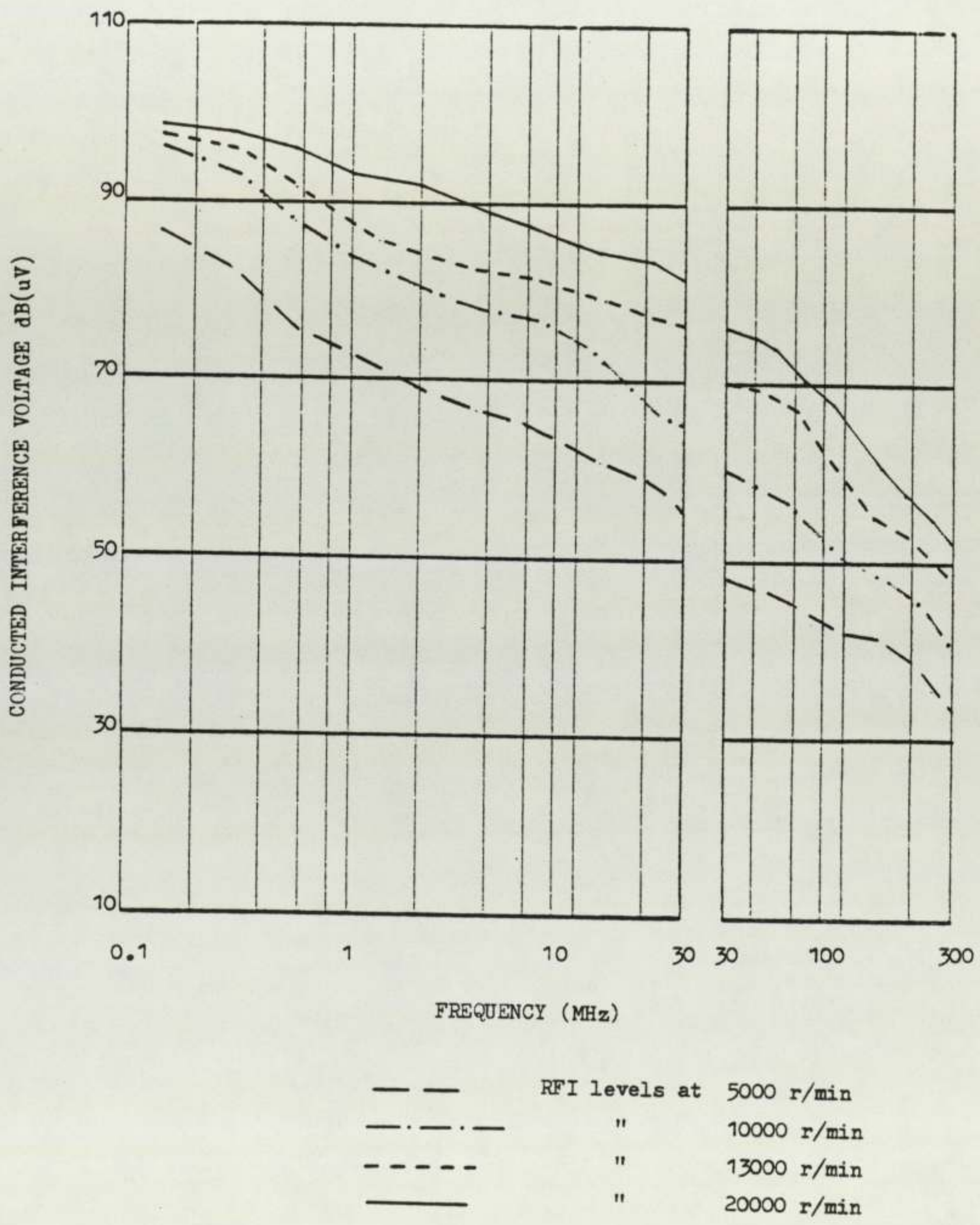

Fig. 6.50

Measured values of active Inductance, L_{comm} with varying brush positions on the 12/24 armature.

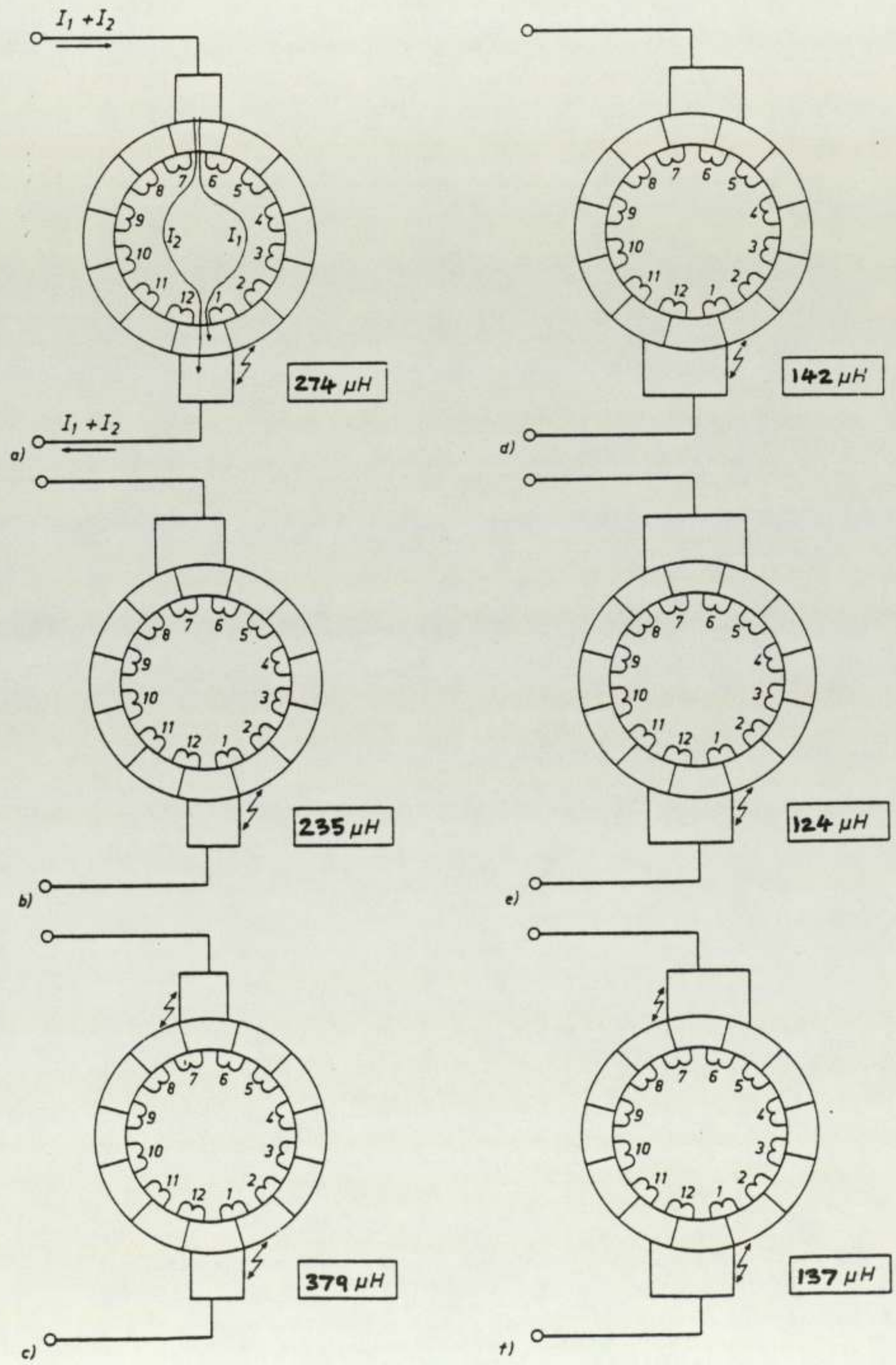

Fig. 6.51

Test rig connection for single winding (a) U-type field using (b) O-type field.

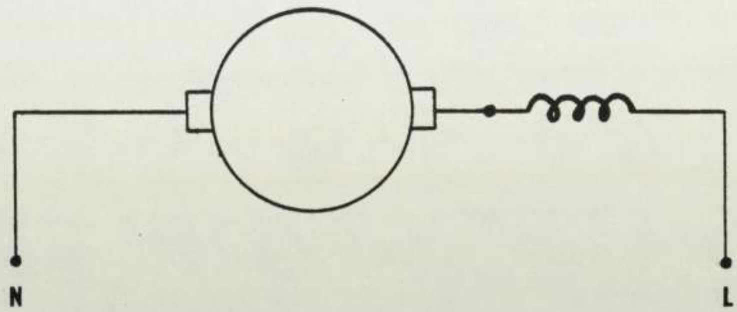

(a)

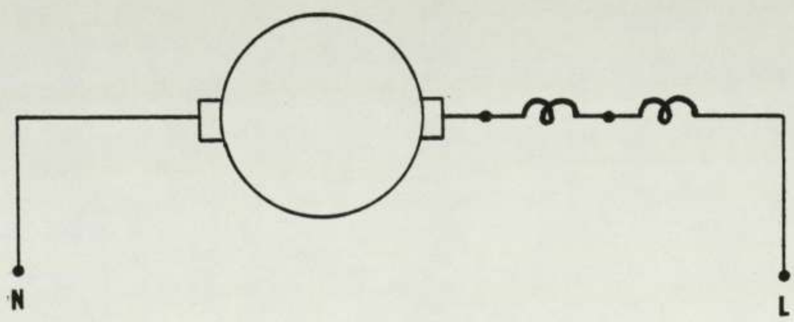

(b)

Fig. 6.52

RFI due to the influence of the physical components of the armature and field:

Measured RFI levels with the field windings connected to the line side of the mains supply using a 12/24 armature and U-type field.

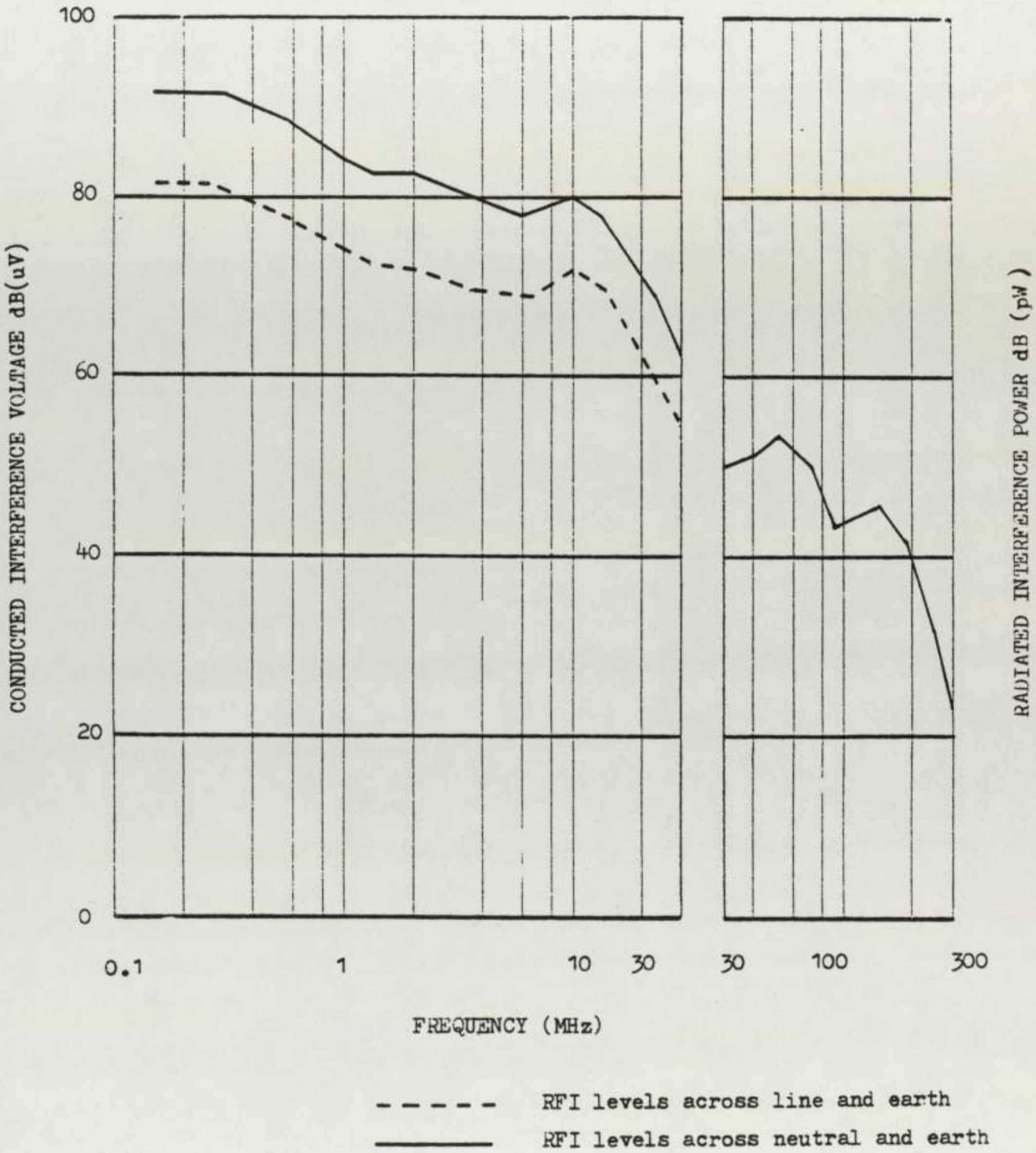

Fig. 6.53

RFI due to the influence of the physical components of the armature and field:
Measured RFI levels with the field windings connected to the neutral side of the mains supply using a 12/24 armature and U-type field.

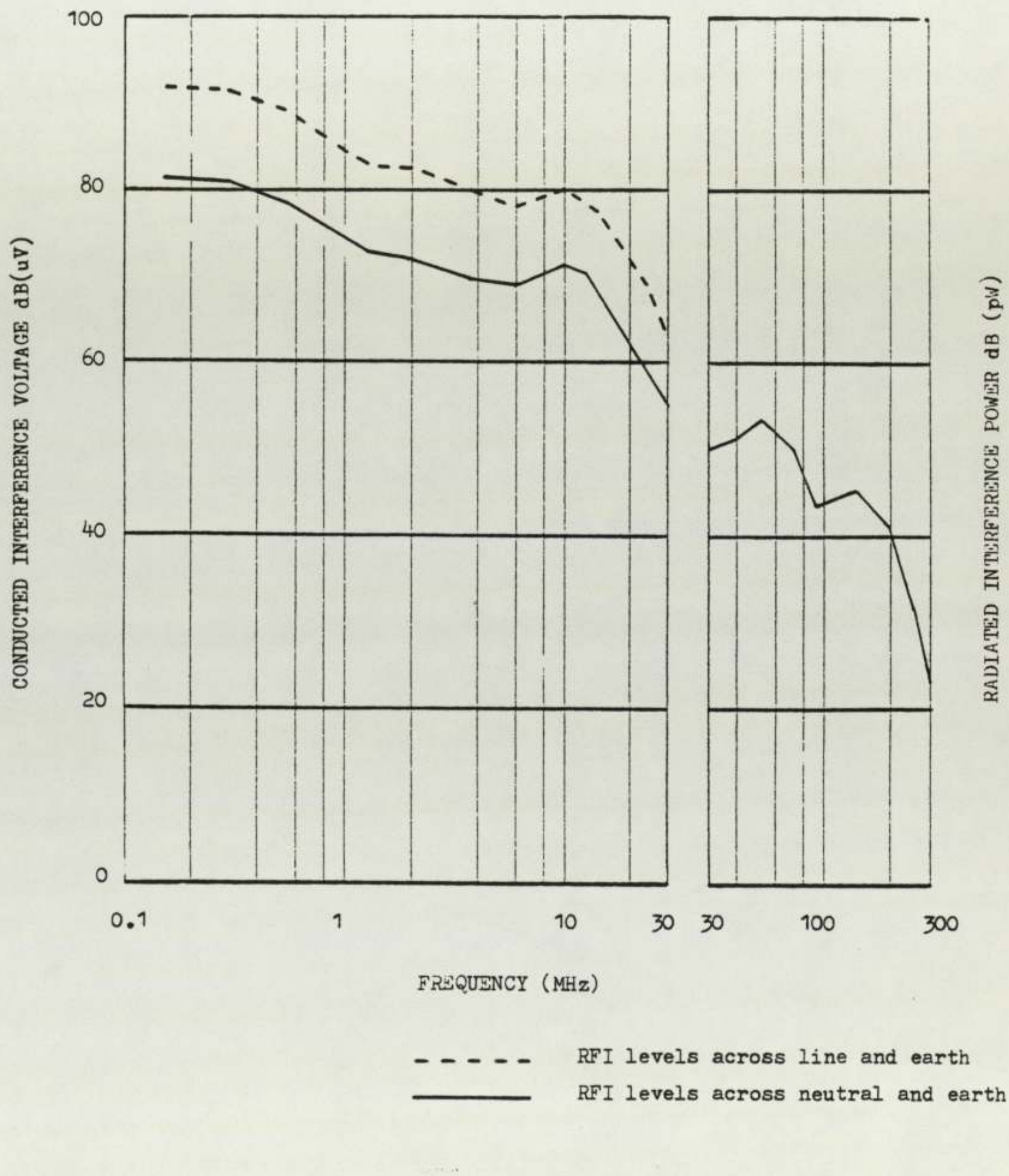

Fig. 6.54

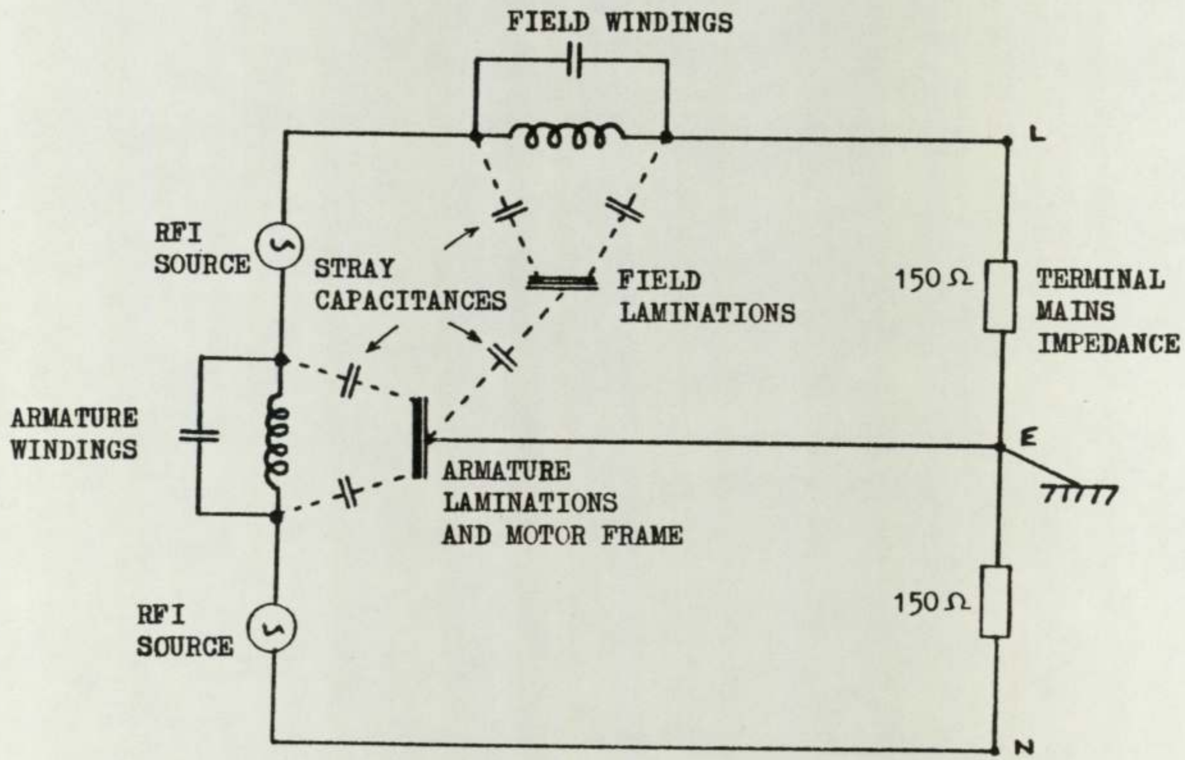

Simple r.f. equivalent circuit of test rig with U-type field windings connected to the line side of the mains supply

Fig. 6.55

R.F. Impedance of the U-type field;
(a) across the windings
(b) between windings and lamination stack.

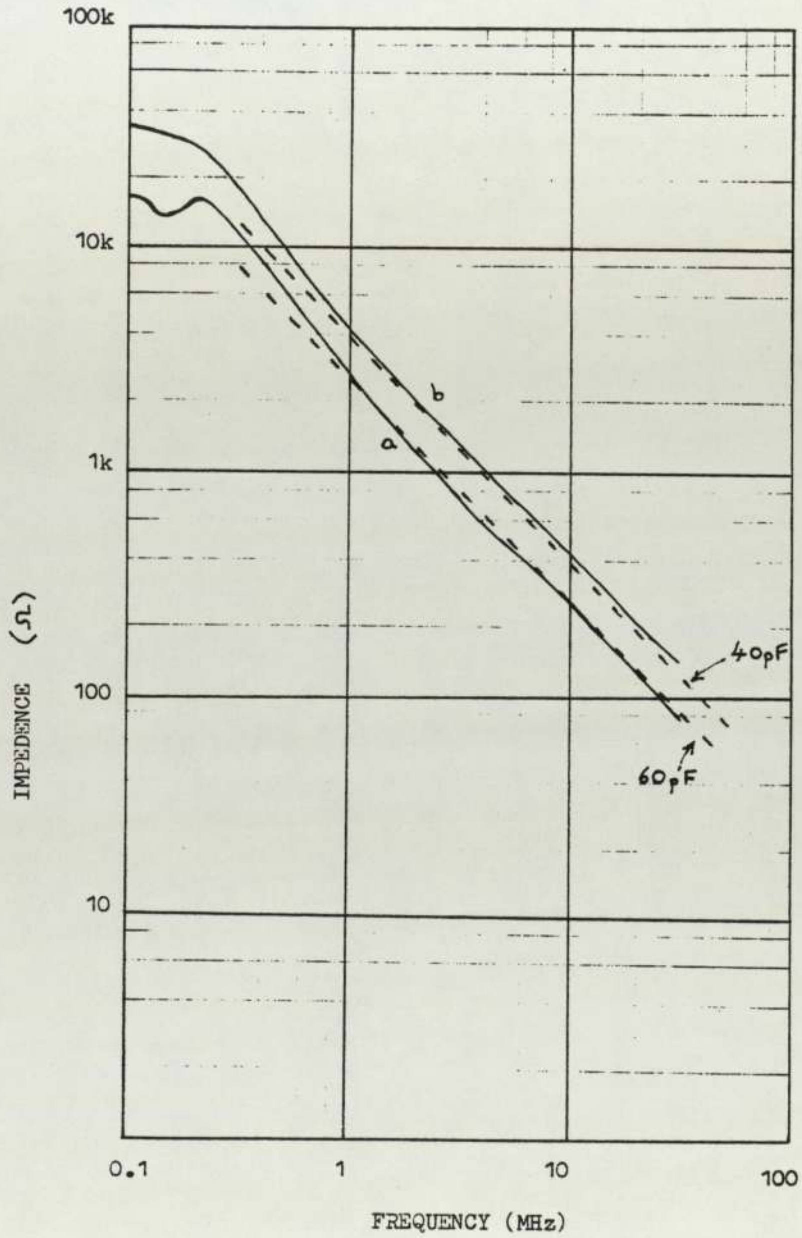

Fig. 6.56

RFI due to the influence of the physical components of the armature and Field:
Measured RFI levels with field windings connected to the line side of mains supply using a 12/24 armature and O-type field.

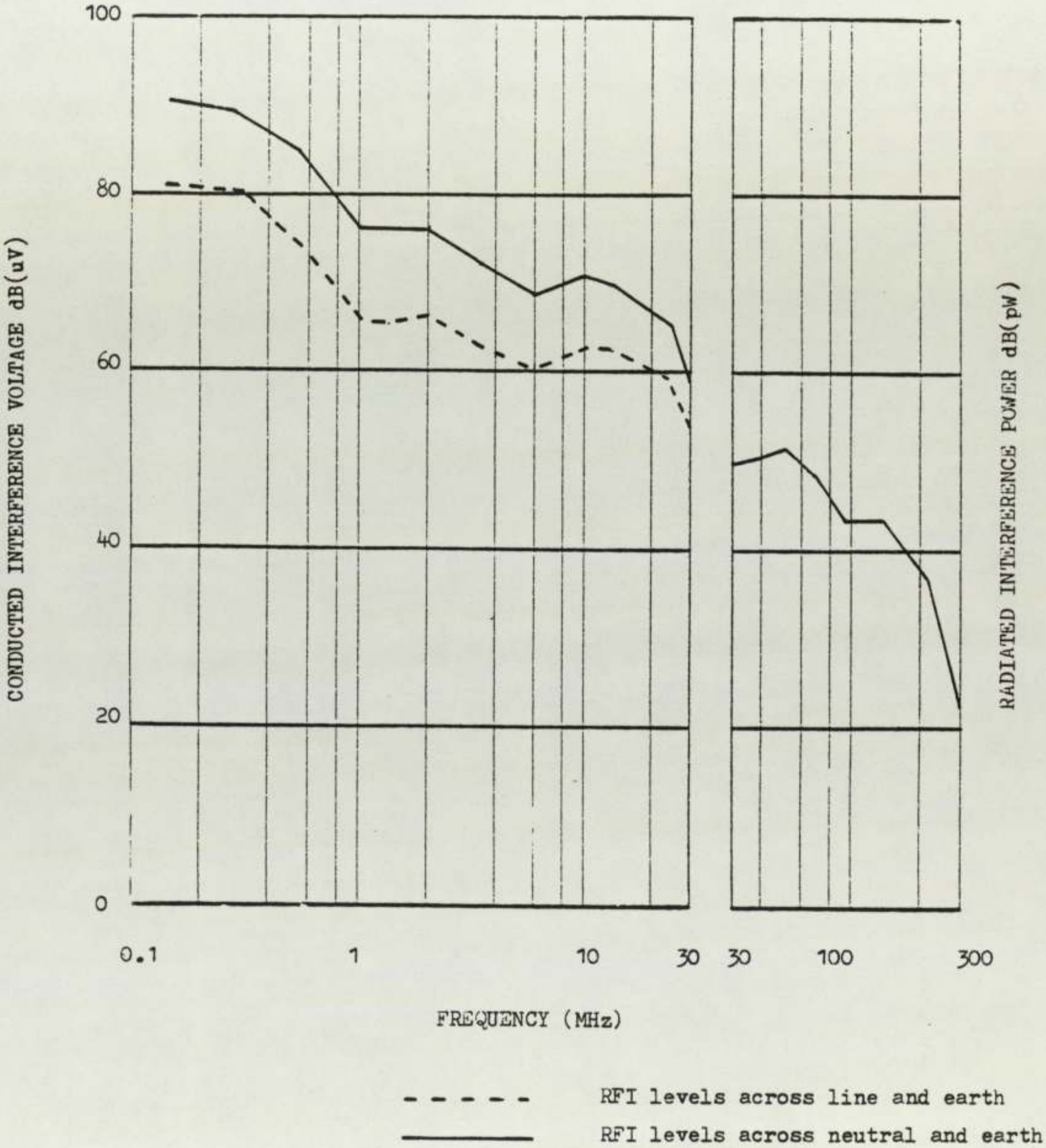

Fig. 6.57

R.F. Impedence of the O-type field windings.

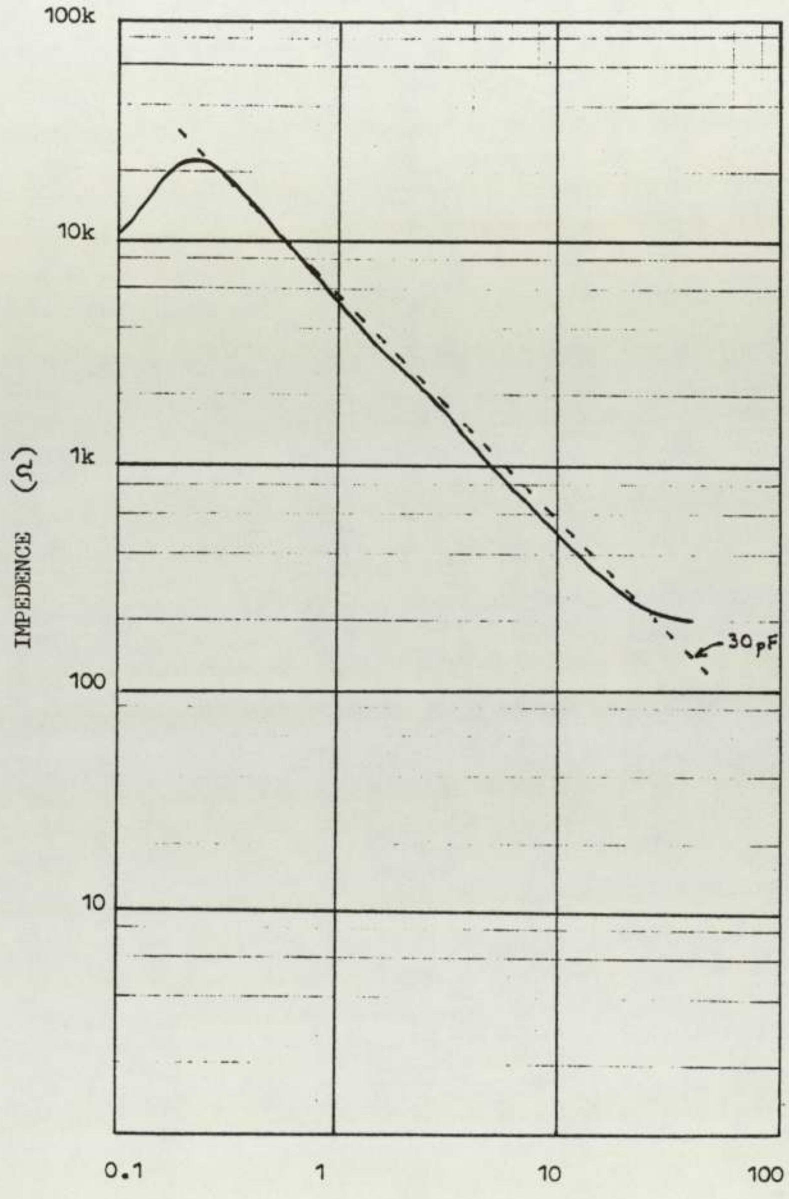

Fig. 6.58

Comparison of measured symmetric interference currents from the test-rig fitted with (a) U-type field and (b) O-type field.

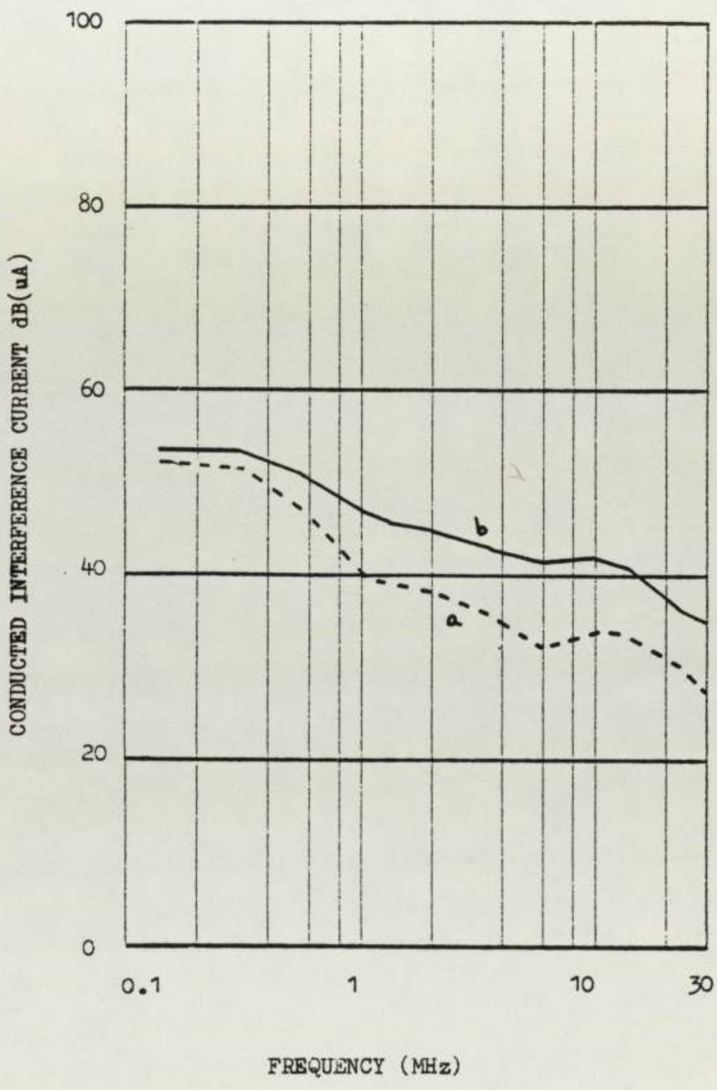

Fig. 6.59

Comparison of measured asymmetric interference currents from the test-rig fitted with (a) U-type field and (b) O-type field.

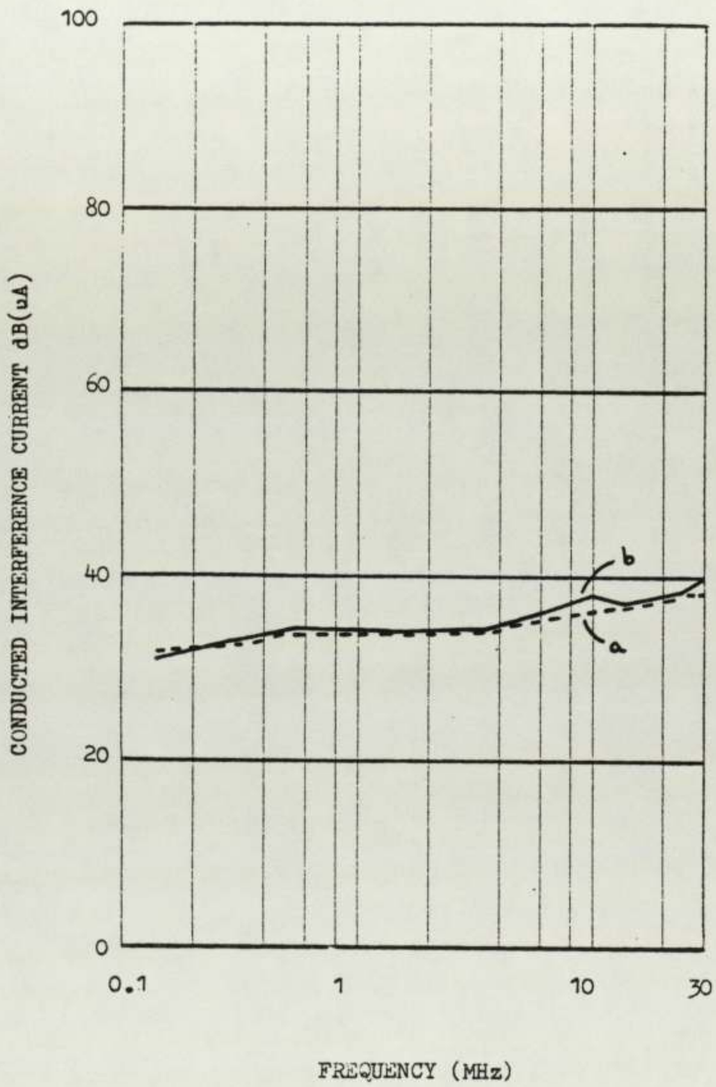

Fig. 6.60

RFI due to the influence of the physical components of the armature and field:

Measured RFI levels with the field windings connected to the line side of the mains supply using a 12/24 armature and U-type field with the earth connection removed.

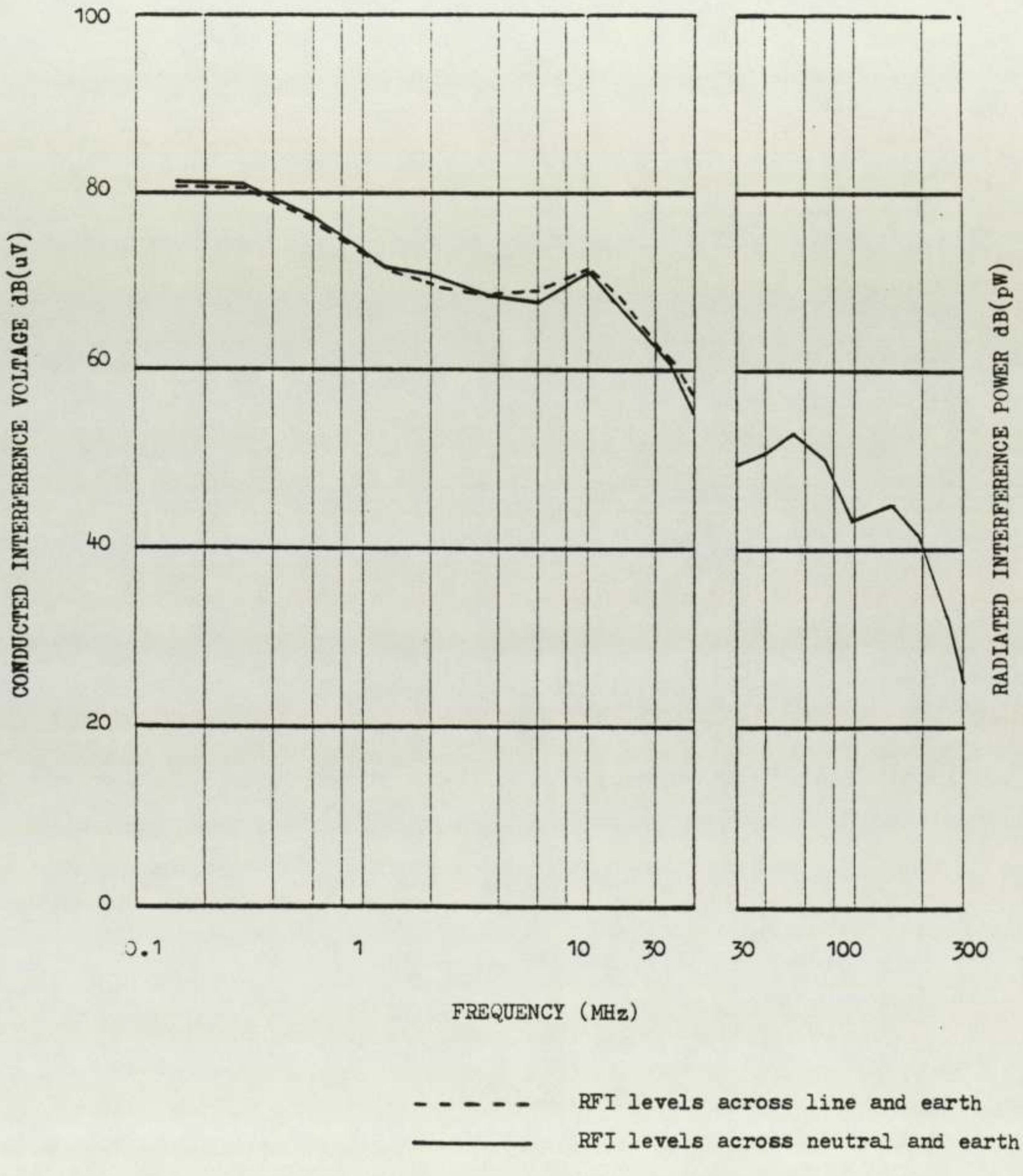

Fig. 6.61

Measured asymmetric and symmetric interference currents from the test-rig fitted with 12/24 armature and U-type field with the earth connection removed.

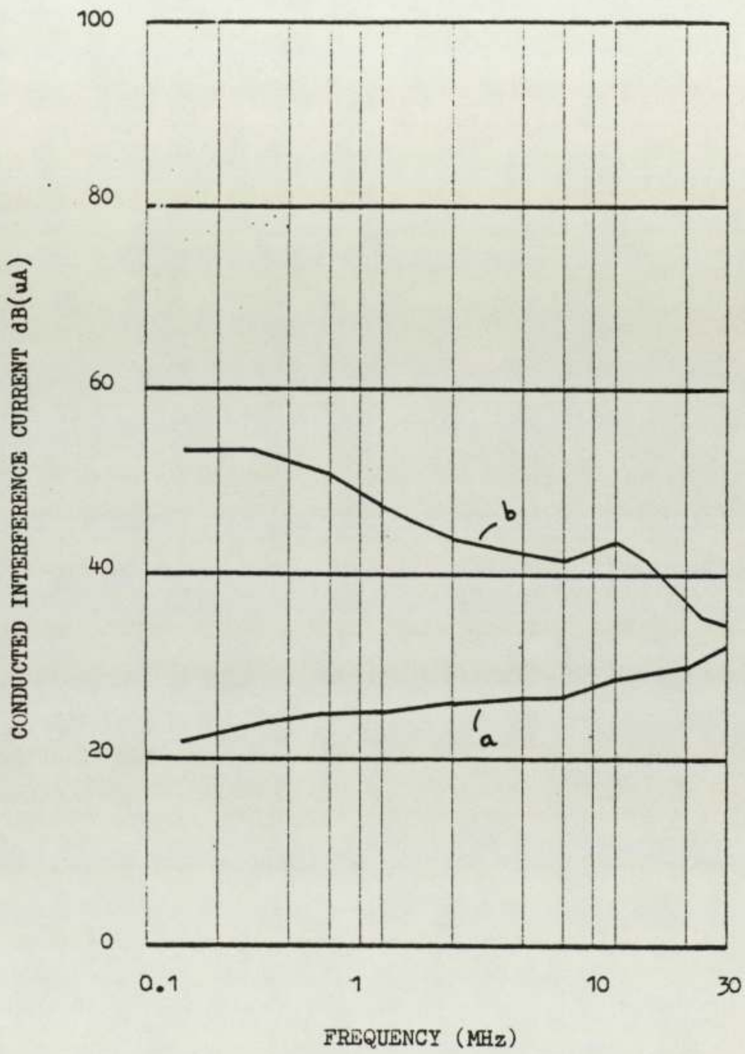

(a) Asymmetric interference current

(b) Symmetric interference current

Fig. 6.62

RFI due to the influence of the physical components of the armature and field:
Measured RFI levels with the field windings connected to the line side of the mains supply using a 12/24 armature and U-type field with the earth connected to the field lamination stack.

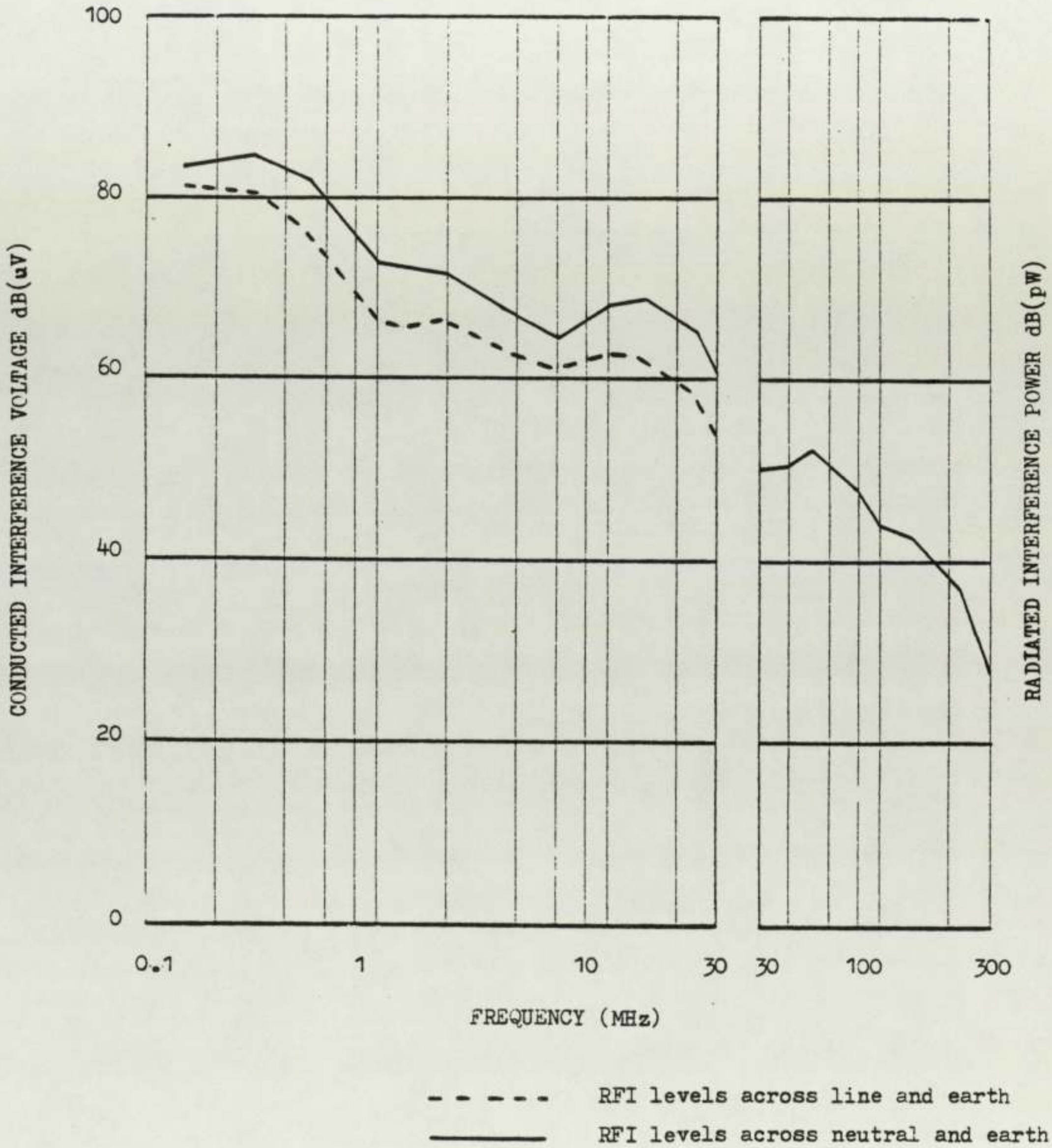

Fig. 6.63

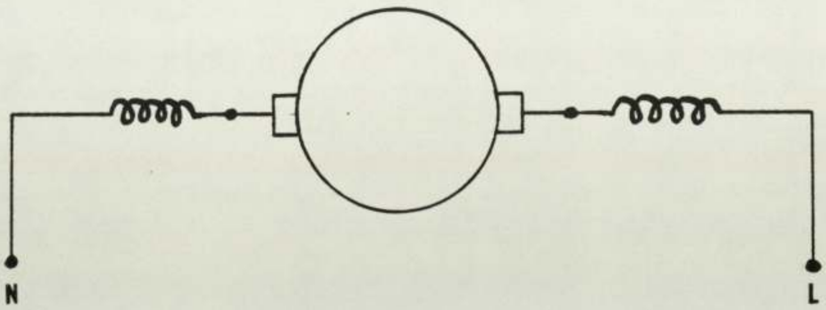

Field connected as a split winding either side of the armature.

Fig 6.64

RFI due to the influence of the physical components of the armature and field:
Comparison of measured RFI levels using the 12/24 armature and O-type field with the windings connected (a) to one side of the armature and (b) in the split winding configuration.

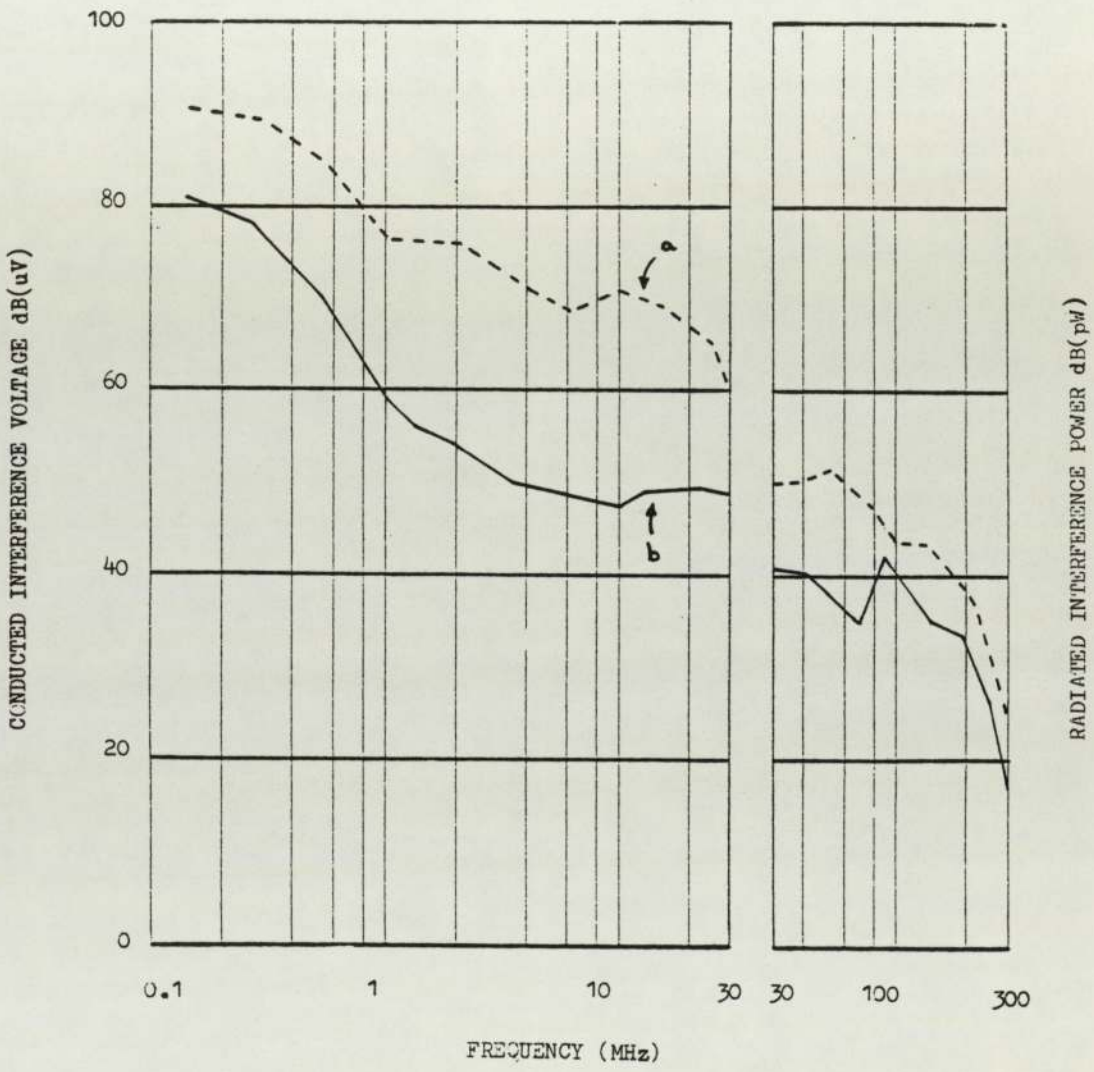

Fig. 6.65

RFI due to the influence of the physical components of the armature and field:

Comparison of measured RFI levels using a 12/24 armature and U-type field with the windings connected (a) to one side of the armature and (b) in the split winding configuration.

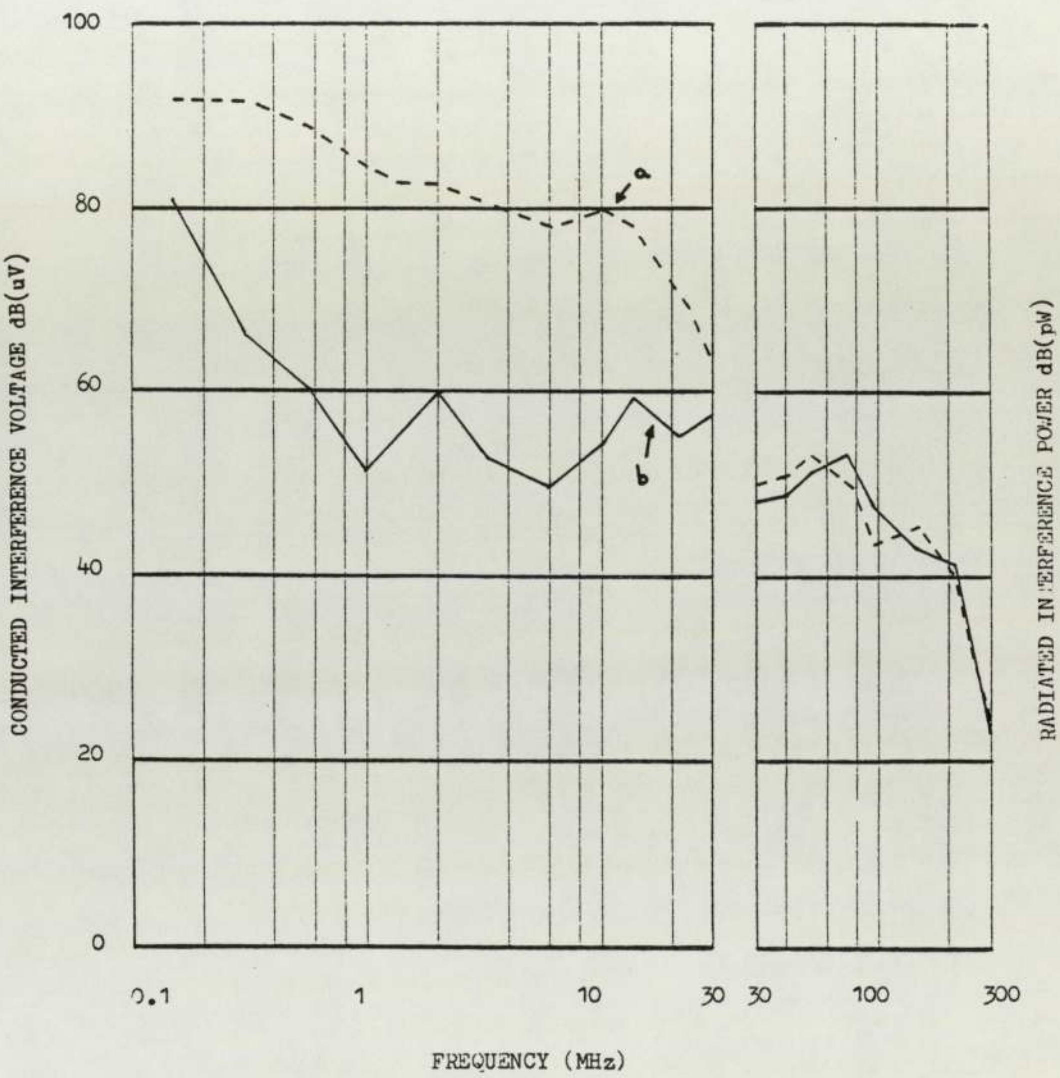

Fig. 6.66

Comparison of measured symmetric interference currents from the test-rig fitted with (a) U-type field and (b) O-type field in the split winding configuration.

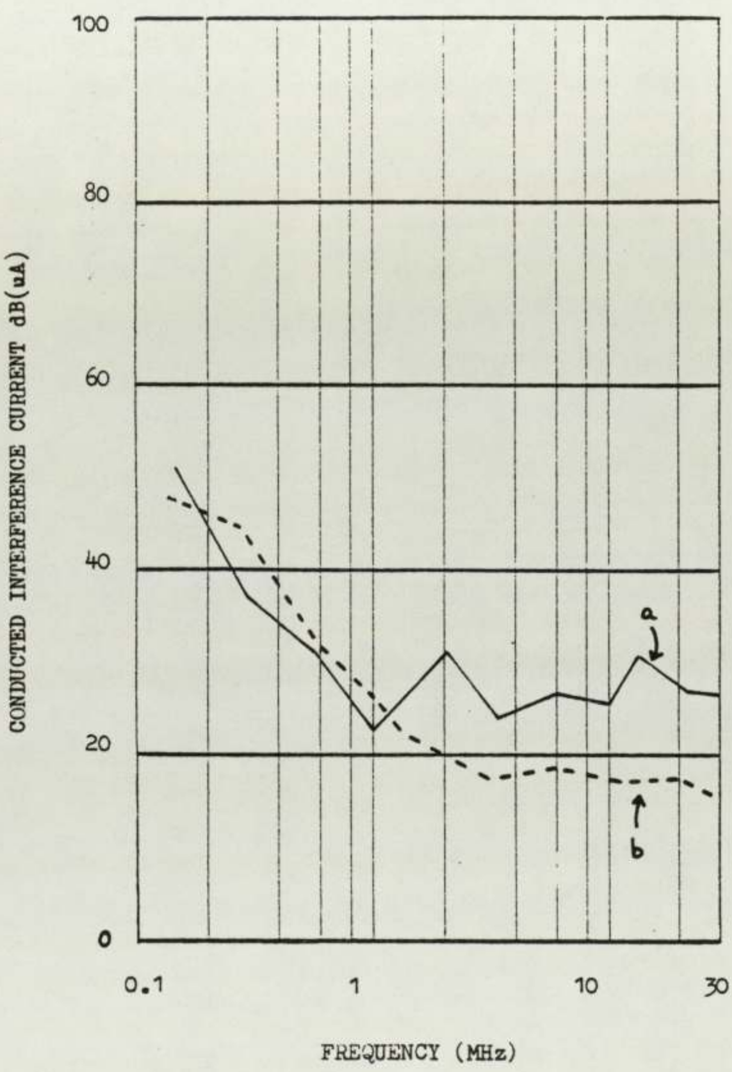

Fig. 6.67

Comparison of measured asymmetric interference currents from the test-rig fitted with (a) U-type field and (b) O-type field in the split winding configuration.

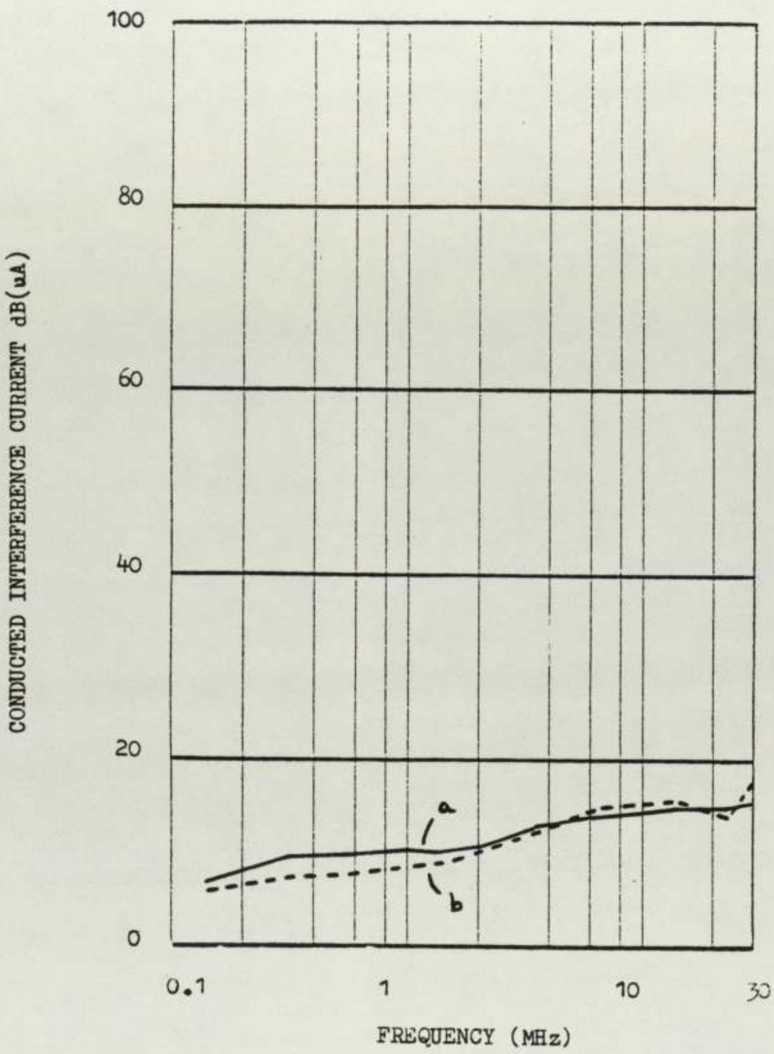

Fig. 6.68

Measured R.F. impedence between split windings of
(a) the O-type field and (b) the U-type field.

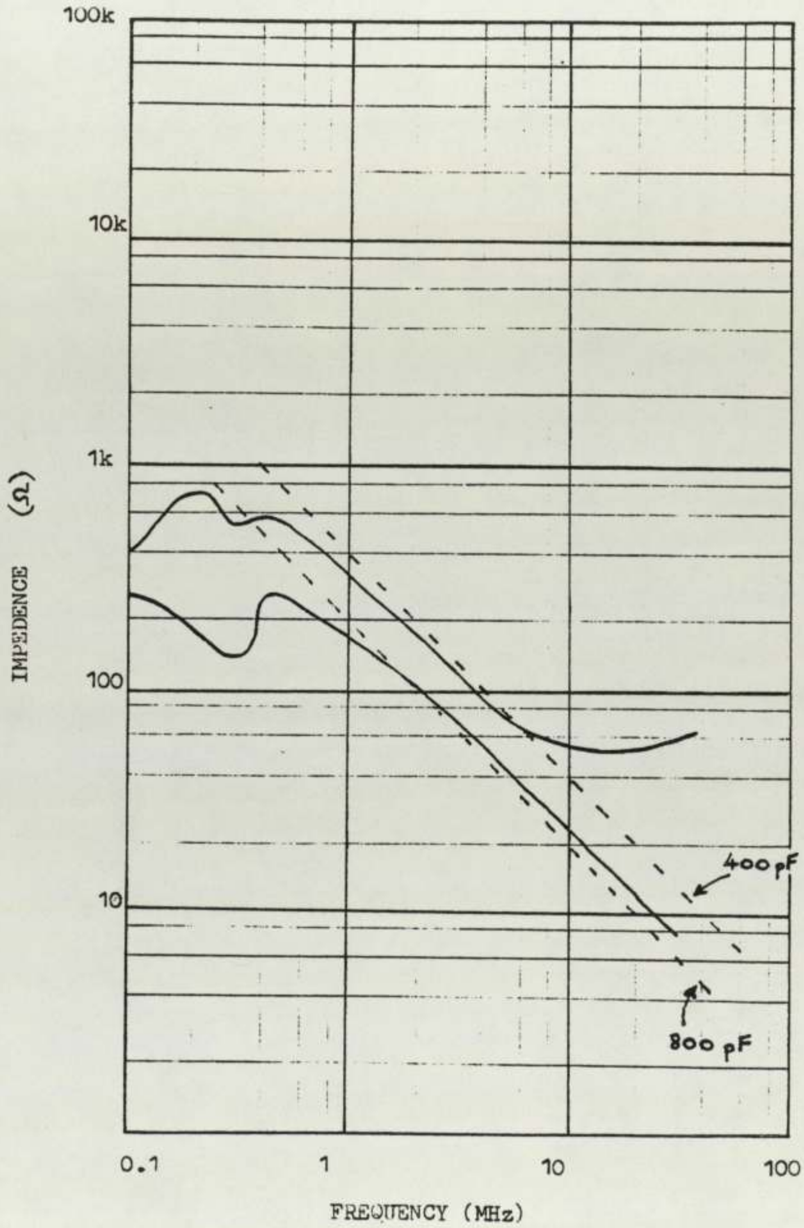

Fig. 6.69

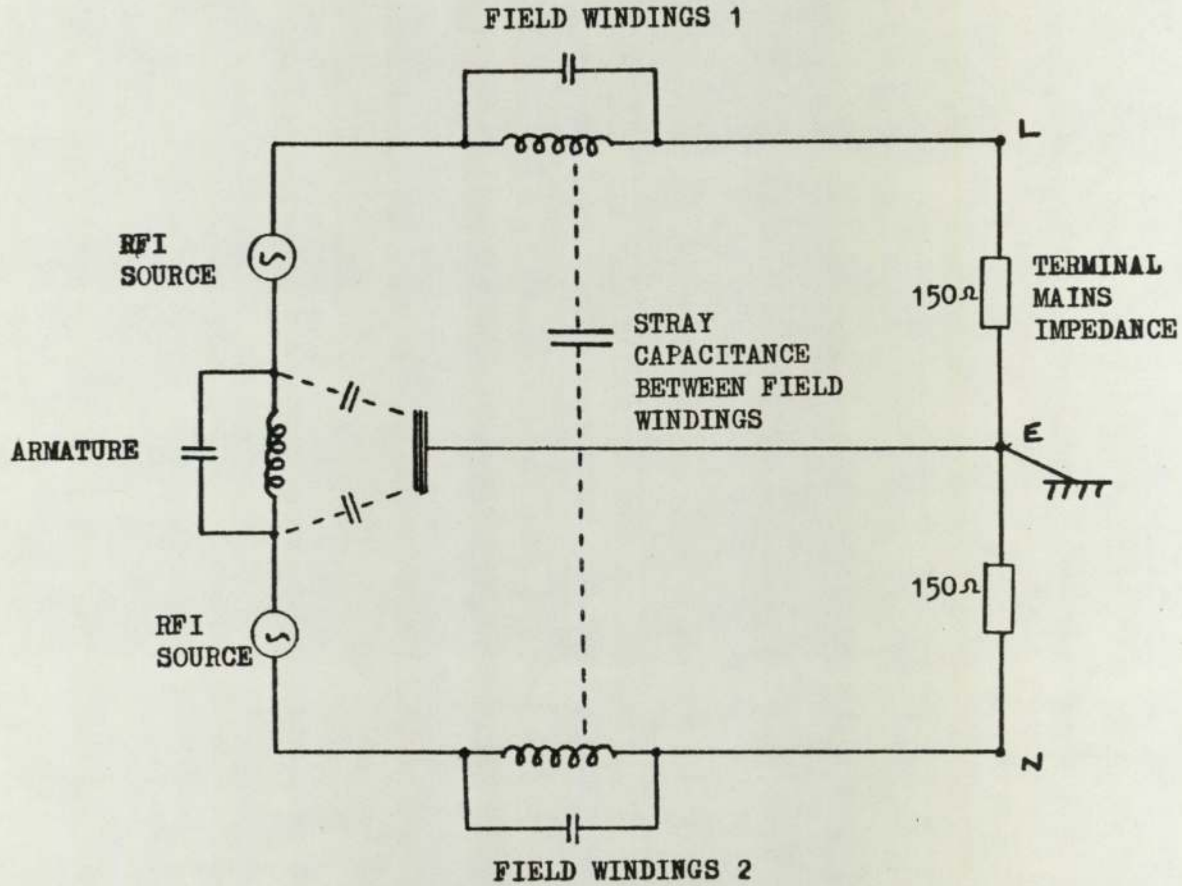

Simple r.f. equivalent circuit of the test rig with Q-type field windings balanced either side of the armature

Fig. 6.70

RFI due to the influence of the physical components of the armature and field:
Comparison of measured RFI levels obtained using a U-type field with different armature configurations.

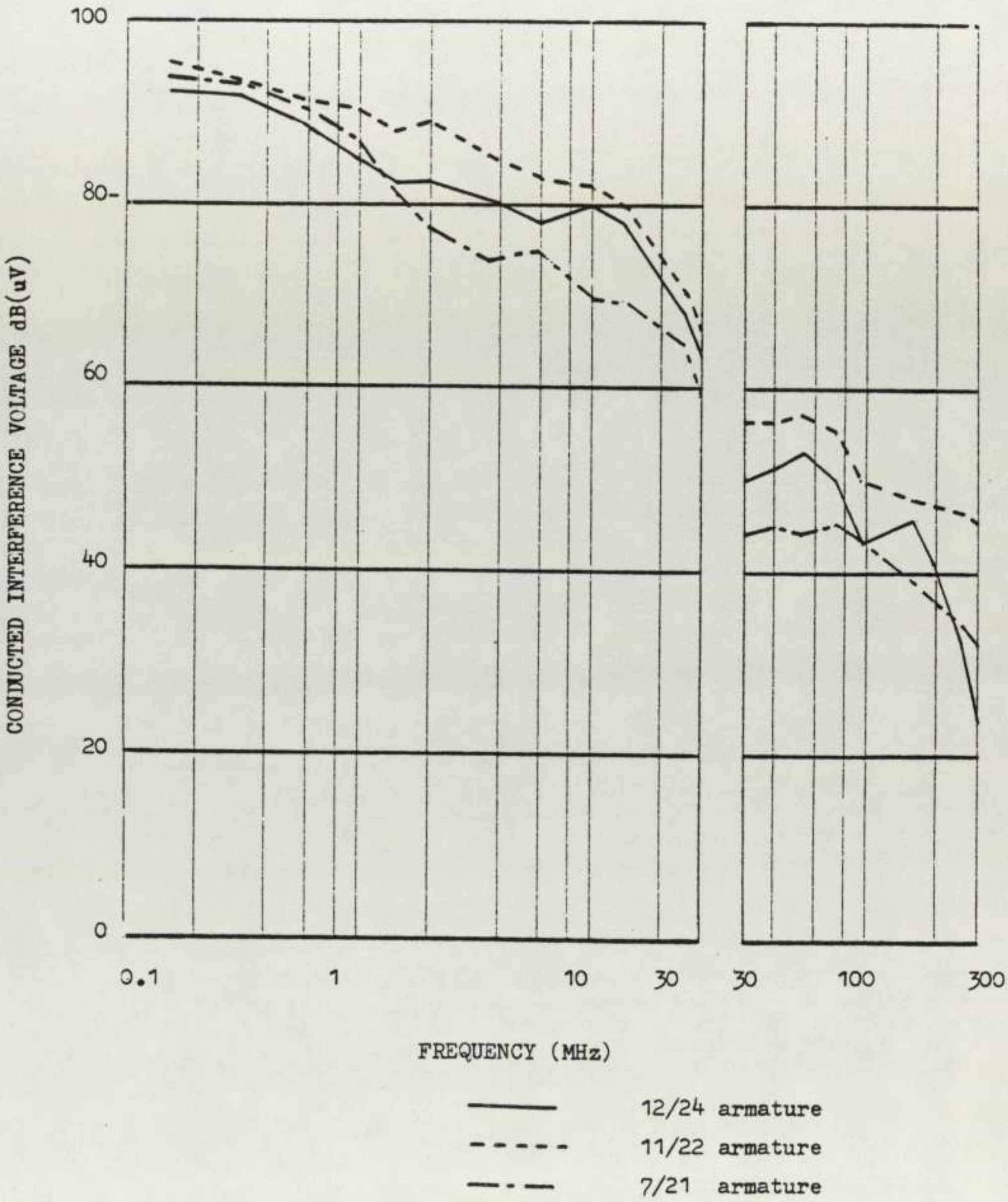

Fig. 6.71

Measured symmetric interference currents from the test-rig with different armature configurations.

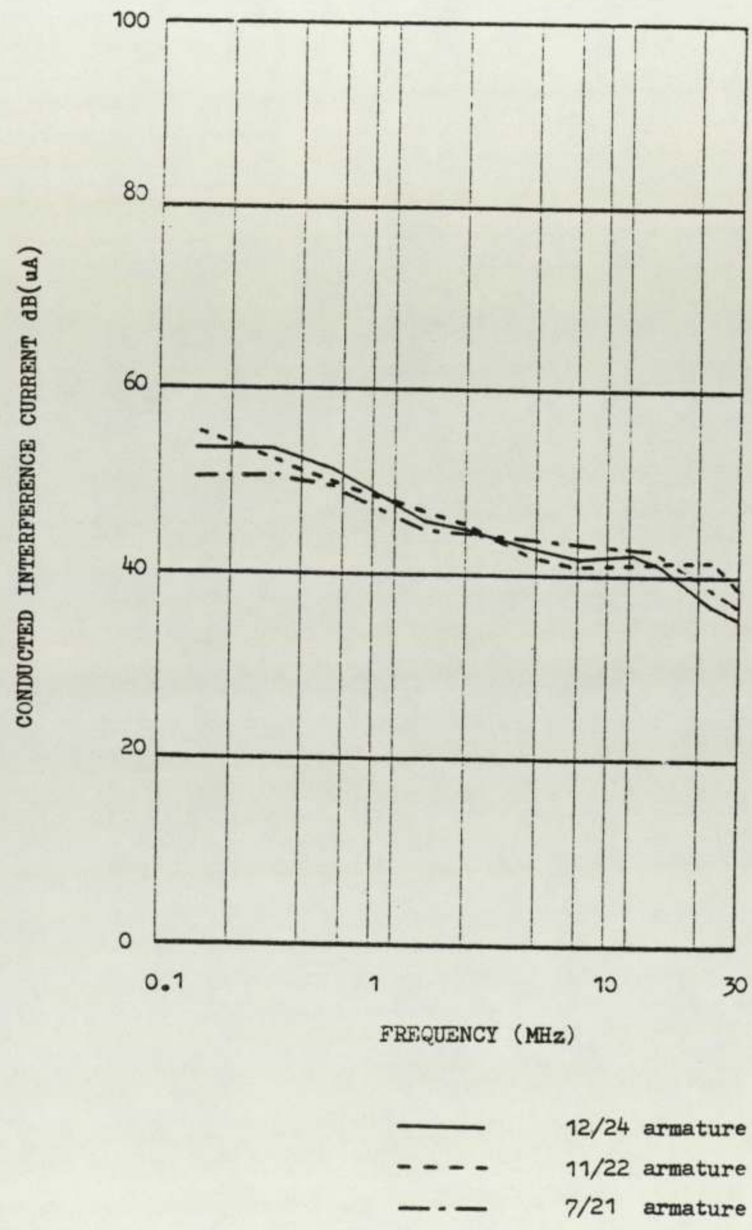

Fig. 6.72

Measured asymmetric interference currents from the test-rig with different armature configurations.

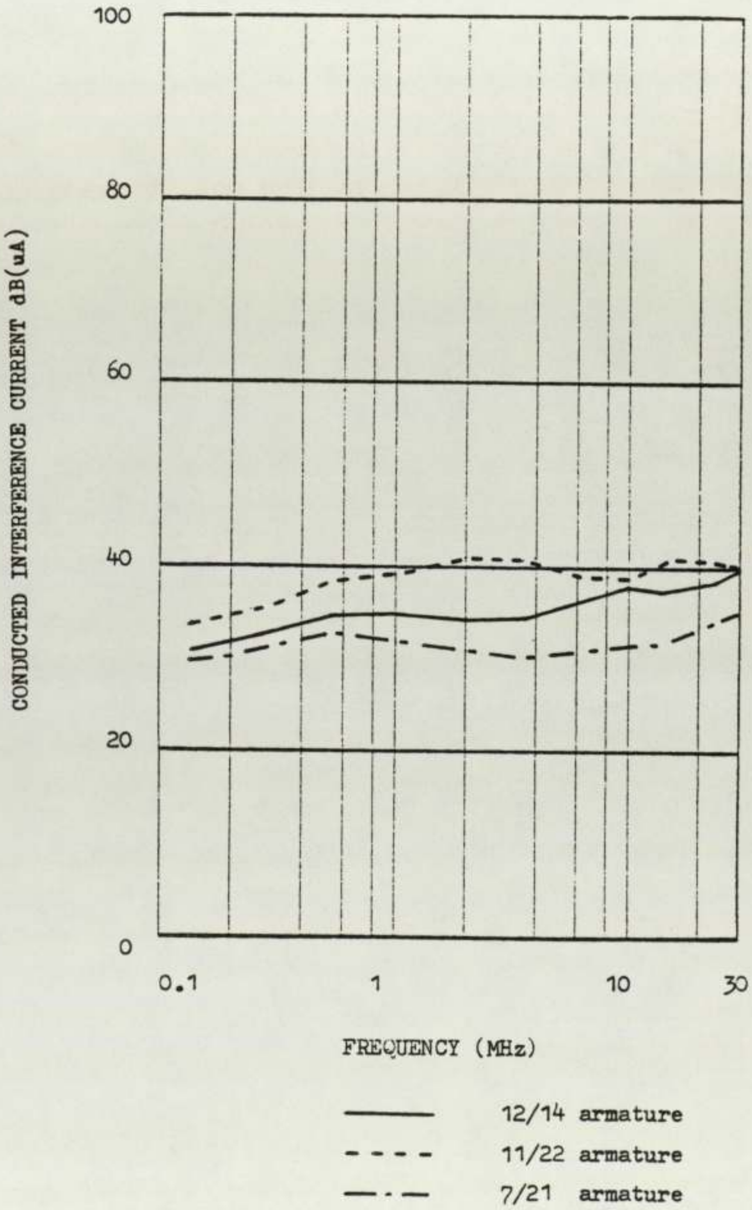

Fig. 6.73

Measured R.F. impedence between armature windings and laminations using (a) 7/21 armature, (b) 12/24 armature and (c) 11/22 armature.

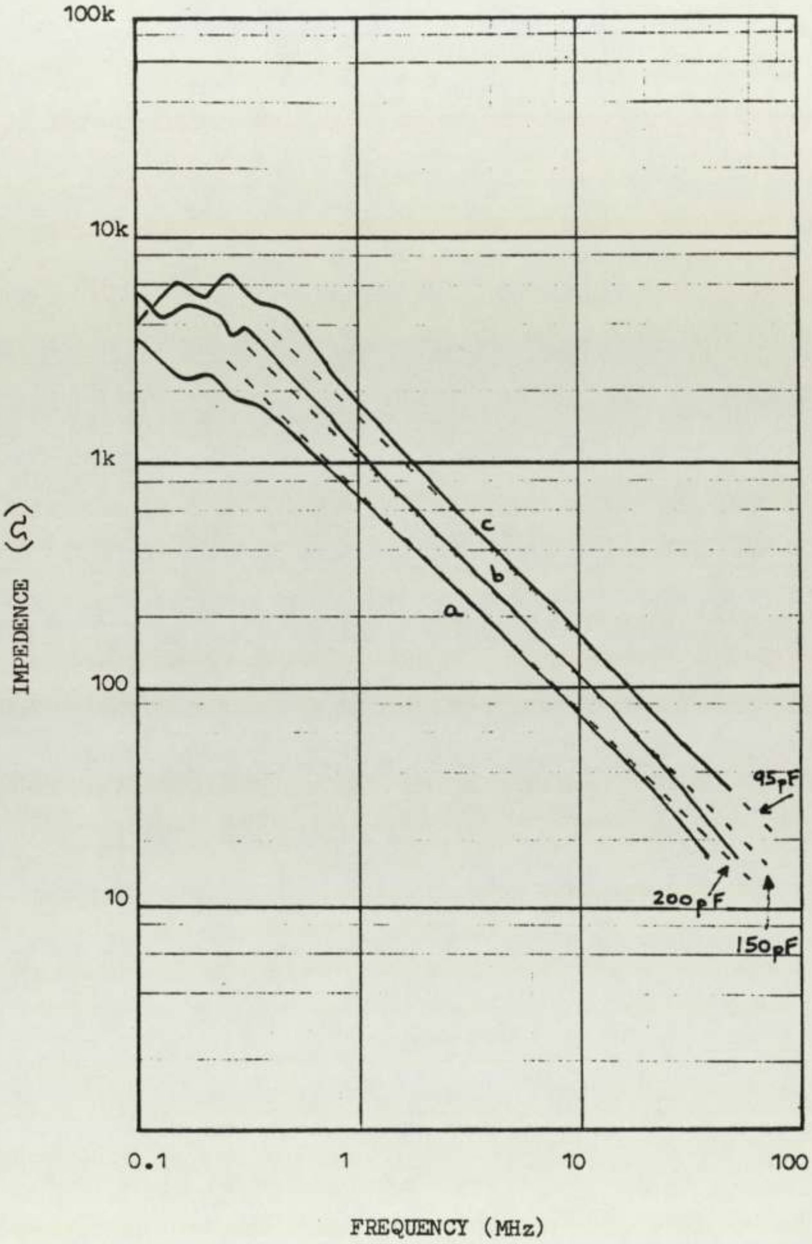

Fig. 6.74

RFI due to the influence of the physical components of the armature and field:
Measured RFI levels with varying armature turns per coil using 12/24 armature and U-type field.

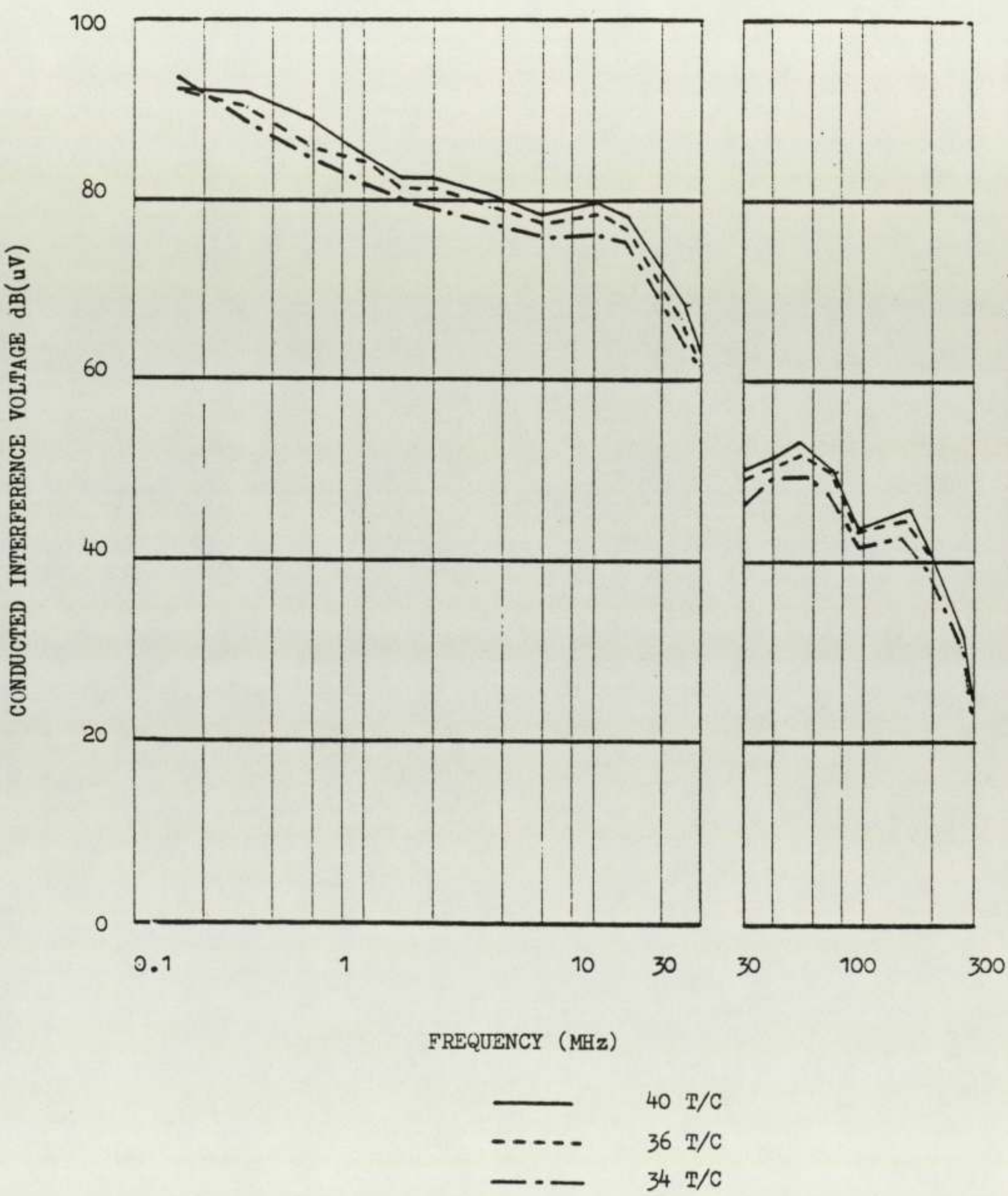

Fig. 6.75

RFI due to the influence of the physical components of the armature and field:
Measured RFI levels with varying armature turns per coil using 7/21 armature and U-type field.

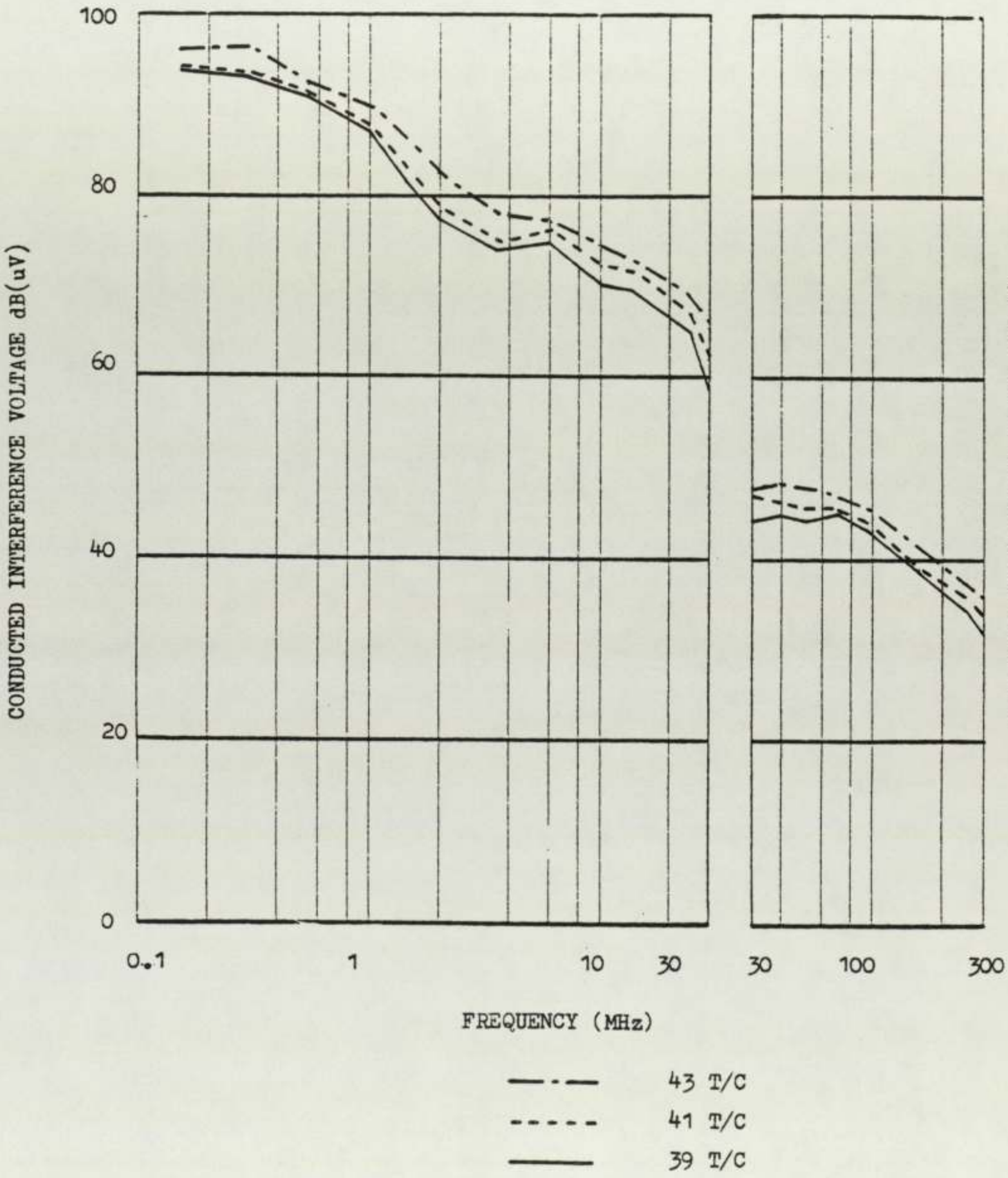

Fig. 6.76

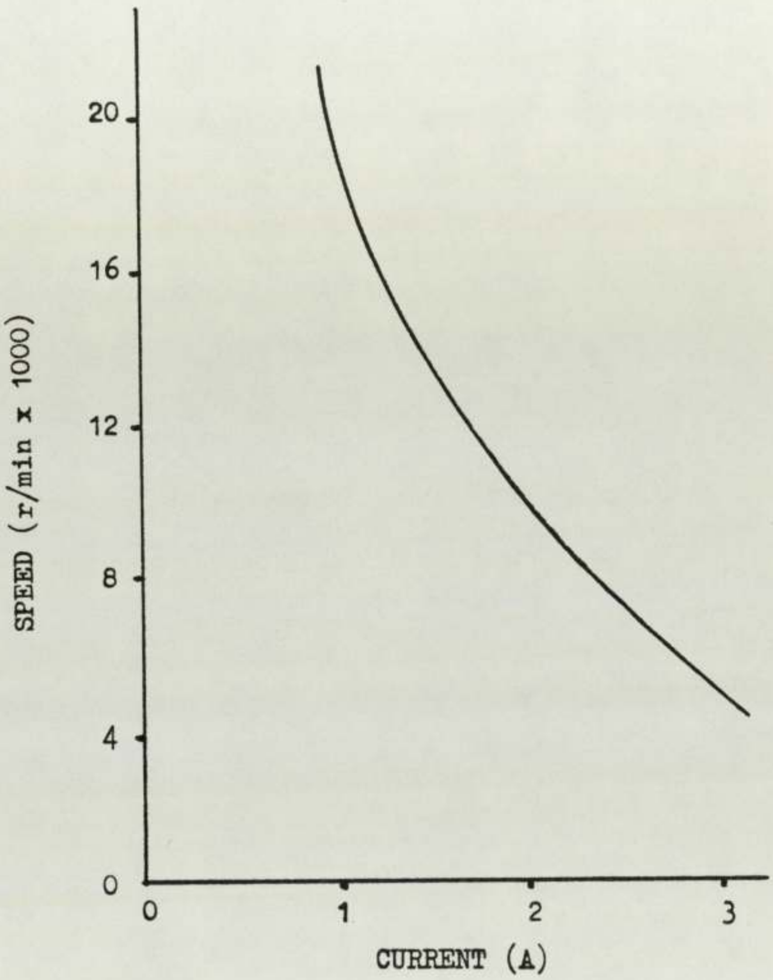

Speed-current characteristics of the test rig fitted with 12/24 armature and U-type field at 240V with varying motor load

Fig. 6.77

RFI due to the influence of the physical components of the armature and field:
Measured RFI levels with varying motor load using 12/24 armature and U-type field.

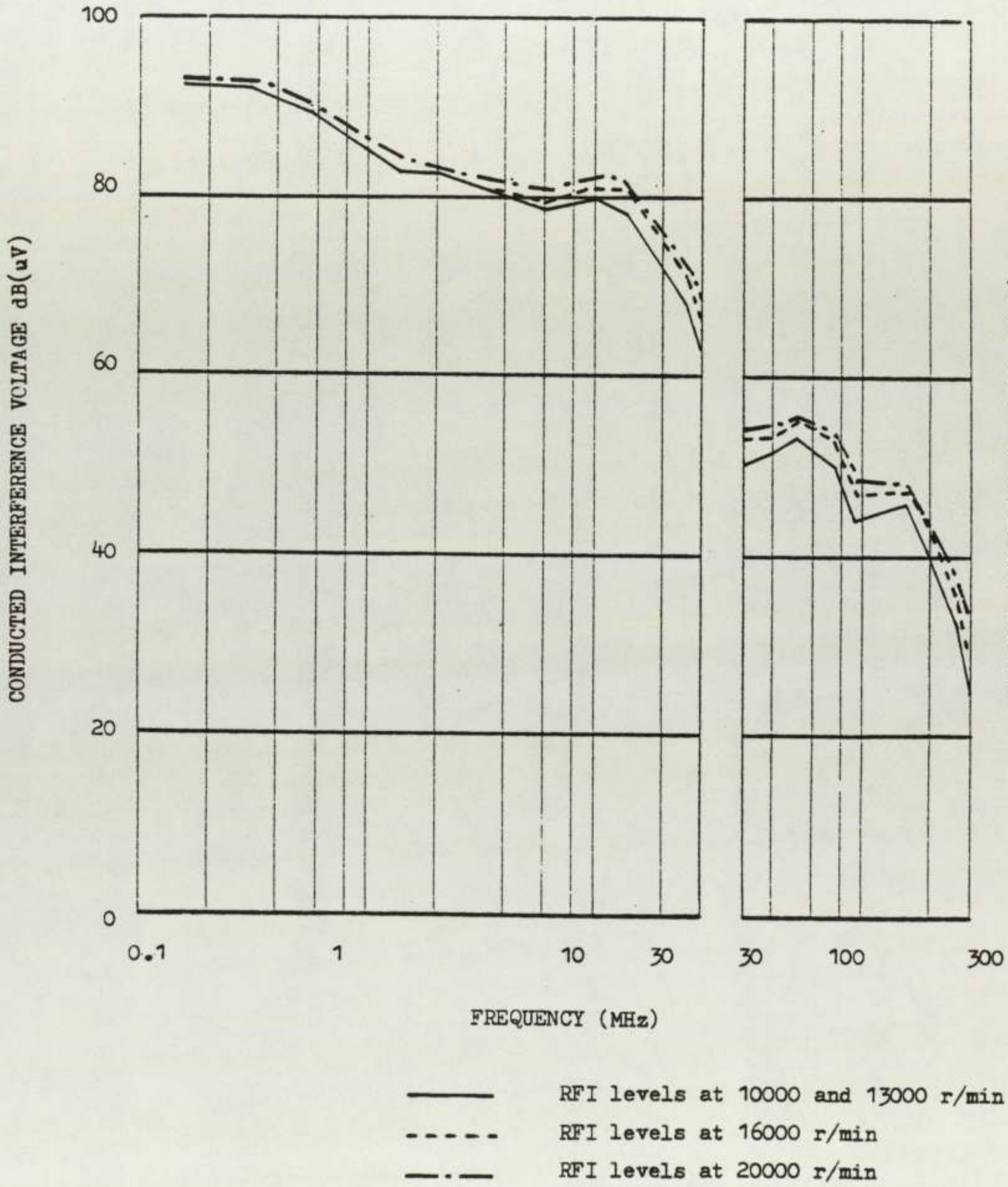

Fig. 6.78

RFI due to the influence of mechanical variations in the motor assembly:
Measured RFI levels with varying armature static out-of-balance at 18000 r/min.

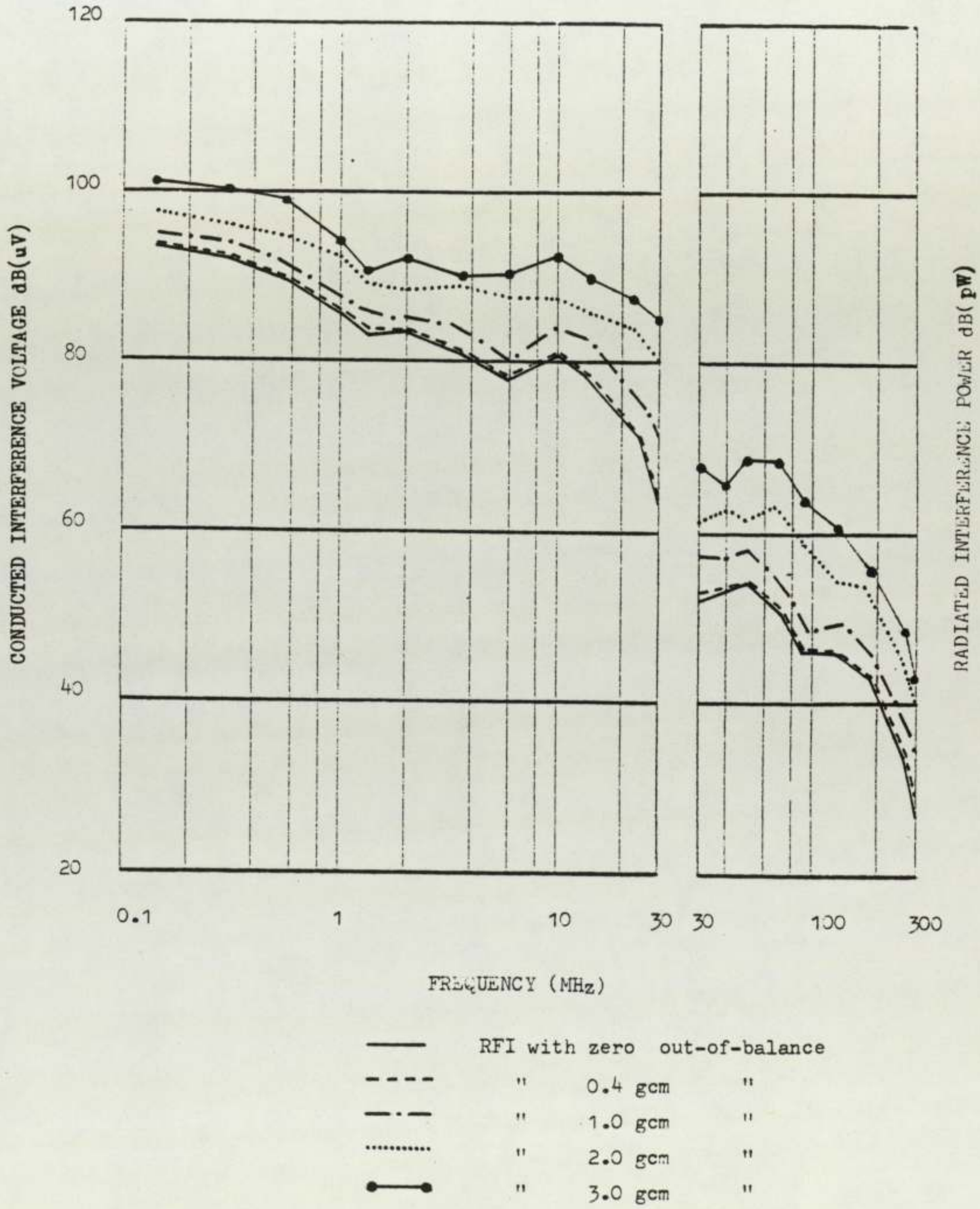

Fig. 6.79

Effect of varying armature static out-of-balance on measured RFI levels at 18000 r/min.

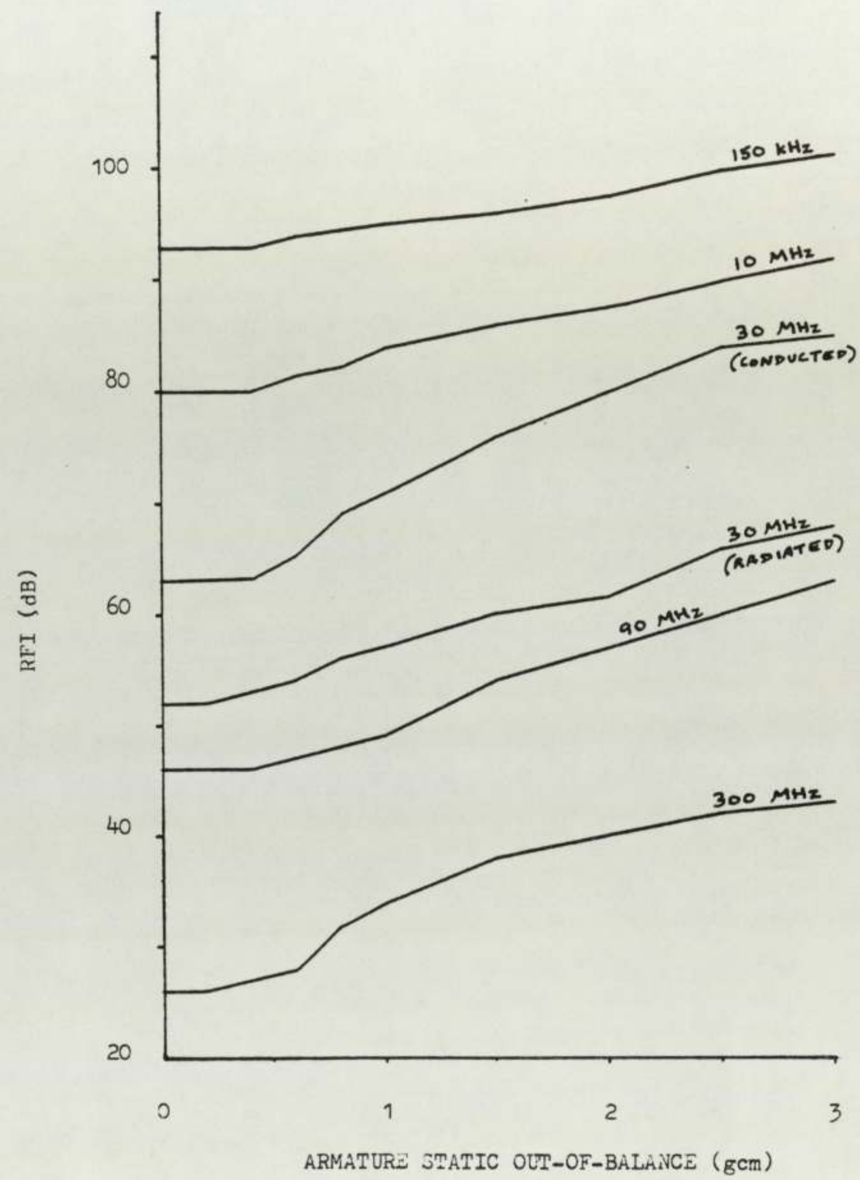

Fig. 6.80

RFI due to the influence of mechanical variations in the motor assembly:

Measured RFI levels with varying armature dynamic out-of-balance at 18000 r/min.

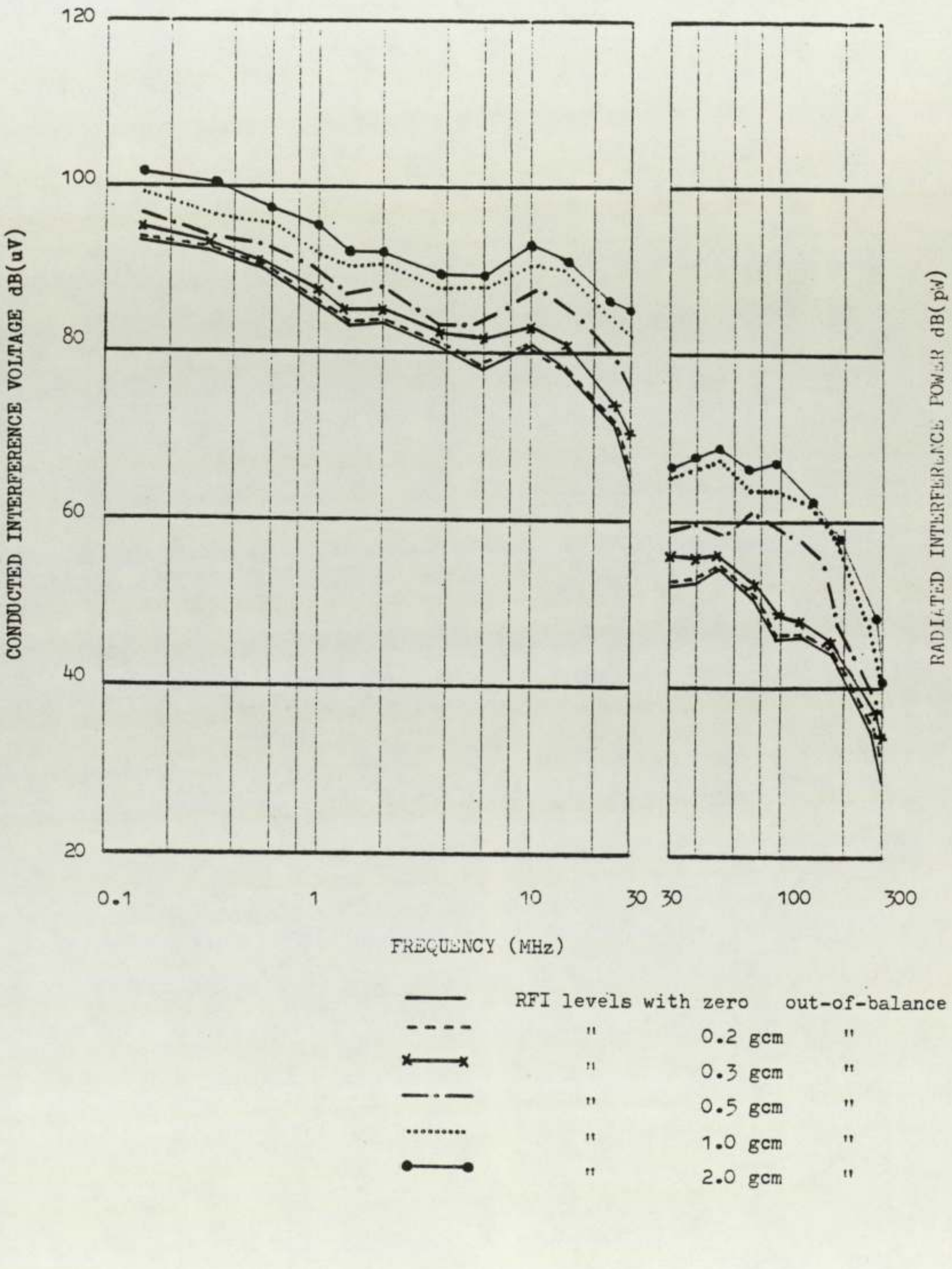

Fig. 6.81

Effect of varying armature dynamic out-of-balance on measured RFI levels at 18000 r/min.

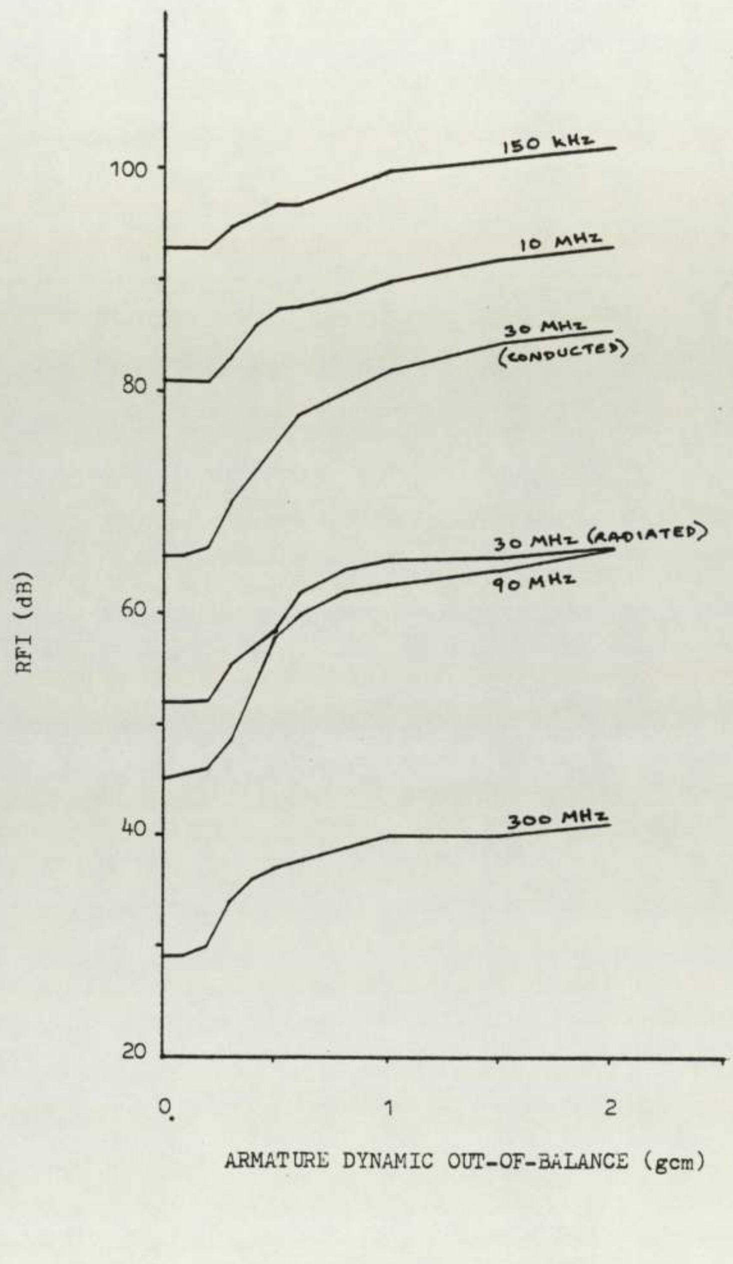

Fig. 6.82

RFI due to the influence of mechanical variations in the motor assembly:

Measured RFI levels with varying spring load at 18000 r/min.

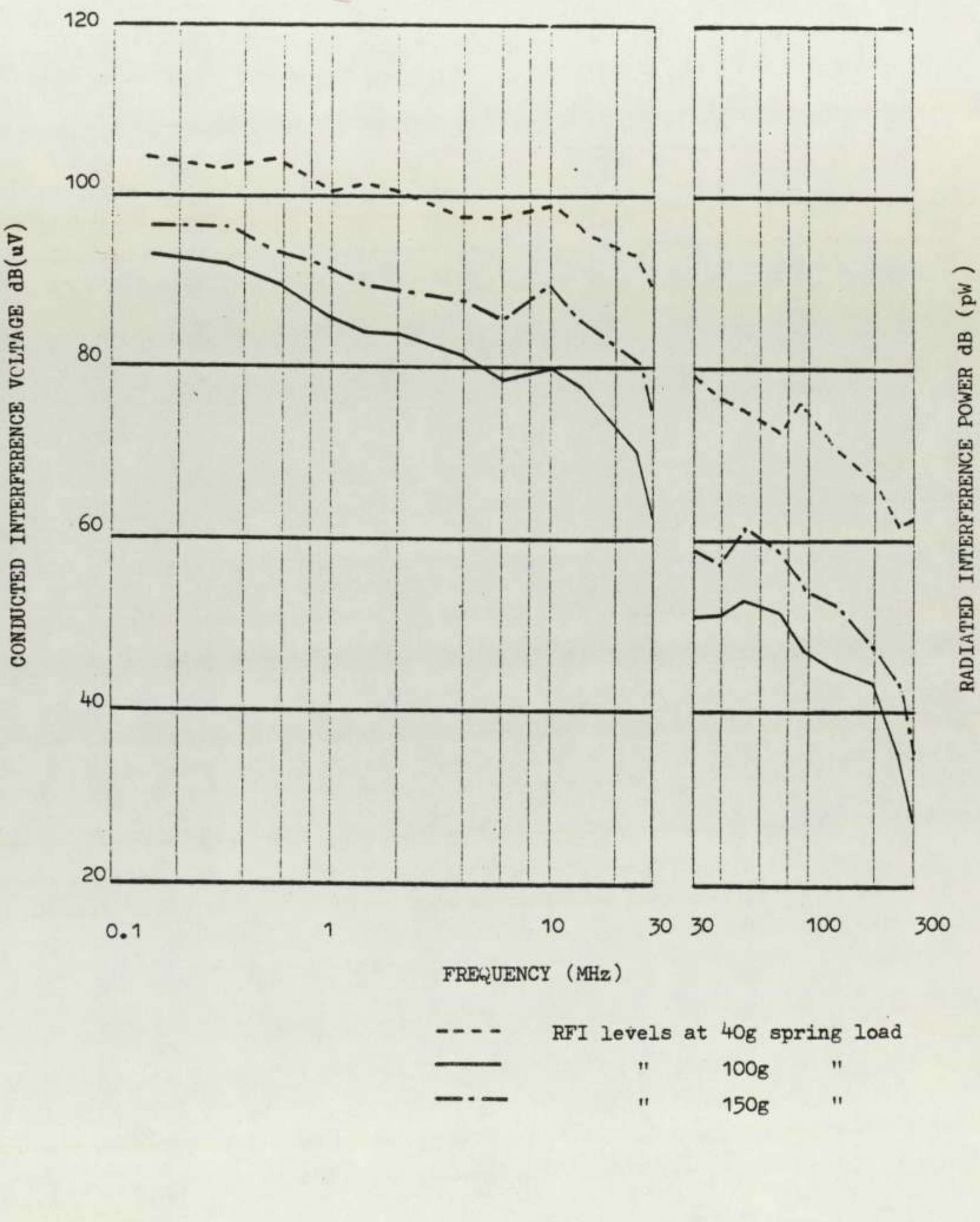

Fig. 6.83

Effect of varying spring load on measured RFI at 18000 r/min.

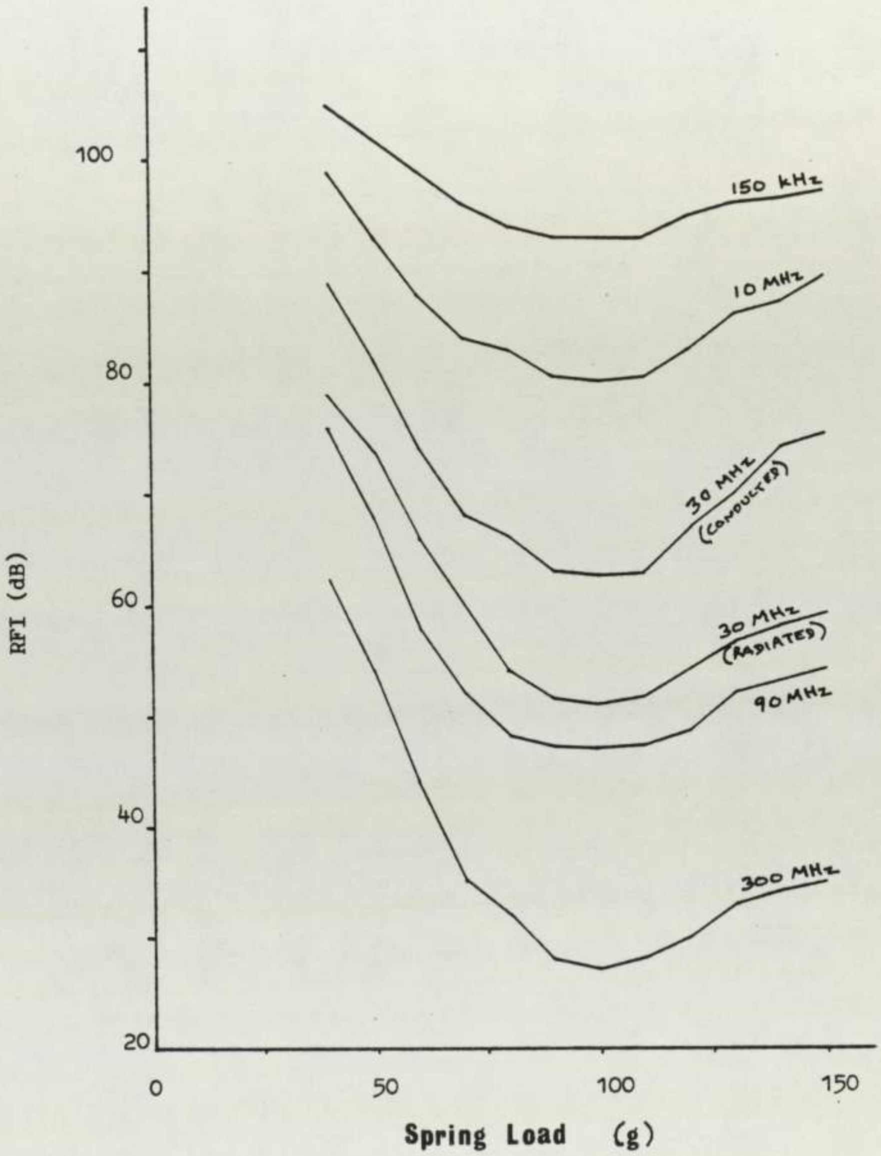

Fig. 6.84

RFI due to the influence of mechanical variations in the motor assembly:
Measured RFI levels with varying brush alignment along the quadrature axis against the direction of rotation.

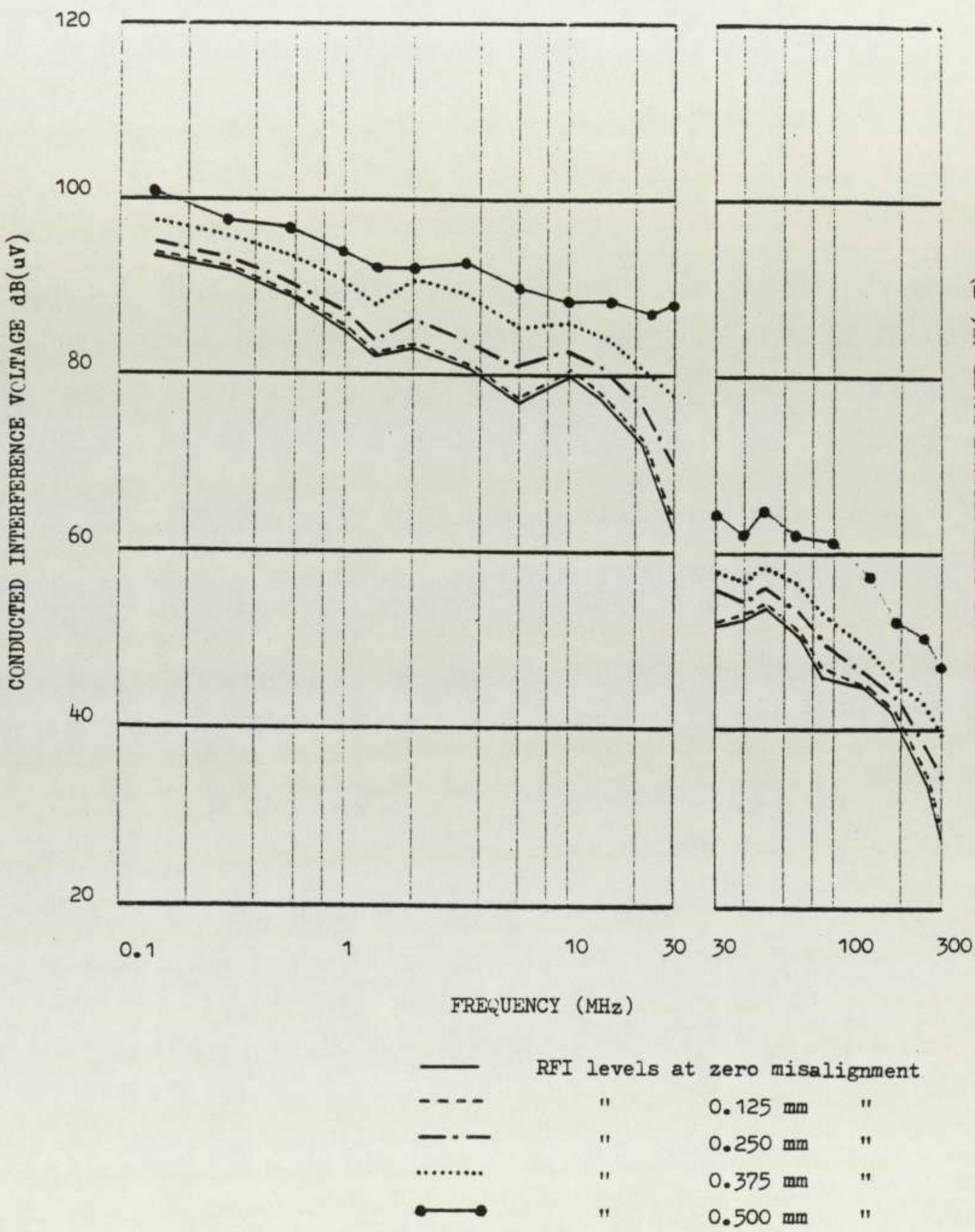

Fig. 6.85

Effect of varying brush alignment along the quadrature axis against the direction of rotation on measured RFI levels.

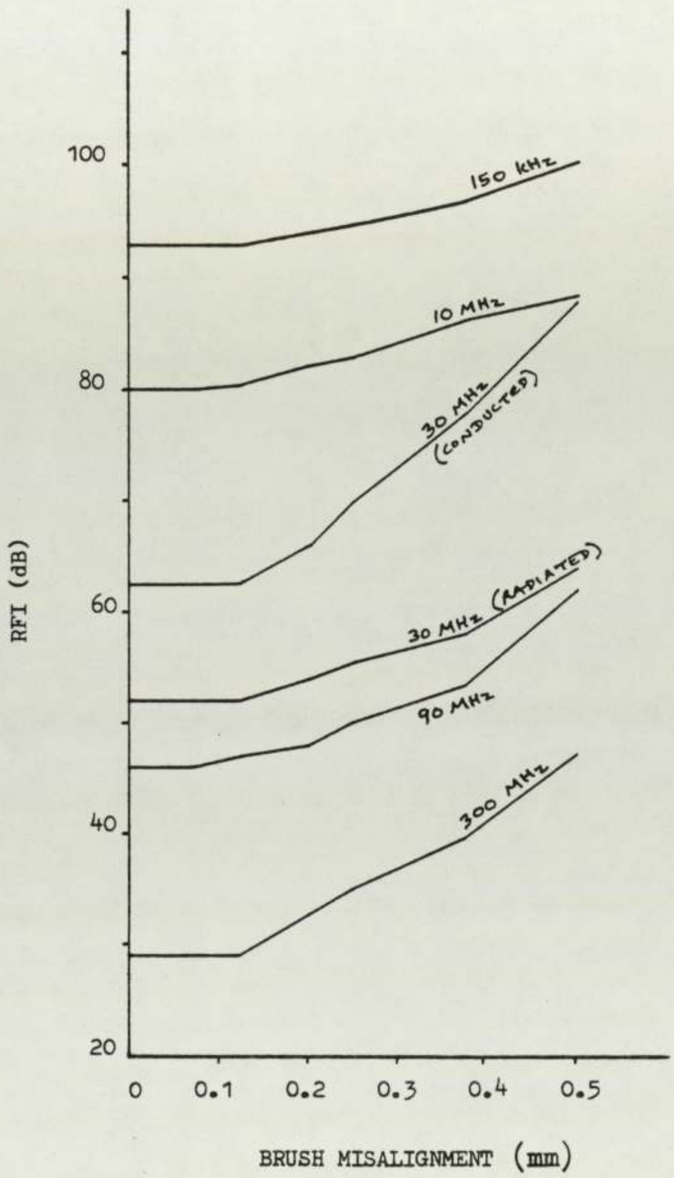

Fig. 6.86

RFI due to the influence of mechanical variations in the motor assembly:
Measured RFI levels with varying brush alignment along the quadrature axis with the direction of rotation.

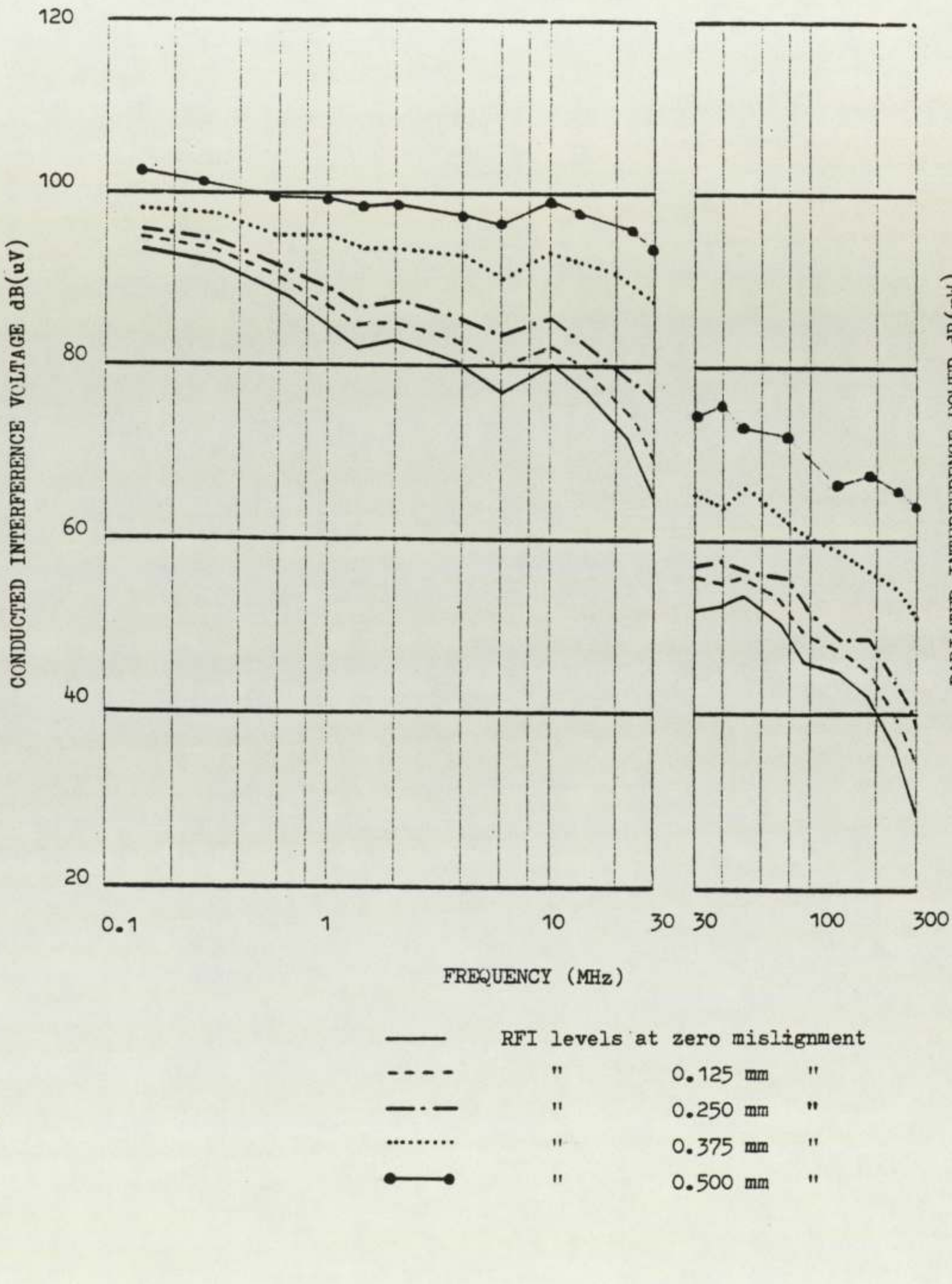

Fig. 6.87

Effect of varying brush alignment along the quadrature axis with the direction of rotation.

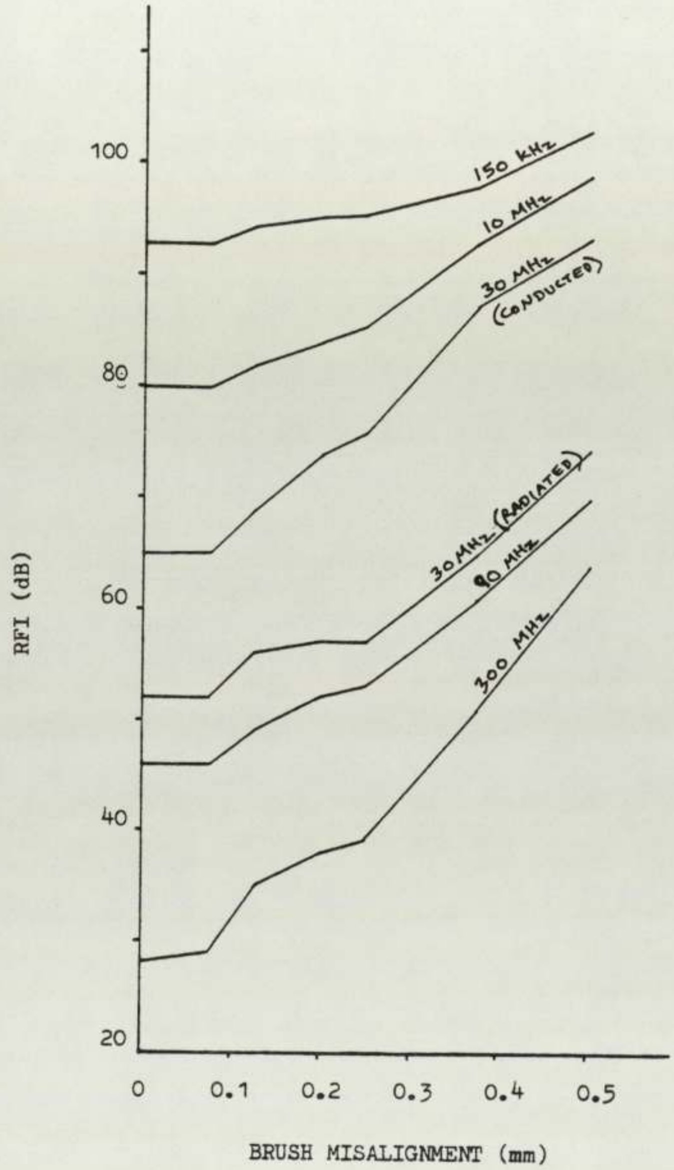

Fig. 6.88

RFI due to the influence of mechanical variations in the motor assembly:
Measured RFI levels with varying heights of proud commutator segments at 18000 r/min.

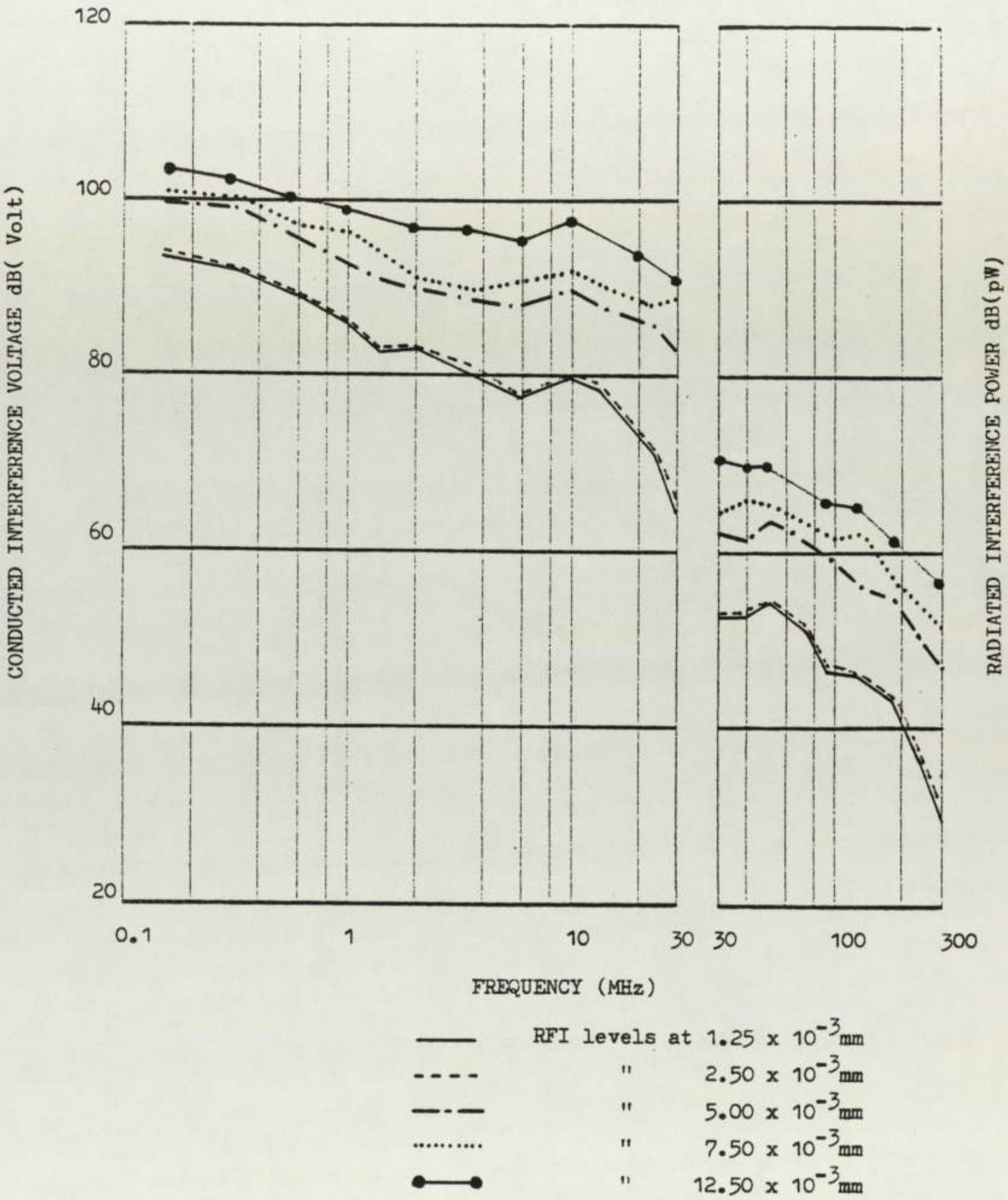

Fig. 6.89

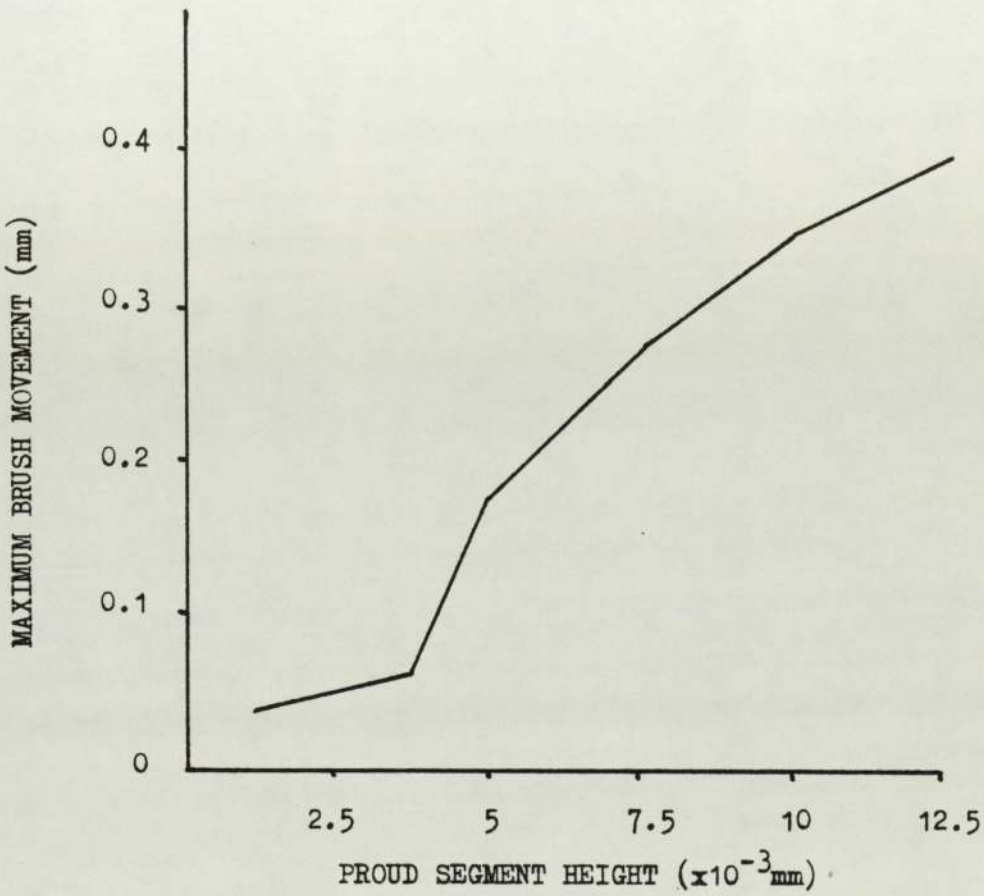

Measured brush movement with varying height of proud commutator segments at 18000 r/min

Fig. 6.90

RFI due to the influence of mechanical variations in the motor assembly:

Measured RFI levels with varying commutator eccentricity at 18000 r/min.

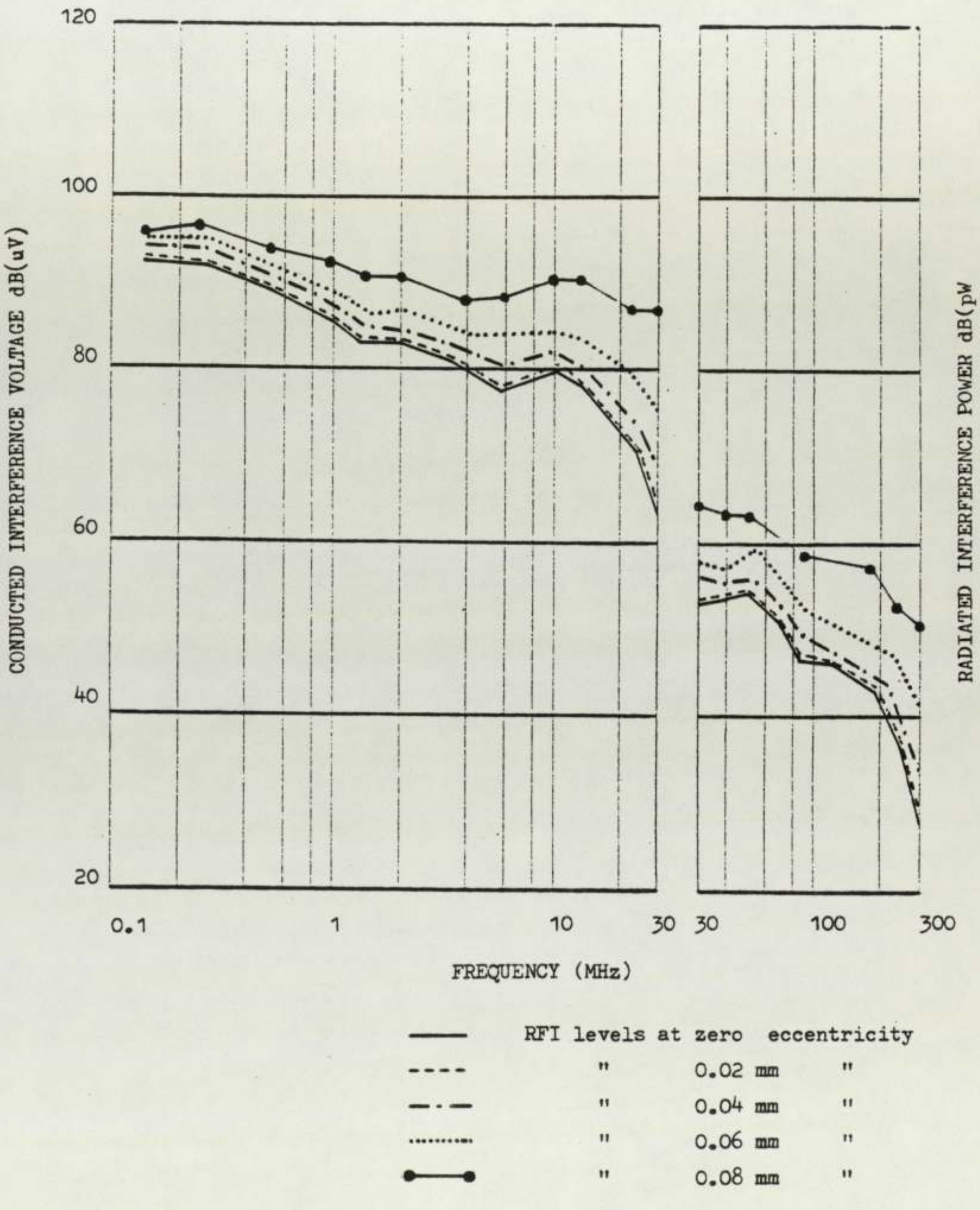

Fig. 6.91

Effect of varying commutator eccentricity on measured RFI levels at 18000 r/min.

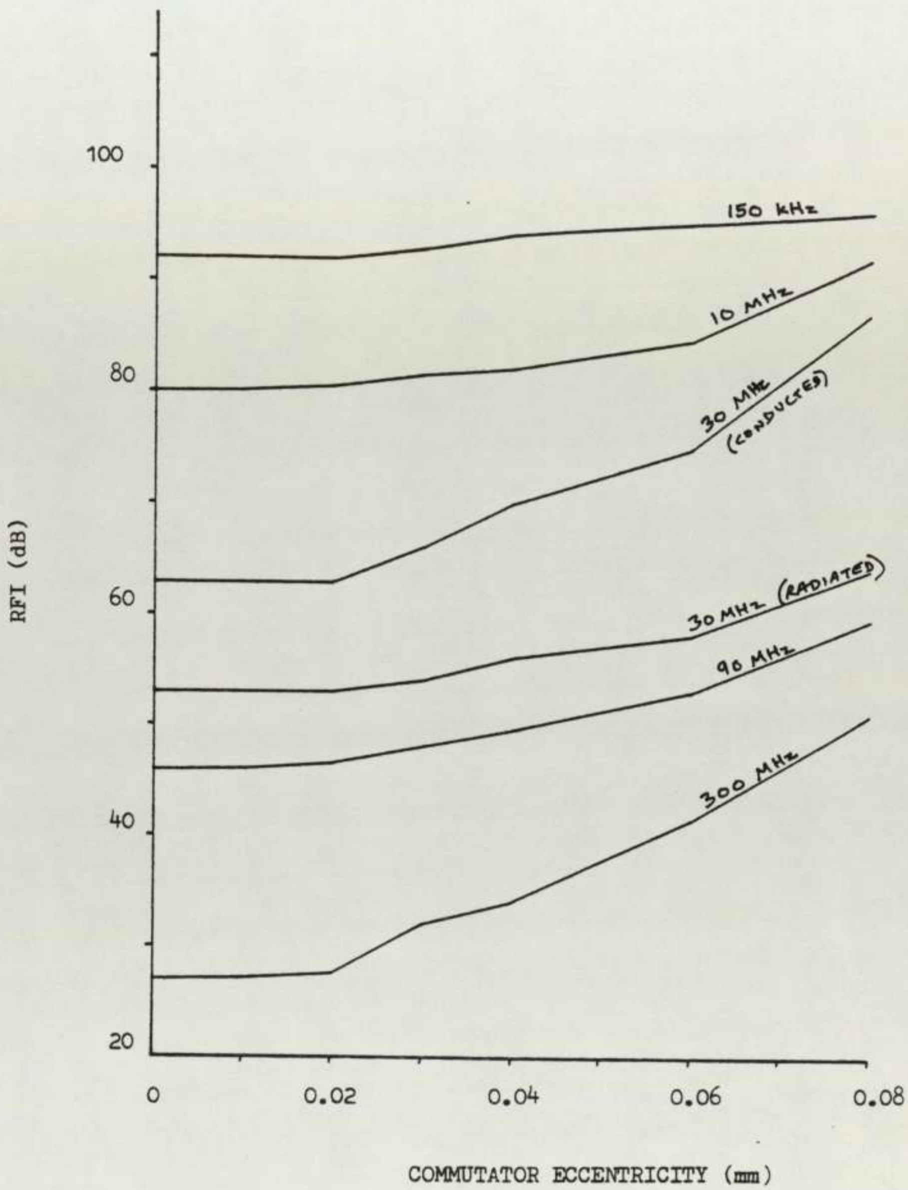

Fig. 6.92

RFI due to the influence of mechanical variations in the motor assembly:
Measured RFI levels with varying commutator surface finishes.

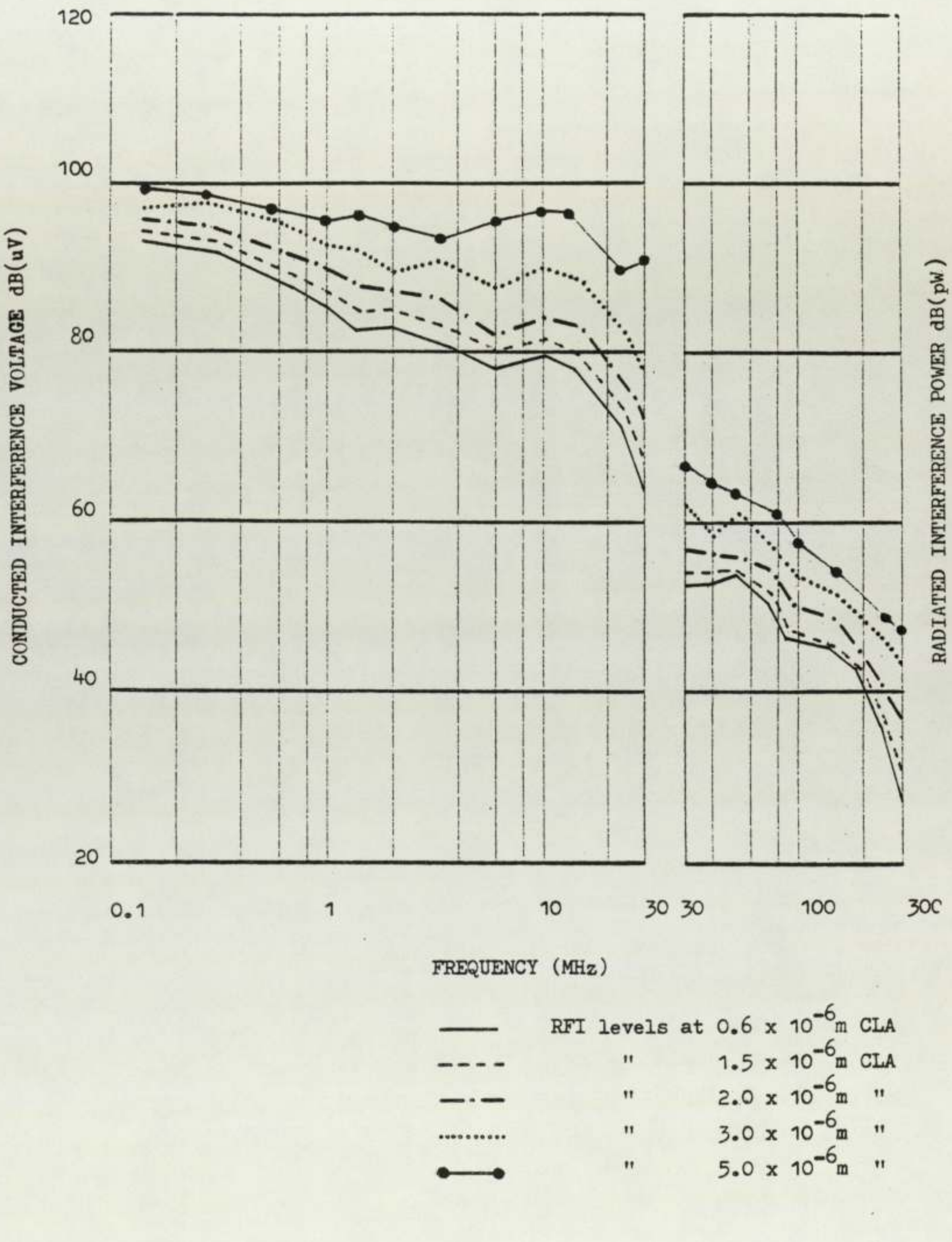

Fig. 6.93

Effect of varying commutator surface finish on measured RFI levels.

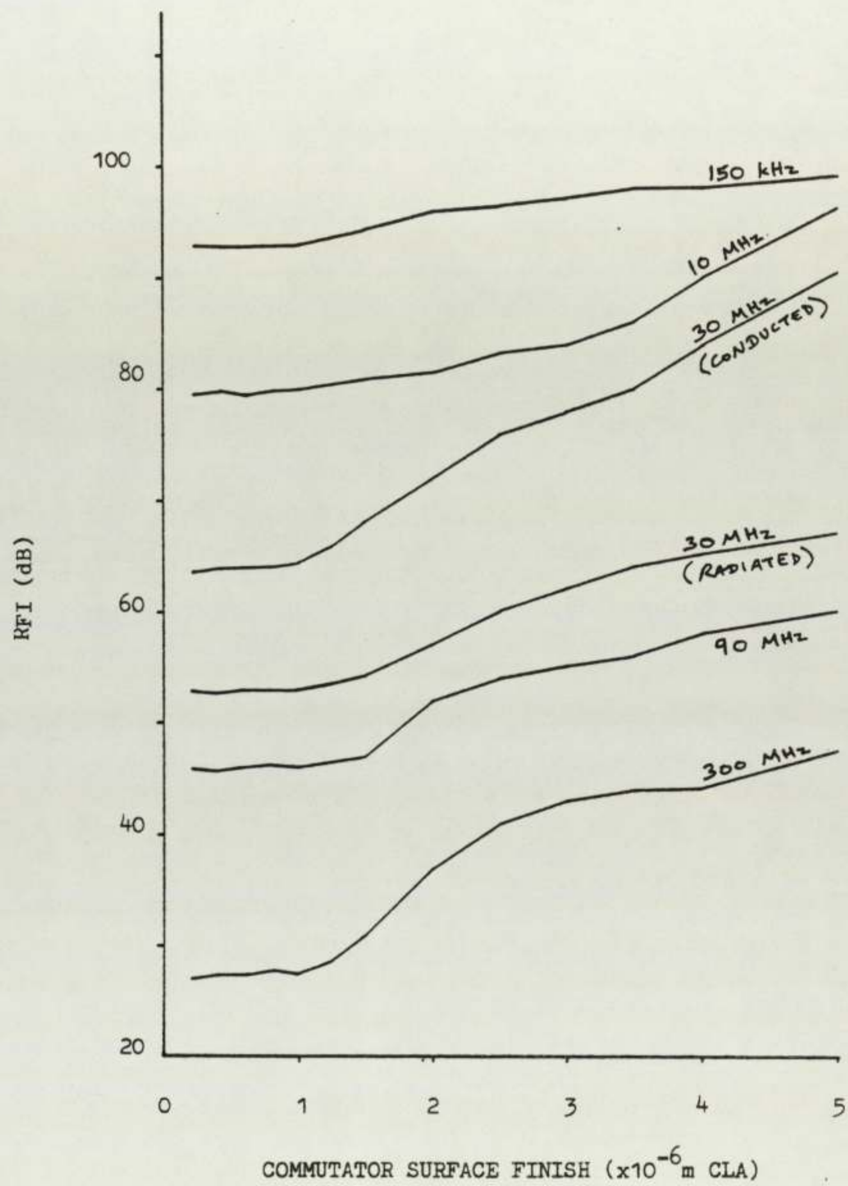

Fig. 6.94

RFI due to the influence of mechanical variations in the motor assembly:
Measured RFI levels with (a) under commutator insulation and (b) flush commutator insulation.

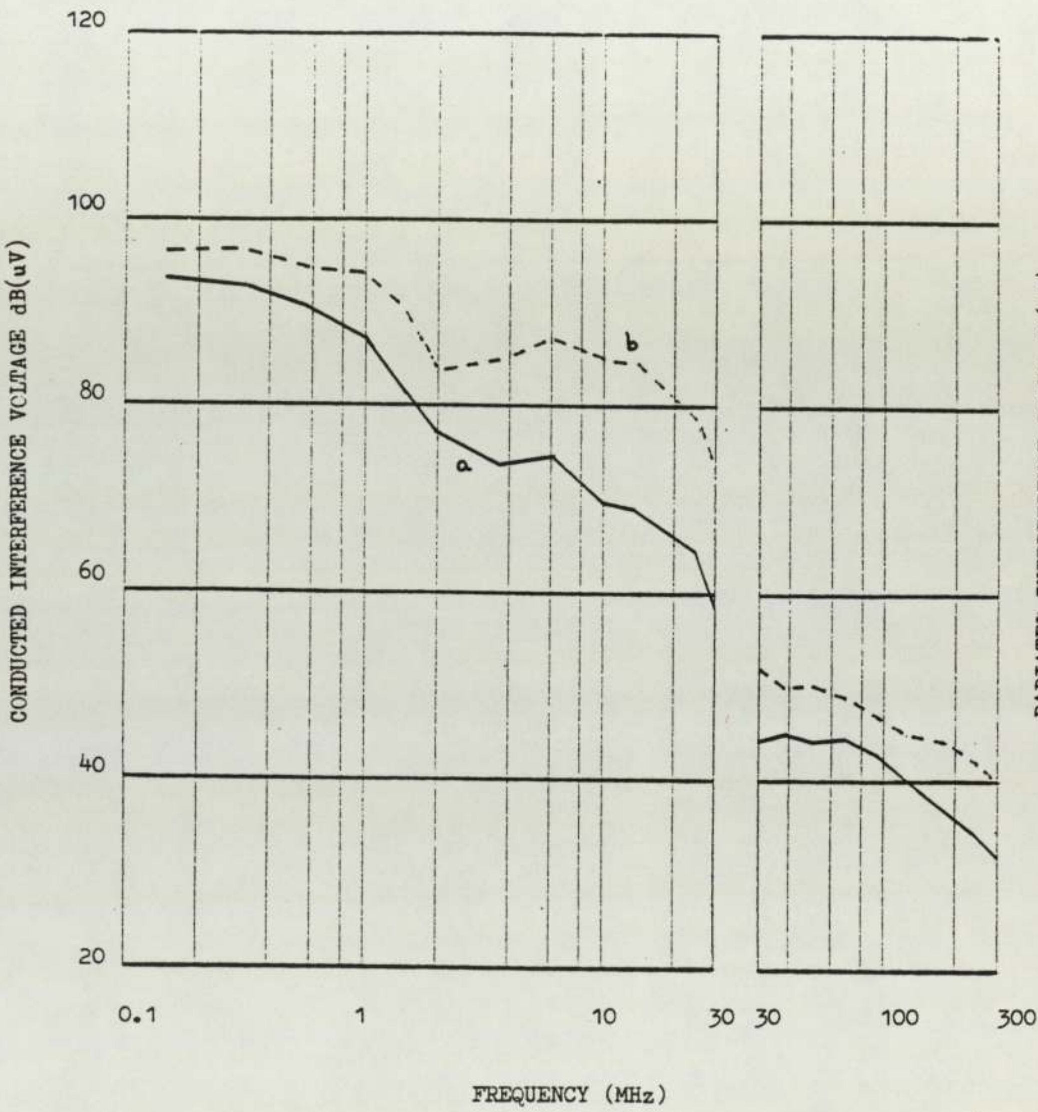

Fig. 6.95

RFI due to the influence of mechanical variations in the motor assembly:

Measured RFI levels with varying brush box and brush clearance in the direction tangential to commutator rotation.

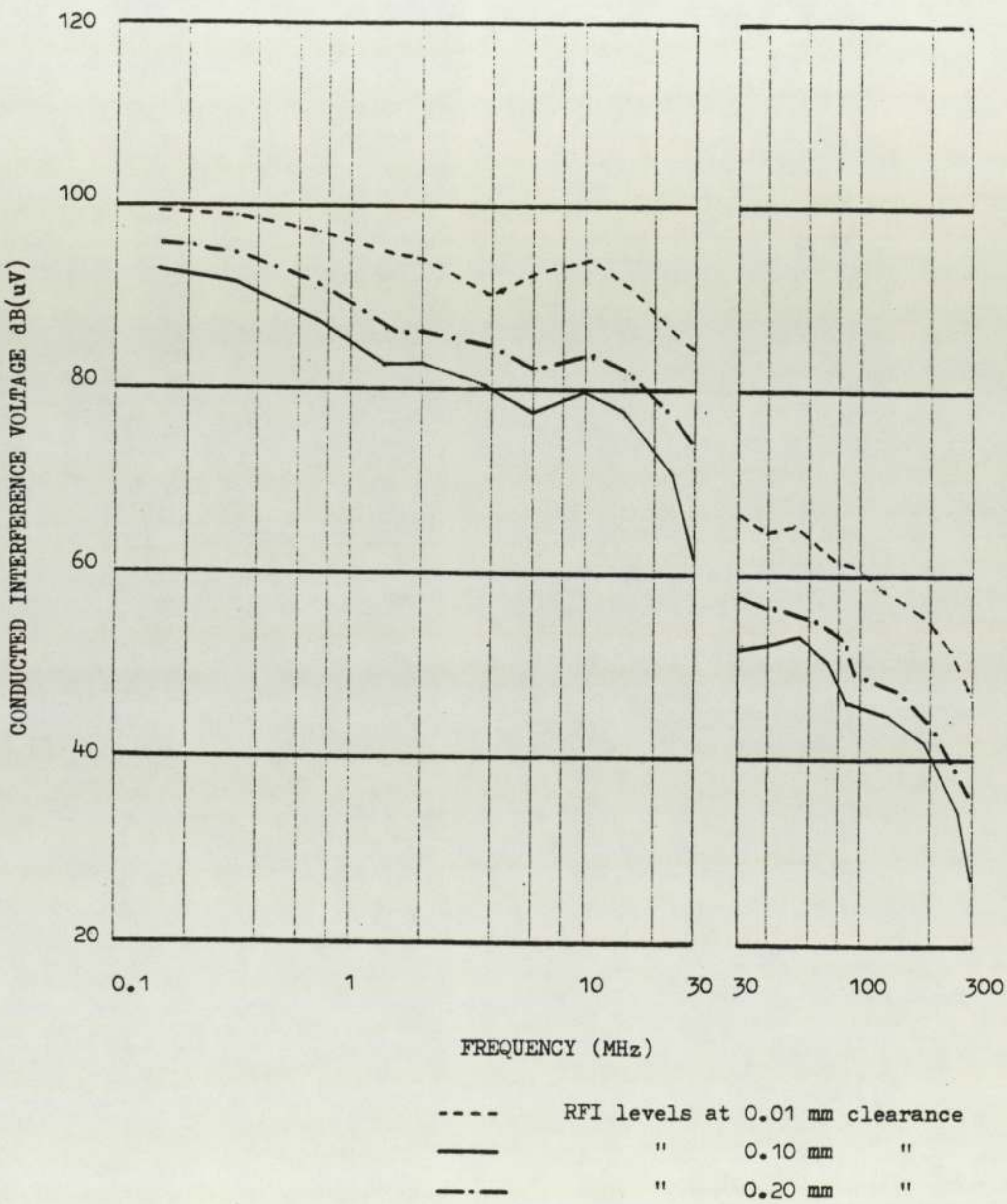

Fig. 6.96

Effect of varying brush box and brush clearance on measured RFI levels.

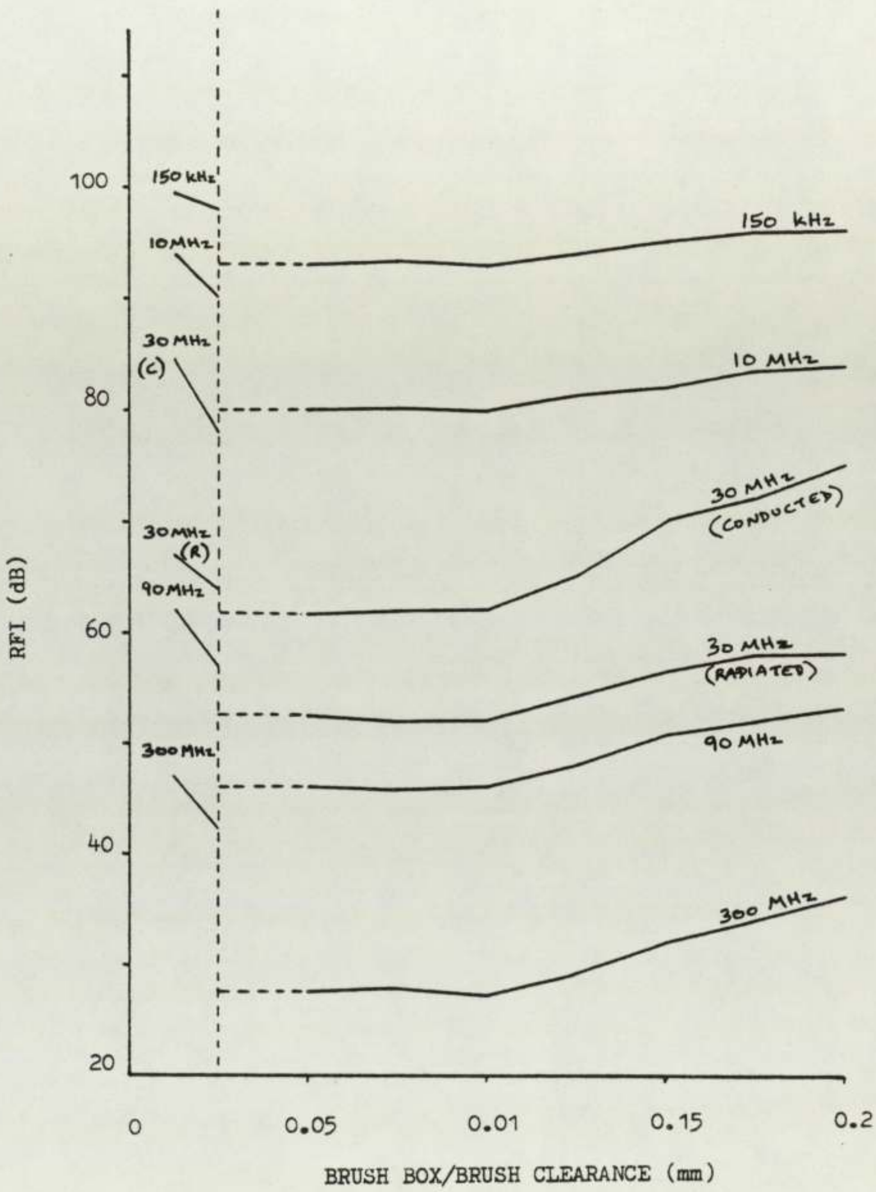

Fig. 6.97

RFI due to the influence of mechanical variations in the motor assembly:
Measured RFI levels with varying brush overhang length at 18000 r/min.

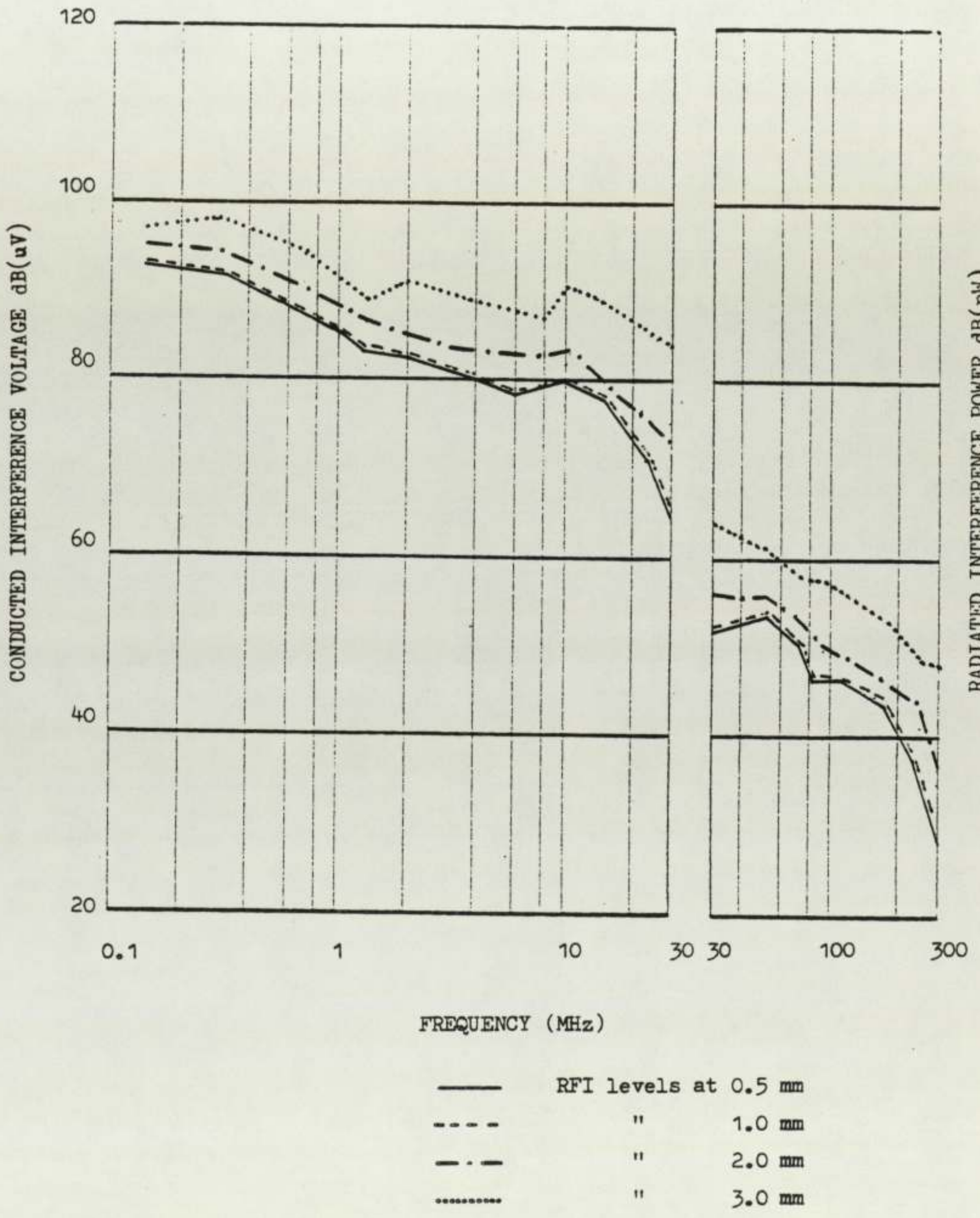

Fig. 6.98

Effect of varying brush overhang length on measured RFI levels.

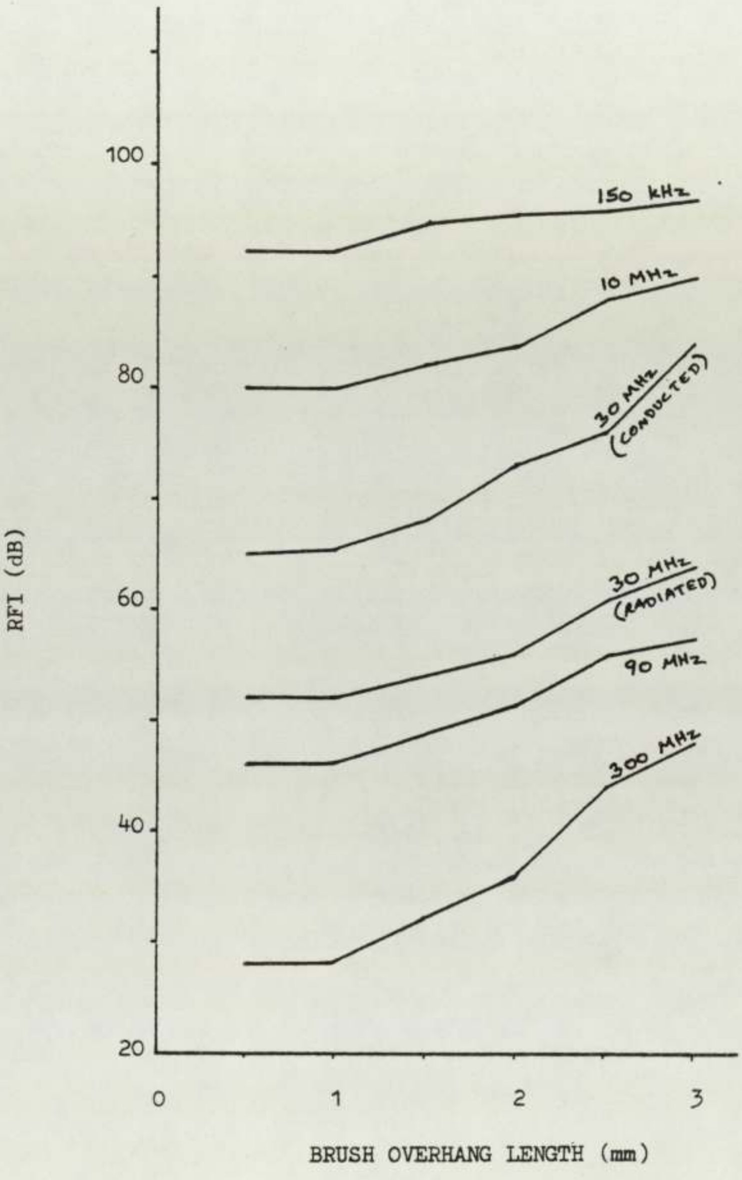

Fig. 6.99

RFI due to the influence of mechanical variations in the motor assembly:
Measured RFI levels with varying bearing misalignment at 18000 r/min.

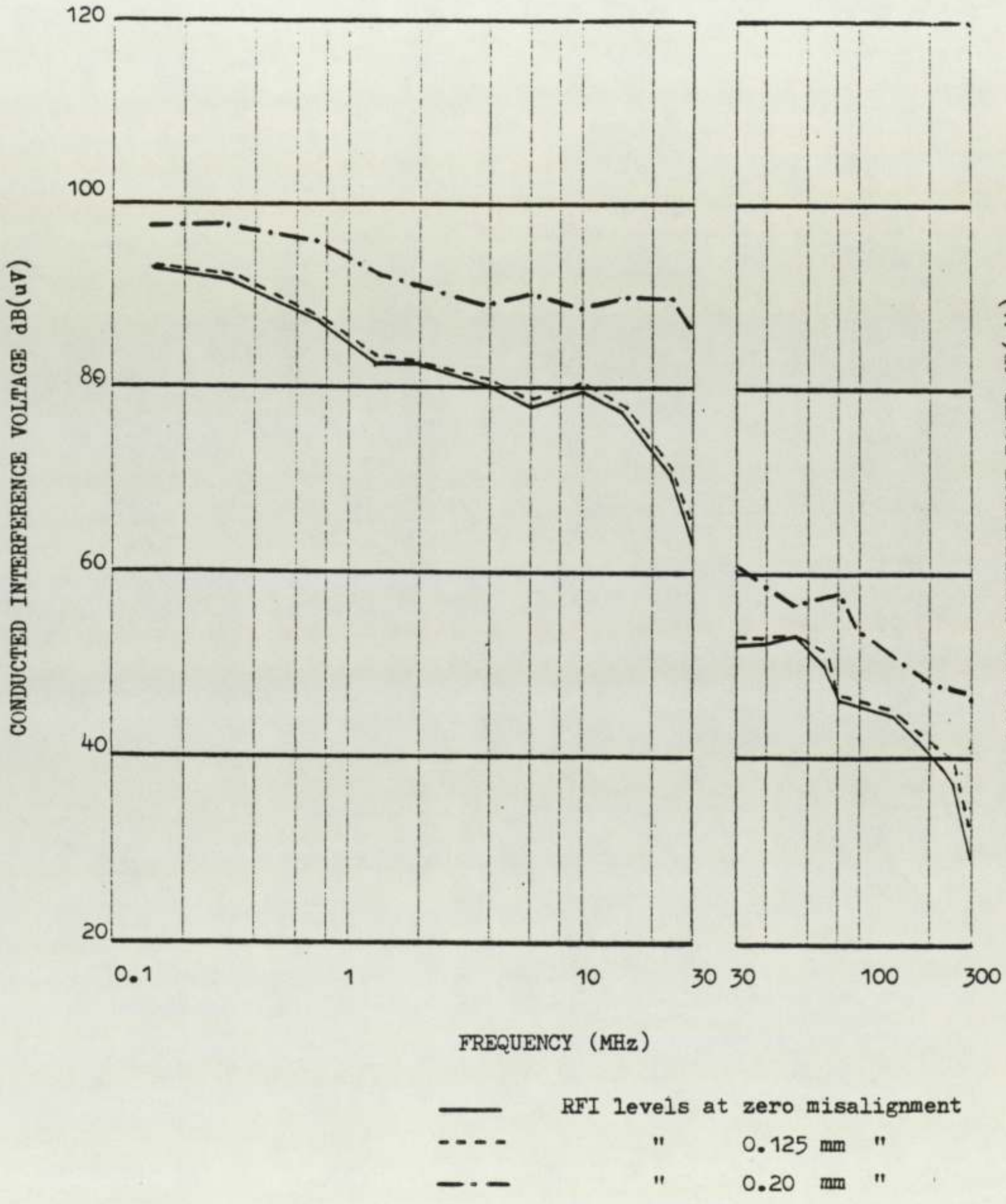

Fig. 6.100

Effect of varying angular brush shift on measured RFI levels at 13000 r/min.

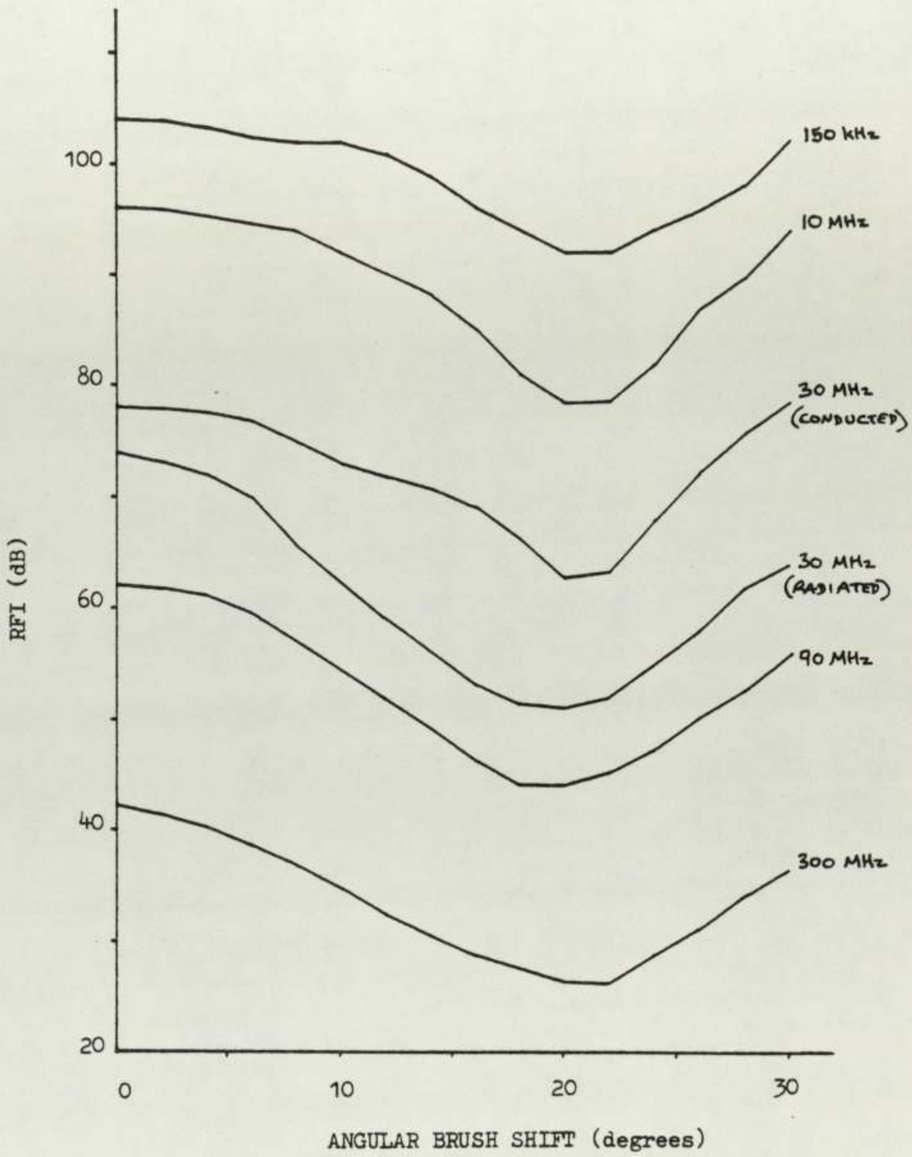

Fig. 6.101

RFI due to the influence of mechanical variations in the motor assembly:

Measured RFI levels with varying bearing journal diameter.

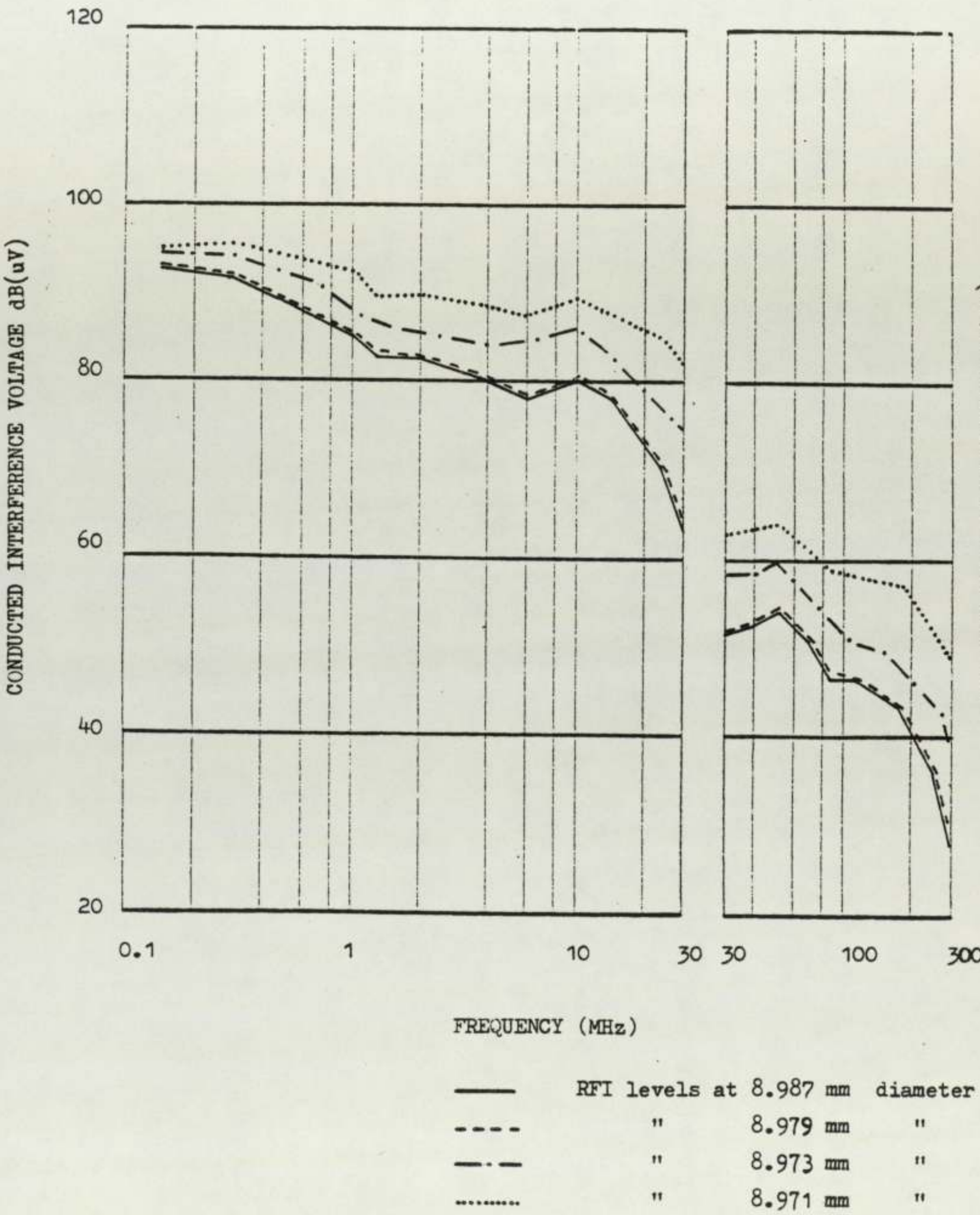

Fig. 6.102

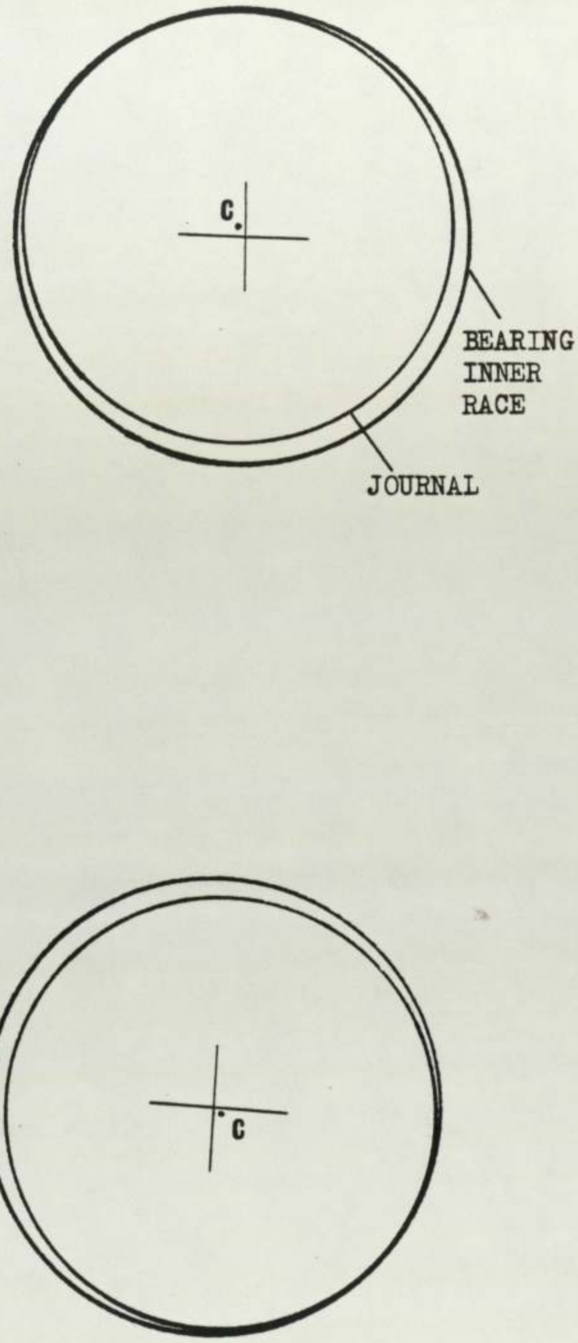

Movement of undersize armature bearing journal inside bearing inner race with rotation

Fig. 6.103

CHAPTER 7

CASE STUDY TO DETERMINE THE SOURCES OF VARIABILITY IN RFI LEVELS FROM MASS PRODUCED MOTORS

7.1 Background to case study

7.2 Manufacturing tolerances

7.3 Factory structure

7.4 General quality monitoring

7.5 Objective manufacturing problems

7.6 Subjective manufacturing problems

7.7 Reduction of variability in RFI levels

CHAPTER 7

CASE STUDY TO DETERMINE THE SOURCES OF VARIABILITY IN RFI LEVELS FROM MASS PRODUCED MOTORS

RFI suppression networks specified for fitting to mass produced motors must ensure that all motor production is capable of conforming to the CISPR/EEC limits. Variability in the levels of RFI generated from these motors, as experienced at Hoover plc, has meant that suppression is often unnecessarily costly due to allownces made to ensure that even motors generating abnormally high RFI levels are adequately suppressed. The case study presented in this chapter was carried out to determine the sources of variability in RFI levels from mass produced motors manufactured at the Hoover Cambuslang factory. It was hoped that once the sources were identified, recommendations to minimise or eliminate their influence could be proposed. This would reduce motor to motor RFI variability and also result in more cost effective suppressor network designs. In the previous chapter, it was shown that mechanical variations in the motor affect the quality of commutation and thus influences the RFI levels generated. The allowable variations determined from the test work, were compared with those found to be used in manufacture and the observations are discussed in section 7.2. Higgs [144] discussed that manufacturing problems fell into two categories, (a) 'subjective' (or indirect) problems and (b) 'objective' (or direct) problems.

'Subjective' problems are those associated with the fundamental manufacturing concepts, although these are difficult to quantify their influences are no less important than 'objective' problems which are generally associated with technical or engineering problems known to exist on the shop floor. Objective and Subjective problems, identified by the case study at the Cambuslang factory together with appropriate recommendations for improvements are presented in section 7.5 and 7.6, respectively.

Finally in section 7.7 it is demonstrated that reduction of motor variability minimises the variation of RFI levels and allows cheaper suppression networks to be used.

7.1 Background to case study

The case study was undertaken at the Hoover Cambuslang factory during spring 1983, the timing is significant since during 1982 the company had undergone a major re-organisation of its U.K. operations. As a result of this, Cambuslang became the centre for all motor production. In addition new products were launched onto the market and also new automated manufacturing techniques had been introduced on the shop floor. In line with the general industrial recession of the period Cambuslang had suffered redundancies in order to affect a 'slimming down' of the work force.

These changes had naturally caused major disruptions at the Cambuslang factory during 1982. In carrying out the cast study, it was thus recognised that (a) operators may be unfamiliar with new manufacturing processes, and (b) 'job loading' throughout the factory departments would be increased. Both of these factors contribute to the subjective problems of the factory; the influence of (a) would no doubt decrease with time but (b) required careful management to ensure that production remained unaffected and is discussed later in section 7.6. 'Teething problems' with the new automated manufacturing equipment were also found to contribute to various assembly difficulties but these were not recorded, as these were considered as only short term problems which would be rectified by production staff in the near future.

The case study considers a manufacturing area at the Cambuslang factory which produces small motors for domestic up-right vacuum cleaners. Two motor designs were manufactured in this area i.e. the 'MC14' and 'EURO', these were studied in parallel since most of their tooling was common. Some machines were alternated to produce parts for the different motors depending on production quota requirements. MC14 components had been used in the test rig for much of the test work described in chapter 6, this motor had originally been made at the Perivale factory but was moved to Cambuslang during the re-organisation period. The motor has a U-type field system and 12/24 type armature.

The EURO was part of the new product range launched in 1983, this motor has an O-type field system and 12/24 type armature. Both motors were of similar rating and suppressed using a parallel 0.1μF capacitor and two in line 6μH inductors. Photographs of the MC14 and EURO motor components are presented in Appendix A6. Figs. 7.1 and 7.2 show the maximum and minimum RFI levels recorded for the MC14 and EURO motors from a selection of production vacuum cleaners. In both cases it was noted that the mean RFI levels recorded were within the CISPR/EEC limits. In the low frequency region the spread of RFI levels from both motors are within the limits, but in the high frequency region particularly around 30 MHz to 90 MHz the variation of RFI levels is such that some motors fall outside the limits. There is a variability of over 30dB in some regions of the spectrum. Of the motors which exhibited the highest RFI levels it was noted that sparking at the brushes was considerably worse than those motors with the lowest recorded RFI levels.

7.2 Manufacturing Tolerances

In section 6.4 the influence on RFI levels due to mechanical variations in the motor structure were examined. In most cases it was observed that it was possible to define an allowable tolerance of the mechanical variation within which RFI levels remained unaffected. Examination of Hoover RFI records showed that variability of RFI levels measured from the production motors such as shown in Fig. 7.1 and 7.2 was caused by a mechanical innaccuracies in the motor assembly. Thus the first task undertaken in the case study was to compare the tolerances specified for the manufacture of motor components and their assembly with those determined from the test results. The intention being to see if the manufacturing tolerances were suitable in the light of the test results; if not, whether it was feasible to recommend tighter manufacturing tolerances with the existing tooling or to see if there was a better production method available. Table 7.1 shows the summary of the tolerances specified for the manufacture of the MC14 and EURO motors and those obtained from the test work.

It can be seen that in most cases the tolerances specified for manufacture are in close agreement with the values determined from the test rig suggesting that their influence on RFI variability is minimal. The notable exceptions are discussed below:

Mechanical variation	Manufacturing tolerance		Allowable tolerance (from test work)
	MC14	EURO	
Static armature out-of-balance	0.432 gcm	-	0.5 gcm
Dynamic armature out-of-balance	-	0.22 gcm	0.3 gcm
Spring Load	73 - 93 g	73 - 93 g	90 g - 110 g
Brush misalignment (with rotation)	-	0.095 mm	0.125 mm
Brush misalignment (against rotation)	-	0.095 mm	0.075 mm
Proud commutator segment	3.8×10^{-3}	3.8×10^{-3}	3.75×10^{-3}mm
Commutator eccentricity	0.01 mm	0.01 mm	0.02 mm
Commutator surface finish	0.8×10^{-6}m CLA	0.8×10^{-6}m CLA	$0.5 - 1 \times 10^{-6}$ CLA
Brush box clearance	0.05 - 0.26 mm	0.05 - 0.26 mm	0.1 mm
Brush overhang length	2.1 mm	1.1 - 2.5 mm	0.5 - 1 mm
Bearing misalignment	0.1 mm	0.1 mm	0.125 mm
Angular brush shift	3^{o}	3^{o}	2^{o}
Bearing journal	0.008 mm	0.006 - 0.008 mm	0.008 mm

Comparison of specified manufacturing tolerances on MC14 and EURO motor assemblies with test results

Table 7.1

(a) Spring load

The nominal spring load specified for both motors is approximately 10g lower than that shown to be required from the test results. Increase of spring load could easily be implemented by increasing the length of helical coil springs - a change of this type could easily be accommodated with the existing spring forming tools used at Cambuslang.

(b) Brush box/brush clearance

The maximum brush box/brush clearance determined from manufacturing drawings is over twice the value found to be acceptable on the test rig. Clearances of this magnitude caused brush vibrations increasing RFI levels by almost 10-15 dB in the high frequency region. Brush box fabrications were bought in from outside suppliers and thus a reduction in clearance could be affected by transmitting tighter tolerances to the source manufacturers.

(c) Brush overhang length

Brush overhang length is determined by the position of the brush box relative to the commutator surface, in both motors it was found that the brush overhang length was almost double the limiting value determined on the test rig. Reduction of this length would require either altering the position of the brush boxes nearer to the commutator, or by increasing the overall brush box length.

(d) Angular brush shift

Brush shift is introduced to the motors by positioning the commutator with the appropriate angular shift on the armature shaft relative to the brush axis. The figure of 3^{o} for the manufacturing tolerance of the brush shift quoted in Table 7.1 was found to have been used in manufacture in the absence of any tolerance specified on motor assembly drawings. The reduction of this tolerance to the value suggested could be implemented by existing manufacturing equipment without difficulty.

Manufacturing tolerances specified for armature out-of-balance, brush alignment, bearing alignment, shaft journal diameters and the commutator variations appear suitable with respect to their influence on RFI levels. However, examination of motors known to generate high RFI levels showed that in many cases the actual variation of these parameters were outside the specified manufacturing tolerances. RFI measurements were recorded from motors taken from different production batches over a period of six weeks. It was observed that causes of high RFI levels could be classified in two broad categories. Firstly, where the cause was other than due to excessive mechanical variations for example varnish or swarf in the commutator slots, absence of grease in bearings, broken brushes. The incidence of these problems were low, motors in this category would normally have been rejected for high brush arcing during a final test stage where the motor performance is checked. Production records showed that the incidence of such rejections was less than 2% of the total production. The second category which was of direct interest to the case-study was where the cause of high RFI levels was due to deviation from the specified manufacturing tolerances. Production records showed that the incidence of such motors rejected at the final stage was on average 10%, but had been known to increase above 20% in exceptional circumstances. However, it was found that in many cases such motors were acceptable in terms of electrical performance and could only be identified as not meeting specifications from RFI tests. In order to demonstrate that the high RFI levels observed were due to poor manufacture, a number of motors which had originally generated high RFI levels were stripped and re-assembled with the defects rectified. In all cases the subsequent RFI levels recorded were lower than seen previously. Figs 7.3, 7.4 and 7.5, show examples of the 'before' and 'after' RFI levels measurements recorded on EURO motors. The maximum mechanical variations recorded for each of the parameters is shown in Table 7.2.

From these preliminary observations, it was clear that the source of RFI variability was the mechanical variations in the motor assemblies being achieved on the shop floor. As discussed above in many cases the variations achieved were in excess of the specified manufacturing tolerances, thus it was planned to follow the production of the MC14 and EURO motors on the shop floor, in order to identify the problem areas. Higgs [144] discussed that problems arising on the shop floor could be loosely classified as follows:

(a) Inadequate or poor facilities

The facilities include machines, tooling, gauges as well as the working environment. Tooling and gauges may be old or poor quality and suffer from lack of maintenance.

Mechanical Variation	Measured Mechanical Variations (MAX)
Static armature out-of-balance	2.5 gcm
Dynamic armature out-of-balance	1.4 gcm
Spring Load	50 g - 180 g
Brush misalignment (with rotation)	0.25 mm
Brush misalignment (against rotation)	0.25 mm
Proud commutator segment	15×10^{-3} mm
Commutator eccentricity	0.04 mm
Commutator surface finish	3×10^{-6} m CLA
Brush box clearance	0.4 mm, (0.01 mm MIN)
Brush overhang length	2.5 mm
Bearing misalignment	0.3 mm
Angular brush shift	6^{o}
Bearing journal	0.015 mm

Summary of maximum mechanical variations recorded from production motors

Table 7.2

(b) Inadequate or poor design, process and material specifications

Motor design and manufacturing process need to be adequately specified in order to reduce complexity of both manufacture and assembly. Materials should be robust to withstand both normal motor requirements and also capable of withstanding manufacturing handling and assembly techniques. Higgs states that problems can creep in if unforseen differences occur between presumed similar products and processes. Production may alter design/process specifications in order to alleviate localised problems without appreciating problems being caused in other manufacturing areas.

(c) Human error

Failures occur even when equipment and specifications are adequate because of human errors. Poor batch identification and quality control results in mistakes going un-noticed and only the final symptoms of the error being observed.

(d) Non-adherence to specified procedures

Higgs states that nearly all manufacturing activities suffer from some operator 'modification' and only intimate knowledge of the daily shop floor situation could reveal them. Poor supervision and quality control make the situation worse as many improper practices can go unchecked. This type of abuse can never be fully quantified because operators, unions and even supervisors are reluctant to acknowledge that such abuse exists.

Information for the case study was gathered by observation of operators at work; by discussions with operators, foremen, quality inspectors and line management; and by examination of various production records. The main problem with case studies of this type, where an outside researcher enters a production environment is ensuring that practices are not 'modified' for the researchers benefit or otherwise. The researcher is often treated with caution as in some quarters he can be viewed as a management 'spy'.

Time was therefore spent in gaining confidence of shop floor personnel in order to obtain useful information. In the event it was surprising how keen and forthcoming the various people were. It was recognised that some information would have to be disregarded due to distortion of facts thus it was ensured that only sound corroborated evidence was recorded. The following sections describe the structure of the manufacturing area and the objective and subjective problems identified within it are discussed. Where possible recommendations are proposed to alleviate the problem areas and thus affect a reduction in the variability of RFI levels from the MC14 and EURO motors.

7.3 Factory Structure

The overall factory structure for the production and assembly of the MC14 and EURO motors can be split into three manufacturing areas, i.e.

1) prime areas

2) sub-assembly areas

3) final assembly and electrical test area

There are three 'prime' areas of manufacture which supply parts to the sub-assembly and final assembly areas, they include (a) a plastic moulding shop which produces motor cases and fans (b) a machining shop for turning and grinding armature shafts and (c) a press shop which produces the motor laminations. Additionally, 'goods inward' can also be considered a prime area for all bought in items including wire, bearings, brush boxes, brushes, suppression components and screw fittings. These parts are stocked and supplied to the factory as required. Components from the prime areas are transported to sub-assembly points for the next stage of the production. The main sub-assembly areas are (a) armature manufacture, (b) field manufacture and (c) brush box and spring manufacture.

The armature and field sub-assemblies are manufactured using semi-automatic production equipment and involve minimal operator handling. The finished sub-assemblies are transferred to the final assembly and electrical test area. Here the components are fitted into the moulded motor cases along with the various bought in items and the motor assembly is completed ready for electrical test. Motors are run for a short period to allow adequate brush bedding before each motor is individually checked for performance and quality of commutation. The motors are then transported to a 'finished products' areas (not examined in the case study) where they are fitted into vacuum cleaner bodies and a selection of these undergo RFI testing.

In each production area there are a number of full time employees working in two eight hour shifts. The employees include:

(a) production work force i.e. operators

(b) local production foremen, responsible for operator supervision and the operators achieving production quotas

(c) local machine setters responsible for setting tools and machinery.

In parallel with the production staff there are the quality control and quality assurance departments and a maintenance department. Quality control is divided into a number of groups which include a quality foreman and 2-3 quality engineers/inspectors. Only two groups are of interest to this study; one covering the MC14 and EURO assembly areas and a second covering plastic moulding and shaft machining areas. Quality assurance covers the inspection of the goods inward and finished products areas and is also responsible for the final RFI testing function. The maintenance department have a group of staff responsible for maintaining and refurbishing electrical and mechanical equipment covering the whole factory area.

7.4 General quality monitoring

Each operator is responsible for the quality control of his/her own manufacturing operation. In some cases, this may involve only a visual inspection, in others they are supplied with appropriate gauges to ensure that components conform to specified manufacturing tolerances. The quality engineers/inspectors carry out random checks on the production line to ensure quality is maintained. Finally, the quality inspectors carry out a rigorous quality audit on batches of finished components. If the audit check reveals poor overall quality, he reports this to the quality foreman who has the right to scrap any item or production batches failing the audit check. Naturally as in any manufacturing environment this can lead to conflict with the local production foreman who is responsible for production quotas being achieved. Thus, if large quantities of production are in question the final responsibility lies with the Quality Superintendent and the Production Manager.

If component quality is poor, there are two possible communication paths by which the machine setter can be summoned, i.e.

(a) If the fault is detected by the operator - he reports it to the local foreman, who can decide whether it is a tool setting problem and call the machine setter but if the problem is more difficult to fathom he may call the quality engineer.

(b) If the fault is detected by the quality engineer/inspector (through their random production checks) he can call the machine setter himself and inform the local foreman of his actions.

7.5 Objective Manufacturing problems

This section describes some of the manufacturing problems observed in the different production areas. The production areas studied include the following:

a) plastic moulding shop (7.5.1)

b) machining shop (7.5.2)

c) press shop (7.5.3)

d) armature manufacture (7.5.4)

e) wound field assembly (7.5.5)

f) brush box and spring manufacture (7.5.6)

g) final assembly and electrical test (7.5.7)

In each case, there is a brief description of the manufacturing processes and techniques used to monitor production quality. The problems observed are discussed and where possible the sources are identified and appropriate recommendations to minimise or eliminate their influence are proposed.

7.5.1 Plastic moulding shop

Motor casings and dirt collecting fans are manufactured in the plastic moulding shop. The accuracy of the casing mouldings is an important feature in the final motor assembly; recesses and slots in the mouldings ensure motor components are located in the correct positions affecting the alignment of the bearings, brush boxes and field assembly. Examination of motors producing high RFI levels had in a number of instances been found due to poor bearing and brush box alignment. The dirt collecting fans were fitted on the armature shaft, these had been found to affect armature out-of-balance.

7.5.1.1 Method of manufacture

All plastic mouldings are made using fully automatic plastic moulding machines. In the machine plastic resin is heated to a molten state which is then injected under pressure into a cavity moulding tool. The plastic is allowed to cool before the moulding is ejected from the cavity, the tool retracts, allowing the mouldings to be removed. The machines typically have three cavities working simultaneously. Tool cycle times, temperatures and speeds have to be set by a machine setter. The machine operator has to remove the new mouldings from the tool when it opens and close it again for the next cycle to begin. The mouldings are placed in omni-crates standing next to the moulding machines. Plastic resin is introduced to the machines at regular intervals via a hopper at the top of the machine by a labourer. Removal of plastic flash and drilling/tapping of holes in the mouldings are carried out in a second operation in an adjoining area.

7.5.1.2 Production monitoring

The operator carries out a visual check on the mouldings inspecting for burning or other surface defect on the plastic. There were no gauging facilities for the operator to carry out any dimensional checks on the mouldings, this was left to quality inspectors who were provided with gauges to check field and bearing alignments on the motor casings. This check should be performed during regular patrol checks and at a final audit inspection on production batches. In the case of the dirt collecting fan mouldings, quality inspectors were provided with a balancing machine to check for fan out-of-balance.

7.5.1.3 Objective problems

Production monitoring in the plastic moulding area, was found to be negligible and moulding quality relied heavily on the machine setters ability to produce components without any visual defects. The gauges provided to the quality inspectors to check bearing and field alignment on the motor cases, were not being used either to monitor production or to check components after tool changes or changes to machine cycle times and temperature settings. The normal practice was to ensure the mouldings were visually free from defects but this meant that small distortions in the mouldings were left undetected only to cause assembly problems later in manufacture or cause the motor to generate high RFI levels observed earlier.

A similar lack of monitoring on the fan mouldings meant that moulding assymetries causing out-of-balances on the armature were not detected. Subsequent measurements showed that fans fitted onto balanced armatures could increase their rotating out-of-balance to over five times the maximum allowable out-of-balance specified for the armature.

Further specific moulding problems are detailed below:

a) inadequate or poor facilities

  i) tooling; examination of the MC14 mouldings showed that there was a thickness error in the field location region causing poor field alignment with respect to the armature. Although variation of air gap was found not to influence RFI levels (see section 6.4.12), this fault had caused a number of problems in the final assembly area. It was found that in some cases, field alignment was so bad such that the armature fouled on the pole face. In many instances this would prevent the armature turning, where however, only slight interference existed it was possible for the motor to turn but the intermittent contact causing arcing at the brushes leading to high RFI levels.

Moulding errors could be caused by inaccurate tool dimensions or by the use of old and worn tools, the fault could only be cleared either by re-grinding the existing moulding tools to the correct dimensions or by replacing them with new tools.

Inspection of motor cases with excessive bearing misalignments showed them to have been moulded in the same tool cavity. Since moulding distortion takes place during cooling, to an experienced machine setter, it was clear that this tool was running too hot. The fault could be cleared by adjustments of the moulding cycle time and temperature settings to ensure adequate cooling of the mould before the tool was opened. Increasing cycle times appeared unpopular with the operators since this would reduce their production rates. Another cause of moulding distortion was the stacking of the hot moulds one on top of another in the omni-crates. The moulds at the bottom of the crates would retain their heat for a long time allowing distortions to develop. This could be improved by the use of 'cooling platens'; as the hot mouldings are removed from the tool, they should be placed on platens which are formed to the shape of the mould and thus as the mould cools its shape cannot distort. Once the mouldings have cooled sufficiently only then can they be stacked as before.

ii) gauging; as described above gauges were provided to check for bearing and field alignment - although not used it must be stated that facilities for checking these dimensions on the mouldings were available. But notably, the absence of any gauge to monitor alignment of the brush box region was of concern. In section 6.4.4 it was shown that brush misalignment increases RFI levels due to sparking caused by excessive brush vibration. The EURO motor has the brush box located in a slot in the casing moulding. Accuracy of the brush box alignment and brush clearance is dependent on the slot position and dimensions, thus, any moulding distortion in this region would impair RFI levels from the motor. It can be summarised from these observations that quality control of moulding needs to be greatly improved in order to reduce the resultant variability of RFI levels from the motors.

b) Inadequate or poor design

The design of the EURO motor fan, although excellent for collecting dirt in the cleaner, was found to cause significant variability in RFI levels due to the out-of-balance it introduced to the armature. Even when the fans were found to be well balanced, subsequent fitting to a balanced armature could cause armature out-of-balance to be greater than the specified manufacturing tolerance. This problem was not evident on the MC14 armature. The difference can be explained from the methods used to fit the fans on the armature shaft. The MC14 fan has a hole at its centre and locates on a journal on the armature shaft and is fixed in position by a nut as shown in Fig. 7.6(a). The centre of the EURO motor fan is drilled and tapped and the fan is screwed directly onto a threaded portion of the armature shaft as shown in Fig. 7.6(b). The threaded fitting meant that the EURO fan cannot be located squarely on the shaft causing unbalance as the armature rotates. Measurements of out-of-balance carried out by Hoover engineers, showed that even small variation loosening or tightening of the fan cause the out-of-balance to increase in magnitude and shift in position on the armature.

The fitting technique used for the MC14 is much better, the machined locating journal ensures that the fan is always positioned squarely on the shaft. It is recommended that a similar design be applied to the EURO dirt collecting fan.

c) Operator malpractices

Operators were paid on a 'piece work' system, this was their incentive for achieving high production rates. It was demonstrated that some operators reduce the machine cycle time and temperature settings in order to increase the rate of moulding production. As mentioned earlier this causes the mouldings to leave the tool without adequate cooling time and the moulds distort as they cool in the omni-crates. Malpractices such as these can go unchecked for long periods without suitable quality control.

The machine temperature and cycle time setting switches were situated in a metal box at the side of the machine, this box should be kept locked at all times but instances of broken locks and box lids were seen.

7.5.2 Machining shop

The machining shop area produces armature shafts for the MC14 and EURO motors. The accuracy of the shaft dimensions is important both in terms of motor assembly and the resultant RFI levels produced by the motor. The armature sub-assembly being semi-automatic relies principly on the accuracy of shoulders and steps along the shaft length for correct positioning of the commutator and laminations. For example, inaccurate positioning of the commutator can cause the brushes to locate on either an unmachined part of the commutator or partially off the commutator surface. In Section 6.4.14, it was discussed that undersize bearing journal diameters cause armature vibrations producing high RFI levels and also reduce motor life. In addition to this, locating journals for the commutator and armature laminations are equally as important; undersize journals can cause loose laminations and oversize journals can lead to stress fractures in the body of the commutator.

7.5.2.1 Methods of manufacture

The armature shafts are made from lengths of round mild steel bar which undergo the following operations;

i) Rough turning

The stock bar is turned in an automatic feed type multispindle turning machine. The bars are loaded by the operator into a barrel at the rear of the machine, the machine automatically pulls the bar into the cutting area where cutting tools descend onto the bar, cut to the rough turning dimensions before the shaft is parted off from the rest of the material falling into a basket below. The machine is then ready to pull the remaining bar to cut the next shaft. All cutting tools are set by a machine setter and the cutting process involves minimal operator intervention.

ii) Grinding and knurling

The rough turned shafts are loaded by an operator into a 'cascade magazine' which feeds one shaft at a time onto centreless grinding wheels to complete a first grinding operation. Dwell angle and time of the grinding wheels is set by a machine setter. As the dwell cycle is completed, the operator removes the shaft from the grinding wheels. From here, shafts are loaded into a hydraulic lettering press to form grooves and knurls on the shaft where necessary and then returned to the grinding machines to grind the shaft bearing journals to their finished dimensions. Finally, the shafts are individually staked in a staking press to form notches in the shaft body to locate the armature laminations.

As with all machines used for shaft manufacture the grinding and knurling tools are set by a machine tool setter.

7.5.2.2 Production monitoring

At each machining stage, the operators are supplied with electronic go, no-go type gauges to check all key journal diameters on the shaft. The requirement is for the operator to do a one in ten item check on shafts produced. Quality inspectors carry out random checks on the shop floor and also a final audit inspection on finished batches.

7.5.2.3 Objective problems

It was reported that shafts were arriving in the assembly area with both undersize and oversize journal diameters and also with incorrect journal lengths causing problems in particular in the semi-automatic armature assembly area. Observation of working practices in the machining area, showed that operators could be running two to three machines at a time, thus inadequate monitoring checks were being carried out. The major problems however, were due to poor machine tool settings. Tool settings were being done using 'make shift' length gauges which were found to be out by as much as 0.5 mm. It was discovered that correct gauges had been supplied to the setters but these were allegedly lost.

The electronic go, no-go gauges used to check the finished shaft diameters were demonstrated to be wholly unsuitable for mass production monitoring. The gauges were easily knocked out of true by rough or continuous handling and were considered unreliable by operators and setters alike. Thus some operators did not bother to use the gauges and others would occassionally accept shafts which had been indicated as faulty, assuming that the gauge was at fault instead. The following two specific problems were observed in the grinding operation area;

(a) inadequate or poor facilities

Electronic go, no-go gauges were provided to monitor shaft journal diameters - their use and reliability has been discussed above. These gauges were designed to check diameters at one point on the journal, thus problems such as journal lobing or tapering could not be discovered. Journal tapering could explain how poor shafts are allowed to be accepted by the gauges. Although the shaft may be correct at the monitoring point its size is incorrect at any appreciable distance away from that point. This is of particular concern for diameters locating the commutator and laminations, e.g. at one end of the shaft the laminations may fit correctly, but, at the other extreme end, they could be loose causing subsequent assembly problems. Journal lobing is more difficult to monitor; at all points the shaft diameter may be correct but the overall journal contour of a lobed shaft is not round as shown in Figure 7.7.

It was observed that lobing of bearing journals gave rise to proud commutator segments monitored in the armature assembly area. The commutators are machined by supporting the armature in V-blocks at the bearing journals, thus the resultant commutator profile is governed by the profile of the journals. Figure 7.8, shows examples of commutator profiles resulting from lobed bearing journals. Proud commutator segments have been shown to have considerable influence on RFI levels and need to be minimised to the specified manufacturing tolerance.

Lobing and tapering of shaft journals are both functions of poor tool settings. Dall [147] describes how lobing can be effectively reduced in centreless grinding by correct setting of the grinding wheel dwell angle. Gauges for checking both parameters should be made available to the operators such that faulty shafts may be detected at the earliest opportunity.

(b) Operator malpractice

The grinding operation is slow and open to operator abuse to increase production rates, it has been noted that certain operators decrease the grinding wheel dwell time, this does not only lead to oversize shafts but also increases the incidence of lobing. The action of centreless grinding is such that the work piece will only be truly round when the complete dwell cycle is performed.

7.5.3 Press Shop Area

The field lamination stacks and armature laminations are manufactured in the press shop area. Loose laminations on the field and armature were shown to increase RFI levels in the low frequency region below around 1 MHz (see section 6.3), thus it is important to ensure the quality control of lamination dimensions and their fixing procedures.

7.5.3.1 Method of manufacture

Strips of sheet steel material are introduced by an operator to a press which pierces and blanks out the armature and field laminations in one operation. The presses have a carbide cutting tool and is able to produce around 400 laminations/minute. The stampings fall into chutes, one collecting armature lamination and the other, the field lamination, The armature laminations are stored for use in the armature sub-assembly area. The field laminations are transferred to the field-stack assembly area. Here the MC14 laminations are placed in a riveting fixture and stacks of approximately 40 laminations are riveted together, these are then drilled and tapped with fixing holes and placed in omni-crates for later use. EURO field laminations were welded together in a welding fixture and the finished stacks were again stacked in omni-crates.

7.5.3.2 Production monitoring

The lamination presses being virtually fully automatic required no operator check. Quality inspectors were provided with plug-gauges to check the bore of the field laminations at regular intervals.

The finished field stacks were again checked with plug gauges to ensure no laminations fitted proud in the stack, here the operators were expected to carry out a one in ten gauge check on the stacks produced.

7.5.3.3 Objective problems

No specific manufacturing problems were found in the press shop area, the presses were new and produced laminations free from edge burrs and of consistent good quality. In the field stack assembly area, there were instances of loose field laminations caused by poor riveting and welding, however, these were few and the stacks were usually rejected by the operators.

7.5.4 Armature Manufacture

The armatures were manufactured using a semi-automatic production line, here the armature shafts manufactured in the machining area are fitted with armature laminations, commutators and the armature windings to produce a complete armature assembly. The main intention for studying this production line was to find the source of problems which had been observed to influence RFI levels e.g. commutator profile, commutator finish and armature out-of-balance. A number of operational problems associated with the automation equipment were observed, e.g. in the areas of epoxy coating of armature laminations, varnishing of windings, staking of windings - but these were not recorded; (a) because it was recognised that this was a new process to the factory and both production engineers and operators needed a longer period to become familiar with its operation, (b) although problems such as varnish in the commutator slots had been found to be causing high RFI levels, these problems could not be quantified within 'manufacturing tolerances'.

7.5.4.1 Method of manufacture

The operations of the mechanised manufacturing process are listed below, after the first operation the armatures are automatically conveyed to and from the various machines;

(1) An operator locates an armature shaft and armature laminations on an assembly tool, a press is activated to force the laminations on to the shaft to complete the armature line assembly. The core is removed from the assembly tool and placed on an automatic conveyor.

(2) The armature core is degreased.

(3) The armature core is epoxy coated - this is an automatic cycle comprising of induction pre-heating of the core, spray coating and post curing.

(4) A commutator is pressed into position on the shaft.

(5) The armature is wound and the connections to the commutator hot staked.

(6) The armature is automatically checked for cross connections, turns count, wire insulation, earths, open circuit and high resistance.

(7) Varnish is drip fed onto the windings and cured.

(8) The commutator is rough turned with the armature supported in V-blocks at the bearing journals.

(9) The armature is balanced by a polar milling operation.

(10) The commutator is machined to its final diameter.

(11) Electrical checks on windings are repeated (as operation 6).

(12) An operator removes the armature from the conveyor and places it in a transport tray.

7.5.4.2 Production monitoring

During the period of the case study, due to continuous process operational problems, armatures were being removed from the automatic line for visual checking after almost every operation. But it was proposed that once the operational problems are cleared, there would only be a final visual check on the completed armature as the operator places it in the transport tray. Quality control, however, would be required to do ramdom checks on armature out-of-balance, commutator profile and commutator finish.

7.5.4.3 Objective problems

The majority of process problems were caused by poor quality armature shafts. The automatic equipment relied on good quality shafts particularly in relation to dimensions of shoulders and steps along the shaft which were used to position the armature components as discussed in section 7.5.2. As discussed earlier, tapering of shaft diameters led to instances of loose armature laminations and lobing of bearing journals had been observed to cause proud commutator segments after the commutator had been machined. Further problems of the armature assembly found to have been caused within the automatic process line are detailed below.

(a) Inadequate or poor facilities

i) maintenance; although the process line was relatively new, there were already signs of lack of maintenance appearing in particular with the tool for commutator machining. For the cutting operation the armature was supported in V-blocks at the bearing journals and rotated by means of a belt drive on the surface of the armature laminations. The belt was seen to be badly frayed and on occassion 'catching' on the armature laminations causing the armature to jump during the machining operation.

Periodic jumping or movement of the armature could lead to excessively proud commutator segments. The V-blocks were found to be worn and damaged with dirt collected at the bottom of the V, this again would aggravate the turning operation, causing commutator eccentricity. Finally, automatic brushes which clear swarf from the commutator area after the cutting operation were so badly worn that they were almost useless in operation. It is clear that regular maintenance of tooling is essential for manufacturing tolerances in this area to be achieved.

ii) tooling; finished commutators were observed to have burrs on the edges of the segments, the cause of this is discussed below. Burrs can cause excessive brush arcing, damaging both the brush and commutator surface and thus need to be removed in the interest of motor life and the reduction of RFI from the motor. Removal of burrs could easily be achieved by the use of a broaching tool to clear out the intersegment slot area. Discussion with production engineers revealed that such a broach had been used at the Perivale factory but, in the subsequent transfer to Cambuslang this tooling had been lost.

(b) Inadequate or poor design and process specifications

i) armature out-of-balance; in section 7.2, it was shown that the armature out-of-balance achieved by production, was outside the specified manufacturing tolerances. Examination of balancing tolerances used in manufacture found them to be acceptable but the cause for excessive out-of-balance can be identified from the process sequence. The armatures are balanced after the first rough machining operation on the commutator, but after balancing, the commutators were again machined to their final dimensions.

It had no doubt been thought that the finishing cut on the commutator would be light and thus have minimal affect on armature balance. But in the event, it was observed that this finishing cut was causing the armature out-of-balance to increase such that in some cases the specified manufacturing tolerances were exceeded. Closer examination of the commutator machining showed that the final cut was almost as deep as the initial rough cut. However, this problem could be alleviated by balancing the armature after the final machining operation on the commutator.

ii) Proud commutator segments; proud commutator segments are caused due to lobing of the bearing journal affecting the profile of the commutator during rotation. This affect could be minimised if instead of rotating the armature in V-blocks, the bearing journals were supported in half-moon type U-blocks. This would not require any large scale change in to implement, but the main requirement would be to ensure that the U-block did not collect dirt or swarf by a regular tool cleaning operation.

iii) Commutator positioning; the angular position of the commutator relative to the armature windings affects the eventual brush shift of the motor. In section 7.2, it was stated that no drawing tolerance on angular brush shift was specified and that production had been using a nominal tolerance of around 3^o. From the RFI results, it was shown that the position for minimum RFI levels only had a tolerance of around 2^{o}, beyond this RFI levels would increase. Thus it was recommended that this figure be implemented in the process specifications.

(c) Non adherance to specified procedure

The finish on the commutator surface has been shown to influence RFI levels from the motor, the specified manufacturing tolerance of 0.8×10^{-6}m CLA surface finish was found to be acceptable with reference to the experimental results. However, the surface finish obtained on the shop floor was found to be poor, with finishes in excess of 1.5×10^{-6}m CLA common place, of even greater concern was that burrs were evident on the edge commutator segments. Poor facilities resulted from incorrect setting of the commutator cutting tool, i.e. the speed and depth of the tool was incorrect. It was observed that the machine setter was setting the tool by eye, although gauging facilities were available. There was no observable difference in the settings used for the rough cut and finishing cut operations on the commutator. The finish cut should have been made using a diamond tipped tool, whereas it was found that an ordinary carbide tool was being used. The carbide tools cannot produce the quality finish required on the commutator surface.

Quality inspectors although aware that armatures with excessive out-of-balance, proud commutator segments and poor commutator surface, were being produced, allowed the situation to persist by not rejecting the armatures.

Recognition of these faults would no doubt have caused the majority of armatures to be rejected which would have caused a major bottle neck in motor production. Thus the need to maintain production quotas meant that in many causes quality control became a secondary consideration.

7.5.5 Wound field assembly

As with the armature assembly, the wound field assembly was also manufactured on a semi-automatic process line. Here field lamination stacks were fitted with plastic insulating bobbins by operators and then located on an automatic conveyor to be wound, terminated and electrically tested. No specific operational problems were observed in this area.

7.5.6 Brush box and spring production

Clearance between the brush the brush box and also the spring load have been shown to influence RFI levels. The production variation of both of these parameters had been found to be in excess of the specified manufacturing tolerances and thus a source of variability in the RFI levels observed from motors.

7.5.6.1 Method of manufacture

Reels of preformed brush boxes were brought in from outside suppliers. The reels are loaded by an operator onto a cutting machine to separate the individual brush boxes. These are then loaded into another fixture to crimp connect a wire onto the body of the brush as shown in Plate A6.7. The brush boxes are then ready for transfer to the final assembly area. The brush springs are coiled on a hand operated former from a reel of wire. The springs are automatically cut to length on the former and again then transferred to the final assembly area.

7.5.6.2 Production monitoring

Production monitoring of both these operations is minimal, with operators looking for visual defects only. No checking on brush box dimensions is done since they should have already been monitored by the 'goods inwards' inspection area responsible for checking bought in items. Quality inspectors carry out random checks on brush spring load and the crimped connection on the brush box body.

7.5.6.3 Objective Problems

The bought in brush boxes being of a closed construction, were found to be of acceptable quality, but the EURO brush boxes which have an open cross section, were found to be arriving distorted as indicated in Figure 7.9(a). Thus the eventual brush box/brush clearance in the final motor assembly would be affected. Observation of brush boxes after the crimping operation showed that the boxes were 'bowed' along their length (see Figure 7.9(b)), this had been known to restrict brush movement causing 'brush sticking', causing arcing during motor operation leading to increased RFI levels. Further brush box distortions were found to occur due to general operator handling. All these problems appear to be due to an inadequate thickness specification of the boxes. Materials should be such that the components not only perform adequately in the motor, but also be able to withstand manufacturing and assembly techniques. The brush boxes clearly do not satisfy this latter requirement and thus a thicker brass material needs to be used. At present a 0.41 mm thickness is used, it is felt that this needs to be increased to a least 0.8mm in order for the higher tolerances recommended in section 6.4.9, can be implemented. Additional operational problems appear to be due to bad tool setting of the brush box cutting fixture and the spring coil winding machine.

Bad tool setting on the cutting fixture leaves a burr on the lip of the front end of the brush box (see Figure 7.9(c)), this burr has been observed to interfere with brush movement causing sparking. On the spring former tool, it was observed that poor settings result in variable lengths of brush springs being manufactured such that at the normal compressed spring length in the brush boxes, the spring load can fall outside the specified manufacturing tolerances. In section 7.2, it was discussed that the specified manufacturing tolerance for spring load was approximately 10g lower than that necessary for the reduction of RFI from the motor. Inspection of the method of spring manufacture showed that there would be no implementation problems for manufacturing longer spring coils to produce the higher spring load, but, spring quality needs to be assured in order that RFI variability is minimised.

7.5.7 Final Assembly and Electrical Test Area

Motor components manufactured in the areas described above, are transported to the final assembly area along with various bought in items including bearings, suppression components and fixing screws.

The assembly is completed on an operator flow line and the finished motors are loaded on to a 'Run-in-Rack'. Here the motors are connected to a power supply terminal and allowed to run for approximately 40 minutes in order to bed the brushes.

The Run-in-Rack is fitted to an automatic conveyor which transports the energised motors to the electrical test area. The motors are then individually checked for electrical performance (i.e. input watts at rated supply voltage) and the quality of commutation is observed.

The various assembly problems arising due to faults on individual components have been discussed in the earlier sections. The final motor assembly operations themselves are relatively problem free, the main area for concern was the final assembly of the brush boxes and this is discussed below. Examination of the Run-in-Rack showed that poor electrical connections on the conveyor resulted in almost 20% of the motors either failing to run or running intermittently. This was found to result from inadequate maintenance of the power supply terminals some of which were loose or broken. Motors with manufacturing problems resulting in poor performance were rejected in the test area. However, very few motors were rejected for poor quality of commutation, it was observed that only motors exhibiting severe arcing at the brushes were rejected. The failure of this subjective testing on commutation was recognised by production engineers and during the course of the study, efforts were being made to install an electronic light detecting device to determine the quality of sparking.

7.5.7.1 Objective problems

Poor design of the EURO motor brush box assembly and fitting resulted in a number of problems that can influence the generation of high RFI levels from the motor. The brush box assembly locates in a square hole in the moulded plastic motor casing. The design was such that the brush box is located in the hole and restrained only by an interference fit of the brush box within the hole. This is wholly inadequate since the rigidity of the brush box is essential to minimise brush vibrations and variability of RFI levels. The inadequacy of this method of assembly are compounded by component problems already discussed i.e. (a) distortion of the brush boxes by operator handling and the crimping operation described in section 7.5.6.4, (b) lack of gauging facilities in the moulding shop to regularly check the dimensions of the brush box hole produced and distortions of casing mouldings as described in section 7.5.1.3. Further evidence of brush box distortion due to operator handling in the final assembly area were observed; a number of operators physically squeezed the brush boxes in order to insert them into the hole, this not only led to loose brush boxes, but also sticking brushes inside the boxes. With the existing design on the EURO motor assembly, there seemed no obvious way to overcome this problem, however, by using a thicker brass brush box fabrication (as recommended in section 7.5.6.3 to overcome brush distortion) it is possible that the boxes could be screw clamped in the moulded hole as shown in Figure 7.10.

7.6 Subjective Manufacturing Problems

The concept of operators being responsible for ensuring the quality of their own manufacturing operation shows a progressive management attitude by not treating manufacture and quality control as two separate functions. However, it is necessary to ensure that factory conditions and facilities would allow such a manufacturing concept to be effective in maintaining good quality control. Preliminary observations of mechanical variations achieved on the shop floor, indicated that adequate quality control was not being achieved. In the previous section manufacturing problems causing these variations observed on the shop floor, were described - this section takes a more global look at the manufacturing environment to determine the suitability of the present quality control procedures. The areas examined were production monitoring and fault prevention.

(a) Production monitoring

The operators are paid on a 'piece-work' system and are paid the same rate whether the components they produce are good or defective. If the operator reports a problem in his manufacturing operation, it is likely that his work will be stopped until repair work is carried out and tool settings are rechecked.

During this time, the operator is paid a 'down-time' rate which probably lower than the rate he would have achieved had he continued working producing defective components. Thus it is clear that high-lighting a manufacturing problem is against the operators own interests. It was observed that many operators make their own value judgment as to how serious a particular defect is and whether attention to it should be brought or not. To guard against cases of operators by-passing the system, quality engineers/inspectors are supposed to carry out random quality checks on the shop floor. However, during the course of the case study it was noted that much of the quality engineers day was taken up with specific day to day production problems such that the random checking function was not always carried out. It is likely that this has come about due to a combination of increased job loading with the reorganisation of motor production and reduction in manpower resulting from the 'slimming down' of work force in 1982. The result of this, is that operator malpractices go undetected and enevitably increase once the operators realise how vulnerable the system is.

The local foremen who are charged with the responsibility for ensuring their production area achieves the production quotas are also known to make value judgements on the usability of faulty components - undermining the quality control concept.

Numerous instances were reported and observed of where batches of rejected components had found their way back into the production area. This practice was particularly prevailent during the night shift where only token quality control staff are employed.

Poor quality is often detected at the final audit stage on production batches before they are moved on to the next production area. Few quality inspectors meant that audit inspections had become less frequent allowing production batches to mount up. By this time, the numbers of faulty components became so large such that rejection of batches would cause a bottle neck in production. Inevitable pressure from the production department usually resulted in the faulty components being used, unless evidence of nonusability could be provided. In these discussions, less tangible quantities such as commutation and RFI levels became secondary considerations.

(b) Fault prevention

Prevention of component faults can only be affected by accurate tool settings and regular machine maintenance to ensure that settings have not been erroded. Many of the objective problems identified in section 7.5 were found to be caused by poor tool settings.

This raises the questions as to the ability of the staff appointed as machine setters. The position of machine setter is obtained by promotion from the shop floor and is always offered to members of staff with the longest company service. This criteria seems wholly unsuitable as the aptitude of the personnel to undertake such a responsible manufacturing function is not considered. Thus it has transpired that the majority of machine setters lack the skills necessary to use tool setting equipment, gauges and to read production drawings - and have little appreciation of manufacturing tolerances and their significance to motor production. Legitimate cases of where staff having been employed to carry out labouring work on the shop floor, had found themselves in line for promotion to be a machine setter on equipment such as the programmable multispindle turning machine were reported. No training courses are available for the newly promoted machine setting staff. The major criticism of both the machine setting and maintenance functions is their ad-hoc usage in the manufacturing system. Machine setters are only summoned by the foremen or quality inspectors when a tooling problem has been identified. Similarly, maintenance staff are only called when a machine is found to be faulty or needing repair. Thus the system relies on the existance of poor quality before any action is taken. Machine setters did not carry out any preventative checking in order to find potential trouble spots, no regular refurbishing of cutting tools and no records as to where and when tool settings or tool changes had been carried out.

Records of tool changes could help predict how often a tool needs to be changed in order to prevent problems before they occur. Records of tool settings could help determine the maximum allowable interval between tool setting checks on different machines.

Similar criticisms can be made of the maintenance procedures; no planned maintenance refurbishing or preventation maintenance checks were carried out. And again the lack of maintenance records results in any machine 'history' being known. The present attitude of 'no need to change anything if everything is working well', is too short sighted and again relies on machine breakdowns before any action is taken.

From the subjective manufacturing problems described above, it can be summarised that in order for the quality control techniques employed at the Cambuslang factory to be successful, the following changes need to be employed:

(a) increase frequency of random quality checks on production by quality inspectors in order that they can be used as a deterent to 'cheating' by operators (this would probably mean increasing the number of quality control staff)

(b) ensure all machine tool setters have suitable skills and motivation

(c) introduce a training course/programme for all new machine setters

(d) introduce preventative tool setting checks

(e) maintain records of where, when and why tool settings are changed

(f) determine tool wear data in order that tools may be changed/refurbished on a regular basis - before failures occur

(g) introduce preventative machine maintenance checks

(h) maintain maintenance records of individual machines.

7.7 Reduction of variability in RFI levels

EURO motors were fitted with RFI suppression networks comprising of a parallel 0.1μF capacitor and two in line series 6μH inductors. The capacitors adequately suppressed the motor in the low frequency region but the inductors were found necessary in order to suppress RFI levels in the high frequency region. Figure 7.11, shows RFI levels measured from a EURO motor constructed to the allowable tolerances determined on the test rig. It can be seen that even without any suppression fitted, RFI levels from the motor above 1MHz lie satisfactorily below the CISPR/EEC limits even in the high frequency region.

Fitting the 0.1μF capacitor alone reduces RFI levels to below the limits throughout the spectrum. Finally, the addition of the inductors results in RFI levels being further reduced by approximately 5 - 10 dB in the high frequency region. These results suggest that by ensuring that the recommended manufacturing tolerances are adhered to, the EURO motor could be adequately suppressed using only the 0.1μF capacitor. This would represent a cost saving both of the inductors and their extra fitting costs totalling between 16p to 20p per motor. However, the major problem with EURO motor assembly as discussed in section 7.5.7.1, is the brush box fitting, this would have to be improved so that loose brush boxes did not influence high RFI levels. Figure 7.12, shows the maximum and minimum RFI levels recorded from twenty EURO motors monitored to have acceptable mechanical variations and fitted with the standard suppression network. It can be seen that the spread of RFI levels of around 10 - 15 dB is almost half that shown in Figure 7.2 of EURO motor samples from the shop floor. The brush boxes of the twenty motors were subsequently glued to the motor cases in order to improve brush stability and the RFI tests repeated; the maximum and minimum levels recorded are shown in Figure 7.13. The combination of improved brush stability and acceptable manufacturing tolerances results in a spread in RFI levels of approximately 5 dB across the spectrum range. Removal of the 6μH inductors from the suppression circuit affected an increase in overall RFI levels of approximately 5 dB in the high frequency region but again the spread in RFI levels remains relatively unaffected, (see Figure 7.14).

From these results, it is clear that by careful mechanical design to improve brush stability and with manufacture controlled in order to achieve the specified mechanical variations in the motor assembly, the resultant improvement in quality of commutation leads to;

(a) lower overall RFI levels

(b) reduction in motor to motor RFI variability

(c) the design of cheaper suppression networks resulting from (a) and (b).

As discussed above, improvements such as this on the EURO motor could reduce suppression costs of between 16p to 20p per motor, representing an annual saving of around £100,000. It is likely that similar improvements on other motors produced at Cambuslang could affect a substantial saving in overall suppression costs. As a spin-off, the reduction in brush sparking can reduce brush wear and thus increase motor life.

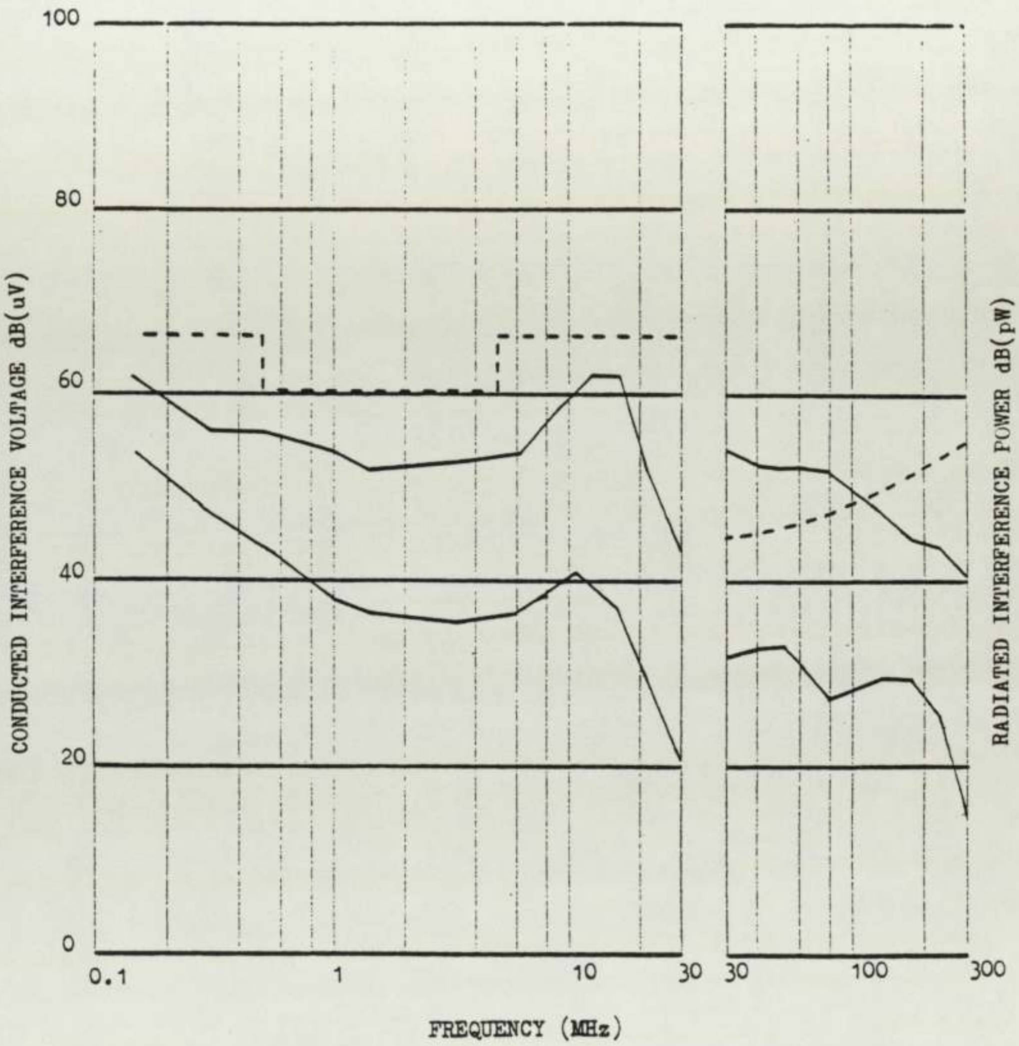

Maximum and minimum RFI levels recorded from a selection of production cleaners fitted with the MC14 motor

Fig. 7.1

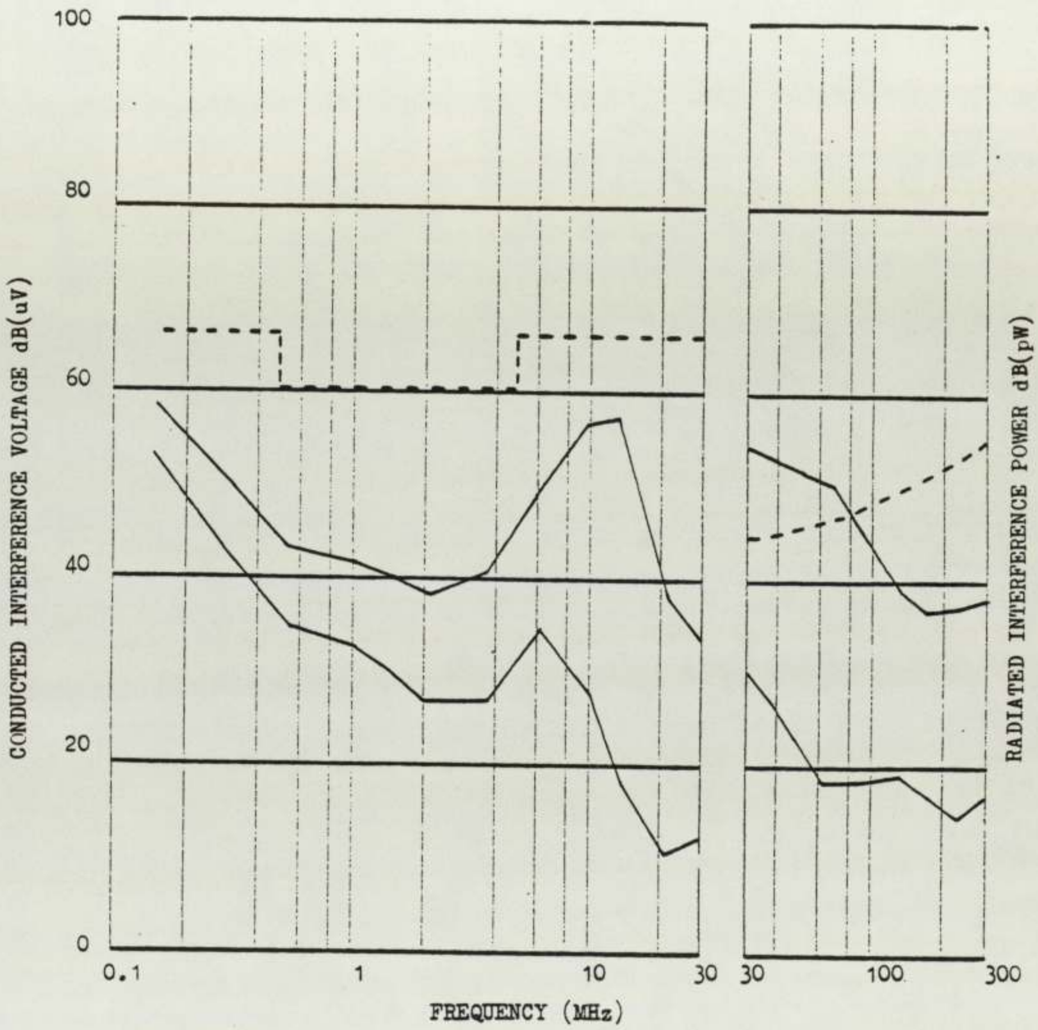

Maximum and minimum RFI levels recorded from a selection of production cleaners fitted with the EURO motor

Fig. 7.2

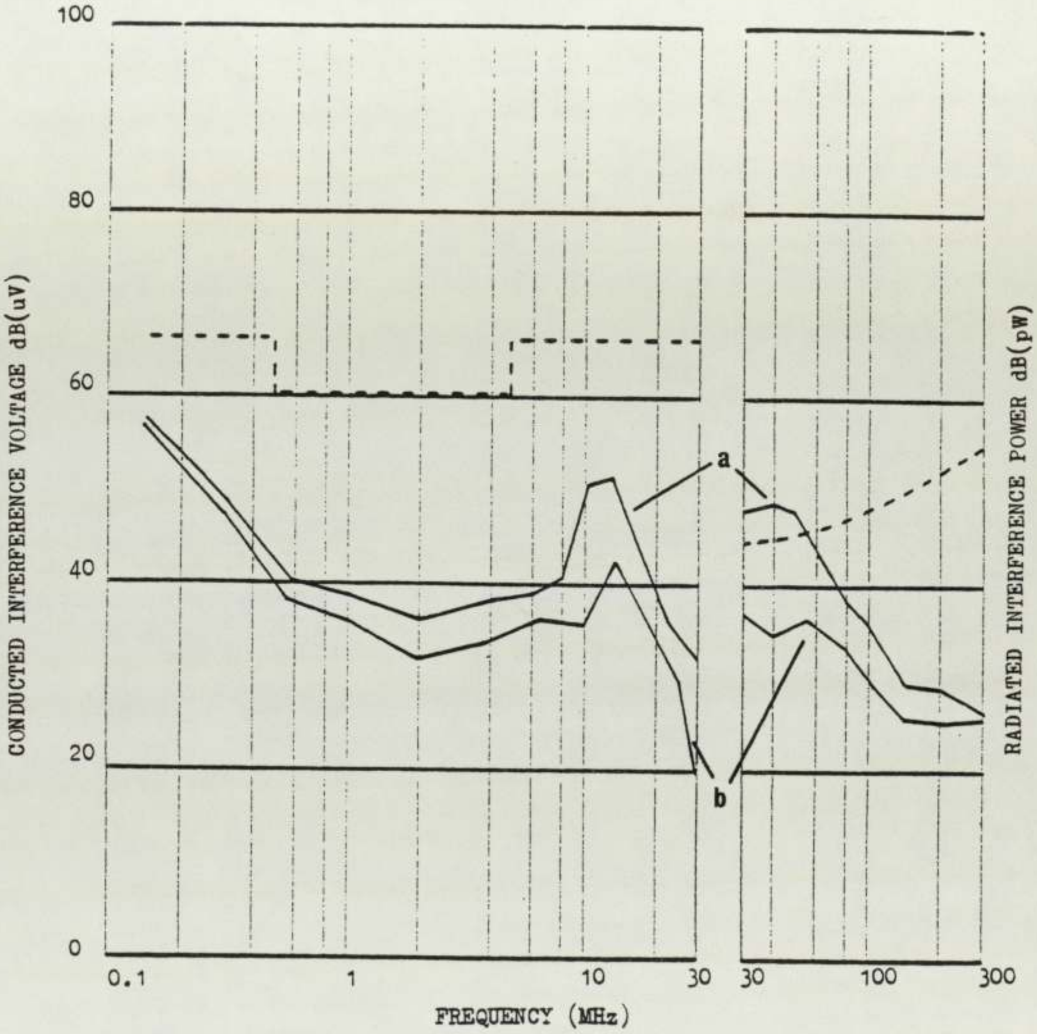

Measured RFI leves from cleaner fitted with EURO motor (a) with sticking brushes (b) after correction

Fig. 7.3

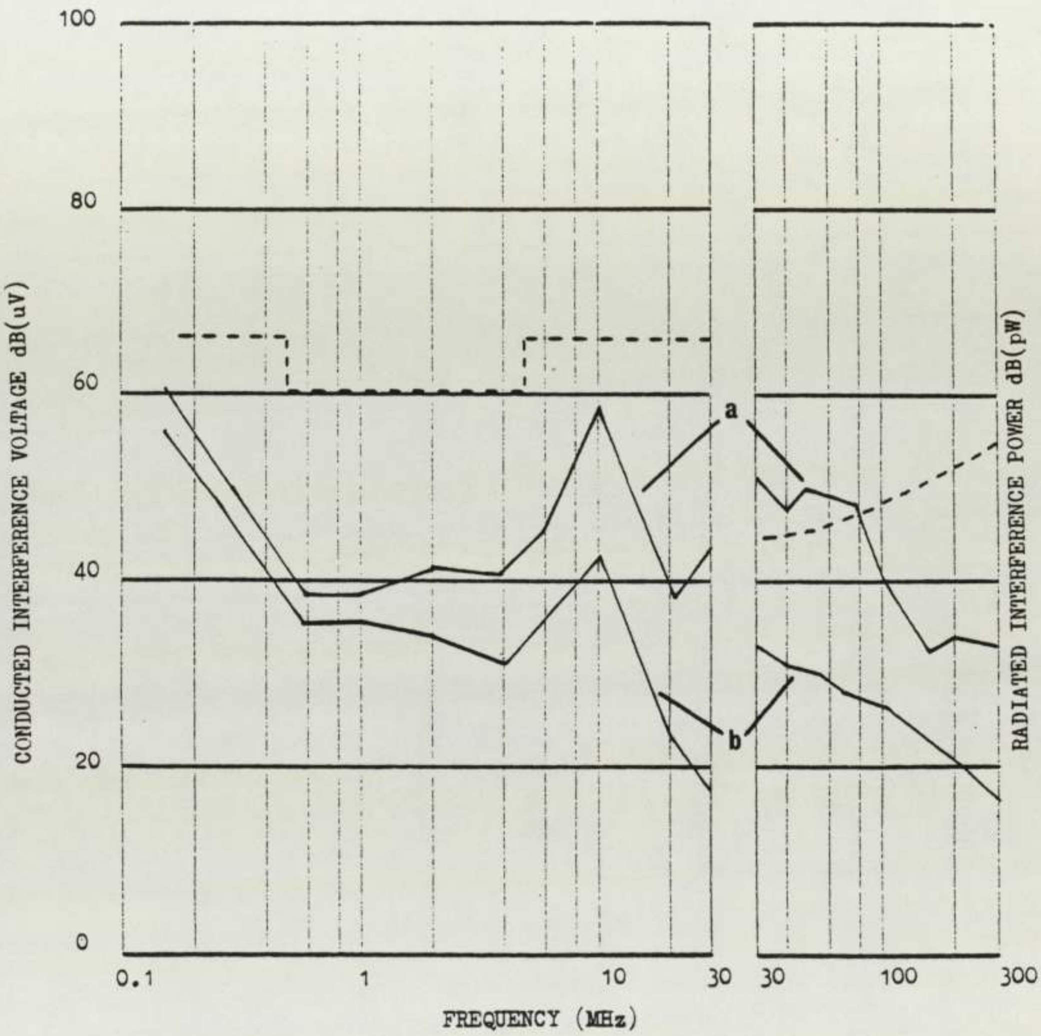

Measured RFI levels from cleaner fitted with EURO motor (a) with proud commutator (b) after correction

Fig. 7.4

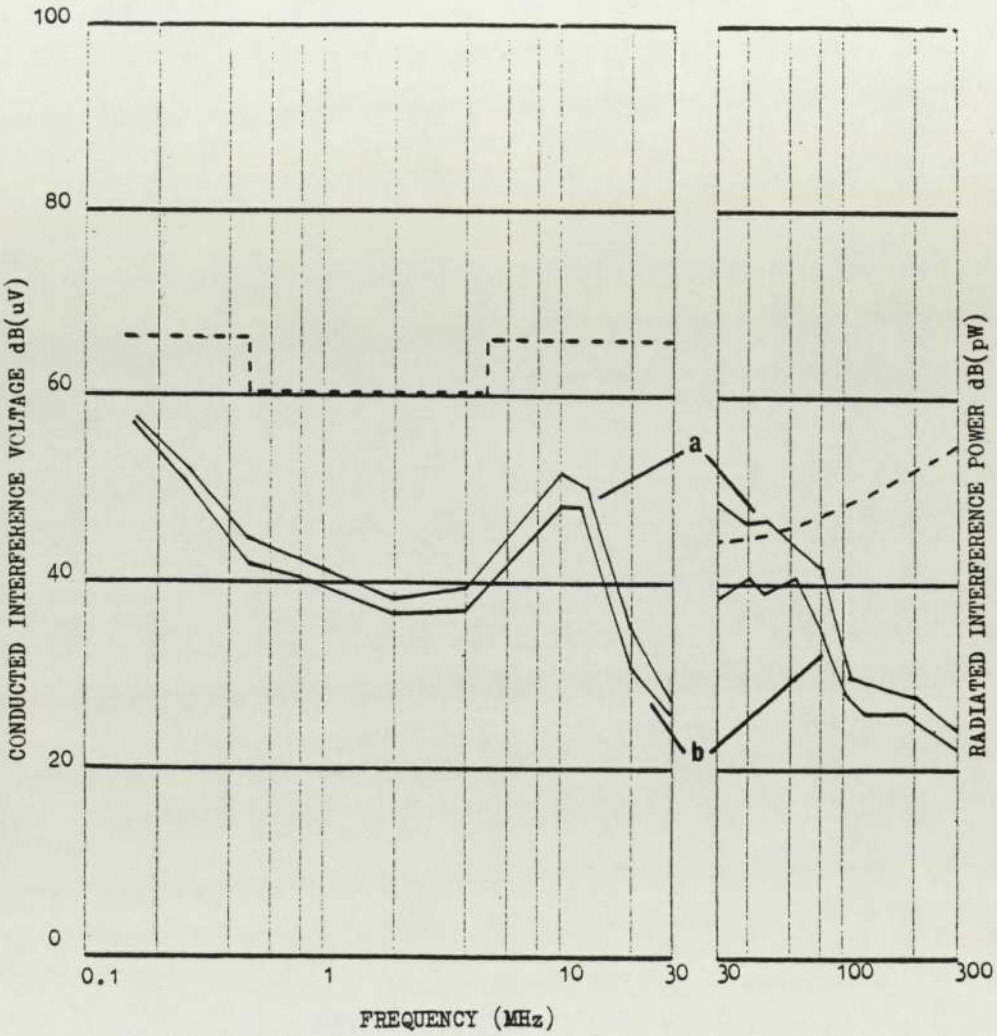

Measured RFI levels from cleaner fitted with EURO motor (a) with armature out-of-balance (b) after correction

Fig. 7.5

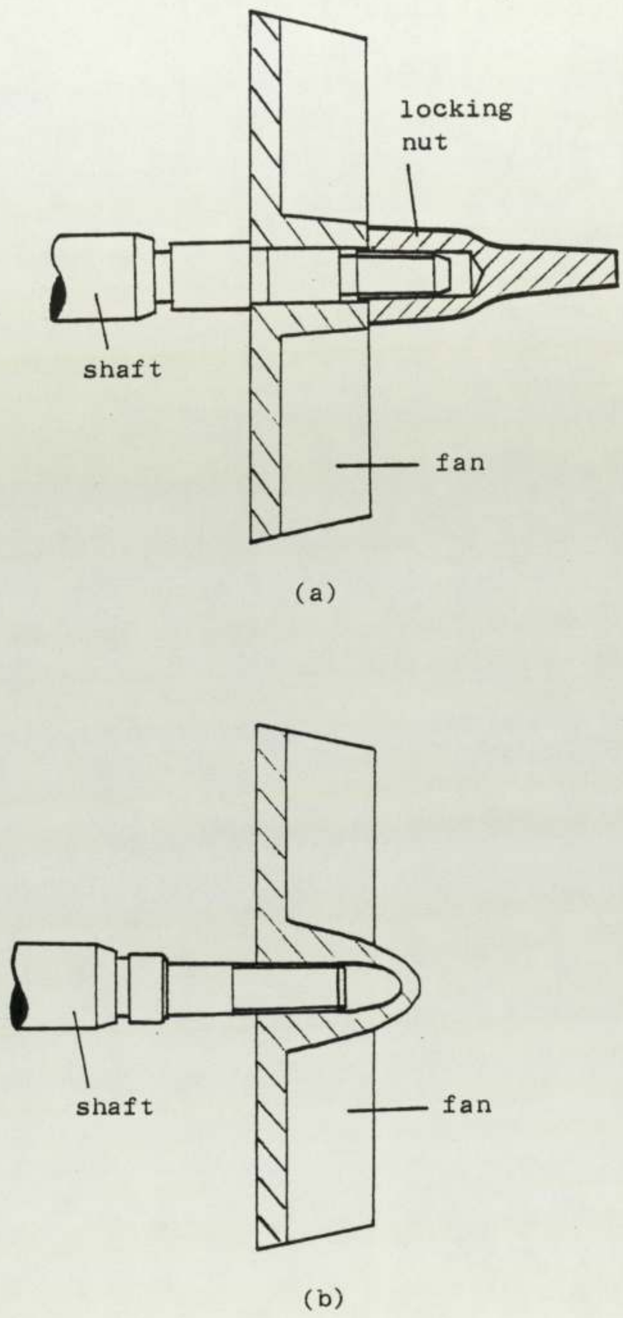

Dirt fan assembly (a) on MC14 armature shaft and (b) on EURO armature shaft

Fig. 7.6

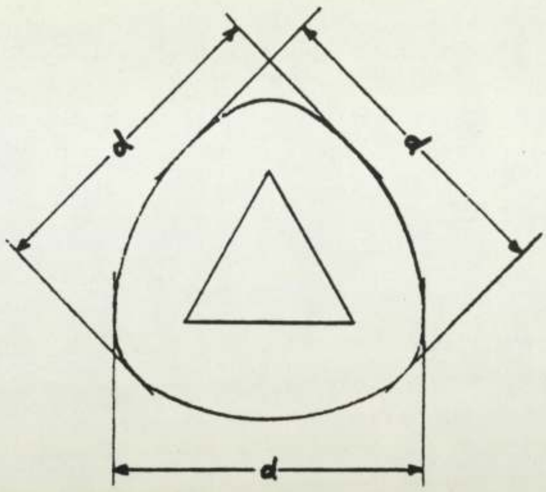

(a) theoretical three lobed journal of diameter "d"

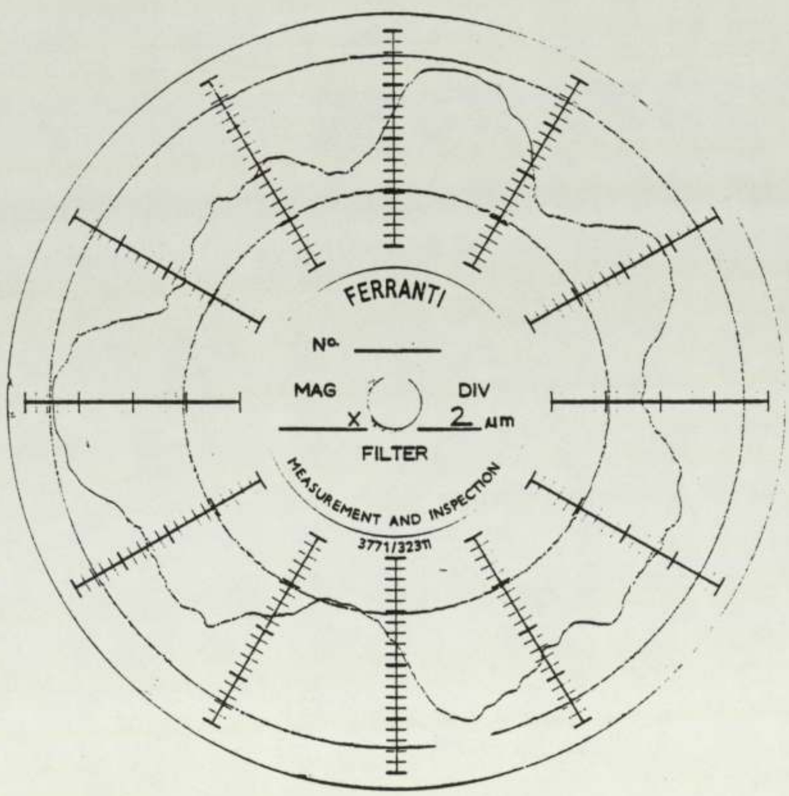

(b) contour of armature bearing journal obtained from shop floor

Lobed journal contours

Fig. 7.7

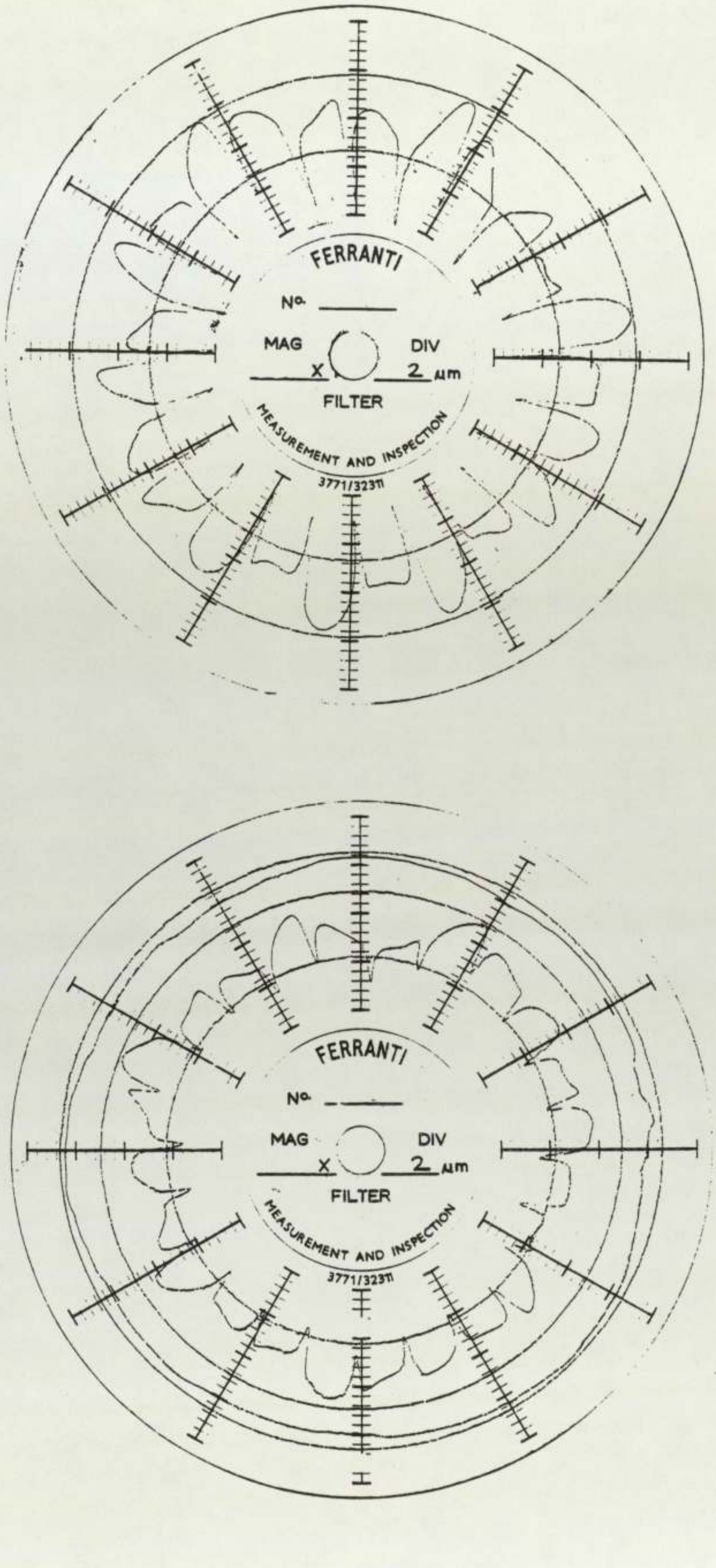

Examples of commutator profiles resulting from lobed bearing journals

Fig. 7.8

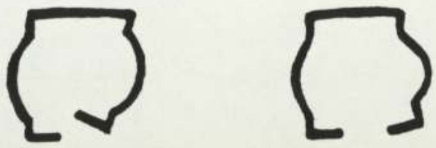

(a) distorted box cross-section

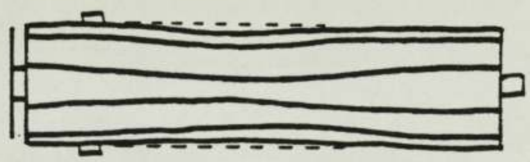

(b) bowed contriction along box length

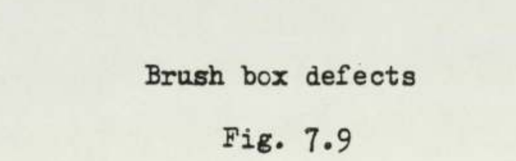

(c) burr on front end of box

Brush box defects

Fig. 7.9

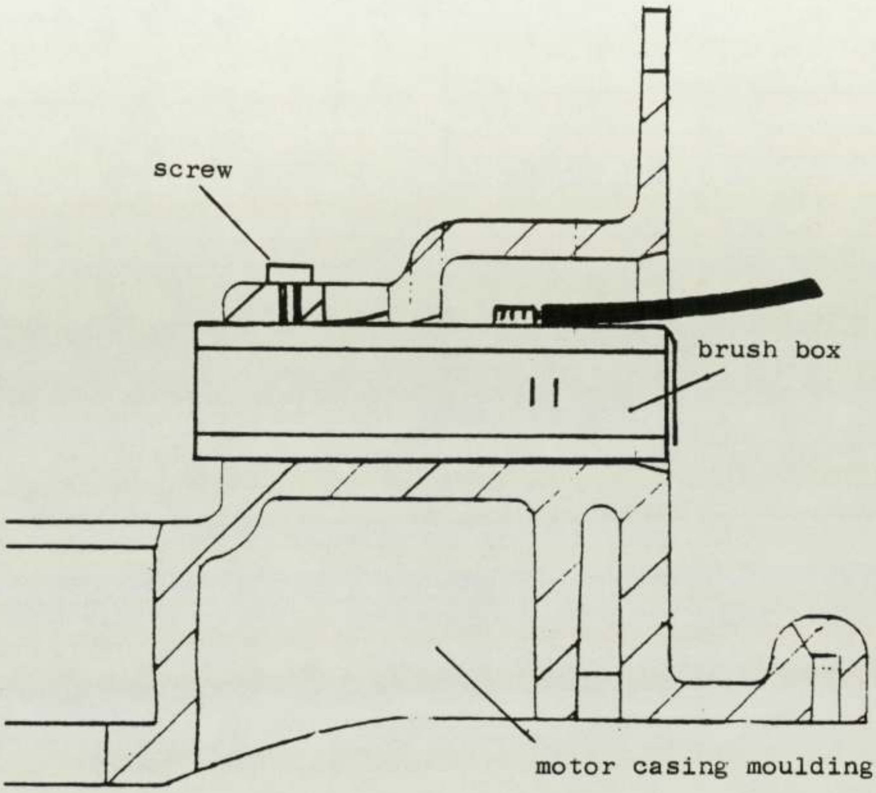

Screw clamping of brush box to motor frame to reduce vibration

Fig. 7.10

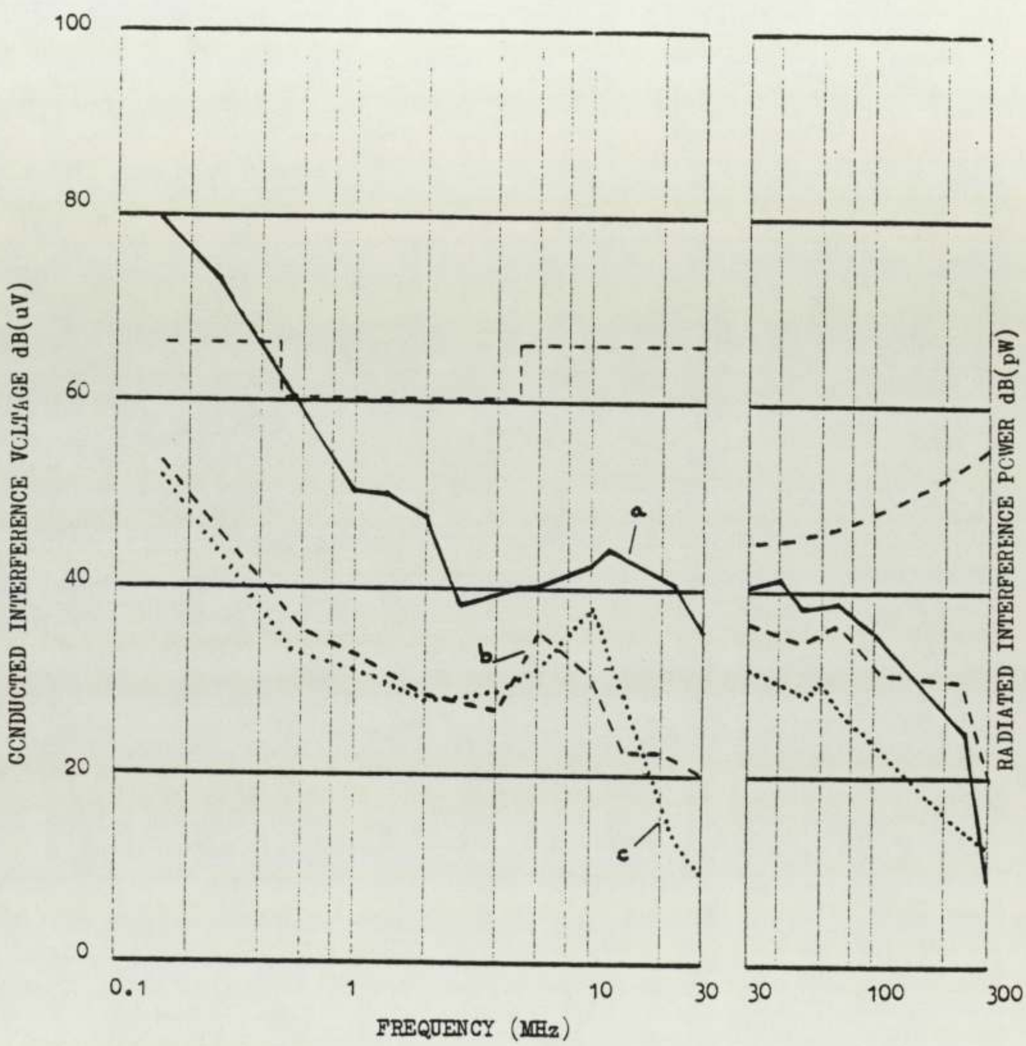

Measured RFI levels from EURO motor constructed to specified tolerances
(a) without suppression
(b) with parallel 0.1 μF capacitor
(c) with parallel 0.1 μF capacitor and two in line 6 μH inductors

Fig. 7.11

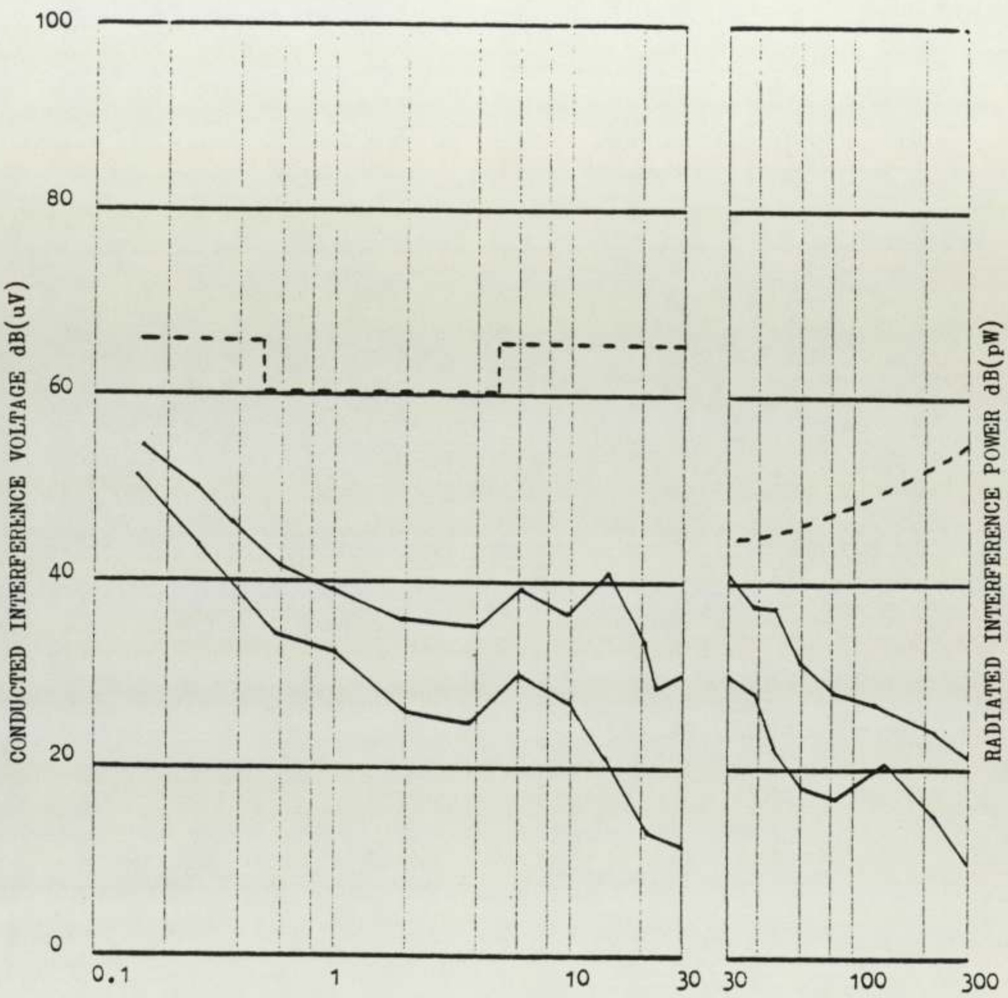

Maximum and minimum RFI levels recorded from cleaners fitted with EURO motors (suppressed) constructed to specified tolerances

Fig. 7.12

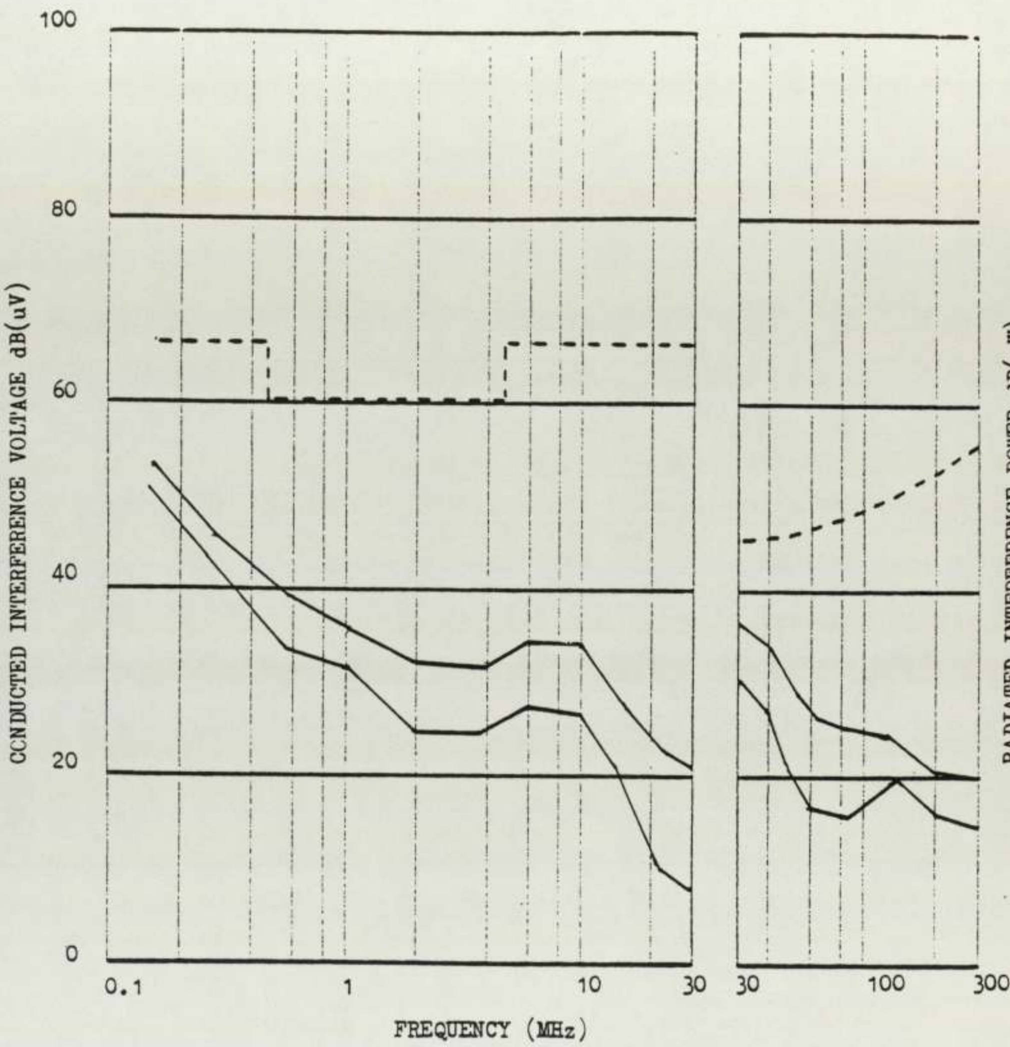

Maximum and minimum RFI levels recorded from cleaners fitted with EURO motors constructed tc specified tolerances and with brush boxes glued to motor frame

Fig. 7.13

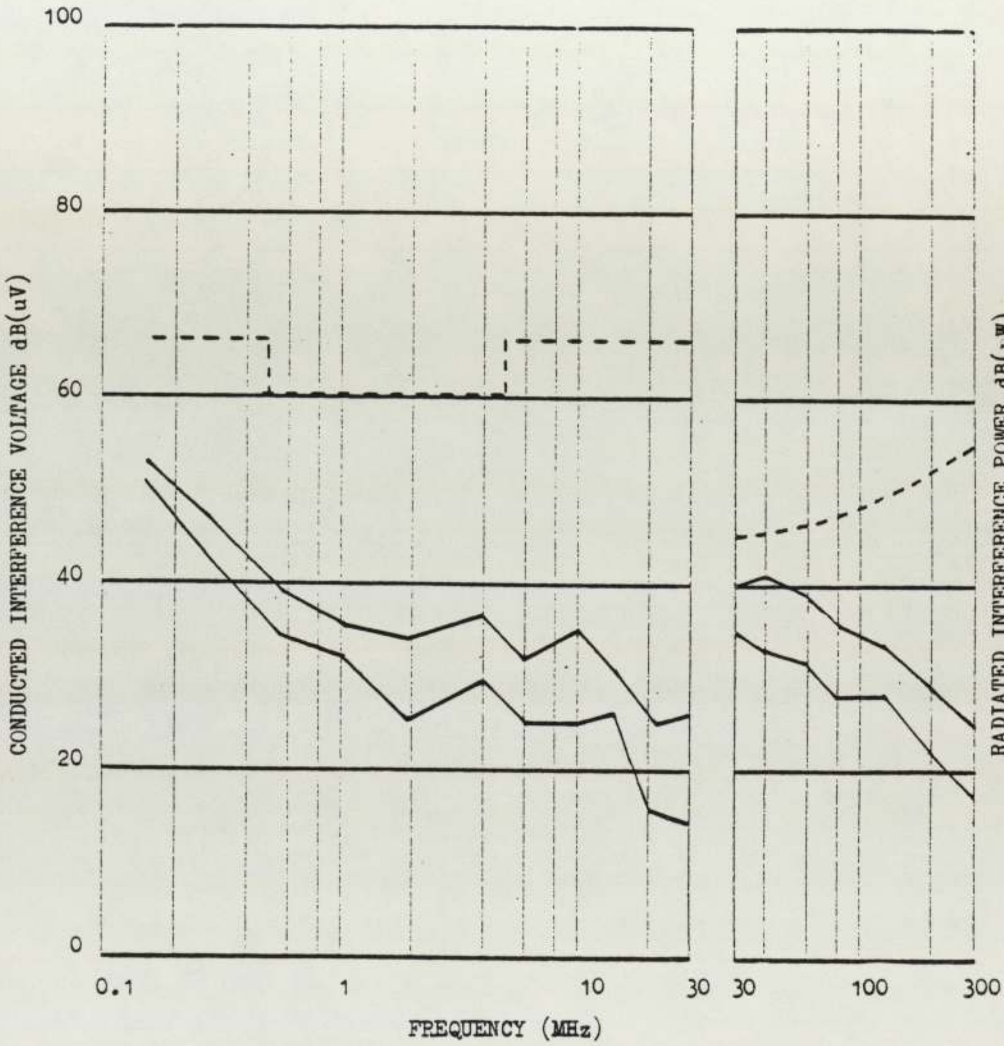

Maximum and minimum RFI levels recorded from cleaners fitted with EURO motors constructed to specified tolerances and only 0.1 μF parallel capacitor suppression

Fig. 7.14

CHAPTER 8

CONCLUSIONS AND RECOMMENDATIONS

8.1 Conclusions from experimental investigations

8.2 Conclusions from case-study

8.3 Recommendations for future work

CHAPTER 8

CONCLUSIONS AND RECOMMENDATIONS

The factors affecting the generation of RFI in the motor design parameters and the influence of mechanical variations in the motor assembly have been studied by experimental means. The experimental work was carried out on a motor test-rig, the results from the test-rig can be considered typical for small motors as used in domestic appliances. Section 8.1 summarises the main conclusions from the investigation and where possible recommendations for the reduction of RFI are suggested. In addition a case-study of the manufacture of small motors at the Hoover plc Cambuslang factory has been carried out in order to identify the causes of motor to motor variability in RFI levels from mass produced motors. The conclusions and recommendations resulting from the case-study are presented in section 8.2. Finally in section 8.3 there is a list of areas in the subject of RFI from small motors which would benefit from further work.

8.1 Conclusions from experimental investigations

The experimental investigations examined the generation and propogation of RFI from the following areas;

i) the commutator switching action.
ii) the variation of the short circuited coil parameters.
iii) the influence of the physical components of the armature and field.
iv) the influence of mechanical variations of the motor assembly.

The conclusions are as follows:-

8.1.1 RFI caused by the commutator switching action

(a) Commutation even without the influence of the short circuited coil parameters and the presence of the armature and field components can generate RFI levels which exceed the CISPR/EEC limits in the low frequency region. As the commutator is an essential component of small motors, it can be considered that these RFI components are an inherent feature of this type of motor.

(b) Surface noise generated between the rotating copper commutator and carbon brush face contributes as much as 20-30 dB RFI in the low frequency region to the overall RFI measured from commutation. Work carried out by the ERA [100] showed that the choice of correct carbon brush grade and lubricant can greatly reduce surface noise and thus reduce overall RFI levels. Nelson and Diehl [94] indicated that chromium plated commutator segments can also reduce surface noise, however this latter observation is not considered to be a practical recommendation for mass produced motors.

(c) At commutation pulse repitition frequencies of greater than around 5kHz the measured RFI levels remain relatively constant. Thus for small motors normally operating at speeds greater than 10000 r/min the measured RFI levels are independent of the number of commutator segments.

(d) Variation of brush current densities in the normal operating region of small motors has no observable influence on measured RFI levels from the commutator. However, at high current densities RFI levels are increased due to excessive heat generated at the brush face causing contact fritting and arcing resulting in increased brush wear and damage to the commutator surface. Most brush manufacturers recommend maximum current densities of approximately 12 A/cm^2 for electrographite brushes.

(e) Low levels of RFI are generated from the rotating brush-commutator contact even when there is no external current source connected. These RFI components increase with speed but are attenuated above around 1 MHz.

8.1.2 RFI caused by the variation of the short circuited coil parameters

(a) Distortion of current by resistance commutation increases overall RFI levels, however the values of coil resistance normally measured on small motors (less than 1Ω) would only cause increases of the order of 2-3dB in the low frequency region.

(b) The influence of reactance voltage (Ldi/dt) generated by the commutating current in the presence of coil inductance is to increase RFI as follows:

i) the reactance voltage delays the commutating current such that there is an abrupt change in current at the end of commutation. This distortion of the commutating current leads to increased RFI components in the low frequency region, attenuating as the frequency is increased.

ii) arcing at the end of commutation as the stored inductive energy ($1/2\ Li^2$) is dissipated generates further RFI components and these have been found to predominate in the region above 10MHz extending across the high frequency region.

The magnitude of reactance voltage is dependent both on rotational speed and the magnitude of the switching current, thus an increase in either parameter further increases the overall RFI levels. Coil inductance can be minimised by reducing the specific permeance of the coil (see equation 3.18). This can be achieved by using short pitched coils, reducing the length of end windings and optimisation of the slot profile. Further recommendations are suggested in section 8.1.3.

(c) The influence of the circulating current generated by the transformer and rotational voltages generated in the commutating coil is to periodically overcommutate and undercommutate the switching current. As above the resulting distortion of current and arcing generate RFI components which increase the overall RFI levels.

Rotational voltage can be adjusted to aid commutation and thus reduce RFI by introducing a brush shift against the direction of rotation (see section 8.1.4). Transformer voltage however can only be reduced by minimising the Turns per coil of the armature windings. The test results indicate that the maximum allowable emf in the coil undergoing commutation in small motors is around 4V.

8.1.3 RFI due to the influence of the physical components of the armature and field.

(a) Magneto-striction of the armature and field laminations causes RFI components to be generated, these components are attenuated with frequency and are not detected above around 1MHz. However at around 0.15MHz RFI levels up to 30 dB were observed and even higher in the case of loose or damaged laminations.

(b) RFI levels measured with the rotor tooth at the centre of the pole face are approximately 5 dB higher than those with the rotor slot in the same position.

(c) There is no observable influence of slot number or slot rotation on measured RFI levels.

(d) Field windings aid the suppression of RFI generated at the brushes by presenting a high impedance path to the flow of interference currents and thus reduce the overall RFI levels measured from the motor. (Field winding impedance is attributed to the reactance of the inter-turn and inter-layer self capacitances of the windings). The h.f. impedance of the windings can be increased by sectionalising the windings in order to reduce the inter-layer capacitance.

(e) Stray capacitance between the field windings and the field laminations provide a path for the interference currents to be diverted away from the motor terminals and thus reduces measured RFI levels.

(f) A symmetrical split field winding configuration is preferred, as it impedes the flow of both the asymmetrical and symmetrical interference currents such that, RFI levels above around 1 MHz are suppressed to below the CISPR/EEC limits without the aid of external suppression components.

The single coil field arrangement although reducing the symmetric interference currents only has minimal effect on asymmetric currents and as such is not as effective as the split winding arrangement.

(g) The number of armature turns per coil should be minimised in order to reduce the active inductance (L_{comm}) of the commutating coil. As a consequence of observations above i.e. the number of commutator segments and rotor slots have no observable influence on RFI at normal operating speeds; it can be concluded that the number of armature coils should be increased to reduce the reactance voltage generated in the commutating coil, and these coils should be distributed in as many rotor slots as is practicable in order to reduce the number of coils per slot. Ref. (145) reported results comparing an armature winding distributed in 12 rotor slots and two coils per slot with those distributed in 24 rotor slots and single coil per slot; the latter winding distribution showed a reduction in measured RFI levels of almost 15 dB across the whole frequency band.

(h) Stray capacitance between the armature windings and the armature laminations should be minimised by suitable choice of insulating material at the bottom of the rotor slots in order to reduce the flow of asymmetrical interference currents.

(i) Both brushes should span at least two commutator segments during commutation; this has been shown to minimise the active inductance of the commutating coil.

(j) Variation of motor load has negligible effect on measured RFI levels due to the speed-current characteristic of small motors.

(k) Where possible the earth connection to the motor frame should be removed since it offers a low impedance path to the flow of asymmetric interference currents. Small motors in domestic appliances are usually of the double insulated type and do not require an earth connection.

8.1.4 RFI due to the influence of mechanical variations in the motor assembly

(a) One of the most influential factors in RFI generation from commutation is the contact stability of the brushes. Brushes make movements and oscillations relative to the brush box; if the magnitude of this vibration is small it has practically no effect on commutation and RFI. However excessive brush movements have an adverse effect on commutation and can increase RFI levels by over 30 dB across the frequency band. The increased RFI components result from;

i) stepped current reversal resulting from the unstable sliding contact.

ii) increased arcing at the brushes

iii) increased brush wear

(b) Brush movements greater than around 0.075mm can cause instantaneous contact break resulting in severe arcing at the brush face, damaging both the brushes and the commutator surface.

(c) Brush stability is influenced by the following mechanical factors in the motor assembly:

i) armature out-of-balance

ii) commutator profile

iii) commutator surface finish

iv) brush box construction

v) brush box alignment

vi) bearing alignment

vii) spring pressure

viii) bearing journal - race clearance

(d) The maximum allowable tolerances of mechanical variations introduced to the test-rig in order to minimise increases in RFI levels due to brush instability are as follows:-

i) static armature out-of-balance, 0.5 gcm max.

ii) dynamic armature out-of-balance, 0.2 to 0.3 gcm max.

iii) brush spring load, 90g to 110g

iv) brush mis-alignment along quadrature axis,
0.125mm max. against rotation
0.075mm max. with rotation

v) proud commutator segments, 3.75×10^{-3}mm max.

vi) commutator eccentricity, 0.02mm max.

vii) commutator surface finish, 0.5×10^{-6} mm CLA min. and 1×10^{-6} CLA max.

viii) brush box clearances, 0.02mm min. and 0.05 to 0.1mm max.

ix) brush overhang length, 0.5mm min. and 1mm max.

x) bearing mis-alignment, 0.125mm max.

xi) bearing journal-race clearance, 8×10^{-3}mm max.

(e) Angular brush shift should be introduced to improve commutation and thus reduce RFI. The maximum allowable variation of brush shift around its optimum position is approx. $\pm 2^{\circ}$.

(f) Undercut intersegmental insulation on the commutator reduces RFI levels by as much as 10-15 dB in comparison with flush insulation.

(g) Asymmetric variation of air-gap has no observable influence on measured RFI levels.

8.2 Conclusions from case-study

The conclusions from the case-study into motor manufacture at the Hoover plc Cambuslang factory are as follows:-

(a) Motor to motor variations in RFI levels from mass produced motors result from mechanical variations in the motor assemblies.

(b) Improvement of brush stability by appropriate mechanical design improves commutation which in turn;

i) reduces overall RFI levels
ii) reduces suppression costs
iii) minimises motor to motor variations in RFI levels
iv) reduces brush wear (and thus increases motor life).

(c) The manufacturing tolerances specified for motor components and their assemblies at Cambuslang are suitable to minimise motor to motor variations in RFI levels.

(d) Deviations from the specified manufacturing tolerances of motor components and assemblies result from:

i) lack of preventative maintenance on tooling and machines.
ii) poor tool settings
iii) poor gauging facilities
iv) operator/tool setter malpractices

v) inadequate brush box material specifications

vi) inadequate brush box fitting in the EURO motor casing

vii) incorrect armature manufacturing sequence (i.e. armature balancing should be the final operation in the armature assembly sequence).

viii) unsuitable dirt fan fitting on the EURO armature shaft (causing armature unbalance).

(e) Poor tool settings and gauging facilities result in the following:-

i) defective moulded motor cases

ii) unsymmetrical dirt fan mouldings

iii) undersize, tapered and/or lobed journals on the armature shafts

iv) incorrect positioning of datum steps along the armature shaft length

v) poor commutator surface finish

vi) burrs on commutator segment edges

vii) proud commutator segments

viii) commutator eccentricity

ix) variable brush spring pressure

x) unbalanced armatures

(f) The quality control of motor components and motor assemblies at Cambuslang can be improved by implementing the following recommendations:

i) increase the frequency of random quality checks on production by quality inspectors in order that they can be used as a deterent to 'cheating' by the operators.

ii) ensure all machine tool setters are qualified tradesmen.

iii) introduce a training course/programme for all new machine setters.

iv) introduce preventative tool setting checks

v) maintain records of where, when and why tool settings changed.

vi) determine tool wear data in order tools may be changed/refurbished on a regular basis - before failures.

vii) introduce preventative maintenance checks.

viii) maintain maintenance records of individual machines.

8.3 Recommendations for future work

Recommendations for future investigations into RFI from small motors which would complement the work presented in this thesis and also benefit the general subject of RFI suppression are listed below:-

a) The influence of motor orientation and wiring in appliances

During experimental investigations it was noted that movement of motor position and its associated wiring could influence measured RFI levels. Similar observations have been made at Hoover plc, finding that motor orientation in an appliance has a bearing on the ultimate electromagnetic compatability of the appliance. Interference sources within the motor are unaltered by such movements thus it is clear that propogation of RFI is affected. Studies are necessary to determine the relevant factors influencing this variation of RFI in order to develop generalised rules for motor positioning and wiring layout for maximum attenuation of RFI within the appliance structure.

b) The influence of variations in the characteristics of the materials used in motor manufacture

This investigation was originally proposed by Hoover plc for inclusion in this thesis, however the work had to be omitted in preference to the work presented. The intent would be to observe the influence of variations in the characteristics of motor construction materials and also the use of alternative materials.

c) The influence of brush grade, laminated brushes, carbon fibre brushes and brush lubrication

A number of references have indicated that choice of correct brush type and brush librication can reduce RFI levels from motors. The subject however requires detailed study such that the advantages and disadvantages of the various alternatives can be assessed.

d) Prediction of RFI from small motors

Holownia [110] demonstrated that circuit analysis techniques could be applied to an equivalent circuit of the motor in order to predict the measured RFI levels. The prediction can be improved by more detailed identification of the r.f. equivalent circuit of the motor. The parameters of the equivalent circuit are frequency dependant, thus it would be necessary to model the various parameters to be representative across the r.f. band. Further work is also required in order to model commutation. In addition to predicting RFI levels, the technique can be applied in order to obtain a better understanding of the modes of RFI propogation and to identify the significant parameters of the r.f. circuit.

e) <u>Determination of the mechanism of RFI generation at the brush-commutator contact at zero current</u>

During RFI investigation it was observed that low levels of RFI were generated from the rotating brush-commutator contact when the circuit was not externally energised. In section 6.1.2 tenuous explanations for this phenomenon were proposed, however further study is necessary in order to accertain the true nature of this noise.

f) <u>RFI suppression network design and optimisation</u>

Suppression network synthesis for small motors utilises empirical and heuristic methods to find optimum circuit parameters. A number of references examining suppression techniques have been reviewed in Chapter 4. However the application of these techniques needs to be demonstrated in order to gain wider acceptance in industry. It is considered that the prediction technique mentioned in above (d) should be applied to determine the effectiveness of various suppression network designs and for the development of an optimisation procedure.

APPENDIX A1

TEST RIG DETAIL DRAWINGS

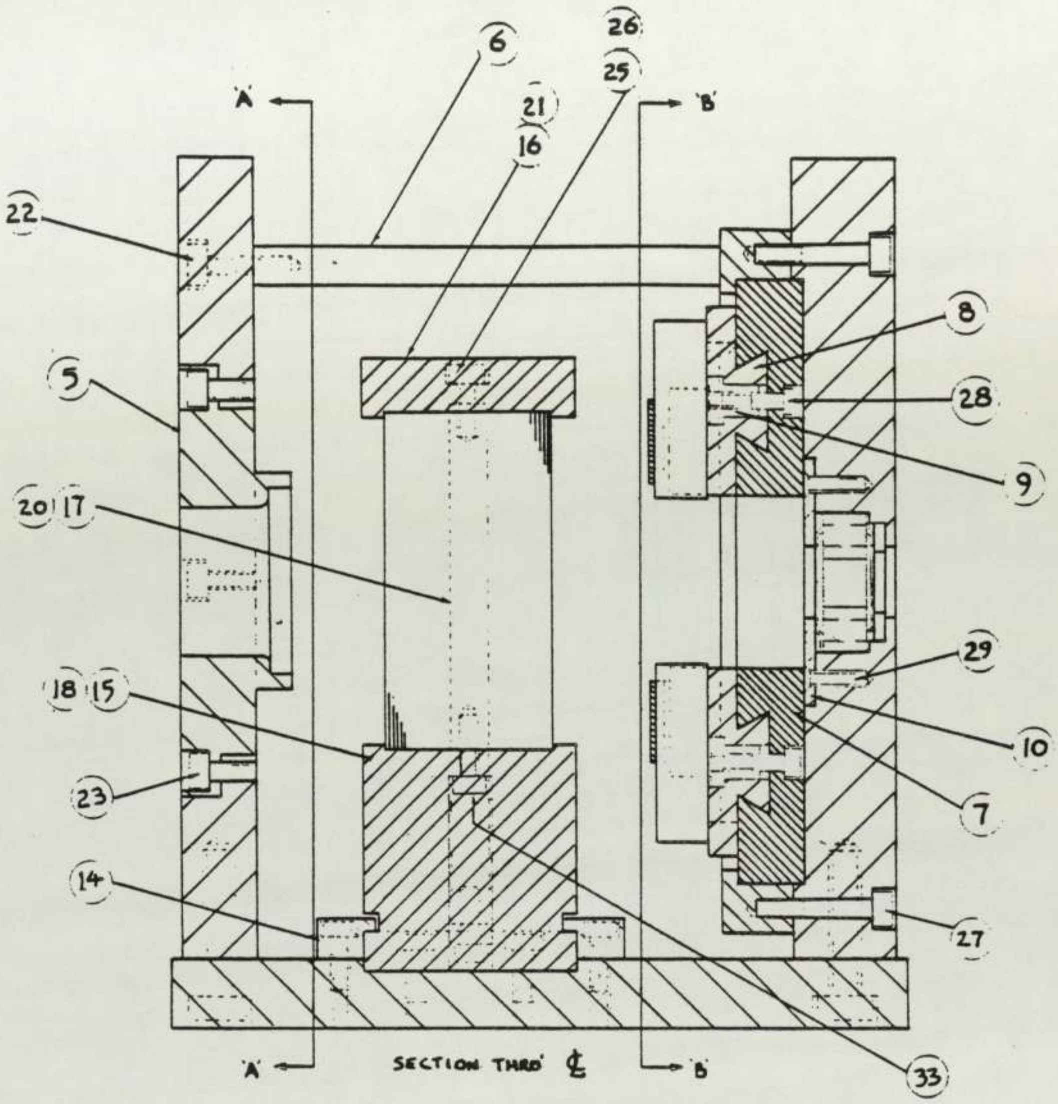

Test-rig general layout 1 (Front elevation - section C/L)

Fig. A1.1(a)

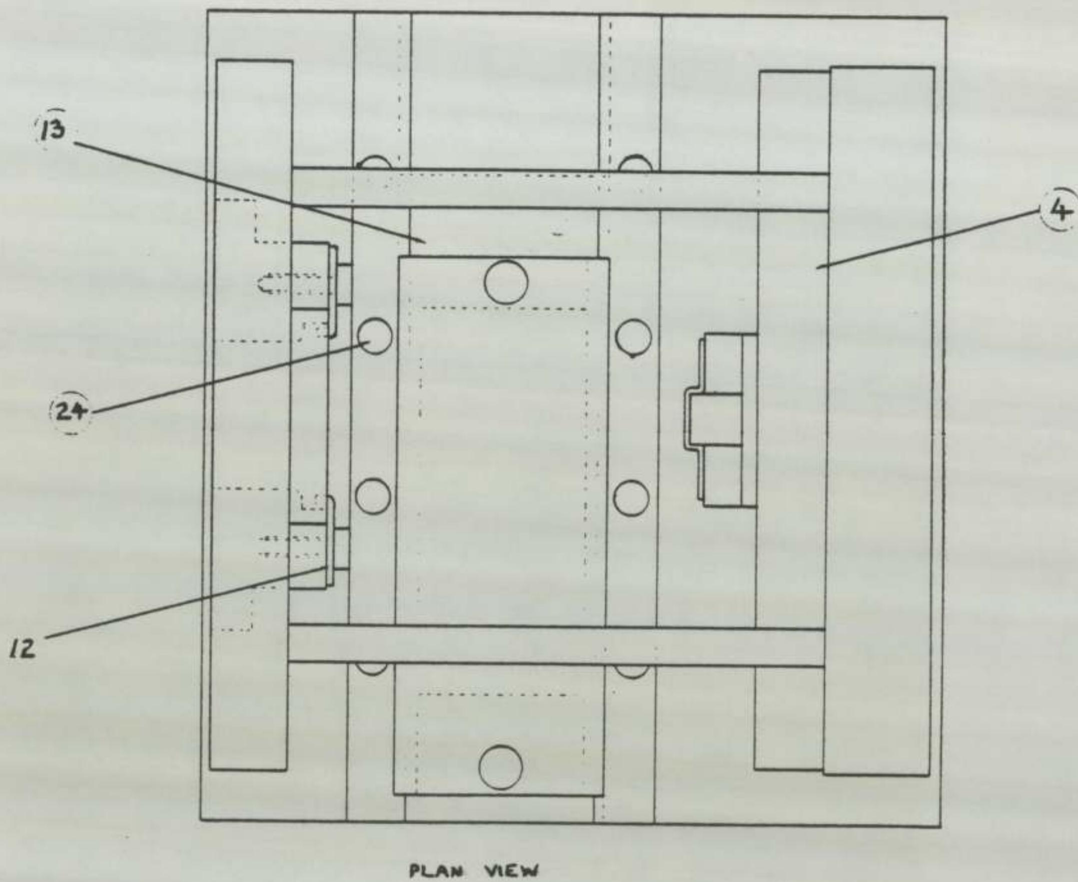

Test-rig general layout 2 (Plan view)

Fig. A1.1(b)

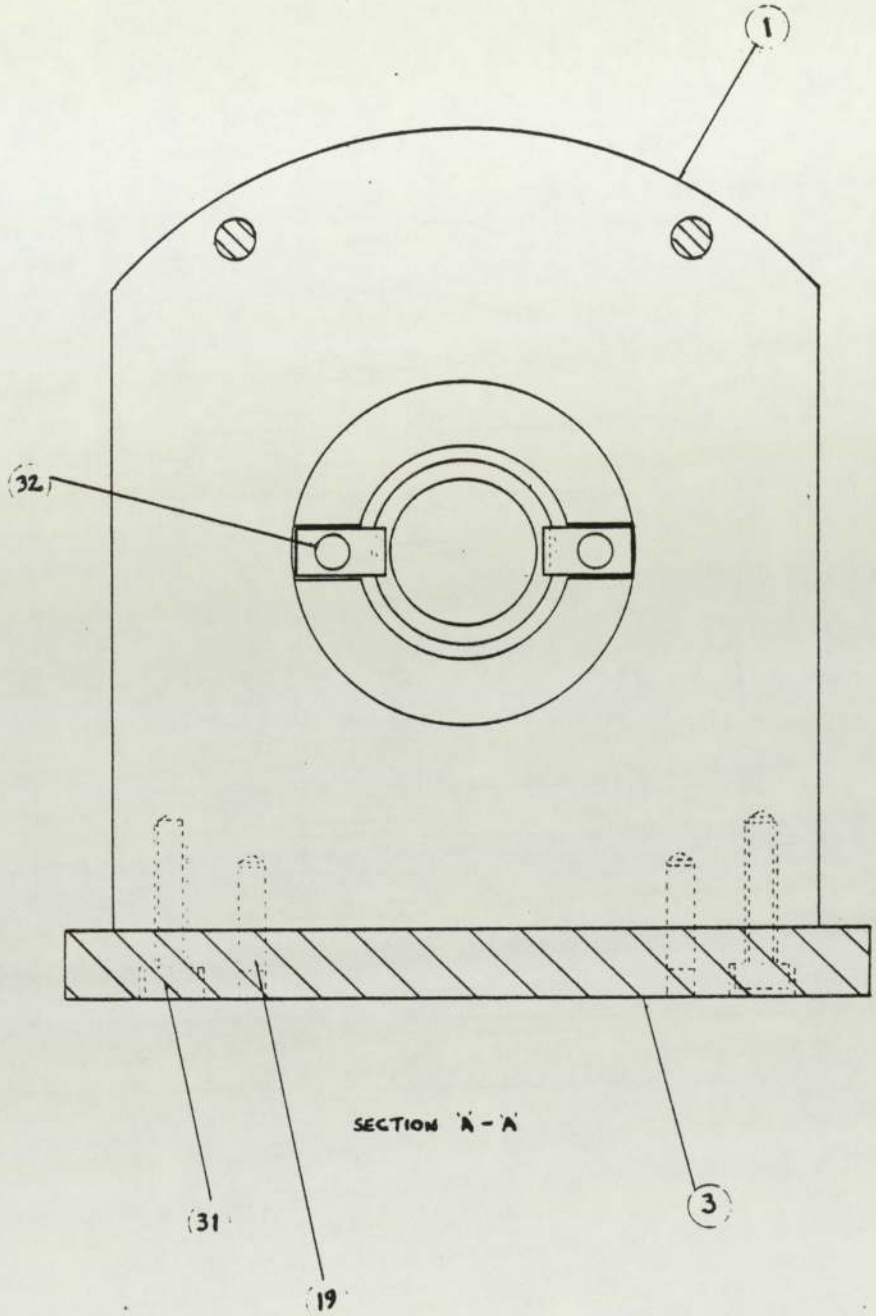

Test-rig general layout 3 (Section A-A)
Fig. A1.2(a)

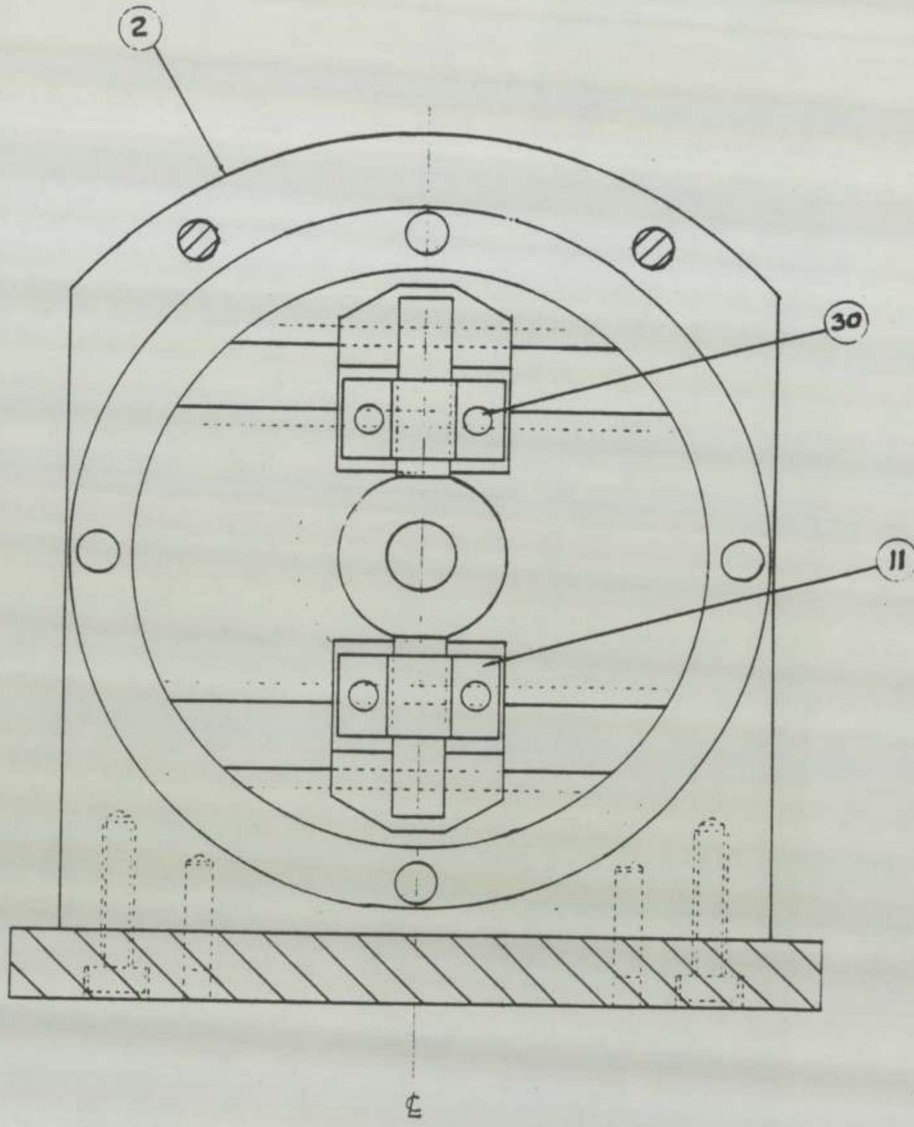

Test-rig general layout 4 (Section B-B)

Fig. 1.2(b)

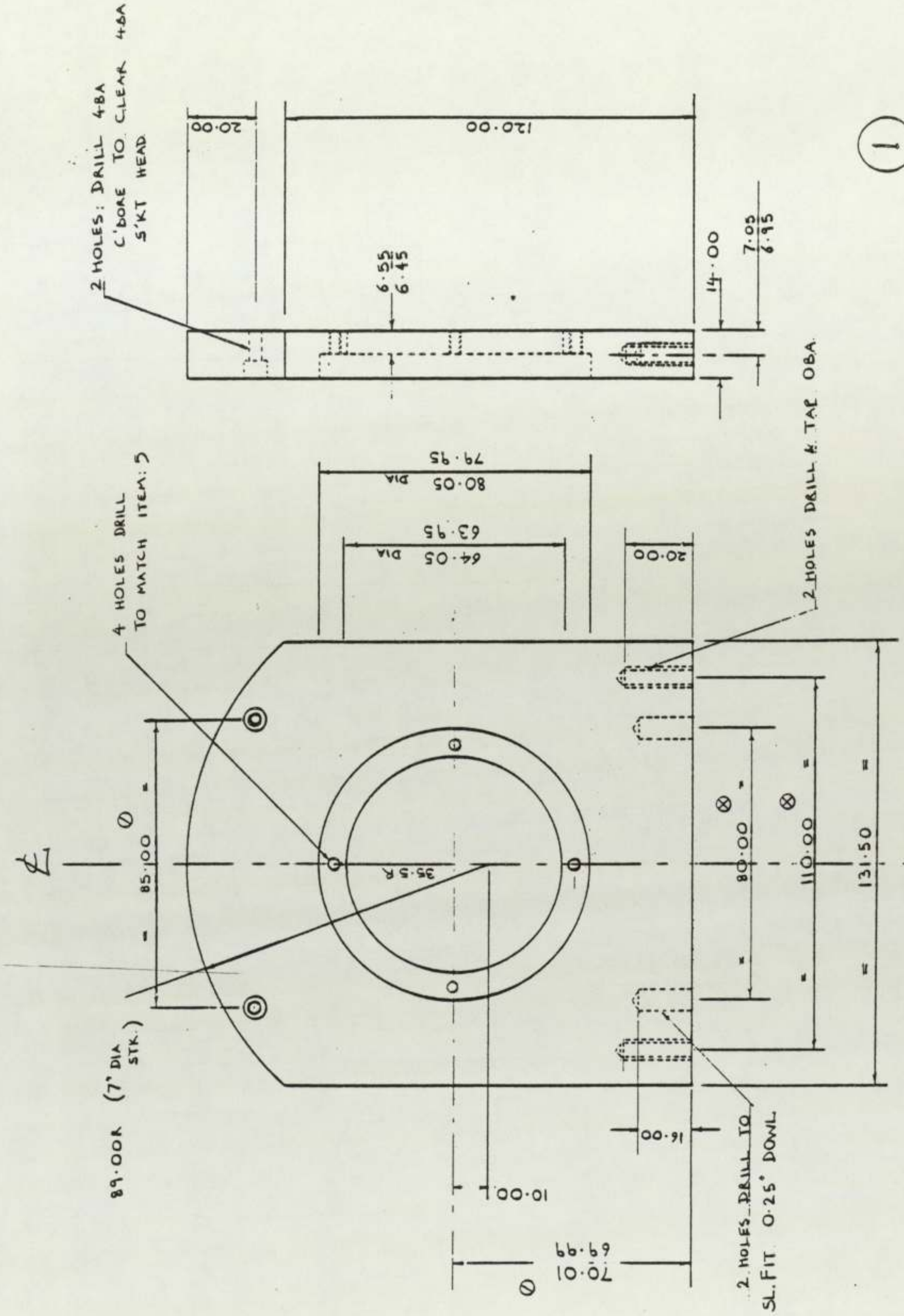

Non-drive end plate

Fig. A1.3

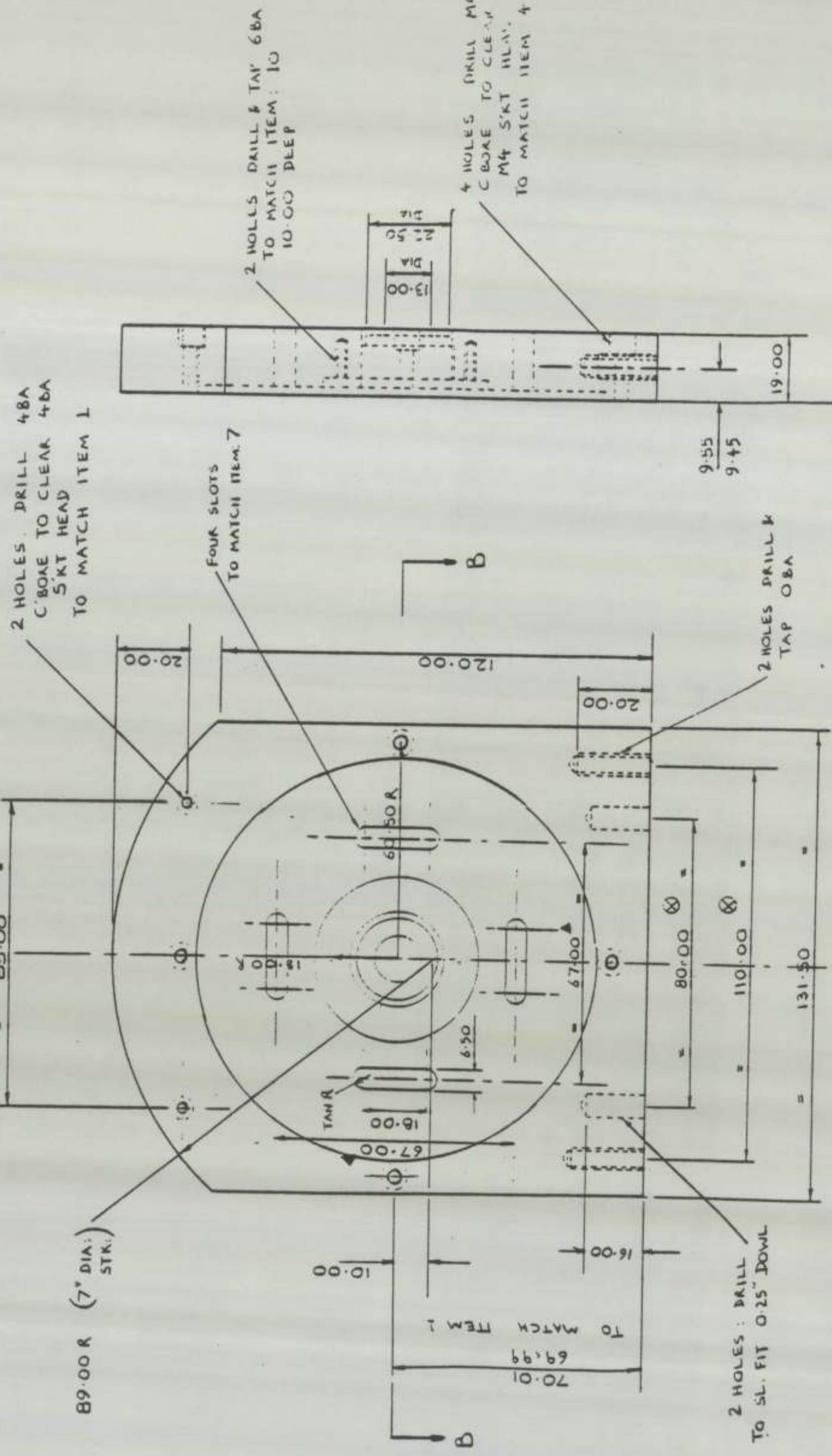

Drive end plate

Fig. A1.4

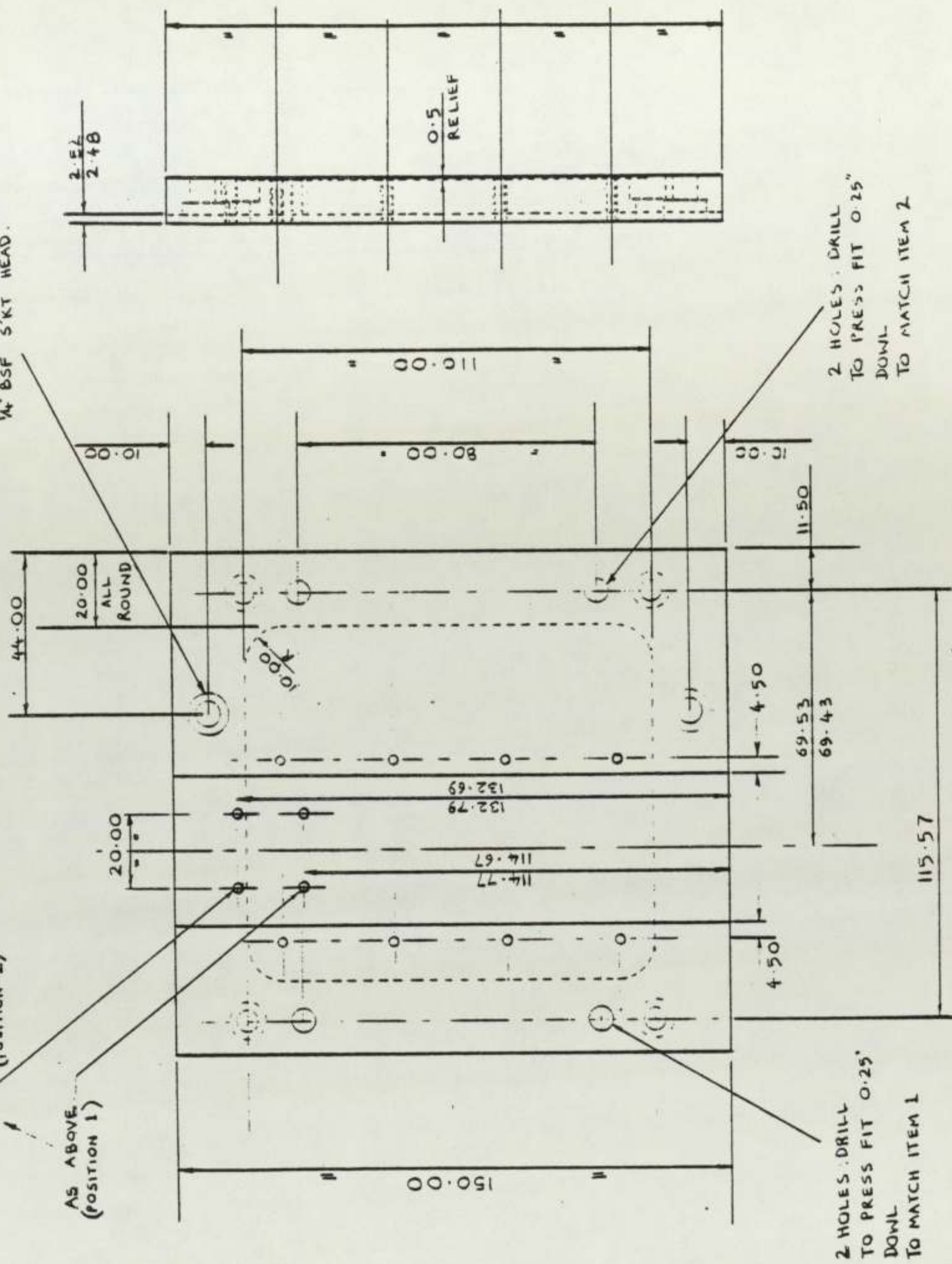

Base plate

Fig. A1.5

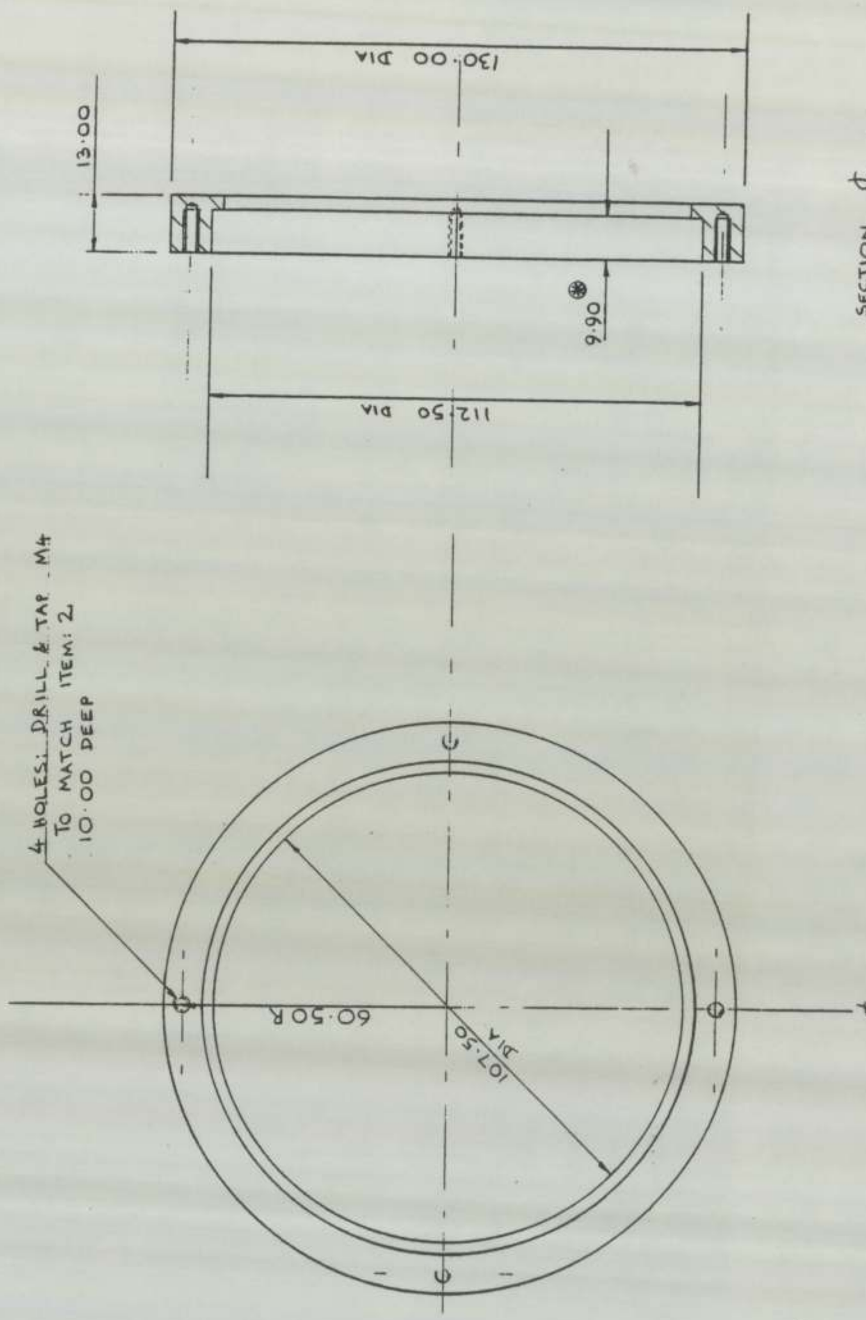

Brush box assembly clamping ring

Fig. A1.6

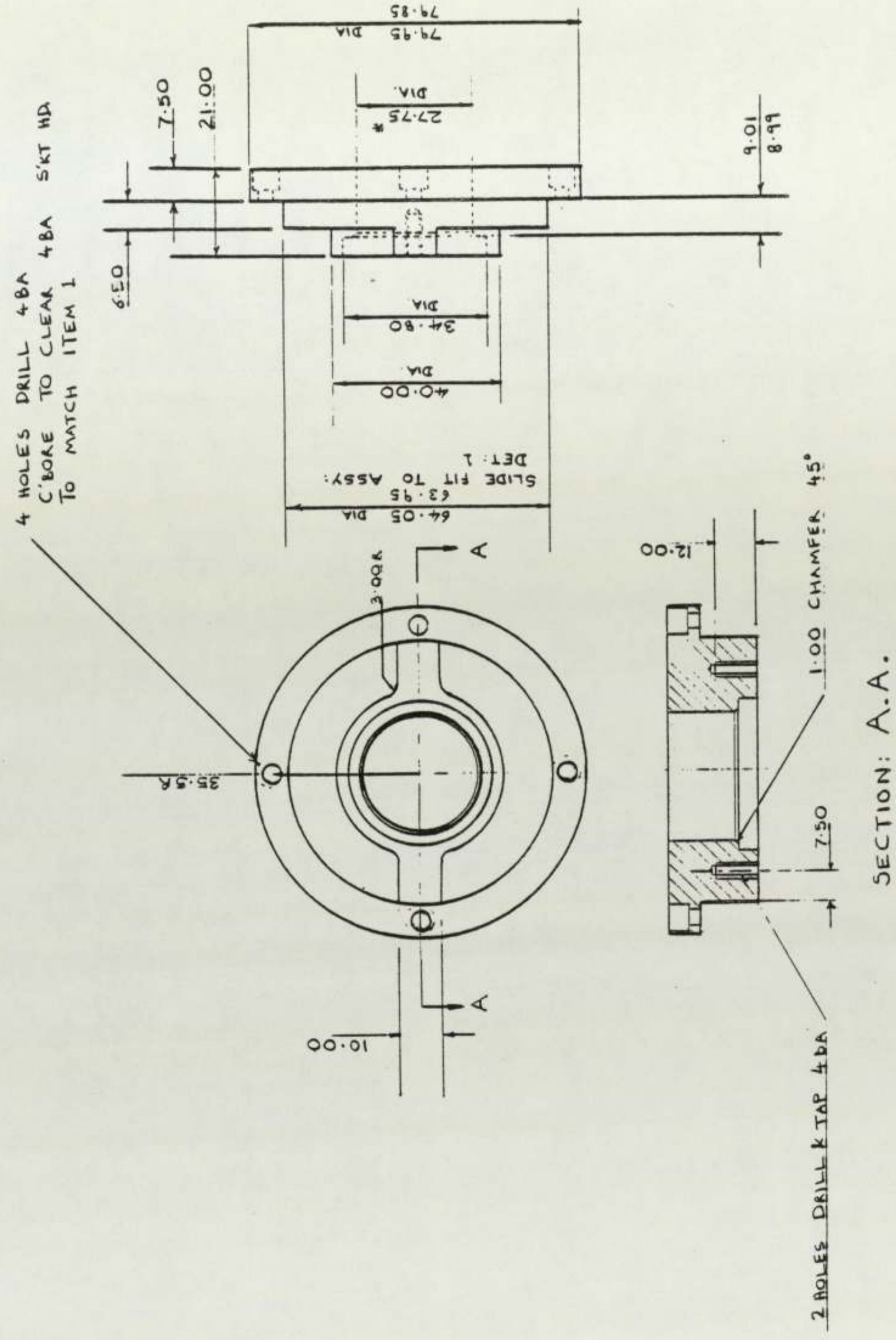

Non-drive end plate detachable central disc

Fig. A1.7

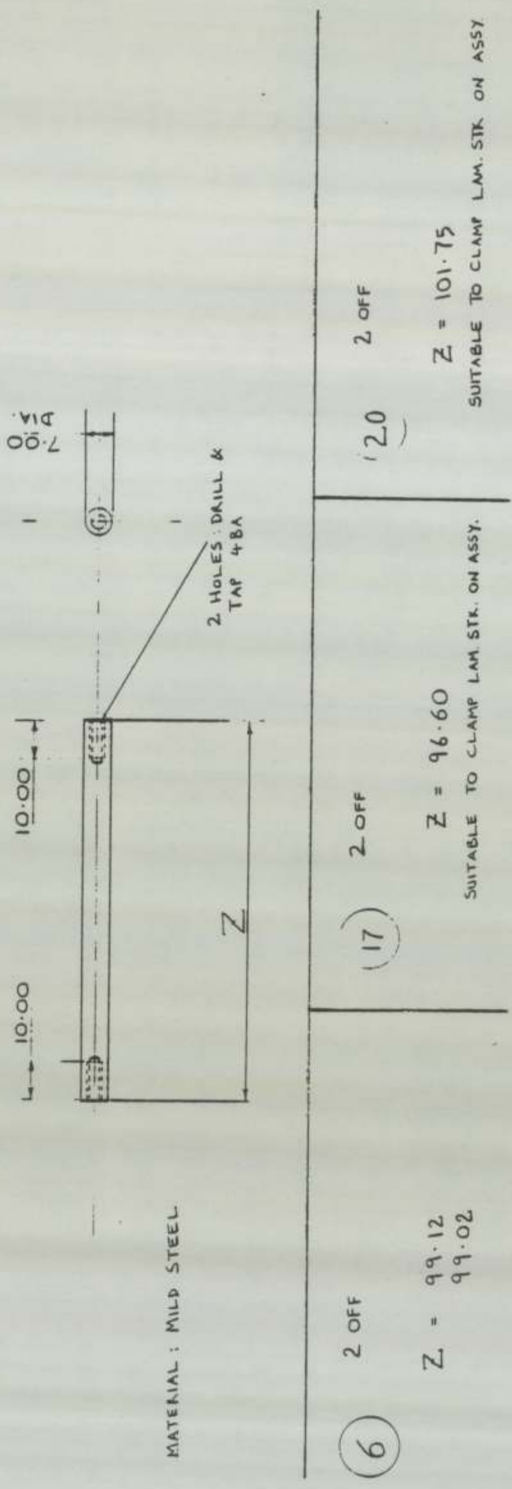

Spacing posts

Fig. A1.8

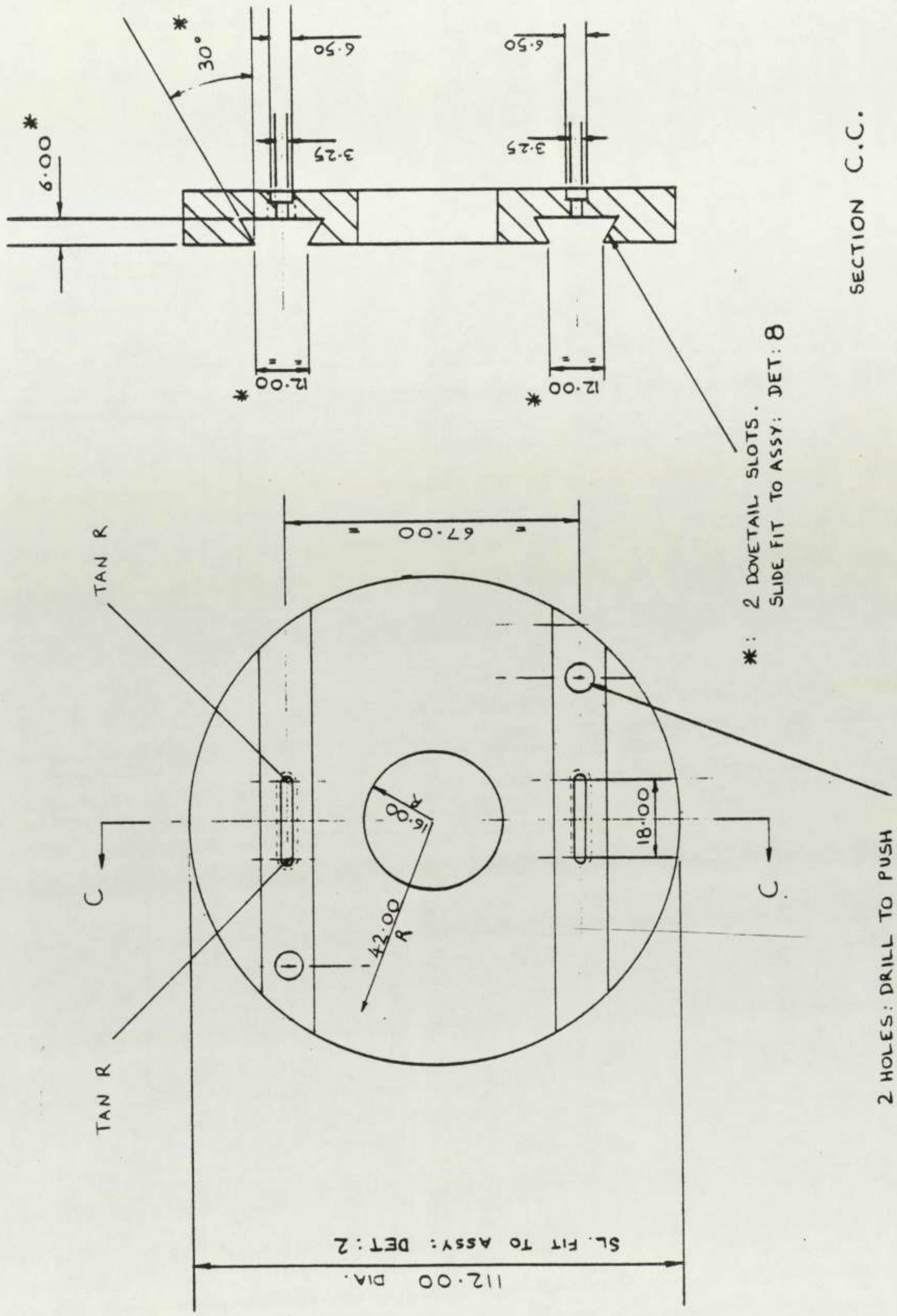

Insulating back plate

Fig. A1.9

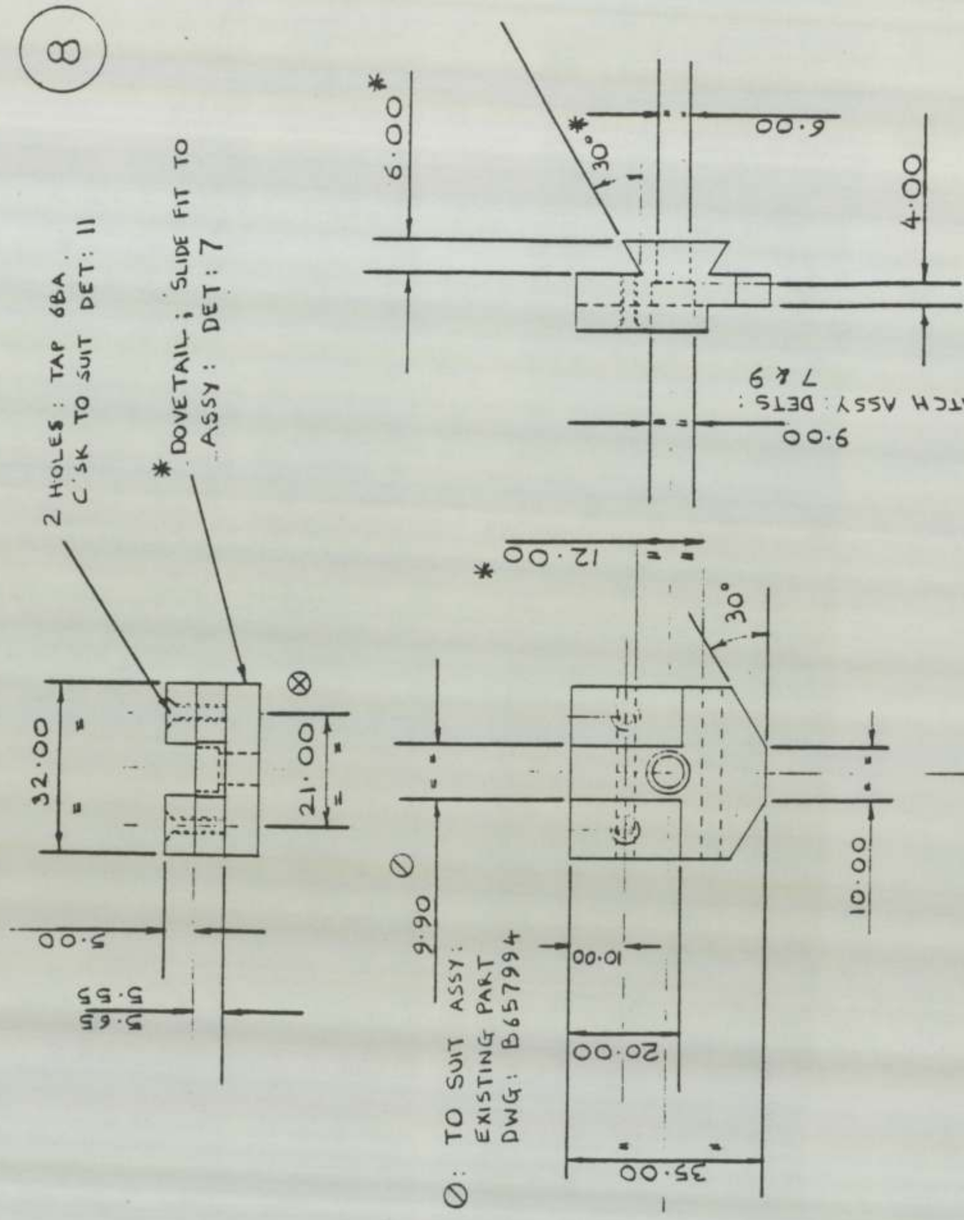

Insulating brush box holder block

Fig. A1.10

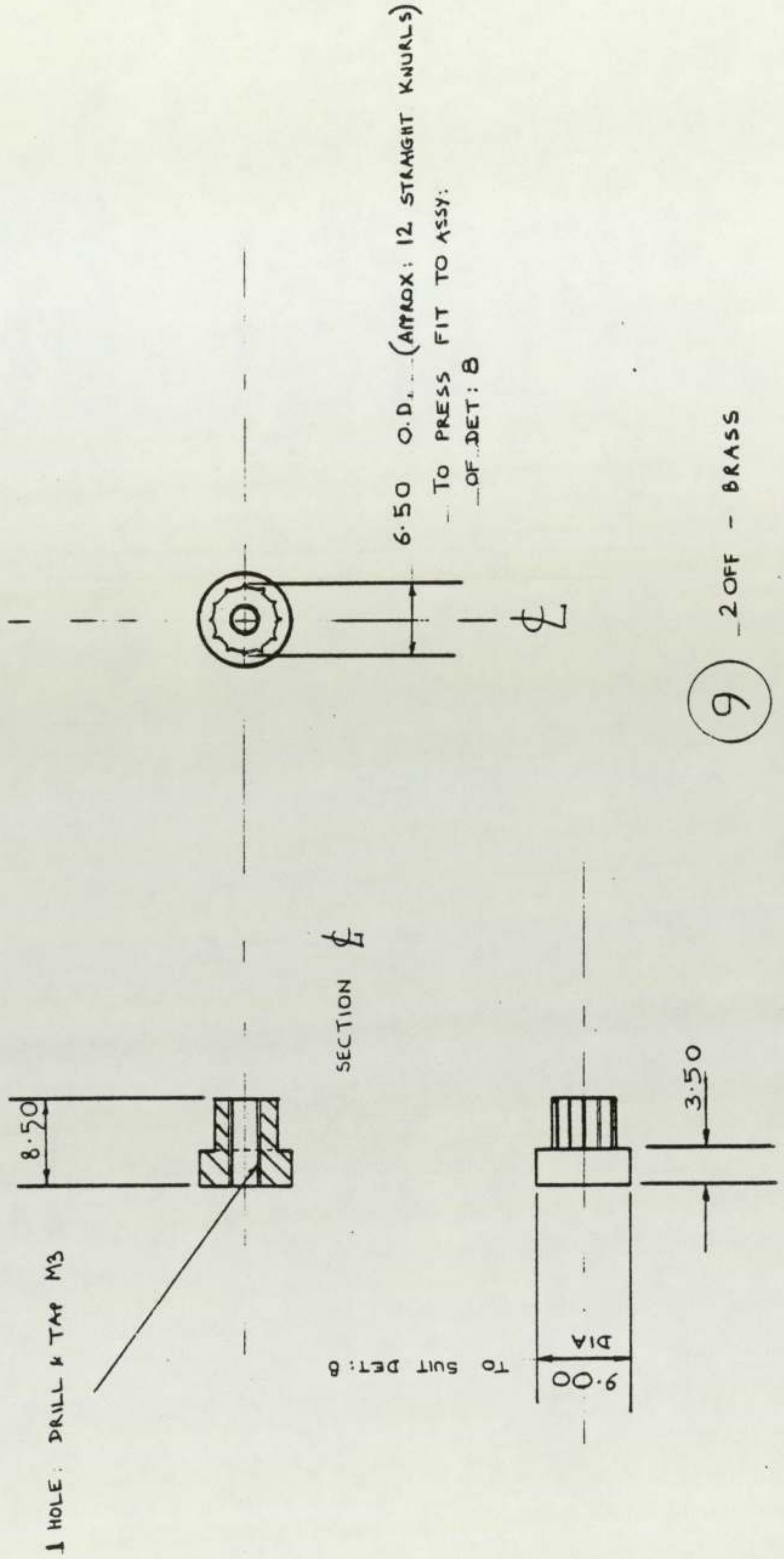

Insulating brush box holder block clamping nut

Fig. A1.11

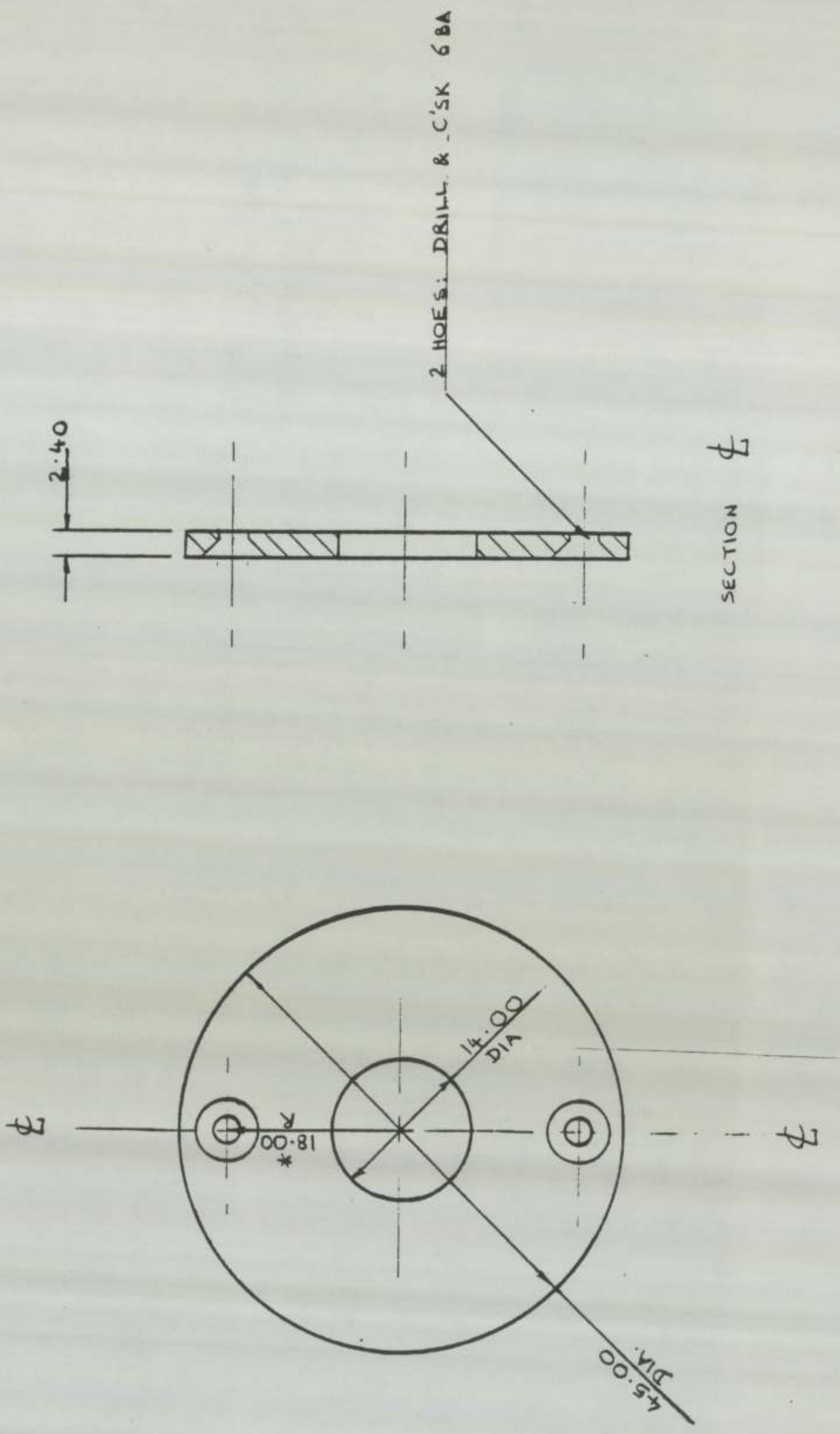

Drive end plate bearing clamping disc

Fig. A1.12

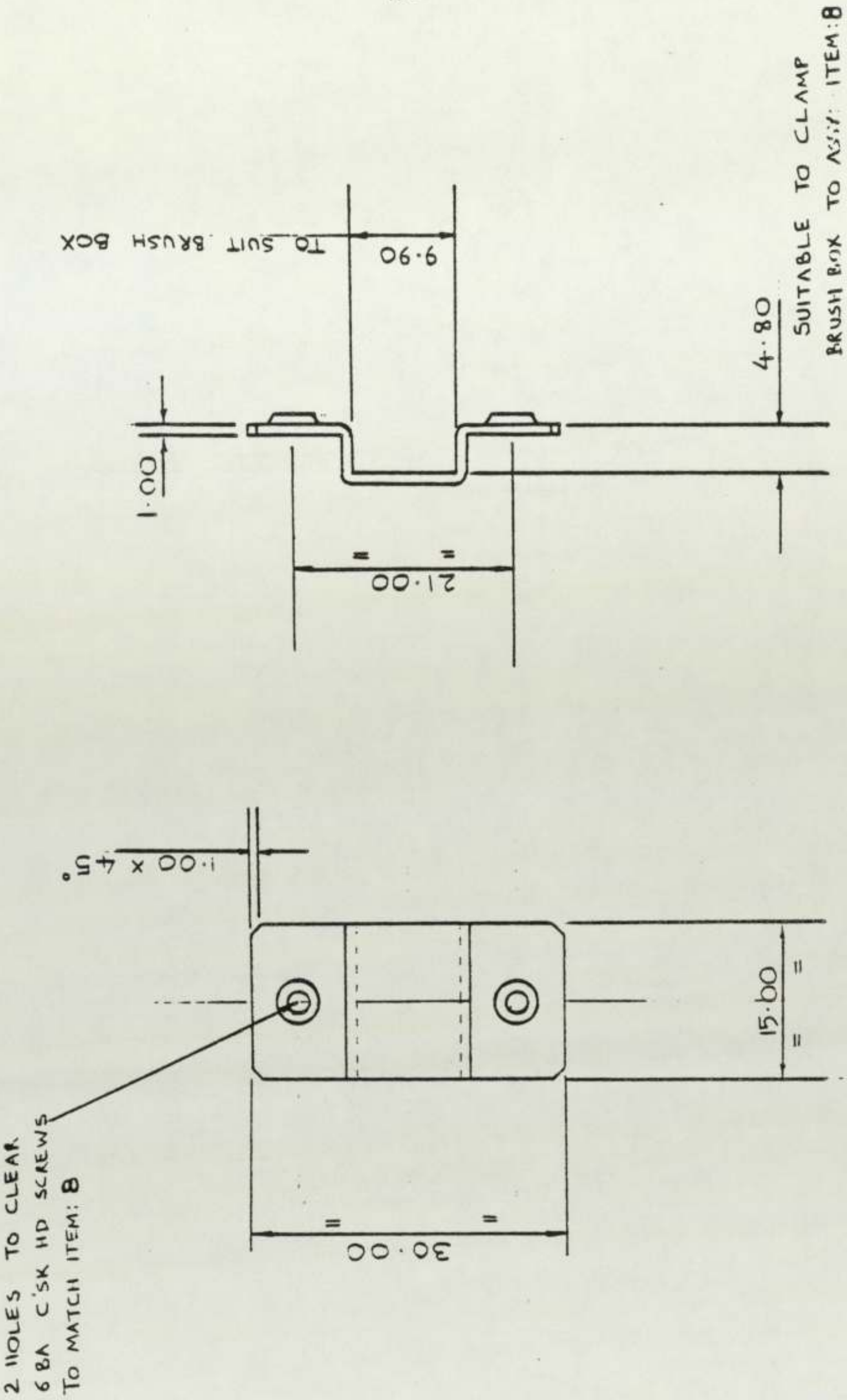

Brush box clamping plate

Fig. A1.13

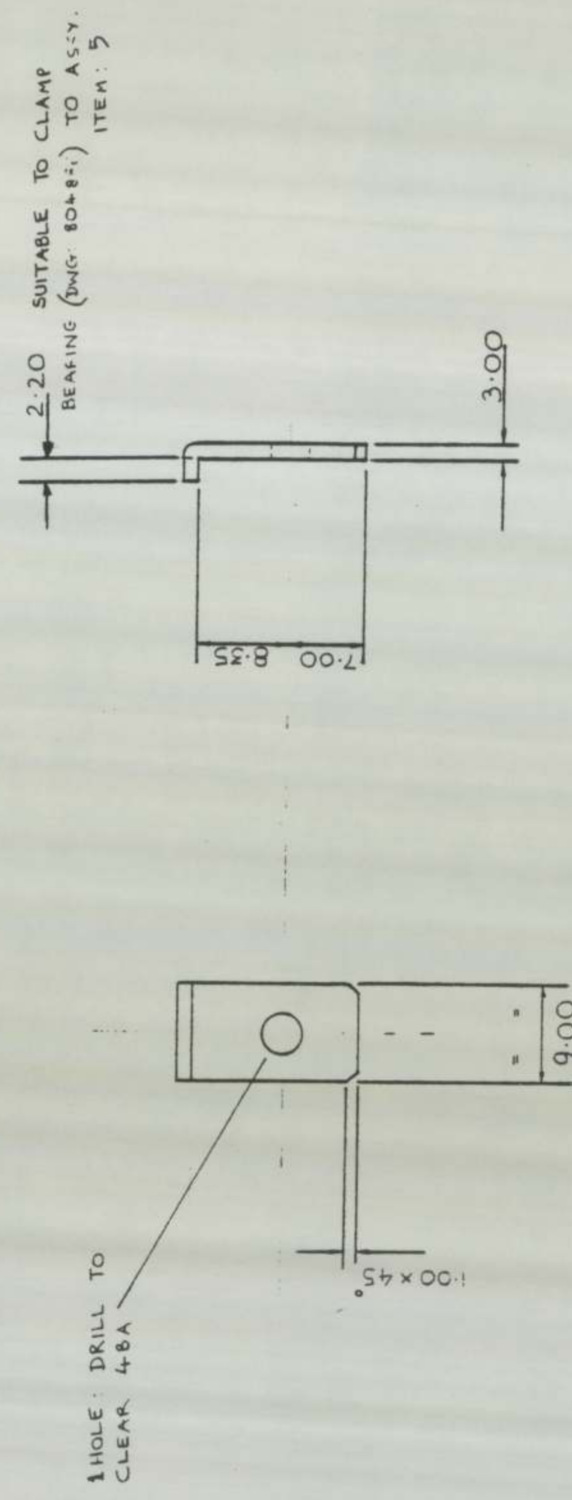

Non-drive end plate bearing cup finger clamp

Fig. A1.14

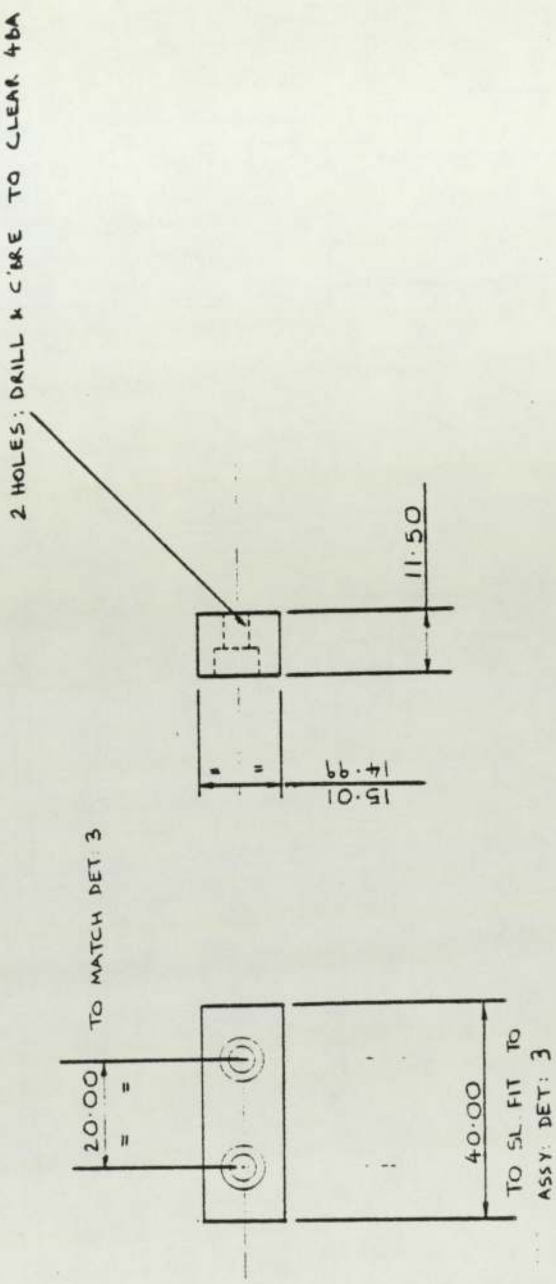

Test-rig framework fixed stop

Fig. A1.15

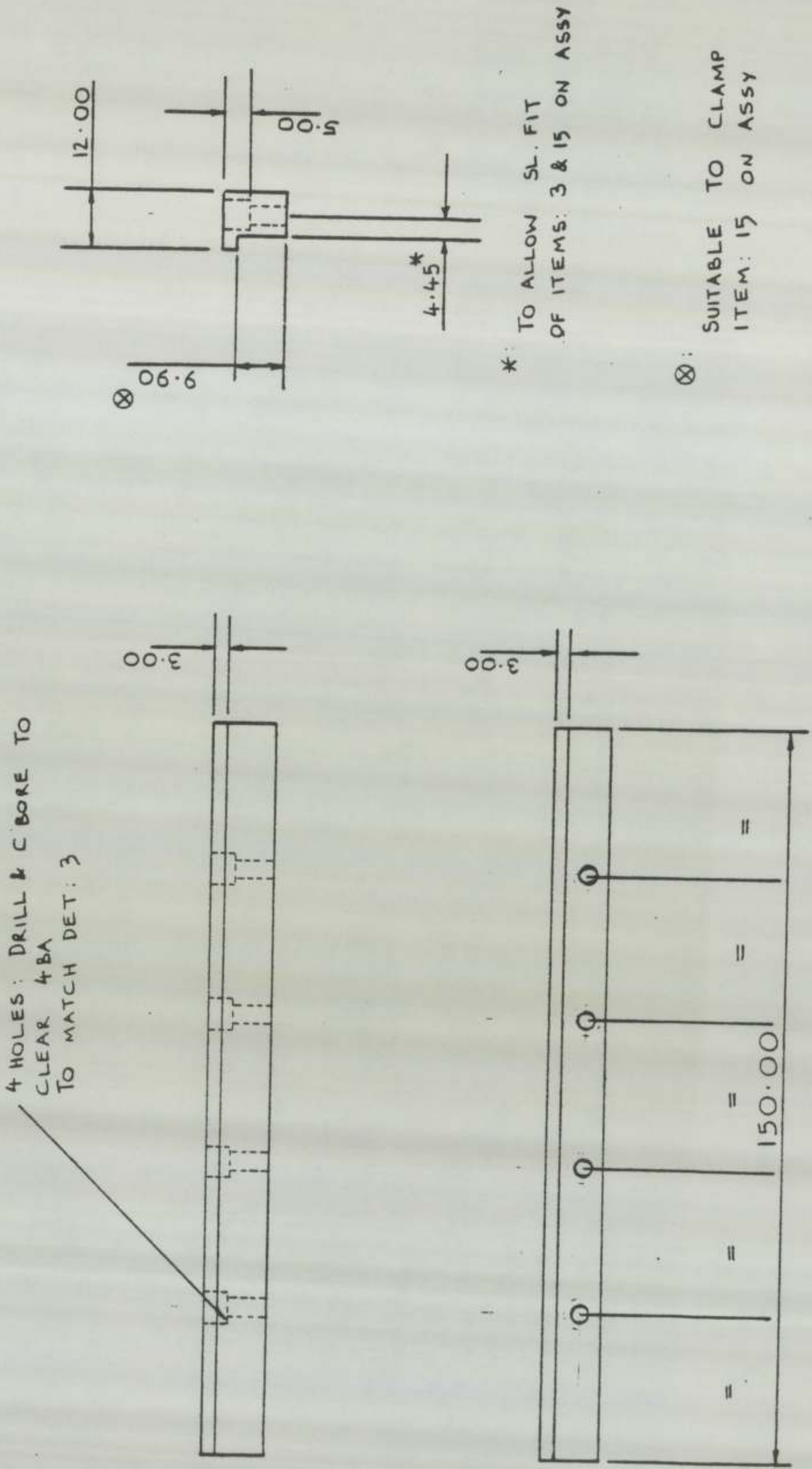

Field assembly clamp

Fig. A1.16

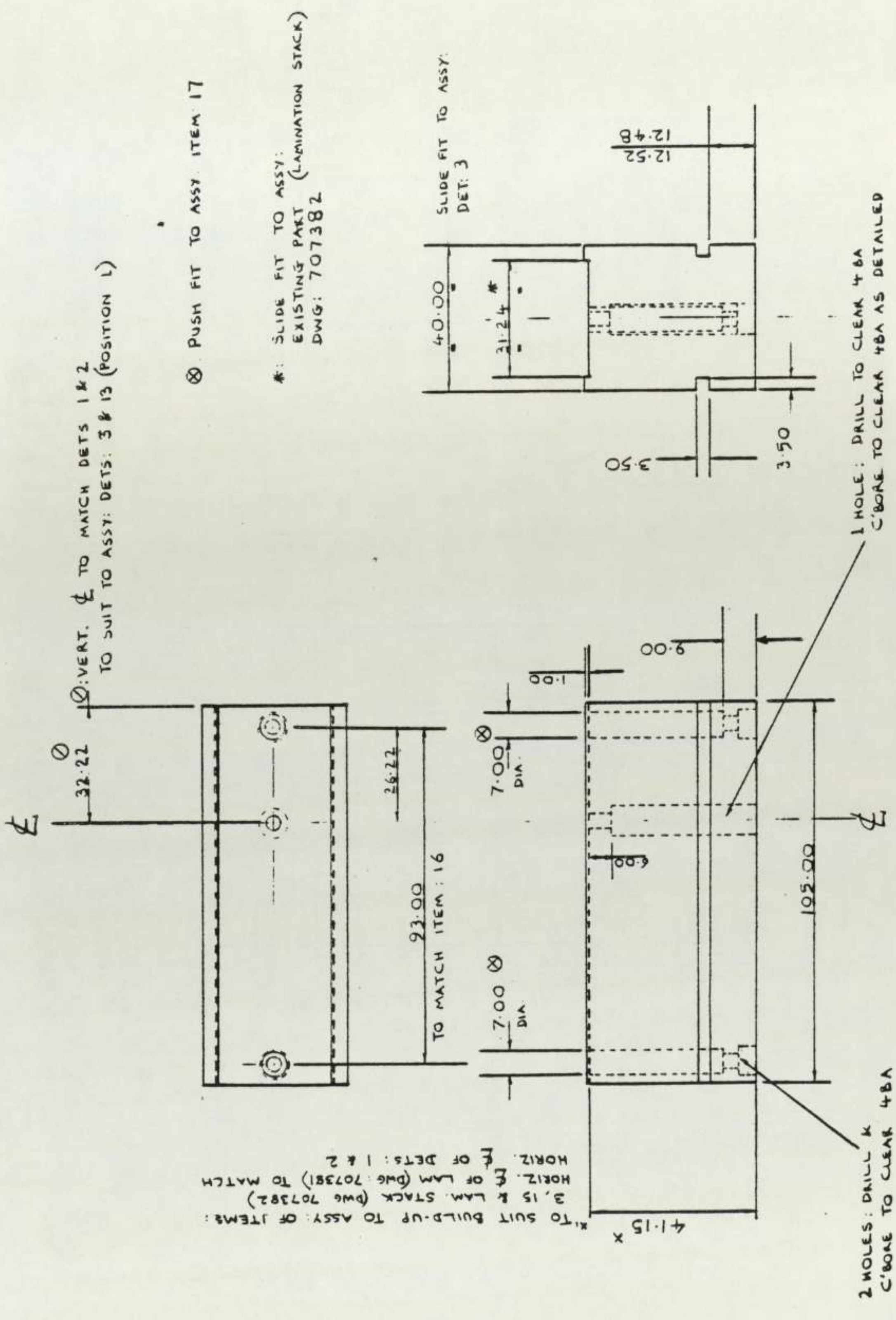

Bottom half field assembly cradle (U-type field)

Fig. A1.17

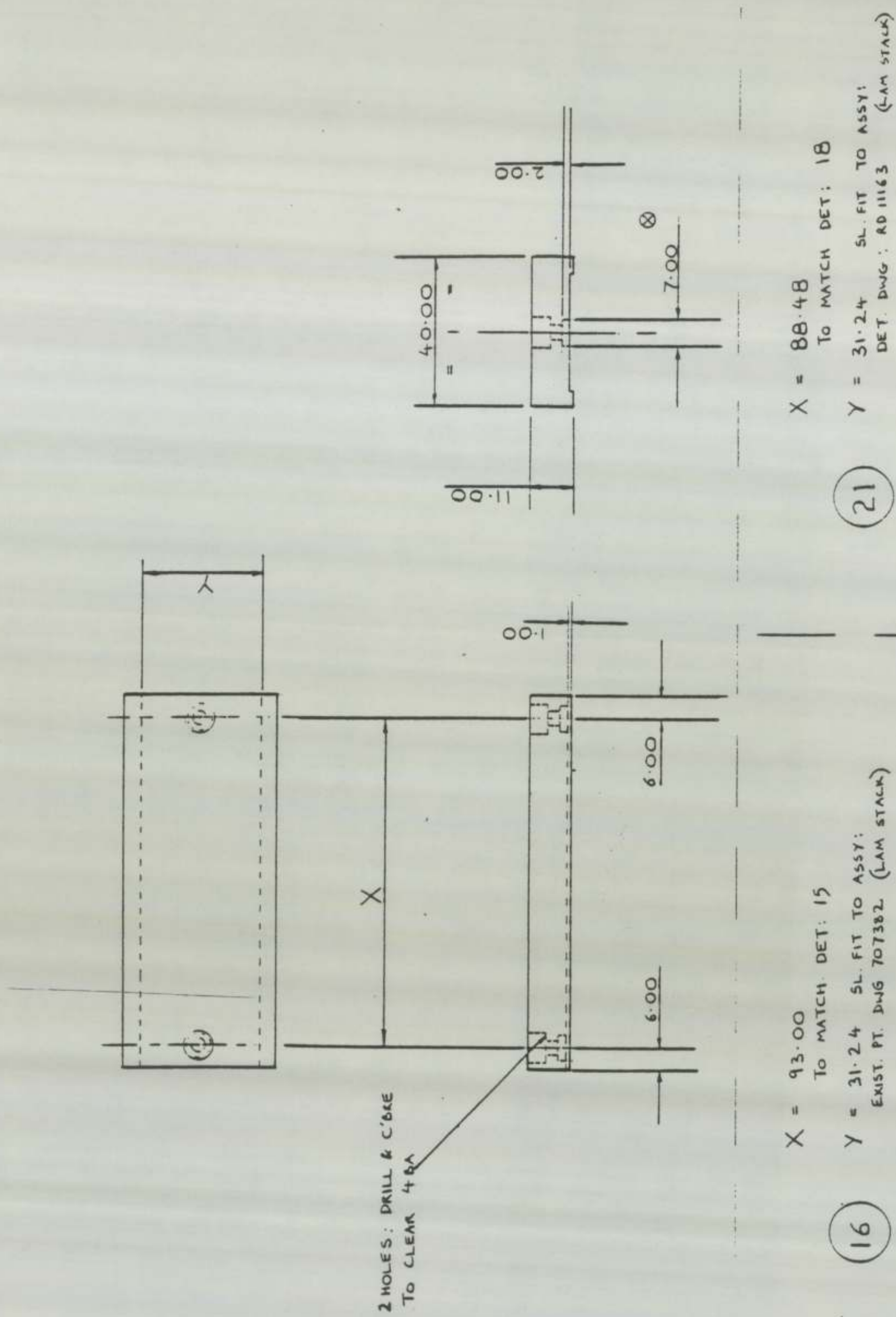

Upper clamping half field assembly cradle

Fig. A1.18

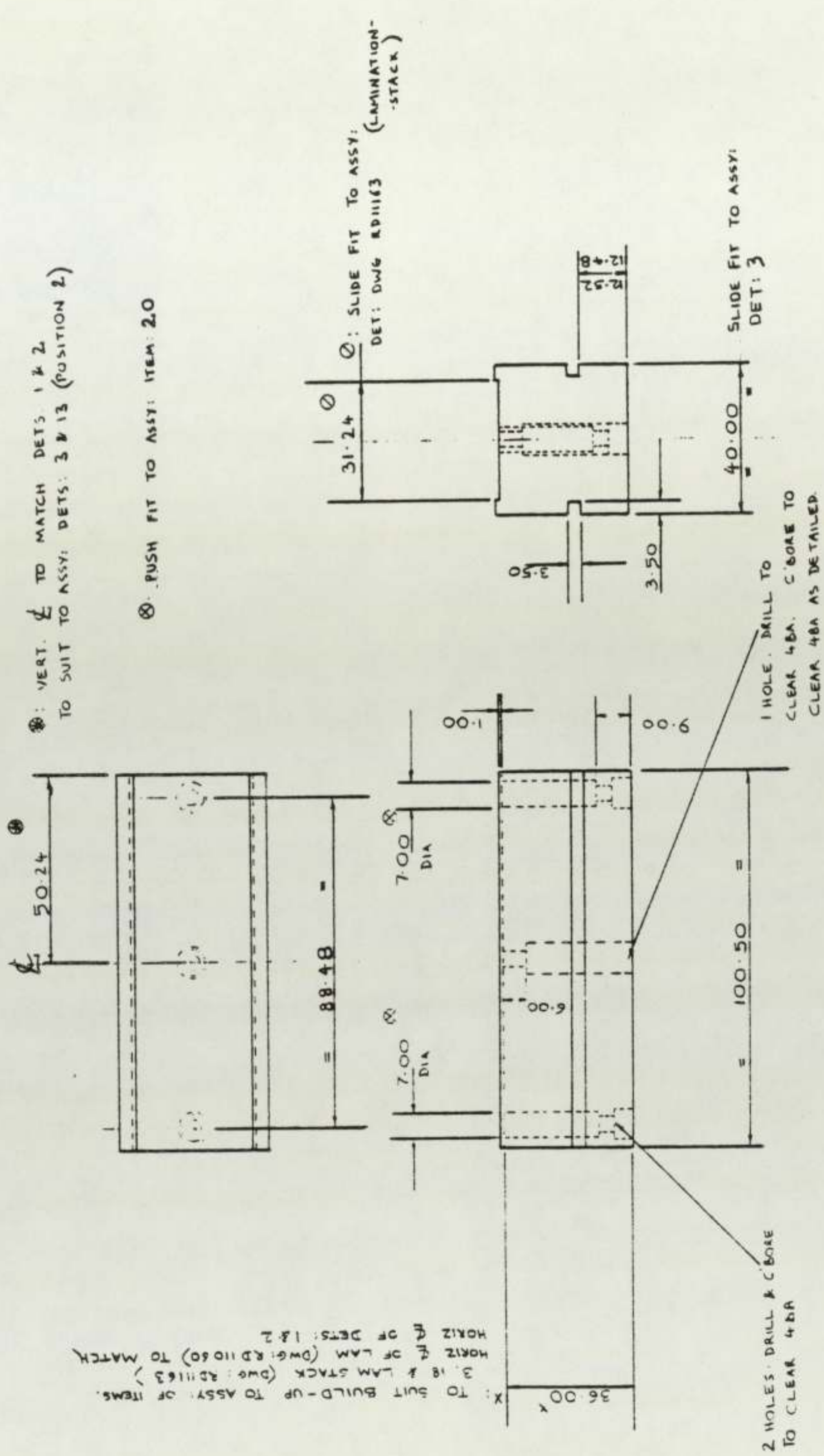

Bottom half field assembly cradle (0-type field)

Fig. A1.19

APPENDIX A2

TEST RESULTS

TABLE A2.1

TITLE: RFI CAUSED BY THE COMMUTATOR SWITCHING ACTION:
MEASURED RFI LEVELS FROM A 24 SEGMENT COMMUTATOR
AT 0.25A SUPPLY CURRENT WITH VARYING SHAFT SPEED

TEST VARIABLE: SPEED (r/min)

TEST NUMBER	1: 2000 r/min	2: 4000	3: 6000	4: 8000	5: 10000	6: 12000
FREQUENCY	RFI CONDUCTED VOLTAGE MEASUREMENTS: dB(uV)					
0.150 MHz	53	67	70	71	71	71
0.160	53	67	69.5	70.5	71	70.5
0.240	46	63	66.5	68	70	70.5
0.550	28.5	42	48	52	54	55
1.000	15.5	30	40.5	42.5	44	44.5
1.400	13	27	38	40	41	42
2.000	15	33	40.5	43	43	43
3.500	21.5	37	45	47	46.5	47.5
6.000	21	36	44	45.5	46	47
10.00	30.5	40	43	46	45.5	46
13.00	30.5	41	46	46	47	47.5
22.00	28	38	44	46.5	46	47
30.00	25	35	41	44	44	43.5
	RFI RADIATED POWER MEASUREMENTS: dB(pW)					
30.00	10.5	22	33	36.5	37	36
40.00	10	21.5	32	36	36.5	36.5
46.00	7	20	33	36.5	36.5	36.5
65.00	7	18.5	29.5	33	34	34
90.00	7	16	22.5	27	27	26.5
150.0	4.5	16	22.5	26	26.5	28
180.0	4	15.5	21	26	26	26
220.0	2	14	21	23	24	23
300.0	1	12	21	22	23	23

TABLE A2.2

TITLE: RFI CAUSED BY THE COMMUTATOR SWITCHING ACTION:
MEASURED RFI LEVELS FROM A 24 SEGMENT COMMUTATOR
AT 0.25A SUPPLY CURRENT WITH VARYING SHAFT SPEED

TEST VARIABLE: SPEED (r/min)

TEST NUMBER	7: 14000 r/min	8: 16000	9: 18000	10: 20000	11: 22000	
FREQUENCY	RFI CONDUCTED VOLTAGE MEASUREMENTS: dB(uV)					
0.150 MHz	70.5	71.5	73	91	93	
0.160	70.5	71	72	91	92.5	
0.240	70.5	70	72	85	88	
0.550	55.5	55.5	58	78	80	
1.000	44.5	43	45	63	66	
1.400	42	43	45	61	64	
2.000	44	45	47	65	68	
3.500	47.5	49	49	70	72	
6.000	47	46.5	49	68	72	
10.00	46	46	46	67	72	
13.00	48	49	54	69	74	
22.00	47	48	53	69	70	
30.00	44	46	49	62	68	
	RFI RADIATED POWER MEASUREMENTS: dB(pW)					
30.00	36.5	37	38	57	63	
40.00	37	37.5	40	57	61	
46.00	37	37.5	40	58	61	
65.00	35	35	36	52	58	
90.00	27.5	27.5	28	46	48	
150.0	27	27.5	28	43	47	
180.0	27	26	29	42	47	
220.0	25	24	26	40	43	
300.0	22.5	23	24	35	38	

TABLE A2.3

TITLE: RFI CAUSED BY THE COMMUTATOR SWITCHING ACTION:
MEASURED RFI LEVELS FROM A 24 SEGMENT COMMUTATOR
AT 1.0A SUPPLY CURRENT WITH VARYING SHAFT SPEED

TEST VARIABLE: SPEED (r/min)

TEST NUMBER	1: 2000 r/min	2: 4000	3: 6000	4: 8000	5: 10000	6: 12000
FREQUENCY	RFI CONDUCTED VOLTAGE MEASUREMENTS: dB(uV)					
0.150 MHz	53	67	70	71	71.5	71
0.160	53	66.5	69.5	71	71	70.5
0.240	46.5	63.5	66.5	68	70.5	70.5
0.550	29	42	48	52	54	55
1.000	15.5	30	41	43	44.5	44.5
1.400	13	27.5	37.5	41	42	42.5
2.000	15	33	41	42	43	43
3.500	21.5	37.5	45	47	46.5	47
6.000	21	36	44	46	45.5	47.5
10.00	31	40.5	43	45.5	47	46.5
13.00	30.5	41	46	46	47	47.5
22.00	28	38	44.5	46.5	46	47
30.00	26	35	41.5	43	44	44
	RFI RADIATED POWER MEASUREMENTS: dB(pW)					
30.00	10	23	33	36	38	37
40.00	10	22	32.5	36	37	36.5
46.00	8	28	32	36	36	36
65.00	7.5	18.5	29	33.5	34	34.5
90.00	7.5	16	22	27.5	27.5	26
150.0	4.5	16	22	26.5	26	27
180.0	4	15.5	21.5	26	26	26
220.0	3	14	21	24	25	24
300.0	1	13	21	23	23	23

TABLE A2.4

TITLE: RFI CAUSED BY THE COMMUTATOR SWITCHING ACTION:
MEASURED RFI LEVELS FROM A 24 SEGMENT COMMUTATOR
AT 1.0A SUPPLY CURRENT WITH VARYING SHAFT SPEED

TEST VARIABLE: SPEED (r/min)

TEST NUMBER	7: 14000 r/min	8: 16000	9: 18000	10: 20000	11: 22000
FREQUENCY	RFI CONDUCTED VOLTAGE MEASUREMENTS: dB(uV)				
0.150 MHz	71	71.5	74	91	93
0.160	70	71	73	90	93
0.240	70.5	71	73	85.5	88
0.550	55	56	59	78.5	81
1.000	44.5	44	47	63	67
1.400	42	43	45	61.5	63.5
2.000	43.5	45	46.5	66	69
3.500	47	48	48.5	70.5	73
6.000	47	47	48	69	73
10.00	46.5	47	47	67.5	72
13.00	48	48.5	56	70	73
22.00	47	48	56	69	71
30.00	44	47	50	63	69
	RFI RADIATED POWER MEASUREMENTS: dB(pW)				
30.00	37	38	40	58	62.5
40.00	37	37.5	39	57	61.5
46.00	37	37.5	38	58	61.5
65.00	36	36	37	53	62
90.00	27	28	29	46.5	58.5
150.0	27	28	29	43.5	49
180.0	26.5	27	28	43	47
220.0	25	25	27	41	45
300.0	22.5	23	26	36	38

TABLE A2.5

TITLE: RFI CAUSED BY THE COMMUTATOR SWITCHING ACTION:
MEASURED RFI LEVELS FROM A 24 SEGMENT COMMUTATOR
AT 1.5A SUPPLY CURRENT WITH VARYING SHAFT SPEED

TEST VARIABLE: SPEED (r/min)

TEST NUMBER	1: 2000 r/min	2: 4000	3: 6000	4: 8000	5: 10000	6: 12000
FREQUENCY	RFI CONDUCTED VOLTAGE MEASUREMENTS: dB(uV)					
0.150 MHz	53.5	67	70	71	71.5	70.5
0.160	53	66	70	71	71	70
0.240	46	63	66.5	68.5	70	70.5
0.550	29	42.5	49	53	54	54.5
1.000	15	31	41	43	44.5	44
1.400	13	28	38	40.5	41	42
2.000	16	34	41.5	43.5	43.5	44
3.500	21.5	37	44.5	47	47	48
6.000	21.5	36	45	46	46	47
10.00	30	40.5	44	46	46	46
13.00	30	40	46.5	46.5	47	48
22.00	28	38	44	47	47	47.5
30.00	25	36	41.5	44	44	44
	RFI RADIATED POWER MEASUREMENTS: dB(pW)					
30.00	10.5	22.5	33.5	37	37.5	36.5
40.00	10	22	32.5	36	37	37
46.00	8	21	33	37	37	37
65.00	7.5	19	29	33	34	34
90.00	7.5	16.5	23	27	27.5	27
150.0	4.5	16	23	27	27	28
180.0	4	16	22	26	26.5	26.5
220.0	2	14	22	23	24	24
300.0	1	12.5	21	23	23	23.5

TABLE A2.6

TITLE: RFI CAUSED BY THE COMMUTATOR SWITCHING ACTION:
MEASURED RFI LEVELS FROM A 24 SEGMENT COMMUTATOR
AT 1.5A SUPPLY CURRENT WITH VARYING SHAFT SPEED

TEST VARIABLE: SPEED (r/min)

TEST NUMBER	7: 14000 r/min	8: 16000	9: 18000	10: 20000	11: 22000	
FREQUENCY	RFI CONDUCTED VOLTAGE MEASUREMENTS: dB(uV)					
0.150 MHz	71	71.5	74	91.5	94	
0.160	70.5	71	73	90	93	
0.240	71	70.5	73	86	89	
0.550	55	56	59	79	81	
1.000	44.5	43.5	45.5	64	67.5	
1.400	42.5	43	45	63	65	
2.000	44.5	45	47.5	66.5	69	
3.500	48	49	51	71	74	
6.000	47.5	47	51	69	72	
10.00	46	46.5	47.5	68	73	
13.00	48.5	49.5	55	71	75	
22.00	47.5	48	54	68	71	
30.00	45	45	50	63.5	67	
	RFI RADIATED POWER MEASUREMENTS: dB(pW)					
30.00	37	37.5	39	57.5	62.5	
40.00	37.5	38	40	58	61.5	
46.00	37.5	38	41	59	62.5	
65.00	35	35	38	53.5	59	
90.00	27.5	28	30	47.5	50	
150.0	28	28	30.5	44	48	
180.0	27	27	30	44	46	
220.0	25	26	27	41.5	44	
300.0	22.5	23.5	24	37.5	39	

TABLE A2.7

TITLE: RFI CAUSED BY THE COMMUTATOR SWITCHING ACTION:
MEASURED RFI LEVELS FROM A 24 SEGMENT COMMUTATOR
AT 2.0A SUPPLY CURRENT WITH VARYING SHAFT SPEED

TEST VARIABLE: SPEED (r/min)

TEST NUMBER	1: 2000 r/min	2: 4000	3: 6000	4: 8000	5: 10000	6: 12000
FREQUENCY	RFI CONDUCTED VOLTAGE MEASUREMENTS: dB(uV)					
0.150 MHz	53	67	70	71	71.5	71.5
0.160	52.5	66.5	70	70.5	71	70
0.240	45.5	63.5	66.5	68.5	69	70
0.550	29	42	50	53.5	54	55.5
1.000	15.5	31	42	43	44	43
1.400	13	28	39	40	42	41.5
2.000	15.5	34.5	41.5	43	44	45.5
3.500	21	36.5	45.5	46	46.5	46.5
6.000	22	36	46	46	46	47
10.00	30	41	44.5	46	45.5	47
13.00	30.5	40.5	46	46.5	46	47.5
22.00	28	38	45	47	48	49
30.00	25.5	37	43	44	44	46
	RFI RADIATED POWER MEASUREMENTS: dB(pW)					
30.00	10.5	24	34	38	37	39.5
40.00	10	23.5	32	37.5	36.5	38
46.00	8.5	23	32	36	36	37
65.00	7	21	29	33	32	34.5
90.00	8	17	23	25	25.5	27
150.0	5.5	17	22	26	27	28
180.0	4.5	16	22	26	26	26.5
220.0	3	14	21	23	25.5	26
300.0	1.5	12	21	22	23	24

TABLE A2.8

TITLE: RFI CAUSED BY THE COMMUTATOR SWITCHING ACTION:
MEASURED RFI LEVELS FROM A 24 SEGMENT COMMUTATOR
AT 2.0A SUPPLY CURRENT WITH VARYING SHAFT SPEED

TEST VARIABLE: SPEED (r/min)

TEST NUMBER	7: 14000 r/min	8: 16000	9: 18000	10: 20000	11: 22000
FREQUENCY	RFI CONDUCTED VOLTAGE MEASUREMENTS: dB(uV)				
0.150 MHz	71	72	74	91	93
0.160	70.5	71	73	90	92
0.240	71	71.5	74	86	87
0.550	56	56	60	79	80
1.000	45	46.5	46	65	67
1.400	42	43	46	64	66
2.000	45	47	47.5	67	69
3.500	48	50	52	72	73
6.000	48	49	51.5	70	71
10.00	46	48	47.5	69.5	73.5
13.00	48	51	55.5	72	76
22.00	48	50	55	68.5	71.5
30.00	46	47	51	64	68
	RFI RADIATED POWER MEASUREMENTS: dB(pW)				
30.00	37	39	41	58	62
40.00	37.5	39	40	59	62
46.00	37.5	38.5	41.5	57	63
65.00	35	37	39	56	59
90.00	27.5	30	31	47	51
150.0	29	29	31	44.5	48.5
180.0	27	27	31	43	47
220.0	25	26.5	29	41	44
300.0	23	23	26	37	39

TABLE A2. 9

TITLE: RFI CAUSED BY THE COMMUTATOR SWITCHING ACTION: MEASURED RFI LEVELS FROM A 24 SEGMENT COMMUTATOR AT 2. 5A SUPPLY CURRENT WITH VARYING SHAFT SPEED

TEST VARIABLE: SPEED (r/min)

TEST NUMBER	1: 2000 r/min	2: 4000	3: 6000	4: 8000	5: 10000	6: 12000
FREQUENCY	RFI CONDUCTED VOLTAGE MEASUREMENTS: dB(uV)					
0.150 MHz	54	67.5	70	71	71	71.5
0.160	53	66	69.5	70	70.5	71
0.240	46	64	67	69	69	70
0.550	29.5	43	49.5	54	54.5	55
1.000	15	32	41.5	44	44.5	44
1.400	13.5	29	39	41	42	42
2.000	16	35	42	44	44.5	46
3.500	22	37	45	46.5	47	47
6.000	21.5	36.5	46	47	47	47.5
10.00	30.5	41.5	45	46.5	47	47.5
13.00	30	41	46.5	47	47.5	47.5
22.00	28.5	38	45	48	48.8	48.5
30.00	26	37	42	45	45	45
	RFI RADIATED POWER MEASUREMENTS: dB(pW)					
30.00	10	23	34	38	38	39
40.00	10.5	23	33	37	38	38
46.00	9	22	33	37	37	37.5
65.00	7.5	21	29.5	33.5	33.5	34
90.00	8	17	23	26	27	27
150.0	5	17.5	22.5	27.5	28	28.5
180.0	4	16	23	26.5	27	27
220.0	2	15	22.5	24	25	25.5
300.0	1.5	13	22	24	23	23

TABLE A2. 10

TITLE: RFI CAUSED BY THE COMMUTATOR SWITCHING ACTION: MEASURED RFI LEVELS FROM A 24 SEGMENT COMMUTATOR AT 2. 5A SUPPLY CURRENT WITH VARYING SHAFT SPEED

TEST VARIABLE: SPEED (r/min)

TEST NUMBER	7: 14000 r/min	8: 16000	9: 18000	10: 20000	11: 22000
FREQUENCY	RFI CONDUCTED VOLTAGE MEASUREMENTS: dB(uV)				
0.150 MHz	72	72	75	92	94
0.160	71	71	75	91	93
0.240	71.5	71	74.5	87	89
0.550	56	56.5	60.5	80	82
1.000	45.5	46	47	66	68
1.400	43.5	43.5	47	64	67
2.000	45.5	46	47.5	67	70
3.500	49	49.5	53	73	74
6.000	48.5	48	52	70	72
10.00	47	47.5	48	69	74
13.00	49.5	50	56	72	76
22.00	48.5	49	56	69	72
30.00	46	46.5	52	65	68
	RFI RADIATED POWER MEASUREMENTS: dB(pW)				
30.00	38	38	42	59	63
40.00	38.5	38.5	41	60	62
46.00	37.5	38	41	59	62
65.00	36	36.5	41	56	60
90.00	28.5	29	32.5	47.5	52
150.0	29	29	32	44	49
180.0	28	28	31	43	49
220.0	26	26.5	29	41.5	45
300.0	23.5	24	27	38	42

TABLE 42.11

TITLE: RFI CAUSED BY THE COMMUTATOR SWITCHING ACTION: MEASURED RFI LEVELS FROM A 24 SEGMENT COMMUTATOR AT 3.0A SUPPLY CURRENT WITH VARYING SHAFT SPEED

TEST VARIABLE: SPEED (r/min)

TEST NUMBER	1: 2000 r/min	2: 4000	3: 6000	4: 8000	5: 10000	6: 12000
FREQUENCY	RFI CONDUCTED VOLTAGE MEASUREMENTS: dB(uV)					
0.150 MHz	62	76	80	82.5	84	84
0.160	60	75	79	82	83	84
0.240	57	72.5	74	77	78	79
0.550	36	47	52	60	63	63.5
1.000	23	38	48.5	54	55.5	56
1.400	23	35	45	54	55	55.5
2.000	26.5	40.5	48	53	55	56
3.500	34	42	50.5	58	60	61.5
6.000	30	42.5	50	59	60	60
10.00	40	47	52	60	61	61.5
13.00	41	46	53	60	61.5	62
22.00	36	46	50	56	57	58
30.00	34	45	48	53	54	55
	RFI RADIATED POWER MEASUREMENTS: dB(pW)					
30.00	22.5	29	39	48.5	49	50
40.00	22	28.5	36.5	48	49	51
46.00	15	28	37	46.5	49	47
65.00	15	27	37	46	47	47
90.00	14.5	24	33.5	34	37	38
150.0	10	23.5	28	33	37	38
180.0	8	22	25	32	36	36.5
220.0	8	21	24	32	33	34
300.0	4	18	22	26	28	29

TABLE 42.12

TITLE: RFI CAUSED BY THE COMMUTATOR SWITCHING ACTION: MEASURED RFI LEVELS FROM A 24 SEGMENT COMMUTATOR AT 3.0A SUPPLY CURRENT WITH VARYING SHAFT SPEED

TEST VARIABLE: SPEED (r/min)

TEST NUMBER	7: 14000	8: 16000	9: 18000	10: 20000	11: 22000
FREQUENCY	RFI CONDUCTED VOLTAGE MEASUREMENTS: dB(uV)				
0.150 MHz	85	86	88	94.5	96
0.160	84	85.5	86	93	96
0.240	80	81	84	89	92
0.550	64	66	69	82	84
1.000	57.5	59	64.5	69	71
1.400	56	56	60	66	69
2.000	57	57	59.5	69	71
3.500	62	64	60	75	78
6.000	60.5	62	66	73	75
10.00	62.5	63	65.5	70	76
13.00	63	64	67	75	79
22.00	59	62	66	74	73
30.00	56	58	60	69	69
	RFI RADIATED POWER MEASUREMENTS: dB(pW)				
30.00	50.5	52	56	63	65
40.00	51	52	55.5	63	64.5
46.00	47.5	49	53.5	62	64
65.00	48	50	53	60	63
90.00	39	40.5	45	50	58
150.0	39	40	44	49.5	52
180.0	37	39	43	49	51
220.0	34	36	40.5	46	49
300.0	30	32	36	40	47

TABLE A2.13

TITLE: RFI CAUSED BY THE COMMUTATOR SWITCHING ACTION: MEASURED RFI LEVELS FROM A 22 SEGMENT COMMUTATOR AT 0.25A SUPPLY CURRENT WITH VARYING SHAFT SPEED

TEST VARIABLE: SPEED (r/min)

TEST NUMBER	1:	2:	3:	4:	5:	6:
	2000 r/min	4000	6000	8000	10000	12000
FREQUENCY	RFI CONDUCTED VOLTAGE MEASUREMENTS: dB(uV)					
0.150 MHz	41.5	59	67	68	71	71
0.160	41	58	66	67	70	70
0.240	34.5	49	57	62	62.5	62.5
0.550	26	42	51.5	57	57.5	57
1.000	10	24	35	41	45	46
1.400	10	23.5	32.5	40	41.5	42.5
2.000	14	29.5	37	46	46	48
3.500	22.5	32	42	48.5	49	49
6.000	18.5	30	40	47	47	49
10.00	22	31.5	42.5	47	51	50.5
13.00	18.5	29	42	48	47	49
22.00	20	32	43	50	50.5	51
30.00	15	26.5	36	43	44.5	45
	RFI RADIATED POWER MEASUREMENTS: dB(pW)					
30.00	8	13	21	26	30	30.5
40.00	8	13	20	26	28.5	29
46.00	7.5	12.5	20	24	28	28
65.00	7	12	19	23	25	26
90.00	6.5	11	18	20	23	25
150.0	3	10	15	19	21	24
180.0	-	7	14	18	21	22
220.0	-	4.5	12	17	20.5	21
300.0	-	3	8	16	20	20

TABLE A2.14

TITLE: RFI CAUSED BY THE COMMUTATOR SWITCHING ACTION: MEASURED RFI LEVELS FROM A 22 SEGMENT COMMUTATOR AT 0.25A SUPPLY CURRENT WITH VARYING SHAFT SPEED

TEST VARIABLE: SPEED (r/min)

TEST NUMBER	7:	8:	9:	10:	11:
	14000 r/min	16000	18000	20000	22000
FREQUENCY	RFI CONDUCTED VOLTAGE MEASUREMENTS: dB(uV)				
0.150 MHz	71	71.5	71.5	71.5	72
0.160	70	70.5	70.5	70.5	71
0.240	63	63	63.5	64	64
0.550	57	57.5	57.5	58	58
1.000	46	46	46.5	46.5	47
1.400	42	43	43	44	44
2.000	47	48	48	48	48
3.500	50	50	50.5	51	52
6.000	48	50	50	50	51
10.00	50	50.5	51	51	51.5
13.00	48	50	50	50.5	50
22.00	50	51	51.5	51	50.5
30.00	46	47	48	49	49
	RFI RADIATED POWER MEASUREMENTS: dB(pW)				
30.00	30.5	31	31	31.5	32
40.00	30	30	31	31.5	31.5
46.00	28	29	31	31	31
65.00	27.5	28	28.5	29	29.5
90.00	25.5	26	26	26	27
150.0	23	23	24	24	25.5
180.0	22.5	23	23	23	23
220.0	21	21.5	21	21.5	22
300.0	20.5	20	21	21	22

TABLE A2.15

TITLE: RFI CAUSED BY THE COMMUTATOR SWITCHING ACTION:
MEASURED RFI LEVELS FROM A 22 SEGMENT COMMUTATOR
AT 1.0A SUPPLY CURRENT WITH VARYING SHAFT SPEED

TEST VARIABLE: SPEED (r/min)

TEST NUMBER	1: 2000 r/min	2: 4000	3: 6000	4: 8000	5: 10000	6: 12000
FREQUENCY	RFI CONDUCTED VOLTAGE MEASUREMENTS: dB(uV)					
0.150 MHz	42	59.5	67	68.5	71.5	71.5
0.160	41.5	58	66	67	71	71
0.240	35	50	56.5	63	63	63.5
0.550	26.5	41.5	51.5	57.5	57	57.5
1.000	10.5	24.5	34	41.5	45	45
1.400	10	24	32.5	41	41.5	42
2.000	14.5	30	37.5	47	46.5	47
3.500	13	32.5	42.5	49	49.5	49.5
6.000	19	31	40	47.5	48	49.5
10.00	22	31.5	42	47	50.5	50.5
13.00	19	30	42	48	48	49.5
22.00	20.5	32.5	43	51	50	51.5
33.00	15.5	27	36.5	44	44.5	45.5
	RFI RADIATED POWER MEASUREMENTS: dB(pW)					
30.00	8.5	13.5	21	26.5	30	31
40.00	8	13	21	26	29	29.5
46.00	8	12	20	24.5	28	28.5
65.00	7.5	12	18.5	23	25.5	26.5
90.00	7	11.5	18	21	24	24
150.0	4	10.5	17	20.5	22	24
180.0	-	7	14	19	21	22.5
220.0	-	5	12	18	21	21
300.0	-	3.5	10	17	19	20

TABLE A2.16

TILTE: RFI CAUSED BY THE COMMUTATOR SWITCHING ACTION:
MEASURED RFI LEVELS FROM A 22 SEGMENT COMMUTATOR
AT 1.0A SUPPLY CURRENT WITH VARYING SHAFT SPEED

TEST VARIABLE: SPEED (r/min)

TEST NUMBER	7: 14000 r/min	8: 16000	9: 18000	10: 20000	11: 22000
FREQUENCY	RFI CONDUCTED VOLTAGE MEASUREMENTS: dB(uV)				
0.150 MHz	71.5	72	71.5	72	72
0.160	70.5	71	71	71.5	71.5
0.240	63.5	63.5	64	64	64.5
0.550	57	57.5	57.5	57.5	58.5
1.000	46.5	46.5	47	47	47.5
1.400	43	43.5	44	44.5	44.5
2.000	48	48.5	48.5	49	49
3.500	50.5	50.5	51	51	52
6.000	50	50	50.5	50.5	51
10.00	50.5	50.5	51	52	52
13.00	48	49	50	51	51
22.00	50.5	51	51	51	51.5
30.00	46.5	48.5	48	48	49
	RFI RADIATED POWER MEASUREMENTS: dB(pW)				
30.00	31	31.5	31.5	32	32
40.00	30	31	31	32	31.5
46.00	28.5	29.5	31	31	31.5
65.00	29	29	29	30	31
90.00	25	26	26	26	27
150.0	23	23.5	24	24.5	26
180.0	23	23	23	24	24
220.0	20	20.5	21	21.5	22
330.0	20.5	21	21	22	22

TABLE A2.17

TITLE: RFI CAUSED BY THE COMMUTATOR SWITCHING ACTION:
MEASURED RFI LEVELS FROM A 22 SEGMENT COMMUTATOR
AT 1.5A SUPPLY CURRENT WITH VARYING SHAFT SPEED

TEST VARIABLE: SPEED (r/min)

TEST NUMBER	1: 2000 r/min	2: 4000	3: 6000	4: 8000	5: 10000	6: 12000
FREQUENCY	RFI CONDUCTED VOLTAGE MEASUREMENTS: dB(uV)					
0.150 MHz	42.5	60	67	69.5	71.5	71
0.160	42	59	66	68	70.5	70
0.240	35	50	57	63	63	63.5
0.550	27	43	52	57	58	58.5
1.000	11	25	35	41.5	45.5	46.5
1.400	10	23	33	41	42	43
2.000	15	30	38	47	47	49
3.500	23	33	43	49	49	50
6.000	19	30	41	48	48	49
10.00	22	31.5	43	47.5	51.5	50.5
13.00	19	29	42.5	48	48	48.5
22.00	21	32.5	44	51	51	51.5
30.00	16	27	37	45	45	46.5
	RFI RADIATED POWER MEASUREMENTS: dB(pW)					
30.00	9	13.5	21.5	27.5	31	31.5
40.00	7.5	13	21	26	29	30
46.00	8.5	12	20	25	28	28
65.00	7	12	19	24	26	27
90.00	6.5	12.0	18	20	24	25.5
150.0	4	9	16	20	23	24
180.0	-	7	15	19	22	23
220.0	-	5	13	17	20	21
300.0	-	4	9.5	16.5	20	20.5

TABLE A2.18

TITLE: RFI CAUSED BY THE COMMUTATOR SWITCHING ACTION:
MEASURED RFI LEVELS FROM A 22 SEGMENT COMMUTATOR
AT 1.5A SUPPLY CURRENT WITH VARYING SHAFT SPEED

TEST VARIABLE: SPEED (r/min)

TEST NUMBER	7: 14000 r/min	8: 16000	9: 18000	10: 20000	11: 22000
FREQUENCY	RFI CONDUCTED VOLTAGE MEASUREMENTS: dB(uV)				
0.150 MHz	72	72	72	71.5	72
0.160	71	71	71	70.5	71
0.240	64	64	64	64	64.5
0.550	58	59	58.5	59	59
1.000	47	47	47	45.5	47.5
1.400	43.5	44	44	45	45
2.000	48.5	49	49	49.5	49.5
3.500	51	51	51.5	52	53
6.000	49	50	50.5	51	52
10.00	50.5	51	51.5	52.5	52
13.00	48.5	50.5	50	51	50
22.00	51	52	51.5	52	51
30.00	47	49	48	50	50
	RFI RADIATED POWER MEASUREMENTS: dB(pW)				
30.00	31	32	32	32.5	33.5
40.00	30.5	31	31.5	32	32
46.00	29	30	31.5	31	32
65.00	29	29	29	30	31
90.00	26	26.5	26.5	26.5	27.5
150.0	24	24	25	25	26
180.0	23	23.5	24	24	24
220.0	20.5	21	21.5	22	22.5
300.0	21	21.5	22	22.5	23

TABLE A2.19

TITLE: RFI CAUSED BY THE COMMUTATOR SWITCHING ACTION:
MEASURED RFI LEVELS FROM A 22 SEGMENT COMMUTATOR
AT 2.0A SUPPLY CURRENT WITH VARYING SHAFT SPEED

TEST VARIABLE: SPEED (r/min)

TEST NUMBER	1: 2000 r/min	2: 4000	3: 6000	4: 8000	5: 10000	6: 12000
FREQUENCY	RFI CONDUCTED VOLTAGE MEASUREMENTS: dB(uV)					
0.150 MHz	43	61	68	69.5	71.5	71.5
0.160	42.5	60	67	68	70.5	70.5
0.240	36	50.5	57	63	63	64
0.550	28	44	53	57.5	58.5	58
1.000	12	26	36	42	46	46.5
1.400	11.5	24	34	41	43	43.5
2.000	15	31	38	47.5	48	48.5
3.500	23.5	33	43	49.5	50	51
6.000	20	30	42	49	50	50
10.00	22	31	42	48	51	50.5
13.00	19	30	42.5	48.5	48.5	48.5
22.00	21.5	33	45	51.5	52	52
30.00	17	28	37.5	46	46	47
	RFI RADIATED POWER MEASUREMENTS: dB(pW)					
30.00	10	14	22	28	30	30.5
40.00	9	13	22	27	29.5	29
46.00	8.5	12.5	21	26	28	28
65.00	8	12	20	25	28	29
90.00	7	11.5	19.5	21	24	25
150.0	5	10	17	20	24	24.5
180.0	-	8	16	19.5	23	23.5
220.0	-	6	14	18	20.5	21
300.0	-	5	10	17	20	20

TABLE A2.20

TITLE: RFI CAUSED BY THE COMMUTATOR SWITCHING ACTION:
MEASURED RFI LEVELS FROM A 22 SEGMENT COMMUTATOR
AT 2.0A SUPPLY CURRENT WITH VARYING SHAFT SPEED.

TEST VARIABLE: SPEED (r/min)

TEST NUMBER	7: 14000 r/min	8: 16000	9: 18000	10: 20000	11: 22000	
FREQUENCY	RFI CONDUCTED VOLTAGE MEASUREMENTS: dB(uV)					
0.150 MHz	72	72.5	72.5	73	73	
0.160	71	72	72	72	72.5	
0.240	64.5	65	65	64.5	65	
0.550	58	58.5	60	59.5	60	
1.000	47	47.5	47.5	48	48	
1.400	44	44	44.5	44	46	
2.000	49	49	49.5	49.5	50	
3.500	51.5	52	53	54	54	
6.000	50	51	52	52.5	53	
10.00	51	51	52	52	52	
13.00	49	49.5	49.5	50	51	
22.00	52	51.5	52	52	52	
30.00	48	48.5	49	49	50	
	RFI RADIATED POWER MEASUREMENTS: dB(pW)					
30.00	30.5	31	32	33	34	
40.00	30	30.5	31	32	32	
46.00	29.5	30	30	30.5	32	
65.00	29	30	30	30.5	31	
90.00	25.5	27	26.5	27	28	
150.0	25	25	26	26.5	27	
180.0	24	24	24	25.5	25	
220.0	21	22	23	23	23	
300.0	21	21	21	22	23	

TABLE A2.21

TITLE: RFI CAUSED BY THE COMMUTATOR SWITCHING ACTION: MEASURED RFI LEVELS FROM A 22 SEGMENT COMMUTATOR AT 2.5A SUPPLY CURRENT WITH VARYING SHAFT SPEED

TEST VARIABLE: SPEED (r/min)

TEST NUMBER	1: 2000 r/min	2: 4000	3: 6000	4: 8000	5: 10000	6: 12000
FREQUENCY	RFI CONDUCTED VOLTAGE MEASUREMENTS: dB(uV)					
0.150 MHz	44	62	68	70	72	72
0.160	43	61	67	69	71	71.5
0.240	37	51	58	63	63	64.5
0.550	28	44.5	54	58	59	58.4
1.000	13	26	36	42	46	46.5
1.400	12	24.5	35	41.5	43.5	43
2.000	15	31	39	48	47.5	49
3.500	24	34	43	50	50	51.5
6.000	21	32	42	49	50	50
10.00	22	32	43	48	50.5	50
13.00	19.5	30	43	48.5	49	49.5
22.00	22	32	45	52	52	52
30.00	18	29	38	46.5	47	48
	RFI RADIATED POWER MEASUREMENTS: dB(pW)					
30.00	10	15	23	29	30	31
40.00	9.5	14	22	28	29.5	30
46.00	9	12.5	21	27	29	29.5
65.00	8.5	12	20	26	29	29
90.00	7	11.5	19.5	22	26	26
150.0	5	11	18	21	25	25
180.0	-	9	15.5	20	24	24.5
220.0	-	7	14	19	22.5	23
300.0	-	6	11	18	21	22

TABLE A2.22

TITLE: RFI CAUSED BY THE COMMUTATOR SWITCHING ACTION: MREASURED RFI LEVELS FROM A 22 SEGMENT COMMUTATOR AT 2.5A SUPPLY CURRENT WITH VARYING SHAFT SPEED

TEST VARIABLE: SPEED (r/min)

TEST NUMBER	7: 14000 r/min	8: 16000	9: 18000	10: 20000	11: 22000	
FREQUENCY	RFI CONDUCTED VOLTAGE MEASUREMENTS: dB(uV)					
0.150 MHz	72.5	72.5	73	73	73	
0.160	72	72	72.5	72.5	72.5	
0.240	65	65.5	65	65	65	
0.550	59	59	59.5	60	61	
1.000	47	47	47.5	48	48.5	
1.400	44	45	45	46	46.5	
2.000	49.5	50	50.5	51	51	
3.500	52	53	53.5	54	54	
6.000	51	51	51.5	52	53	
10.00	51	51	51	51.5	52	
13.00	49	50	50	50.5	51	
22.00	53	53	53	52.5	53	
30.00	49	49	49	49.5	50	
	RFI RADIATED POWER MEASUREMENTS: dB(pW)					
30.00	31	32	33	34	34.5	
40.00	30	30	31	32	32.5	
46.00	29.5	30	31	31.5	32	
65.00	29.5	31	31	31	31.5	
90.00	26	27	28	28.5	29	
150.0	25.5	26	27	27.5	28	
180.0	24.5	26	27	26	26	
220.0	22	23	24	24	24	
300.0	21.5	22	22	22.5	23	

TABLE A2.23

TITLE: RFI CAUSED BY THE COMMUTATOR SWITCHING ACTION:
MEASURED RFI LEVELS FROM A 22 SEGMENT COMMUTATOR
AT 3.0A SUPPLY CURRENT WITH VARYING SHAFT SPEED

TEST VARIABLE: SPEED (r/min)

TEST NUMBER	1: 2000 r/min	2: 4000	3: 6000	4: 8000	5: 10000	6: 12000
FREQUENCY	RFI CONDUCTED VOLTAGE MEASUREMENTS: dB(uV)					
0.150 MHz	63	79	85	87	89.5	90
0.160	62	78	84	86.5	89	89
0.240	54	70.5	77.5	80	82	82
0.550	47.5	63	71	73	75	75.5
1.000	28	45	53	55.5	57	57
1.400	26	42	50	52	54	53
2.000	30	44	52.5	55	57	57.5
3.500	36	52	58	60	61	61
6.000	33	49	55	57.5	59	59.5
10.00	36	55	63.5	65	67	67
13.00	33	50.5	58	60	62	62.5
22.00	32	49	58	60.5	61	61
30.00	30	44	53	55	57	57.5
	RFI RADIATED POWER MEASUREMENTS: dB(pW)					
30.00	24	34	40.5	42	44	44
40.00	23.5	33	40	41	43	43
46.00	23	30	39	40	43	43
65.00	15	28	38.5	40	41	41
90.00	12	27	33	34	36	36
150.0	10	27	31	32	34	34
180.0	8	24	30.5	32	32	32
220.0	7	22	29	30	30	30
300.0	3	19	23	25	27	27

TABLE A2.24

TITLE: RFI CAUSED BY THE COMMUTATOR SWITCHING ACTION:
MEASURED RFI LEVELS FROM A 22 SEGMENT COMMUTATOR
AT 3.0A SUPPLY CURRENT WITH VARYING SHAFT SPEED

TEST VARIABLE: SPEED (r/min)

TEST NUMBER	7: 14000 r/min	8: 16000	9: 18000	10: 20000	11: 22000
FREQUENCY	RFI CONDUCTED VOLTAGE MEASUREMENTS: dB(uV)				
0.150 MHz	90	91	93	93.5	93.5
0.160	89	90	92	92	93
0.240	82	83	84	86	86
0.550	76	76	78	80	80.5
1.000	57.5	58	60	61	62
1.400	53	54	56	57	57
2.000	58	58	59	60	60
3.500	62	63	64	64	64
6.000	60	61	62	63	63.5
10.00	67.5	68	69	70	71
13.00	63	64	66	67	67
22.00	62	63	65	65	66
30.00	58	59	60	60	60.5
	RFI RADIATED POWER MEASUREMENTS: dB(pW)				
30.00	45	46	48	49	50
40.00	44	45	44	46	50
46.00	43	43	43	44	46
65.00	41	41	41	43	44
90.00	35	36	37	40	42
150.0	33	35	37	39	40
180.0	32	33	35	37	38
220.0	30	33	33	35	36
300.0	27.5	31	32	35	35

TABLE A2.25

TITLE: RFI CAUSED BY THE COMMUTATOR SWITCHING ACTION: MEASURED RFI LEVELS FROM A 21 SEGMENT COMMUTATOR AT 0.25A SUPPLY CURRENT WITH VARYING SHAFT SPEED

TEST VARIABLE: SPEED (r/min)

TEST NUMBER	1: 2000 r/min	2: 4000	3: 6000	4: 8000	5: 10000	6: 12000
FREQUENCY	RFI CONDUCTED VOLTAGE MEASUREMENTS: dB(uV)					
0.150 MHz	40.5	58	66.5	65	73	73
0.160	40	57	65.5	68	72	72
0.240	25	41	51	54	57	57
0.550	18	32	42	45	48.5	48
1.000	7.5	16	31.5	38	40	40.5
1.400	7	18.5	29	36.5	38	38
2.000	6.5	19	29.5	36	36.5	36.5
3.500	14	25.5	34	40.5	41	41
6.000	22	33	42	45	47	47.5
10.00	20	32	40	44	46	47
13.00	22.5	32.5	41	45	47	47.5
22.00	22	34	41	45	47	47.5
30.00	17	28	35	41.5	45	46
	RFI RADIATED POWER MEASUREMENTS: dB(pW)					
30.00	2.5	15	22	29.5	31	32
40.00	3	15.5	23	31	30	31
46.00	1	13	21	27	29	28
65.00	-	12.5	18	26.5	28	27.5
90.00	-	9	13	24	28	27
150.0	-	9	14	23	26	25
180.0	-	7.5	12	21	25	24
220.0	-	7	10	17	23	22
300.0	-	4.5	6	15	22	21

TABLE A2.26

TITLE: RFI CAUSED BY THE COMMUTATOR SWITCHING ACTION: MEASURED RFI LEVELS FROM A 21 SEGMENT COMMUTATOR AT 0.25A SUPPLY CURRENT WITH VARYING SHAFT SPEED

TEST VARIABLE: SPEED (r/min)

TEST NUMBER	7: 14000 r/min	8: 16000	9: 18000	10: 20000	11: 22000
FREQUENCY	RFI CONDUCTED VOLTAGE MEASUREMENTS: dB(uV)				
0.150 MHz	73	73	74	74	74.5
0.160	72.5	72	73.5	73	74
0.240	57.5	58	58	58.5	58.5
0.550	48	48.5	49	50	50
1.000	41	40.5	41	41.5	41
1.400	39	39	39.5	39.5	40
2.000	37	38	37.5	38	38
3.500	41.5	42	41.5	42	43
6.000	48	47.5	48	48	48
10.00	47.5	47.5	47	47.5	47
13.00	48	48	48	49	49
22.00	48	48	48.5	49	49
30.00	46	47	47	47.5	48
	RFI RADIATED POWER MEASUREMENTS: dB(pW)				
30.00	32	32	32.5	33	33
40.00	31	31	31.5	32	32
46.00	28.5	29	29	31	31.5
65.00	28	29	28.5	31	31.5
90.00	28	28	28	29	29
150.0	26	26	27	28	28
180.0	24	24	25	26	27
220.0	22.5	23	23	26	27
300.0	21.5	21.5	22	23	24

TABLE A2.27

TITLE: RFI CAUSED BY THE COMMUTATOR SWITCHING ACTION:
MEASURED RFI LEVELS FROM A 21 SEGMENT COMMUTATOR
AT 1.0A SUPPLY CURRENT WITH VARYING SHAFT SPEED

TEST VARIABLE: SPEED (r/min)

TEST NUMBER	1: 2000 r/min	2: 4000	3: 6000	4: 8000	5: 10000	6: 12000
FREQUENCY	RFI CONDUCTED VOLTAGE MEASUREMENTS: dB(uV)					
0.150 MHz	41	58	66	69	73	73.5
0.160	40	57	65.5	68.5	72	72
0.240	25	41.5	51	54	57.5	57
0.550	17	32.5	42	45.5	49	48.5
1.000	7.5	16.5	32	38	40	41
1.400	7	18.5	29.5	37	38.5	38
2.000	6.5	19	29.5	37	37	37
3.500	14	26	34	41	40.5	40.5
6.000	22	33	42.5	45	46	47
10.00	20.5	32	40.5	44	46.5	47
13.00	23	33	41	45.5	47	46.5
22.00	22	24	41	45.5	47	46.5
30.00	18	28.5	35	41	45.5	46
	RFI RADIATED POWER MEASUREMENTS: dB(pW)					
30.00	3	16	22	29.5	31	32
40.00	3	15.5	23.5	30.5	31	31
46.00	1	13	21.5	26	29.5	29
65.00	-	13	18	25	28.5	28
90.00	-	9.5	13.5	23	28	28.5
150.0	-	9	14	23	26	26.5
180.0	-	8	12	21	25	25.5
220.0	-	7	10	17.5	24	24
300.0	-	5	7	15.5	23	22.5

TABLE A2.28

TITLE: RFI CAUSED BY THE COMMUTATOR SWITCHING ACTION:
MEASURED RFI LEVELS FROM A 21 SEGMENT COMMUTATOR
AT 1.0A SUPPLY CURRENT WITH VARYING SHAFT SPEED

TEST VARIABLE: SPEED (r/min)

TEST NUMBER	7: 14000 r/min	8: 16000	9: 18000	10: 20000	11: 22000
FREQUENCY	RFI CONDUCTED VOLTAGE MEASUREMENTS: dB(uV)				
0.150 MHz	74	74	74.5	74.5	75
0.160	73	73	73	73.5	74.5
0.240	57.5	57	57.5	58	58.5
0.550	48	49	50	49.5	50
1.000	41.5	41	41.5	42	41.5
1.400	38.5	39	38.5	39	40
2.000	38.5	38.5	38.5	39	39
3.500	41	41	42.5	42.5	42.5
6.000	48.5	48	49	48	48.5
10.00	48.5	47	47.5	47.5	47.5
13.00	47.5	48	48	48	49
22.00	47.5	48	48	48	49
30.00	46	47	47.5	47.5	48
	RFI RADIATED POWER MEASUREMENTS: dB(pW)				
30.00	32.5	32.5	33	33.5	34
40.00	31	31.5	32	32	33
46.00	29	30	30	31	32
65.00	29	30	30	31	31
90.00	29	29	28.5	28	29
150.0	27	27	27	27.5	28.5
180.0	26	26.5	26.5	27.5	27
220.0	25	26	26.5	27	27
300.0	22.5	23	24	23	24

TABLE A2.29

TITLE: RFI CAUSED BY THE COMMUTATOR SWITCHING ACTION:
MEASURED RFI LEVELS FROM A 21 SEGMENT COMMUTATOR
AT 1.5A SUPPLY CURRENT WITH VARYING SHAFT SPEED

TEST VARIABLE: SPEED (r/min)

TEST NUMBER	1: 2000 r/min	2: 4000	3: 6000	4: 8000	5: 10000	6: 12000
FREQUENCY	RFI CONDUCTED VOLTAGE MEASUREMENTS: dB(uV)					
0.150 MHz	41	58	66	69.5	73	72.5
0.160	40.5	57	65.5	68	72	72
0.240	25	42	51	55	57	57.5
0.550	17	33	42	46	48	49
1.000	8	17	32	39	41	42
1.400	7	19	30	37	38	38.5
2.000	7	19	30	36.5	37	38
3.500	15	26	35	41	41.5	42
6.000	23	34	43	46	47	48
10.00	20	32	41	45	46.5	48.5
13.00	23	34	41	45	47	47
22.00	22	34	41	45	47	47
30.00	18	29	36	42	46	46
	RFI RADIATED POWER MEASUREMENTS: dB(pW)					
30.00	2	15	22.5	30	32	32.5
40.00	3	16	24	32	31	31
46.00	1	13	22	28	29.5	30
65.00	-	13	19	27	29	29
90.00	-	10	14	25	29	28.5
150.0	-	9	15	24	27	27
180.0	-	8	12	21	26	26.5
220.0	-	7	10	17	24	25
300.0	-	5	6.5	15	22.5	24

TABLE A2.30

TITLE: RFI CAUSED BY THE COMMUTATOR SWITCHING ACTION:
MEASURED RFI LEVELS FROM A 21 SEGMENT COMMUTATOR
AT 1.5A SUPPLY CURRENT WITH VARYING SHAFT SPEED

TEST VARIABLE: SPEED (r/min)

TEST NUMBER	7: 14000 r/min	8: 16000	9: 18000	10: 20000	11: 22000
FREQUENCY	RFI CONDUCTED VOLTAGE MEASUREMENTS: dB(uV)				
0.150 MHz	74	73.5	75	74	75.5
0.160	73	72.5	74	73	74
0.240	58	58	58.5	59	59
0.550	48.5	49	50	51	50.5
1.000	41.5	41	42	42.5	42
1.400	39	39	40	40	40.5
2.000	39	38	38.5	39	39
3.500	41.5	42	42.5	43	43
6.000	48.5	48	48.5	49	48.5
10.00	47.5	47	47.5	47.5	47
13.00	47.5	48	49	50	49.5
22.00	47.5	48	49	49	49.5
30.00	46.5	47	47	48	48
	RFI RADIATED POWER MEASUREMENTS: dB(pW)				
30.00	32	31	33	33	34
40.00	30.5	31	31	33	32
46.00	30	30	30.5	32.5	32
65.00	29.5	30	30	31	31.5
90.00	29	29	28.5	29	29.5
150.0	27.5	27	27	28	28
180.0	26.5	26.5	27	28	27.5
220.0	24.5	25	26.5	27	27.5
300.0	23	24	24.5	23.5	24.5

TABLE A2.31

TITLE: RFI CAUSED BY THE COMMUTATOR SWITCHING ACTION:
MEASURED RFI LEVELS FROM A 21 SEGMENT COMMUTATOR
AT 2.0A SUPPLY CURRENT WITH VARYING SHAFT SPEED

TEST VARIABLE: SPEED (r/min)

TEST NUMBER	1: 2000 r/min	2: 4000	3: 6000	4: 8000	5: 10000	6: 12000
FREQUENCY	RFI CONDUCTED VOLTAGE MEASUREMENTS: dB(uV)					
0.150 MHz	42	58	66.5	70	73	73
0.160	41	57.5	66	69	72	72.5
0.240	25	42	52	56	58	58
0.550	17	33.5	43	46	48	49
1.000	8	17.5	32	39.5	41	42
1.400	7.5	20	31	38	38	38.5
2.000	7.5	19	30	37	37	38
3.500	17	26.5	36	41	41	41.5
6.000	24	34.5	44	46	48.5	48.5
10.00	21	33	42	45.5	46.5	47
13.00	23	34	41	45.5	47	47
22.00	23	34	41.5	45	47	47
30.00	18	29	37	42	45.5	46
	RFI RADIATED POWER MEASUREMENTS: dB(pW)					
30.00	4	16	23	31	33	32.5
40.00	5	17	24	32	32	32
46.00	1	13	23	30	29	29.5
65.00	-	12	20	28	29	29
90.00	-	11	15	26	28.5	28.5
150.0	-	10	15	25	28	28
180.0	-	9	12	22	27	27
220.0	-	8	10	18	25	24.5
300.0	-	5.5	6.5	16	23	22.5

TABLE A2.32

TITLE: RFI CAUSED BY THE COMMUTATOR SWITCHING ACTION:
MEASURED RFI LEVELS FROM A 21 SEGMENT COMMUTATOR
AT 2.0A SUPPLY CURRENT WITH VARYING SHAFT SPEED

TEST VARIABLE: SPEED (r/min)

TEST NUMBER	7: 14000 r/min	8: 16000	9: 18000	10: 20000	11: 22000
FREQUENCY	RFI CONDUCTED VOLTAGE MEASUREMENTS: dB(uV)				
0.150 MHz	74	73.5	74	75	75
0.160	73	72.5	74	74	74.5
0.240	58	58	58	59	59
0.550	49	49	49	51	51
1.000	42	41	42	43	43
1.400	39.5	39	40	41	41.5
2.000	39	38	39	40	40
3.500	42	42.5	43	44	43
6.000	49	49	49	49	49.5
10.00	47.5	47.5	48	48	48.5
13.00	47.5	48	50	50	50
22.00	47	48	49	49.5	49.5
30.00	46	47	48.5	49	49
	RFI RADIATED POWER MEASUREMENTS: dB(pW)				
30.00	33	33	33	33	34
40.00	31	32	32	32	33
46.00	30	30.5	31	32	32
65.00	29.5	30	30	31.5	31
90.00	29	29	29	29	30
150.0	28	27	27.5	28	29
180.0	27	26	27	27.5	27.5
220.0	25	25	26	27	27
300.0	23	22	24	25	25

TABLE A2.33

TITLE: RFI CAUSED BY THE COMMUTATOR SWITCHING ACTION: MEASURED RFI LEVELS FROM A 21 SEGMENT COMMUTATOR AT 2.5A SUPPLY CURRENT WITH VARYING SHAFT SPEED

TEST VARIABLE: SPEED (r/min)

TEST NUMBER	1: 2000 r/min	2: 4000	3: 6000	4: 8000	5: 10000	6: 12000
FREQUENCY	RFI CONDUCTED VOLTAGE MEASUREMENTS: dB(uV)					
0.150 MHz	42.5	58	67	69.5	73	73.5
0.160	42	58	66	69	73	73
0.240	25	43	53	57	57.5	58
0.550	18	34	43	48	48.5	49
1.000	8.5	18	33	39	41.5	42.5
1.400	8	20	32	38	38.5	39
2.000	8	19	30	38	38	38
3.500	17	27	36	41.5	42	41.5
6.000	24	35	44.5	46	48	48.5
10.00	21	33	43	46	47	47
13.00	23.5	34.5	42	46	47.5	47.5
22.00	23.5	34.5	42	43	47.5	47.5
30.00	19	30	38	42	46	46.5
	RFI RADIATED POWER MEASUREMENTS: dB(pW)					
30.00	4	18	24	32	33	33
40.00	4.5	18	24	31.5	34	32
46.00	1.5	14	23	30	30.5	30
65.00	-	12	20	29	29.5	30
90.00	-	10.5	15	27	28	29
150.0	-	10	14.5	26	28	29
180.0	-	10	12	24	28	27.5
220.0	-	9	10	19	25	25
300.0	-	6	7	17	24	24

TABLE A2.34

TITLE: RFI CAUSED BY THE COMMUTATOR SWITCHING ACTION: MEASURED RFI LEVELS FROM A 21 SEGMENT COMMUTATOR AT 2.5A SUPPLY CURRENT WITH VARYING SHAFT SPEED

TEST VARIABLE: SPEED (r/min)

TEST NUMBER	7: 14000 r/min	8: 16000	9: 18000	10: 20000	11: 22000	
FREQUENCY	RFI TERMIMAL VOLTAGE MEASUREMENTS: dB(uV)					
0.150 MHz	75	74.5	75	75	75.5	
0.160	74.5	74	75	74.5	75	
0.240	59	59	59.5	59.5	60	
0.550	49	49.5	50	51	51	
1.000	43	44	44.5	44.5	44.5	
1.400	40	41	41	41.5	42	
2.000	39.5	40	40	39.5	40	
3.500	43	44	44	44.5	44.5	
6.000	50	50	49.5	50	50	
10.00	48	48.5	48.5	49	49	
13.00	49	49.5	49	49.5	50	
22.00	49	49.5	49	49.5	50	
30.00	46	47	48	48	48.5	
	RFI RADIATED POWER MEASUREMENTS: dB(pW)					
30.00	34	34	34	34.5	34.5	
40.00	32	33	33	34	34	
46.00	30	32	32	33	33	
65.00	30	31	31.5	32	32	
90.00	30	30	30.5	30.5	30.5	
150.0	29	30	30	30	29.5	
180.0	28	29	29.5	29	28	
220.0	26	26	26	26.5	27	
300.0	24	23	23	23.5	24	

TABLE A2.35

TITLE: RFI CAUSED BY THE COMMUTATOR SWITCHING ACTION:
MEASURED RFI LEVELS FROM A 21 SEGMENT COMMUTATOR
AT 3.0A SUPPLY CURRENT WITH VARYING SHAFT SPEED

TEST VARIABLE: SPEED (r/min)

TEST NUMBER	1:	2:	3:	4:	5:	6:
	2000 r/min	4000	6000	8000	10000	12000
FREQUENCY	RFI CONDUCTED VOLTAGE MEASUREMENTS: dB(uV)					
0.150 MHz	54	71	79	82	86	86
0.160	53	70.5	78	81	85	85.5
0.240	35	51	60	64	69	69
0.550	28	43	53	56	60	61
1.000	20	28.5	44	50	52	53
1.400	19	30	41.5	49	50	49.5
2.000	9	21	40	48	49	49.5
3.500	31	43	51	58	42	52.5
6.000	32	44	52	59	60	59
10.00	34	46	54	58	61	61.5
13.00	26	38	55	59.5	60	60
22.00	34	37	54	59.5	60	60
30.00	31	41	48	54	59	59.5
	RFI RADIATED POWER MEASUREMENTS: dB(pW)					
30.00	12	25	33	40.5	43	43
40.00	10	24	32	41	42	42
46.00	8	20	28	37	40	41
65.00	2	18	26	36	40	40
90.00	1	15	22	34	36.5	36.5
150.0	-	15	23	33	34	35
180.0	-	12	19	31	33	33.5
220.0	-	9	15	28	32	32.5
300.0	-	6	8	26	30	31

TABLE A2.36

TITLE: RFI CAUSED BY THE COMMUTATOR SWITCHING ACTION:
MEASURED RFI LEVELS FROM A 21 SEGMENT COMMUTATOR
AT 3.0A SUPPLY CURRENT WITH VARYING SHAFT SPEED

TEST VARIABLE: SPEED (r/min)

TEST NUMBER	7:	8:	9:	10:	11:
	14000 r/min	16000	18000	20000	22000
FREQUENCY	RFI CONDUCTED VOLTAGE MEASUREMENTS: dB(uV)				
0.150 MHz	86.5	86.5	88	88	90
0.160	86	86	87.5	87.5	89
0.240	70	72	72	73	74
0.550	60.5	61	62	62	62
1.000	53	54	54	54.5	55
1.400	50	50	50.5	51	52
2.000	50	49.5	49.5	50	51
3.500	52.5	53	53	53.5	54
6.000	59.5	60	60	61	61
10.00	62.5	62	62.5	63	63
13.00	61	61.5	62	63	62.5
22.00	61	61	61	61.5	62
30.00	60	59.5	60	60	60.5
	RFI RADIATED POWER MEASUREMENTS: dB(pW)				
30.00	44	44.5	45	45	45.5
40.00	42.5	43	44	44.5	44
46.00	40.5	40.5	41	41.5	42
65.00	40.5	40	40	41	41.5
90.00	37.5	38	38.5	39	39
150.0	35.5	36	37	37	37.5
180.0	34	34	35	35	36
220.0	33	33.5	34	34	35
300.0	30.5	31	32	32.5	33

TABLE A2.37

TITLE: RFI CAUSED BY THE COMMUTATOR SWITCHING ACTION:
MEASURED RFI LEVELS FROM A COPPER SLIP RING
AT 1.5A SUPPLY CURRENT WITH VARYING SHAFT SPEED

TEST VARIABLE SPEED (r/min)

TEST NUMBER	1: 2000 r/min	2: 4000	3: 6000	4: 8000	5: 10000	6: 12000
FREQUENCY	RFI CONDUCTED VOLTAGE MEASUREMENTS: dB(uV)					
0.150 MHz	15	17	19.5	23.5	26	29
0.160	14	16	18	22	25	28
0.240	11	13	15	18	21	25
0.550	8	10	12	14	15.5	17
1.000	6.5	8.5	10	11.5	12	15
1.400	4.5	7	8.5	9	10.5	12
2.000	3.5	5	7	8.5	10.5	13
3.500	3.5	5.5	7	8	10.5	14
6.000	2	4	6.5	7.5	9	13
10.00	3	6	8	10	11	16
13.00	1	3	5	6	7.5	11
22.00	1.5	3	5	7	8	12
30.00	2.5	2.5	5	6	7	10
	RFI RADIATED POWER MEASUREMENTS: dB(pW)					
30.00	-	-	0.5	1	1	1.5
40.00	-	-	-	1	1	1
46.00	-	-	-	-	-	1
65.00	-	-	-	-	-	-
90.00	-	-	-	-	-	-
150.0	-	-	-	-	-	-
180.0	-	-	-	-	-	-
220.0	-	-	-	-	-	-
300.0	-	-	-	-	-	-

TABLE A2.38

TITLE: RFI CAUSED BY THE COMMUTATOR SWITCHING ACTION:
> MEASURED RFI LEVELS FROM A COPPER SLIP RING
AT 1.5A SUPPLY CURRENT WITH VARYING SHAFT SPEED

TEST VARIABLE: SPEED (r/min)

TEST NUMBER	7: 14000 r/min	8: 16000	9: 18000	10: 20000	11: 22000
FREQUENCY	RFI CONDUCTED VOLTAGE MEASUREMENTS: dB(uV)				
0.150 MHz	33	36.5	37.5	40	42
0.160	32	36	37	39	41
0.240	29	31	32	34	35
0.550	19.5	23	24	25	26.5
1.000	16	19	20	20.5	21
1.400	15	18	19	20.5	20.5
2.000	15	17.5	19	19.5	20
3.500	16	20	21	22	23
6.000	16.5	21	22	23	24
10.00	17.5	22	22.5	24	25
13.00	15	21	21.5	23	24
22.00	14	18.5	19	19.5	21
30.00	12	16.5	17	18	20
	RFI RADIATED POWER MEASUREMENTS: dB(pW)				
30.00	2	4	5	6	7.5
40.00	1.5	3	4	5.5	6
46.00	1	2	3.5	5	5.5
65.00	0.5	1	2	3	4
90.00	-	-	1	2	3
150.0	-	-	-	1	1.5
180.0	-	-	-	-	-
220.0	-	-	-	-	-
300.0	-	-	-	-	-

TABLE A2.39

TITLE: RFI CAUSED BY THE COMMUTATOR SWITCHING ACTION:
MEASURED RFI LEVELS FROM A COPPER SLIP RING
AT 18000 r/min WITH VARYING SUPPLY CURRENT

TEST VARIABLE: CURRENT (A)

TEST NUMBER	1: 0.25A	2: 1.0A	3: 1.5A	4: 2.0A	5: 2.5A	6: 3.0A
FREQUENCY	RFI CONDUCTED VOLTAGE MEASUREMENTS: dB(uV)					
0.150 MHz	35	36.5	37.5	38.5	40	45
0.160	34.5	36	37	38	39	44
0.240	30	31	32	33	35	40
0.550	22	23	24	25	27	30
1.000	17.5	19.5	20	20.5	22.5	24.5
1.400	16	18	19	20	22	24
2.000	16	18	19	20	22	24
3.500	18	20.5	21	22.5	23.5	26
6.000	18.5	21	22	23	24	27
10.00	22	22.5	22.5	24	26	28
13.00	21	21.5	21.5	23	25	27.5
22.00	19	19	19	21	23	27.5
30.00	17	17	17	18	19.5	21
	RFI RADIATED POWER MEASUREMENTS: dB(pW)					
30.00	4.5	5	5	5.5	6.5	9
40.00	3.5	4	4	4.5	5	8.5
46.00	3	3	3.5	3.5	4	5.5
65.00	1.5	1.5	2	2.5	3	4.5
90.00	-	-	1	1.5	2.5	3
150.0	-	-	-	-	1	1
180.0	-	-	-	-	-	-
220.0	-	-	-	-	-	-
300.0	-	-	-	-	-	-

TABLE A2.40

TITLE: RFI CAUSED BY THE COMMUTATOR SWITCHING ACTION:
MEASURED RFI LEVELS FROM A COPPER SLIP RING
AT 18000 r/min WITH VARYING SUPPLY CURRENT

TEST VARIABLE: CURRENT (A)

TEST NUMBER	7: 3.5A	8: 4.0A				
FREQUENCY	RFI CONDUCTED VOLTAGE MEASUREMENTS: dB(uV)					
0.150 MHz	48	55				
0.160	47.5	53				
0.240	44	51				
0.550	35	43				
1.000	29	35				
1.400	28.5	35				
2.000	28	36				
3.500	35	37				
6.000	36.5	37				
10.00	32	37.5				
13.00	32	35				
22.00	30	35				
30.00	29	32				
	RFI RADIATED POWER MEASUREMENTS: dB(pW)					
30.00	14	19				
40.00	13	17				
46.00	10.5	15				
65.00	10	13.5				
90.00	8	10				
150.0	6	8.5				
180.0	3	5				
220.0	1	2				
300.0	-	1				

TABLE A2.41

TITLE: RFI CAUSED BY THE COMMUTATOR SWITCHING ACTION:
MEASURED RFI LEVELS FROM A 24 SEGMENT COMMUTATOR
AT ZERO SUPPLY CURRENT WITH VARYING SHAFT SPEED

TEST VARIABLE: SPEED (r/min)

TEST NUMBER	1: 2000 r/min	2: 4000	3: 6000	4: 8000	5: 10000	6: 12000
FREQUENCY	RFI CONDUCTED VOLTAGE MEASUREMENTS: dB(uV)					
0.100 MHz	8	9.5	11.5	13	15	15.5
0.150	5	5.5	6.25	7	7.5	8.5
0.240	2.25	2.5	3	3	3.5	4
0.550	2	2.25	2.5	2.5	2.75	3
1.000	0.5	0.75	1	1	1.25	1.5
1.400	-	-	-	-	0.5	0.75
2.000	-	-	-	-	-	-
3.500	-	-	-	-	-	-
6.000	-	-	-	-	-	-
10.00	-	-	-	-	-	-
13.00	-	-	-	-	-	-
22.00	-	-	-	-	-	-
30.00	-	-	-	-	-	-
	RFI RADIATED POWER MEASUREMENTS: dB(pW)					
30.00	-	-	-	-	-	-
40.00	-	-	-	-	-	-
46.00	-	-	-	-	-	-
65.00	-	-	-	-	-	-
90.00	-	-	-	-	-	-
150.0	-	-	-	-	-	-
180.0	-	-	-	-	-	-
220.0	-	-	-	-	-	-
300.0	-	-	-	-	-	-

TABLE A2.42

TITLE: RFI CAUSED BY THE COMMUTATOR SWITCHING ACTION:
MEASURED RFI LEVELS FROM A 24 SEGMENT COMMUTATOR
AT ZERO SUPPLY CURRENT WITH VARYING SHAFT SPEED

TEST VARIABLE: SPEED (r/min)

TEST NUMBER	7: 14000 r/min	8: 16000	9: 18000	10: 200000	11: 22000
FREQUENCY	RFI CONDUCTED VOLTAGE MEASUREMENTS: dB(uV)				
0.100 MHz	18	20	22	23.5	25.5
0.150	9.5	11	11.5	12	12.5
0.240	4.5	4.75	5	6.25	6.5
0.550	3.25	3.5	4	4.5	4.5
1.000	1.5	1.75	2	2	2
1.400	0.75	1	1	1.5	1.5
2.000	0.5	0.5	0.75	1	1
3.500	0.5	0.5	0.5	1	1
6.000	-	-	-	0.5	0.5
10.00	-	-	-	-	-
13.00	-	-	-	-	-
22.00	-	-	-	-	-
30.00	-	-	-	-	-
	RFI RADIATED POWER MEASUREMENTS: dB(pW)				
30.00	-	-	-	-	-
40.00	-	-	-	-	-
46.00	-	-	-	-	-
65.00	-	-	-	-	-
90.00	-	-	-	-	-
150.0	-	-	-	-	-
180.0	-	-	-	-	-
220.0	-	-	-	-	-
300.0	-	-	-	-	-

TABLE A2.43

TITLE: RFI CAUSED BY THE COMMUTATOR SWITCHING ACTION:
MEASURED RFI LEVELS FROM A 22 SEGMENT COMMUTATOR
AT ZERO SUPPLY CURRENT WITH VARYING SHAFT SPEED

TEST VARIABLE: SPEED (r/min)

TEST NUMBER	1: 2000 r/min	2: 4000	3: 6000	4: 8000	5: 10000	6: 12000
FREQUENCY	RFI CONDUCTED VOLTAGE MEASUREMENTS: dB(uV)					
0.100	7.5	9	12	13	15	19
0.150	4.5	5.25	6.5	7	7.5	10
0.240	2.5	2.5	3	3.5	3.5	4.5
0.550	2	2.25	2.5	2.5	2.5	3
1.000	0.5	1	1	1	1.5	1.5
1.400	-	-	0.5	0.5	1	1
2.000	-	-	-	-	0.5	0.5
3.500	-	-	-	-	-	0.5
6.000	-	-	-	-	-	-
10.00	-	-	-	-	-	-
13.00	-	-	-	-	-	-
22.00	-	-	-	-	-	-
30.00	-	-	-	-	-	-
	RFI RADIATED POWER MEASUREMENTS: dB(pW)					
30.00	-	-	-	-	-	-
40.00	-	-	-	-	-	-
46.00	-	-	-	-	-	-
65.00	-	-	-	-	-	-
90.00	-	-	-	-	-	-
150.0	-	-	-	-	-	-
180.0	-	-	-	-	-	-
220.0	-	-	-	-	-	-
300.0	-	-	-	-	-	-

TABLE A2.44

TITLE: RFI CAUSED BY THE COMMUTATOR SWITCHING ACTION:
MEASURED RFI LEVELS FROM A 22 SEGMENT COMMUTATOR
AT ZERO SUPPLY CURRENT WITH VARYING SHAFT SPEED

TEST VARIABLE: SPEED (r/min)

TEST NUMBER	7: 14000 r/min	8: 16000	9: 18000	10: 20000	11: 22000
FREQUENCY	RFI CONDUCTED VOLTAGE MEASUREMENTS: dB(uV)				
0.100 MHz	19	20	23	24	26
0.150	10	11.5	12	13	14
0.240	4.5	5	5.5	6	7
0.550	3	4	4	5	6
1.000	1.5	2	2	3	4
1.400	1	1	1.5	2	2
2.000	0.5	0.5	0.75	1	1.5
3.500	0.5	0.5	1	1	1
6.000	-	-	-	0.5	0.5
10.00	-	-	-	-	-
13.00	-	-	-	-	-
22.00	-	-	-	-	-
30.00	-	-	-	-	-
	RFI RADIATED POWER MEASUREMENTS: dB(pW)				
30.00	-	-	-	-	-
40.00	-	-	-	-	-
46.00	-	-	-	-	-
65.00	-	-	-	-	-
90.00	-	-	-	-	-
150.0	-	-	-	-	-
180.0	-	-	-	-	-
220.0	-	-	-	-	-
300.0	-	-	-	-	-

TABLE A2.45

TITLE: RFI CAUSED BY THE COMMUTATOR SWITCHING ACTION:
MEASURED RFI LEVELS FROM A 21 SEGMENT COMMUTATOR
AT ZERO SUPPLY CURRENT WITH VARYING SHAFT SPEED

TEST VARIABLE: SPEED (r/min)

TEST NUMBER	1: 2000 r/min	2: 4000	3: 6000	4: 8000	5: 10000	6: 12000
FREQUENCY	RFI CONDUCTED VOLTAGE MEASUREMENTS: dB(uV)					
0.100 MHz	9	10	12	14	16	17
0.150	6	6	7	8	9	9.5
0.240	3	3.5	3.5	4	4	4.5
0.550	2	2	2	3	3	3
1.000	1	1	1.5	1.5	1.5	1.5
1.400	0.5	0.5	0.5	0.5	1	1
2.000	-	-	-	0.25	0.5	0.5
3.500	-	-	-	-	0.5	0.5
6.000	-	-	-	-	-	-
10.00	-	-	-	-	-	-
13.00	-	-	-	-	-	-
22.00	-	-	-	-	-	-
30.00	-	-	-	-	-	-
	RFI RADIATED POWER MEASUREMENTS: dB(pW)					
30.00						
40.00						
46.00						
65.00						
90.00						
150.0						
180.0						
220.0						
300.0						

TABLE A2.46

TITLE: RFI CAUSED BY THE COMMUTATOR SWITCHING ACTION:
MEASURED RFI LEVELS FROM A 21 SEGMENT COMMUTATOR
AT ZERO SUPPLY CURRENT WITH VARYING SHAFT SPEED

TEST VARIABLE: SPEED (r/min)

TEST NUMBER	7: 14000 r/min	8: 16000	9: 18000	10: 20000	11: 22000	
FREQUENCY	RFI CONDUCTED VOLTAGE MEASUREMENTS: dB(uV)					
0.100 MHz	19	21	23	24	25	
0.150	10	11	11.5	12	12	
0.240	5	6	7	7.5	8	
0.550	3.5	4	4	4.5	5	
1.000	2	2.5	3	3	3.5	
1.400	1	2	2	2	2.5	
2.000	0.5	1.5	1.5	2	2.25	
3.500	0.5	1	1.5	1.5	2	
6.000	-	0.5	0.5	1	1	
10.00	-	-	-	-	0.5	
13.00	-	-	-	-	-	
22.00	-	-	-	-	-	
30.00	-	-	-	-	-	
	RFI RADIATED POWER MEASUREMENTS: dB(pW)					
30.00	-	-	-	-	-	
40.00	-	-	-	-	-	
46.00	-	-	-	-	-	
65.00	-	-	-	-	-	
90.00	-	-	-	-	-	
150.0	-	-	-	-	-	
180.0	-	-	-	-	-	
220.0	-	-	-	-	-	
300.0	-	-	-	-	-	

TABLE A2.47

TITLE. RFI CAUSED BY THE VARIATION OF THE SHORT-CIRCUITED COIL PARAMETERS:
MEASURED RFI LEVELS WITH VARYING RESISTANCE (Rs) AT 5000 r/min AND 0.5A SUPPLY CURRENT (Ls=0, e=0)

TEST VARIABLE: RESISTANCE (Ohms)

TEST NUMBER	1: ZERO Ohms	2: 0.2	3: 0.5	4: 1.0	5: 2.0	6: 3.0
FREQUENCY	RFI CONDUCTED VOLTAGE MEASUREMENTS: dB(uV)					
0.150 MHz	65.5	66.5	67.5	71	74.5	78
0.160	65	66	67	70	74	77
0.240	61	62.5	63.5	69	71	75
0.550	51.5	53	54	57	61	67
1.000	46	46.5	47	49	57	61
1.400	44	45	45.5	47	50	56
2.000	44	44	44.5	45	48	48
3.500	46	46	46.5	46.5	48	48.5
6.000	46	46	46.5	46.5	47	48
10.00	43.5	44	44.5	44.5	45	46
13.00	43	43	44	44	44	45
22.00	34.5	34.5	35	35	35.5	36
30.00	26	26	27	28.5	30	31
	RFI RADIATED POWER MEASUREMENTS: dB(pW)					
30.00	22	22	22.5	23	25.5	26
40.00	21.5	21.5	22	22	24	24
46.00	21	21	21.5	22	23	23
65.00	19	19	19	19.5	20	22
90.00	17	17	17.5	18.5	19	20
150.0	17	17	17	17	18	19
180.0	15	15	15	15.5	16	16
220.0	13	13	13	13	14	15
300.0	12	12	12	12	13	13

TABLE A2.48

TITLE: RFI CAUSED BY THE VARIATION OF THE SHORT-CIRCUITED COIL PARAMETERS:
MEASURED RFI LEVELS WITH VARYING RESISTANCE (Rs) AT 5000 r/min AND 0.5A SUPPLY CURRENT (Ls=0, e=0)

TEST VARIABLE: RESISTANCE (Ohms)

TEST NUMBER	7: 5.0 Ohms	8: 6.0	9: 8.0	10: 10.0	11: 15.0	12: 20.0
FREQUENCY	RFI CONDUCTED VOLTAGE MEASUREMENTS: dB(uV)					
0.150 MHz	82	84	84	85	85	86
0.160	81	83.5	84	84	84.5	85.5
0.240	80	81	81	82	82.5	83
0.550	72	74	75	75	76	76
1.000	67	70	71	71	71	71.5
1.400	63	67	69	70	71	71
2.000	57	62	66	67	67	68.5
3.500	49	53	62	65	67	68
6.000	49	50	58	62	63	65
10.00	46	50	57	61	62	63.5
13.00	45	48	54	58	60	61.5
22.00	38	40	45	50	53	55
30.00	33	34	38	40	49	52
	RFI RADIATED POWER MEASUREMENTS: dB(pW)					
30.00	27	29	31	35	44	46
40.00	26	28	30	34.5	42	45
46.00	24	25	27	33	41	44
65.00	22	23	26	31	38	41
90.00	21	20	25	30	38	40
150.0	20	20	23	30	36	38
180.0	17	18	20	28	34	35
220.0	16	18	19	24	30	33
300.0	13	14	16	20	28	31

*

* TABLE A2.49

*

TITLE: RFI CAUSED BY THE VARIATION OF THE SHORT-CIRCUITED COIL PARAMETERS:
MEASURED RFI LEVELS WITH VARYING RESISTANCE (Rs) AT 5000 r/min AND 1.5A SUPPLY CURRENT (Ls=0, e=0)

*

TEST VARIABLE: RESISTANCE (Ohms)

*

TEST NUMBER	1:	2:	3:	4:	5:	6:
	ZERO	0.2 Ohms	0.5	1.0	2.0	3.0
FREQUENCY	RFI CONDUCTED VOLTAGE MEASUREMENTS: dB(uV)					
0.150 MHz	66	67	68	72	76	80
0.160	65	66	68	71	75	80
0.240	61.5	63	64	70	72	77
0.550	52	53.5	55	58	62	69
1.000	46	47	48	50	56	63
1.400	44.5	45	45.5	48	51	58
2.000	44	44.5	45	46	48.5	50.5
3.500	46.5	46.5	47	47	48	49
6.000	46	46	46	46.5	47.5	48
10.00	44	44	44.5	44.5	45	46
13.00	43	43	43	43.5	44	45
22.00	34	34	35	35	36	37
30.00	26	26	27	28.5	30.5	33
	RFI RADIATED POWER MEASUREMENTS: dB(pW)					
30.00	22	22	22.5	23	26	27
40.00	22	22	22	22.5	25	26
46.00	21	21	21.5	22	24	25
65.00	19	19	19	19.5	21	22
90.00	17.5	17.5	18	18.5	19	20
150.0	17	17	17	18	19	19
180.0	15	15	15	16	17	17
220.0	13	13	13	13	14	16
300.0	12	12	12	13	13	13

*

*

*

*

* TABLE A2.50

*

TITLE: RFI CAUSED BY THE VARIATION OF THE SHORT-CIRCUITED COIL PARAMETERS:
MEASURED RFI LEVELS WITH VARYING RESISTANCE (Rs) AT 5000 r/min AND 1.5A SUPPLY CURRENT (Ls=0, e=0)

*

TEST VARIABLE: RESISTANCE (Ohms)

*

TEST NUMBER	7:	8:	9:	10:	11:	12:
	5.0 Ohms	6.0	8.0	10.0	15.0	20.0
FREQUENCY	RFI CONDUCTED VOLTAGE MEASUREMENTS: dB(uV)					
0.150 MHz	84	86	87.5	87.5	88	88
0.160	84	85	87	86.5	87	88
0.240	81	83	84	84.5	84.5	85
0.550	74	76	77	77	78	78
1.000	69.5	72	73	73.5	73.5	73.5
1.400	65	69	71	72	72	73
2.000	58	64.5	69	71	71	71.5
3.500	50	55	64	68	69	70
6.000	49	53	60	65.5	66	67
10.00	47	52	59	64	64	65
13.00	46	50	56	61	62	63
22.00	39	42.5	47	52	54	56
30.00	35	36	40	42	51	53
	RFI RADIATED POWER MEASUREMENTS: dB(pW)					
30.00	28	31	35	38	45	47
40.00	26	30	34	36	44	46
46.00	25	27	32	35	43	45
65.00	23	25	30	32	40	41
90.00	22	25	30	30	40	40
150.0	20	23	29	29.5	38	39
180.0	19.5	20	27	27	35	36
220.0	17	19	24	24	33	34
300.0	14	16	20	22	30	31

*

*

*

TABLE A2.51

TITLE: RFI CAUSED BY THE VARIATION OF THE SHORT-CIRCUITED COIL PARAMETERS:
MEASURED RFI LEVELS WITH VARYING RESISTANCE (Rs) AT 5000 r/min AND 2.5A SUPPLY CURRENT (Ls=0, e=0)

TEST VARIABLE: RESISTANCE (Ohms)

TEST NUMBER	1:	2:	3:	4:	5:	6:
	ZERO	0.2 Ohms	0.5	1.0	2.0	3.0
FREQUENCY	RFI CONDUCTED VOLTAGE MEASUREMENTS: dB(uV)					
0.150 MHz	66.5	67.5	69	73	78	82
0.160	65	67	68.5	72	77	81
0.240	62	63	64	71.5	74	79
0.550	52	54	55.5	59	64	71
1.000	46	47.5	49	51	58	66
1.400	45	46	46.5	49	50.5	61.5
2.000	44	45	45.5	47	48.5	54
3.500	47	47	47.5	47.5	48	50
6.000	46	46	46.5	46.5	47.5	48
10.00	44	44	45	45.5	46	46.5
13.00	43	43	44	44	45	46
22.00	35	35	36	36	37	37
30.00	27	27	28	29	31	33
	RFI RADIATED POWER MEASUREMENTS: dB(pW)					
30.00	23	23	23.5	24	25	27
40.00	22	22	22	23	24	26
46.00	21	21	21.5	22	23	26
65.00	19	19	19	20	21	23
90.00	18	18	18	19	20	21
150.0	17	17	17	18	19	20
180.0	15	15	15	16	17	18
220.0	13	13	13	13	14	17
300.0	12	12	12	13	13	14

TABLE A2.52

TITLE: RFI CAUSED BY THE VARIATION OF THE SHORT-CIRCUITED COIL PARAMETERS:
MEASURED RFI LEVELS WITH VARYING RESISTANCE (Rs) AT 5000 r/min AND 2.5A SUPPLY CURRENT (Ls=0, e=0)

TEST VARIABLE: RESISTANCE (Ohms)

TEST NUMBER	7:	8:	9:	10:	11:	12:
	5.0 Ohms	6.0	8.0	10.0	15.0	20.0
FREQUENCY	RFI CONDUCTED VOLTAGE MEASUREMENTS: dB(uV)					
0.150 MHz	87	89	90	90	91	92
0.160	86	88	89	89.5	90	91
0.240	84	86	87.5	87	88	89
0.550	77	79	90	81	82.5	83
1.000	72	75	76	77	77.5	78
1.400	68	72	74	74	75	76
2.000	60	67	71	72	73	74
3.500	52	57	67	69	71	73.5
6.000	48	55	62	67	71	72
10.00	47	55	62	66	69	70
13.00	46	53	59	63	64	66
22.00	40	45	50	56	57	59
30.00	36	38	44	46	54	57
	RFI RADIATED POWER MEASUREMENTS: dB(pW)					
30.00	29	35	40	45	49	51
40.00	27	34	38	43	48	50
46.00	26	31.5	38	40	47	49
65.00	24	29	34	38	42	44
90.00	22	29	31	38	41	43
150.0	21	27	30	34	38	40
180.0	18	27	29	30	36	37
220.0	17	24	26	29	35	36
300.0	14	20	22	26	33	34

TABLE A2.53

TITLE: RFI CAUSED BY THE VARIATION OF THE SHORT-CIRCUITED COIL PARAMETERS:
MEASURED RFI LEVELS WITH VARYING RESISTANCE (Rs) AT 10000 r/min AND 0.5A SUPPLY CURRENT (Ls=0, e=0)

TEST VARIABLE: RESISTANCE (Ohms)

TEST NUMBER	1: ZERO	2: 0.2 Ohms	3: 0.5	4: 1.0	5: 2.0	6: 3.0
FREQUENCY	RFI CONDUCTED VOLTAGE MEASUREMENTS: dB(uV)					
0.150 MHz	74	74.5	75.5	79	82	83.5
0.160	73	74	75	78	81.5	83
0.240	69.5	70	71	76.5	78.5	81
0.550	64.5	65	66	68	70	72.5
1.000	58	58	58.5	62	63.5	65
1.400	57	57	58	60	61	62
2.000	55.5	56	56	56.5	57	58
3.500	56	56	56	56	56	57
6.000	57	57	57	57	57.5	59
10.00	59	59	59	59.5	60	60.5
13.00	59.5	60	60.5	60.5	61	61
22.00	54.5	55	55	55	55.5	56
30.00	48.5	49	49.5	50	51	51
	RFI RADIATED POWER MEASUREMENTS: dB(pW)					
30.00	39.5	40	40.5	41	41	42
40.00	38.5	38.5	39	40	40	41
46.00	38	38	38	39	39	39.5
65.00	36	36	36.5	37	37	38
90.00	33.5	33.5	34	35	35	36
150.0	33.5	33.5	33.5	34	34.5	35
180.0	32	32	32	32	34	34
220.0	29	29	29	30	30	31
300.0	25	25.5	25.5	26	26.5	28

TABLE A2.54

TITLE: RFI CAUSED BY THE VARIATION OF THE SHORT-CIRCUITED COIL PARAMETERS:
MEASURED RFI LEVELS WITH VARYING RESISTANCE (Rs) AT 10000 r/min AND 0.5A SUPPLY CURRENT (Ls=0, e=0)

TEST VARIABLE: RESISTANCE (Ohms)

TEST NUMBER	7: 5.0 Ohms	8: 6.0	9: 8.0	10: 10.0	11: 15.0	12: 20.0
FREQUENCY	RFI CONDUCTED VOLTAGE MEASUREMENTS: dB(uV)					
0.150 MHz	87.5	90	91	92	92	93
0.160	87	89	90.5	91.5	91.5	92.5
0.240	84.5	86.5	87	89	90	92
0.550	75.5	77.5	80	81.5	83	85
1.000	66	69	72.5	75	77	81
1.400	63	67	68	70	72	78
2.000	59	61	64	65.5	70	77
3.500	58	60	60.5	62	66	75
6.000	59.5	59.5	61	61	65.5	74
10.00	61	61	61	61.5	65	70
13.00	62	62	62	62	63	68
22.00	57	57.5	57.5	58	58	63
30.00	52	52.5	53	54	56	59
	RFI RADIATED POWER MEASUREMENTS: dB(pW)					
30.00	42.5	43	43.5	44	46	52
40.00	42	42.5	43	43	46	51
46.00	41	41	42	42	44	48
65.00	38	38	39	40	43	47
90.00	36.5	37	37.5	38	40.5	44
150.0	35	36	37	37	39	44
180.0	34	35	36	37	38	40
220.0	32	33	34.5	35	35	38
300.0	28	28	28.5	30	31	33

TABLE A2.55

TITLE: RFI CAUSED BY THE VARIATION OF THE SHORT-CIRCUITED COIL PARAMETERS:
MEASURED RFI LEVELS WITH VARYING RESISTANCE (Rs) AT 10000 r/min AT 1.5A SUPPLY CURRENT (Ls=0, e=0)

TEST VARIABLE: RESISTANCE (Ohms)

TEST NUMBER	1:	2:	3:	4:	5:	6:
	ZERO	0.2 Ohms	0.5	1.0	2.0	3.0
FREQUENCY	RFI CONDUCTED VOLTAGE MEASUREMENTS: dB(uV)					
0.150 MHz	74	75	76	80	82	84
0.160	73	74.5	75	79	81	83.5
0.240	70	70.5	71.5	77	79	81
0.550	65	65.5	67	69.5	70.5	73
1.000	58	58.5	59	63	64	65.5
1.400	57	57	57.5	60.5	61	62
2.000	56	56	56	57	57.5	58.5
3.500	56	56	56	56.5	56.5	57
6.000	57.5	57.5	57.5	58	58	59
10.00	59.5	59.5	59.5	60	60.5	61
13.00	60	60	60	60.5	61	61.5
22.00	55	55	55	55.5	56	56.5
30.00	49	49	50	50	51	51.5
	RFI RADIATED POWER MEASUREMENTS: dB(pW)					
30.00	40	40	40.5	41	41	42
40.00	39	39	40	40	40.5	41
46.00	38	38	39	39	39.5	40
65.00	36	36	36.5	37	37	38
90.00	34	34	34.5	35	35	36
150.0	34	34	34	34	35	35
180.0	32	32	32	33	34	34
220.0	29	29	29	30	30	31
300.0	26	26	26	27	27	28

TABLE A2.56

TITLE: RFI CAUSED BY THE VARIATION OF THE SHORT-CIRCUITED COIL PARAMETERS:
MEASURED RFI LEVELS WITH VARYING RESISTANCE (Rs) AT 10000 r/min AND 1.5A SUPPLY CURRENT (Ls=0, e=0)

TEST VARIABLE:

TEST NUMBER	7:	8:	9:	10:	11:	12:
	5.0 Ohms	6.0	8.0	10.0	15.0	20.0
FREQUENCY	RFI CONDUCTED VOLTAGE MEASUREMENTS: dB(uV)					
0.150 MHz	88	90	91.5	93	93.5	94
0.160	87	89	91	92	93	93.5
0.240	85	87	87.5	90	91	92.5
0.550	76	78	80	82.5	84	86
1.000	67	70	73	76	79	81.5
1.400	63	67	69	71	73	79
2.000	59.5	61	64.5	66	70	78
3.500	58	60	61	62.5	66	76
6.000	60	60	61	62	66	74.5
10.00	61.5	62	62	62	65.5	71
13.00	62	62.5	63	63	64	69
22.00	57	58	58	58.5	59	63.5
30.00	52	52.5	53	54	57	60
	RFI RADIATED POWER MEASUREMENTS: dB(pW)					
30.00	42.5	43	44	44	47	53
40.00	42	42	43.5	43.5	46	52
46.00	41	41	42	42.5	45	49
65.00	38	38	39	40	43	47
90.00	36.5	37	38	39	41	45
150.0	35.5	36	38	38	40	44
180.0	34.5	35	36	37	39	42
220.0	32	33	34	35	36	39
300.0	28	29	29	30	32	35

TABLE A2.57

TITLE: RFI CAUSED BY THE VARIATION OF THE SHORT-CIRCUIT COIL PARAMETERS:
MEASURED RFI LEVELS WITH VARYING RESISTANCE (Rs) AT 10000 r/min AND 2.5A SUPPLY CURRENT (Ls=0, e=0)

TEST VARIABLE: RESISTANCE (Ohms)

TEST NUMBER	1:	2:	3:	4:	5:	6:
	ZERO	0.2 Ohms	0.5	1.0	2.0	3.0
FREQUENCY	RFI CONDUCTED VOLTAGE MEASUREMENTS: dB(uV)					
0.150 MHz	74.5	75.5	77	81	83	84.5
0.160	74	75	76	80	81.5	84
0.240	70	71	72	78	79	82
0.550	65.5	66	67	70	71	74
1.000	58.5	59	60	64	64.5	66
1.400	57.5	58	59	61	61	63
2.000	57	57.5	57.5	58	58.5	59
3.500	57	57	57.5	58	57	58
6.000	58	58	58.5	59	59	60
10.00	60	60	60.5	61	61.5	61.5
13.00	60.5	60.5	61	61	62	62
22.00	59.5	55.5	56	56	57	57.5
30.00	49	49	50	50	51.5	52
	RFI RADIATED POWER MEASUREMENTS: dB(pW)					
30.00	40	40	41	41	42	42.5
40.00	39.5	39.5	40.5	40.5	41	42
46.00	38	38	39	39	40	41
65.00	36.5	36.5	37	37.5	38	39
90.00	34.5	35	35	36	36	37
150.0	34	34	34.5	35	35.5	36
180.0	33	33	33	33.5	34	35
220.0	30	30	30.5	31	31	32
300.0	26.5	26.5	27	27.5	28	29

TABLE A2.58

TITLE: RFI CAUSED BY THE VARIATION OF THE SHORT-CIRCUITED COIL PARAMETERS:
MEASURED RFI LEVELS WITH VARYING RESISTANCE (Rs) AT 10000 r/min AND 2.5A SUPPLY CURRENT (Ls=0, e=0)

TEST VARIABLE: RESISTANCE (Ohms)

TEST NUMBER	7:	8:	9:	10:	11:	12:
	5.0 Ohms	6.0	8.0	10.0	15.0	20.0
FREQUENCY	RFI CONDUCTED VOLTAGE MEASUREMENTS: dB(uV)					
0.150 MHz	89	90.5	92	94	94.5	95
0.160	88	89	91	93	94	95
0.240	86	88	89.5	92	93	93.5
0.550	77	80	81.5	83	85	86
1.000	68	71	74	77	79	82
1.400	64	68	70	72.5	74	79.5
2.000	60	62	65	67	71	79.5
3.500	58	61	62	63	67	78
6.000	60.5	61.5	62.5	63	67	75
10.00	63	62	62.5	63	66	72
13.00	63	63	63	63.5	64	70
22.00	58	58	59	59	59.5	64
30.00	53	53	54	55	58	60
	RFI RADIATED POWER MEASUREMENTS: dB(pW)					
30.00	43	44	45	46	49	54
40.00	42	43	44.5	45	48	53
46.00	41	42	42	43	46	49.5
65.00	39	39	40	41	44	47.5
90.00	37	38	39	40	42	46
150.0	36.5	37	38	39.5	41	45
180.0	35	37	38.5	39	40	43
220.0	33	34	35	36	37	40
300.0	29	30	31.5	32	33	36

TABLE 42.59

TITLE: RFI CAUSED BY THE VARIATION OF THE SHORT-CIRCUITED COIL PARAMETERS:
MEASURED RFI LEVELS WITH VARYING RESISTANCE (Rs) AT 15000 r/min AND 0.5A SUPPLY CURRENT (Ls=0, e=0)

TEST VARIABLE: RESISTANCE (Ohms)

TEST NUMBER	1: ZERO	2: 0.2 Ohms	3: 0.5	4: 1.0	5: 2.0	6: 3.0
FREQUENCY	RFI CONDUCTED VOLTAGE MEASUREMENTS: dB(uV)					
0.150 MHz	76	76	76	79	81.5	83
0.160	74.5	75	75.5	78	81	83
0.240	72	73	73.5	76	78	79
0.550	64.5	64	65	67.5	70	71
1.000	58	58	59	63	64	67
1.400	57	57.5	58	61.5	63	65
2.000	58	58	59	60	62	63
3.500	58	58	58	59	60	60
6.000	57	57	57	58.5	59	60
10.00	62	62	62	62	62	62.5
13.00	61.5	62	62	62	62	62
22.00	59	59.5	60	60	60	60
30.00	54	54	54	54.5	54.5	54.5
	RFI RADIATED POWER MEASUREMENTS: dB(pW)					
30.00	44	44	44.5	45	45	45.5
40.00	43	43.5	44	44	44.5	45
46.00	42.5	43	43	43	43	43
65.00	40	40	40.5	40.5	41	41
90.00	40	40	40	40.5	40.5	41
150.0	38	38	38	38.5	39	40
180.0	36	36	36	36	36.5	37
220.0	35	35	35	35	35	35.5
300.0	31.5	31.5	31.5	32	32	32.5

TABLE 42.60

TITLE: RFI CAUSED BY THE VARIATION OF THE SHORT-CIRCUITED COIL PARAMETERS:
MEASURED RFI LEVELS WITH VARYING RESISTANCE (Rs) AT 15000 r/min AND 0.5A SUPPLY CURRENT (Ls=0, e=0)

TEST VARIABLE: RESISTANCE (Ohms)

TEST NUMBER	7: 5.0 Ohms	8: 6.0	9: 8.0	10: 10.0	11: 15.0	12: 20.0
FREQUENCY	RFI CONDUCTED VOLTAGE MEASUREMENTS: dB(uV)					
0.150 MHz	88	90	92	94	95	96
0.160	87	89.5	91	93.5	94.5	95
0.240	84	86	89	91	91.5	93
0.550	77	78	83	84.5	86	88
1.000	71.5	73	75	77.5	81	83
1.400	67	69	72.5	74	77	81.5
2.000	65.5	67	68	69.5	74	79
3.500	62	63.5	65	66	70	77
6.000	62	63	64	64.5	68	74
10.00	62.5	62.5	63.5	64	67	72.5
13.00	62	62.5	63.5	64	66	70
22.00	60.5	60.5	61	62	63.5	67
30.00	56	58	59	61	62.5	65
	RFI RADIATED POWER MEASUREMENTS: dB(pW)					
30.00	47	49	51.5	54	56	59
40.00	46	48	51	53	55.5	58
46.00	44	46	50	52	53	54
65.00	42	44.5	46.5	48	51	52
90.00	42	43	46	47.5	48	49
150.0	41	41.5	42	46	47	48
180.0	38	39	40	44	45	45.5
220.0	36	37	39	43	44	44.5
300.0	33	35	37	40	41	42

TABLE A2.61

TITLE: RFI CAUSED BY THE VARIATION OF THE SHORT-CIRCUITED COIL PARAMETERS:
MEASURED RFI LEVELS WITH VARYING RESISTANCE (Rs) AT 15000 r/min AND 1.5A SUPPLY CURRENT (Ls=0, e=0)

TEST VARIABLE: RESISTANCE (Ohms)

TEST NUMBER	1:	2:	3:	4:	5:	6:
	ZERO	0.2 Ohms	0.5	1.0	2.0	3.0
FREQUENCY	RFI CONDUCTED VOLTAGE MEASUREMENTS: dB(uV)					
0.150 MHz	76	76	77	80	82	84
0.160	75	75	76	79	81.5	83.5
0.240	72.5	73	74	77	79.5	80
0.550	65	65	66	69	71	72
1.000	59	59	60	64	64.5	67
1.400	58	58	59	62	63.5	65
2.000	59	59	60	61	62.5	64
3.500	59	59	59	60	60.5	61
6.000	57	57	57	59	60	61
10.00	61.5	62	62	62	62.5	62.5
13.00	62	62	62	62	62.5	62.5
22.00	60	60	60	60	60.5	60.5
30.00	55	55.5	55	55	55.5	55.5
	RFI RADIATED POWER MEASUREMENTS: dB(pW)					
30.00	45	45	45	45.5	46	46
40.00	44	44	44.5	44.5	45	45
46.00	43	43	43	43	44	44
65.00	40	40	40.5	40.5	41	41
90.00	40.5	40.5	41	41	41	41.5
150.0	38	38	39	39	40	40
180.0	36	36	36	36	36.5	37
220.0	35	35	35	35	35	36
300.0	32	32	32	32	32	33

TABLE A2.62

TITLE: RFI CAUSED BY THE VARIATION OF THE SHORT-CIRCUITED COIL PARAMETERS:
MEASURED RFI LEVELS WITH VARYING RESISTANCE (Rs) AT 15000 r/min AND 1.5A SUPPLY CURRENT (Ls=0, e=0)

TEST VARIABLE: RESISTANCE (Ohms)

TEST NUMBER	7:	8:	9:	10:	11:	12:
	5.0 Ohms	6.0	8.0	10.0	15.0	20.0
FREQUENCY	RFI CONDUCTED VOLTAGE MEASUREMENTS: dB(uV)					
0.150 MHz	89	91	93	95	96	97
0.160	88	90	92	94	95	96
0.240	85	87	90	91.5	92	94
0.550	78	79	83	85	86.5	89
1.000	72	74	76	78	81	84
1.400	68	70	73	75	78	82
2.000	66	68	69	70	74	80
3.500	63	65	66	67	70.5	78
6.000	63	64	64	65	69	75
10.00	63.5	64	64	65	67.5	73
13.00	63.5	64	64	64	66	70
22.00	61	61	62	63	64	67
30.00	57	59	60	62	63	66
	RFI RADIATED POWER MEASUREMENTS: dB(pW)					
30.00	48	50	52	55	57	60
40.00	47	49	51	54	56	58
46.00	45	47	50	52	54	54.5
65.00	42	45	47	49	52	53
90.00	43	44	46	49	49.5	50
150.0	41	42	43	47	47	48
180.0	38	39	41	45	45.5	46
220.0	37	38	40	44	44.5	45
300.0	34	36	39	41	42	42

TABLE A2.63

TITLE: RFI CAUSED BY THE VARIATION OF THE SHORT-CIRCUITED COIL PARAMETERS:
MEASURED RFI LEVELS WITH VARYING RESISTANCE (Rs) AT 15000 r/min AND 2.5A SUPPLY CURRENT (Ls=0, e=0)

TEST VARIABLE: RESISTANCE (Ohms)

TEST NUMBER	1:	2:	3:	4:	5:	6:
	ZERO	0.2 Ohms	0.5	1.0	2.0	3.0
FREQUENCY	RFI CONDUCTED VOLTAGE MEASUREMENTS: dB(uV)					
0.150 MHz	76.5	77	78	81	83	84.5
0.160	76	76	77	79.5	82	84
0.240	72.5	73	74	78	80	82
0.550	66	67	68	69	72	74
1.000	59	60	61.5	64.5	67	68
1.400	58	58.5	61	62.5	64	66
2.000	59.5	60	61	61	63	65
3.500	59.5	60	60.5	61	61	62
6.000	57.5	58	58	59.5	60	61
10.00	62	62.5	62.5	63	63.5	64
13.00	62	62.5	63	63	63	63
22.00	61	61	61	61	61.5	62
30.00	56	56	56	56.5	57	57
	RFI RADIATED POWER MEASUREMENTS: dB(pW)					
30.00	45.5	46	46.5	46.5	47	47
40.00	45	45	45	46	46	46.5
46.00	44	44	44.5	45	45	45
65.00	42	42.5	42.5	42.5	43	43
90.00	41	42	41	41.5	42	42
150.0	38.5	39	39	39	40	40.5
180.0	36	36	36	36.5	37	37
220.0	35	35	35	35	36	36
300.0	32	32	32.5	33	33.5	33.5

TABLE A2.64

TITLE: RFI CAUSED BY THE VARIATION OF THE SHORT-CIRCUITED COIL PARAMETERS:
MEASURED RFI LEVELS WITH VARYING RESISTANCE (Rs) AT 15000 r/min AND 2.5A SUPPLY CURRENT (Ls=0, e=0)

TEST VARIABLE: RESISTANCE (Ohms)

TEST NUMBER	7:	8:	9:	10:	11:	12:
	5.0 Ohms	6.0	8.0	10.0	15.0	20.0
FREQUENCY	RFI CONDUCTED VOLTAGE MEASUREMENTS: dB(uV)					
0.150 MHz	90	92.5	94	96.5	97	97.5
0.160	89	91	93.5	96	96	96
0.240	86	88	90.5	92	92.5	94.5
0.550	79	80	84	86	87	90
1.000	73	75	78	79.5	82	86
1.400	69	70.5	75	77	80	84
2.000	68	68.5	70	71	75	82
3.500	64.5	65	66.5	69	72.5	79
6.000	64	64.5	65	67	69	76
10.00	64	64	64	67.5	69	74
13.00	64	64	64.5	66	68.5	70
22.00	63	63	64	64	66	68
30.00	57.5	58	62	63	65	68
	RFI RADIATED POWER MEASUREMENTS: dB(pW)					
30.00	48	51.5	53.5	57	59	62
40.00	47	50	52	56	58	61
46.00	46	48	52	54	55	56
65.00	44	46	48	53	53	55
90.00	42.5	45	47	50	52	54
150.0	41	42	45	48	48	50
180.0	39	39.5	40	46	46	47
220.0	37	38	39.5	45	45.5	46
300.0	34	36	38	43	44	46

TABLE A2.65

TITLE: RFI CAUSED BY THE VARIATION OF THE SHORT-CIRCUITED COIL PARAMETERS:
MEASURED RFI LEVELS WITH VARYING RESISTANCE (Rs) AT 20000 r/min AND 0.5A SUPPLY CURRENT (Ls=0, e=0)

TEST VARIABLE: RESISTANCE (Ohms)

TEST NUMBER	1:	2:	3:	4:	5:	6:
	ZERO	0.2 Ohms	0.5	1.0	2.0	3.0
FREQUENCY	RFI CONDUCTED VOLTAGE MEASUREMENTS: dB(uV)					
0.150 MHz	76.5	76	77	80	81.5	84
0.160	75	75.5	76	79	81	83
0.240	72.5	73	74	77	79	80
0.550	65	65	66	69	70.5	72
1.000	58.5	58.5	60	64	65	67.5
1.400	57.5	57.5	59	62	64	65
2.000	58	58	59	61	62	63
3.500	58.5	59	59	60	60.5	61
6.000	57	57	57	58.5	59	60
10.00	62	62	62	62.5	63	62
13.00	62.5	63	63	63	63	63
22.00	59.5	60	60	60.5	61	61
30.00	55	54.5	55	55	56	56
	RFI RADIATED POWER MEASUREMENTS: dB(pW)					
30.00	44	44	45	45	46	46
40.00	44	44	44.5	45	45	45.5
46.00	43	43	43	43	44	44.5
65.00	41	40.5	41	41	41.5	42
90.00	40.5	40.5	41	41	41	42
150.0	38	38	38	38.5	39	40
180.0	36	36	36	36.5	37	37
220.0	35	35	35	35	35.5	36
300.0	32	32	32.5	33	33.5	34

TABLE A2.66

TITLE: RFI CAUSED BY THE VARIATION OF THE SHORT-CIRCUITED COIL PARAMETERS:
MEASURED RFI LEVELS WITH VARYING RESISTANCE (Rs) AT 20000 r/min AND 0.5A SUPPLY CURRENT (Ls=0, e=0)

TEST VARIABLE: RESISTANCE (Ohms)

TEST NUMBER	7:	8:	9:	10:	11:	12:
	5.0 Ohms	6.0	8.0	10.0	15.0	20.0
FREQUENCY	RFI CONDUCTED VOLTAGE MEASUREMENTS: dB(uV)					
0.150 MHz	88	90	93	95	96	97
0.160	88	89	92	94	95	96
0.240	85.5	87	90	91	92	93.5
0.550	78	79	85	85	87	89
1.000	72.5	74	76	78	82	84
1.400	68	71	74	76	78	81
2.000	65	69	69	71	75	80
3.500	61.5	64	66	67.5	71	78
6.000	61	62	64	66	69.5	75
10.00	63	63	64	65	68	73
13.00	63.5	64	65	65	67	70
22.00	61.5	63	63.5	63	64	68
30.00	57	59	61	62	63	66
	RFI RADIATED POWER MEASUREMENTS: dB(pW)					
30.00	47.5	48	52	56	57.5	61
40.00	47	47.5	52	54.5	56	60
46.00	45	46	51	52	54.5	57
65.00	43	45	49	49	51	53
90.00	43	45	47	49	49	50
150.0	41	42	42.5	47.5	49	49
180.0	38	39	40	46	46	47
220.0	37	38	39	43	44	46
300.0	34.5	36	37	41	42	44

*
*   TABLE A2.67
*

TITLE: RFI CAUSED BY THE VARIATION OF THE SHORT-CIRCUITED COIL PARAMETERS:
MEASURED RFI LEVELS WITH VARYING RESISTANCE (Rs) AT 20000 r/min AND 1.5A SUPPLY CURRENT (Ls=0, e=0)

TEST VARIABLE: RESISTANCE (Ohms)

TEST NUMBER	1:	2:	3:	4:	5:	6:
	ZERO	0.2 Ohms	0.5	1.0	2.0	3.0
FREQUENCY	RFI CONDUCTED VOLTAGE MEASUREMENTS: dB(uV)					
0.150 MHz	76.5	76.5	77.5	81	82	85
0.160	76	76	77	80.5	81.5	84
0.240	73	73.5	75	78	80	81
0.550	65.5	66	67	70	71	73
1.000	59	59	60	65	65	68
1.400	58	58	59.5	63	64	66
2.000	59	59	60	62	63	64
3.500	59.5	59.5	60	60.5	61	61.5
6.000	57	57	57	59.5	60	61
10.00	62	62	62.5	63	63	63
13.00	62.5	63	63	63.5	64	64
22.00	60	60	60.5	61	61	61.5
30.00	55	55	55.5	55.5	56	57
	RFI RADIATED POWER MEASUREMENTS: dB(pW)					
30.00	45	45.5	46	46	47	47
40.00	44.5	45	45.5	45	45.5	46
46.00	43	43	43	43	44	45
65.00	41	41.5	41	41	42	43
90.00	41	41	40.5	40.5	41.5	42
150.0	38.5	38.5	39	39	40	40
180.0	36	36	36.5	36.5	37	37
220.0	36	35	35	35	36	36
300.0	33	33	33.5	33.5	34	34

*
*   TABLE A2.68
*

TITLE: RFI CAUSED BY THE VARIATION OF THE SHORT-CIRCUITED COIL PARAMETERS:
MEASURED RFI LEVELS WITH VARYING RESISTANCE (Rs) AT 20000 r/min AND 1.5A SUPPLY CURRENT (Ls=0, e=0)

TEST VARIABLE: RESISTANCE (Ohms)

TEST NUMBER	7:	8:	9:	10:	11:	12:
	5.0 Ohms	6.0	8.0	10.0	15.0	20.0
FREQUENCY	RFI CONDUCTED VOLTAGE MEASUREMENTS: dB(uV)					
0.150 MHz	90	92	94	95.5	97	97.5
0.160	89	91	93.5	95	96	97
0.240	86	88	92	92.5	93	94
0.550	79	80	84	86	88	90
1.000	73	75	77	79.5	83	85
1.400	69	71	74	77	79	83
2.000	66	69	70	72	76	81
3.500	62	66	67	68	72	80
6.000	62	63	64	67	71	77
10.00	64	64.5	65	67	69	75
13.00	64	64	65	66	68	72
22.00	62	63	64	64	66	69
30.00	58	59.5	62	63	65	68
	RFI RADIATED POWER MEASUREMENTS: dB(pW)					
30.00	48.5	49.5	53	56	59	62
40.00	47	49.5	52	55	58	61
46.00	45	47.5	51	53	56	58
65.00	43.5	46	49	50	52	55
90.00	43.5	45	47	49	51	52
150.0	41.5	42	43	48	49	50
180.0	38	39	40	46	47	48
220.0	37.5	38	40	45	46	47
300.0	35.5	36.5	38	43	46	46.5

*
*
*

TABLE A2.69

TITLE: RFI CAUSED BY THE VARIATION OF THE SHORT-CIRCUITED COIL PARAMETERS:
MEASURED RFI LEVELS WITH VARYING RESISTANCE (Rs) AT 20000 r/min AND 2.5A SUPPLY CURRENT (Ls=0, e=0)

TEST VARIABLE: RESISTANCE (Ohms)

TEST NUMBER	1: ZERO	2: 0.2 Ohms	3: 0.5	4: 1.0	5: 2.0	6: 3.0
FREQUENCY	RFI CONDUCTED VOLTAGE MEASUREMENTS: dB(uV)					
0.150 MHz	77	77.5	78	81.5	83	86
0.160	76.5	77	77.5	81	82	85
0.240	73	74	75.5	79	81	82
0.550	66	67	68	71	72	75
1.000	59.5	59.5	61.5	66	68	69
1.400	58	58.5	61.5	64	65	67
2.000	59.5	60	61	62.5	64	65.5
3.500	60	60	60.5	61	62	62
6.000	57	57	57.5	59.5	61	61
10.00	62	62	62.5	63	63	63.5
13.00	63	63	63	63.5	64	64
22.00	61	61.5	61.5	62	62	62
30.00	56	56.5	56.5	57	57	58
	RFI RADIATED POWER MEASUREMENTS: dB(pW)					
30.00	46	46	46.5	47	47	48
40.00	45	45.5	46	46	46.5	47
46.00	44	44	44	45	45	46
65.00	42.5	43	43	43.5	44	45
90.00	41	41	41	42	42	42.5
150.0	39	39.5	39.5	39.5	40	42
180.0	36.5	37	37	37	38	39
220.0	36	36	36	36	37	38
300.0	33	33	33.5	34	35	36

TABLE A2.70

TITLE: RFI CAUSED BY THE VARIATION OF THE SHORT-CIRCUITED COIL PARAMETERS:
MEASURED RFI LEVELS WITH VARYING RESISTANCE (Rs) AT 20000 r/min AND 2.5A SUPPLY CURRENT (Ls=0, e=0)

TEST VARIABLE: RESISTANCE (Ohms)

TEST NUMBER	7: 5.0 Ohms	8: 6.0	9: 8.0	10: 10.0	11: 15.0	12: 20.0
FREQUENCY	RFI CONDUCTED VOLTAGE MEASUREMENTS: dB(uV)					
0.150 MHz	91	93	95	97	98	98
0.160	90	92	94	96	97.5	97.5
0.240	87	90	94	95	95	95.5
0.550	80	81	85	88	89.5	92
1.000	74	76	79	80	84	87
1.400	70	71.5	76	79	80.5	85
2.000	69	70	71	72.5	77	83
3.500	62	67	68	69	73	80.5
6.000	62.5	63	65	67	72	78.5
10.00	64	64.5	65	67.5	70	76
13.00	65	65	66	67	69	74
22.00	62.5	63	64.5	66	68	70
30.00	58.5	60	63	64	66	69
	RFI RADIATED POWER MEASUREMENTS: dB(pW)					
30.00	51	54	56	58	60	64
40.00	50	52	54.5	57	59	63
46.00	47	50	52	55	57	59.5
65.00	45	47	49	50	54	56
90.00	44	46.5	49	50	52	54
150.0	43	45	47	49	50	52
180.0	40	42	45	47	49	50
220.0	39	41	44	46	46.5	48
300.0	37	40	42	43.5	46	47

TABLE A2.71

TITLE: RFI CAUSED BY THE VARIATION OF THE SHORT-CIRCUITED COIL PARAMETERS:
MEASURED RFI LEVELS WITH VARYING INDUCTANCE (Ls) AT 5000 r/min AND 0.5A SUPPLY CURRENT (Rs=RL=0.15, e=0)

TEST VARIABLE: INDUCTANCE (uH)

TEST NUMBER	1: 25uH	2: 50	3: 100	4: 250	5: 500	6: 1000	7: 1300
FREQUENCY	RFI CONDUCTED VOLTAGE MEASUREMENTS: dB(uV)						
0.150 MHz	70	74	78	81	82.5	84	85
0.160	70	74	77	80	82	83	84
0.240	67	70	76	77	80	81	81.5
0.550	60	63	69	72	73	73.5	74
1.000	56	58	64	67	68	70	71
1.400	54.5	57	62	66	67	68	69
2.000	54	56	61	64	65	66	67
3.500	53	55	60	62.5	64	65	66
6.000	50	53	56	60	62	63	64
10.00	46	50	53	56	60	61	64
13.00	45	47	50	54	57.5	60	64
22.00	36	39	44	48	54	56	61
30.00	30	32	36	45	51	55	59
	RFI RADIATED POWER MEASUREMENTS: dB(pW)						
30.00	25	27.5	32	41	44	48.5	52
40.00	24.5	27	32	40	44	46	52
46.00	23	24.5	30	39	43	45.5	50
65.00	22	23	30	36	40	43	48
90.00	20	20	28	35	39	42	46
150.0	19	20	28	35	37	41	43
180.0	15	17	26	33	37	40	42.5
220.0	15	16	23	28	31	35	36.5
300.0	13	14	19	25	30	32	35

TABLE A2.72

TITLE: RFI CAUSED BY THE VARIATION OF THE SHORT-CIRCUITED COIL PARAMETERS:
MEASURED RFI LEVELS WITH VARYING INDUCTANCE (Ls) AT 5000 r/min AND 1.5A SUPPLY CURRENT (Rs=RL=0.15, e=0)

TEST VARIABLE: INDUCTANCE (uH)

TEST NUMBER	1: 25 uH	2: 50	3: 100	4: 250	5: 500	6: 1000	7: 1300
FREQUENCY	RFI CONDUCTED VOLTAGE MEASUREMENTS: dB(uV)						
0.150 MHz	71	75	79	81.5	84	85	85.5
0.160	70.5	74.5	79	81	83	84	85
0.240	68	71	76.5	78.5	80.5	81.5	82
0.550	61	64	70	73	73.5	74.5	75.5
1.000	56.5	59	65	67.5	69	70.5	71.5
1.400	55	57.5	63	66.5	67.5	68	69
2.000	54	57	62	64.5	66.5	67.5	68
3.500	53	55.5	61	63.5	65.5	66	67
6.000	51	53.5	58	61	64	64.5	65.5
10.00	47.5	50	56	58.5	62	63	66.5
13.00	45.5	48	53	56	60	62.5	66
22.00	37	40	47	50.5	55.5	58.5	62.5
30.00	30.5	33	39.5	47	53	57	60
	RFI RADIATED POWER MEASUREMENTS: dB(pW)						
30.00	26	28	35	43	46	50	54
40.00	25	28	34	41	45	48	54
46.00	23.5	25	32	40	45	48	52
65.00	22	23	31	37	41	45	50
90.00	20	21	30	36	40	44	48
150.0	20	21	31	36	38	42	45
180.0	16	18	28	34	37	42	45
220.0	15	16	25	30	33	36	38
300.0	13	14	21	27	30	33	37

TABLE A2.73

TITLE: RFI CAUSED BY THE VARIATION OF THE SHORT-CIRCUITED COIL PARAMETERS:
MEASURED RFI LEVELS WITH VARYING INDUCTANCE (Ls) AT 5000 r/min AND 2.5A SUPPLY CURRENT (Rs=RL=0.15, e=0)

TEST VARIABLE: INDUCTANCE (uH)

TEST NUMBER	1: 25 uH	2: 50	3: 100	4: 250	5: 500	6: 1000	7: 1300
FREQUENCY	RFI CONDUCTED VOLTAGE MEASUREMENTS: dB(uV)						
0.150 MHz	72	75.5	79.5	82	84.5	85	86
0.160	71	75	78	81.5	84	84	85
0.240	69	72	77	79	81	82	83
0.550	61.5	64	70.5	74	74.5	75	76
1.000	57	59.5	65	68	69	71	72
1.400	55	58	63	67	68	69	70
2.000	54	57.5	62	65	67	68	69
3.500	53	56	62	64	66	67.5	68.5
6.000	51.5	54	59	63	65.5	66	67
10.00	48	51	57.5	60	63.5	65	68
13.00	46	49	54	58	62	64	68
22.00	37	41	48	52	57	60	64
30.00	31	33	41	48	55	60	63
	RFI RADIATED POWER MEASUREMENTS: dB(pW)						
30.00	26.5	29	36	44.5	47.5	52	57
40.00	25	28	36	42.5	47	50	56.5
46.00	24	25	33	42	46.5	49	55
65.00	22	23	32	39	43	47	53
90.00	20	21.5	31	38	42	46.5	51
150.0	20	20.5	31	37	40	44	48
180.0	16.5	19	29	36	39	43	47
220.0	15	18	26	32	35	38	40
300.0	13	16	22	29	32	35	39

TABLE A2.74

TITLE: RFI CAUSED BY THE VARIATION OF THE SHORT-CIRCUITED COIL PARAMETERS:
MEASURED RFI LEVELS WITH VARYING INDUCTANCE (Ls) AT 10000 r/min AND 0.5A SUPPLY CURRENT (Rs=RL=0.15, e=0)

TEST VARIABLE: INDUCTANCE (uH)

TEST NUMBER	1: 25 uH	2: 50	3: 100	4: 250	5: 500	6: 1000	7: 1300
FREQUENCY	RFI CONDUCTED VOLTAGE MEASUREMENTS: dB(uV)						
0.150 MHz	82	85.5	92	95	97	99	99.5
0.160	81	85	91.5	94.5	96.5	98	99
0.240	78.5	83	89	92	94	95	96
0.550	73	78	83	86	88	89	89
1.000	70	73	80	82	83	84	84.5
1.400	68	71	79	80	82	83	83
2.000	67	69.5	77	79.5	81	82	83
3.500	66	69	74.5	78	80	81	82
6.000	65	67.5	72	75	77.5	79	81
10.00	64	66	70	71	74	77	81.5
13.00	62	63.5	68	69	70	75	79
22.00	56	58	61	63	66	71	76
30.00	49	52	59	60	65	70	75
	RFI RADIATED POWER MEASUREMENTS: dB(pW)						
30.00	43.5	45.5	54	55	60.5	62	67
40.00	42	43.5	53	54.5	60	61.5	67
46.00	41	43	51	53	58	61	66
65.00	37.5	40	48	50	54	57	60
90.00	36	39	46	47.5	51	54	58.5
150.0	35	38	43	45	49	50	52
180.0	33	36	43	43	47	49	50
220.0	31	33	35	36	43	44	47
300.0	27	30	33.5	34.5	40	43	45

TABLE A2.75

TITLE: RFI CAUSED BY THE VARIATION OF THE SHORT-CIRCUITED COIL PARAMETERS:
MEASURED RFI LEVELS WITH VARYING INDUCTANCE (Ls) AT 10000 r/min AND 1.5A SUPPLY CURRENT (Rs=RL=0.15, e=0)

TEST VARIABLE: INDUCTANCE (uH)

TEST NUMBER	1: 25 uH	2: 50	3: 100	4: 250	5: 500	6: 1000	7: 1300
FREQUENCY	RFI CONDUCTED VOLTAGE MEASUREMENTS: dB(uV)						
0.150 MHz	82	86	92.5	95.5	97.5	99.5	100
0.160	81.5	85.5	92	95	97	99	99.5
0.240	79	83	89.5	92	94.5	96	96.5
0.550	73.5	78	83.5	86.5	88.5	89.5	89.5
1.000	70	73	80	82.5	84	85	85
1.400	68.5	71.5	79	80.5	82.5	83.5	83.5
2.000	67.5	70	77	80	82	82.5	83
3.500	66	69	75	78	81	81.5	82.5
6.000	65.5	68	73.5	76.5	79	81	82
10.00	64	66	71	73	75.5	79	83
13.00	62	64	69	70	72	77	81
22.00	56	58	62.5	64	68	73	78
30.00	50	52.5	60	61	67	72	77
	RFI RADIATED POWER MEASUREMENTS: dB(pW)						
30.00	44	46	55	57	62	64	69
40.00	42	44	54	55	61	64	68
46.00	41	44	52	54	60	63	68
65.00	38	40	49	51	56	58	62
90.00	36	40	47	49	53	55	60
150.0	35	38	44	46	50	52	54
180.0	34	36	43	44	48	50	52
220.0	31	33	36	37	44	46	49
300.0	28	30	36	36.5	42	45	47

TABLE A2.76

TITLE: RFI CAUSED BY THE VARIATION OF THE SHORT-CIRCUITED COIL PARAMETERS:
MEASURED RFI LEVELS WITH VARYING INDUCTANCE (Ls) AT 10000 r/min AND 2.5A SUPPLY CURRENT (Rs=RL=0.15, e=0)

TEST VARIABLE: INDUCTANCE (uH)

TEST NUMBER	1: 25 uH	2: 50	3: 100	4: 250	5: 500	6: 1000	7: 1300
FREQUENCY	RFI CONDUCTED VOLTAGE MEASUREMENTS: dB(uV)						
0.150 MHz	82	86	93	96	98	100	100.5
0.160	82	86	92	95	97.5	99	99.5
0.240	79.5	84	90	92	94.5	96	97
0.550	74	78	84	87	89	90	90
1.000	70	73.5	80	83	85	85	85.5
1.400	69	72	79	81	83	84	84.5
2.000	68	70	77	80	82	83	83
3.500	66	69.5	76	80	82	82.5	84
6.000	66	68	75	78	81	83	84
10.00	64	66	72	75	77	81	85
13.00	62.5	64.5	70.5	72	74	79	82
22.00	56	58	64	66	70	75	79.5
30.00	50.5	53	61	63	69	75	79
	RFI RADIATED POWER MEASUREMENTS: dB(pW)						
30.00	44	46.5	57	59	63	67	71.5
40.00	42.5	45	55	57	62.5	66	71
46.00	42	44	53	56	62	65	70
65.00	38.5	40.5	50	53	58	60	64.5
90.00	36	40	48	50	55	56.5	62
150.0	35	38	45	47.5	52	53	56
180.0	34	36	44	46	50	51.5	54
220.0	31	33	37	39	46	48	51.5
300.0	28.5	31	37	38.5	44	47	50

TABLE A2.77

TITLE: RFI CAUSED BY THE VARIATION OF THE SHORT-CIRCUITED COIL PARAMETERS:
MEASURED RFI LEVELS WITH VARYING INDUCTANCE (Ls) AT 15000 r/min AND 0.5A SUPPLY CURRENT (Rs=RL=0.15, e=0)

TEST VARIABLE: INDUCTANCE (uH)

TEST NUMBER	1:	2:	3:	4:	5:	6:
	10 uH	25	50	100	250	500
FREQUENCY	RFI CONDUCTED VOLTAGE MEASUREMENTS: dB(uV)					
0.150 MHz	80	85	90	93.5	96	97.5
0.160	79.5	84	89.5	93	95	97
0.240	78	83	88	91	93	96
0.550	74	78.5	85	87	89	91
1.000	71	76	82	84	86	88
1.400	70	74	82	83	84	86.5
2.000	68	72	78.5	81.5	83	85
3.500	67	72	76.5	79	80.5	82.5
6.000	65.5	71	75	77	79	81
10.00	65	70	74	75	77	80
13.00	64	68	72	74	75	79
22.00	61	64	67.5	70	73	77
30.00	56	61	66	67	71	76
	RFI RADIATED POWER MEASUREMENTS: dB(pW)					
30.00	47	54	60.5	62	63.5	69
40.00	47	54	60	61.5	63.5	68
46.00	45	52	58.5	60	63	67
65.00	41.5	50	54	55	58	61.5
90.00	42	49	52	53	55	60
150.0	40	46.5	48.5	50	52	54
180.0	38	44	47	48	51	53
220.0	37	42	43	45	47	49
300.0	34	40	41.5	43	45	46.5

TABLE A2.78

TITLE: RFI CAUSED BY THE VARIATION OF THE SHORT-CIRCUITED COIL PARAMETERS:
MEASURED RFI LEVELS WITH VARYING INDUCTANCE (Ls) AT 15000 r/min AND 0.5A SUPPLY CURRENT (Rs=RL=0.15, e=0)

TEST VARIABLE: INDUCTANCE (uH)

TEST NUMBER	7:	8:				
	1000 uH	1300				
FREQUENCY	RFI CONDUCTED VOLTAGE MEASUREMENTS: dB(uV)					
0.150 MHz	99.5	100				
0.160	99	99.5				
0.240	96.5	98				
0.550	92	92				
1.000	88	89				
1.400	86	87				
2.000	85	86				
3.500	83	84				
6.000	82	83				
10.00	81.5	85				
13.00	81	84				
22.00	80	83				
30.00	80	83.5				
	RFI RADIATED POWER MEASUREMENTS: dB(pW)					
30.00	72	77				
40.00	71.5	76				
46.00	70	73.5				
65.00	64	66.5				
90.00	61.5	65				
150.0	55	58				
180.0	54	56				
220.0	50.5	52				
300.0	47	48				

*
*   TABLE A2.79
*

TITLE: RFI CAUSED BY THE VARIATION OF THE SHORT-CIRCUITED COIL PARAMETERS.
MEASURED RFI LEVELS WITH VARYING INDUCTANCE (Ls) AT 15000 r/min AND 1.5A SUPPLY CURRENT (Rs=Ls=0.15, e=0)

TEST VARIABLE: INDUCTANCE (uH)

TEST NUMBER	1:	2:	3:	4:	5:	6:
	10 uH	25	50	100	250	500
FREQUENCY	RFI CONDUCTED VOLTAGE MEASUREMENTS: dB(uV)					
0.150 MHz	80.5	85	[illegible]	94	96	98
0.160	80	84.5	90		95	97.5
0.240	78	83.5	88	91.[illegible]	[illegible]3.5	96.5
0.550	74	79	85	87	89	
1.000	71.5	76	82	84.5	86	[illegible]
1.400	70	74	80	83	84.5	87
2.000	68.5	72.5	79	82	83	85
3.500	67	72.5	77	80	81.5	84
6.000	66	71	75.5	78	80	83
10.00	65	70	74	76	78	81.5
13.00	64	68.5	72	74.5	76	81
22.00	61	64	68	71	74	79
30.00	56.5	61	66	68	72.5	78.5
	RFI RADIATED POWER MEASUREMENTS: dB(pW)					
30.00	48	55	61	63	65	71
40.00	47	54	60	63	65	70
46.00	45	52	59	61	64	69
65.00	42	50	54	56	59	63
90.00	43	49	52	54	56	61
150.0	40	47	49	51	53	55
180.0	38	44	47	49	52	54
220.0	37	43	43	46	48	50
300.0	34	40	42	44	46	48

*
*   TABLE A2.80
*

TITLE: RFI CAUSED BY THE VARIATION OF THE SHORT-CIRCUITED COIL PARAMETERS:
MEASURED RFI LEVELS WITH VARYING INDUCTANCE (Ls) AT 15000 r/min AND 1.5A SUPPLY CURRENT (Rs=RL=0.15, e=0)

TEST VARIABLE: INDUCTANCE (uH)

TEST NEMBER	7:	8:				
	1000 uH	1300				
FREQUENCY	RFI CONDUCTED VOLTAGE MEASUREMENTS: dB(uV)					
0.150 MHz	100	101				
0.160	99	100				
0.240	97	98				
0.550	92	92.5				
1.000	88.5	89				
1.400	87	87.5				
2.000	85.5	86.5				
3.500	84.5	85				
6.000	84	85				
10.00	83	86				
13.00	82.5	86				
22.00	81.5	85.5				
30.00	81	85				
	RFI RADIATED POWER MEASUREMENTS: dB(pW)					
30.00	74	79				
40.00	73	78				
46.00	71	75				
65.00	65	69				
90.00	63	66				
150.0	57	60				
180.0	56	58				
220.0	52	54				
300.0	49	50				

TABLE A2.81

TITLE: RFI CAUSED BY THE VARIATION OF THE SHORT-CIRCUITED COIL PARAMETERS:
MEASURED RFI LEVELS WITH VARYING INDUCTANCE (Ls) AT 15000 r/min AND 2.5A SUPPLY CURRENT (Rs=RL=0.15, e=0)

TEST VARIABLE: INDUCTANCE (uH)

TEST NUMBER	1:	2:	3:	4:	5:	6:
	10 uH	25	50	100	250	500
FREQUENCY	RFI CONDUCTED VOLTAGE MEASUREMENTS: dB(uV)					
0.150 MHz	81	85	91	94	96	98.5
0.160	80	85	90	94	95.5	98
0.240	78	84	88.5	92	94	97
0.550	74	79	86	87	89	91.5
1.000	72	76.5	82.5	85	87	88
1.400	71	74	80	83	85	87
2.000	69	73	79	83	83.5	85.5
3.500	67	73	77	82	82.5	84.5
6.000	66.5	72	76	80.5	82	84
10.00	65	70.5	75	79	80	83
13.00	64	69	73	77	79	83
22.00	62	64	69	73	77.5	82
30.00	57	61	66.5	70	75	81
	RFI RADIATED POWER MEASUREMENTS: dB(pW)					
30.00	48	55	61.5	65	67.5	74
40.00	48	54	61	64.5	67	73.5
46.00	45.5	53	59	63	67	71
65.00	43	51	55	58	60.5	65
90.00	43	49	53	56	58	63
150.0	40	47	49	53	54	57.5
180.0	38	44.5	47	51.5	54	56
220.0	37	43	43.5	48	50	53
300.0	34	39	42	46	48	50

TABLE A2.82

TITLE: RFI CAUSED BY THE VARIATION OF THE SHORT-CIRCUITED COIL PARAMETERS:
MEASURED RFI LEVELS WITH VARYING INDUCTANCE (Ls) AT 15000 r/min AND 2.5A SUPPLY CURRENT (Rs=RL=0.15, e=0)

TEST VARIABLE: INDUCTANCE (uH)

TEST NUMBER	7:	8:				
	1000 uH	1300				
FREQUENCY	RFI CONDUCTED VOLTAGE MEASUREMENTS: dB(uV)					
0.150 MHz	100	101				
0.160	99	101				
0.240	97.5	98				
0.550	92	93				
1.000	89	90				
1.400	87.5	88				
2.000	86.5	87				
3.500	86	86				
6.000	86	87.5				
10.00	85	88				
13.00	85.5	89				
22.00	85	88				
30.00	83.5	86.5				
	RFI RADIATED POWER MEASUREMENTS: dB(pW)					
30.00	76.5	80.5				
40.00	75	79.5				
46.00	73	77				
65.00	67	70.5				
90.00	65	68				
150.0	59	62				
180.0	58	60				
220.0	54	56				
300.0	51	53				

TABLE A2.83

TITLE: RFI CAUSED BY THE VARIATION OF THE SHORT-CIRCUITED COIL PARAMETERS:
MEASURED RFI LEVELS WITH VARYING INDUCTANCE (Ls) AT 20000 r/min
AND 0.5A SUPPLY CURRENT (Rs=RL=0.15, e=0)

TEST VARIABLE: INDUCTANCE (uH)

TEST NUMBER	1:	2:	3:	4:	5:	6:
	5 uH	10	25	50	100	500
FREQUENCY	RFI CONDUCTED VOLTAGE MEASUREMENTS: dB(uV)					
0.150 MHz	81.5	87	92.5	95.5	97	98.5
0.160	81	86	92	95	97	98
0.240	79	85	91	93.5	96	98
0.550	75	82	88	91	93	96
1.000	72.5	80	86	89	91	93
1.400	71	79	85	88	90	92
2.000	70	78	83	87	88	91
3.500	68	75	80	88	88	89
6.000	68	75	79	85	85.5	87
10.00	67	72	77.5	81	84	85
13.00	67	71	76	78	80	84
22.00	64	68	71	74	81	82
30.00	61.5	65	69	72	76	81
	RFI RADIATED POWER MEASUREMENTS: dB(pW)					
30.00	55	60	63	65	68	73
40.00	54	59.5	63	65	68	72
46.00	52	58	63	64	66	71.5
65.00	49	53	57	60	60.5	68
90.00	48	50	55	57	59	63
150.0	46	48.5	52	54	55	58
180.0	43	47	50	52	52	55
220.0	42	43	47	49	49	50
300.0	38	41.5	50	47	47	48

TABLE A2.84

TITLE: RFI CAUSED BY THE VARIATION OF THE SHORT-CIRCUITED COIL PARAMETERS:
MEASURED RFI LEVELS WITH VARYING INDUCTANCE (Ls) AT 20000 r/min
AND 0.5A SUPPLY CURRENT (Rs=RL=0.15, e=0)

TEST VARIABLE: INDUCTANCE (uH)

TEST NUMBER	7:	8:
	1000 uH	1300
FREQUENCY	RFI CONDUCTED VOLTAGE MEASUREMENTS: dB(uV)	
0.150 MHz	101	102
0.160	100	101
0.240	99	100
0.550	97	97.5
1.000	95	96
1.400	94	95
2.000	92	93.5
3.000	90	91
6.000	88	89
10.00	86	88
13.00	86	89
22.00	84	88
30.00	83	87
	RFI RADIATED POWER MEASUREMENTS: dB(pW)	
30.00	78.5	83
40.00	78	82
46.00	74	78
65.00	68.5	74
90.00	65	68
150.0	60	63
180.0	57	59
220.0	54	57
300.0	50	53

TABLE A2.85

TITLE: RFI CAUSED BY THE VARIATION OF THE SHORT-CIRCUITED COIL PARAMETERS:
MEASURED RFI LEVELS WITH VARYING INDUCTANCE (Ls) AT 20000 r/min AND 1.5A SUPPLY CURRENT (Rs=RL=0.15, e=0)

TEST VARIABLE: INDUCTANCE (uH)

TEST NUMBER	1: 5 uH	2: 10	3: 25	4: 50	5: 100	6: 500
FREQUENCY	RFI CONDUCTED VOLTAGE MEASUREMENTS: dB(uV)					
0.150 MHz	82	87	93	96	97.5	99
0.160	81.5	87	92.5	95	97	99
0.240	79	85	91.5	94	96	98.5
0.550	75	82	88.5	91	93.5	96
1.000	73	80.5	86	89	91.5	93.5
1.400	71.5	79	85	88.5	90.5	92.5
2.000	70	78	83	88	89	92
3.500	69.5	76	80.5	88	88.5	90
6.000	69	75	79	85	86.5	88.5
10.00	68	72.5	78	81	83	87
13.00	67	71	76.5	79	81.5	86
22.00	64.5	68	71.5	74	79	84
30.00	62	65.5	70	72.5	78	83
	RFI RADIATED POWER MEASUREMENTS: dB(pW)					
30.00	56	60.5	64	66	70	75
40.00	55	60	64	65	70	74
46.00	53	58	63	65	68	74
65.00	50	53	57	60	62	70
90.00	49	51	55	57	60	65
150.0	47	49	52	54	56	60
180.0	44	47	50	52	53	57
220.0	43	43	47	49	50	53
300.0	39	42	45	47	48	50

TABLE A2.86

TITLE: RFI CAUSED BY THE VARIATION OF THE SHORT-CIRCUITED COIL PARAMETERS:
MEASURED RFI LEVELS WITH VARYING INDUCTANCE (Ls) AT 20000 r/min AND 1.5A SUPPLY CURRENT (Rs=RL=0.15, e=0)

TEST VARIABLE: INDUCTANCE (uH)

TEST NUMBER	7: 1000 uH	8: 1300				
FREQUENCY	RFI CONDUCTED VOLTAGE MEASUREMENTS: dB(uV)					
0.150 MHz	101.5	102.5				
0.160	101	102				
0.240	99	100.5				
0.550	97	98				
1.000	95	96				
1.400	94	95				
2.000	92.5	93				
3.500	91	91.5				
6.000	89.5	90.5				
10.00	88.5	89.5				
13.00	88	90				
22.00	86	90				
30.00	85.5	89.5				
	RFI RADIATED POWER MEASUREMENTS: dB(pW)					
30.00	80	84				
40.00	80	83				
46.00	76	79				
65.00	71	74				
90.00	67	69				
150.0	62	65				
180.0	59	60				
220.0	56	58				
300.0	52	54				

TABLE A2.87

TITLE: RFI CAUSED BY THE VARIATION OF THE SHORT-CIRCUITED COIL PARAMETERS:
MEASURED RFI LEVELS WITH VARYING INDUCTANCE (Ls) AT 20000 r/min AND 2.5A SUPPLY CURRENT (Rs=RL=0.15, e=0)

TEST VARIABLE: INDUCTANCE (uH)

TEST NUMBER	1:	2:	3:	4:	5:	6:
	5 uH	10	25	50	100	500
FREQUENCY	RFI CONDUCTED VOLTAGE MEASUREMENTS: dB(uV)					
0.150 MHz	82	88	93.5	96	98	99.5
0.160	82	87	93	95	97	99
0.240	79	85.5	92	94	96.5	99
0.550	76	83	89	91.5	94	96
1.000	74	81	86	90	92	94
1.400	72	79	85	89	91	93
2.000	71	78	83	88.5	90	93
3.500	70	76.5	81	89.5	90	91.5
6.000	69	75	79	87	88	90
10.00	68	73	78	83	85	89
13.00	68	71	77	81.5	84	88
22.00	65	68	72	76	82	86.5
30.00	63	66	70	75	80.5	85
	RFI RADIATED POWER MEASUREMENTS: dB(pW)					
30.00	57	61	64.5	68	73	80
40.00	56	60	64.5	68	72	79
46.00	54	58	63	67	70	75
65.00	51	53	58	62	66	69
90.00	50	52	56	59	63	66
150.0	48	49	53	56	59	61
180.0	45	47	51	54	56	58
220.0	44	43	48	51	53	55
300.0	40	42	46	49	50	51

TABLE A2.88

TITLE: RFI CAUSED BY THE VARIATION OF THE SHORT-CIRCUITED COIL PARAMETERS:
MEASURED RFI LEVELS WITH VARYING INDUCTANCE (Ls) AT 20000 r/min AND 2.5A SUPPLY CURRENT (Rs=RL=0.15, e=0)

TEST VARIABLE: INDUCTANCE (uH)

TEST NUMBER	7:	8:				
	1000	1300				
	uH					
FREQUENCY	RFI CONDUCTED VOLTAGE MEASUREMENTS: dB(uV)					
0.150 MHz	102	103				
0.160	101	102				
0.240	99	101				
0.550	97.5	99				
1.000	96	97				
1.400	94	96				
2.000	94	94.5				
3.500	92.5	93				
6.000	91.5	93				
10.00	91	92.5				
13.00	90	92				
22.00	89.5	93				
30.00	87.5	92				
	RFI RADIATED POWER MEASUREMENTS: dB(pW)					
30.00	85	87				
40.00	84.5	86				
46.00	79	82				
65.00	75	76				
90.00	70	71.5				
150.0	66	67				
180.0	60	62				
220.0	58	60				
300.0	54	56				

TABLE A2.89

TITLE: RFI CAUSED BY THE VARIATION OF THE SHORT-CIRCUITED COIL PARAMETERS:
MEASURED RFI LEVELS WITH VARYING INDUCTANCE (Ls) AT 5000 r/min AND 1.5A SUPPLY CURRENT (Rs=0.3 Ohms, e=0)

TEST VARIABLE: INDUCTANCE (uH)

TEST NUMBER	1:	2:	3:	4:	5:	6:	7:
	25 uH	50	100	250	500	1000	1300
FREQUENCY	RFI CONDUCTED VOLTAGE MEASUREMENTS: dB(uV)						
0.150 MHz	71	75	79	82	84	85	86
0.160	71	75	78	81	83	84	85
0.240	68	71	77	79	81	82	82
0.550	61	64	70	73	74	75	76
1.000	57	59	65	68	69	71	72
1.400	55	58	63	67	68	68	69
2.000	54	57	62	65	67	68	68
3.500	53	56	61	64	66	66	67
6.000	51	54	58	61	64	65	66
10.00	47.5	50	56	59	62	63	67
13.00	45.5	48	53	56	60	63	66
22.00	37	40	47	51	56	59	63
30.00	30.5	33	39.5	47	53	57	60
	RFI RADIATED POWER MEASUREMENTS: dB(pW)						
30.00	26	28	35	43	46	50	54
40.00	25	28	34	41	45	48	54
46.00	23.5	25	32	40	45	48	52
65.00	22	23	31	37	41	45	50
90.00	20	21	30	36	40	44	48
150.0	20	21	31	36	38	42	45
180.0	16	18	28	34	37	42	45
220.0	15	16	25	30	33	36	38
300.0	13	14	21	27	30	33	37

TABLE A2.90

TITLE: RFI CAUSED BY THE VARIATION OF THE SHORT-CIRCUITED COIL PARAMETERS:
MEASURED RFI LEVELS WITH VARYING INDUCTANCE (Ls) AT 10000 r/min AND 1.5A SUPPLY CURRENT (Rs=0.3 Ohms, e=0)

TEST VARIABLE: INDUCTANCE (uH)

TEST NUMBER	1:	2:	3:	4:	5:	6:	7:
	25 uH	50	100	250	500	1000	1300
FREQUENCY	RFI CONDUCTED VOLTAGE MEASUREMENTS: dB(uV)						
0.150 MHz	82	86	93	96	98	100	100
0.160	82	86	92	95	97	99	100
0.240	79	83	89	92	95	96	97
0.550	74	78	84	87	89	89	89
1.000	70	73	80	83	84	85	85
1.400	69	72	79	81	83	84	84
2.000	68	70	77	80	82	83	83
3.500	66	69	75	78	81	82	83
6.000	66	68	74	77	79	81	82
10.00	64	66	71	73	76	79	83
13.00	62	64	69	70	72	77	81
22.00	56	58	63	64	68	73	78
30.00	50	53	60	61	67	72	77
	RFI RADIATED POWER MEASUREMENTS: dB(pW)						
30.00	44	46	55	57	62	64	69
40.00	42	44	54	55	61	64	68
46.00	41	44	52	54	60	63	68
65.00	38	40	49	51	56	58	62
90.00	36	40	47	49	53	55	60
150.0	35	38	44	46	50	52	54
180.0	34	36	43	44	48	50	52
220.0	31	33	36	37	44	46	49
300.0	28	30	36	36.5	42	45	47

TABLE A2.91

TITLE: RFI CAUSED BY THE VARIATION OF THE SHORT-CIRCUITED COIL PARAMETERS:
MEASURED RFI LEVELS WITH VARYING INDUCTANCE (Ls) AT 15000 r/min AND 1.5A SUPPLY CURRENT (Rs=0.3 Ohms, e=0)

TEST VARIABLE: INDUCTANCE (uH)

TEST NUMBER	1: 10 uH	2: 25	3: 50	4: 100	5: 250	6: 500
FREQUENCY	RFI CONDUCTED VOLTAGE MEASUREMENTS: dB(uV)					
0.150 MHz	81	85	91	94	96	98
0.160	80	85	90	93	95	98
0.240	78	84	88	92	94	97
0.550	74	79	85	87	89	91
1.000	72	76	82	85	86	88
1.400	70	74	80	83	85	87
2.000	69	73	79	82	83	85
3.500	67	73	77	80	82	84
6.000	66	71	76	78	80	83
10.00	65	70	74	76	78	82
13.00	64	69	72	75	76	81
22.00	61	64	68	71	74	79
30.00	57	61	66	68	73	79
	RFI RADIATED POWER MEASUREMENTS: dB(pW)					
30.00	48	55	61	63	65	71
40.00	47	54	60	63	65	70
46.00	45	52	59	61	64	69
65.00	42	50	54	56	59	63
90.00	43	49	52	54	56	61
150.0	40	47	49	51	53	55
180.0	38	44	47	49	52	54
220.0	37	43	43	46	48	50
300.0	34	40	42	44	46	48

TABLE A2.92

TITLE: RFI CAUSED BY THE VARIATION OF THE SHORT-CIRCUITED COIL PARAMETERS:
MEASURED RFI LEVELS WITH VARYING INDUCTANCE (Ls) AT 15000 r/min AND 1.5A SUPPLY CURRENT (Rs=0.3 Ohms, e=0)

TEST VARIABLE: INDUCTANCE (uH)

TEST NUMBER	7: 1000 uH	8: 1300				
FREQUENCY	RFI CONDUCTED VOLTAGE MEASUREMENTS: dB(uV)					
0.150 MHz	100	101				
0.160	99	100				
0.240	97	98				
0.550	92	93				
1.000	89	89				
1.400	87	88				
2.000	86	87				
3.500	85	85				
6.000	84	85				
10.00	83	86				
13.00	83	86				
22.00	82	86				
30.00	81	85				
	RFI RADIATED POWER MEASUREMENTS: dB(pW)					
30.00	74	79				
40.00	73	78				
46.00	71	75				
65.00	65	69				
90.00	63	66				
150.0	57	60				
180.0	56	58				
220.0	52	54				
300.0	49	50				

TABLE A2.93

TITLE: RFI CAUSED BY THE VARIATION OF THE SHORT-CIRCUITED COIL PARAMETERS:
MEASURED RFI LEVELS WITH VARYING INDUCTANCE (Ls) AT 20000 r/min AND 1.5A SUPPLY CURRENT (Rs=0.3 Ohms, e=0)

TEST VARIABLE: INDUCTANCE (uH)

TEST NUMBER	1: 5 uH	2: 10	3: 25	4: 50	5: 100	6: 500
FREQUENCY	RFI CONDUCTED VOLTAGE MEASUREMENTS: dB(uV)					
0.150 MHz	82	87	93	96	98	99
0.160	82	87	93	95	97	99
0.240	79	85	92	94	96	99
0.550	75	82	89	91	94	96
1.000	73	81	86	89	92	94
1.400	72	79	85	89	91	93
2.000	70	78	83	88	89	92
3.500	70	76	81	88	89	90
6.000	69	75	79	85	87	89
10.00	68	73	78	81	83	87
13.00	67	71	77	79	82	86
22.00	65	68	72	74	79	84
30.00	62	66	70	73	78	83
	RFI RADIATED POWER MEASUREMENTS: dB(pW)					
30.00	56	61	64	66	70	75
40.00	55	60	64	65	70	74
46.00	53	58	63	65	68	74
65.00	50	53	57	60	62	70
90.00	49	51	55	57	60	65
150.0	47	49	52	54	56	60
180.0	44	47	50	52	53	57
220.0	43	43	47	49	50	53
300.0	39	42	45	47	48	50

TABLE A2.94

TITLE: RFI CAUSED BY THE VARIATION OF THE SHORT-CIRCUITED COIL PARAMETERS:
MEASURED RFI LEVELS WITH VARYING INDUCTANCE (Ls) AT 20000 r/min AND 1.5A SUPPLY CURRENT (Rs=0.3 Ohms, e=0)

TEST VARIABLE: INDUCTANCE (uH)

TEST NUMBER	7: 1000 uH	8: 1300
FREQUENCY	RFI CONDUCTED VOLTAGE MEASUREMENTS: dB(uV)	
0.150 MHz	101.5	102.5
0.160	101	102
0.240	99	101
0.550	97	98
1.000	95	96
1.400	94	95
2.000	93	93
3.500	91	92
6.000	89	91
10.00	89	89
13.00	88	90
22.00	86	90
30.00	86	89
	RFI RADIATED POWER MEASUREMENTS: dB(pW)	
30.00	80	84
40.00	80	83
46.00	76	79
65.00	71	74
90.00	67	69
150.0	62	65
180.0	59	60
220.0	56	58
300.0	52	54

TABLE A2.95

TITLE: RFI CAUSED BY THE VARIATION OF THE SHORT-CIRCUITED COIL PARAMETERS:
MEASURED RFI LEVELS WITH VARYING INDUCTANCE (Ls) AT 5000 r/min AND 1.5A SUPPLY CURRENT (Rs=0.65 Ohms, e=0)

TEST VARIABLE: INDUCTANCE (uH)

TEST NUMBER	1:	2:	3:	4:	5:	6:	7:
	25 uH	50	100	250	500	1000	1300
FREQUENCY	RFI CONDUCTED VOLTAGE MEASUREMENTS: dB(uV)						
0.150 MHz	71	75	79	83.5	85.5	85	87.5
0.161	71	75	79.5	81	83	85.5	85
0.240	69.5	71	77	79	81	83.5	82
0.550	61	65.5	71.5	73	75.5	75	77.5
1.000	57	59	65	69.5	69	71	73.5
1.400	55	59.5	63	67	69.5	69.5	69
2.000	55.5	57	63.5	65	67	69.5	68
3.500	53	57.5	61	65.5	67.5	67.5	67
6.000	51	55.5	59.5	61	65.5	65	67.5
10.00	47.5	50	57.5	59	63.5	63	67
13.00	45.5	48	53	57.5	61.5	63	66
22.00	37	40	47	51	57.5	59	63
30.00	30.5	33	39.5	47	53	57	60
	RFI RADIATED POWER MEASUREMENTS: dB(pW)						
30.00	26	28	35	43	46	50	54
40.00	25	28	34	41	45	48	54
46.00	23.5	25	32	40	45	48	52
65.00	22	23	31	37	41	45	50
90.00	20	21	30	36	40	44	48
150.0	20	21	31	36	38	42	45
180.0	16	18	28	34	37	42	45
220.0	15	16	25	30	33	36	38
300.0	13	14	21	27	30	33	37

TABLE A2.96

TITLE: RFI CAUSED BY THE VARIATION OF THE SHORT-CIRCUITED COIL PARAMETERS:
MEASURED RFI LEVELS WITH VARYING INDUCTANCE (Ls) AT 10000 r/min AND 1.5A SUPPLY CURRENT (Rs=0.65 Ohms, e=0)

TEST VARIABLE: INDUCTANCE (uH)

TEST NUMBER	1:	2:	3:	4:	5:	6:	7:
	25 uH	50	100	250	500	1000	1300
FREQUENCY	RFI CONDUCTED VOLTAGE MEASUREMENTS: dB(uV)						
0.150 MHz	83.5	87.5	93	97.5	99.5	100	100
0.161	83.5	87.5	93.5	95	97	99	100
0.240	79	83	89	93.5	95	97.5	97
0.550	75.5	79.5	85.5	87	89	89	89
1.000	71.5	73	81.5	83	85.5	85	85
1.400	69	73.5	79	81	83	85.5	85.5
2.000	69.5	71.5	77	81.5	83.5	83	83
3.500	67.5	69	75	79.5	81	83.5	83
6.000	67.5	69.5	75.5	77	79	81	82
10.00	65.5	67.5	71	73	77.5	79	83
13.00	63.5	65.5	69	71.5	73.5	77	81
22.00	57.5	59.5	63	65.5	69.5	73	78
30.00	50	53	61.5	61	67	73.5	77
	RFI RADIATED POWER MEASUREMENTS: dB(pW)						
30.00	44	46	55	57	63.5	65.5	69
40.00	42	44	55.5	55	61	65.5	68
46.00	41	44	53.5	55.5	61.5	63	68
65.00	38	40	49	51	57.5	59.5	62
90.00	36	40	47	49	53	55	60
150.0	35	38	44	46	50	53.5	54
180.0	34	36	43	44	48	50	52
220.0	31	33	36	37	44	46	49
300.0	28	30	36	36.5	42	45	47

*
*
TABLE A2.97

*

TITLE: RFI CAUSED BY THE VARIATION OF THE SHORT-CIRCUITED COIL PARAMETERS:
MEASURED RFI LEVELS WITH VARYING INDUCTANCE (Ls) AT 15000 r/min AND 1.5A SUPPLY CURRENT (Rs=0.65 Ohms, e=0)

TEST VARIABLE: INDUCTANCE (uH)

TEST NUMBER	1: 10 uH	2: 25	3: 50	4: 100	5: 250	6: 500
FREQUENCY	RFI CONDUCTED VOLTAGE MEASUREMENTS: dB(uV)					
0.150 MHz	81	85	91	95.5	97.5	99.5
0.161	81.5	85	91.5	93	95	99.5
0.240	79.5	85.5	89.5	93.5	95.5	97
0.550	75.5	79	85	87	89	91
1.000	73.5	77.5	83.5	85	87.5	89.5
1.400	71.5	75.5	81.5	83	85	87
2.000	69	73	79	83.5	83	85
3.500	67	73	77	81.5	83.5	85.5
6.000	67.5	71	77.5	79.5	81.5	83
10.00	65	71.5	75.5	77.5	79.5	83.5
13.00	65.5	69	73.5	75	77.5	81
22.00	61	65.5	69.5	71	75.5	79
30.00	57	61	67.5	69.5	73	79
	RFI RADIATED POWER MEASUREMENTS: dB(pW)					
30.00	48	55	61	63	65	71
40.00	47	55.5	61.5	63	65	71.5
46.00	45	53.5	59	61	65.5	69
65.00	42	50	55.5	57.5	59	63
90.00	43	49	53.5	55.5	57.5	61
150.0	40	47	49	51	53	55
180.0	38	44	47	49	53.5	55.5
220.0	37	43	43	46	48	50
300.0	34	40	42	44	46	48

*
*
TABLE A2.98

*

TITLE: RFI CAUSED BY THE VARIATION OF THE SHORT-CIRCUITED COIL PARAMETERS:
MEASURED RFI LEVELS WITH VARYING INDUCTANCE (Ls) AT 15000 r/min AND 1.5A SUPPLY CURRENT (Rs=0.65 , e=0)

TEST VARIABLE: INDUCTANCE (uH)

TEST NUMBER	7: 1000 uH	8: 1300				
FREQUENCY	RFI CONDUCTED VOLTAGE MEASUREMENTS: dB(uV)					
0.150 MHz	100	101				
0.161	99	100				
0.240	97	99.5				
0.550	93.5	93				
1.000	89	89				
1.400	87	89.5				
2.000	87.5	87				
3.500	85	85				
6.000	85.5	85				
10.00	83	87.5				
13.00	83	87.5				
22.00	83.5	87.5				
30.00	81	85				
	RFI RADIATED POWER MEASUREMENTS: dB(pW)					
30.00	75.5	79				
40.00	73	79.5				
46.00	71	75				
65.00	65	69				
90.00	63	67.5				
150.0	57	61.5				
180.0	57.5	59.5				
220.0	53.5	55.5				
300.0	49	50				

TABLE A2.99

TITLE. RFI CAUSED BY THE VARIATION OF THE SHORT-CIRCUITED COIL PARAMETERS:
MEASURED RFI LEVELS WITH VARYING INDUCTANCE (Ls) AT 20000 r/min AND 1.5A SUPPLY CURRENT (Rs=0.65 Ohms, e=0)

TEST VARIABLE: INDUCTANCE (uH)

TEST NUMBER	1:	2:	3:	4:	5:	6:
	5 uH	10	25	50	100	500
FREQUENCY	RFI CONDUCTED VOLTAGE MEASUREMENTS: dB(uV)					
0.150 MHz	83.5	87	93	97.5	99.5	99
0.161	83.5	87	93	95	97	99
0.240	79	85	93.5	95.5	97.5	99
0.550	75	83.5	89	91	95.5	97.5
1.000	73	81	87.5	89	93.5	95.5
1.400	73.5	79	85	89	91	93
2.000	71.5	79.5	83	89.5	89	93.5
3.500	71.5	77.5	81	89.5	89	91.5
6.000	69	75	79	85	87	89
10.00	69.5	73	79.5	81	83	87
13.00	67	71	77	79	83.5	87.5
22.00	65	69.5	73.5	75.5	79	85.5
30.00	63.5	67.5	71.5	73	79.5	83
	RFI RADIATED POWER MEASUREMENTS: dB(pW)					
30.00	57.5	61	65.5	67.5	71.5	75
40.00	55	61.5	65.5	65	71.5	75.5
46.00	53	59.5	63	65	69.5	75.5
65.00	50	53	57	61.5	63.5	71.5
90.00	49	51	55	57	61.5	65
150.0	47	49	53.5	55.5	57.5	61.5
180.0	44	47	50	53.5	53	57
220.0	43	43	47	49	50	53
300.0	39	42	45	47	48	50

TABLE A2.100

TITLE: RFI CAUSED BY THE VARIATION OF THE SHORT-CIRCUITED COIL PARAMETERS:
MEASURED RFI LEVELS WITH VARYING INDUCTANCE (Ls) AT 20000 r/min AND 1.5A SUPPLY CURRENT (Rs=0.65 Ohms, e=0)

TEST VARIABLE: INDUCTANCE (uH)

TEST NUMBER	7:	8:
	1000 uH	1300
FREQUENCY	RFI CONDUCTED VOLTAGE MEASUREMENTS: dB(uV)	
0.150 MHz	100	102.5
0.161	101	102
0.240	99	101
0.550	97	99.5
1.000	95	97.5
1.400	95.5	95
2.000	93	93
3.500	91	93.5
6.000	89	91
10.00	89	89
13.00	89.5	91.5
22.00	87.5	91.5
30.00	87.5	89
	RFI RADIATED POWER MEASUREMENTS: dB(pW)	
30.00	81.5	85.5
40.00	81.5	83
46.00	77.5	79
65.00	71	75.5
90.00	67	69
150.0	63.5	65
180.0	59	61.5
220.0	57.5	59.5
300.0	53.5	55.5

TABLE A2.101

TITLE: RFI CAUSED BY THE VARIATION OF THE SHORT-CIRCUITED COIL PARAMETERS:
MEASURED RFI LEVELS WITH VARYING CIRCUIT VOLTAGE (e) AT 15000 r/min, 1.5A SUPPLY CURRENT AND PHI=0 (Ls=230uH, Rs=0.17 Ohms)

TEST VARIABLE: VOLTAGE 'e' (V)

TEST NUMBER	1:	2:	3:	4:	5:	6:
	0	2	3	4	6	8
FREQUENCY	RFI CONDUCTED VOLTAGE MEASUREMENTS: dB(uV)					
0.150 MHz	95.5	95.5	96	99	103	105
0.160	94.5	95	95.5	98	103	104.5
0.240	93	93	95	96.5	102	103
0.550	88	88.5	89	92	96	98
1.000	86	86	86.5	88	93.5	95
1.400	84	85	86	87	91	92
2.000	83	83	83.5	85	88	90
3.500	81	81.5	82	82	85.5	87
6.000	79	80	80	80.5	83	85.5
10.00	77	77.5	77.5	78	81.5	84
13.00	75	75	75	75	80	84
22.00	73	73	73	74	77	84
30.00	71.5	71.5	72	72	73.5	83
	RFI RADIATED POWER MEASUREMENTS: dB(pW)					
30.00	65	65	65.5	66	69	75
40.00	64	64.5	65	65	67	74.5
46.00	63.5	64	64	65	67	74
65.00	58	58	58.5	59	62.5	68
90.00	55.5	56	56	57	59	64
150.0	53	53	53	54	58	59
180.0	52	52	52	53	55	57
220.0	47	47	47	48	50	53
300.0	45.5	45.5	46	46.5	47	51

TABLE A2.102

TITLE: RFI CAUSED BY THE VARIATION OF THE SHORT-CIRCUITED COIL PARAMETERS:
MEASURED RFI LEVELS WITH VARYING CIRCUIT VOLTAGE (e) AT 15000 r/min, 1.5A SUPPLY CURRENT AND PHI=45 (Ls=230uH, Rs=0.17 Ohms)

TEST VARIABLE: VOLTAGE 'e' (V)

TEST NUMBER	1:	2:	3:	4:	5:	6:
	0V	2	3	4	6	8
FREQUENCY	RFI CONDUCTED VOLTAGE MEASUREMENTS: dB(uV)					
0.150 MHz	95.5	96	97	100	105	106
0.160	94.5	95	96	99	105	106
0.240	93	94	95	98	103	105
0.550	88	89	90	93	98	99
1.000	86	86.5	87	90	95	96
1.400	84	85	86	88	92	93
2.000	83	83.5	84	86	90	90.5
3.500	81	81.5	82	83	87	89
6.000	79	80	80	81	85	88
10.00	77	78	78	79	83	85
13.00	75	76	76	77	81	86
22.00	73	73.5	74	75	78	85
30.00	71.5	72	72	72	74	85
	RFI RADIATED POWER MEASUREMENTS: dB(pW)					
30.00	65	66	66	67	70.5	79
40.00	64	65	65	66	69	78
46.00	63.5	64	64.5	65.5	68	76
65.00	58	59	59	60	63	68
90.00	55.5	56	56.5	57	60	66
150.0	53	54	54	55	58	61
180.0	52	52	52.5	53.5	57	59
220.0	47	48	48	49	51	54
300.0	45.5	46	46	47	49	52

TABLE A2.103

TITLE: RFI CAUSED BY THE VARIATION OF THE SHORT-CIRCUITED COIL PARAMETERS:
MEASURED RFI LEVELS WITH VARYING CIRCUIT VOLTAGE (e) AT 15000 r/min, 1.5A SUPPLY CURRENT AND PHI=90 (Ls=230uH, Rs=0.17 Ohms)

TEST VARIABLE: VOLTAGE 'e' (V)

TEST NUMBER	1: 0	2: 2V	3: 3	4: 4	5: 6	6: 8
FREQUENCY	RFI CONDUCTED VOLTAGE MEASUREMENTS: dB(uV)					
0.150 MHz	95.5	96	96	102	107	108
0.160	94.5	95	95.5	101	106	107
0.240	93	94	94	100	105	107
0.550	88	89	89	95	100	101
1.000	86	87	88	92	97	99
1.400	84	85	85.5	89	94	96
2.000	83	84	84	89	92	94
3.500	81	82	82	84	89	91
6.000	79	80	80.5	82.5	87	89
10.00	77	78	78	80	85	86
13.00	75	76	76.5	79	83	88
22.00	73	74	74	78	83	87
30.00	71.5	72	73	75	82	87
	RFI RADIATED POWER MEASUREMENTS: dB(pW)					
30.00	65	66	66	71	76	80
40.00	64	65	65	69	75	78
46.00	63.5	64	64	68	74	77
65.00	58	59	59.5	62	68	70
90.00	55.5	56	57	59	66	68
150.0	53	54	54	58	60	62
180.0	52	52	52	56	59	60
220.0	47	48	48	50	53	56
300.0	45.5	46	47	49	51	54

TABLE A2.104

TITLE: RFI CAUSED BY THE VARIATION OF THE SHORT-CIRCUITED COIL PARAMETERS:
MEASURED RFI LEVELS WITH VARYING CIRCUIT VOLTAGE (e) AT 15000 r/min, 1.5A SUPPLY CURRENT AND PHI=0 (Ls=500uH, Rs=0.32 Ohms)

TEST VARIABLE: CIRCUIT VOLTAGE 'e' (V)

TEST NUMBER	1: 0	2: 2V	3: 3	4: 4	5: 6	6: 8
FREQUENCY	RFI CONDUCTED VOLTAGE MEASUREMENTS: dB(uV)					
0.150 MHz	98	98	98.5	101	105	107
0.160	97.5	97.5	78	101	104.5	107
0.240	96.5	96.5	97	99.5	103	105
0.550	91	91	91.5	93	97	100
1.000	88	88.5	89	90.5	92.5	97
1.400	87	87	87.5	90	92	93
2.000	85	85	85.5	87	90	91
3.500	84	84	85	86	88	89.5
6.000	83	83	83	84.5	86	88
10.00	81.5	81.5	82	83	84	86
13.00	81	81	81.5	82.5	84	85
22.00	79	79	80	81	82.5	86
30.00	78.5	79	79.5	80	81	87
	RFI RADIATED POWER MEASUREMENTS: dB(pW)					
30.00	71	71	71.5	72	75	78
40.00	70	70	70.5	71.5	73.5	78
46.00	69	69	70	71	73	77
65.00	63	63	63	64	66	68
90.00	61	61	61	63	63.5	66.5
150.0	55	55	55.5	56.5	58	61
180.0	54	54	54	55	58	60
220.0	50	50	50.5	51	54	55
300.0	48	48	49	50	52	52

TABLE A2.105

TITLE: RFI CAUSED BY THE VARIATION OF THE SHORT-CIRCUITED COIL PARAMETERS:
MEASURED RFI LEVELS WITH VARYING CIRCUIT VOLTAGE (e) AT 15000 r/min, 1.5A SUPPLY CURRENT AND PHI=45 (Ls=500uH, Rs=0.32 Ohms)

TEST VARIABLE: VOLTAGE 'e' (V)

TEST NUMBER	1:	2:	3:	4:	5:	6:
	0	2V	3	4	6	8
FREQUENCY	RFI CONDUCTED VOLTAGE MEASUREMENTS: dB(uV)					
0.150 MHz	98	98	99	102	106	109
0.160	97.5	97.5	98.5	101	105	108
0.240	96.5	97	97.5	100	104	107
0.550	91	91.5	92	95	98	100
1.000	88	88	89	91	94	98
1.400	87	87	88	90	93	95
2.000	85	85.5	86	88	90.5	92
3.500	84	84	85	86	88	90
6.000	83	83	84	85	86	89
10.00	81.5	82	83	84	85	87
13.00	81	81.5	82	83	85	86
22.00	79	79	80	81	83	87
30.00	78.5	79	79.5	80	82	87
	RFI RADIATED POWER MEASUREMENTS: dB(pW)					
30.00	71	71.5	72	73	76	80
40.00	70	70	71	72	74	79
46.00	69	69	70	71	73	77
65.00	63	63	64	65	67	69
90.00	61	61.5	62	63	65	67
150.0	55	55	56	57	59	61.5
180.0	54	54	55	56	58	60
220.0	50	50	51	52	54	55
300.0	48	48	49	50	52	53

TABLE A2.106

TITLE: RFI CAUSED BY THE VARIATION OF THE SHORT-CIRCUITED COIL PARAMETERS:
MEASURED RFI LEVELS WITH VARYING CIRCUIT VOLTAGE (e) AT 15000 r/min, 1.5A SUPPLY CURRENT AND PHI=90 (Ls=500uH, Rs=0.32 Ohms)

TEST VARIABLE: VOLTAGE 'e' (V)

TEST NUMBER	1:	2:	3:	4:	5:	6:
	0	2V	3	4	6	8
FREQUENCY	RFI CONDUCTED VOLTAGE MEASUREMENTS: dB(uV)					
0.150 MHz	98	98	99	105	107	110
0.160	97	97.5	98	104	106	109
0.240	96	97	97.5	102	105	108
0.550	91	92	92	97	100	102
1.000	88	88	89	93	98	100
1.400	87	87.5	88	92	95	98
2.000	85	85.5	86	90	93	94
3.500	84	85	85	87	90	92
6.000	83	84	84.5	86	88	90
10.00	81.5	82	82.5	85	86	88
13.00	81	81.5	82	84	87	89
22.00	79	79	79	84	86	87
30.00	78.5	79	79	84	86	88
	RFI RADIATED POWER MEASUREMENTS: dB(pW)					
30.00	71	71.5	72	78	80	82
40.00	70	70	70	77	78	80
46.00	69	69	69.5	75	76	78
65.00	63	63	63	67	69	74
90.00	61	62	62	65	67	69
150.0	55	55	56	60	63	65
180.0	54	54	55	58	60	62
220.0	50	50	50	53	55	56
300.0	48	48	48	51	53	54

TABLE A2.107

TITLE: RFI CAUSED BY THE VARIATION OF THE SHORT-CIRCUITED COIL PARAMETERS:
MEASURED RFI LEVELS WITH VARYING CIRCUIT VOLTAGE (e) AT 15000 r/min, 1.5A SUPPLY CURRENT AND PHI=0 (Ls=1000uH, Rs=0.32 Ohms)

TEST VARIABLE: VOLTAGE 'e' (V)

TEST NUMBER	1:	2:	3:	4:	5:	6:
	0	2V	3	4	6	8
FREQUENCY	RFI CONDUCTED VOLTAGE MEASUREMENTS: dB(uV)					
0.150 MHz	100	100	100	103	105	109
0.160	99	99	99.5	102.5	104	107.5
0.240	97	97	98	100	103	107
0.550	92	92	92.5	94	98	100
1.000	88.5	88.5	89	91	94	96
1.400	87	87	87	90	91	93
2.000	85.5	85.5	86	87	90	91.5
3.500	84.5	84.5	85	86	87	89
6.000	84	84	85	85.5	87	89
10.00	83	83	84	84.5	86	87
13.00	82.5	82.5	83	85	86.5	88
22.00	81.5	81.5	82	82	83	86
30.00	81	81	81	81.5	83	85.5
	RFI RADIATED POWER MEASUREMENTS: dB(pW)					
30.00	74	74	74.5	75	76	80
40.00	73	73	74	74	75.5	78
46.00	71	71	72	72.5	75	76
65.00	65	65	65.5	66	68	70
90.00	63	63	63.5	64	65	66.5
150.0	57	57	57	58	60	61
180.0	56	56	56	57	58.5	59
220.0	52	52	52	53.5	54	55
300.0	49	49	49.5	50	51	53

TABLE A2.108

TITLE: RFI CAUSED BY THE VARIATION OF THE SHORT-CIRCUITED COIL PARAMETERS:
MEASURED RFI LEVELS WITH VARYING CIRCUIT VOLTAGE (e) AT 15000 r/min, 1.5A SUPPLY CURRENT AND PHI=45 (Ls=1000uH, Rs=0.32 Ohms)

TEST VARIABLE: VOLTAGE 'e' (V)

TEST NUMBER	1:	2:	3:	4:	5:	6:
	0	2V	3V	4	6	8
FREQUENCY	RFI CONDUCTED VOLTAGE MEASUREMENTS: dB(uV)					
0.150 MHz	100	100	101	104	107	110
0.160	99	99	100	103	106	109
0.240	97	97	98.5	101	105	108
0.550	92	92	93	96	99.5	101
1.000	88.5	89	90	93	96	99
1.400	87	87	88	90.5	93.5	96
2.000	85.5	86	86.5	89	92	93
3.500	84.5	85	86	87	89	91
6.000	84	84	85	86	88	90
10.00	83	84	84	85	87	89.5
13.00	82.5	83	84	85.5	87	89
22.00	81.5	81.5	82	82.5	84	88
30.00	81	81	82	82	83.5	88
	RFI RADIATED POWER MEASUREMENTS: dB(pW)					
30.00	74	74	75	75.5	77	81
40.00	73	73	74	74.5	77	80
46.00	71	71	72	73	76	78
65.00	65	65	66	67	69	71
90.00	63	63	63	64	66	68
150.0	57	57	58	59	61	62
180.0	56	56	57	58	60	61
220.0	52	52	53	54	56	56
300.0	49	49	50	51	52	54

TABLE A2.109

TITLE: RFI CAUSED BY THE VARIATION OF THE SHORT-CIRCUITED COIL PARAMETERS:
MEASURED RFI LEVELS WITH VARYING CIRCUIT VOLTAGE (e) AT 15000 r/min, 1.5A SUPPLY CURRENT AND PHI=90 (Ls=1000uH, Rs=0.32 Ohms)

TEST VARIABLE: VOLTAGE 'e' (V)

TEST NUMBER	1:	2:	3:	4:	5:	6:
	0	2V	3	4	6	8
FREQUENCY	RFI CONDUCTED VOLTAGE MEASUREMENTS: dB(uV)					
0.150 MHz	100	100	101	106	108	111
0.160	99	99	99.5	105	108	110
0.240	97	97	98	103	106	109
0.550	92	92	93	98	100	102
1.000	88.5	89	90	94	98	100
1.400	87	87	87.5	93	95	99
2.000	85.5	86	87	90	94	95
3.500	84.5	85	86	88	91	93
6.000	84	84	84	87	89	91
10.00	83	83.5	84	86	86	90
13.00	82.5	83	83	87	87	91
22.00	81.5	82	82	86	86	89
30.00	81	81	82	86	87	88
	RFI RADIATED POWER MEASUREMENTS: dB(pW)					
30.00	74	74	75	79	80	82
40.00	73	73	74.5	77	79	81
46.00	71	71	72	75	77	79
65.00	65	65	67	68	69	76
90.00	63	63	63.5	66	68	70
150.0	57	57	57	64	64	66
180.0	56	56	56	60	61	64
220.0	52	52	53	55	55	57
300.0	49	49	49.5	53	53	55

TABLE A2.110

TITLE: RFI CAUSED BY THE VARIATION OF THE SHORT-CIRCUITED COIL PARAMETERS:
MEASURED RFI LEVELS WITH VARYING CIRCUIT VOLTAGE (e) AT 15000 r/min, 0.5A SUPPLY CURRENT AND PHI=45 (Ls=230uH, Rs=0.32 Ohms)

TEST VARIABLE: VOLTAGE 'e' (V)

TEST NUMBER	1:	2:	3:	4:	5:	6:	7:
	0	1V	2	3	4	6	8
FREQUENCY	RFI CONDUCTED VOLTAGE MEASUREMENTS: dB(uV)						
0.150 MHz	95	95	97	98	100	104	106
0.160	94.5	94.5	96	97	99	104	105
0.240	92	92	94	95	97	102	104
0.550	88	88	90	91	93	96	98
1.000	85	85	87	87.5	90	94	96
1.400	84	84	85.5	86	88	91	93
2.000	83	83	85	86	87	90	91
3.500	80	81	83	85	85	87	88
6.000	78	78	79	80	81	84	86
10.00	76	76	78	79	79	82	85
13.00	74	74	76	77	78	80	83
22.00	72	72	74	76	76	78	84
30.00	70	70	72	74	74	75	84
	RFI RADIATED POWER MEASUREMENTS: dB(pW)						
30.00	63	63	65	66	67	70	77
40.00	62	62.5	64	65	66	68	76
46.00	62	62	64	64.5	65	67.5	74
65.00	57	57	60	60	61	64	66
90.00	54	54	56	57	58	60	64
150.0	51	52	54	55	56	58	61
180.0	51	51	53	54	55	57	59
220.0	48	48	51	51	51	52	54
300.0	45	45	47	47	48	49	51

TABLE A2.111

TITLE: RFI CAUSED BY THE VARIATION OF THE SHORT-CIRCUITED COIL PARAMETERS:
MEASURED RFI LEVELS WITH VARYING CIRCUIT VOLTAGE (e) AT 15000 r/min. 2.5A SUPPLY CURRENT AND PHI=45 (Ls=230uH, Rs=0.32 Ohms)

TEST VARIABLE: VOLTAGE 'e' (V)

TEST NUMBER	1: 0	2: 1V	3: 2	4: 3	5: 4	6: 6	7: 8
FREQUENCY	RFI CONDUCTED VOLTAGE MEASUREMENTS: dB(uV)						
0.150 MHz	96	96	96.5	97	100	105	107
0.160	95	95	95.5	96	99.5	105	106
0.240	94	94.5	95	95.5	98	103	106
0.550	88	88.5	89	90	94	99	100
1.000	87	87	87.5	88	91	96	98
1.400	85	85	85.5	86	88	93	94
2.000	83	83	83.5	84	86	91	93
3.500	82	82	82	82.5	84	89	91
6.000	81	81	81.5	82	83	88	92
10.00	80	80	80	81	82	85	87
13.00	79	79	79.5	80	81	86	88
22.00	77	77	77	78	79	84	87
30.00	75	75	75	76	77	84	86
	RFI RADIATED POWER MEASUREMENTS: dB(pW)						
30.00	67	67	67	67.5	68	78	80
40.00	66	66	66	66	67	77	79
46.00	65	65	65	65.5	66	75	79
65.00	60	61	61	61	62	66	70
90.00	57	57	57	58	59	64	68
150.0	54	54	54	55	56	60	63
180.0	53	53	53	54	55	58	60
220.0	50	50	50	51	52	54	56
300.0	47	47	47	48	49	50	54

TABLE A2.112

TITLE: RFI DUE TO THE INFLUENCE OF THE PHYSICAL COMPONENTS OF THE ARMATURE AND FIELD:
MEASURED RFI LEVELS FROM THE U-TYPE FIELD SYSTEM WITH VARYING EXCITATION CURRENT

TEST VARIABLE: CURRENT (A)

TEST NUMBER	1: 0.5A	2: 1.0	3: 1.5	4: 2.0			
FREQUENCY	RFI CONDUCTED VOLTAGE MEASUREMENTS: dB(uV)						
0.100 MHz	0.5	2	4.5	9			
0.120	0.25	1.5	4.5	6.5			
0.150	-	1	3.5	5.5			
0.180	-	-	1.5	3.5			
0.200	-	-	-	2			
0.220	-	-	-	-			
0.240	-	-	-	-			
0.300	-	-	-	-			
0.350	-	-	-	-			
0.400	-	-	-	-			
0.500	-	-	-	-			
0.550	-	-	-	-			
1.000	-	-	-	-			

TABLE A2.113

TITLE: RFI DUE TO THE INFLUENCE OF THE PHYSICAL COMPONENTS OF THE ARMATURE AND FIELD:
MEASURED RFI LEVELS FROM THE O-TYPE FIELD SYSTEM WITH VARYING EXCITATION CURRENT

TEST VARIABLE: CURRENT (A)

RFI CONDUCTED VOLTAGE MEASUREMENTS: dB(uV)

TEST NUMBER / FREQUENCY	1: 0.5A	2: 1.0	3: 1.5	4: 2.0			
0.100 MHz	0.5	1.5	4	8			
0.120	0.25	1	3.5	6			
0.150	-	0.5	3	4			
0.180	-	-	1.5	3			
0.200	-	-	0.5	1.5			
0.220	-	-	-	0.5			
0.240	-	-	-	-			
0.300	-	-	-	-			
0.350	-	-	-	-			
0.400	-	-	-	-			
0.500	-	-	-	-			
0.550	-	-	-	-			
1.000	-	-	-	-			

TABLE A2.114

TITLE: RFI DUE TO THE INFLUENCE OF THE PHYSICAL COMPONENTS OF THE ARMATURE AND FIELD:
MEASURED RFI LEVELS FROM THE U-TYPE FIELD SYSTEM WITH VARYING EXCITATION CURRENT (FIELD CORE WITH LOOSE LAMINATIONS)

TEST VARIABLE: CURRENT (A)

RFI CONDUCTED VOLTAGE MEASUREMENTS: dB(uV)

TEST NUMBER / FREQUENCY	1: 0.5A	2: 1.0	3: 1.5	4: 2.0			
0.100 MHz	1.0	3.5	8	14.5			
0.120	0.5	3	6.5	13			
0.150	0.25	2	6	11			
0.180	-	0.5	3.5	6.5			
0.200	-	-	1	4			
0.220	-	-	-	-			
0.240	-	-	-	-			
0.300	-	-	-	-			
0.350	-	-	-	-			
0.400	-	-	-	-			
0.500	-	-	-	-			
0.550	-	-	-	-			
1.000	-	-	-	-			

TABLE A2.115

TITLE: RFI DUE TO THE INFLUENCE OF THE PHYSICAL COMPONENTS OF THE ARMATURE AND FIELD:
MEASURED RFI LEVELS FROM THE U-TYPE FIELD AND STATIONARY UNWOUND 12 SLOT ARMATURE WITH VARYING EXCITATION CURRENT (ROTOR SLOT ON DIRECT AXIS)

TEST VARIABLE: CURRENT (A)

RFI CONDUCTED VOLTAGE MEASUREMENTS: dB(uV)

TEST NUMBER / FREQUENCY	1: 0.5A	2: 1.0	3: 1.5	4: 2.0			
0.100 MHz	4.5	10	25	35			
0.120	3.5	9	22.5	33			
0.150	3	8	20	31			
0.180	1	5	11	22			
0.200	1	4	9	20			
0.220	-	1	5.5	13			
0.240	-	0.5	3	8			
0.300	-	-	1.5	5.5			
0.350	-	-	-	-			
0.400	-	-	-	-			
0.500	-	-	-	-			
0.550	-	-	-	-			
1.000	-	-	-	-			

TABLE A2.145

TITLE: RFI DUE TO THE INFLUENCE OF MECHANICAL VARIATIONS IN THE MOTOR ASSEMBLY:
MEASURED RFI LEVELS WITH VARYING ARMATURE STATIC OUT-OF-BALANCE AT 18000 r/min

TEST VARIABLE: OUT-OF-BALANCE (gcm)

TEST NUMBER	7:	8:	9:	10:
	1.5 gcm	2.0	2.5	3.0
FREQUENCY	RFI CONDUCTED VOLTAGE MEASUREMENTS: dB(uV)			
0.150 MHz	96	98	100	102
0.160	96	97	99	101
0.240	95	96	98	100.5
0.550	93	95	97	99.5
1.000	89	90	91	94
1.400	87.5	89	89.5	91
2.000	86	88	90	92
3.500	87	89	89	90
6.000	85	88	89	90.5
10.00	86	87.5	89.5	92
13.00	84	86	88	90
22.00	80	84	85	87.5
30.00	75	80	84	85.5
	RFI RADIATED POWER MEASUREMENTS: dB(pW)			
30.00	60	61.5	65	68
40.00	61	62.5	63	65
46.00	60	61.5	67	69
65.00	59	63	66	69
90.00	53	58	61	64
150.0	52.5	54.5	58	61
180.0	49	54	55	56
220.0	41	45	47	48
300.0	38	40	42	43

TABLE A2.146

TITLE: RFI DUE TO THE INFLUENCE OF MECHANICAL VARIATIONS IN THE MOTOR ASSEMBLY:
MEASURED RFI LEVELS WITH VARYING DYNAMIC ARMATURE OUT-OF-BALANCE AT 13000 r/min

TEST VARIABLE: OUT-OF-BALANCE (gcm)

TEST NUMBER	1:	2:	3:	4:	5:	6:
	0.1 gcm	0.2	0.3	0.4	0.5	0.6
FREQUENCY	RFI CONDUCTED VOLTAGE MEASUREMENTS: dB(uV)					
0.150 MHz	92.5	92.5	92.5	93	94	95
0.160	92	92.5	92.5	92.5	93	94.5
0.240	91	91	91.5	91.5	92.5	93
0.550	89	89	89	89.5	90	92
1.000	85	85	85.5	85.5	86.5	87
1.400	81	81.5	82	82	83	85
2.000	81	81	81	82	82	84
3.500	79	79.5	79.5	80	81	83
6.000	76	76	76	76.5	78	80
10.00	78	78	78.5	79	80	83
13.00	76	76	76	77	78	80
22.00	70	70	70	71	72	74
30.00	61	61.5	62	63	64	66
	RFI RADIATED POWER MEASUREMENTS: dB(pW)					
30.00	50	50.5	50.5	51	52	53
40.00	51	51	51	51	52	53
46.00	52	52	52	52.5	53	54
65.00	50	50	50	51	52	54
90.00	45	45.5	45.5	46	48	49.5
150.0	45	45	45	45	46	48
180.0	41	41	41	42	42	46
220.0	31	31.5	32	33	34	38
300.0	25	25	26	27	29	30

*
*   TABLE A2.116
*

TITLE: RFI DUE TO THE INFLUENCE OF THE PHYSICAL COMPONENTS OF THE ARMATURE AND FIELD:
MEASURED RFI LEVELS FROM THE U-TYPE FIELD AND STATIONARY UNWOUND 12 SLOT ARMATURE WITH VARYING EXCITATION CURRENT (ROTOR TOOTH ON DIRECT AXIS)

*
TEST VARIABLE: CURRENT (A)
*

TEST NUMBER	1: 0.5A	2: 1.0	3: 1.5	4: 2.0			
FREQUENCY	RFI CONDUCTED VOLTAGE MEASUREMENTS: dB(uV)						
0.100 MHz	7	12	30	40.5			
0.120	5.5	11	24	39			
0.150	5	10	23.5	36			
0.180	3	8	16	26			
0.200	1.5	6	14	25			
0.220	1	2.5	9	17			
0.240	-	1	7	13.3			
0.300	-	0.5	4	12			
0.350	-	-	3	5.5			
0.400	-	-	1.5	3			
0.500	-	-	0.5	1.5			
0.550	-	-	-	0.5			
1.000	-	-	-	-			

*
*
*

*
*   TABLE A2.117
*

TITLE: RFI DUE TO THE INFLUENCE OF THE PHYSICAL COMPONENTS OF THE ARMATURE AND FIELD:
MEASURED RFI LEVELS FROM THE U-TYPE FIELD AND STATIONARY UNWOUND 11 SLOT ARMATURE WITH VARYING EXCITATION CURRENT (ROTOR SLOT ON DIRECT AXIS)

*
TEST VARIABLE: CURRENT (A)
*

TEST NUMBER	1: 0.5A	2: 1.0	3: 1.5	4: 2.0			
FREQUENCY	RFI CONDUCTED VOLTAGE MEASUREMENTS: dB(uV)						
0.100 MHz	5	12	27	37			
0.120	4.5	10	24	34			
0.150	3	9	21	31.5			
0.180	1.5	7	11.5	23			
0.200	1	5	10	21			
0.220	0.5	2.5	6.5	15			
0.240	-	1	4	9			
0.300	-	-	2.5	7			
0.350	-	-	1.0	1.5			
0.400	-	-	-	-			
0.500	-	-	-	-			
0.550	-	-	-	-			
1.000	-	-	-	-			

*
*
*

*
*   TABLE A2.118
*

TITLE: RFI DUE TO INFLUENCE OF THE PHYSICAL COMPONENTS OF THE ARMATURE AND FIELD:
MEASURED RFI LEVELS FROM THE U-TYPE FIELD AND STATIONARY UNWOUND 11 SLOT ARMATURE WITH VARYING EXCITATION CURRENT (ROTOR TOOTH ON DIRECT AXIS)

*
TEST VARIABLE: CURRENT (A)
*

TEST NUMBER	1: 0.5A	2: 1.0	3: 1.5	4: 2.0			
FREQUENCY	RFI CONDUCTED VOLTAGE MEASUREMENTS: dB(uV)						
0.100 MHz	8.5	16	32.5	43			
0.120	8	15	29	39			
0.150	7	13.5	28	36			
0.180	4	11	19.5	29			
0.200	2	9	16	27			
0.220	1	7	11	20			
0.240	0.5	4	9	13			
0.300	-	2.5	4.5	11			
0.350	-	0.5	4	6			
0.400	-	-	2.5	5			
0.500	-	-	1	3			
0.550	-	-	-	1			
1.000	-	-	-	-			

*
*
*

TABLE A2.119

TITLE: RFI DUE TO THE INFLUENCE OF THE PHYSICAL COMPONENTS OF THE ARMATURE AND FIELD:
MEASURED RFI LEVELS FROM THE U-TYPE FIELD AND STATIONARY UNWOUND 7 SLOT ARMATURE WITH VARYING EXCITATION CURRENT (ROTOR SLOT ON DIRECT AXIS)

TEST VARIABLE: CURRENT (A)

TEST NUMBER	1: 0.5A	2: 1.0	3: 1.5	4: 2.0
FREQUENCY	RFI CONDUCTED VOLTAGE MEASUREMENTS: dB(uV)			
0.100 MHz	3.5	8	21	33
0.120	2	7.5	20	31
0.150	1.5	6	19	27
0.180	1	4	9	21
0.200	0.5	3	7	18
0.220	-	1.5	6	12
0.240	-	0.5	2.5	0.5
0.300	-	-	1	4
0.350	-	-	-	-
0.400	-	-	-	-
0.500	-	-	-	-
0.550	-	-	-	-
1.000	-	-	-	-

TABLE A2.120

TITLE: RFI DUE TO THE INFLUENCE OF THE PHYSICAL COMPONENTS OF THE ARMATURE AND FIELD:
MEASURED RFI LEVELS FROM THE U-TYPE FIELD AND STATIONARY UNWOUND 7 SLOT ARMATURE WITH VARYING EXCITATION CURRENT (ROTOR TOOTH ON DIRECT AXIS)

TEST VARIABLE: CURRENT (A)

TEST NUMBER	1: 0.5A	2: 1.0	3: 1.5	4: 2.0
FREQUENCY	RFI CONDUCTED VOLTAGE MEASUREMENTS: dB(uV)			
0.100 MHz	8	13	29	41
0.120	6	11.5	25	40
0.150	5.5	10	21	35.5
0.180	3	9	15	30
0.200	2	6.5	14	28
0.220	1	3	9	20
0.240	-	1	7.5	15
0.300	-	0.5	5	13
0.350	-	-	3.5	5
0.400	-	-	2	4
0.500	-	-	1.0	2
0.550	-	-	-	1.0
1.000	-	-	-	-

TABLE A2.121

TITLE: RFI DUE TO THE INFLUENCE OF THE PHYSICAL COMPONENTS OF THE ARMATURE AND FIELD:
MEASURED RFI LEVELS FROM THE U-TYPE FIELD AND STATIONARY UNWOUND 12 SLOW ARMATURE WITH VARYING EXCITATION CURRENT (ROTOR TOOTH ON DIRECT AXIS AND LOOSE ARMATURE LAMINATIONS)

TEST VARIABLE: CURRENT (A)

TEST NUMBER	1: 0.5A	2: 1.0	3: 1.5	4: 2.0
FREQUENCY	RFI CONDUCTED VOLTAGE MEASUREMENTS: dB(uV)			
0.100 MHz	23	32	47	55
0.120	11	26	44	52
0.150	7	23	41	50
0.180	4.5	19	33	43
0.200	1.0	11	28	40
0.220	0.5	7	26	31
0.240	-	3	24	29
0.300	-	2	19	28
0.350	-	1.5	13	25
0.400	-	0.5	4	8
0.500	-	-	0.5	1.5
0.550	-	-	-	0.5
1.000	-	-	-	-

TABLE A2.122

TITLE: RFI DUE TO THE INFLUENCE OF THE PHYSICAL COMPONENTS OF THE ARMATURE AND FIELD:
MEASURED RFI LEVELS FROM THE U-TYPE FIELD AND UNWOUND 12 SLOT ARMATURE AT 1.5A EXCITATION CURRENT WITH VARYING SHAFT SPEED

TEST VARIABLE: SPEED (r/min)

TEST NUMBER	1: 5000 r/min	2: 10000	3: 20000			
FREQUENCY	RFI CONDUCTED VOLTAGE MEASUREMENTS: dB(uV)					
0.100 MHz	27	27	27			
0.120	23	23	22.5			
0.150	21	21	21			
0.180	14.5	14.5	14			
0.200	12	12	12			
0.220	6.5	6.5	6.5			
0.240	5.5	5.5	5.5			
0.300	2.5	2.5	2			
0.350	1	1	1			
0.400	0.5	0.5	0.5			
0.500	0.25	0.25	-			
0.550	-	-	-			
1.000	-	-	-			

TABLE A2.123

TITLE: RFI DUE TO THE INFLUENCE OF THE PHYSICAL COMPONENTS OF THE ARMATURE AND FIELD:
MEASURED RFI LEVELS FROM THE U-TYPE FIELD AND UNWOUND 11 SLOT ARMATURE AT 1.5A EXCITATION CURRENT WITH VARYING SHAFT SPEED

TEST VARIABLE: SPEED (r/min)

TEST NUMBER	1: 5000 r/min	2: 10000	3: 20000			
FREQUENCY	RFI CONDUCTED VOLTAGE MEASUREMENTS: dB(uV)					
0.100 MHz	29	29	29			
0.120	26	26	26			
0.150	23.5	23	23			
0.180	14.5	14.5	14			
0.200	12	12	11.5			
0.220	8	8	8			
0.240	6	6	6			
0.300	3	3	3			
0.350	2	2	1.5			
0.400	1.0	1.0	1.0			
0.500	0.5	0.25	0.25			
0.550	-	-	-			
1.000	-	-	-			

TABLE A2.124

TITLE: RFI DUE TO THE INFLUENCE OF THE PHYSICAL COMPONENTS OF THE ARMATURE AND FIELD:
MEASURED RFI LEVELS FROM THE U-TYPE FIELD AND UNWOUND 7 SLOT ARMATURE AT 1.5A EXCITATION CURRENT WITH VARYING SHAFT SPEED

TEST VARIABLE: SPEED (r/min)

TEST NUMBER	1: 5000 r/min	2: 10000	3: 20000			
FREQUENCY	RFI CONDUCTED VOLTAGE MEASUREMENTS: dB(uV)					
0.100 MHz	24	24	23.5			
0.120	22	22	22			
0.150	20	20	20			
0.180	11.5	11	11			
0.200	9.5	9.5	9			
0.220	7.5	7	7			
0.240	5	5	5			
0.300	3	3	3			
0.350	1.5	1.5	1.25			
0.400	1.0	1.0	1.0			
0.500	0.5	0.5	0.25			
0.550	-	-	-			
1.000	-	-	-			

TABLE A2.125

TITLE: RFI DUE TO THE INFLUENCE OF THE PHYSICAL COMPONENTS OF THE ARMATURE AND FIELD:
MEASURED RFI LEVELS FROM A 12/24 ARMATURE (FIELD SYSTEM REMOVED) AT 1.5A SUPPLY CURRENT WITH VARYING SPEED

TEST VARIABLE: SPEED (r/min)

TEST NUMBER	1: 5000 r/min	2: 10000	3: 13000	4: 20000
FREQUENCY	RFI CONDUCTED VOLTAGE MEASUREMENTS: dB(uV)			
0.150 MHz	87	97	98	99.5
0.160	86	96.5	97	99
0.240	82.5	93.5	96.5	98.5
0.550	76	88	92	97
1.000	73	84	88	93.5
1.400	70.5	82	86	92.5
2.000	69	81	84.5	92
3.500	66	78	82.5	90
6.000	64	77	82	88
10.00	62	74	80.5	86
13.00	60	72	79.5	85
22.00	58	66.5	77	84
30.00	55.5	65.5	76	82
	RFI RADIATED POWER MEASUREMENTS: dB(pW)			
30.00	48	60	70	76.5
40.00	47	58	69.5	75.5
46.00	46	57.5	68	74
65.00	44	55	66	70.5
90.00	42	51.5	61	68
150.0	41.5	48.5	55	61
180.0	40	47	54	58
220.0	36	44.5	51	55.5
300.0	33.5	41	48	51.5

TABLE A2.126

TITLE: RFI DUE TO THE INFLUENCE OF THE PHYSICAL COMPONENTS OF THE ARMATURE AND FIELD:
MEASURED RFI LEVELS FROM TEST RIG FITTED WITH 12/24 ARMATURE AND U-TYPE FIELD CONNECTED AS A SINGLE LUMPED WINDING

TEST VARIABLE: FIELD WINDINGS CONNECTED TO THE LINE SIDE OF MAINS SUPPLY (TEST RIG FRAME EARTHED)

TEST NUMBER	1: RFI @ L-E	2: RFI @ N-E
FREQUENCY	RFI CONDUCTED VOLTAGE MEASUREMENTS: dB(uV)	
0.150 MHz	82	92
0.160	82	92
0.240	81.5	92
0.550	78	88.5
1.000	74	84
1.400	72	82.5
2.000	71.5	82.5
3.500	69.5	80
6.000	69	78
10.00	72	80
13.00	70	78
22.00	59	68
30.00	54	62
	RFI RADIATED POWER MEASUREMENTS: dB(pW)	
30.00	50	50
40.00	51	51
46.00	54	54
65.00	50	50
90.00	43.5	43.5
150.0	45.5	45.5
180.0	41.5	41
220.0	32	32
300.0	23	23

*
* TABLE A2.127
*

TITLE: RFI DUE TO THE INFLUENCE OF THE PHYSICAL COMPONENTS OF THE ARMATURE AND FIELD:
MEASURED RFI LEVELS FROM TEST RIG FITTED WITH 12/24 ARMATURE AND U-TYPE FIELD CONNECTED AS A SINGLE LUMPED WINDING

TEST VARIABLE: FIELD WINDINGS CONNECTED TO THE NEUTRAL SIDE OF MAINS SUPPLY (TEST RIG FRAME EARTHED)

TEST NUMBER	1: RFI @ L-E	2: RFI @ N-E					
FREQUENCY	RFI CONDUCTED VOLTAGE MEASUREMENTS: dB(uV)						
0.150 MHz	92	82					
0.160	92	82					
0.240	92	81.5					
0.550	88.5	78					
1.000	84	74					
1.400	82.5	72					
2.000	82.5	71.5					
3.500	80	69.5					
6.000	78	69					
10.00	80	72					
13.00	78	70					
22.00	68	59					
30.00	62	54					
	RFI RADIATED POWER MEASUREMENTS: dB(pW)						
30.00	50	50					
40.00	51	51					
46.00	54	54					
65.00	50	50					
90.00	43.5	43.5					
150.0	43.5	43.5					
180.0	41.5	41.5					
220.0	32	32					
300.0	23	23					

*
* TABLE A2.128
*

TITLE: RFI CAUSED BY THE VARIATION OF THE SHORT-CIRCUITED COIL PARAMETERS:
MEASURED RFI LEVELS FROM TEST RIG FITTED WITH 12/24 ARMATURE AND U-TYPE FIELD CONNECTED AS A SINGLE LUMPED WINDING

TEST VARIABLE: FIELD WINDINGS CONNECTED TO THE LINE SIDE OF MAINS SUPPLY AND EARTH CONNECTION REMOVED

TEST NUMBER	1: RFI @ L-E	2: RFI @ N-E					
FREQUENCY	RFI CONDUCTED VOLTAGE MEASUREMENTS: dB(uV)						
0.150 MHz	81	81.5					
0.160	81	81					
0.240	81	81					
0.550	77.5	77.5					
1.000	73	73					
1.400	71	71					
2.000	69.5	70.5					
3.500	68	68					
6.000	69	68					
10.00	79.5	79					
13.00	68	67					
22.00	61	61					
30.00	57	55.5					
	RFI RADIATED POWER MEASUREMENTS: dB(pW)						
30.00	49.5	49.5					
40.00	50.5	50.5					
46.00	53	53					
65.00	50	50					
90.00	41.5	41.5					
150.0	45	45					
180.0	41.5	41.5					
220.0	33	33					
300.0	25.5	25.5					

*
*
*

TABLE A2.129

TITLE: RFI CAUSED BY THE VARIATION OF THE SHORT-CIRCUITED COIL PARAMETERS:
MEASURED RFI LEVELS FROM TEST RIG FITTED WITH 12/24 ARMATURE AND U-TYPE FIELD CONNECTED AS A SINGLE LUMPED WINDING

TEST VARIABLE: FIELD WINDINGS CONNECTED TO THE LINE SIDE OF MAINS SUPPLY AND EARTH CONNECTED TO FIELD LAMINATIONS

TEST NUMBER	1: RFI @ L-E	2: RFI @ N-E
FREQUENCY	RFI CONDUCTED VOLTAGE MEASUREMENTS: dB(uV)	
0.150 MHz	82	84.5
0.160	81.5	84
0.240	80	85
0.550	77	84
1.000	73.5	80
1.400	72	78
2.000	72	77
3.500	70.5	74.5
6.000	69	73
10.00	71	78
13.00	69	75.5
22.00	59	64
30.00	53	60
	RFI RADIATED POWER MEASUREMENTS: dB(pW)	
30.00	49	49
40.00	50.5	50.5
46.00	53	53
65.00	48	48
90.00	46	46
150.0	45	45
180.0	40	40
220.0	34	34
300.0	25	25

TABLE A2.130

TITLE: RFI DUE TO THE INFLUENCE OF THE PHYSICAL COMPONENTS OF THE ARMATURE AND FIELD:
MEASURED RFI LEVELS FROM TEST RIG FITTED WITH 12/24 ARMATURE AND O-TYPE FIELD CONNECTED AS A SINGLE LUMPED WINDING

TEST VARIABLE: FIELD WINDING CONNECTED TO THE LINE SIDE OF MAINS SUPPLY (TEST RIG FRAME EARTHED)

TEST NUMBER	1: RFI @ L-E	2: RFI @ N-E
FREQUENCY	RFI CONDUCTED VOLTAGE MEASUREMENTS: dB(uV)	
0.150 MHz	81	90.5
0.160	80.5	90
0.240	80	89.5
0.550	74	85
1.000	65	76
1.400	65	76
2.000	66	76
3.500	62	72
6.000	60	78.5
10.00	62.5	71
13.00	62.5	70
22.00	59	65
30.00	54	59
	RFI RADIATED POWER MEASUREMENTS: dB(pW)	
30.00	50	50
40.00	51	51
46.00	51.5	51.5
65.00	48	48
90.00	44	44
150.0	44	44
180.0	40	40
220.0	37	37
300.0	23	23

TABLE A2.131

TITLE: RFI DUE TO THE INFLUENCE OF THE PHYSICAL COMPONENTS OF THE ARMATURE AND FIELD:
MEASURED RFI LEVELS FROM TEST RIG FITTED WITH 12/24 ARMATURE AND O-TYPE FIELD CONNECTED AS A SINGLE LUMPED WINDING

TEST VARIABLE: FIELD WINDING CONNECTED TO THE NEUTRAL SIDE OF MAINS SUPPLY (TEST RIG FRAME EARTHED)

TEST NUMBER	1: RFI @ L-E	2: RFI @ N-E					
FREQUENCY	RFI CONDUCTED VOLTAGE MEASUREMENTS: dB(uV)						
0.150 MHz	90.5	81					
0.160	90	80.5					
0.240	89.5	80					
0.550	85	74					
1.000	76	65					
1.400	76	65					
2.000	76	66					
3.500	72	62					
6.000	70.5	60					
10.00	71	62.5					
13.00	70	62.5					
22.00	65	59					
30.00	59	54					
	RFI RADIATED POWER MEASUREMENTS: dB(pW)						
30.00	50	50					
40.00	51	51					
46.00	51.5	51.5					
65.00	48	48					
90.00	44	44					
150.0	44	44					
180.0	40	40					
220.0	37	37					
300.0	23	23					

TABLE A2.132

TITLE: RFI DUE TO THE INFLUENCE OF THE PHYSICAL COMPONENTS OF THE ARMATURE AND FIELD:
MEASURED RFI LEVELS FROM TEST RIG FITTED WITH 12/24 ARMATURE AND O-TYPE FIELD CONNECTED AS A SINGLE LUMPED WINDING

TEST VARIABLE: FIELD WINDINGS CONNECTED TO THE LINE SIDE OF MAINS SUPPLY AND EARTH CONNECTION REMOVED

TEST NUMBER	1: RFI @ L-E	2: RFI @ N-E					
FREQUENCY	RFI CONDUCTED VOLTAGE MEASUREMENTS: dB(uV)						
0.150 MHz	81.5	81.5					
0.160	81	81					
0.240	79	79.5					
0.550	73	73					
1.000	65	65					
1.400	65.5	65.5					
2.000	67	67					
3.500	63	63					
6.000	60	60.5					
10.00	63	63.5					
13.00	62	62					
22.00	57	57					
30.00	53	52.5					
	RFI RADIATED POWER MEASUREMENTS: dB(pW)						
30.00	48	48					
40.00	49	49					
46.00	50.5	50.5					
65.00	47	47					
90.00	43	43					
150.0	42	42					
180.0	39	39					
220.0	35	35					
300.0	23	23					

TABLE A2.133

TITLE: RFI DUE TO THE INFLUENCE OF THE PHYSICAL COMPONENTS OF THE ARMATURE AND FIELD:
MEASURED RFI LEVELS FROM TEST RIG FITTED WITH 12/24 ARMATURE AND O-TYPE FIELD CONNECTED AS A SINGLE LUMPED WINDING

TEST VARIABLE: FIELD WINDINGS CONNECTED TO THE LINE SIDE OF MAINS SUPPLY AND EARTH CONNECTED TO FIELD LAMINATIONS

TEST NUMBER	1: RFI @ L-E	2: RFI @ N-E
FREQUENCY	RFI CONDUCTED VOLTAGE MEASUREMENTS: dB(uV)	
0.150 MHz	81	83.5
0.160	80.5	83.5
0.240	80.5	84.5
0.550	76	82
1.000	66	73
1.400	65	72
2.000	66	72
3.500	63	68
6.000	61	64
10.00	62	68
13.00	62	69
22.00	58	65
30.00	54	61
	RFI CONDUCTED POWER MEASUREMENTS: dB(pW)	
30.00	51	51
40.00	51	51
46.00	52	52
65.00	48	48
90.00	44	44
150.0	42.5	42.5
180.0	39.5	39.5
220.0	37	37
300.0	28	28

TABLE A2.134

TITLE: RFI CAUSED BY THE VARIATION OF THE SHORT-CIRCUITED COIL PARAMETERS:
MEASURED RFI LEVELS FROM TEST RIG FITTED WITH 11/22 ARMATURE AND U-TYPE FIELD CONNECTED AS A SINGLE LUMPED WINDING

TEST VARIABLE: FIELD WINDINGS CONNECTED TO THE LINE SIDE OF MAINS SUPPLY (TEST RIG FRAME EARTHED)

TEST NUMBER	1: RFI @ L-E	2: RFI @ N-E
FREQUENCY	RFI CONDUCTED VOLTAGE MEASUREMENTS: dB(uV)	
0.150 MHz	84	96
0.160	83.5	95.5
0.240	82	93.5
0.550	79	91.5
1.000	79	90.5
1.400	78	88
2.000	79	89
3.500	76	85.6
6.000	75.5	83
10.00	75.5	82
13.00	70	80
22.00	66	70
30.00	59	66
	RFI RADIATED POWER MEASUREMENTS: dB(pW)	
30.00	56	56
40.00	56	56
46.00	57	57
65.00	55.5	55.5
90.00	50	50
150.0	48	48
180.0	46.5	46.5
220.0	46	46
300.0	45.5	45.5

TABLE A2.135

TITLE: RFI CAUSED BY THE VARIATION OF THE SHORT-CIRCUITED COIL PARAMETERS:
MEASURED RFI LEVELS FROM TEST RIG FITTED WITH 7/21 ARMATURE AND U-TYPE FIELD CONNECTED AS A SINGLE LUMPED WINDING

TEST VARIABLE: FIELD WINDINGS CONNECTED TO THE LINE SIDE OF MAINS SUPPLY (TEST RIG FRAME EARTHED)

TEST NUMBER	1: RFI @ L-E	2: RFI @ N-E
FREQUENCY	RFI CONDUCTED VOLTAGE MEASUREMENTS: dB(uV)	
0.150 MHz	83.5	94
0.160	83.5	93.5
0.240	82	93
0.550	81	91
1.000	79	87
1.400	77.5	81
2.000	67.5	77
3.500	64	73.5
6.000	64	74
10.00	64	69.5
13.00	59	69
22.00	56.5	64
30.00	51	59
	RFI RADIATED POWER MEASUREMENTS: dB(pW)	
30.00	44	44
40.00	45	45
46.00	44.5	44.5
65.00	44	44
90.00	43.5	43.5
150.0	39	39
180.0	37.5	37.5
220.0	34	34
300.0	32	32

TABLE A2.136

TITLE: RFI DUE TO THE INFLUENCE OF THE PHYSICAL COMPONENTS OF THE ARMATURE AND FIELD:
MEASURED RFI LEVELS FROM TEST RIG FITTED WITH 12/24 ARMATURE AND U-TYPE FIELD CONNECTED AS A SPLIT WINDING (a) WITH TEST RIG EARTHED . (b) NOT EARTHED

TEST VARIABLE: (a),(b)

TEST NUMBER	1:(a) RFI @ L-E	2:(a) RFI @ N-E	3:(b) RFI @ L-E	4:(b) RFI @ N-E
FREQUENCY	RFI CONDUCTED VOLTAGE MEASUREMENTS: dB(uV)			
0.150 MHz	81	81	80.5	80.5
0.160	80	80.5	80	80
0.240	66	66	65	65.5
0.550	60	59.5	60	59.5
1.000	52	52	51	51
1.400	56	56	55	55.5
2.000	60	59.5	59	59
3.500	53	52.5	52	52.5
6.000	50	50	49	49
10.00	54.5	55	54	54.5
13.00	59	59	58	58
22.00	55	55.5	54	54
30.00	57	57	56	56
	RFI RADIATED POWER MEASUREMENTS: dB(pW)			
30.00	48	48	47	47
40.00	48.5	48.5	47	47
46.00	51	51	50	50
65.00	53.5	53.5	51	51
90.00	48	48	47	47
150.0	43	43	44	44
180.0	42	42	40	40
220.0	41	41	41	41
300.0	23	23	24	24

TABLE A2.137

TITLE: RFI DUE TO THE INFLUENCE OF THE PHYSICAL COMPONENTS OF THE ARMATURE AND FIELD:
MEASURED RFI LEVELS FROM TEST RIG FITTED WITH 12/24 ARMATURE AND D-TYPE FIELD CONNECTED AS A SPLIT WINDING (a) WITH TEST RIG EARTHED , (b) NOT EARTHED

TEST VARIABLE: (a),(b)

TEST NUMBER	1:(a) RFI @ L-E	2:(a) RFI @ N-E	3:(b) RFI @ L-E	4:(b) RFI @ N-E
FREQUENCY	RFI CONDUCTED VOLTAGE MEASURMENTS: dB(uV)			
0.150 MHz	81	81	81	81.5
0.160	80.5	80.5	80	81
0.240	78	78	77.5	78
0.550	70	69.5	70	70
1.000	59	58	57	57
1.400	56	56	55	55.5
2.000	54	53.5	52	53
3.500	50	50	50	51
6.000	49	49	48	48.5
10.00	47.5	47	46	47
13.00	49	49	49	49
22.00	49.5	49	49	49
30.00	49	49	48	47.5
	RFI RADIATED POWER MEASUREMENTS: dB(pW)			
30.00	41	41	40	40
40.00	40.5	40.5	40	40
46.00	38	38	37	37
65.00	35	35	34	34
90.00	42	42	40	40
150.0	35	35	36	36
180.0	34	34	33	33
220.0	26	26	28	28
300.0	17	17	18	18

TABLE A2.138

TITLE: RFI DUE TO THE INFLUENCE OF THE PHYSICAL COMPONENTS OF THE ARMATURE AND FIELD:
COMPARISON OF MEASURED RFI LEVELS OBTAINED USING A U-TYPE FIELD WITH DIFFERENT ARMATURE CONFIGURATIONS

TEST VARIABLE: ARMATURE (ROTOR SLOTS/COMMUTATOR SEGMENTS)

TEST NUMBER	1: 12/24	2: 11/22	3: 7/21
FREQUENCY	RFI CONDUCTED VOLTAGE MEASUREMENTS: dB(uV)		
0.150 MHz	92	96	94
0.160	92	95.5	93.5
0.240	91.5	93.5	93
0.550	89	91.5	91
1.000	85	90.5	87
1.400	82	88	81
2.000	82	89	77
3.500	80.5	85.6	73.5
6.000	78	83	74
10.00	80	82	69.5
13.00	78	80	69
22.00	68	70	64
30.00	63	66	59
	RFI RADIATED POWER MEASUREMENTS: dB(pW)		
30.00	50	56	44
40.00	51	56	45
46.00	53.5	57	44.5
65.00	50	55.5	45
90.00	43.5	50	43.5
150.0	45.5	48	39
180.0	42	46.5	37.5
220.0	31	46	34
300.0	24	45.5	32

*
*
TABLE A2.139
*

TITLE: RFI DUE TO THE INFLUENCE OF THE PHYSICAL COMPONENTS OF THE ARMATURE AND FIELD:
MEASURED RFI LEVELS WITH VARYING ARMATURE TURNS PER COIL USING A U-TYPE FIELD AND 12/24 ARMATURES

*

TEST VARIABLE: ARMATURE TURNS/COIL (T/C)

*

TEST NUMBER	1: 34 T/C	2: 36	3: 40				
FREQUENCY	RFI CONDUCTED VOLTAGE MEASUREMENTS: dB(uV)						
0.150 MHz	94	92	92				
0.160	93	91.5	92				
0.240	88.5	90	91.5				
0.550	85	86	89				
1.000	82	84	85				
1.400	80	81	82.5				
2.000	79	81	82				
3.500	77.5	79	80.5				
6.000	76	77.5	78				
10.00	76	78	80				
13.00	75	76.5	78				
22.00	63	65	68				
30.00	61.5	62	63				
	RFI RADIATED POWER MEASUREMENTS: dB(pW)						
30.00	46	49	50				
40.00	49	50	51				
46.00	49	51.5	53				
65.00	46.5	50	50				
90.00	41.5	43.5	44				
150.0	42	44.5	45.5				
180.0	38	41	41				
220.0	30	32	32				
300.0	24	25	25				

*
*
*

*
*
TABLE A2.140
*

TITLE: RFI DUE TO THE INFLUENCE OF THE PHYSICAL COMPONENTS OF THE ARMATURE AND FIELD:
MEASURED RFI LEVELS WITH VARYING ARMATURE TURNS PER COIL USING A U-TYPE FIELD AND 7/21 ARMATURES

*

TEST VARIABLE: ARMATURE TURNS/COIL (T/C)

*

TEST NUMBER	1: 39 T/C	2: 41	3: 43				
FREQUENCY	RFI CONDUCTED VOLTAGE MEASUREMENTS: dB(uV)						
0.150 MHz	94	94	96				
0.160	94	94	96				
0.240	93.5	93.5	96.5				
0.550	91	91.5	92				
1.000	87	87.5	90				
1.400	81	83	86				
2.000	79	77.5	82.5				
3.500	74	75	78				
6.000	74.5	76	77				
10.00	70	72	74				
13.00	70	72	73.5				
22.00	64	66	70.5				
30.00	59	62.5	66				
	RFI RADIATED POWER MEASUREMENTS: dB(pW)						
30.00	44	47	48				
40.00	45	46	48.5				
46.00	44	45.5	48				
65.00	45	45.5	47				
90.00	43	43.5	45.5				
150.0	39	39	42				
180.0	38	37	42				
220.0	34.5	36	37				
300.0	32	34	36				

*
*
*

TABLE A2.141

TITLE: RFI DUE TO THE INFLUENCE OF THE PHYSICAL COMPONENTS OF THE ARMATURE AND FIELD:
MEASURED RFI LEVELS WITH VARYING MOTOR LOAD USING A U-TYPE FIELD AND A 12/24 ARMATURE

TEST VARIABLE: SPEED (r/min)

TEST NUMBER	1:	2:	3:	4:
	10000 r/min	13000	16000	20000
FREQUENCY	RFI CONDUCTED VOLTAGE MEASUREMENTS: dB(uV)			
0.150 MHz	92	92	92	93
0.160	92	92	92	93
0.240	92	92	92	93
0.550	90	90	90	91
1.000	85	85	85	86.5
1.400	83	83	83	84.5
2.000	83	83	83	83.5
3.500	81	81	81	82
6.000	78.5	78.5	79.5	81
10.00	80	30	81	82
13.00	78	78	81	81.5
22.00	68	68	71	72.5
30.00	63	63	66	68
	RFI RADIATED POWER MEASUREMENTS: dB(pW)			
30.00	50	50	53	54
40.00	51	51	53	54.5
46.00	53	53	55	55
65.00	50	50	53	54
90.00	44	44	47	49
150.0	45.5	45.5	47	48
180.0	41	41	44	44
220.0	32	32	35	37
300.0	25	25	30	34

TABLE A2.142

TITLE: RFI DUE TO THE INFLUENCE OF MECHANICAL VARIATIONS IN THE MOTOR ASSEMBLY:
MEASURED RFI LEVELS WITH VARYING ARMATURE STATIC OUT-OF-BALANCE AT 13000 r/min

TEST VARIABLE: OUT-OF-BALANCE (gcm)

TEST NUMBER	1:	2:	3:	4:	5:	6:
	ZERO	0.2	0.4	0.6	0.8	1.0
FREQUENCY	RFI CONDUCTED VOLTAGE MEASUREMENTS: dB(uV)					
0.150 MHz	92.5	92.5	93	93	94	95
0.160	92	92	92.5	92.5	93	94
0.240	91	91	91	91.5	92	93
0.550	89	89	89.5	89.5	90	91.5
1.000	85	85	85	85	86	87
1.400	81	81	81	81.5	82	84
2.000	81	81	81	81	82	83
3.500	79	79	79.5	80	80.5	81.5
6.000	76	76	76	76	77	78
10.00	78	78	78.5	79	80	82
13.00	76	76	76.5	76.5	77	79.5
22.00	70	70	71	71	71.5	73
30.00	61	61	61.5	62	63	65
	RFI RADIATED POWER MEASUREMENTS: dB(pW)					
30.00	50	50	50.5	50.5	51.5	53
40.00	51	51	51	51	52	54
46.00	52	52	52	52	52	53.5
65.00	50	50	50.5	50.5	51	53
90.00	45	45	46	46	47	49
150.0	45	45	45	45	46	47
180.0	41	41	41	41	42	44
220.0	31	31	31.5	31.5	33	36
300.0	25	25	26	26	28	29.5

TABLE A2.143

TITLE: RFI DUE TO THE INFLUENCE OF MECHANICAL VARIATIONS IN THE MOTOR ASSEMBLY:
MEASURED RFI LEVELS WITH VARYING ARMATURE STATIC OUT-OF-BALANCE AT 13000 r/min

TEST VARIABLE: OUT-OF-BALANCE (gcm)

TEST NUMBER	7: 1.5 gcm	8: 2.0	9: 2.5	10: 3.0		
FREQUENCY	RFI CONDUCTED VOLTAGE MEASUREMENTS: dB(uV)					
0.150 MHz	95	96	97	99		
0.160	94.5	95	97	99		
0.240	94	95	96.5	98		
0.550	92	93	94	96		
1.000	87	89	90	91		
1.400	85	87	88	89		
2.000	84	86.5	87	89		
3.500	84	86.5	88	89		
6.000	80	83	88	89		
10.00	84	86	87	90		
13.00	81	83	85	86		
22.00	76	81.5	83	84.5		
30.00	70	75	78	84		
	RFI RADIATED POWER MEASUREMENTS: dB(pW)					
30.00	56	60	61	63		
40.00	57	60	62	63		
46.00	55.5	60	61	65		
65.00	55	59	61	65		
90.00	51	53	56	60		
150.0	49.5	51	54	59		
180.0	46	48	50	56		
220.0	39	40	43	45		
300.0	31	36	39	40		

TABLE A2.144

TITLE: RFI DUE TO THE INFLUENCE OF MECHANICAL VARIATIONS IN THE MOTOR ASSEMBLY:
MEASURED RFI LEVELS WITH VARYING ARMATURE STATIC OUT-OF-BALANCE AT 18000 r/min

TEST VARIABLE: OUT-OF-BALANCE (gcm)

TEST NUMBER	1: ZERO	2: 0.2 gcm	3: 0.4	4: 0.6	5: 0.8	6: 1.0
FREQUENCY	RFI CONDUCTED VOLTAGE MEASUREMENTS: dB(uV)					
0.150 MHz	93.5	93.5	93.5	94	94.5	95
0.160	92.5	92.5	92.5	93	94	94.5
0.240	92	92	92	93	93.5	94
0.550	90	90	90	91	91.5	91.5
1.000	86	86	86	87.5	87.5	88
1.400	83	83.5	83.5	85	85	86
2.000	83	83	83.5	84.5	84.5	85
3.500	81	81	81.5	83	84	84
6.000	77.5	78	78	80	80	80
10.00	80	80	80	82	82.5	84
13.00	78	78	78	80.5	81	82
22.00	71	71	71	73	74	76
30.00	63	63	63	65	69	71.5
	RFI RADIATED POWER MEASUREMENTS: dB(pW)					
30.00	52	52	53	54	56	57
40.00	53.5	54	54	54.5	56	57
46.00	54	54	54	55	57	58
65.00	51	51	51.5	52	53	54.5
90.00	46.5	46.5	46.5	47	48	49
150.0	46	46	46	47	48	49
180.0	43	43	43	44	45	46
220.0	33	33	33	34	36	38
300.0	26	26	27	28	32	34.5

TABLE A2.147

TITLE: RFI DUE TO THE INFLUENCE OF MECHANICAL VARIATIONS IN THE MOTOR ASSEMBLY:
MEASURED RFI LEVELS WITH VARYING DYNAMIC ARMATURE OUT-OF-BALANCE AT 13000 r/min

TEST VARIABLE: OUT-OF-BALANCE (gcm)

TEST NUMBER	7: 0.8 gcm	8: 1.0	9: 1.5	10: 2.0
FREQUENCY	RFI CONDUCTED VOLTAGE MEASUREMENTS: dB(uV)			
0.150 MHz	96	96.5	98	100
0.160	95	96	97.5	100
0.240	95	95.5	97	99
0.550	93	94	96	98
1.000	88.5	90	91	93
1.400	86	88	89	90
2.000	86	87	89	91
3.500	85	87	87	87.5
6.000	81	84	86	87
10.00	85	87	89	91
13.00	83	85	87	89
22.00	77	81	82	84
30.00	74	76	78	81
	RFI RADIATED POWER MEASUREMENTS: dB(pW)			
30.00	58	60	63	64.5
40.00	58	61	63.5	64
46.00	57	60.5	64	66
65.00	56	60	63	67
90.00	52	54	59	61
150.0	50	53	57	60
180.0	48	49	54	55
220.0	39.5	41	46	47
300.0	33	38	40	40

TABLE A2.148

TITLE: RFI DUE TO THE INFLUENCE OF MECHANICAL VARIATIONS IN THE MOTOR ASSEMBLY:
MEASURED RFI LEVELS WITH VARYING DYNAMIC ARMATURE OUT-OF-BALANCE AT 18000 r/min

TEST VARIABLE: OUT-OF-BALANCE (gcm)

TEST NUMBER	1: 0.1 gcm	2: 0.2	3: 0.3	4: 0.4	5: 0.5	6: 0.6
FREQUENCY	RFI CONDUCTED VOLTAGE MEASUREMENTS: dB(uV)					
0.150 MHz	93.5	93.5	95	96	97	97
0.160	93	93	94.5	95	96.5	97
0.240	92	92	93	93.5	94	95
0.550	90	90	91	92	93	94.5
1.000	86	86	87.5	89	90	90
1.400	83.5	83.5	85	86	87	88
2.000	83.5	84	85	87	88	89
3.500	81	81	82	82	83	85
6.000	77.5	79	81.5	82	84	85
10.00	81	81	83	86.5	88	88
13.00	78	78	81	84	85.5	86
22.00	72	72	73.5	76	80	81
30.00	65	65.5	70	72.5	75	78
	RFI RADIATED POWER MEASUREMENTS: dB(pW)					
30.00	52	52	55.5	57.5	58.5	61.5
40.00	53	53	55.5	57	60	61.5
46.00	54	54.5	56	57	58	60
65.00	52	52	53	56	61	61
90.00	45	45.5	46	49	59	60
150.0	46	46	48	51	58	59
180.0	42	43	44	46	47	51
220.0	33	34	36.5	37	38	40
300.0	29	30	33.5	36.5	37	38

TABLE A2.149

TITLE: RFI DUE TO THE INFLUENCE OF MECHANICAL VARIATIONS IN THE MOTOR ASSEMBLY:
MEASURED RFI LEVELS WITH VARYING DYNAMIC ARMATURE OUT-OF-BALANCE AT 18000 r/min

TEST VARIABLE: OUT-OF-BALANCE (gcm)

TEST NUMBER	7:	8:	9:	10:			
	0.8 gcm	1.0	1.5	2.0			
FREQUENCY	RFI CONDUCTED VOLTAGE MEASUREMENTS: dB(pW)						
0.150 MHz	99	100	101	102			
0.160	98.5	99	100	101.5			
0.240	97	97	98.5	101			
0.550	95	96	98	98.5			
1.000	90.5	92	93	95.5			
1.400	89	90.5	91	92			
2.000	90	90.5	91	92			
3.500	86	88	89	89.5			
6.000	87	88	88	89.5			
10.00	88.5	90	92	93			
13.00	87.5	90	90	91			
22.00	83	84	85	86			
30.00	80	82	84	85			
	RFI RADIATED POWER MEASUREMENTS: dB(pW)						
30.00	64	65	65	66			
40.00	63	66	67	68			
46.00	63	67	68.5	69			
65.00	62	63.5	64	65.5			
90.00	62	62.5	64	66			
150.0	61	62	62	63			
180.0	57	58	58	58.5			
220.0	42	44	47	48			
300.0	39	40	40	41			

TABLE A2.150

TITLE: RFI DUE TO THE INFLUENCE OF MECHANICAL VARIATIONS IN THE MOTOR ASSEMBLY:
MEASURED RFI LEVELS WITH VARYING SPRING LOAD AT 18000 r/min

TEST VARIABLE: SPRING LOAD (g)

TEST NUMBER	1:	2:	3:	4:	5:	6:
	40 g	50	60	70	80	90
FREQUENCY	RFI CONDUCTED VOLTAGE MEASUREMENTS: dB(uV)					
0.150 MHz	105	101.5	99	96	94	93
0.160	105	101	98	95	93.5	92
0.240	103	99	95	94	93	92
0.550	104	99	94	93	92	90
1.000	101	96	92	87	86	85
1.400	102	97	92	86	85	83
2.000	101	95	90	85	84	82
3.500	98	88	82	82	81	80.5
6.000	98	87	81	80	79	77
10.00	99	93	88	84	83	80.5
13.00	96	91	84	83	81	78
22.00	93	87	80	75	73	71.5
30.00	89	82	74.5	68.5	66.5	63.5
	RFI RADIATED POWER MEASUREMENTS: dB(pW)					
30.00	79	74	66	60	54.5	52
40.00	76	71	63	57	54	53
46.00	75	70	61	55	54.5	54
65.00	73	68	60	54	53	50
90.00	76	68	58	53	48	47
150.0	72	66	57	51	49	46
180.0	68	61	53	47	45	42
220.0	62	55	46	39	36	34
300.0	62.5	54	44	35	32	28

TABLE A2.151

TITLE: RFI DUE TO THE INFLUENCE OF MECHANICAL VARIATIONS IN THE MOTOR ASSEMBLY:
MEASURED RFI LEVELS WITH VARYING SPRING LOAD AT 18000 r/min

TEST VARIABLE: SPRING LOAD (g)

TEST NUMBER	7: 100 g	8: 110	9: 120	10: 130	11: 140	12: 150
FREQUENCY	RFI CONDUCTED VOLTAGE MEASUREMENTS: dB(uV)					
0.150 MHz	93	93	94.5	96	96.5	97.5
0.160	93	92.5	93	95	96	97
0.240	91.5	92	92	94	95	96.5
0.550	89	90	92	93	93	93
1.000	86	87	88	89.5	90	91.5
1.400	84	84.5	85	87	89	90
2.000	84	84	85	86.5	87	89
3.500	81.5	82	83.5	85	86	88
6.000	78	78	79	81	83	86
10.00	80	80.5	83	86	87	90
13.00	77	78	81.5	84	84	85
22.00	70	70.5	74	77	79.5	80
30.00	63	63	67	70	74.5	76
	RFI RADIATED POWER MEASUREMENTS: dB(pW)					
30.00	51	52	54.5	57	58	59.5
40.00	51.5	52	54	56	57	57.5
46.00	52.5	52.5	55	56	58	61
65.00	51.5	52	54	56	57	58
90.00	46.5	47	49	52	53.5	55
150.0	45	45	47	50	51	53
180.0	42	43	44	47	48	48.5
220.0	35	36	38	39.5	40	43
300.0	27	28	30	33	34	35

TABLE A2.152

TITLE: RFI DUE TO THE INFLUENCE OF MECHANICAL VARIATIONS IN THE MOTOR ASSEMBLY:
MEASURED RFI LEVELS WITH VARYING BRUSH ALIGNMENT ALONG THE QUADRATURE AXIS AGAINST THE DIRECTION OF ROTATION

TEST VARIABLE: BRUSH MISALIGNMENT (mm)

TEST NUMBER	1: ZERO	2: 0.075 mm	3: 0.125	4: 0.200	5: 0.250	6: 0.375	7: 0.500
FREQUENCY	RFI CONDUCTED VOLTAGE MEASUREMENTS: dB(uV)						
0.150 MHz	93	93	93	94	94.5	97	100.5
0.160	92.5	92.5	92.5	93.5	94	96	100
0.240	92	92	92	93	93	96	98
0.550	89	89	89	90	91	94	97
1.000	85	85	85	86	87	90.5	94
1.400	82	82	82	83	84	88	92
2.000	83	83.5	83.5	85	86	91	92
3.500	81	81	81	83	84	89.5	92.5
6.000	77	77	77	80	81	86	90
10.00	80	80	80.5	82	83	86	88.5
13.00	77	77	77.5	79	81	84.5	90
22.00	72	72	72	74.5	76	80	87
30.00	63	63	63	66	70	78	88
	RFI RADIATED POWER MEASUREMENTS: dB(pW)						
30.00	52.5	52.5	52.5	54.5	55.5	58.5	64
40.00	50	51	51	53	54.5	56.5	62
46.00	54	54	54	55	56	58	64.5
65.00	50	50.5	50.5	52.5	54	56	62
90.00	46	46	46.5	48	50	53	62
150.0	45	45	45	46	46	50	58
180.0	42	42	42	43	44	45	52
220.0	34	34	34	36.5	38	42	51
300.0	29	29	29	33	35	39.5	47

TABLE A2.153

TITLE: RFI DUE TO THE INFLUENCE OF MECHANICAL VARIATIONS IN THE MOTOR ASSEMBLY:
MEASURED RFI LEVELS WITH VARYING BRUSH ALIGNMENT ALONG THE QUADRATURE AXIS WITH THE DIRECTION OF ROTATION

TEST VARIABLE: BRUSH MISALIGNMENT (mm)

TEST NUMBER	1: ZERO	2: 0.075 mm	3: 0.125	4: 0.200	5: 0.250	6: 0.375	7: 0.500
FREQUENCY	RFI CONDUCTED VOLTAGE MEASUREMENTS: dB(uV)						
0.150 MHz	93	93	94	95	95.5	98	103
0.160	92.5	92.5	93	94.5	95	97	102
0.240	92	92	93	97	95	98	101
0.550	89	89	89.5	90	91	95	99.5
1.000	85	85	87	88	89	95	99.5
1.400	82	82.5	84.5	86	87	94	99
2.000	83	83.5	84.5	86	87.5	93.5	99
3.500	81	81	83	85	86	93	98
6.000	77	77	80	83	84	90	97
10.00	80	80	82	84	85	93	99
13.00	77	77.5	80	81	82	92	98
22.00	72	72	74	76	78	90	96
30.00	65	65	69	74	75	87.5	93
	RFI RADIATED POWER MEASUREMENTS: dB(pW)						
30.00	52.5	52.5	56	57.5	57.5	65	84.5
40.00	50	50	55	57.5	58	64	76
46.00	54	54	56	56	57	66	74
65.00	50	50.5	54	55.5	56	63	72
90.00	46	46	49	52	53.5	61	70
150.0	45	45	47.5	48	49	59	66
180.0	42	42	45	47	49	56.5	68
220.0	34	34	38	40	43	54	66
300.0	28	29	35	38	39	51	64

TABLE A2.154

TITLE: RFI DUE TO THE INFLUENCE OF MECHANICAL VARIATIONS IN THE MOTOR ASSEMBLY:
MEASURED RFI LEVELS WITH VARYING HEIGHTS OF PROUD COMMUTATOR SEGMENTS AT 13000 r/min

TEST VARIABLE: PROUD COMMUTATOR HEIGHT (mm *E-3)

TEST NUMBER	1: 1.25 E-3 MM	2: 2.50 E-3	3: 3.75 E-3	4: 5.00 E-3	5: 7.50 E-3	6: 10.0 E-3	7: 12.5 E-3
FREQUENCY	RFI CONDUCTED VOLTAGE MEASUREMENTS: dB(uV)						
0.150 MHz	92	92	93	93.5	97	98	101
0.160	91.5	92	92.5	93	96	98	100
0.240	91	91	92	92	95	96	99
0.550	89	89	89.5	90	94	95	99
1.000	84.5	85	86	87	89.5	90	94
1.400	81	82	82.5	83	88	89	92
2.000	81	81	82	83	86	87	92
3.500	78.5	79	80	81	87	88	94
6.000	75	76	77	78	83	88	93
10.00	77.5	78	79	80	86	87	91
13.00	76	76	78.5	79.5	84	86	89
22.00	70	70	72	72	82	84	87
30.00	61.5	62	64	64	75	78	84
	RFI RADIATED POWER MEASUREMENTS: dB(pW)						
30.00	50	50	52	52	60	61	66
40.00	50	50.5	52	53	61	62	65
46.00	51.5	51.5	52	52	60	62	68
65.00	49	49.5	50	51	58	61	65
90.00	45	46	47	47.5	53	58	61
150.0	44.5	45	46	46	52	54	57
180.0	41	41	43	43	47	52	55
220.0	30	31	33	33	40	43	49
300.0	24	25	27	28	35	40	51

TABLE A2.155

TITLE: RFI DUE TO THE INFLUENCE OF MECHANICAL VARIATIONS IN THE MOTOR ASSEMBLY:
MEASURED RFI LEVELS WITH VARYING HEIGHTS OF PROUD COMMUTATOR SEGMENTS AT 18000 r/min

TEST VARIABLE: PROUD COMMUTATOR HEIGHT (mm *E-3)

TEST NUMBER	1: 1.25 E-3 MM	2: 2.50 E-3	3: 3.75 E-3	4: 5.00 E-3	5: 7.50 E-3	6: 10.0 E-3	7: 12.5 E-3
FREQUENCY	RFI CONDUCTED VOLTAGE MEASUREMENTS: dB(uV)						
0.150 MHz	93	94	94	99.5	101	102	104
0.160	93	93	93.5	99	101	101.5	103.5
0.240	92	92	93	99	100	101	102
0.550	89	89	89	96	98	99	100.5
1.000	86	86	86	93	97.5	98	99
1.400	82	82.5	83	91	94	97	98.5
2.000	83	83	83	90	91	95	97.5
3.500	80	81	81	89	90	95	97
6.000	77	77	77.5	88	91	93	96
10.00	80	80	80.5	90	92	94	98
13.00	78	79	79	88	90.5	94	96.5
22.00	71	71	71	86	88	90	93
30.00	64	65	65	83	89	90	91
	RFI RADIATED POWER MEASUREMENTS: dB(pW)						
30.00	52	52	52	62	64	70	71
40.00	53	53.5	54	61.5	66	68	70
46.00	54	54	54	63	65	68	70
65.00	51	51	51	61	63	65	67
90.00	46	46.5	47	60	61.5	64	66
150.0	46	46	46	59	62	63	65
180.0	43	43.5	43.5	55	57	59	61.5
220.0	36	36	36	50.5	54	57	59
300.0	30	31	31	46	52	55	57

TABLE A2.156

TITLE: RFI DUE TO THE INFLUENCE OF MECHANICAL VARIATIONS IN THE MOTOR ASSEMBLY:
MEASURED RFI LEVELS WITH VARYING COMMUTATOR ECCENTRICITY AT 13000 r/min

TEST VARIABLE: COMMUTATOR ECCENTRICITY (mm)

TEST NUMBER	1: ZERO	2: 0.01	3: 0.03	4: 0.04	5: 0.05	6: 0.06	7: 0.08
FREQUENCY	RFI CONDUCTED VOLTAGE MEASUREMENTS: dB(uV)						
0.150 MHz	92	92	92.5	92.5	92.5	94	95
0.160	91.5	92	92	92	92.5	93	94.5
0.240	91	91	91.5	91.5	92	93	94
0.550	88	88	88.5	88.5	89	90	91
1.000	84	84	84.5	84.5	85	87	90
1.400	82	82	82	82	82	84	87
2.000	81	81.5	81.5	82	82	85	88
3.500	79	79	79	79	79.5	83	85
6.000	75	75	75.5	75.5	76	82	85
10.00	78	78.5	78.5	78.5	78.5	82	90
13.00	76	76	76.5	77	77.5	81	87
22.00	70	70	70.5	70.5	71	87	84
30.00	62	62	63	63	63	73	84
	RFI RADIATED POWER MEASUREMENTS: dB(pW)						
30.00	50	50.5	50.5	51	51	55	60
40.00	50.5	50	50.5	50.5	51	56	61
46.00	51	51	52	52	52	56	60
65.00	49	49.5	50	50	50	55	58
90.00	46.	46	47	47	47.5	51	55
150.0	45	45.5	46	46	46	50	54
180.0	41	42	43	43	43	46	53
220.0	30	31	32	32	32	44	51
300.0	24	25	27	28	28	37	48

TABLE A2.157

TITLE: RFI DUE TO THE INFLUENCE OF MECHANICAL VARIATIONS IN THE MOTOR ASSEMBLY:
MEASURED RFI LEVELS WITH VARYING COMMUTATOR ECCENTRICITY AT 18000 r/min

TEST VARIABLE: COMMUTATOR ECCENTRICITY (mm)

TEST NUMBER	1:	2:	3:	4:	5:	6:	7:
	ZERO	0.01 mm	0.02	0.03	0.04	0.06	0.08
FREQUENCY	RFI CONDUCTED VOLTAGE MEASUREMENTS: dB(uV)						
0.150 MHz	92	92	92	93	94	95	96
0.160	91.5	91.5	91.5	92.5	94	95	97
0.240	91.5	91.5	91.5	93	94	95	97.5
0.550	89	89	89	90	91	92	94
1.000	85	85	85.5	86.5	87	89	92
1.400	83	83	83	85	85.5	87	91
2.000	83	83	83	84	84.5	87.5	91
3.500	81	81	81	82	83	85	88
6.000	77.5	77.5	78	79	80.5	84	88.5
10.00	80	80	80.5	81.5	82	84.5	92
13.00	78	78	78	79	80	84	90.5
22.00	70	70	70	72	73	89	89
30.00	63	63	63	66	70	75	87
	RFI RADIATED POWER MEASUREMENTS: dB(pW)						
30.00	53.5	53.5	53.5	54.5	56	58	64
40.00	54	54	54	54.5	55	57	63.5
46.00	55	55	55	56	56	59.5	63.5
65.00	51	51	51	53	53	56	61
90.00	46	46.5	46.5	48	49.5	53	59
150.0	46	46	46	47	48	51	58
180.0	43	43.5	43.5	44	45	48	57
220.0	36	36	36.5	38	40	46	53
300.0	27	27	27.5	32	34	41.5	51

TABLE A2.158

TITLE: RFI DUE TO THE INFLUENCE OF MECHANICAL VARIATIONS IN THE MOTOR ASSEMBLY:
MEASURED RFI LEVELS WITH VARYING COMMUTATOR SURFACE FINISHES

TEST VARIABLE: SURFACE FINISH (mm*E-6 CLA)

TEST NUMBER	1:	2:	3:	4:	5:	6:
	0.1 mm*E-6 CLA	0.6 E-6	1.5 E-6	2.0 E-6	3.0 E-6	5.0 E-6
FREQUENCY	RFI CONDUCTED VOLTAGE MEASUREMENTS: dB(uV)					
0.150 MHz	93	93	94	96	97.5	99.5
0.160	92	92.5	94	95.5	98	99
0.240	91.5	92	93	95	98	99
0.550	88	88.5	90	92	96	97.5
1.000	85	86	87.5	90	92.5	96
1.400	82	82	85	88	92	96.5
2.000	82.5	82.5	85	87.5	90	95
3.500	81	81	83	86	91	94
6.000	77.5	78	80	82	88	96
10.00	79.5	79.5	81	84	90	97
13.00	78	78	80	83	89	97
22.00	71	71	73	75	83	90
30.00	63	63	67	72	78	91
	RFI RADIATED POWER MEASUREMENTS: dB(pW)					
30.00	52	52	54	56.5	62	66
40.00	52	52.5	54	56	58	64
46.00	53.5	54	54.5	56	61	63
65.00	50	50	52	54	56.5	61
90.00	46	46	47	50	54	59
150.0	44.5	45	45.5	49	52	54.5
180.0	43	43	43	45	50	52
220.0	36	36	37	41	46	49
300.0	26	27	31	37	44	48

TABLE A2.159

TITLE: RFI DUE TO THE INFLUENCE OF MECHANICAL VARIATIONS IN THE MOTOR ASSEMBLY:
MEASURED RFI LEVELS WITH VARYING DEPTH OF COMMUTATOR INSULATION UNDERCUT

TEST VARIABLE: UNDERCUT DEPTH INSULATION (mm)

TEST NUMBER	1: ZERO (FLUSH)	2: 0.5 mm	3: 1.0	4: 1.5		
FREQUENCY	RFI CONDUCTED VOLTAGE MEASUREMENTS: dB(uV)					
0.150 MHz	97	94	94	94.5		
0.160	97	94	93.5	94		
0.240	97.5	92.5	93	93		
0.550	94.5	91	91	91		
1.000	94	87	88	87		
1.400	91	82	82	81.5		
2.000	84	77	77.5	77		
3.500	85	73	72	72		
6.000	87	74	73.5	73		
10.00	85.5	69	68	68		
13.00	85	68.5	69	68		
22.00	78	64	64	64		
30.00	74	59.5	59	59		
	RFI RADIATED POWER MEASUREMENTS: dB(pW)					
30.00	52	44	44.5	44		
40.00	50	45	45	45		
46.00	50	44	44	44		
65.00	49	44.5	44	44		
90.00	47	43	43	43		
150.0	45	40	40	40		
180.0	44	37	36	36		
220.0	42	34	34	34		
300.0	40	32	31	31		

TABLE A2.160

TITLE: RFI DUE TO THE INFLUENCE OF MECHANICAL VARIATIONS IN THE MOTOR ASSEMBLY:
MEASURED RFI LEVELS WITH VARYING BRUSH/BRUSH BOX CLEARANCE IN THE DIRECTION TANGENTIAL TO COMMUTATOR ROTATION

TEST VARIABLE: BRUSH/BRUSH BOX CLEARANCE (mm)

TEST NUMBER	1: 0.010 mm	2: 0.020	3: 0.050	4: 0.075	5: 0.100	6: 0.125
FREQUENCY	RFI CONDUCTED VOLTAGE MEASUREMENTS: dB(uV)					
0.150 MHz	99.5	98	93	93	93	94
0.160	99.5	97	92.5	92.5	92.5	94
0.240	99	96	92	92	92.5	94
0.550	98	96	87	87.5	87.5	88
1.000	96	91	84.5	84.5	85	86.5
1.400	95	91	82	82	82	83
2.000	94	90	82	82	82	83
3.500	91	89	80	80	80.5	81
6.000	92.5	89	78	78	78.5	80
10.00	94	90	80	80	80	81.5
13.00	92	87	77.5	77.5	77.5	79
22.00	86	82	70	70.5	70.5	72
30.00	84.5	78	62	62	62	65
	RFI RADIATED POWER MEASUREMENTS: dB(pW)					
30.00	67	64	53	52	52	54.5
40.00	64	63	52	52	52	53
46.00	65	64	53	53	53	54.5
65.00	62	60	51	51	51	53
90.00	63	57	46	45.5	46	48
150.0	58	54	45.5	45	45.5	47
180.0	56	54	42	42	42	44
220.0	52	48	33	33	34	36
300.0	47	42.5	27.5	28	27	29

TABLE A2.161

TITLE: RFI DUE TO THE INFLUENCE OF MECHANICAL VARIATIONS IN THE MOTOR ASSEMBLY:
MEASURED RFI LEVELS WITH VARYING BRUSH/BRUSH BOX CLEARANCE IN THE DIRECTION TANGENTIAL TO COMMUTATOR ROTATION

TEST VARIABLE: BRUSH/BRUSH BOX CLEARANCE (mm)

TEST NUMBER	7: 0.150 mm	8: 0.175	9: 0.200			
FREQUENCY	RFI CONDUCTED VOLTAGE MEASUREMENTS: dB(uV)					
0.150 MHz	95	96	96			
0.160	94	95	95.5			
0.240	94.5	95	95			
0.550	89	90	91			
1.000	87	88	89.5			
1.400	85	86.5	87			
2.000	84	85	86			
3.500	82	84	85			
6.000	80	81	82			
10.00	82	83.5	84			
13.00	80	81	82			
12.00	74	76	77			
30.00	70	72	75			
	RFI RADIATED POWER MEASUREMENTS: dB(pW)					
30.00	57	58	58			
40.00	55	56	57			
46.00	55	56	56			
65.00	53.5	54	54			
90.00	51	52	53.5			
150.0	48	48	48.5			
180.0	45	46	46			
220.0	37	40	38			
300.0	32	34	36			

TABLE A2.162

TITLE: RFI DUE TO THE INFLUENCE OF MECHANICAL VARIATIONS IN THE MOTOR ASSEMBLY:
MEASURED RFI LEVELS WITH VARYING BRUSH OVERHANG LENGTH AT 18000 r/min

TEST VARIABLE: BRUSH OVERHANG (mm)

TEST NUMBER	1: 0.5 mm	2: 1.0	3: 1.5	4: 2.0	5: 2.5	6: 3.0
FREQUENCY	RFI CONDUCTED VOLTAGE MEASUREMENTS: dB(uV)					
0.150 MHz	92	92.5	94.5	95	96	97
0.160	91.5	92	94	95	96	97.5
0.240	91.5	92	93	94	96	98.5
0.550	89	89	90	91.5	94	96
1.000	86	86	87	88.5	90	92
1.400	83	83.5	85	87	88	89
2.000	82	82	84	85	89	91
3.500	81	81	82	83.5	87	90
6.000	78	78.5	80	83	85	88
10.00	80	80	82	84	88	90
13.00	78	78	79	80	89	99
22.00	71	71.5	74	76	80	86
30.00	65	65.5	68	73	76	84
	RFI RADIATED POWER MEASUREMENTS: dB(pW)					
30.00	52.5	52.5	54	56	61	64
40.00	53	53.5	55	56	58	63
46.00	53	54	54	56	58	61
65.00	50	50	51	53.5	56	58
90.00	46	46	49	51.5	56	58
150.0	46	46	48	49.5	50	57
180.0	44	45	46	46.5	50	54
220.0	37	37.5	40	44	47	49
300.0	28	28	32	35.5	44	48

TABLE A2.163

TITLE: RFI DUE TO THE INFLUENCE OF MECHANICAL VARIATIONS IN THE MOTOR ASSEMBLY:
MEASURED RFI LEVELS WITH VARYING BEARING MISALIGNMENT ALONG DIRECT AXIS

TEST VARIABLE: BEARING MISALIGNMENT (mm)

TEST NUMBER	1: ZERO	2: 0.075 mm	3: 0.100	4: 0.125	5: 0.150	6: 0.200
FREQUENCY	RFI CONDUCTED VOLTAGE MEASUREMENTS: dB(uV)					
0.150 MHz	93	93	93	93	95	98
0.160	92.5	92.5	93	93	94	98
0.240	92	92	92	92	93	98.5
0.550	89	89	89	89	91	96
1.000	86	86	86	86	87	94
1.400	82	82	82.5	82.5	84	92
2.000	82	82	82	83	85	91
3.500	81	81	81	81	83	89
6.000	77.5	77.5	78	78	78.5	90
10.00	79.5	79.5	79.5	80	82	88
13.00	77.5	77.5	77.5	78	80	90
22.00	71	71	71	71.5	73	90
30.00	63	63	63	64	66	86
	RFI RADIATED POWER MEASUREMENTS: dB(pW)					
30.00	52	52	52	52.5	55	61
40.00	52	52	52.5	53	54	58
46.00	53	53	53	53	53	56
65.00	50	50	50	51	53	58
90.00	46	46	46	46	48	55
150.0	45	45	45	45	47	51
180.0	43	43	43	44	46	49
220.0	38	38	38	39.5	41	48
300.0	30	30	30	32	35	47

TABLE A2.164

TITLE: RFI DUE TO THE INFLUENCE OF MECHANICAL VARIATIONS IN THE MOTOR ASSEMBLY:
MEASURED RFI LEVELS WITH VARYING BEARING MISALIGNMENT ALONG QUADRATURE AXIS

TEST VARIABLE: BEARING MISALIGNMENT (mm)

TEST NUMBER	1: 0.075 mm	2: 0.100	3: 0.125	4: 0.150	5: 0.200		
FREQUENCY	RFI CONDUCTED VOLTAGE MEASUREMENTS: dB(uV)						
0.150 MHz	93	93	93.5	97	MOTOR		
0.160	92.5	92.5	93	95.5	FAIL		
0.240	92	92	92	94			
0.550	89	89.5	89.5	92			
1.000	86	87	87	88			
1.400	82	82	82	84			
2.000	82	82	82	86			
3.500	81	81.5	82	84			
6.000	78	79	79	79			
10.00	79.5	80	80	83			
13.00	78	78	78	81.5			
22.00	72	72.5	72.5	74			
30.00	63	64	64	66			
	RFI RADIATED POWER MEASUREMENTS: dB(pW)						
30.00	52	53	54	56			
40.00	52	52	53	55			
46.00	53	53	53	54			
65.00	50	50	50	53			
90.00	46	46	46.5	48			
150.0	45	45	45	48			
180.0	43	44	44	47			
220.0	38	38	38	42			
300.0	29	30	30	34			

TABLE A2.165

TITLE: RFI DUE TO THE INFLUENCE OF MECHANICAL VARIATIONS IN THE MOTOR ASSEMBLY:
MEASURED RFI LEVELS WITH VARYING ANGULAR BRUSH SHIFT (AGAINST THE DIRECTION OF ROTATION FROM MAGNETIC NEUTRAL AXIS)

TEST VARIABLE: BRUSH SHIFT (DEGREES)

TEST NUMBER	1: 0 DEG	2: 2	3: 4	4: 6	5: 8	6: 10
FREQUENCY	RFI CONDUCTED VOLTAGE MEASUREMENTS: dB(uV)					
0.150 MHz	104	104	103	102	101.5	101.5
0.160	103	103	102	101.5	100	100
0.240	102	102	101	101	100	99
0.550	100	100	99	99	98	97
1.000	99	99	98	98	97	97
1.400	98	97	97	97	94	95
2.000	97	96	96	95	91	91
3.500	97	95	95	95	90	89
6.000	96	95	94	93	90	88
10.00	96	96	95	94.5	94	91.5
13.00	96.5	94	94	94	93	90
22.00	86	83	82	80	78	77
30.00	78.5	78.5	78	77	75	73
	RFI RADIATED POWER MEASUREMENTS: dB(pW)					
30.00	74	73	72	70	65.5	62
40.00	72	71	70	68	66	61.5
46.00	70	69	68	68	65	63
65.00	64	64	63	63	63	61
90.00	62.5	62	61	60	57	54.5
150.0	61	61	61	60	57	54
180.0	59	58	58	57	57	55
220.0	50	48	46	45	45	45
300.0	42	41.5	40	38.5	36	34.5

TABLE A2.166

TITLE: RFI DUE TO THE INFLUENCE OF MECHANICAL VARIATIONS IN THE MOTOR ASSEMBLY:
MEASURED RFI LEVELS WITH VARYING ANGULAR BRUSH SHIFT (AGAINST THE DIRECTION OF ROTATION FROM MAGNETIC NEUTRAL AXIS)

TEST VARIABLE: BRUSH SHIFT (DEGREES)

TEST NUMBER	7: 12 DEG	8: 14	9: 16	10: 18	11: 20	12: 22
FREQUENCY	RFI CONDUCTED VOLTAGE MEASUREMENTS: dB(uV)					
0.150 MHz	101	99	96	93.5	92	92
0.160	100	98	95	93	91	91.5
0.240	99	97	94	92	90	90
0.550	96	96	92	89	87	87
1.000	96	95	88	86	84	84
1.400	95	95	85	82	80	80
2.000	90	90	85	82	81	81
3.500	89	88	83	81	81	80.5
6.000	87	87	78	78	76	76
10.00	90	88	85	81	79	79
13.00	90	86	82	78	76	77
22.00	75	75	74	72	70	71
30.00	72	70.5	69	66	63	63.5
	RFI RADIATED POWER MEASUREMENTS: dB(pW)					
30.00	59	56	53.5	51.5	51	52
40.00	60	58	53	52	51	51.5
46.00	61	55	53	53	52	52
65.00	60	53	51	50	49	50
90.00	52	49	46	44	44	45
150.0	51	48	45	44	42	43
180.0	48	47	44	43	41	41
220.0	40	40	39	38	36	34
300.0	32	30	29	27.5	26	26

TABLE A2.167

TITLE: RFI DUE TO THE INFLUENCE OF MECHANICAL VARIATIONS IN THE MOTOR ASSEMBLY:
MEASURED RFI LEVELS WITH VARYING ANGULAR BRUSH SHIFT (AGAINST THE DIRECTION OF ROTATION FROM MAGNETIC NEUTRAL AXIS)

TEST VARIABLE: BRUSH SHIFT (DEGREES)

TEST NUMBER	13: 24 DEG	14: 26	15: 28	16: 30
FREQUENCY	RFI CONDUCTED VOLTAGE MEASUREMENTS: dB(uV)			
0.150 MHz	94	96	98	102
0.160	93.5	95.5	98	101.5
0.240	93	95	97	101
0.550	90	93	96	100
1.000	86	88	93	99.5
1.400	83	86	92	99
2.000	82	85	89	98
3.500	81	84	88	95
6.000	78	79	87	93
10.00	82	87	90	94
13.00	79	84	87	94
22.00	73	76	76	80
30.00	68.5	73	76	79
	RFI RADIATED POWER MEASUREMENTS: dB(pW)			
30.00	55.5	59	62	64
40.00	57	60	60	66
46.00	54	61	57	65
65.00	52	60	55	63
90.00	47	50	53	56
150.0	47	50	52	56
180.0	47	48	50	56
220.0	40	40	42	45
300.0	29	31	34	36

TABLE A2.168

TITLE: RFI DUE TO THE INFLUENCE OF MECHANICAL VARIATIONS IN THE MOTOR ASSEMBLY:
MEASURED RFI LEVELS WITH VARYING BEARING JOURNAL DIAMETER

TEST VARIABLE: BEARING JOURNAL (mm)

TEST NUMBER	1: 8.987 mm	2: 8.985	3: 8.981	4: 8.979	5: 8.975	6: 8.973	7: 8.971
FREQUENCY	RFI CONDUCTED VOLTAGE MEASUREMENTS: dB(uV)						
0.150 MHz	92	92	92	92	93	94	95
0.160	91.5	91.5	91.5	91.5	92	94	95.5
0.240	91.5	91.5	92	92	92	94	96
0.550	88	88	88	88	89	91.5	94
1.000	85	85	85.5	85.5	86	88	92
1.400	82.5	83	83	83	84	87	90
2.000	82.5	82.5	82.5	82.5	83	85.5	90
3.500	81	81	81	81	82	84.5	89
6.000	78	78	78	78	80	84	88
10.00	80	80.5	80.5	80.5	81	86	89.5
13.00	78	78	78	78	80	82	88
22.00	70	70	70	70	71	77	85.5
30.00	63	63	64	64	72	75	82
	RFI RADIATED POWER MEASUREMENTS: dB(pW)						
30.00	51.5	51.5	51.5	51.5	53	58	62.5
40.00	52.5	52.5	53	53	54	58	63
46.00	54	54	54.5	54.5	56	60	64
65.00	51	51	51	51.5	53	56	61
90.00	46	46	46	46.5	50	54	59
150.0	46	46	46	46	48	50	58
180.0	43	43	43	43	44	48	57
220.0	36	36	36	36	37	44	52
300.0	28	29	29	30	32	40	49

APPENDIX A3

PROPERTIES OF THE FOURIER TRANSFORM

(reproduced from EVANS [5])

Coherent Noise Analysis

Coherent or impulse noise spectrums can be analysed using the Fourier Transform

By means of the Fourier Transform a function can be described in two ways; in the time-domain and in the frequency-domain. The equations defining the Fourier transform are given

$$F(\omega) = \int_{-\infty}^{\infty} f(t) e^{-j\omega t} dt \qquad \ldots(1)$$

and
$$f(t) = \frac{1}{2} \int_{-\infty}^{\infty} F(\omega) e^{j\omega t} d\omega \qquad \ldots(2)$$

Transformation between the two domains can be freely made and can be denoted by a double arrow

thus
$$f(t) \longleftrightarrow F(\omega) \qquad \ldots(3)$$

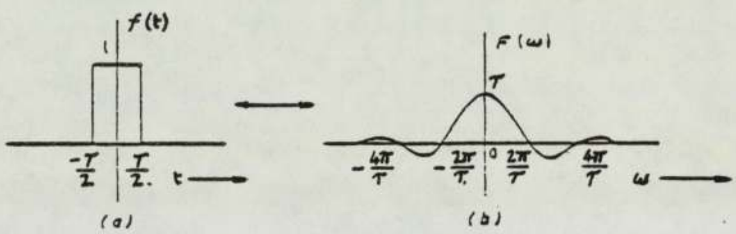

Fig. 2

indicates that $F(\omega)$ is the direct Fourier transform of $f(t)$ and that $f(t)$ is the inverse Fourier transform of $F(\omega)$.

Certain properties of the Fourier Transform are of particular interest to us in the measurement of impulse noise.

1. A gate function, which may be represented by a pulse of unit height and width can be translated into a Sampling Function of the form

$$Sa(x) = \frac{\sin x}{x} \qquad \ldots(4)$$

2. The Symmetry Property is expressed by

$$f(t) \longleftrightarrow 2\, f(-\omega) \qquad \ldots(5)$$

and

3. The Scaling Property is expressed by

$$f(at) \longleftrightarrow \frac{1}{a} F\left(\frac{\omega}{a}\right) \qquad \ldots(6)$$

The Scaling Property shows that compression in the time domain is equivalent to an expansion in the frequency domain and this phenomenon enables us to define the level of broadband noise in terms of voltage and bandwidth. This is illustrated in Figure 3.

The Symmetry Property shows that the Fourier transform of a gate function is a sampling function, whereas the Fourier transform of a sampling function is a gate function.

It should also be noted that the Fourier transform of a Gaussian response is another Gaussian response.

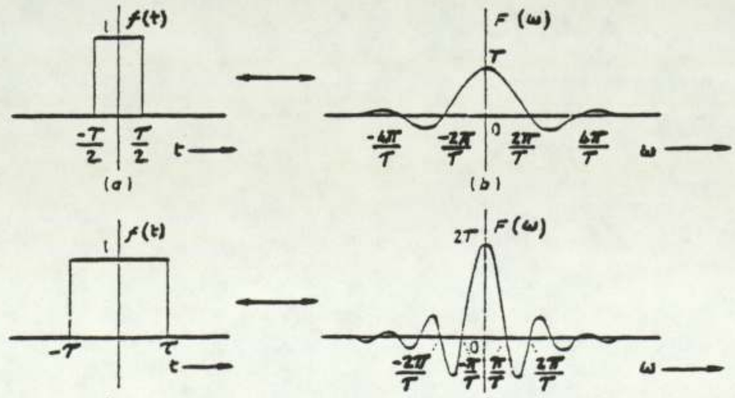

Fig. 3

APPENDIX A4

ESSON'S FORMULA

(reproduced from DIJKEN [28])

The internal power (P) of a D.C. commutator motor can be described by Esson's formula ;

$$P = \frac{\pi^2 \, n \, d_r \, l_r \, S \, B}{k_{pole} \, k_{car}}$$

where S = specific load in amperes per radian

B = air gap flux density

d_r = rotor diameter

l_r = length of rotor stack

n = rotor speed

k_{pole} = relative pole arc ratio

k_{car} = Carter factor

APPENDIX A5

<u>THE USE OF THE MICROWAVES IN OBSERVING BRUSH MOVEMENT IN FRACTIONAL HORSEPOWER COMMUTATOR MOTORS</u>

Paper presented at the "Transducer-Tempcon" Conference, Harrogate, November 1984

THE USE OF MICROWAVES IN OBSERVING BRUSH MOVEMENT IN FRACTIONAL HORSEPOWER COMMUTATOR MOTORS

T.S. BILKHU, B. JAMES, D.S. PALMER

Summary

The theory and operation of a method using microwave and waveguide components to observe single axis vibrations/ movements of less than 3 mm is presented. The technique was developed to measure the movement of carbon brushes in small a.c. commutator motors. Previous methods used to observe this movement are reviewed and the particular problems associated with observing brush movements are discussed. The method used to calibrate the apparatus is described and a discussion on the advantages and limitations of the measurement technique are presented.

1 INTRODUCTION

The operating life of small a.c. commutator motors (often called fractional horsepower commutator motors) of the type used in domestic appliances is determined by their brush life. Brush life in turn is a function of the rate of brush wear and the quality of commutation, both of which have been shown to be affected by brush movement during motor operation.[1,2]

Brushes supply current to the rotating armature via a sliding commutator contact, they are supported in rigid brush holders which are mounted on the motor framework. Fig. 1.1 shows an example of a brush mounting arrangement commonly used in small motors. The brush is able to slide radially in the holder and is restrained on the commutator surface by a helical coil spring. The spring force is such that the brush may ride over small irregularities on the commutator surface and still maintain an effective electrical contact. However, during motor operation, mechanical factors can cause vibrations which result in excessive brush movement. These mechanical factors include;

- i) friction induced vibration at the brush/commutator contact
- ii) impact of the commutator segments
- iii) commutator eccentricity
- iv) misalignment of the brush holder
- v) unbalance of the motor
- vi) width of insulation between commutator segments
- vii) vibration of the drive shaft
- viii) malfunction of the bearings

The brush movement becomes a complex function of the oscillation frequencies generated by the mechanical disturbance involved. In most small motors a combination of these factors are always present. Excessive brush movement increases both the mechanical and electrical wear of the brush.[3]

Mechanical wear is due to the rubbing action of the sliding contact. In normal conditions the sliding contact produces a smooth black film on the commutator surface which greatly reduces the sliding friction but excessive brush movement deteriorates the smooth surface into an abrasive film which greatly increases the mechanical wear.

Electrical wear results from sparking at the brush contact and is increased by heavy sparking at the brush edge caused by brush instability deteriorating the commutation process. In many cases heavy sparking also damages the surface film, thus creating further mechanical wear. The measurement of brush movement during motor operation is difficult, a number of techniques have been used in large machines but they are not readily applicable to small motors. The problems experienced and some of the general techniques and some of the general techniques used in the past are discussed below.

1.1 Limited access to the brushes

The brush being enclosed in the brush holder makes acess to observe brush movement difficult. The holder itself is usually compactly constructed in the motor framework and only the rear of the brush holder is accessable from outside - this only to allow replacement of the brush without dismantling the complete motor. Ryan and Summers[4] described a method using microwaves and waveguide equipment to measure commutator irregularities and suggested that they could be applied to measure brush movements. Their test arrangement required the vibrating surface to be in close proximty (less than 3 mm) to an open end of a waveguide section. In a small motor this arrangement would be virtually impossible to configure since the brush is deep inside the holder and too far from the waveguide to have any effect. However in a large motor where the brush holder dimensions approach those of the open end of the waveguide itself, it is possible that the brush holder could form part of the waveguide section to enable the technique to be applied.

1.2 Small size of brushes

In small motors the brush weight is often less than 1 g to 2 g. Thus the use of accelerometers or strain gauges attached to the body of the brush as recommended by Lewis and Walkden[5] for use in large machines cannot be applied to small machines. It is important to ensure that the dynamic behaviour of the brush is not significantly altered by the additional mass of the transducers themselves.

1.3 Mains potentials

The brush is connected to the mains supply and during operation conducts current in the range 0.5 A to around 2.5 A. Any brush contact device developed to measure movement must be able to withstand both the mains potentials and high temperatures existing at the brush surface.

1.4 Radio frequency interference (RFI)

The commutating current in the armature coils and the resulting arcing at the trailing edge of the brush generates RFI.[6] RFI corruption of measurement equipment and its associated wiring is one of the most significant problems in measuring brush movement. Reduction of RFI can only be achieved with adequate shielding and r.f. filter cicuits in the measurement circuitry, but in this case since the source of RFI is the commutating brush itself, it becomes impossible to shield the transducer from the RFI. Clauss and Vogelsberg [7] detected brush movement by attaching a piezo-electric record player pick-up to the brush surface. Although they make no mention of RFI problems, it is apparent that the pick-up would be corrupted by their test arrangement. Knights [8] carried out brush vibration tests on a washing machine motor using an optical technique. The test rig arrangement is shown in Fig. 1.2. A hole drilled through the brush and brush holder is used as a light shutter sandwiched between a rigidly mounted bulb (light source) and photo-transistor. The brush movement causing variation of the light falling on the photo-transistor, the output of which was detected on an oscilloscope. Even after attention was given to the problem of RFI, it was found that RFI still accounted for as much as ten per cent of the detected signal.

2 PRINCIPLE OF OPERATION

Fig. 2.1 illustrates the basic principles involved and the components used to measure radial brush movement. A thin metallic probe connected to the back of the brush extends into a rectangular waveguide through a slot in the broad face. The waveguide is energised by a microwave oscillator at end A and a crystal detector is mounted on the opposite end (B) where the waveguide is terminated by a reflexionless load. The dimensions of the waveguide are such that the oscillator gives rise to a transverse electric field in the intervening space.

An obstacle in the waveguide (such as the probe) disturbs the flow of energy along the waveguide, the new field created resolves into the following components;

i) the original transverse electric field
ii) scattered waves from the probe which propogate themselves toward the load and also back to the source oscillator
iii) a series of 'evanescent' modes

Evanescent modes have frequencies which are below the cut-off frequency of the waveguide. This means that they are unable to propogate themselves along the waveguide and are rapidly attenuated. They create a 'reservoir' in the vicinity of the obstacle into which energy is absorbed during one half cycle. Thus the obstacle fulfils the function of a reactance in storing energy [9]. This stored energy is partly in the electric and partly the magnetic fields of the evanesent modes. If the storage field is predominantly electric the obstacle behaves as a capacitance, conversely if the storage field is predominantly magnetic the obstacle behaves as an inductance. Resonance occurs when the energies stored in the electric and magnetic fields are equal.

Obstacles in a waveguide, provided they do not take up any appreciable distance along it's length, can thus be represented as lumped shunt impedences in a transmission line equivalent circuit of the microwave system. Huxley [10] showed that the admittance, y, of such an obstacle can be expressed;

$$y = -2h/(1 + h)$$

where h is the scattering coefficient of the obstacle dependent on its dimensions and positioning. It follows that the admittance of the probe is dependent on its dimensions and the depth to which it is inserted into the waveguide. No adequate theoretical treatment has been given to the susceptance of probes extending part way into waveguides, but their behaviour has been determined from experimental work.

As the probe is introduced into the waveguide, it behaves as a shunt capacitance, its susceptance increases with the depth of insertion. However, as the distance of insertion becomes an appreciable function of the microwave wavelength, λ, the probe acts as an inductance and capacitance in series shunted across the waveguide. When the length of the probe is approximately one quarter wavelength($\lambda/4$), resonance occurs and the susceptance tends to infinity. With still greater distance of insertion the susceptance becomes negative and the probe appears as a shunt inductance. Fig. 2.2 shows the variation of susceptance with increasing depth of a 0.5 mm probe in a waveguide of cross section 2.54 cm x 1.27 cm operated at a wavelength of 3.25 cm. Similar results are obtained with probes of different thicknesses.[10] Schelkunoff [11] discussed that at the neighbourhood of resonance, the susceptance depends critically on the probe dimensions and the oscillation frequency. He also calculated the inductance of a thin wire positioned across the waveguide and verified his calculated value with that obtained by experiment.

As a result of this brief review of the characteristics of a transverse probe in the waveguide, the operation of the apparatus in Fig. 2.1 may be understood. The movement of the probe acts as a varying shunt reactance in the waveguide. The transmission line representation of the system (Fig. 2.3) shows that variation of the probe reactance,Z_p, gives rise to a variation of the voltage measured at the reflectionless load,Z_l.

3 TEST EQUIPMENT AND CALIBRATION

Tests were carried out using an 'X-band' waveguide of length 25cm and cross section 2.54 cm x 1.27 cm. A slot was cut in the broad face of the waveguide as shown in Fig. 2.1. A bar and post waveguide transformer fitted to end A was excited by a sweep oscillator tuned to approximately 10.4 GHz creating a transverse electric field of wavelength λ= 3 cm. The crystal detector, fitted at end B is mounted in a reflesionless load, the output of which is observed on an oscilloscope.

Steel probes of various thicknesses were introduced into the waveguide through the slot. The probes were made of high tensile steel as used in hyperdermic needles, making them light-weight and of high stiffness. Fig. 3.1 shows the detector output obtained using a probe, of 0.6 mm for increasing probe depths at different positions along the slot. The greatest output deflection occurs for increasing probe depths at a position coinciding with the peak of the transverse field. Fig.3.2 shows the decrease in output voltage for increasing probe depth set at a position for maximum deflection. It can be seen that as the susceptance of the probe increases up to approximately 4mm probe depth, no significant change in output voltage is obtained. In the region from 4mm to 8mm the susceptance rises sharply creating an almost linear change at the output. at a probe depth of between 8.5 mm to 9 mm,probe resonance occurs and the incident electric wave is virtually completely reflected thus producing a minimum voltage detection at the terminating load. Beyond this, as the susceptance of the probe becomes negative giving the appearance of a shunt inductance in the waveguide, there is a small rise in output voltage as the probe touches the bottom face of the waveguide.

From these test results it became apparent that the linear change of output between 4 mm and 8 mm probe depth could be readily calibrated to measure small movements of the probe as could be expected from the brush motor operation. Fig 3.3, shows the apparatus used to calibrate the probe-waveguide system. The probe is shown located into the back of a carbon brush which was glued to an accelerometer mounted on a vibration exciter. Probe displacement amplitude and frequency was controlled by a signal generator connected to the exciter. Tests were carried out with the probe inserted into the waveguide to a depth of 6 mm i.e. at the linear portion of the detector output curve (Fig. 3.2), and then excited to give small displacements around the stationary position. Fig. 3.4 presents the results obtained of detector output with increasing probe movements for a number of different probe thicknesses. It was also observed that the detector output is independent of the probe displacement frequency. The linear response observed indicates that the detector output voltage can be calibrated directly to measure actual probe movements provided the deflection is along the axis of the probe and within approximately 3mm peak to peak.

4 DISCUSSION ON OPERATION

Fig. 4.1, shows the arrangement to measure radial movements of the left hand brush on a test rig motor using the techniques described above. The waveguide system being clamped to the motor framework in a position such that the slot in the broad face of the waveguide is in line with the back of the brush holder. A small hole drilled in the back of the brush holder allows the probe implanted in the back of the brush to be threaded through the helical coil spring and out into the waveguide. This arrangement effectively overcomes the problem of limited access to the vibrating brush surface.

The position of the slot is adjusted such that the probe gives a maximum detector output deflection, the depth of the probe in the stationary state is 6mm as discussed above. Since the brush and probe are at mains potential during operation, to avoid the probe touching the walls of the waveguide a small plastic ferrule was inserted into the waveguide slot as indicated.

The probe represented an increase in brush mass, of approximately 3 per cent, but the effect of this would be small considering the brush and brush spring as a complete system. RFI from the motor had no measurable effect on the detector output, even though the equipment is in close proximity to the noise source. The high cut-off frequency (approximately 10 GHz) of the waveguide ensured that no RFI component can corrupt the electric field in the waveguide. Co-axial cables from the detector to the oscilloscope ensured that there is no RFI pick-up in the connecting equipment.

Measurements of peak to peak brush movements were taken from the oscilloscope trace of the detector output voltage for a number of different mechanical conditions of the motor test rig. The movements were found rarely to exceed 0.25 mm and could be measured to a high degree of resolution from the oscilloscope trace. The technique proved satisfactory to measure brush movements for motor speeds greater than 1000 r/min. Below these speeds, readings were distorted due to excessive brush rocking and brush chatter.

The technique has also proved successful in observing vibrations of light rods in small scale model structure. In this case, it was found that conventional accelerometers attached to the rods could change their natural frequency. It was found that the probe should be kept as short as possible to minimise vibration flextures within the probe itself. The high tensile steel probes used in the test procedure, proved satisfactory and their flextures were virtually negligible in comparision to the vibrations observed.

5 CONCLUSIONS

The technique of using microwaves and waveguide components for measuring brush movement proved satisfactory, overcoming the major problems associated with measurement of brush movement i.e.

i) Limited access to the brushes
ii) Small size of brushes
iii) Mains potentials
iv) Radio frequency interference (RFI)

With reasonable care the method can be readily adapted to measure most types of single axis vibrations of less than 3 mm peak to peak. The apparatus described was capable of giving a measurement resolution of apprximately 1μV detector output equivalent to 5×10^{-9}m probe movement independent of displacement frequency.

6 REFERENCES

1 Nellin, V I et al; 'The effect that external vibrations has on sparking in small commutator machines', Electrotechnika (USSR), No. 4, April 1965, pp. 44-46

2 Weinert, H; 'Factors which affect carbon brushes wear in small motors', Ringsdorff-Werke GmbH, Vol. 1, 1967, pp. 14-20

3 Schobert II, E I; 'Carbon brushes', Chemical Publishing Co. Inc., New York, USA, 1965

4 Ryan, A H and Summers, S D; 'The use of microwaves in observing commutator and slip ring surfaces during operation', AIEE Trans., PAS, Vol. 73, pp.92-96

5 Lewis, D L and Walkden, A J; 'Mechanical aspects of commutation in traction motors', GEC Jour. Sci. and Tech., Vol. 40, 1973

6 Hall, J K and Quelch, M W; ' R.F. interference generated by a thyristor-controlled, hand held drill motor', IERE Conf. Proc. on EMC, No. 47, September 1980, pp. 353-362

7 Carson, R W; 'Cutting down ziggle makes brushes last longer',

Product Engg., June 1967, pp.93-96

8 Knights, D E; 'Drives for domestic appliances', ERA Report No. 74-1195, December 1974

9 Macfarlane, G G; 'Quasi-stationary field theory and its application to diaphragms and junctions in transmission lines and waveguides', Elect. Eng., Vol. 93, Part IIIA, No. 4, 1946

10 Huxley, L G H; 'A survey of the principles and practice of waveguides', Cambridge University Press, 1947

11 Schelkunoff, S A; 'Impedance of a transverse wire in a waveguide', Quart. Appl. Math., Vol. 1, April 1943, pp. 78-85

B. James and D.S. Palmer are with the University of ASTON in Birmingham

T.S. Bilkhu is with GEC Electrical Projects Ltd., Rugby

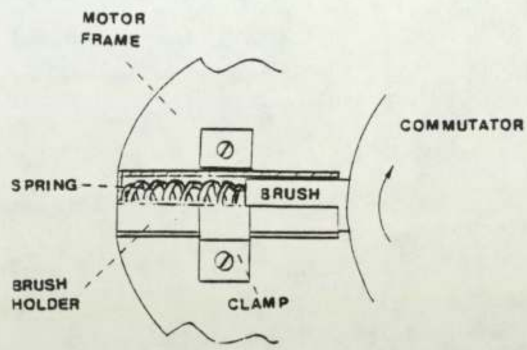

Fig. 1.1 Typical brush mounting arrangement in small a.c. commutator motors

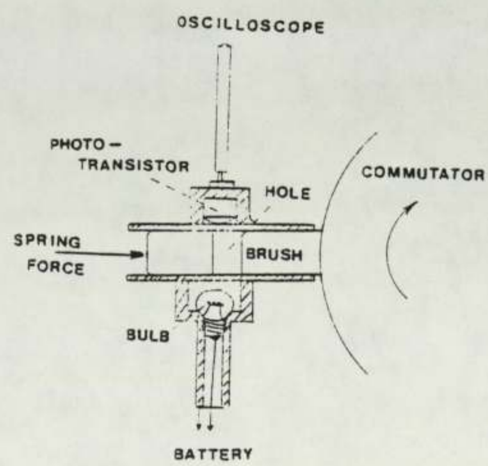

Fig. 1.2 Brush vibration rig assembly used by Knights [8]

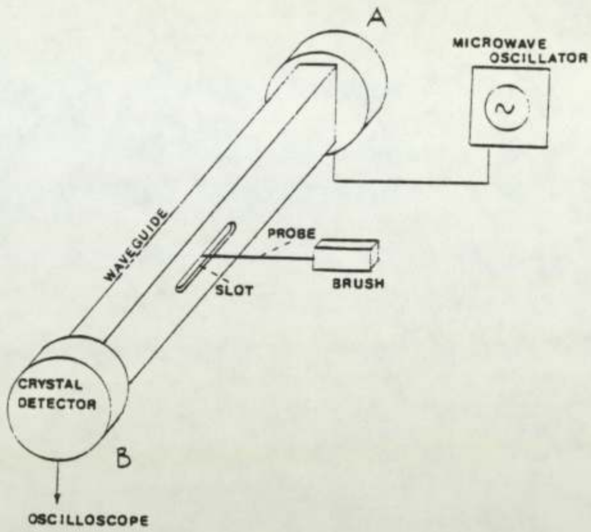

Fig. 2.1 Brush movement measuring equipment

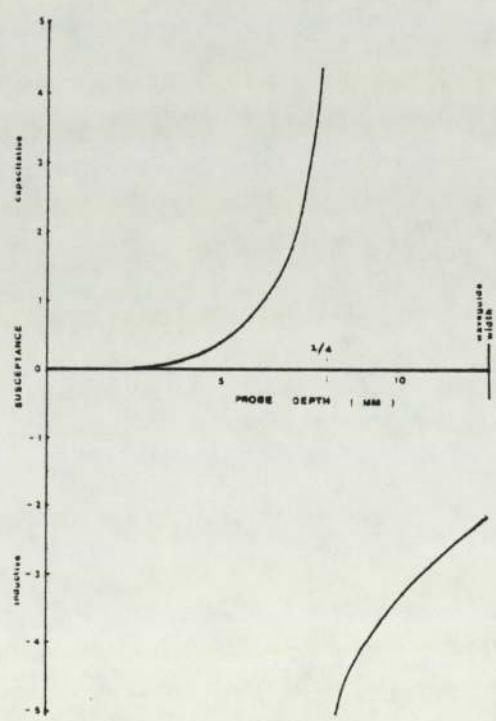

Fig. 2.2 Variation of probe susceptance with probe depth in the waveguide

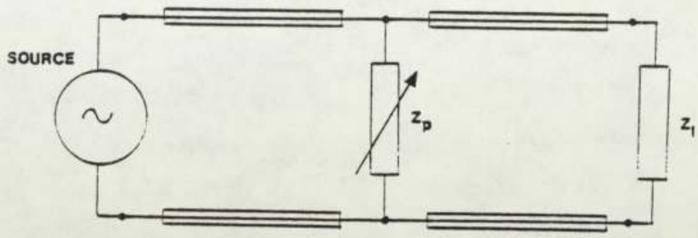

Fig. 2.3 Transmission line equivalent circuit of the microwave system

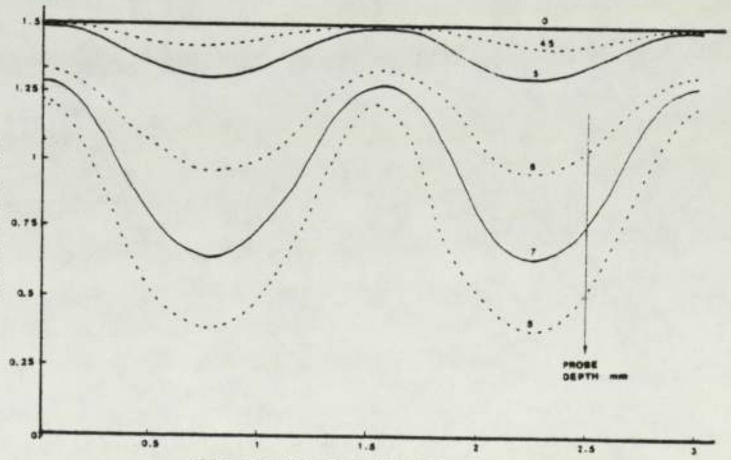

Fig. 3.1 Variation of detector output with depth of probe insertion along the waveguide slot

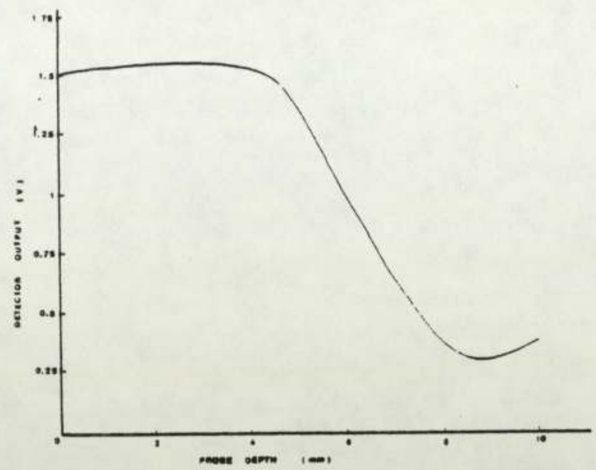

Fig. 3.2 Variation of detector output with depth of probe insertion (probe position along waveguide slot adjusted for maximum output variation)

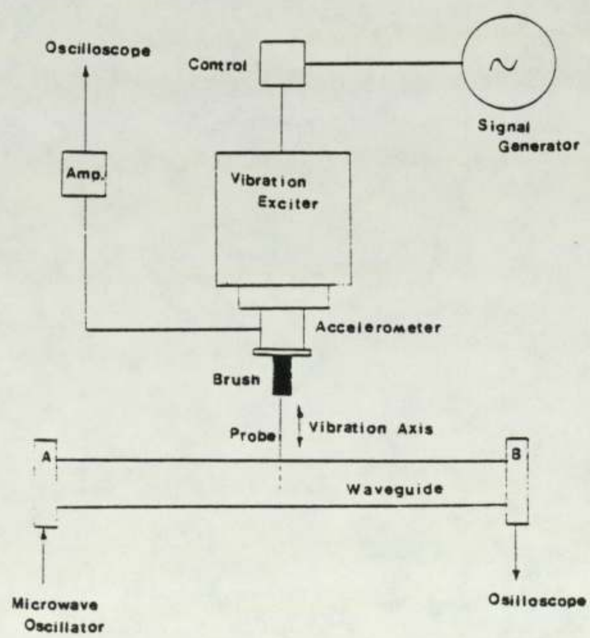

Fig. 3.3 Test rig calibration equipment

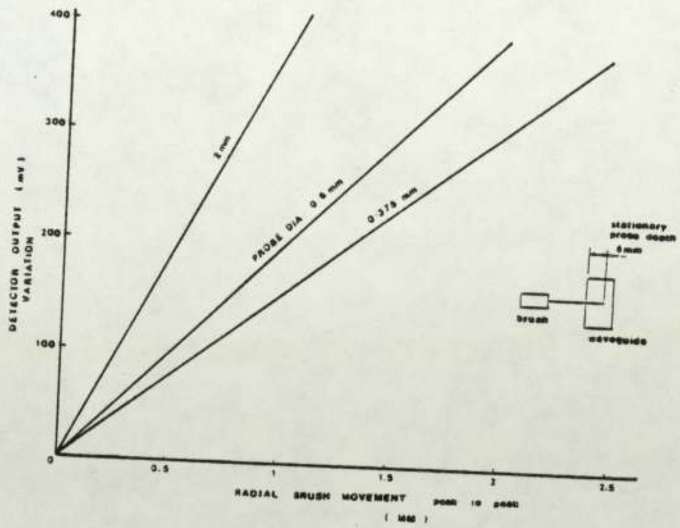

Fig. 3.4 Variation of detector output with small probe movements (probe set at stationary depth of 6 mm)

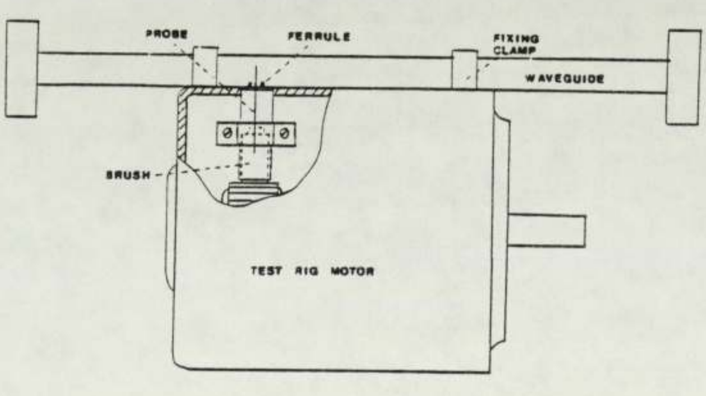

Fig. 4.1 Test arrangement for measurng brush movement on test rig motor

APPENDIX A6

PHOTOGRAPHS

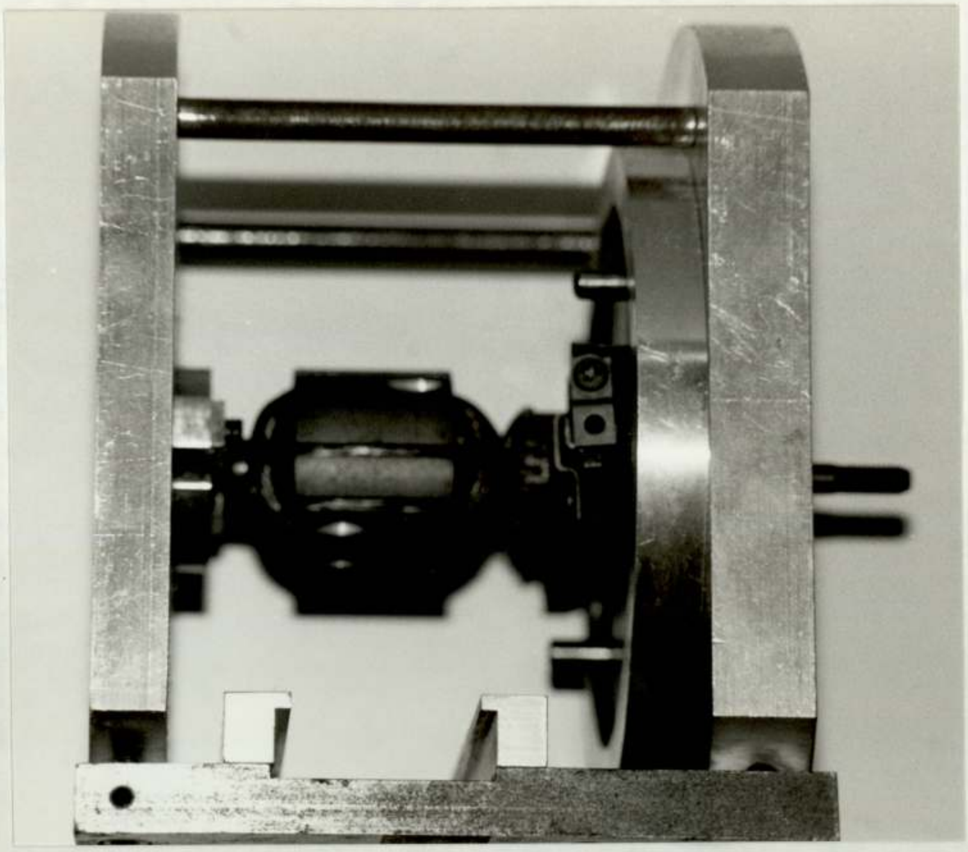

Plate A6.1   Test rig assembly (with field removed)

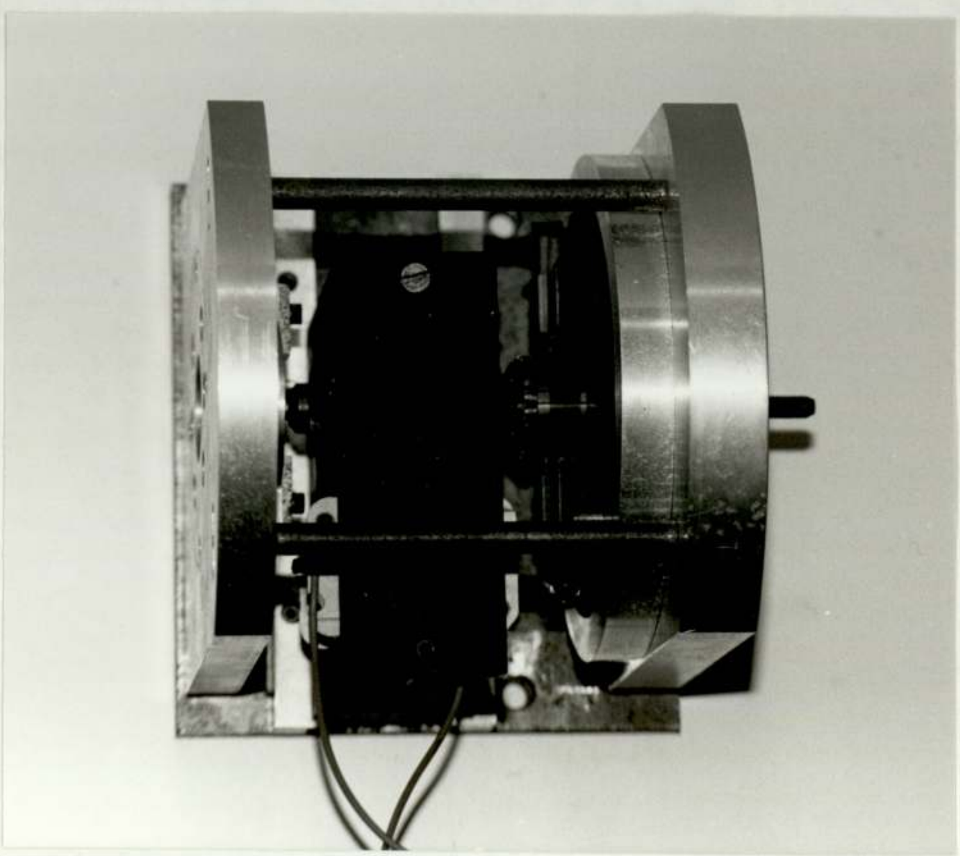

Plate A6.2   Test rig (plan view)

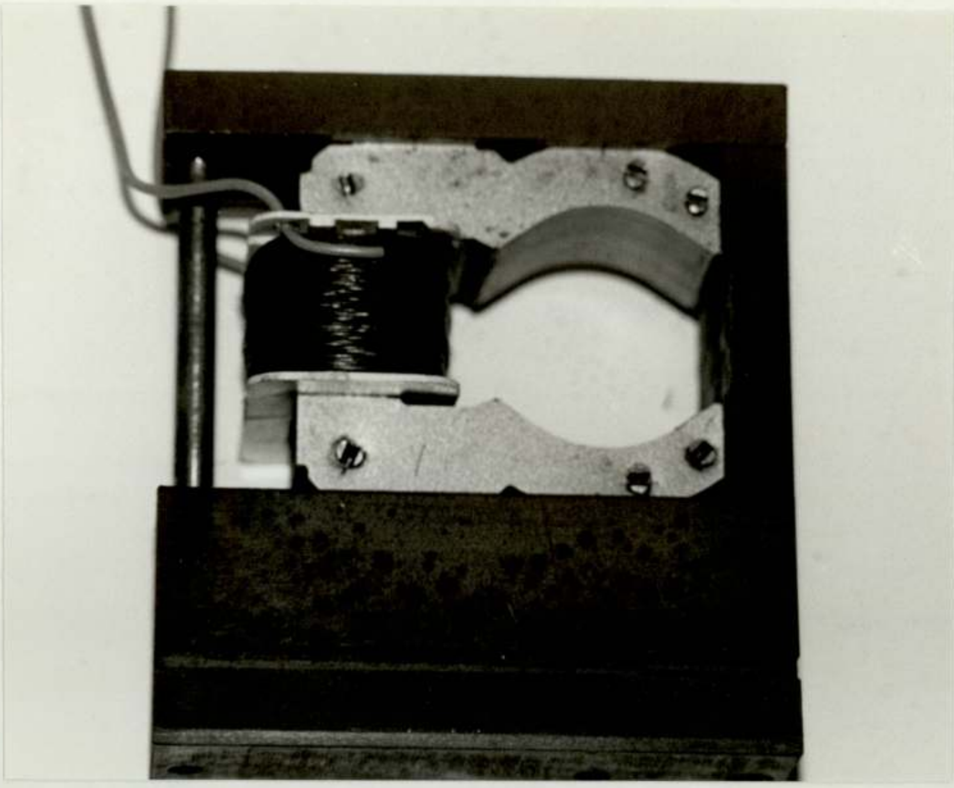

Plate A6.3 U-type field assembly

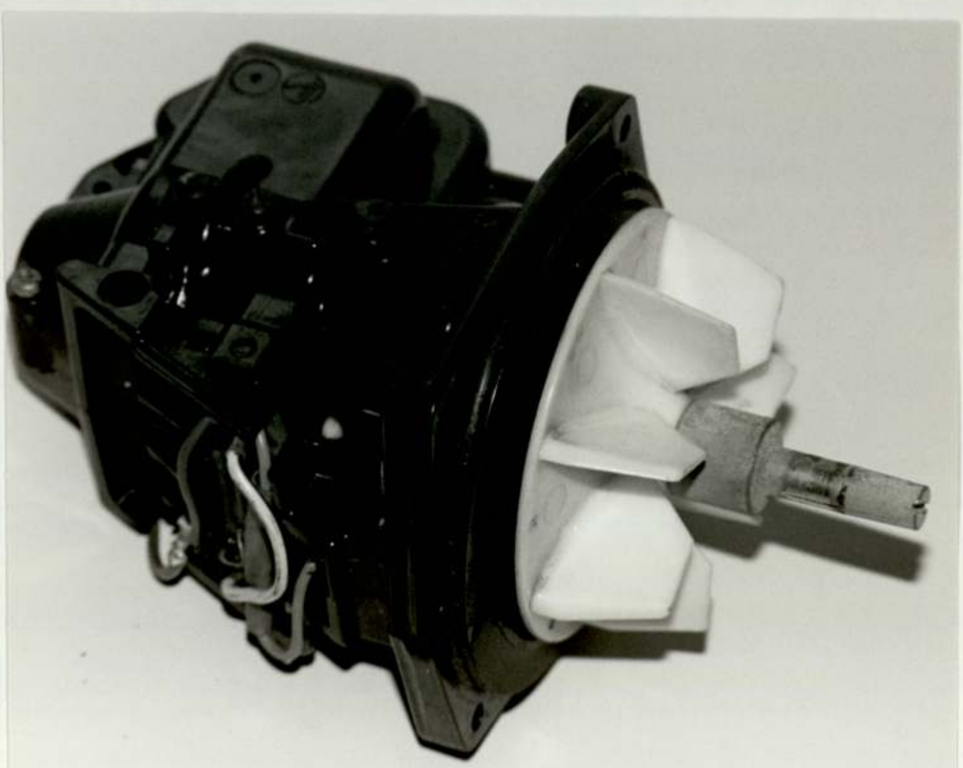

Plate A6.4 Hoover MC14 motor

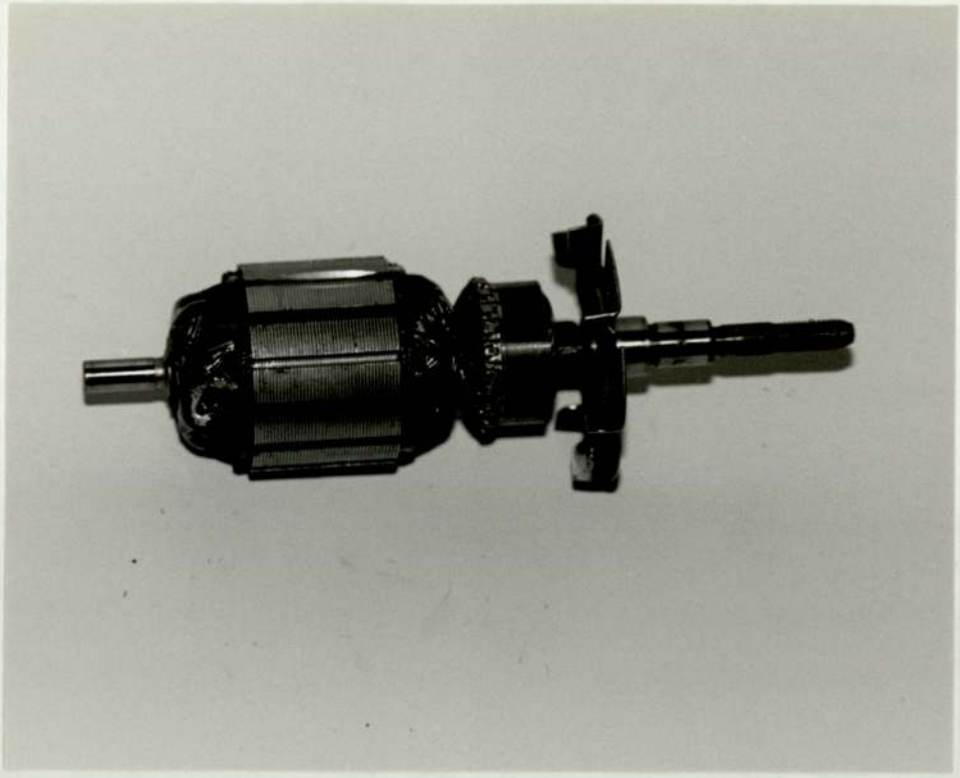

Plate A6.5   MC14 armature assembly

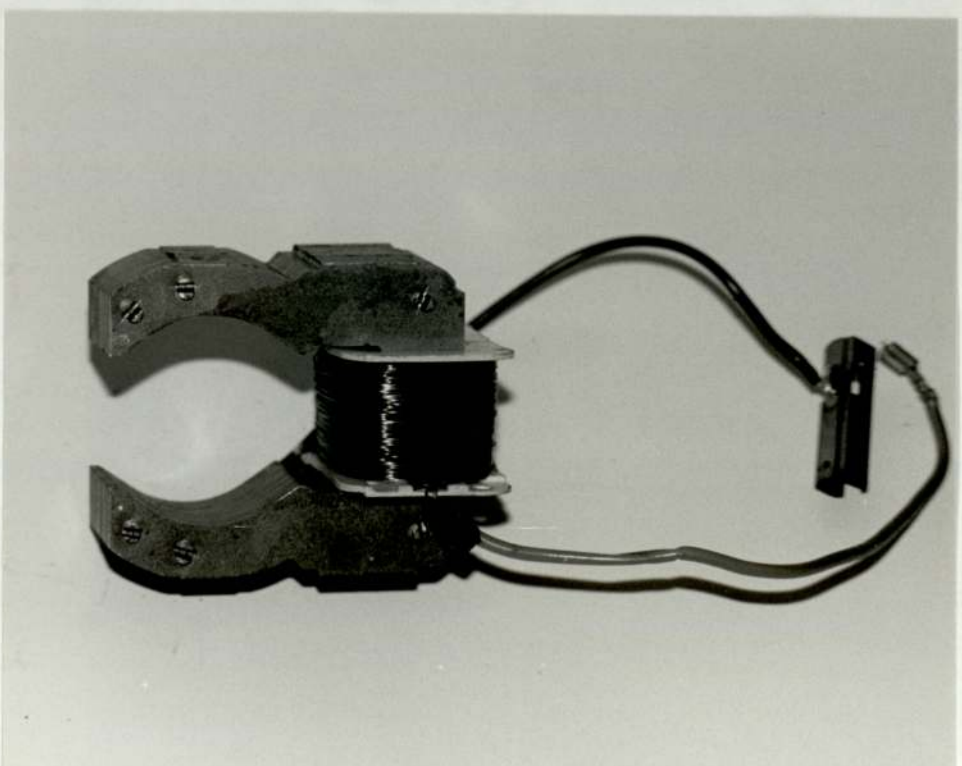

Plate A6.6   U-type field

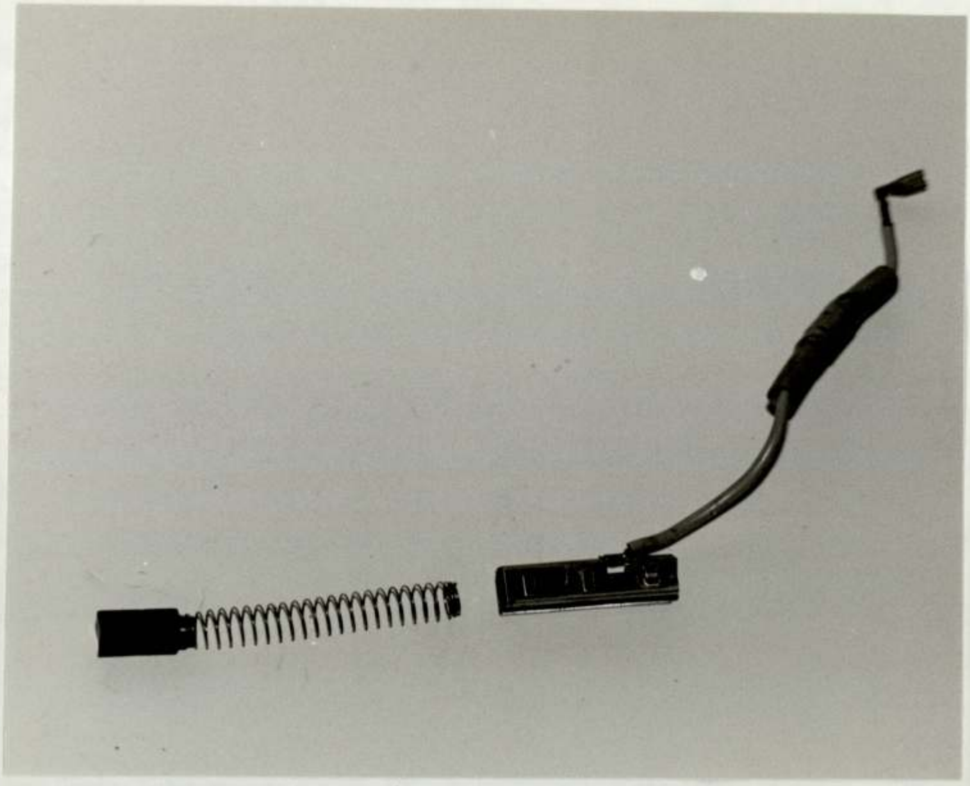

Plate A6.7 MC14 brush assembly

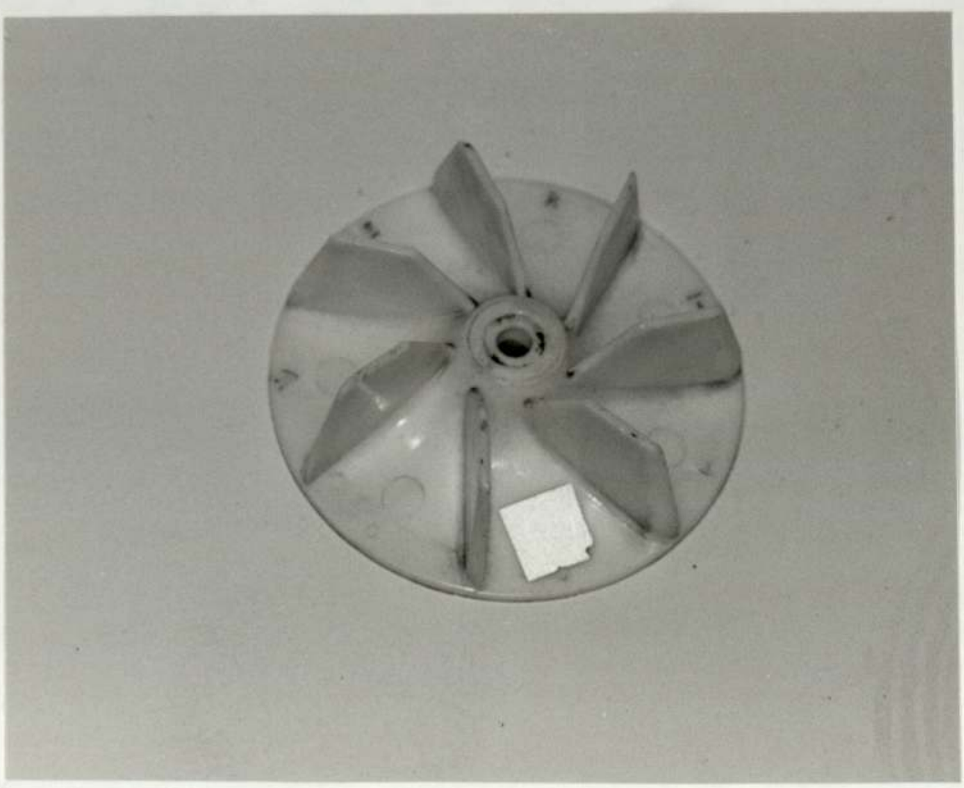

Plate A6.8 MC14 dirt fan

Plate A6.9 Hoover EURO motor

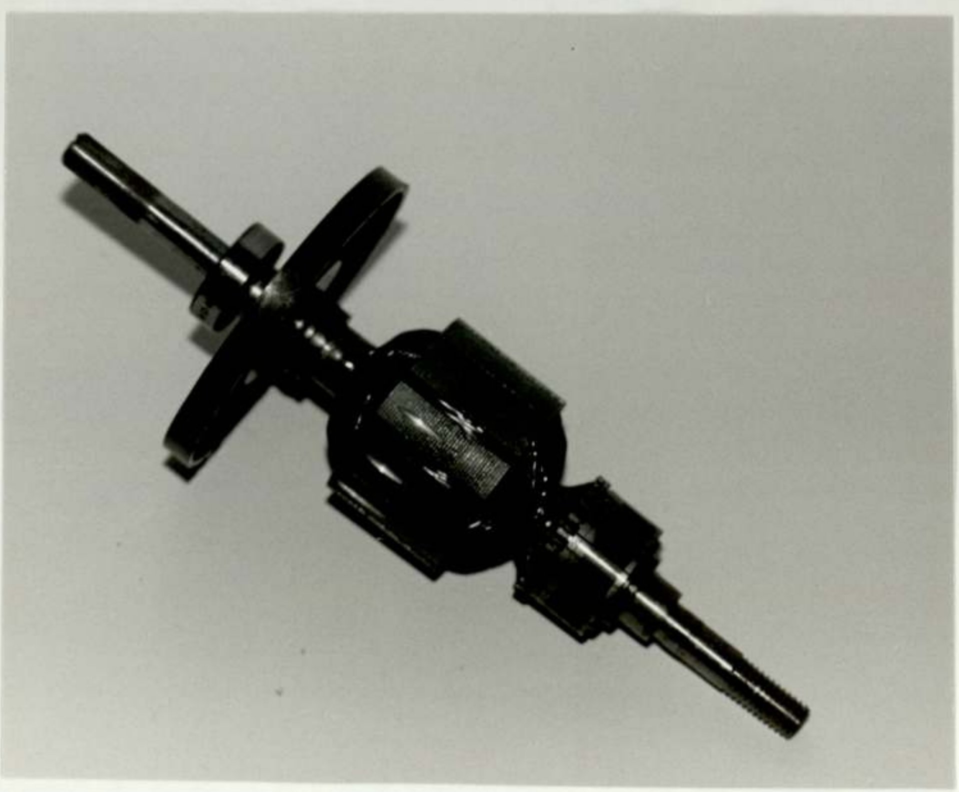

Plate A6.10 EURO armature assembly

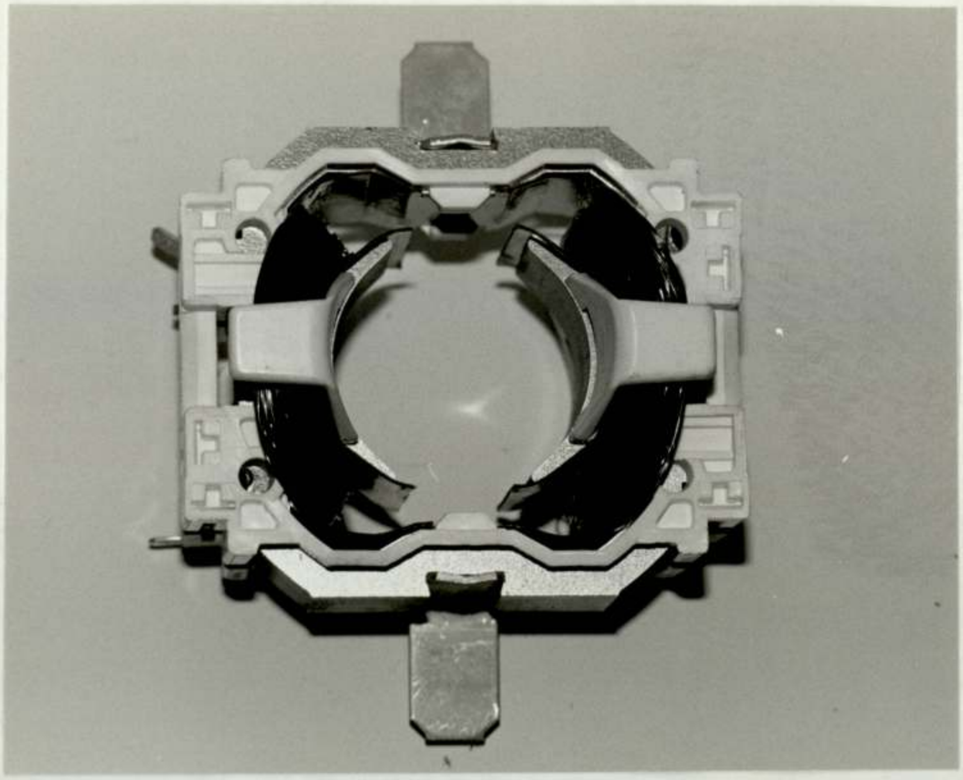

Plate A6.11 EURO O-type field

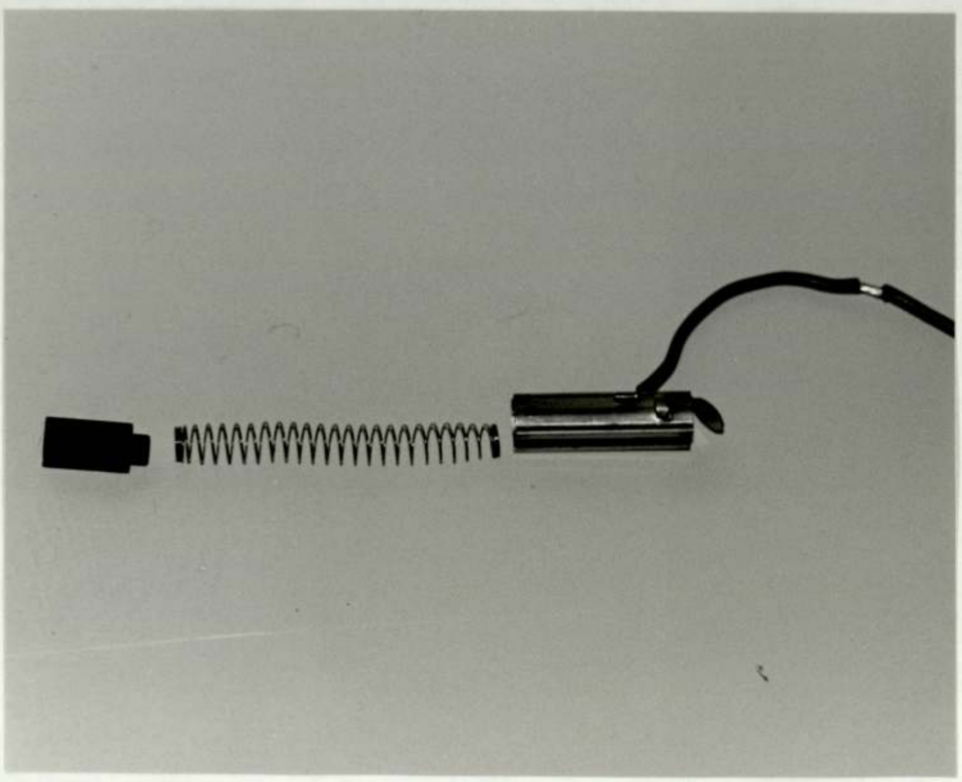

Plate A6.12 EURO brush assembly

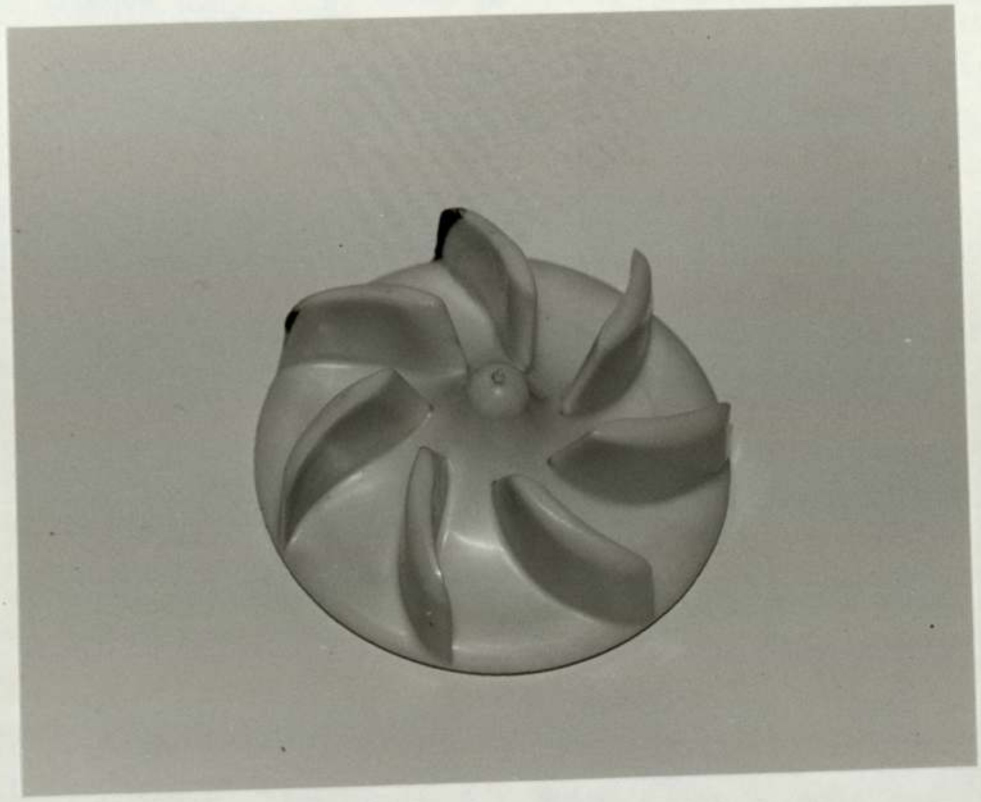

Plate A6.13 EURO dirt fan

REFERENCES

1. Motter, D.P.; "Control of radio influence voltage in D.C. rotating electrical machines". Armour Research Foundation, Proc. of Conf. on Radio Interference Reduction, Chicago, Dec., 1954, pp. 20-34.

2. White, D.; "Electromagnetic Interference and Compatibility" Vol.3, Don White Consultants, 1st Edition, 1973, pp. 1.1-1.3.

3. Ibid., pp. 2.1-2.46.

4. Ibid., pp. 14.6-14.22.

5. Evans, R.H.; "Broadband noise measurement in EMC control". IEEE, 1st Symp. & Tech. Exhib. on EMC, Montreux, May, 1975, pp. 433-437.

6. Lathi, B.P., "Signals, systems and communications". Wiley, 1967.

7. McLachlan, A.S., Ainley, J.H. and Harry, R.J.; "Radio Interference - a review". Wireless World, June, 1974, pp. 191-195.

8. Popovic, B.D., "Introductory Engineering Electromagnetics". Addison - Wesley Pub. Co., 1971, pp.582-589.

9. Feldt, L.; "Radio frequency interference measurements in accordance with CISPR recommendations". Appliance Engineer, Vol.8. No.5, 1974, pp. 14-17.

10. Hall, J.K. and Quelch, M.W.; "R.F. interference generated by a thyristor controlled, hand held drill motor". IERE, EMC Conf. Proc., No.47, Southampton, Sept. 1980, pp. 353-362.

11. German, J.P.; "Characteristics of electromagnetic radiation from gap type spark discharges on electric power distribution lines". IEEE Trans., Vol. EMC-11, No.2, May, 1969, pp.83-89.

12. Knights, D.E.; "Drives for domestic appliances". ERA Report No.74-1195, December, 1974, pp. 26-39.

13. Ibid., pp. 76-82.

14. Livshits, D.M.; "Suppression of radio interference from equipment having commutator motors". Elektrotekhnita, No.7, 1971, pp. 31-35.

15. Stephens, G.L., "Radio interference suppression". Iliffe and Sons Ltd., 2nd edition, 1952, pp. 11-26.

16. Ibid., pp. 27-82.

17. The Wireless Telegraphy Act, 1949, H.M.S.O.

18. British Standard 727; "Specification for Radio Interference measuring apparatus for the frequency range 0.015MHz to 1000MHz". H.M.S.O., 1967.

19. British Standard 800; "Specification for Radio Interference limits and measurements for equipment embodying small motors and control devices". H.M.S.O. 1980.

20. Home Office DRT Technical Memorandum, No. I.25, 1979.

21. Whittingham, K.C., "Small motors, Radio Interference and the Law". ERA Technical Seminar, London, January, 1979.

22. European Economic Community, Directive 76/889/EEC, "On the approximation of the laws of the member states relating to radio interference caused by electrical household appliances, portable tools and similar equipment". 1976.

23. European Economic Community, Directive 82/499/EEC, "Commission Directive adapting to the Directive 76/889/EEC", June 1982.

24. Liwschitz - Garik, M. and Whipple, C.C.; "Electric Machinery". Vol.1, Van Nostrand, 2nd edition 1947.

25. Taylor, E.O.; "The performance and design of A.C. commutator motors". Pitman and Sons Ltd., London, 1958.

26. Say, M.G.; "Alternating current machines". Pitman publishing Ltd., London, 1983.

27. Puchstein A.F. and Kimberley E.E.; "Universal electric motors". The Ohio State University, Ohio, Engineering Experimentation Station, Bulletin 53, 1930.

28. Dijken, R.H.; "Optimisation of small A.C. series commutator motors". Thesis, Eindhoven University, October 1971, pp. 1-6.

29. Ibid., pp. 67-105.

30. Bond, N.; "RFI - one of the undesirables". Electronic Engineering, August, 1971, pp. 31-35.

31. Mayer, F.; "RFI suppression components: State of the Art; New developments". IEEE Trans. on EMC, Vol. EMC-18, No.2, May, 1976, pp. 59-70.

32. Cowdell, R.B.; "Graphic aids simplify bypass and feedthrough capacitor filter design".

33. Shifman, J.C., "A graphical method for the analysis and synthesis of electromagnetic interference filters". IEEE Trans. on EMC, September, 1965, pp. 297-318.

34. Montgomerie, G.A.; "Total Technology at Aston - a retrespect". IHD Publication, University Aston Birmingham, January, 1984.

35. Chang, S.S.; "The Interdisciplinary Higher degrees scheme". Chartered Mechanical Eng., June, 1973, pp. 78-80.

36. Nickolson, S.; "Motor brush spring part No. 815551". Hoover plc memorandum, August, 1982.

37. Schobert, E.I.; "Carbon brushes". Chemical Publishing Co.Inc., New York, USA, 1965, pp.76-99.

38. Ibid., pp. 5-77.

39. Ibid., pp. 43-44.

40. Ibid., pp. 156-160

41. Moullin, E.B., "Electromagentic principles of the Dynamo". Clarendon Press, Oxford, 1955.

42. Clayton, A.E.; "The performance and design of direct current motors". Pitman and Sons Ltd., 1939.

43. Kostenko, M. and Piotrovsky, L.; "Electrical Machines". Foreign Languages Publishing House, Moscow, USSR, Pt.1, pp.129-192.

44. Ademoglu, D.Y., "Problems in D.C. Machine representation". Thesis, University of Birmingham, 1976.

45. Mohr, A.W.; "Commutation in Universal Motors". Thesis, Stuttgart, 1957.

46. Davies, W; "The sliding contact of graphite and copper". IEE Monograph 271U.

47. Watson, A.F.; "Commutator films and brush operation". Elec. Rev., Vol.173, No.9, August, 1963, pp. 339-342.

48. ERA; "Commutation in fractional-horse-power machines; Survey of published work". Ref. 69/8.7/T4, March 1969.

49. Grossman, M.I. et al; "On the stability of the brush commutator assembly of an electric machine to vibration". Electrotekhnika, Vol. 38, No.12, 1967.

50. Maslov, P.F. et al; "Analysis of vibrations of the brushes of traction motors relative to the collector". Izv. Vuz Electromekh. No.10, 1971, pp.1123-1130.

51. Ichnki, T.; "The effects of brush riding stability on commutation". Proc. Eng. Seminar on Electric Contact Phenomena, Illinois, Chicago, Nov. 1967, pp. 101-107.

52. Volkman, W.; "The dynamic behaviour of carbon brushes". Schunk and Ebe GmbH, Giessen, Vol.21, November, 1965, pp.5-14.

53. Nellin, V.I. et al; "The effect of external vibration has on sparking in small commutator machines". Electrotechnika, No.9, 1965, pp. 49-53.

54. Hancock, M.; "Mechanical factors in commutation". Direct Current, Vol. 10, Feb., 1965, pp. 36-39.

55. Harris, C.M. and Crede, C.E.; "Shock and Vibration handbook". McGraus-Hill Book Co., USA, 1976, 2nd edition, pp.39.1-39.31.

56. Weinert, H.; "Factors which affect carbon brush wear in small motors". Ringsdorff-Werke GmbH, Vol.1, 1967, pp.14-20.

57. Knights, D.E., "An assessment of the effect of vibration on commutation". ERA Report No.76-1, June 1976.

58. Bates, C.; "Choosing and testing carbon brushes for domestic appliances". Electrical Engineer, October 1971, pp.33-35.

59. Lewis, D.L. and Walkden, A.J.; "Mechanical aspects of commutation in traction motors". GEC J.Sci. and Tech., Vol.40, No.3, 1973, pp.99-106.

60. Carson, R.W.; "Cutting down ziggle makes brushes last longer". Prod. Eng., June 1967, pp.93-96.

61. Ryan, A.H. and Summers, S.D.; "The use of microwaves in observing commutator and slipring surfaces during operation". AIEE Trans. PAS, Vol.73, pp.92-96.

62. Knights, D.E., "The effect of thyristor and triac control on commutation in series motors". ERA Report No. 73-1071, July 1973.

63. Binder, K.; "Limiting conditions of arcing during commutation". ETZ-A, Vol.81, No.60, August, 1960, pp. 558-562.

64. Dickin-Zangger, C.W.; "Calculation and measurement of commutation in FHP Universal motors". IEEE District Meeting, Ohio, May 1963.

65. Mohr, A.W.; "The spark free speed and load range with Universal motors". ETZ-A, Vol.81, No.23, November 1960, pp.812-816.

66. Gray, A.; "Electrical Machine Design". McGraw-Hill Book Co., 1926, pp.78-109.

67. Lancaster, J.K.; "The influence of arcing on wear of carbon brushes on copper".

68. Padmanobhan, K. and Sirivasan, A.; "Some important aspects in the phenomenon of commutator sparking". IEEE Trans., Vol. PAS-84, May, 1965, p.396.

69. Tait, P.G.; "Encyclopedia Brittanica". Donnelley and Sons Co., Vol.15, 1943, pp.119-120.

70. Singer, C.; "A history of technology". Clarendon Press, Vol.5, Oxford, 1958, pp.227-229.

71. McClure, C.L.; "Dynamo current interference with telephone systems and means of relief". Electrical World, Vol.12, 1888, pp. 140-142.

72. Mirabelli, B.; "Note sur les pertubations produites par la traction electique sur les fils telegraphiques". Journal Telgraphique, Vol. 33, 1909, pp. 177-182.

73. Klewe, J.R.H.; "Interference between power systems and telecommunication lines". Arnold Ltd., London, 1958.

74. Jackson G.A.; "Peak versus Quasi-Peak". IEEE Conference on EMC, Lausanne, Oct., 1971.

75. Thomas, L.W.; "Spectrum Signatures". Armour Research Found., 4th Conf. on RIR, October, 1958.

76. Myers, H.A.; "Industrial Equipment spectrum signatures". IEEE Trans. on RFI, March, 1963, pp.30-42.

77. Skomal, E.N.; "Man-made radio noise". Van Nostrand Reinhold Co., New York, 1978.

78. Ibid., pp.147-156.

79. Ibid., pp.75-120.

80. Ibid., pp.21-24.

81. Ibid., pp.56-67.

82. Hsu, H.P.; "Automative Ignition interference". IEEE Trans. on EMC, October, 1964. pp. 15-20.

83. Oranc, H.S.; "Ignition noise measurements in the VHF/UHF Bands". IEEE Trans. oin EMC, Vol. EMC-17, No.2, May 1975, pp.54-64.

84. Burgett, R.R. et al; "Relationship between spark plugs and engine radiated electromagnetic interference". IEEE Trans. on EMC, Vol. EMC-16, No.3 August 1974, pp.160-172.

85. Keith Howell, E.; "How switches produce electrical noise". IEEE Trans. on EMC, Vol. EMC-21, No.3, August, 1979, pp.162-170.

86. Hyde, F.J.; "Physical basis of electrical noise". Conf. on Phys. aspects of noise in elect. devices, 1968.

87. Hall, J.K. and Palmer D.S.; "Electrical noise generated by thyristor control". IEE Proc., Vol. 123, No.8, August, 1976, pp. 781-786.

88. ERA; "Radio Interference from semi-conductor controls". Report No. 80-4R, 1980.

89. ERA; "Radio Interference from contact devices". Report No. 80-7R, 1980.

90. Stannard, G.E. and Krackhardt, R.H.; "Contact noise and problems of its suppression". Armour Research Foundation, Proc. of Conf. on Radio Interference Reduction, Chicago, December 1954, pp.108-219.

91. Short, B.H.; "Vehicular radio noise suppression". Armour Research Foundation, Proc. of Conf. on Radio Interference Reduction, Chicago, December 1954, pp. 12-19.

92. ERA; "Characteristics of universal motors at radio frequency part 1". Report No. 3031/51, June 1972.

93. Motter, D.P.; "Commutation of D-C Machines and its effect on Radio Influence Voltage Generation". AIEE Trans., Vol. 68, 1949, pp.491-496.

94. Nelson, R.E. and Diehl, J.E.; "Radio Interference from Carbon brush operation". Electro-Technology, July 1963, pp. 53-57.

95. ERA; "Factors affecting the generation of radio interference in appliances containing commutator motors". Report No. 3031/118, 1976.

96. ERA; "Interim report on Commutator Interference". Report No. 3031/27, November 1970.

97. ERA; "Variation in radio interference generated by universal motors during continuous running". Report no. 3031/33, August 1971.

98. ERA; "Investigation into radio interference generated by universal motors". Report no. 3031/34, August 1971.

99. ERA; "Radio interference generated by food mixers". Report No. 3031/40, November 1971.

100. ERA; "Further measurement and analysis of results on the effects of brush grade and lubrication on appliances containing small motors". Report no. 3031/124, Dec., 1977.

101. ERA; "Investigation into the effects of lubrication of brushes and response to suppression components in small permanent magnet motors". Report No. 3031/127, April, 1978.

102. ERA; "Investigation into the effects due to different lubricant constituents used in the lubrication of brushes in small motors". Report No. 3031/130, April, 1978.

103. ERA; "Interim report of proprogation of interference in small motors". Report No. 3031/106.

104. ERA; "Characteristics of universal motors at radio frequency part 2". Report No. 3031/64, Jan. 1973.

105. ERA; "Further investigations into the propogation of interference by small motors". Report No. 3031/109.

106. ERA; "Summary of investigations into the propogation of radio interference in appliances containing small motors". Report no. 3031/111.

107. ERA; "Radio interference suppression in appliances. Its independence on source impedance and mode of current propogation". Report No. 3594/2, April 1980.

108. Andone, B.; "Graphical harmonic analysis". IEEE Trans. on EMC, Vol. EMC-15, No.2, May 1973, pp.72-74.

109. Babcock, E.F. and Sagasta, P.J.; "Simplified prediction of conducted and radiated interference levels for pulses and step functions". IEEE Trans. on EMC, Vol. EMC-8, No.2 June 1966, pp.97-101.

110. Holownia, J.; "Frequency spectrum generators". Technical University of Wroclaw, Wroclaw, Poland, 1964.

111. Holownia, J.; "A state space analysis example of transient noise generation in electrical circuits". IEEE Trans. on EMC, Vol. EMC-18, No.3, August 1976, pp. 97-105.

112. White, D.R.J.; "A handbook on electrical filters - Synthesis, design and applications". Don White Consultants, 1970.

113. ERA; "Measurements of the insertion loss of suppressors". Report no. 3031/77.

114. ERA; "Interim report on methods of assessment of filter performance". Report no. 3031/91.

115. ERA; "Aspects of radio interference suppression". Report No. 3031/116.

116. CISPR; "Reports and Study Questions of the CISPR". Publication 8, 2nd Edition, Report No.33, 1969, pp.55-66.

117. Jackson, G.A.; "Towards standardisation of radio interference measuring equipment and techniques". IERE-IEE Conf. on R.F. Measurements and Standards, Teddington, November, 1967.

118. Haber, F.; "Response of Q.P. detector to periodic impulses with random amplitudes". IEEE Trans, Vol. EMC-9, No.1 March, 1967, pp. 1-6.

119. Cook, J.H.; "Quasi-Peak to RMS voltage conversion". IEEE Trans., Vol. EMC-21, No.1, Feb., 1974, pp. 9-12.

120. Hsu H.P. et al; "Measured Amplitude Distribution of automatic ignition noise". IEEE Trans. on EMC, Vol. EMC-16, No.2, May, 1974, pp. 57-63.

121. Hsu, H.P.; "Quasi-Peak and peak ignition noise measurements and degradation effects of ignition noise on communication systems". IEEE 1st Symp. and Tech. Exhib. on EMC, Switzerland, May, 1975, pp.177-181.

122. Nano, E.; "Correlation factors for Quasi-Peak Measurements with spectrum analyser". IEEE 1st Symp. and Tech. Exhib. on EMC, Switzerland, May, 1975, pp.156-161.

123. Frich, C.W.; "The Quasi-Peak Voltmeter". AIEE Trans. Vol.73, November, 1954, pp.417-42.

124. CISPR; "Limits and methods of measurements of radio interference characteristics of household electrical appliances, portable tools and similar electrical appliances". Pub. 14, 1975.

125. ERA; "Historical survey of the developments of A.M.N.'s". Report No. 3031/60, November 1972.

126. Illingworth, G.; "Interim report on the effect of the proposed change from the CISPR (1) to CISPR (11) Network for terminal voltage measurements on domestic appliances in the frequency range 0.15-30 MHz.". ERA Report No. 3594/15, Feb., 1981.

127. ERA; "Report to Sponsors". Report no. 69/3/T1, March 1969.

128. De Jong.; "Comparison between the methods of measuring radio interference in the VHF range caused by domestic appliances". CISPR/WG1 (De Jong-Neth)3, Feb. 1967.

129. Meyer, J. and Bersier, R.; "The absorbing clamp - a new measuring method of interference in the metric wave bands". CISPR (Swiss) 334, March, 1969, pp.96-104.

130. Meyer, J.; "Mode D'emploi de la pince absorbant MDS". CISPR/GT6 (Meyer-CH)205, Dec., 1968.

131. Meyer, J.; "Pince Absorbant V34.419". CISPR/GT6 (Meyer-CH) 66.4, March 1966.

132. Fromy.; "Contribution a la possibilite d'eviter les mesures en plein air des rayonnements perturbateurs". CISPR/GT1 (Fromy-France)6, Dec., 1966.

133. Meyer J.; "Comparison experimentale de diverses methodes de mesure du pouvoir perturbateur d'apparieils en ondes metriques". CISPR/GT1 (Meyer-CH) 66.3, March 1966.

134. Pietranik.; "Comments on MDS clamp input Impedance". CISPR/A-WG1 (Pietranik-Poland)2, Dec., 1976.

135. McLachlan.; "Contribution to Study Question 32/1". CISPR/WG6 (McLachlan-U.K.)15, March 1969.

136. De Jong.; "Investigations on absorbing clamps". CISPR/WG1 (De Jong-Neth)5, March 1968.

137. Konstannov, A.S.; "Determination of the commutation characteristics of electrical brushes". Vestn. Electroprom., Vol.28, No.2, 1957, pp.22-24.

138. ERA; "Radio interference suppression in appliances. Its dependence on source impedance and mode of current propogation". ERA Report no. 3594/2, April, 1980.

139. Rose-Innes, A.; "Static electricity - an ancient enigma". New Scientist, Vol.94, No.1394, May, 1982, pp. 346-348.

140 Gregory, D.P.; "Metal-Air batteries'. MKB Monograph CE/16, Mills and Boon Ltd, London, 1972.

141 Allis-Chalmers; "Transformer Reference Book". Allis-Chalmers Mfg. Co., Wisconsia, USA, 1951, pp.79-83.

142. Kitter, D.; "Euro motor brush spring". Hoover plc memorandum, October 1982.

143. Radia, S.; "Motor life tests with varying bearing journal diameters on EURO motor shafts". Hoover plc test report, January, 1982.

144. Higgs, R.P.; "Rubber to metal bond failure during the manufacture of concentric brushes". Thesis, University of Aston in Birmingham, April, 1981.

145. Private communication.

146. Mackay, D.; "Factors in A.C. commutator motor design and manufacture influencing radio frequency noise generation". Hoover plc Project proposal, July, 1980.

147. Dall, A.H.; "Rounding effect in centreless grinding". The American Society of Mechanical Engineers, Cincinnati, Ohio.